Bone Densitometry in Clinical Practice
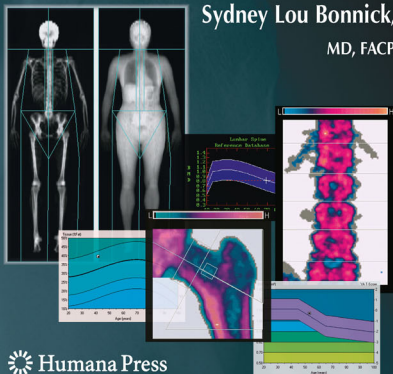
Application and Interpretation

THIRD EDITION

Sydney Lou Bonnick,

MD, FACP

CD-ROM Included

Humana Press

BONE DENSITOMETRY IN CLINICAL PRACTICE

BONE DENSITOMETRY IN CLINICAL PRACTICE

APPLICATION AND INTERPRETATION

THIRD EDITION

SYDNEY LOU BONNICK, MD, FACP

Clinical Research Center of North Texas, Denton, TX

Foreword by

PAUL D. MILLER, MD, FACP

Colorado Center for Bone Research, Lakewood, CO

Sydney Lou Bonnick, MD, FACP
Clinical Research Center of North Texas
2921 Country Club Road, #101
Denton, TX
USA
sbonnickcrcnt@verizon.net

Printed on acid-free paper

springer.com

Foreword

The third edition of Bone Densitometry in Clinical Practice by Dr. Sydney Lou Bonnick is the crown jewel in her seminal efforts to educate us all in the fundamentals as well as the advanced applications of bone densitometry. This edition shares common themes of her life's work: accuracy in all she does and precision in her science. One cannot, put very simply, find another book on bone densitometry that compares to the thoroughness of her work, and, in that regard, this book should be on the shelf of every medical library, medical student, house-officer, academic faculty member, practicing clinician, and radiology technologist – this edition offers each and every one at every level the latest and greatest in bone densitometry.

Since her pioneering work in bone densitometry which preceded by years the publication of her First edition of Bone Densitometry in Clinical Practice in 1998, Dr Bonnick has provided us an enduring education of how the science of DXA can be applied in the management of osteoporosis as well as distinctly different metabolic diseases traditionally not considered for DXA use. These include, for example, aortic calcium scoring in assessing risk for cardiovascular disease and the associations between BMD levels and breast cancer; body composition with assessment of visceral fat, an increasingly important measurement in the diagnosis and management of the "metabolic syndrome" as science keys in on the links between the adipocyte and bone metabolism. Body composition measurements also take on more importance at the other extreme: in the management of diseases associated with very low body mass index (e.g. anorexia, bulimia, the athletic triad) and will evolve as a means to study the associations between muscle mass and bone mass as pharmaceuticals are developed that influence the sarcolemma and bone cells. The expanded DXA application of hip structural analysis (HSA) has now allowed DXA to be used in measuring interventions that affect the cross-sectional moment of inertia and cortical bone size by assessing the effect of newer pharmacologicals and the mechanostats that influence bone strength by mechanisms independent of areal BMD.

There is more guidance in this third edition in assessing fracture risk beyond bone mineral density measurements alone but still emphasis that the highly under detected prior vertebral fracture, like all low-trauma fractures, carries the greatest weight in fracture risk prediction. Thus, DXA's improved application of vertebral fracture assessment (VFA) using higher resolution imaging is the best and lowest radiation technique to detect the highly prevalent non-clinical vertebral compression fracture. Wider implementation of VFA, whose CMS recognized indications for performance were spearheaded by The International Society for Clinical Densitometry (ISCD), should enable all involved in the management of osteoporosis patients to better select those patients at highest fracture risk. In that regard, Dr. Bonnick discusses the evolution as well as the pros and cons of the available fracture risk assessment tools that incorporate independent risk factors for fracture risk assessment (such as FRAX[TM] and FRAX[TM] precursors) as well as the National Osteoporosis Foundation's Clinicians Guide, that help guide clinicians in deciding on pharmacological intervention for osteoporosis at a broader level than simply provided by FRAX[TM].

In this pivotal textbook there are new chapters on radiation safety and assessment for secondary causes of bone fragility – issues that are important to all primary care and specialists who perform bone mass measurements and advise patient management decisions.

Finally, Dr. Bonnick has incorporated the recent ISCD Position Development Conferences (PDCs), both the fourth adult and the first pediatric into her text and has an entire appendix entirely devoted to the PDCs, which serve to advance the unanswered questions concerning DXA applications.

Bone densitometry quality control and performance and its subsequent clinical application are an entire science in their own right. If individuals performing DXA follow the advice provided by Dr. Bonnick in this third edition, patient care will be elevated to a very high quality. Health care professionals and payers of medical services who study this book will realize that DXA output goes far, far beyond a printed computer sheet. Proper DXA performance demands detail and clinical application and Dr. Bonnick's text provides the steps to achieve this excellence.

As I stated in the final sentences of the FOREWARD of her second edition, I am deeply honored to be asked by her to contribute to this introduction of a text that is symbolic of Dr. Sydney Bonnick's devotion to this field. I continue to learn from her and anyone who is privileged enough to know her and also read this outstanding piece of work will also benefit from her tremendous grasp of bone densitometry science and clinical application.

<div align="right">

Paul D. Miller, MD, FACP
Distinguished Clinical Professor of Medicine
University of Colorado Health Sciences Center
Medical Director
Colorado Center for Bone Research
Lakewood, Colorado

</div>

Preface

Bone densitometry is a fascinating field of medicine. Even in its earliest phases of development, densitometry incorporated aspects of imaging, physics, quantitative analysis, statistics, and computer technology that were applied in the diagnosis and management of multiple disease states. This extraordinary combination of attributes, however, left densitometry without a well-defined niche in clinical medicine. Imaging has traditionally been the purview of the radiologist. Quantitative analysis is more familiar to the pathologist. Metabolic bone disease has been the concern of the internist, rheumatologist, or endocrinologist and occasionally the nephrologist and orthopedist. And of course, physics, statistics, and computer technology have been left to those hardy souls who enjoy such things.

In 1988, when X-ray-based densitometers began to rapidly replace isotope-based densitometers, the door was opened for any medical specialty to perform densitometry. And yet, without a well-defined niche, without a specialty to champion the technology, there were no physicians who, by training, were immediately experts in the utilization of the technology.

In 1983, when I began working with dual-photon absorptiometry, the manufacturers provided a 4-hour inservice at the time of machine installation along with a brief operator's manual and the promise of technical support whenever it was needed. There were no ongoing programs of continuing education in the performance of densitometry or in the interpretation of the data that it generated. There was no supply of trained densitometry technologists. Conferences on osteoporosis were infrequent and lectures on densitometry were decidedly rare. As a clinical tool, densitometry was viewed with skepticism. None of the notable fracture trials had yet been published. Indeed, these would not come for approximately 10 years. Clinicians, unable to noninvasively measure bone density in the past, saw little need for the ability to do so. The one disease in which densitometry seemed most applicable, osteoporosis, was largely viewed as an unalterable component of aging making the measurement of bone density superfluous.

Certainly much has changed since then, both for good and for ill. With the ability to measure bone density, many disease states are now known to be characterized, at least in part, by demineralization. Suddenly, it is not only osteoporosis for which the technology can provide information crucial to disease management. And osteoporosis itself is certainly no longer viewed as unassailable. The fracture trials are published. Therapeutic and preventive efficacy of many drugs has now been documented. And the disease itself can now be defined based on the measured level of bone density. Although the technology is still properly viewed as a quantitative analytical technique, imaging with densitometry is progressing so rapidly that the time has come when some aspects of plain skeletal radiography are being superseded by imaging densitometry.

But as strange as it may seem, the technology itself is in danger of becoming so devalued that improvements in accessibility and advances in applications may be lost. Although densitometry is still underutilized, the number of devices has steadily increased. The number of individuals involved in the performance of densitometry has

steadily increased. But insistence on quality densitometry has not kept pace. There are those who perform bone densitometry for whom it is ultimately of little importance. There may be no attention to quality control of the devices, no learned supervision of the technologist, and little concern for the ramifications of inaccurate or obsolete reporting of densitometry results. In these circumstances, little value and attention is given to bone densitometry. Not surprisingly then, third party payers, the public, and our non-densitometrist physician colleagues have begun to attach little value to densitometry as well. This is a tragedy, as the advances of the last 20 years may be potentially wasted.

In 1990, Dr. Paul Miller and I independently began teaching courses in bone densitometry for the physician and technologist. The physicians who attended these courses came from all specialties. The technologists were RTs, MRTs, RNs, PAs, and nursing assistants. With the publication of the first edition of *Bone Densitometry in Clinical Practice* in 1998, I hoped to reach many more physicians and technologists who wished to become proficient in the application and interpretation of bone densitometry. In 2002, my technologist, Lori Lewis, and I published the first edition of *Bone Densitometry for Technologists*. This volume was intended solely for technologists, regardless of background, who worked in the field of densitometry. Although much of the requisite information and skill in densitometry are common to physicians and technologists alike, the unique demands placed on the densitometry technologist made such a volume both appropriate and necessary. The second edition of *Bone Densitometry for Technologists* was published in 2006. The second edition of *Bone Densitometry in Clinical Practice* was published in 2004.

Some, but not all, of our concerns in 2009 are vastly different from 1998. Unlike the situation in 1998, there are few locales in which bone densitometry is not available. Many physicians, clinics, and hospitals own densitometers. The number and types of devices have proliferated at a remarkable rate. It is rare to encounter a physician who does not yet know that fracture risk can be predicted with a single bone mass measurement. Our concerns are no longer access to densitometry and convincing the practicing physician that fracture risk can be predicted. But some concerns remain the same. Should every woman have a bone density measurement and if so, when? Can the World Health Organization criteria for the diagnosis of osteoporosis in postmenopausal Caucasian women be used to diagnose osteoporosis in women of other races or men of any race? Should the diagnosis of osteoporosis be restricted to bone density measurements of the proximal femur? Can peripheral skeletal sites be used to diagnose osteoporosis? How should an individual's risk of fracture be expressed? Can or should bone densitometry be used to determine efficacy of therapeutic agents in the treatment of osteoporosis? None of these concerns are new or esoteric. They go straight to the heart of how and when we use densitometry and interpret the data in the care of our patients. Whether you are new to the field or have worked in densitometry for 20 years, the issues are the same. All of us must ensure that quality control procedures are instituted and followed, precision studies are done, and data are properly interpreted. In 2009, however, perhaps because we are victims of our own success, the increase in the number of devices and number of individuals involved in densitometry has contributed to occasional misuse of the technology and lapses in quality, which have raised the specter of devaluation.

The third edition of *Bone Densitometry in Clinical Practice* is substantially larger than the first. New chapters have been added, even since the second edition of the book, which reflect both the new applications for densitometry and the evolving needs of the

densitometrist. Chapter 1 is a review of densitometry technologies that spans the earliest attempts to quantify bone density in the mandible in the late 1800s to the modern technologies of DXA, QCT, and QUS. Chapter 2 looks at the unique aspects of gross skeletal anatomy in densitometry and aspects of bone physiology relevant to the interpretation of bone density data. Chapter 3, which deals with statistics, is intended as an overview only. While most clinicians are familiar with statistical concepts like the mean, standard deviation, and significance, there are few if any areas of clinical medicine in which the application of statistical principles has assumed such a prominent role as in bone densitometry. As the reader will find, an understanding of some basic statistical concepts is imperative in the practice of densitometry. Chapter 3 is not intended to replace a review of more thorough statistical texts, but it is intended to ease the pain that the contemplation of such texts can engender. Chapter 4 reviews issues of machine quality control that are often underappreciated in clinical settings but which profoundly affect the validity of the data generated by the densitometers. Chapter 5 is new to this edition and is a review of radiation safety issues for the non-radiologist. Although radiation safety in clinical practice is not a major concern for the densitometrist, knowledge of radiation safety issues is requisite in the practice of densitometry. Chapter 6 addresses the differences in bone density measurements among the various manufacturers and the attempts at standardization of bone density measurements among manufacturers when bone density is measured at the same skeletal site on devices from different manufacturers.

Two of the last eight chapters in this edition are new to this volume. Chapters 7 and 8 deal with the selection of patients for densitometry measurements. Chapter 7 discusses and compares the guidelines from major organizations as they have evolved over the years. Chapter 8 deals with the various questionnaires and indices that have been developed to help patients identify themselves as candidates for bone mass measurements. These indices are deceptively simple in their final form, belying the very complex development process behind them. Consequently, the initial skepticism with which most of these indices have been met is understandable. Nevertheless, they are extremely useful in many circumstances. Chapters 9, 10, and 11 deal with the specific densitometry applications of diagnosis of osteoporosis, fracture risk prediction, and monitoring changes in bone density. Diagnosis and fracture risk prediction are separate entities and both remain the subject of some controversy, as previously noted. Chapter 11, which deals with monitoring changes in bone density, has been updated and expanded and includes a discussion of the statistical concept of regression to the mean and its relevance, or lack thereof, to monitoring bone density. It is an important concept to understand as it is still incorrectly used to diminish the value of monitoring changes in bone density. Chapter 12, which addresses secondary causes of bone loss, is new to this edition, replacing the chapter in earlier editions in which various articles relating to causes of bone loss were abstracted. When low bone density or osteoporosis is identified, the referring physician may look to the densitometrist for guidance in the evaluation of the patient to exclude secondary causes of bone loss. In this chapter, some of the more common differential diagnoses and the relevant evaluations to exclude each are reviewed. Chapter 12 is intended for the non-metabolic bone disease specialist densitometrist. Chapter 13 is also new to this edition and focuses on the new applications for DXA such as vertebral fracture assessment, aortic calcification scoring, hip structure analysis, and assessment of visceral fat. Finally, the challenge of bringing all this information to bear on the interpretation of the numerical densitometry data is addressed in Chapter 14. Although it is

one of the shorter chapters in the book, its importance should not be underestimated. The reality is that an inadequate or unread report will negate the expertise of the densitometrist and technologist as well as the promise of the technology. Finally, in Chapter 15, the technical specifications of densitometry devices currently approved for use in the United States are listed. These specifications may change without notice; so, the reader is encouraged to contact the manufacturer directly if more information is desired. Contact information for the various manufacturers can be found in Appendix I.

The appendices are an attempt to pull together reference information in a convenient location to enable the physician to refer to the information quickly, without searching the text. An entire appendix, Appendix V, has been devoted to the 2007 ISCD guidelines. The 1998 NHANES III reference database and native databases from the major manufacturers of central DXA devices will be found in Appendices IX-XII. The CD-ROM that accompanies this book contains several files that the densitometrist should find useful in every day practice as well as a study guide that can be completed for continuing education credit. The contents of the CD are described in Appendix XIV.

In a few circumstances in this text, data has been presented from published abstracts, rather than from peer-reviewed, published articles. This was done in the interest of providing information rapidly. The reader should be cautioned that data presented in abstract form might change slightly when it is finally published in a peer-reviewed journal. Some data presented in abstract form is never published in a peer-reviewed journal for a variety of reasons.

As this text has evolved over the years, it has essentially become a text on the use of DXA in clinical practice. Other technologies are discussed and should not be dismissed by the clinician. Some technologies provide measurements that are biologically different from those obtained with DXA. All of the technologies are remarkably accurate and when utilized correctly, very precise. But the evolution of the clinical criteria for the diagnosis of osteoporosis and the prediction of fracture risk have created a circumstance in which DXA measurements of the spine and proximal femur are the measurements that are ultimately clinically useful. It is perhaps unfortunate that this is so, in that truly remarkable technologies consequently have little practical clinical use. Nevertheless, it is the circumstance in which we find ourselves and is reflected in the focus of this book.

Bone densitometry is an extraordinary clinical tool. It provides a safe, non-invasive window to the skeleton. Through that window a physician can obtain vital clinical information that enhances the management of the patient that cannot currently be obtained in any other way. So, to whom in medicine does densitometry belong? To no one specialty in particular and to every specialty in general as long as the physician and technologist are committed to learning the unique aspects of this technology and the proper interpretation of the data that it generates. The technology itself is superb. Bone density can be measured with superior accuracy in virtually every region of the skeleton. The machines are capable of the finest precision of any quantitative technique in use in clinical medicine today. But the machines will perform only to the level of the expertise of those who operate them. And the data that they generate will only be as useful as the clarity of the interpretation that is provided by the densitometrist. It is hoped that this volume will be useful in helping the densitometrist fulfill the potential that the technology holds for contributing to the highest quality of patient care and disease prevention and management.

Sydney Lou Bonnick, MD, FACP

Acknowledgments

Numerous individuals have contributed to the content of this edition of Bone Densitometry in Clinical Practice. My gratitude is extended to all of them and in particular to: Tom Sanchez and Kathy Dudzek of Norland Medical Systems, a CooperSurgical Company; Dr. Mary Porter of Procter & Gamble; Dr. Howard Barden and Sean O'Sullivan of GE Healthcare; Mary Ann Barrick, RT and Dr. Kevin Wilson of Hologic, Inc.; Jakob Algulin of Sectra Imtec AB; Thomas Hessel of Osteometer Meditech; Chrystele Zawislack of Orthometrix; Imbar Vana of Sunlight Medical, Ltd; Roger Schulte of Image Analysis, Inc.; Dr. Ken Faulkner; Dr. Harry Genant; Dr. Richard Wasnich; Dr. Elliot Schwartz; Dr. Majorie Luckey; Dr. Michael McClung; and Dr. Paul Miller.

I would also like to thank those authors and publishers who allowed me to reproduce their work in the interest of continuing education.

And a special word of thanks to my editor, Paul Dolgert of Humana Press.

DEDICATION

For Margery Winston and Eliza Calvert Hall
and Cora Jane Spiller and Lynn Niedermeier, who helped me find them.

Contents

Continuing Medical Education

RELEASE DATE
September 1, 2009

EXPIRATION DATE
September 1, 2012

ESTIMATED TIME TO COMPLETE
30 Hours

Accreditation

We are pleased to award category 1 credit(s) toward the AMA Physician's Recognition Award. By reading the instructions in Appendix XIV and by completing the review in the CD-ROM companion, you are eligible for up to 30 hours of category 1 credit. After answering all of the questions correctly, complete the review evaluation and enter the required identifying information on the certificate of course completion. *This certificate is not valid until signed with authorized signature at the Foundation for Osteoporosis Research*. The certificate may be printed one time only. Send the certificate and the required fee to the Foundation for Osteoporosis Research and Education for awarding of continuing education credits.

This activity is offered by the Foundation for Osteoporosis Research and Education, a CMA accredited provider. Physicians completing this course may report up to 30 hours of category 1 credits toward the California Medical Association's Certification in Continuing Education and the American Medical Association's Physician's Recognition award. Each physician should claim only those hours of credit that he/she actually spent in the activity.

This activity has been planned and implemented in accordance with the essential areas and policies of the Accreditation Council for Continuing Medical Education (ACCME) through the joint sponsorship of the Foundation for Osteoporosis Research and Education and Humana Press, a part of Springer Science+Business Media. The Foundation for Osteoporosis Research and Education is accredited by the California Medical Association to provide continuing medical education for physicians.

Method of Participation

Read the book carefully. Complete the posttest and evaluation/certificate to be found on the companion CD-ROM. There is a $150 fee for this activity. Credit for the activity

is available until September 1, 2012. Additional directions for obtaining credit can be found on the companion CD-ROM.

Faculty and Disclosure

Sydney Lou Bonnick, MD

Clinical Research Center of North Texas
2921 Country Club Road, Ste. 101
Denton, Texas

Faculty for CME activities are expected to disclose to the activity audience any real or apparent conflict(s) of interest related to the content of the material they present. The following relationships have been disclosed:
Dr. Bonnick has nothing to disclose.

Provider Disclosure

The Foundation for Osteoporosis Research and Education is an independent organization that does not endorse specific products of any pharmaceutical concern and therefore has nothing to disclose. Humana Press does not endorse specific products of any pharmaceutical concern and therefore has nothing to disclose.

Intended Audience

This book is designed for physicians and technologists involved in the application of bone densitometry.

Overall Goal

The overall goal of this activity is to update the scientific knowledge and skills of physicians and technologists who manage patients with established osteoporosis or patients who may be at risk for developing osteoporosis.

Learning Objectives

Upon completion of this continuing medical education activity, participants should have improved overall knowledge, skills, and attitudes concerning the use of bone densitometry. Specifically, the objectives are:

1. To review the most clinically relevant aspects of interpreting bone density data.
2. To familiarize the physician with the resources found in the third edition of *Bone Densitometry in Clinical Practice*.
3. To emphasize potential pitfalls in interpreting and reporting densitometry results.

4. To familiarize the physician with current recommendations and standards for patient selection for testing and for densitometry reporting
5. To review the similarities and differences among the various densitometry techniques used in clinical practice
6. To review aspects of human anatomy unique to the field of densitometry

Unlabeled/Unapproved use Disclosure

In accordance with ACCME standards for commercial support, the audience is advised that this CME activity may contain references to unlabeled or unapproved uses of drugs or devices.

1   Densitometry Techniques

CONTENTS

Clinical densitometry is relatively new but densitometry itself is actually quite old. It was first described over 100 years ago in the field of dental radiology as dentists attempted to quantify the bone density in the mandible (*1, 2*). With today's techniques bone density can be quantified in almost every region of the skeleton. The extraordinary technical advances in recent years have expanded the realm of densitometry from that of a quantitative technique to that of an imaging technique as well. But even the oldest techniques remain both viable and valuable with computer modernization. Densitometry technologies have evolved as our understanding of relevant disease processes has increased. In a complimentary fashion, our understanding of the disease processes has increased as the technologies have evolved.

PLAIN RADIOGRAPHY IN THE ASSESSMENT OF BONE DENSITY

The earliest attempts to quantify bone density utilized plain skeletal radiography. When viewed by the unaided eye, plain skeletal radiographs can only be used in an extremely limited fashion to quantify bone density. Demineralization becomes visually apparent only after 40% or more of the bone density has been lost (*3*). If demineralization is suspected from a plain film, a great deal of demineralization is presumed to have occurred. A more precise statement cannot be made. Plain radiographs have been used for qualitative and quantitative skeletal morphometry. Plain radiographs were also used to assess bone density based on the optical densities of the skeleton when compared to simultaneously X-rayed standards of known density

made from ivory or aluminum. With the advent of photon absorptiometric techniques, most of these early methods, as originally performed, have fallen into disuse. Nevertheless, a brief review of these techniques should enhance the appreciation of the capabilities of modern testing and provide a background for understanding modern technologies.

QUALITATIVE MORPHOMETRY

Qualitative Spinal Morphometry

Qualitative morphometric techniques for the assessment of bone density have been in limited use for over 50 years. Grading systems for the spine relied on the appearance of the trabecular patterns within the vertebral body and the appearance and thickness of the cortical shell (*4*). Vertebrae were graded from IV down to I as the vertical trabecular pattern became more pronounced with the loss of the horizontal trabeculae and the cortical shell became progressively thinned. The spine shown in Fig. 1-1 demonstrates a pronounced vertical trabecular pattern. The cortical shell appears as though it was outlined in white around the more radiotranslucent vertebral body. These vertebrae would be classified as Grade II.

Fig. 1-1. Quantitative spine morphometry. The vertebrae on this lateral lumbar spine X-ray demonstrate marked accentuation of the vertical trabecular pattern and thinning of the cortical shell. This is a Grade 2 spine.

The Singh Index

The Singh Index is a qualitative morphometric technique that was similarly based on trabecular patterns, but based on those seen in the proximal femur (*5*). Singh and others had noted that there was a predictable order in the disappearance of the five groups of trabeculae from the proximal femur in osteoporosis. Based on the order of disappearance, radiographs of the proximal femur could be graded 1–6 with lower values indicating a greater loss of the trabecular patterns normally seen in the proximal femur. Studies evaluating prevalent fractures demonstrated an association between Singh Index values of 3 or less and the presence of fractures of the hip, spine, or wrist. Figure 1-2 shows a proximal femur with a Singh Index of 2. Only the trabecular pattern known as the principle compressive group, which extends from the medial cortex of the shaft to the upper portion of the head of the femur, remains. This patient was known to have osteoporotic spine fractures as well as a contralateral proximal femur fracture. Later attempts to demonstrate an association between Singh Index values and proximal femur bone density measured by dual-photon absorptiometry were not successful (*6*).

Fig. 1-2. The Singh Index and *calcar femorale* thickness. A Grade 2 Singh Index would be assessed based on having only remnants of the principle compressive group visible. This is indicative of osteoporosis. The arrow points to the *calcar femorale*, which measured 4 mm in thickness. Values <5 mm are associated with hip fracture. This patient had experienced a contralateral hip fracture.

Both of these qualitative morphometric techniques are highly subjective. In general, the best approach to their use required the creation of a set of reference radiographs of the various grades of vertebrae for spinal morphometry or proximal femurs for the Singh Index to which all other radiographs could be compared.

QUANTITATIVE MORPHOMETRIC TECHNIQUES

Calcar Femorale Thickness

A little known quantitative morphometric technique involved the measurement of the thickness of the *calcar femorale*. The *calcar femorale* is the band of cortical bone immediately above the lesser trochanter in the proximal femur. In normal subjects, this thickness is greater than 5 mm. In femoral fracture cases, it is generally less than 5 mm in thickness (*7*). The arrow seen in Fig. 1-2 is pointing to the *calcar femorale*. This patient had previously suffered a femoral neck fracture. The thickness of the *calcar femorale* measured 4 mm.

Radiogrammetry

Radiogrammetry is the measurement of the dimensions of the bones using skeletal radiographs. Metacarpal radiogrammetry has been in use for almost 50 years. As originally practiced, the dimensions of the metacarpals were measured using a plain radiograph of the hand and fine calipers or a transparent ruler. The total width and medullary width of the metacarpals of the index, long, and ring fingers were measured at the midpoint of the metacarpal. The cortical width was calculated by subtracting the medullary width from the total width. Alternatively, the cortical width could be measured directly. A variety of different calculations were then made such as the metacarpal index (MI) and the hand score (HS). The MI is the cortical width divided by the total width. The HS, which is also known as the percent cortical thickness, is the metacarpal index expressed as a percentage. Measurements of the middle three metacarpals of both hands were also made and used to calculate the six metacarpal hand score (6HS). Other quantities derived from these measurements included the percent cortical area (%CA), the cortical area (CA), and the cortical area to surface area ratio (CA/SA). The main limitation in all of these measurements is that they were based on the false assumption that the point at which these measurements were made on the metacarpal was a perfect hollow cylinder. Nevertheless, using these measurements and knowledge of the gravimetric density of bone, the bone density could be calculated. The correlation[1] between such measurements and the weight of ashed bone was good, ranging from 0.79 to 0.85 (*8,9*). The precision of metacarpal radiogrammetry was quite variable depending upon the measurement used.[2] The measurement of total width is very reproducible. The measurement of medullary width or the direct measurement of cortical width is less reproducible because the delineation between the cortical bone and medullary canal is not as distinct as the delineation between the cortical bone and soft tissue. Precision was variously

---

[1] Correlation indicates the strength of the association between two values or variables. The correlation value is denoted with the letter "r." A perfect correlation would be indicated by an r-value of +1.00 or −1.00.

[2] Techniques are compared on the basis of accuracy and precision, which can be described using the percent coefficient of variation (%CV). The %CV is the standard deviation divided by the average of replicate measurements expressed as a percentage. The lower the %CV, the better the accuracy or precision. See Chapters 3 and 11 for a detailed discussion of precision and accuracy.

reported as excellent to poor, but in expert hands it was possible to achieve a precision of 1.9% (*10*).

Although metacarpal radiogrammetry is an old technique and somewhat tedious to perform, it remains a viable means of assessing bone density in the metacarpals. Metacarpal radiogrammetry demonstrates a reasonably good correlation to bone density at other skeletal sites measured with photon absorptiometric techniques (*11*). The technique is very safe as the biologically significant radiation dose from a hand X-ray is extremely low at only 1 mrem.

Radiogrammetry can also be performed at other sites such as the phalanx, distal radius, and femur (*12–14*). Combined measurements of the cortical widths of the distal radius and the second metacarpal are highly correlated with bone density in the spine, as measured by dual-photon absorptiometry (*12*).

Today, plain films of the hand and forearm can be digitized using flatbed optical scanners and radiogrammetry performed with computerized analysis of the digitized images. Using such a digital radiogrammetry (DXR) system, Bouxsein et al. (*15*) evaluated the utility of metacarpal radiogrammetry in predicting fracture risk and the correlation between metacarpal DXR-BMD and BMD measured by other techniques at other sites. The authors used a case–cohort approach to identify three groups of 200 women based on their having experienced a hip fracture, wrist fracture, or spine fracture during the first 5 years of the Study of Osteoporotic Fractures (*16*). DXR-BMD of the metacarpals was strongly correlated with distal and proximal radial BMD measured by single-photon absorptiometry[3] ($r = 0.68$ and 0.75, respectively). The correlation with femoral neck and lumbar spine BMD measured by dual-energy X-ray absorptiometry[3] was more modest ($r = 0.50$ and 0.44, respectively). Metacarpal DXR-BMD predicted spine and wrist fracture risk as well as single-photon absorptiometry BMD measurements of the distal or proximal radius or heel or dual-energy X-ray absorptiometry of PA lumbar spine or femoral neck. The increase in risk for wrist fracture was 1.6 for each standard deviation decline in DXR-BMD and 1.9 for spine fracture. Although femoral neck BMD was the strongest predictor of hip fracture risk, metacarpal DXR-BMD predicted hip fracture risk as well as the other BMD measurements with an increase in risk of 1.8 for each standard deviation decline in BMD. This type of DXR system is available commercially from Sectra Pronosco in Denmark as part of a PACS[4] system.

The Radiologic Osteoporosis Score

The radiologic osteoporosis score combined aspects of both quantitative and qualitative morphometry (*14*). Developed by Barnett and Nordin, this scoring system utilized radiogrammetry of the femoral shaft and metacarpal as well as an index of biconcavity of the lumbar vertebrae. In calculating what Barnett and Nordin called a peripheral score, the cortical thickness of the femoral shaft divided by the diameter of the shaft and expressed as a percentage was added to a similar measurement of the metacarpal. A score of 88 or less was considered to indicate peripheral osteoporosis. The biconcavity index was calculated by dividing the middle height of the third lumbar vertebra by

---

[3] This technique is discussed later in this chapter.
[4] Picture Archiving and Communications System.

its anterior height and expressing this value as a percentage. A biconcavity index of 80 or less indicated spinal osteoporosis. Combining both peripheral score and biconcavity index resulted in the total radiologic osteoporosis score, which indicated osteoporosis if the value was 168 or less.

Radiographic Texture Analysis (RTA) and Spatial Anisotropy Analysis Utilizing Plain Radiography

The Singh Index (*5*), which was described earlier in this chapter, utilized plain radiographs of the proximal femur to assign a grade, based on the orderly disappearance of trabecular bundles in the femoral neck. Although the index was not characterized at the time in terms of radiographic texture analysis (RTA) or spatial anisotropy, it was not far removed in concept from today's approaches which utilize sophisticated mathematics such as fractal analysis, principal component analysis, and fast Fourier transform analysis of images from skeletal radiographs (*17–21*). The logistical advantage to these approaches, just as was the logistical advantage of the Singh Index, is the utilization of both existing and widely available non-invasive technology to acquire the original data. The logistical disadvantage of these newer approaches is that the mathematical iterations generally require specific expertise and exportation of the image into complex computer programs, which are not widely available. RTA and spatial anisotropy are not measurements of density; they are included here because they represent a highly sophisticated return to plain radiography in the assessment of bone strength.

RADIOGRAPHIC TEXTURE ANALYSIS

Radiographic texture analysis (RTA) of either plain films or DXA images is an analysis of patterns in the two-dimensional images of three-dimensional bones rather than an analysis of individual trabeculae. Fractal mathematics is used to quantify qualitative changes in the texture patterns. These patterns can differ between strong and fragile bones. RTA has been shown in cross-sectional studies to differentiate between patients with vertebral fracture and non-fractured controls, based even in subgroups with overlapping proximal femur bone density values (*17*). Pothauad et al. employed fractal mathematics to analyze plain films of the calcaneus in 39 postmenopausal women with vertebral crush fractures compared to 39 non-fractured postmenopausal women. The area under the receiver-operating curve (AUROC)[5] for the fractal statistic, called the H_{mean} (Hurst exponent mean), was statistically significantly greater than for femoral neck BMD. Interestingly, in a sub-group analysis, the H_{mean} was significantly lower in the fracture patients compared to controls, even though the femoral neck and trochanteric bone densities were overlapping. In a larger cross-sectional study, Benhamou et al. (*18*) utilized plain films of the calcaneus and fractal analysis to perform RTA in 197 controls and 107 fracture patients. BMD was measured with DXA. The fracture patients had experienced spine, hip, or wrist fractures. In this study, the H_{mean} was significantly lower in the spine and hip fracture patients compared to controls, even after adjustment for spine or femoral neck BMD.

---

[5] See Chapter 3 for a discussion of the AUROC.

Plain radiographs of the proximal femur were utilized by Gregory et al. (*19*) to perform RTA in a small group of 26 hip fracture patients and 24 non-fractured controls. In this study, both fractal analysis and another mathematical approach called principal components analysis (PCA), a data-reduction technique, were used to perform RTA and bone density was measured at the femoral neck with DXA. Not surprisingly, femoral neck BMD was significantly lower in the fracture patients compared to controls. Both the fractal analysis and the PCA were also able to discriminate between the fracture patients and controls and neither was significantly correlated with femoral neck BMD, age, or body mass index (BMI). The results of this study and that of Benhamou et al. (*18*) suggested that RTA provided insight into skeletal fragility that was not apparent from BMD or age.

Measurements of Spatial Anisotropy

In a sense, quantifying spatial anisotropy in bone is an extension of RTA. It is generally acknowledged that the strength of the bone is not isotropic (*22*). Instead, bone strength is anisotropic; that is, bone is stronger when loaded in one direction versus another. The orientation of the trabeculae is generally viewed as an indication of the preferred spatial anisotropy. The original Singh Index could thus be viewed as an early assessment of spatial anisotropy. Chappard et al. (*19*) proposed a measure of spatial anisotropy called the degree of anisotropy (DA). This was calculated from digitized images of calcaneal radiographs, using fast Fourier transform (FFT) spectrum data. From these data the spreading angles of the longitudinal trabeculae, called the dispersion longitudinal index (DLI), and the spreading angles of the horizontal trabeculae, called the dispersion transverse index (DTI), could be calculated. The DA is the ratio of π (pi) divided by the sum of the DLI and DTI. Chappard et al. applied this analysis in a cross-sectional study of 39 postmenopausal women with vertebral fractures and 70 non-fracture controls. The study subjects also underwent DXA bone density measurements at the PA lumbar spine and femoral neck. In this same study, RTA was performed and the H_{mean} fractal statistic reported. The best discrimination between fracture patients and non-fracture controls was seen for the DA and H_{mean} with AUROCs of 0.765 and 0.683, respectively, compared to those for lumbar spine and femoral neck BMD of 0.614 and 0.591, respectively. In a similar study of 22 patients with a variety of osteoporotic fractures who were then matched with 44 non-fracture controls, the DA was significantly higher in the fracture patients (*21*). The higher DA suggests greater anisotropy, which would theoretically result from a loss of some directional trabeculae. In evaluating the ability of the various parameters to discriminate between the fracture patients and controls, the authors found that the AUROCs for the DA, lumbar spine BMD, femoral neck BMD, and total hip BMD were 0.77, 0.64, 0.62, and 0.65, respectively.

The logistical limitations of the measurement of spatial anisotropy are the same as those for RTA. The mathematical calculations are extremely complex and such expertise is not commonly found. The attractiveness of the approach lies in its ability to utilize data from plain radiography. Both RTA and spatial anisotropy appear to provide complementary information to that obtained from the BMD, which could potentially be used to better predict fracture risk. At present, however, data are limited to cross-sectional studies looking at the ability to discriminate fracture patients from non-fracture controls.

RADIOGRAPHIC PHOTODENSITOMETRY

Much of the development of the modern techniques of single- and dual-photon absorptiometry and dual-energy X-ray absorptiometry actually came from early work on the X-ray-based method of photodensitometry (*23*). In photodensitometry, broad-beam X-ray exposures of radiographs were obtained and the density of the skeletal image was quantified using a scanning photodensitometer. One such early device at Texas Woman's University is shown in Fig. 1-3. The effects of variations in technique such as exposure settings, beam energy, and film development were partially compensated by the simultaneous exposure of a step wedge of known densities on the film. An aluminum wedge was most often used, but other materials such as ivory were also employed (*13*). This technique could only be applied to areas of the skeleton in which the soft tissue coverage was less than 5 cm such as the hand, forearm, and heel. This restriction was necessary because of technical limitations from scattered radiation in thicker parts of the body and "beam hardening" or the preferential attenuation of the softer energies of the polychromatic X-ray beam as it passed through the body. Photodensitometry was also used in cadaver studies of the proximal femur (*24*). Such studies noted the predictive power for hip fracture of the density of the region in the proximal femur known as Ward's triangle[6] 30 years before studies using the modern technique of dual-energy X-ray absorptiometry in 1993 (*25*). The accuracy of such measurements was fairly good with a %CV of 5%. The correlation between metacarpal photodensitometry and ashed bone was also high at 0.88 (*8*), which was a slightly better correlation than seen with metacarpal radiogrammetry. The precision of photodensitometry was not as good, however, ranging from 5
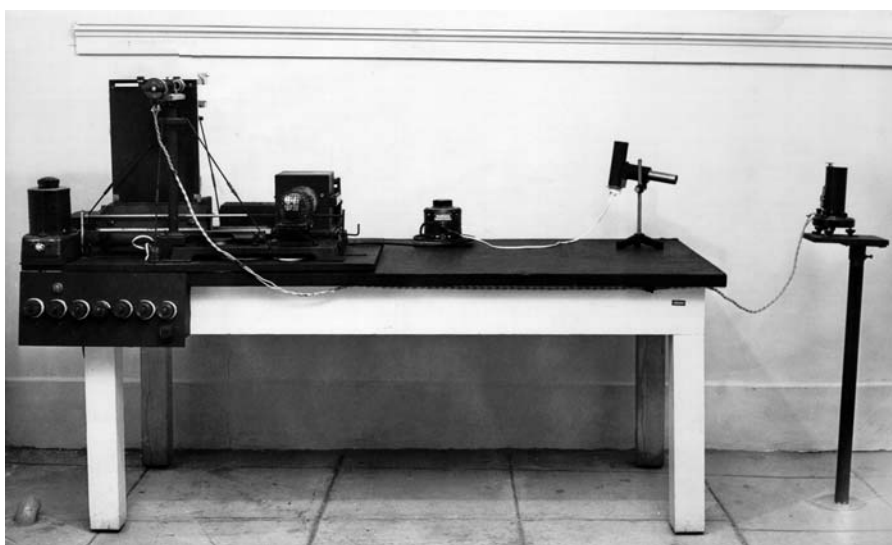
Fig. 1-3. A radiographic photodensitometer at Texas Woman's University from the early 1950s.

---

[6] Ward's triangle was first described by F.O. Ward in *Outlines of Human Osteology*, London; Henry Renshaw, 1838. It is a triangular region created by the intersection of three groups of trabeculae in the femoral neck.

to 15% (*26*). In this regard, the six metacarpal radiogrammetry hand score was superior (*4*). Radiation dose to the hand was the same for metacarpal radiogrammetry and radiographic photodensitometry. In both cases, the biologically significant radiation dose was negligible.

Radiographic photodensitometry was developed and used extensively by researchers Pauline Beery Mack and George Vose (*27*). Many of the original studies of the effects of weightlessness on the skeleton in the Gemini and Apollo astronauts were performed by Pauline Beery Mack and her colleagues at Texas Woman's University (*28*). The photodensitometry hand film of one of the Gemini astronauts is shown in Fig. 1-4.

Fig. 1-4. A radiographic photodensitometry hand film taken in 1965 of one of the Gemini astronauts. The Texas Woman's University aluminum wedge is seen next to the little finger.

RADIOGRAPHIC ABSORPTIOMETRY

Radiographic absorptiometry (RA) is the modern-day descendent of radiographic photodensitometry (*29, 30*). The ability to digitize high-resolution radiographic images and to perform computerized analysis of such images largely eliminated the errors introduced by differences in radiographic exposure techniques and overlying soft tissue thickness. In an early version of RA, two X-rays of the left hand using non-screened film were taken at slightly different exposures. Standard X-ray equipment was used to perform the hand films. The initial recommended settings were 50 kVp at 300 mA for

1 sec and 60 kVp at 300 mA for 1 sec. The exact settings varied slightly with the equipment used and were adjusted so that the background optical density of each of the two hand films matched a quality control film. An aluminum alloy reference wedge was placed on the film prior to exposure, parallel to the middle phalanx of the index finger. After development, the films were sent to a central laboratory where they were digitized and analyzed by computer. The average bone mineral density in arbitrary RA units of the middle phalanges of the index, long, and ring fingers was reported. Figure 1-5 illustrates the X-ray appearance of the hand and aluminum alloy reference wedge.

Fig. 1-5. A radiographic absorptiometry hand film. The small aluminum wedge, originally known as the Fel's wedge, is seen next to the index finger.

In cadaveric studies, the accuracy of RA for the assessment of bone mineral content of the middle phalanges was good at 4.8% (*31*). The authors of this study noted that very thick soft tissue that might be seen in very obese subjects could potentially result in an underestimation of RA values. The correlation between the RA values and the ashed weight in the phalanges was excellent with r = 0.983. The short-term reproducibility of these measurements was also excellent at 0.6%.

The ability to predict bone density at other skeletal sites from hand radiographic absorptiometry is as good as that seen with other techniques such as single-photon absorptiometry, dual-photon absorptiometry, dual-energy X-ray absorptiometry, or quantitative computed tomography of the spine (*29, 32*). This does not mean that RA hand values can be used to accurately predict bone density at other skeletal sites. Although the correlations between different sites as measured by various techniques are correctly said to be statistically significant, the correlations are too weak to allow

clinically useful predictions of bone mass or density at one site from measurement at another.

The utility of modern-day radiographic absorptiometry in predicting hip fracture risk was suggested by an analysis of data acquired during the first National Health and Nutrition Examination Survey (NHANES I, 1971–1975). During this survey, 1559 hand radiographs of Caucasian women were obtained with the older technique of photodensitometry using the Texas Woman's University wedge (*33*). During a median follow-up of 14 years that extended through 1987, 51 hip fractures occurred. Based on radiographic photodensitometry of the second phalanx of the small finger of the left hand the risk for hip fracture per standard deviation decline in bone density increased 1.66-fold. These films were then reanalyzed using radiographic absorptiometry with some compensation for the differences in technique. This reanalysis yielded an increase in the risk for hip fracture per standard deviation decline in RA bone density of 1.81-fold. Huang and colleagues (*34*) evaluated the utility of RA in the prediction of vertebral fractures. They followed 560 postmenopausal women, average age 73.7 years, for an average of 2.7 years in the Hawaii Osteoporosis Study. The risk for vertebral fracture in this study using RA was 3.41-fold for each standard deviation decline in bone density.

RA systems are commercially available. The automated Osteogram® system from CompuMed, Inc. consists of the computer hardware, software, and film cassette with hand template and reference wedge needed to perform radiographic absorptiometry of the phalanges. A film-less, self-contained system is also in development. The Metriscan™ from Alara, Inc. is a self-contained device that utilizes storage phosphor technology in place of X-ray film to perform RA of the phalanges. Both systems are discussed in Chapter 15.

PHOTON ABSORPTIOMETRY TECHNIQUES

In radiology, attenuation refers to a reduction in the number and energy of photons in an X-ray beam. Attenuation, then, is a reduction in an X-ray beam's intensity. To a large extent, the attenuation of X-rays is determined by tissue density. The difference in tissue densities is responsible for creating the images seen on an X-ray. The more dense the tissue, the more electrons it contains. The number of electrons in the tissue determines the ability of the tissue to either attenuate or transmit the photons in the X-ray beam. The differences in the pattern of transmitted or attenuated photons create the contrast necessary to discern images on the X-ray. If all the photons were attenuated (or none were transmitted), no image would be seen because the film would be totally white. If all of the photons were transmitted (or none were attenuated), no image would be seen because the film would be totally black. The difference in the attenuation of the X-ray photon energy by different tissues is responsible for the contrast on an X-ray, which enables the images to be seen. If the degree of attenuation could be quantified, it would be possible to quantitatively assess the tissue density as well. This is the premise behind the measurement of bone density with photon absorptiometric techniques. The earliest photon absorptiometric techniques employed radionuclides to generate photon energy. These radionuclide-based techniques have given way to X-ray based techniques. The basic principles on which they operate, however, remain the same.

Single-Photon Absorptiometry

Writing in the journal *Science* in 1963, Cameron and Sorenson (*35*) described a new method for determining bone density in vivo by passing a monochromatic or single-energy photon beam through bone and soft tissue. The amount of mineral encountered by the beam could be quantified by subtracting the beam intensity after passage through the region of interest from the initial beam intensity. In these earliest single-photon absorptiometry (SPA) units, the results of multiple scan passes at a single location, usually the mid-radius, were averaged (*36*). In later units, scan passes at equally spaced intervals along the bone were utilized such that the mass of mineral per unit of bone length could be calculated. A scintillation detector was used to quantify the photon energy after attenuation by the bone and soft tissue in the scan path. After the photon attenuation was quantified, a comparison to the photon attenuation seen with a calibration standard derived from dried defatted human ashed bone of known weight was made in order to determine the amount of bone mineral.

The photon beam and the detector were highly "collimated" or restricted in size and shape. The beam source and detector moved in tandem across the region of interest on the bone, coupled by a mechanical drive system. Iodine-125 at 27.3 keV or americium-241 at 59.6 keV was originally used to generate the single-energy photon beam although most SPA units subsequently developed in the United States employed only [125]I.

The physical calculations for SPA determinations of bone mineral were valid only when there was uniform thickness of the bone and soft tissue in the scan path. In order to artificially create this kind of uniform thickness, the limb to be studied had to be submerged in a water bath or surrounded by a tissue-equivalent material. As a practical matter, this limited SPA to measurements of the distal appendicular skeleton such as the radius and later, the calcaneus. Figure 1-6 is a photograph of an old SPA device, the Norland 2780 that was in use in the 1980s.
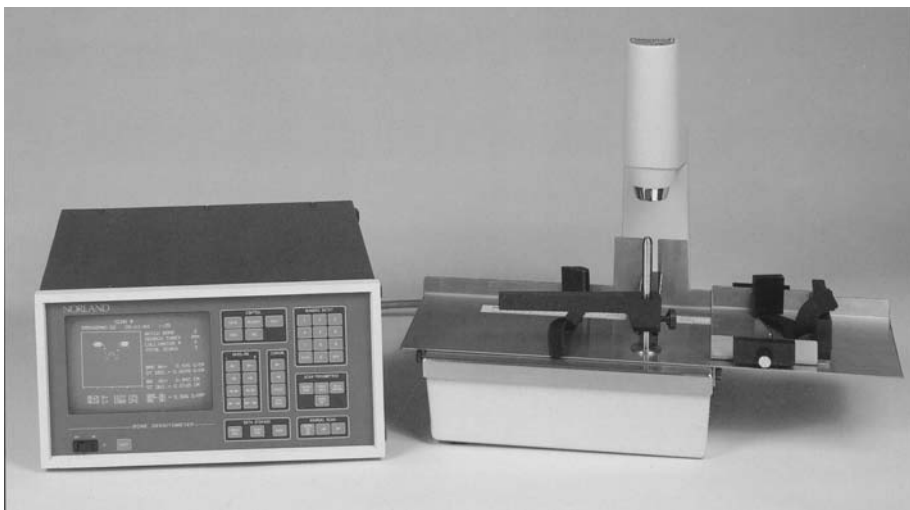
Fig. 1-6. An early Norland model 2780 single photon absorptiometer. This device utilized ^{125}I to generate photon energy. Photo courtesy of Norland, a CooperSurgical Company, Ft. Atkinson, WI.

Single-photon absorptiometry was both accurate and precise although the parameters varied slightly with the site studied. For SPA measurements of the mid-radius accuracy ranged from 3 to 5% and precision from 1 to 2% (*35–39*). Early measurements of the distal and ultra-distal radius with SPA did not demonstrate the same high degree of precision primarily due to the marked changes in the composition of the bone with very small changes in location within the distal and ultra-distal radius.[7] With later instruments that employed computer-enhanced localization routines and rectilinear scanning, SPA measurements of the distal and ultra-distal radius approached a precision of 1% (*40*). Accuracy and precision of measurements at the calcaneus with SPA were reported to be less than 3% (*38*). The skin radiation dose for both the radius and calcaneus was 5–10 mrem (*38, 39*). The biologically important radiation dose, the effective dose, was negligible. Results were reported as either bone mineral content (BMC) in g or as bone mineral content per unit length (BMD/l) in g/cm. The time required to perform such studies was approximately 10 minutes (*41*).

SPA is rarely performed today, having been supplanted first by single-energy X-ray absorptiometry (SXA) and now dual-energy X-ray absorptiometry. The demise of SPA was due to improvements in ease of use and precision seen with SXA and DXA. SPA was an accurate technology that could be used to predict fracture risk. The ability to predict the risk of appendicular fractures with SPA measurements of the radius was convincingly established (*42–44*). SPA measurements of the radius were also good predictors of spine fracture risk and global[8] fracture risk (*42, 45, 46*). Indeed, the longest fracture trials published to date, demonstrating the ability of a single bone mass measurement to predict fracture, were performed using SPA measurements of the radius.

Dual-Photon Absorptiometry

The basic principle involved in dual-photon absorptiometry (DPA) for the measurement of bone density was the same as for single-photon absorptiometry: quantifying the degree of attenuation of a photon energy beam after passage through bone and soft tissue. In dual-photon systems, however, an isotope, which emitted photon energy at two distinct photoelectric peaks, or two isotopes, each emitting photon energy at separate and distinct photoelectric peaks, were used. When the beam was passed through a region of the body containing both bone and soft tissue, attenuation of the photon beam occurred at both energy peaks. If one energy peak was preferentially attenuated by bone, however, the contributions of soft tissue to beam attenuation could be mathematically subtracted (*47*). As in single-photon absorptiometry, the remaining contributions of beam attenuation from bone were quantified and then compared to standards created from ashed bone. The ability to separate bone from soft tissue in this manner finally allowed quantification of the bone density in those areas of the skeleton which were surrounded by large or irregular soft tissue masses, notably the spine and proximal femur. DPA was also used to determine total body bone density. The development of

---

[7] See Chapter 2 for a discussion of the composition of the radius and ulna.

[8] Global fracture risk refers to the risk of having any and all types of fractures combined. This is in contrast to a site-specific fracture risk prediction in which the risk for a fracture at a specific skeletal site is given, such as spine fracture risk or hip fracture risk.

DPA and its application to the spine, proximal femur, and total body is attributed to a number of investigators: B.O. Roos, G.W. Reed, R.B. Mazess, C.R. Wilson, M. Madsen, W. Peppler, B.L. Riggs, W.L. Dunn, and H.W. Wahner (*48–53*).

The isotope most commonly employed in dual-photon absorptiometry in the United States was gadolinium-153, which naturally emitted photon energy at two photoelectric peaks, 44 and 100 keV. At the photoelectric peak of 44 keV bone preferentially attenuated the photon energy. The attenuated photon beams were detected by a NaI scintillation detector and quantified after passage through pulse-height analyzers set at 44 and 100 keV. The shielded holder for the ^{153}Gd source, which was collimated and equipped with a shutter that was operated by a computer, moved in tandem with the NaI detector in a rectilinear scan path over the region of interest. A point-by-point calculation of bone density in the scan path was made. Figure 1-7 is an intensity-modulated image of the spine, created with an early DPA device.
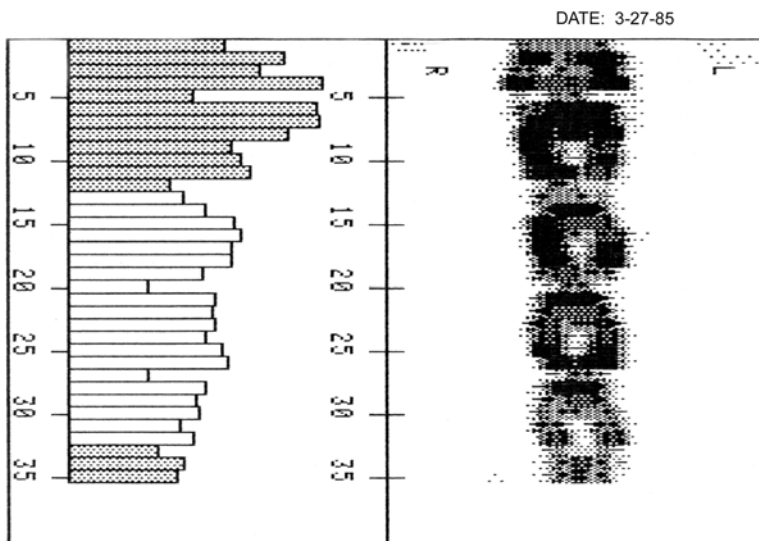
Fig. 1-7. A dual-photon absorptiometry PA spine study obtained on a device as shown in Fig. 1-8. The spine image is upside down. The histogram on the *right* was used to place the intervertebral disc space markers. The *shortest bar* in the vicinity of the disc space was identified and the marker was placed there.

DPA bone density studies of the lumbar spine were performed with the photon energy beam passing in a posterior to anterior direction. Because of the direction of the beam, the vertebral body and the posterior elements were included in the scan path. The transverse processes were eliminated. This resulted in a combined measurement of cortical and trabecular bone, or an integral measurement, that included the more trabecular vertebral body surrounded by its cortical shell and the highly cortical posterior elements. The results were reported as an areal density in g/cm^2. The bone mineral density of the proximal femur was also an areal density that was acquired with the beam passing in a posterior to anterior direction. Figure 1-8 shows an early dual-photon absorptiometer with the patient positioned for a study of the lumbar spine.

DPA studies of the spine required approximately 30 minutes to complete. Studies of the proximal femur took 30–45 minutes to perform. Total body bone density studies with DPA required 1 hour. Skin radiation dose was low during spine or proximal femur

Fig. 1-8. An early Lunar DP3 dual-photon absorptiometer. This device utilized ^{153}Gd to generate photon energy. Photo courtesy of GE Healthcare, Madison, WI.

studies at 15 mrem. Accuracy of DPA measurements of the spine ranged from 3 to 6% and for the proximal femur 3 to 4% (*54*). Precision for measurements of spine bone density was 2–4% and around 4% for the femoral neck.

Dual-photon absorptiometry was considered a major advance from single-photon absorptiometry because it allowed the quantification of bone density in the spine and proximal femur. DPA did have several limitations, however. Machine maintenance was expensive. The ^{153}Gd source had to be replaced yearly at a cost of $5000.00 or more. It had also been noted that as the radioactive source decayed, values obtained with DPA increased by as much as 0.6% per month (*55*). With replacement of the source, values could fall by as much as 6.2%. Although mathematical formulas were developed to compensate for the effect of source decay, it remained a cause for concern, potentially affecting both accuracy and precision. The precision of 2–4% for DPA measurements of the spine and proximal femur limited its application in detecting changes in bone density. With a precision of 2%, a change of at least 5.5% from the baseline value had to be seen before one could be certain at the 95% confidence level that any change had occurred at all (*56*). With a precision of 4%, this figure increased to 11.1%. At a lower 80% confidence level, the required change for precision values of 2 and 4% were 3.6 and 7.2%, respectively. As a practical matter, this meant that DPA bone density studies would not show significant changes for up to 5 years. This was too long a period to wait to be clinically useful.

In DPA spine bone density studies in which the photon beam passed in a PA direction the highly trabecular vertebral body could not be separated from its more cortical posterior elements. In addition, the cortical shell of the vertebral body could not be separated from its trabecular interior. Calcifications in the overlying soft tissue or abdominal aorta will attenuate such a beam, falsely elevating the bone density values. Arthritic changes in the posterior elements of the spine also affect the measurement (*57*). These effects are discussed in greater detail in Chapters 2 and 9. PA dual-energy X-ray absorptiometry

(DXA) studies of the spine are not immune to these effects either but lateral DXA spine studies can be performed to overcome these limitations. Studies of the spine in the lateral projection were never available with DPA.

The ability to make site-specific predictions of fracture risk of the spine and proximal femur or global fracture risk predictions with dual-photon absorptiometry was established in prospective trials (*25*, *45*). Like SPA, DPA is rarely performed in the United States now, because of the availability of DXA with its technological improvements.

Dual-Energy X-ray Absorptiometry

The underlying principles of dual-energy X-ray absorptiometry (DXA) are the same as those of dual-photon absorptiometry. With DXA, however, the radioactive isotope source of photon energy has been replaced by an X-ray tube. There are several advantages of X-ray sources over radioactive isotopes. There is no source decay that would otherwise require costly replacement of the radioactive source. Similarly, there is no concern of a drift in patient values due to source decay. The greater source intensity or "photon flux" produced by the X-ray tube and the smaller focal spot allows for better beam collimation resulting in less dose overlap between scan lines and greater image resolution. Scan times are faster and precision is improved.

Because X-ray tubes produce a beam that spans a wide range of photon energies, the beam must be narrowed in some fashion in order to produce the two distinct photo-electric peaks necessary to separate bone from soft tissue. The major manufacturers of central dual-energy X-ray absorptiometers in the United States have chosen to do this in one of two ways. GE Healthcare of Madison, WI, and Norland, a CooperSurgical Company of Fort Atkinson, WI, use rare earth K-edge filters to produce two distinct photoelectric peaks. Hologic, Inc. of Bedford, MA, uses a pulsed power source to the X-ray tube to create the same effect.

K-edge filters produce an X-ray beam with a high number of photons in a specific range. The energy range that is desired is the energy range that is just above the K-absorption edge of the tissue in question. The K-edge is the binding energy of the K-shell electron. This energy level varies from tissue to tissue. The importance of the K-edge is that at photon energies just above this level, the transmission of photons through the tissue in question drops dramatically. That is, the photons are maximally attenuated at this energy level (*58*). Therefore, to separate bone from soft tissue in a quantifiable fashion, the energy of the photon beam should be just above the K-edge of bone or soft tissue for maximum attenuation. GE Healthcare uses a cerium filter in its central[9] devices that has a K-shell absorption edge at 40 keV. A cerium-filtered X-ray spectrum at 80 kV will contain two photoelectric peaks at about 40 and 70 keV. The samarium K-edge filter employed by Norland in its central devices has a K-shell absorption edge of 46.8 keV. The samarium-filtered X-ray beam at 100 kV produces a low-energy peak at 46.8 keV. In the Norland system, the high-energy peak is variable because the system employs selectable levels of filtration but the photons are limited

---

[9] A central device is a bone densitometer that can be used to quantify bone density in the spine and proximal femur. The distinction between central and peripheral devices is discussed in Chapter 2.

to less than 100 keV by the 100 kV employed. The K-edge of both cerium and samarium results in a low-energy peak that approximates the 44 keV low-energy peak of gadolinium-153 used in old dual-photon systems.

Hologic central DXA devices utilize a different system to produce the two photoelectric peaks necessary to separate bone from soft tissue. Instead of employing K-edge filtering of the X-ray beam, Hologic employs alternating pulses to the X-ray source at 70 and 140 kV.

Most regions of the skeleton are accessible with dual-energy X-ray absorptiometry. Studies can be made of the spine in both an anteroposterior[10] and lateral projection. Lumbar spine studies acquired in the lateral projection have the ability to eliminate the confounding effects of dystrophic calcification on densities measured in the PA direction (*59*). Lateral scans also eliminate the highly cortical posterior elements which contribute as much as 47% of the mineral content measured in the PA direction (*60*). The utility of lateral DXA lumbar spine studies can be limited by rib overlap of L1 and L2 and pelvic overlap of L4, more so when performed in the left lateral decubitus position than the supine position (*59, 61*). Bone density in the proximal femur, forearm, calcaneus, and total body can also be measured with DXA.

Scan times are dramatically shorter with DXA compared to DPA. Early DXA units required approximately 4 minutes for studies of the PA lumbar spine or proximal femur. Total body studies required 20 minutes in the medium scan mode and only 10 minutes in the fast scan mode. Newer DXA units scan even faster, with studies of the AP spine or proximal femur requiring less than a minute to perform.

The values obtained with dual-energy X-ray studies of the skeleton are highly correlated with values from earlier studies performed with dual-photon absorptiometry. Consequently, the accuracy of DXA is considered comparable to that of DPA (*62–65*). DXA spine values and Hologic and Norland DXA proximal femur values are consistently lower than values obtained previously with DPA. There are also differences in the values obtained with DXA equipment from the three major manufacturers.[11] Values obtained with either a Hologic or Norland DXA unit are consistently lower than those obtained with a Lunar DXA unit although all are highly correlated with each other (*66–68*). Comparison studies using all three manufacturer's central DXA devices have resulted in the development of formulas that make it possible to convert values for the lumbar spine and femoral neck obtained on one manufacturer's device to the expected value on another manufacturers' device (see Appendix II) (*69*). The margin of error in such conversions is still too great to use such values in following a patient over time, however. Such values should only be viewed as "ball park" figures. Another set of formulas makes possible the conversion of any manufacturer's BMD value at the lumbar spine or total hip to a second value called the "standardized bone mineral density" or

---

[10] Although spine bone density studies with dual-energy X-ray absorptiometry are often referred to as AP spine studies, the beam actually passes in a posterior to anterior direction. Such studies are correctly characterized as PA spine studies, but an accepted convention is to refer to them as AP spine bone density studies. The Lunar Expert, a fan-array DXA scanner, does acquire spine bone density studies in the AP projection.

[11] See Chapter 6 for a detailed discussion of the difference in values obtained using central devices from different manufacturers, conversions equations, and the development of the sBMD.

sBMD (see Appendix II) (*69, 70*). The sBMD is always reported in mg/cm^2 to distinguish it from the manufacturer's BMD, which is reported in g/cm^2.

Perhaps the most significant advance seen with DXA compared to DPA is the marked improvement in precision. Expressed as a coefficient of variation, short-term precision in normal subjects has been reported as low as 0.9% for the PA lumbar spine and 1.4% for the femoral neck (*62*). Precision studies over the course of 1 year have reported values of 1% for the PA lumbar spine and 1.7–2.3% for the femoral neck (*65*).

Radiation exposure is extremely low for all types of DXA scans. Expressed as skin dose, radiation exposure during a PA lumbar spine or proximal femur study is only 2–5 mrem.[12] The biologically important effective dose or whole-body equivalent dose is only 0.1 mrem (*71*).

Dual-energy X-ray absorptiometry has been used in prospective studies to predict fracture risk. In one of the largest studies of its kind, DXA studies of the proximal femur were demonstrated to have the greatest short-term predictive ability for hip fracture compared to measurements at other sites with SPA or DPA (*25*).

DXA central devices are called "pencil-beam" or "fan-array" scanners. Examples of pencil-beam scanners are the Lunar DPX® Plus, DPX®-L, DPX-IQ™, DPX®-SF, DPX®-A, DPX-MD™, DPX-MD+™, and DPX-NT™, the Hologic QDR® 1000 and QDR®2000, and the Norland XR-36™, XR-46™, Excell™, and Excell™plus.[13] Examples of fan-array DXA scanners are the Lunar Expert®, Bravo™, Duo™, Prodigy™, and iDXA™ and the Hologic QDR® 4500 A, QDR® 4500 C, QDR® 4500 W, QDR® 4500 SL, Delphi™, Discovery™, and Explorer™. The difference between the pencil-beam and fan-array scanners is illustrated in Figs. 1-9 and 1-10. Pencil-beam scanners employ a collimated or narrowed X-ray beam (narrow like a pencil) that moves in tandem in a rectilinear pattern with the detector(s). Fan-array scanners utilize a much broader or fan-shaped beam and an array of detectors, so that an entire scan line can be instantly quantified. Scan times are reduced to as little as 30 sec for a PA study of the lumbar spine. Image resolution is also enhanced with the fan-array scanners as shown in the extraordinary images in Fig. 1-11. This has created a new application for bone densitometry scanning called morphometric X-ray absorptiometry or MXA. With MXA, images of the spine obtained in the lateral projection can be used for computer analysis of the vertebral dimensions and diagnosis of vertebral fracture.[14] Fan-array scanners have also been developed to image the lateral spine in its entirety to allow a visual assessment of vertebral size and shape. Examples of scanners with this capability are the Hologic Delphi™ and the Lunar Prodigy™. Figures 1-12 and 1-13 are lateral spine images from the Lunar Prodigy™. In the LVA™ (lateral vertebral assessment)[15] image in Fig. 1-12 a fracture is suggested at T12. In Fig. 1-13, the dimensions of the suspect vertebra are measured with morphometry. Figures 1-14 and

---

[12] See Chapter 15 for a listing of radiation dose according to device and scan type.

[13] Specific descriptions and photographs of these scanners can be found in Chapter 15.

[14] This application is discussed in detail in Chapter 13.

[15] This application on newer GE Healthcare devices is now called DVA (Dual-energy vertebral assessment). An image of the spine in the PA projection can be obtained in addition to the lateral view with DVA.
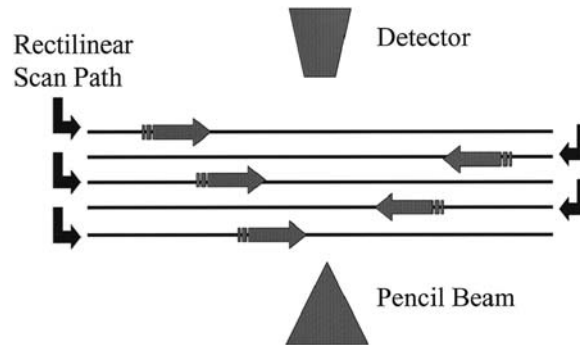
Fig. 1-9. Pencil-beam DXA densitometers. The single detector or sequential detectors move in tandem with the narrowed X-ray beam in a rectilinear scan path.
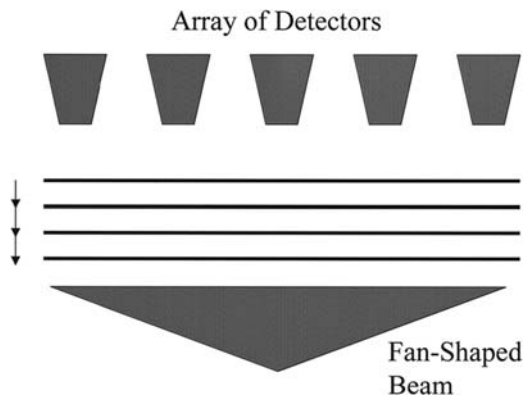
Fig. 1-10. Fan-array DXA densitometers. An array of detectors and fan-shaped beam make possible the simultaneous acquisition of data across an entire scan line.
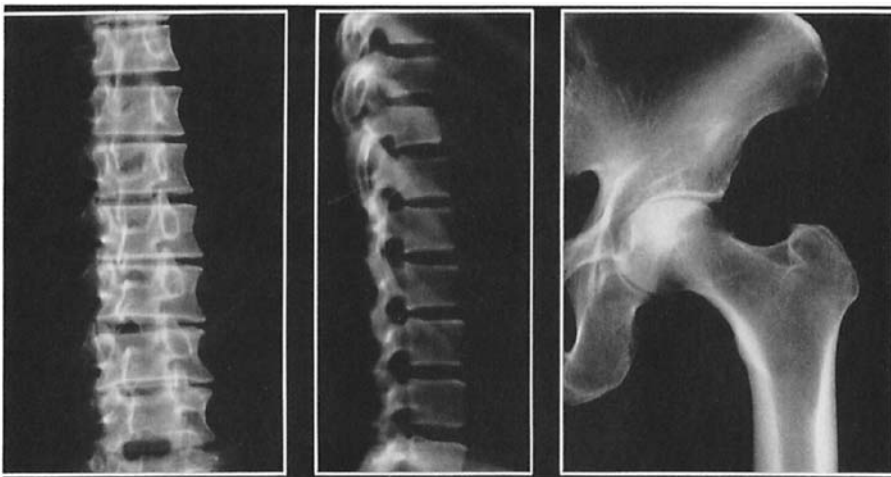
Fig. 1-11. Images from the fan-array imaging densitometer, the Lunar EXPERT-XL. Images courtesy of GE Healthcare, Madison, WI.
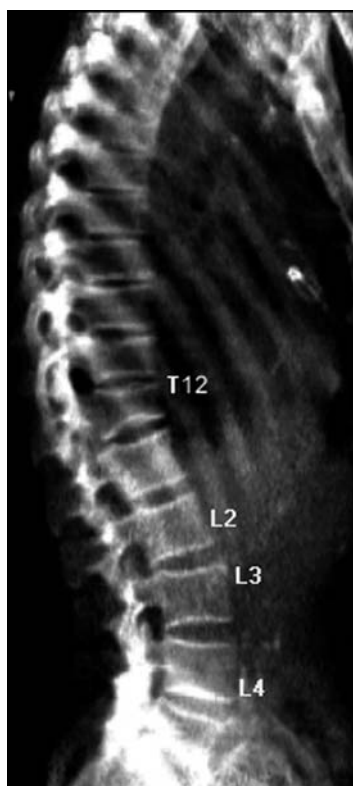
Fig. 1-12. LVA[TM] image acquired on the Lunar Prodigy[TM]. A fracture is apparent at T12. A safety pin is also seen over the anterior chest. Case courtesy of GE Healthcare, Madison, WI.

1-15 are IVA[TM] (instant vertebral assessment) images[16] from the Hologic Delphi[TM]. No fractures are apparent in Fig. 1-14. Note the multiple thoracic deformities in Fig. 1-15.

DXA has effectively replaced DPA in both research and clinical practice. The shortened scan times, improved image resolution, lower radiation dose, improved precision, application to more skeletal sites, and lower cost of operation with DXA have relegated DPA to an honored place in densitometry history.

Peripheral DXA

Dual-energy X-ray technology is also employed in portable devices dedicated to the measurement of one or two appendicular sites. As such, these devices are characterized as "peripheral" devices or pDXA devices. Because these devices employ dual-energy X-ray, they do not require a water bath or tissue-equivalent gel surrounding the region of the skeleton being studied. As a consequence, they are somewhat easier to maintain

---

[16] A new version of this application is called high-definition instant vertebral assessment or IVA-HD and is available as a standard or optional application, depending on the model of Hologic DXA device.

Fig. 1-13. LVA[TM] image acquired on the Lunar Prodigy[TM]. Morphometric software allows the user to define the vertebral edges and measure the vertebral heights to quantitatively diagnose fracture. Case courtesy of GE Healthcare, Madison, WI.

and use than SXA devices. Examples of pDXA units are the Lunar PIXI[®], the Norland pDEXA[®] and the Norland Apollo[TM], the Schick accuDEXA[TM] and the Osteometer DexaCare DTX-200, and G4. These devices are discussed in detail in Chapter 15.

Single-Energy X-ray Absorptiometry

Single-energy X-ray absorptiometry (SXA) is the X-ray based counterpart of single-photon absorptiometry, much as dual-energy X-ray absorptiometry is the X-ray based counterpart of dual-photon absorptiometry. SXA units were used to measure bone density in the distal radius and ulna and calcaneus. Like their DXA counterparts, SXA units did not utilize radioactive isotopes but did require a water bath or tissue-equivalent gel surrounding the region of the skeleton being measured. The accuracy and precision of SXA were comparable to SPA (*72*). With the development of portable DXA devices for the measurement of forearm and heel bone density that do not require a water bath or tissue-equivalent gel, SXA is largely obsolete, just like its predecessor SPA.

Quantitative Computed Tomography

Although quantitative computed tomography (QCT) is a photon absorptiometric technique like SPA, SXA, DPA, and DXA, it is unique in that it provides a three-dimensional or volumetric measurement of bone density and a spatial separation of trabecular from
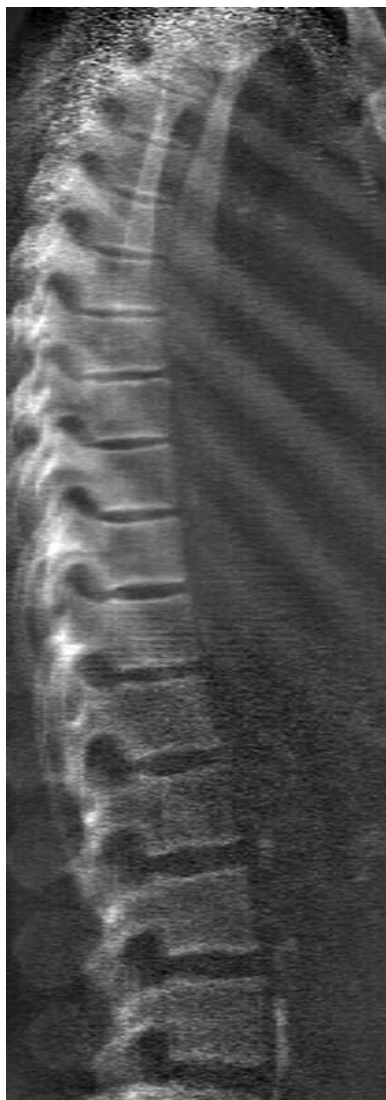
Fig. 1-14. IVA™ image acquired on the Hologic Delphi™. No fractures are apparent in the thoracic and lumbar spine although aortic calcification is seen anterior to the lumbar spine. Case courtesy of Hologic, Inc., Bedford, MA.

cortical bone. In 1976, Ruegsegger et al. (*73*) developed a dedicated peripheral quantitative CT scanner using ^{125}I for measurements of the radius. Cann and Genant (*74*, *75*) are credited with adapting commercially available CT scanners for the quantitative assessment of spinal bone density. It is this approach that has received the most widespread use in the United States, although dedicated CT units for the measurement of the peripheral skeleton, or pQCT units, are in use in clinical centers. QCT studies of the spine utilize a reference standard or phantom that is scanned simultaneously with the patient. The phantom contains varying concentrations of K_2HPO_4 and is placed underneath the patient during the study. A scout view is required for localization and then an 8- to 10-mm-thick slice is measured through the center of two or more vertebral

Fig. 1-15. IVA™ image acquired on the Hologic Delphi™. There are multiple deformities in the thoracic spine as well as osteophytes in the lower lumbar spine. Aortic calcification is also seen anterior to the lumbar spine. Case courtesy of Hologic, Inc., Bedford, MA.

bodies that are generally selected from T12 to L3 (*76*). A region of interest within the anterior portion of the vertebral body is analyzed for bone density and is reported as mg/cm^3 K$_2$HPO$_4$ equivalents. This region of interest is carefully placed to avoid the cortical shell of the vertebral body. The result is a three-dimensional trabecular density unlike the two-dimensional areal mixed cortical and trabecular densities reported with PA studies of the spine utilizing DPA or DXA (Figs. 1-16 and 1-17).

A study of the spine with QCT requires about 30 minutes (*41*). The skin radiation dose is generally 100–300 mrem. This overestimates the biologically important effective dose because only a small portion of marrow is irradiated during a QCT study of the
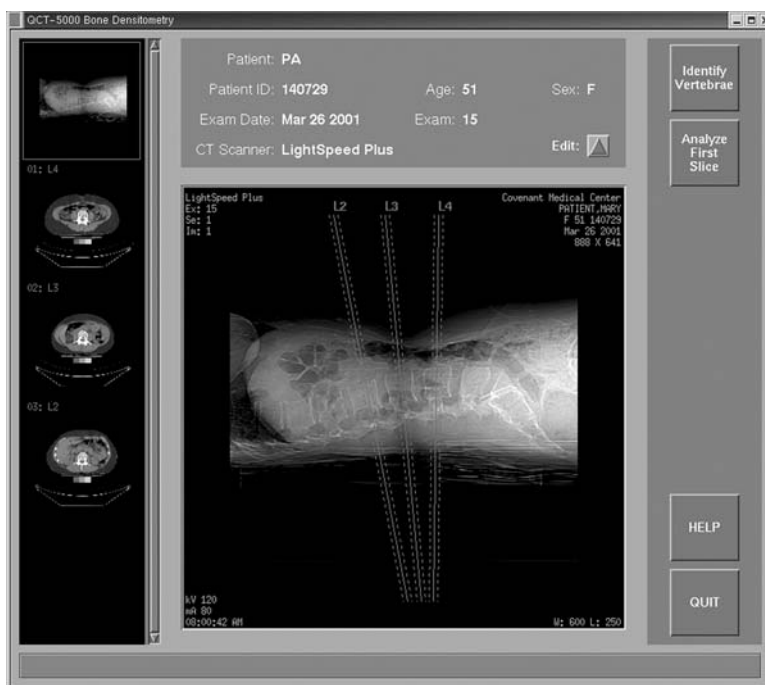
Fig. 1-16. QCT-5000[TM] scout image. Reproduced courtesy of Image Analysis, Inc., Columbia, KY.
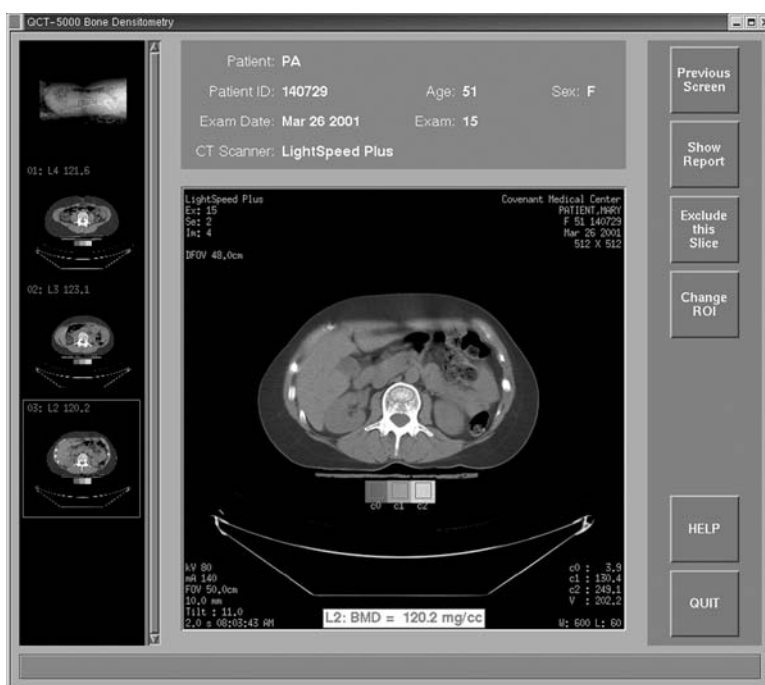
Fig. 1-17. QCT-5000[TM] axial spine image. This is a three-dimensional volumetric measurement, reported in mg/cm^3 or mg/cc. The L2 BMD shown here is 120.2 mg/cc. This measurement is 100% trabecular. Reproduced courtesy of Image Analysis, Inc., Columbia, KY.

spine (*71*). The effective dose or whole-body equivalent dose is generally in the range of only 3 mrem (30 µSv). The localizer scan that precedes the actual QCT study will add an additional 3 mrem to the effective dose. These values are quite acceptable in the context of natural background radiation of approximately 20 mrem per month. Older CT units, which by their design are unable to utilize low kVp settings for QCT studies, may deliver doses 3–10 times higher.

The accuracy of QCT for measurements of spine bone mineral density can be affected by the presence of marrow fat (*76–78*). Marrow fat increases with age resulting in an increasingly large error in the accuracy of spine QCT measurements in older patients. The accuracy of QCT is reported to range from 5 to 15%, depending upon the age of the patient and percentage of marrow fat. The presence of marrow fat results in an underestimation of bone density in the young of about 20 mg/cm^3 and as much as 30 mg/cm^3 in the elderly (*76*). The error introduced by marrow fat can be partially corrected by applying data on vertebral marrow fat with aging originally developed by Dunnill et al. (*79*). In an attempt to eliminate the error introduced by marrow fat, dual-energy QCT or DEQCT was developed by Genant and Boyd (*80*). This method clearly reduced the error introduced by the presence of marrow fat to as low as 1.4% in cadaveric studies (*77, 78*). In vivo, the accuracy with DEQCT is 3–6% (*41, 76*). Radiation dose with DEQCT is increased approximately 10-fold compared to regular or single-energy QCT (SEQCT) but precision is not as good. The precision of SEQCT for vertebral measurements in expert hands is 1–3% and for DEQCT 3–5% (*76, 81*).

The measurement of bone density in the proximal femur with QCT has become more available in recent years. Using both dedicated QCT and standard CT units, investigators have utilized QCT for measurements of the proximal femur as shown in Fig. 1-18 (*82, 83*). Some QCT proximal femur software applications will also provide DXA-equivalent values. QCT proximal femur hip structural analysis software has also been developed and is discussed in Chapter 13.

QCT of the spine has been used in studies of prevalent osteoporotic fractures and it is clear that such measurements can distinguish osteoporotic individuals from normal individuals as well or even better than DPA (*84–87*). Fractures are rare with values above 110 mg/cm^3 and extremely common below 60 mg/cm^3 (*88*). Because QCT can isolate and measure trabecular bone, which is more metabolically active than cortical bone, rates of change in disease states observed with QCT spine measurements tend to be greater than those observed with PA spine studies performed with DPA or DXA (*74, 89*). This greater magnitude of change partially offsets the effects of the poorer precision seen with QCT compared to DXA.[17] The correlations between spine bone density measurements with QCT and skeletal sites measured with other techniques are statistically significant but too weak to allow accurate prediction of bone density at another site from measurement of the spine with QCT (*32, 86, 87*). This is no different, however, from attempting to use BMD at the spine obtained with DXA to predict BMD at other skeletal sites.

---

[17] See Chapter 11 for a detailed discussion on the interaction between precision and rate of change in determining the time interval required between measurements to demonstrate significant change.

Fig. 1-18. QCT proximal femur study. The study on the *upper right* is a three-dimensional volumetric measurement, reported in mg/cm^3 or mg/cc. On the *lower right*, this study provides DXA values in g/cm^2. Reproduced courtesy of Image Analysis, Inc., Columbia, KY.

Peripheral QCT

Peripheral QCT (pQCT) is becoming more widely available. pQCT devices are utilized primarily for the measurement of bone density in the forearm. Like QCT scans of the spine, pQCT makes possible true three-dimensional or volumetric measurements of bone density in the forearm, which may be particularly useful when the size of the bone is changing, as in pediatric populations. Information on commercially available pQCT devices, such as the Stratec XCT 2000L^{TM} and XCT 3000^{TM}, can be found in Chapter 15.

High-Resolution Quantitative Computed Tomography

High-resolution quantitative computed tomography (HS-QCT) is a newer generation of QCT in which the spatial resolution has been increased to allow imaging of individual trabeculae (*90*, *91*) Volumetric measures of BMD can still be obtained with HS-QCT just as they are with QCT. HS-QCT, however, can also be used to quantify the structural parameters of trabecular number, trabecular spacing, trabecular thickness, and distribution. At present, HS-QCT is limited to the radius and tibia and is thus more correctly characterized as HS-pQCT. With this approach, a nominal isotropic voxel size of 82 μm can be obtained.

In early work from Laib et al. (*90*) HS-pQCT structural parameters were shown to be highly correlated with structural parameters from iliac crest bone biopsies assessed with μCT. HS-pQCT was employed by Boutroy et al. (*91*) to obtain both three-dimensional measures of bone density as well as structural parameters at the distal radius and distal tibia in 256 pre- and postmenopausal women. DXA of the lumbar spine and femoral neck was also performed. Short-term precision[18] was assessed in 15 healthy women who underwent three HS-pQCT scans of the radius and tibia. Precision for the structural parameters of trabecular number (TbN), thickness (TbTh), spacing (TbSp), trabecular spacing standard deviation (TbSpSD), and cortical thickness (CTh) ranged from 0.9 to 4.4% at both the distal radius and tibia. In the postmenopausal women at both skeletal sites, trabecular and cortical density measured by HS-pQCT were significantly lower than in the premenopausal women. Postmenopausal women also had a significantly lower trabecular number and thickness and increased trabecular separation. There were 113 postmenopausal women who were considered osteopenic on the basis of the DXA T-score at either the lumbar spine or femoral neck. Among these osteopenic women, the HS-pQCT parameters of trabecular bone volume fracture (BV/TV) and TbSpSD were significantly different in the women with spine fractures compared to the non-fracture women, whereas BMD at the spine and femoral neck by DXA were not.

HR-pQCT of the distal radius and tibia was also used to evaluate volumetric density and architecture in a case–control study of 101 women with spine and non-spine fractures followed for 13 years as part of the OFELY[19] cohort (*92*). These women also underwent DXA of the ultradistal radius and proximal femur. Compared to age-matched controls, the women with fractures had significantly lower BV/TV, CTh, and TbN and TbSp, and increased TbSpSD. After adjustment for DXA BMD, there was a trend toward a continued significant difference for TbN, TbSp, and TbSpSD. At the tibia, even after adjusting for DXA BMD, TbTh remained significantly decreased in the fracture patients compared to controls.

An attractive feature of HS-pQCT is that it provides both volumetric bone density as well as structural parameters. Because this is QCT, it does expose the patient to ionizing radiation but the exposure is less than 5 μSv. Scan times are also acceptably short at approximately 3 minutes. Commercially available equipment exists to perform HS-pQCT but it remains an investigational procedure in the United States.

QUANTITATIVE ULTRASOUND BONE DENSITOMETRY

Research in quantitative ultrasound bone densitometry (QUS) has been ongoing for over 40 years. Only in the last few years, however, has QUS begun to play a role in the clinical evaluation of the patient. Ultrasound technologies in clinical medicine have traditionally been imaging technologies used, for example, to image the gall bladder or the ovaries. Like photon absorptiometric technologies, however, the application of ultrasound in bone densitometry is not primarily directed at producing an image of the

---

[18] See Chapter 11 for a discussion of short-term precision.

[19] OFELY is a prospective study of the determinants of bone loss, involving over 1000 women aged 31–89 years from France.

bone. Instead, a quantitative assessment of bone density is desired with the image being secondary in importance.

In theory, the speed with which sound passes through bone is related not only to the density of the bone but to the quality of the bone as well. Both bone density and bone quality determine a bone's resistance to fracture. Therefore, the speed of sound through bone can be related to the risk of fracture. These relationships can be illustrated mathematically. For example, the bone's ability to resist fracture (R) can be described as the amount the bone deforms when it is subjected to a force (F) that is moderated by the bone's ability to resist that force, the elastic modulus (E) as shown in Equation 1:

$$R = \frac{F}{E} \tag{1}$$

Studies have shown that the elastic modulus, E, is determined by both bone density and bone quality. Mathematically this is represented in Equation 2, where K is a constant representing bone quality and ρ represents bone density:

$$E = K\rho^2 \tag{2}$$

From such an equation, it becomes clear that the bone's ability to resist a force and not fracture is determined by changes in bone density and bone quality. When ultrasound passes through a material, the velocity of the sound wave is also related to the elastic modulus (*93*, *94*) and density of the material as shown in Equation 3:

$$V = \sqrt{\frac{E}{\rho}} \tag{3}$$

When Equations 2 and 3 are combined, it becomes clear that the velocity of ultrasound through bone is directly related to the square root of the product of bone density and bone quality:

$$V = \sqrt{\frac{K\rho^2}{\rho}} \tag{4}$$

$$V = \sqrt{K\rho} \tag{5}$$

The velocity with which ultrasound passes through normal bone is quite fast and varies depending upon whether the bone is cortical or trabecular. Speeds of 3000–3600 m/sec are typical in cortical bone with speeds of 1650–2300 m/sec typical of trabecular bone.

In order to calculate velocity, ultrasound densitometers must measure the distance between two points and the time required for the sound wave to travel between these two points. The velocity is reported as the speed of sound (SOS). Higher values of SOS indicate greater values of bone density.

A second ultrasound parameter is broadband ultrasound attenuation (BUA). This parameter is reported in decibels per megahertz (dB/MHz). BUA is perhaps best understood using the analogy of a child's slinky toy. When the toy is stretched out and then suddenly released, the energy imparted to the rings by stretching them causes the rings to oscillate for a period of time, with the oscillations becoming progressively less

and then finally stopping as the energy is lost. The same thing happens to the sound wave as it passes through bone. Some of the energy is lost from the sound wave and the oscillations of the sound wave are diminished. How much energy is lost is again related to the density of the bone and to architectural qualities such as porosity and trabecular connectivity (*93*, *94*). Like SOS, higher BUA values indicate greater bone density.

Most devices report both SOS and BUA. However, one manufacturer has mathematically combined SOS and BUA into a proprietary index called the Stiffness Index. Another manufacturer reports a proprietary index called the Quantitative Ultrasound Index (QUI) and an estimated BMD that is derived from the measurements of SOS and BUA. QUS devices are considered peripheral devices and are generally quite portable. They employ no ionizing radiation, unlike their SXA or DXA peripheral counterparts. The calcaneus is the most common skeletal site assessed with QUS, but devices exist that can be applied to the radius, finger, and tibia. In heel QUS measurements, heel width apparently has little, if any, effect on BUA but may have a slight effect on SOS (*95*). Most ultrasound devices require some type of coupling medium between the transducers and the bone. This is often accomplished with water when the heel is placed directly into a water bath. Ultrasound gel may be used in place of direct contact with water for heel measurements and measurements at other skeletal sites. Systems that utilize water baths into which the foot is placed are called "wet" systems. Systems that do not require water submersion but utilize gel instead are called "dry" systems. There is one system for the heel in which neither water submersion nor gel is required, making it truly "dry." The Lunar Achilles+^{TM}, the Lunar Achilles Express^{TM}, the Lunar Insight^{TM}, the Sunlight Omnisense^{TM} 7000S and 8000S, the Quidel QUS-2^{TM}, the McCue C.U.B.A. Clinical^{TM}, the Hologic Sahara^{TM} Clinical Bone Sonometer, and the Osteometer Ultrasure DTU-one are all examples of QUS densitometers currently available for clinical use. These devices are discussed in more detail in Chapter 15.

The technical differences between QUS devices from various manufacturers are even greater than those seen with DXA devices. Different frequency ranges and transducer sizes may be employed from device to device. Within the same skeletal site, slightly different regions of interest may be measured. As a consequence, values obtained on one QUS device are not necessarily comparable to values obtained on another QUS device.

The physics of ultrasound suggests that it should provide information about the bone that goes beyond a simple measurement of mass or density. Clinical research has tended to confirm this assumption, although perhaps not to the extent that was originally hoped. In a very large study of 5662 older women, both SOS and BUA predicted the risk of hip fracture as well or better than did measurements of BMD at the femoral neck using DXA (*96*). Similar findings were reported in the Study of Osteoporotic Fractures by Bauer et al. (*97*).

The precision of QUS measurements is generally excellent. In addition, because of the speed with which measurements can be made and the lack of any ionizing radiation, measurements can be made in duplicate or triplicate at any one examination. The average value of such replicate studies can be used, which dramatically improves precision. In a study from Njeh et al. (*98*) in which the precision of 6 different calcaneal QUS devices was determined, the short-term precision for SOS, expressed as the root-mean-square percent coefficient of variation (RMS-%CV), ranged from 0.11 to

0.42. For BUA, the RMS-%CV ranged from 1.39 to 6.30. Typically, better precision values are seen for SOS than for BUA.

REFERENCES

1. Dennis J. A new system of measurement in X-ray work. Dental Cosmos 1897;39:445–454.
2. Price WA. The science of dental radiology. Dental Cosmos 1901;43:483–503.
3. Johnston CC, Epstein S. Clinical, biochemical, radiographic, epidemiologic, and economic features of osteoporosis. Orthop Clin North Am 1981;12:559–569.
4. Aitken M. Measurement of bone mass and turnover. Osteoporosis in clinical practice. Bristol: John Wright & Sons Ltd, 1984:19–20.
5. Singh J, Nagrath AR, Maini PS. Changes in trabecular pattern of the upper end of the femur as an index of osteoporosis. J Bone Joint Surg Am 1970;52-A:457–467.
6. Bohr H, Schadt O. Bone mineral content of femoral bone and lumbar spine measured in women with fracture of the femoral neck by dual photon absorptiometry. Clin Ortho 1983;179:240–245.
7. Nordin BEC. Osteoporosis with particular reference to the menopause. In: Avioli LV, ed. The osteoporotic syndrome. New York: Grune & Stratton, 1983:13–44.
8. Shimmins J, Anderson JB, Smith DA, et al. The accuracy and reproducibility of bone mineral measurements "in vivo." (a) The measurement of metacarpal mineralisation using an X-ray generator. Clin Radiol 1972;23:42–46.
9. Exton-Smith AN, Millard PH, Payne PR, Wheeler EF. Method for measuring quantify of bone. Lancet 1969;2: 1153–1154.
10. Dequeker J. Precision of the radiogrammetric evaluation of bone mass at the metacarpal bones. In: Dequeker J, Johnston CC, eds. Non-invasive bone measurements: methodological problems. Oxford: IRL Press, 1982, 27–32.
11. Aitken JM, Smith CB, Horton PW, et al. The inter-relationships between bone mineral at different skeletal sites in male and female cadavera. J Bone Joint Surg Br 1974;56B:370–375.
12. Meema HE, Meindok H. Advantages of peripheral radiogrammetry over dual-photon absorptiometry of the spine in the assessment of prevalence of osteoporotic vertebral fractures in women. J Bone Miner Res 1992;7:897–903.
13. Bywaters EGL. The measurement of bone opacity. Clin Sci 1948;6:281–287.
14. Barnett E, Nordin BEC. Radiologic assessment of bone density. 1.-The clinical and radiological problem of thin bones. Br J Radiol 1961;34:683–692.
15. Bouxsein ML, Palermo L, Yeung C, Black DM. Digital X-ray radiogrammetry predicts hip, wrist and vertebral fracture risk in elderly women: a prospective analysis from the Study of Osteoporotic Fractures. Osteoporos Int 2002;12:358–365.
16. Cummings S, Black D, Nevitt M, et al. Appendicular bone density and age predict hip fractures in women. JAMA 1990;263:665–668.
17. Pothuaud L, Lespessailles E, Harba R, et al. Fractal analysis of trabecular bone texture on radiographs: discriminant value in postmenopausal osteoporosis. Osteoporos Int 1998;(6):618–25.
18. Benhamou CL, Poupon S, Lespessailles E, Loiseau S, Jennane R, Siroux V, et al. Fractal analysis of radiographic trabecular bone texture and bone mineral density: two complementary parameters related to osteoporotic fractures. J Bone Miner Res 2001:16(4)697–704.
19. Gregory JS, Stewart A, Undrill PE, Reid DM, Aspden RM. Identification of hip fracture patients from radiographs using Fourier analysis of the trabecular structure: a cross-sectional study. BMC Med Imaging 2004;4(1):4.
20. Chappard C, Brunet-Imbault B, Lemineur G, et al. Anisotropy changes in post-menopausal osteoporosis: characterization by a new index applied to trabecular bone radiographic images. Osteoporos Int 2005:16(10)1193–202.
21. Brunet-Imbault B, Lemineur G, Chappard C, Harba R, Benhamou CL. A new anisotropy index on trabecular bone radiographic images using the fast Fourier transform. BMC Med Imaging 2005 May 31;5:4.
22. van der Linden JC, Weinans H. Effects of microarchitecture on bone strength. Curr Osteoporos Rep 2007;5(2)56–61.

23. Mack PB, Brown WN, Trapp HD. The quantitative evaluation of bone density. Am J Roentgenol Rad Ther 1949;61:808–825.
24. Vose GP, Mack PB. Roentgenologic assessment of femoral neck density as related to fracturing. Am J Roentgenol Rad Ther Nucl Med 1963;89:1296–1301.
25. Cummings SR, Black DM, Nevitt MC, et al. Bone density at various sites for prediction of hip fractures. Lancet 1993;341:72–75.
26. Mazess RB. Noninvasive methods for quantitating trabecular bone. In: Avioli LV, ed. The osteoporotic syndrome. New York: Grune & Stratton, 1983:85–114.
27. Mack PB, O'Brien AT, Smith JM, Bauman AW. A method for estimating degree of mineralization of bones from tracings of roentgenograms. Science 1939;89:467.
28. Mack PB, Vogt FB. Roentgenographic bone density changes in astronauts during representative Apollo space flight. Am J Roentgenol Rad Ther Nucl Med 1971;113:621–633.
29. Cosman F, Herrington B, Himmelstein S, Lindsay R. Radiographic absorptiometry: a simple method for determination of bone mass. Osteoporos Int 1991;2:34–38.
30. Yates AJ, Ross PD, Lydick E, Epstein RS. Radiographic absorptiometry in the diagnosis of osteoporosis. Am J Med 1995;98:41S–47S.
31. Yang S, Hagiwara S, Engelke K, et al. Radiographic absorptiometry for bone mineral measurement of the phalanges: precision and accuracy study. Radiology 1994;192:857–859.
32. Kleerekoper M, Nelson DA, Flynn MJ, Pawluszka AS, Jacobsen G, Peterson EL. Comparison of radiographic absorptiometry with dual-energy X-ray absorptiometry and quantitative computed tomography in normal older white and black women. J Bone Miner Res 1994;9:1745–1749.
33. Mussolino ME, Looker AC, Madans JH, et al. Phalangeal bone density and hip fracture risk. Arch Intern Med 1997;157:433–438.
34. Huang C, Ross PD, Yates AJ, et al. Prediction of fracture risk by radiographic absorptiometry and quantitative ultrasound: a prospective study. Calcif Tissue Int 1998;6:380–384.
35. Cameron JR, Sorenson G. Measurements of bone mineral in vivo: an improved method. Science 1963;142:230–232.
36. Vogel JM. Application principles and technical considerations in SPA. In: Genant HK, ed. Osteoporosis update 1987. San Francisco: University of California Printing Services, 1987:219–231.
37. Johnston CC. Noninvasive methods for quantitating appendicular bone mass. In: Avioli L, ed. The osteoporotic syndrome. New York: Grune & Stratton, 1983:73–84.
38. Barden HS, Mazess RB. Bone densitometry of the appendicular and axial skeleton. Top Geriatric Rehabi. 1989;4:1–12.
39. Kimmel PL. Radiologic methods to evaluate bone mineral content. Ann Intern Med 1984;100:908–911.
40. Steiger P, Genant HK. The current implementation of single-photon absorptiometry in commercially available instruments. In: Genant HK, ed. Osteoporosis update 1987. San Francisco: University of California Printing Services, 1987:233–240.
41. Chesnut CH. Noninvasive methods for bone mass measurement. In: Avioli L, ed. The Osteoporotic syndrome. 3rd ed. New York: Wiley-Liss, 1993:77–87.
42. Gardsell P, Johnell, O, Nilsson BE. The predictive value of bone loss for fragility fractures in women: a longitudinal study over 15 years. Calcif Tissue Int 1991;49:90–94.
43. Hui SL, Slemenda CW, Johnston CC. Baseline measurement of bone mass predicts fracture in white women. Ann Intern Med 1989;111:355–361.
44. Ross PD, Davis JW, Vogel JM, Wasnich RD. A critical review of bone mass and the risk of fractures in osteoporosis. Calcif Tissue Int 1990;46:149–161.
45. Melton LJ, Atkinson EJ, O'Fallon WM, Wahner HW, Riggs BL. Long-term fracture prediction by bone mineral assessed at different skeletal sites. J Bone Miner Res 1993;8:1227–1233.
46. Black DM, Cummings SR, Genant HK, Nevitt MC, Palermo L, Browner W. Axial and appendicular bone density predict fracture in older women. J Bone Miner Res 1992;7:633–638.
47. Nord RH. Technical considerations in DPA. In: Genant HK., ed. Osteoporosis update 1987. San Francisco: University of California Printing Services, 1987:203–212.
48. Dunn WL, Wahner HW, Riggs BL. Measurement of bone mineral content in human vertebrae and hip by dual photon absorptiometry. Radiology 1980;136:485–487.

49. Reed GW. The assessment of bone mineralization from the relative transmission of [241]Am and ^{137}Cs radiations. Phys Med Biol 1966;11:174.

50. Roos B, Skoldborn H. Dual photon absorptiometry in lumbar vertebrae. I. Theory and method. Acta Radiol Ther Phys Biol 1974;13:266–290.

51. Mazess RB, Ort M, Judy P. Absorptiometric bone mineral determination using [153]Gd. In: Cameron JR, ed. Proceedings of bone measurements conference. U.S. Atomic Energy Commission, 1970: 308–312.

52. Wilson CR, Madsen M. Dichromatic absorptiometry of vertebral bone mineral content. Invest Radiol 1977;12:180–184.

53. Madsen M, Peppler W, Mazess RB. Vertebral and total body bone mineral content by dual-photon absorptiometry. Calcif Tissue Res 1976;2:361–364.

54. Wahner WH, Dunn WL, Mazess RB, et al. Dual-photon Gd-153 absorptiometry of bone. Radiology 1985;156: 203–206.

55. Lindsay R, Fey C, Haboubi A. Dual-photon absorptiometric measurements of bone mineral density increase with source life. Calcif Tissue Int 1987;41:293–294.

56. Cummings SR, Black DB. Should perimenopausal women be screened for osteoporosis? Ann Intern Med 1986;104:817–823.

57. Drinka PJ, DeSmet AA, Bauwens SF, Rogot A. The effect of overlying calcification on lumbar bone densitometry. Calcif Tissue Int 1992;50:507–510.

58. Curry TS, Dowdey JE, Murry RC. Christensen's physics of diagnostic radiology. Philadelphia: Lea & Febiger, 1990, 1–522.

59. Rupich RC, Griffin MG, Pacifici R, Avioli LV, Susman N. Lateral dual-energy radiography: artifact error from rib and pelvic bone. J Bone Miner Res 1992;7:97–101.

60. Louis O, Van Den Winkel P, Covens P, Schoutens A, Osteaux M. Dual-energy X-ray absorptiometry of lumbar vertebrae: relative contribution of body and posterior elements and accuracy in relation with neutron activation analysis. Bone 1992;13:317–320.

61. Peel NFA, Johnson A, Barrington NA, Smith TWD, Eastell R. Impact of anomalous vertebral segmentation of measurements of bone mineral density. J Bone Miner Res 1993;8:719–723.

62. Lees B, Stevenson JC. An evaluation of dual-energy X-ray absorptiometry and comparison with dual-photon absorptiometry. Osteoporos Int. 1992;2:146–152.

63. Kelly TL, Slovik DM, Schoenfeld DA, Neer RM. Quantitative digital radiography versus dual photon absorptiometry of the lumbar spine. J Clin Endocrinol Metab 1988;76:839–844.

64. Holbrook TL, Barrett-Connor E, Klauber M, Sartoris D. A population-based comparison of quantitative dual-energy X-ray absorptiometry with dual-photon absorptiometry of the spine and hip. Calcif Tissue Int 1991;49:305–307.

65. Pouilles JM, Tremollieres F, Todorovsky N, Ribot C. Precision and sensitivity of dual-energy X-ray absorptiometry in spinal osteoporosis. J Bone Miner Res 1991;6:997–1002.

66. Laskey MA, Cirsp AJ, Cole TJ, Compston JE. Comparison of the effect of different reference data on Lunar DPX and Hologic QDR-1000 dual-energy X-ray absorptiometers. Br J Radiol 1992;65:1124–1129.

67. Pocock NA, Sambrook PN, Nguyen T, Kelly P, Freund J, Eisman J. Assessment of spinal and femoral bone density by dual X-ray absorptiometry: comparison of Lunar and Hologic instruments. J Bone Miner Res 1992;7:1081–1084.

68. Lai KC, Goodsitt MM, Murano R, Chesnut CC. A comparison of two dual-energy X-ray absorptiometry systems for spinal bone mineral measurement. Calcif Tissue Int 1992;50:203–208.

69. Genant HK, Grampp S, Gluer CC, et al. Universal standardization for dual X-ray absorptiometry: patient and phantom cross-calibration results. J Bone Miner Res 1994;9:1503–1514.

70. Hanson J. Standardization of femur BMD. J Bone Miner Res 1997;12:1316–1317.

71. Kalender WA. Effective dose values in bone mineral measurements by photon-absorptiometry and computed tomography. Osteoporos Int 1992;2:82–87.

72. Kelly TL, Crane G, Baran DT. Single x-ray absorptiometry of the forearm: precision, correlation, and reference data. Calcif Tissue Int 1994;54:212–218.

73. Ruegsegger P, Elsasser U, Anliker M, Gnehn H, Kind H, Prader A. Quantification of bone mineralisation using computed tomography. Radiology 1976;121:93–97.

74. Genant HK, Cann CE, Ettinger B, Gorday GS. Quantitative computed tomography of vertebral spongiosa: a sensitive method for detecting early bone loss after oophorectomy. Ann Intern Med 1982;97:699–705.

75. Cann CE, Genant HK. Precise measurement of vertebral mineral content using computed tomography. J Comput Assist Tomogr 1980;4:493–500.

76. Genant HK, Block JE, Steiger P, Gluer C. Quantitative computed tomography in the assessment of osteoporosis. In: Genant HK, ed. Osteoporosis update 1987. San Francisco: University of California Printing Services, 1987:49–72.

77. Laval-Jeantet AM, Roger B, Bouysse S, Bergot C, Mazess RB. Influence of vertebral fat content on quantitative CT density. Radiology 1986;159:463–466.

78. Reinbold W, Adler CP, Kalender WA, Lente R. Accuracy of vertebral mineral determination by dual-energy quantitative computed tomography. Skeletal Radiol 1991;20:25–29.

79. Dunnill MS, Anderson JA, Whitehead R. Quantitative histological studies on age changes in bone. J Pathol Bacteriol 1967;94:274–291.

80. Genant HK, Boyd D, Quantitative bone mineral analysis using dual energy computed tomography. Invest Radiol 1977;12:545–551.

81. Cann CE. Quantitative computed tomography for bone mineral analysis: technical considerations. In: Genant HK, ed. Osteoporosis update 1987. San Francisco: University of California Printing Services, 1987:131–144.

82. Sartoris DJ, Andre M, Resnick C, Resnick D. Trabecular bone density in the proximal femur: quantitative CT assessment. Radiology 1986;160:707–712.

83. Reiser UJ, Genant HK. Determination of bone mineral content in the femoral neck by quantitative computed tomography. 70th Scientific Assembly and Annual Meeting of the Radiological Society of North America, Washington, DC, 1984.

84. Gallagher C, Golgar D, Mahoney P, McGill J. Measurement of spine density in normal and osteoporotic subjects using computed tomography: relationship of spine density to fracture threshold and fracture index. J Comput Assist Tomogr 1985;9:634–635.

85. Raymaker JA, Hoekstra O, Van Putten J, Kerkhoff H, Duursma SA. Osteoporosis fracture prevalence and bone mineral mass measured with CT and DPA. Skeletal Radiol 1986;15:191–197.

86. Reinbold WD, Reiser UJ, Harris ST, Ettinger B, Genant HK. Measurement of bone mineral content in early postmenopausal and postmenopausal osteoporotic women. A comparison of methods.Radiology 1986;160:469–478.

87. Sambrook PN, Bartlett C, Evans R, Hesp R, Katz D, Reeve J. Measurement of lumbar spine bone mineral: a comparison of dual photon absorptiometry and computed tomography. Br J Radiol 1985;58:621–624.

88. Genant HK, Ettinger B, Harris ST, Block JE, Steiger P. Quantitative computed tomography in assessment of osteoporosis. In: Riggs BL, Melton LJ, eds. Osteoporosis: etiology, diagnosis and management. New York: Raven Press, 1988, 221–249.

89. Richardson ML, Genant HK, Cann CE, et al. Assessment of metabolic bone disease by quantitative computed tomography. Clin Orth Rel Res 1985;195:224–238.

90. Laib A, Ruegsegger P. Calibration of trabecular bone structure measurements of in vivo three-dimensional peripheral quantitative computed tomography with 28-micron-resolution microcomputed tomography. Bone 1999:24(1)35–9.

91. Boutroy S, Bouxsein ML, Munoz F, Delmas PD. In vivo assessment of trabecular bone microarchitecture by high-resolution peripheral quantitative computed tomography. J Clin Endocrinol Metab 2005:90(12)6508–6515.

92. Sornay-Rendu E, Boutroy, S, Munoz F, Delmas PD. Alterations of cortical and trabecular architecture are associated with fractures in postmenopausal women, partially independent of decreased BMD measured by DXA: the OFELY study. J Bone Miner Res 2007;22:425–433.

93. Gluer C, Wu C, Jergas M, Goldstein S, Genant H. Three quantitative ultrasound parameters reflect bone structure. Calcif Tissue Int 1994;55:46–52.

94. Nicholson P, Haddaway M, Davie M. The dependence of ultrasonic properties on orientation in human vertebral bone. Phys Med Biol 1994;39:1013–1024.

95. Njeh CF, Boivin CM, Langton CM. The role of ultrasound in the assessment of osteoporosis: a review. Osteoporos Int 1997;7:7–22.

96. Hans D, Dargent-Molina P, Schott AM, et al. Ultrasonographic heel measurements to predict hip fracture in elderly women: the EPIDOS prospective study. Lancet 1996;348:511–514.
97. Bauer DC, Gluer CC, Cauley JA, et al. Bone ultrasound predicts fractures strongly and independently of densitometry in older women: a prospective study. Arch Intern Med 1997;157:629–634.
98. Njeh CF, Hans D, Li J, et al. Comparison of six calcaneal quantitative ultrasound devices: precision and hip fracture discrimination. Osteoporos Int 2000;11:1051–1062.

2 Skeletal Anatomy in Densitometry

CONTENTS

Densitometry is primarily a quantitative measurement technique rather than a skeletal imaging technique. Nevertheless, there are unique aspects of skeletal anatomy in densitometry that must be appreciated to properly utilize the technology and interpret the quantitative results as well as the skeletal images.

CHARACTERIZING THE SKELETON IN DENSITOMETRY

The bones of the skeleton can be described by four characteristics, one of which is unique to densitometry. The characterizations are important, as this often determines which skeletal site is the most desirable to measure in a given clinical situation. A skeletal site may be described as axial or appendicular, weight bearing or non-weight bearing, central or peripheral, and predominantly cortical or trabecular.

The Axial and Appendicular Skeleton

The axial skeleton includes the skull, ribs, sternum, and spine (*1*) as shown in Fig. 2-1. In densitometry, the phrase "axial skeleton" or "axial bone density study" has traditionally referred to the lumbar spine and PA lumbar spine bone density studies. This limited use is no longer appropriate since the lumbar spine can also be studied in the lateral projection and the thoracic spine can be measured as well. The skull and the ribs are quantified only as part of a total body bone density study and as a consequence, the phrase "axial bone density study" has never implied a study of those bones although they are part of the axial skeleton. The appendicular skeleton includes the extremities and the limb girdles as shown in Fig. 2-1. The scapulae and the pelvis are therefore
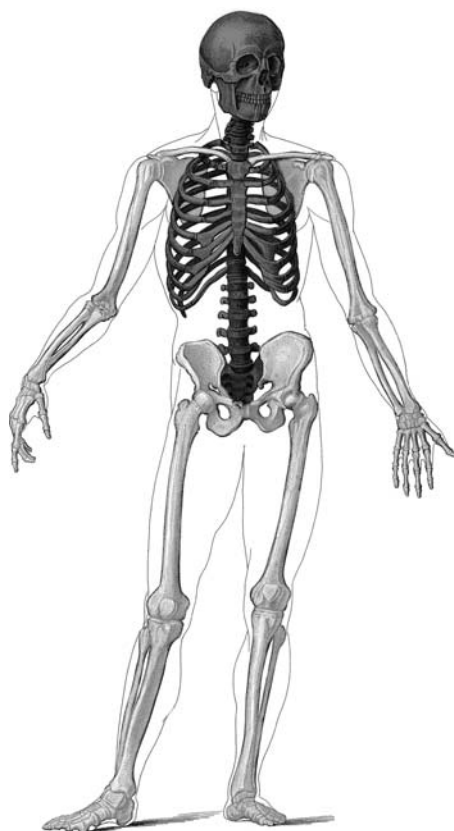
Fig. 2-1. The axial and appendicular skeleton. The *darker-shaded* bones comprise the axial skeleton. The *lighter-shaded* bones comprise the appendicular skeleton. Image adapted from EclectiCollections™.

part of the appendicular skeleton. The proximal femur is also obviously part of the appendicular skeleton, although it is often mistakenly described as being part of the axial skeleton. Contributing to this confusion is the current practice of including dual-energy X-ray bone density studies of the proximal femur and pelvis under the same Current Procedural Technology (CPT) code[1] of 77080 used for DXA spine bone density studies in which the studies are described as studies of the axial skeleton (*2*).

The Weight-Bearing and Non-weight-Bearing Skeleton

Regions of the skeleton are also characterized as weight bearing or non-weight bearing. This division is obvious but not without clinical significance. The cervical, thoracic, and lumbar spine and lower extremities are weight-bearing regions of the skeleton. Portions of the pelvis are weight-bearing. The small calcaneus is also part of the weight-bearing skeleton and is perhaps the most sensitive of all the bones to the effects of weight-bearing forces. The remainder of the skeleton is non-weight-bearing.

[1] See Appendix VIII for a list of CPT codes used in bone densitometry.

The Central and Peripheral Skeleton

Skeletal sites may also be characterized as central or peripheral. This classification is unique to densitometry. The spine, in either the PA or lateral projection, is considered a central site. The proximal femur is also a central site even though it is not part of the axial skeleton like the spine. The calcaneus and the various forearm sites are all peripheral sites although the calcaneus is a weight-bearing site while the forearm sites are not. As an extension of this terminology, bone densitometers that are used to measure bone density in the spine, hip, or both are called "central" machines even though the machines may also have software that allows them to be used to measure a peripheral site like the forearm. The description of a bone densitometer as a central machine is generally reserved for dual-energy X-ray and older dual-photon absorptiometry devices. Although quantitative computed tomography (QCT) is used clinically to measure bone density in the spine, as a matter of convention QCT is rarely described as a central technique, although it would be appropriate to do so. Densitometers that can *only* be used to measure the distal appendicular skeleton like the forearm or calcaneus are called "peripheral" machines. Because there is no current application of quantitative ultrasound (QUS) for the central skeleton, it is understood that QUS devices are peripheral devices. As a consequence, it is not necessary to distinguish between central and peripheral QUS devices, so the term peripheral is not used in conjunction with QUS devices. Figure 2-2 illustrates the central and peripheral skeleton.

The Trabecular/Cortical Composition of the Skeleton

The skeleton is composed of two types of bone: cortical bone and trabecular bone. Cortical bone is also called compact bone or haversian bone. It is typically found in the shafts of long bones and the vertebral endplates. Trabecular bone is also called cancellous bone and is primarily found in the vertebral bodies, pelvis, and distal ends of long bones. Trabecular bone contains hematopoietic or fatty marrow. Eighty percent of the skeleton is cortical bone. The remaining 20% is trabecular bone. Trabecular bone consists of plates, arches, and struts with marrow occupying the spaces between these structures. Cortical bone is a more solid structure forming the outer casing of the bones (*1*).

Skeletal metabolism as a whole is roughly equally distributed between the two types of bones even though the skeleton is 80% cortical bone. This is because trabecular bone has a higher metabolic rate per unit of volume than cortical bone (*3*). In any one bone, however, rates of change in bone density may be greater at sites that are predominantly trabecular in composition compared to sites that are predominantly cortical. Rates of change are also greater in axial trabecular bone than in appendicular trabecular bone. If a patient is being followed over time to look for changes in the bone mineral density from a disease process or therapeutic intervention, the greatest magnitude of change will generally be seen at a site that is predominantly trabecular bone. There are certain disease processes, however, which seem to have a predilection for sites that are predominantly cortical in composition. Hyperparathyroidism, for example, may cause demineralization at predominantly cortical sites, like the femoral neck or 33% radial site. Conversely, Cushing's disease may preferentially destroy the trabecular bone of the axial skeleton. In a disease like acromegaly, hypogonadism may cause a profound decrease in the trabecular bone of the spine while excessive growth hormone causes an increase in the density of the cortical bone of the appendicular skeleton.

A   **B**
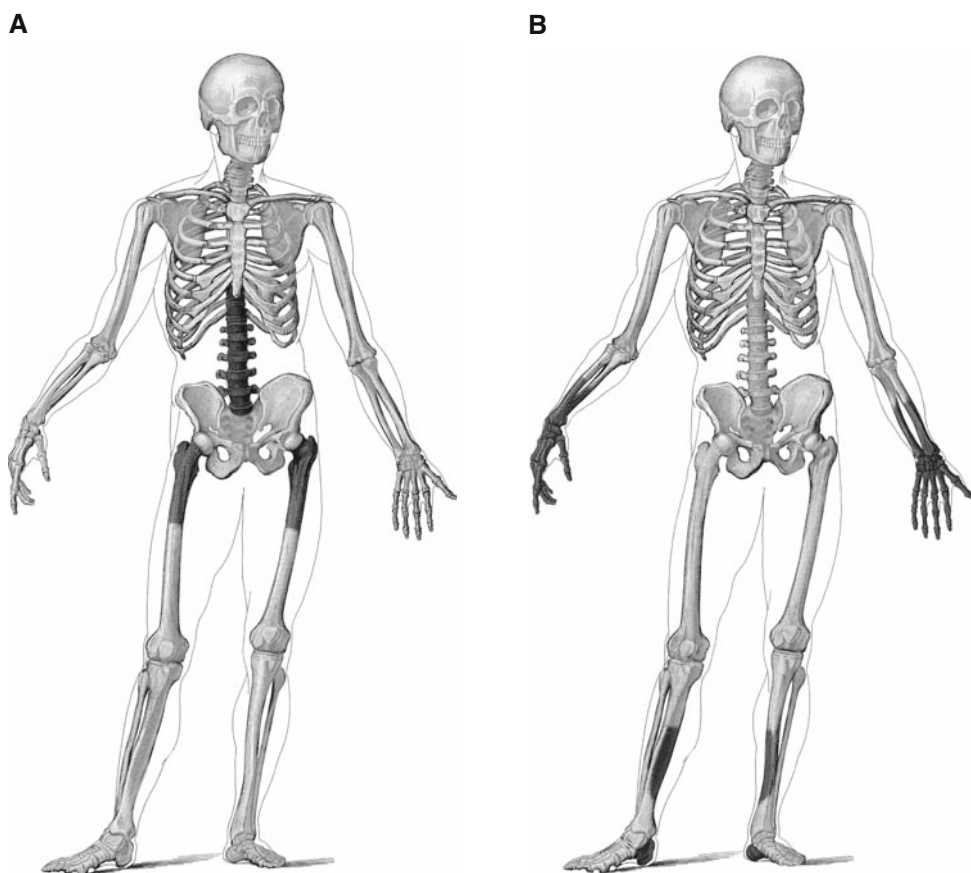
Fig. 2-2. (A) and **(B)**. The central and peripheral skeleton. The *darker-shaded* bones in **(A)** comprise the central skeleton. The *darker-shaded* bones in **(B)** comprise the peripheral skeleton. Images adapted from EclectiCollections™.

FOREARM COMPOSITION

The exact percentage of trabecular and cortical bone of many of the sites used in densitometry remains controversial. In a classic study, Schlenker and VonSeggen (*4*) quantified the average percentage of cortical and trabecular bone along the length of the radius and ulna in four cadaveric female forearms. The forearms were taken from women aged 21, 43, 63, and 85 years. The distribution and percentage of trabecular bone in the radius and ulna were similar. The maximum percentage of trabecular bone was seen in the first two centimeters proximal to the radial and ulnar styloids. The percentage of trabecular bone then dropped precipitously in both bones in a transitional region which lay between 2- and 3 cm proximal to either styloid and remained very small throughout the remainder of the proximal radius and ulna. The percentage of trabecular bone in the four subjects in the most distal 10% of the radius ranged from 50 to 67% while in the region that represented 30 to 40% of the total length measured from the styloid tip, the percentage of trabecular bone ranged from only 0.6 to 6.8%.

VERTEBRAL COMPOSITION

The composition of whole vertebra or the isolated vertebral body remains in dispute. The traditional view is that 55–75% of the calcium content of the whole vertebra is in trabecular bone. These figures are largely derived from early anatomic studies in which the methods used to arrive at such conclusions were poorly described (*5, 6*). The traditional view was challenged in 1987 by Nottestad et al. (*7*) who performed anatomic dissections of 24 vertebrae taken from 14 normal individuals, 10 of whom were women with an average age of 72 years and 4 of whom were men with an average age of 63. The vertebrae were ashed and the calcium content was assayed using atomic absorption spectrophotometry. Nottestad et al., found that trabecular bone accounted for only 24.4% of the calcium content of whole female vertebrae. Trabecular calcium accounted for 41.8% of the calcium content in the vertebral body. The percentages were less in men, averaging 18.8 and 33.5%, respectively. Eastell et al. (*8*) refuted this finding based on anatomic dissections of L2 from 13 individuals, 6 men whose average age was 38.5 years and 7 women whose average age was 40.9. In this study, cortical and trabecular contributions to calcium content were determined by microdensitometry and by dissection and ashing. They reported that the whole vertebra was 72% trabecular bone in women and 80% trabecular bone in men. Adjusting these figures to compensate for the expected difference between the two-dimensional measurements that were actually performed and the three-dimensional structure of whole vertebrae, the percentages of trabecular bone in whole vertebrae dropped slightly to 69% in women and 77% in men.

FEMORAL COMPOSITION

The composition of the commonly measured sites in the proximal femur was briefly studied by Baumel (Heaney RP. Personal communication, November 23, 1994) using anatomic dissection of the upper end of the femur in six cadavers (age at death 49–79 years). In this small study the percentage of trabecular bone in the femoral neck was 36.45% (±.85%) and in the trochanter 39.06% (±3.79%). Using QCT, Kuiper et al. (*9*) studied the amount and distribution of cortical and trabecular bone in the femoral neck of 20 cadaveric specimens. The average age of the individuals from whom the specimens were taken was 83.2 years. In this study, trabecular bone mass accounted for 33% of the total bone mass at the mid-neck. In an earlier study from Werner et al. (*10*) trabecular bone mineral content at the mid-femoral neck was reported as 23.5% from 20 cadaveric specimens taken from individuals with an average age of 75 years. In the study from Kuiper et al. (*9*) the authors noted that trabecular bone mass appeared to decrease at a rate of 2.5% for every 1 mm increment from the femoral head to the trochanter. This raises the possibility that markedly different locations for the femoral neck region of interest among DXA manufacturers may result in the measurement of differing amounts of trabecular and cortical bone.

ALL SITES

In spite of these controversies, clinically useful characterizations of the composition of densitometry sites can be made. Table 2-1 lists the most commonly assessed skeletal sites and their relative proportions of trabecular and cortical bone (*11*). Note that the spine, when measured with QCT, is described as 100% trabecular bone. This is because the three-dimensional volumetric measure that is obtained with QCT allows the center of the vertebral body to be isolated from its cortical shell and the highly cortical

Table 2-1
Percentage of Trabecular Bone at Central and Peripheral Sites

PA Spine[a]	66%
Lateral Spine[b]	?
Femoral Neck	25%
Trochanter	50%
Ward's[b]	?
Total Body	20%
Calcaneus	95%
33% Radius or Ulna[c]	1%
10% Radius or Ulna[d]	20%
8-mm Radius or Ulna[e]	25%
5-mm Radius or Ulna[e]	40%
4-5% Radius or Ulna[f]	66%
Phalanges	40%

[a]These percentages are for DXA PA spine studies only. A volumetric measurement of 100% trabecular bone could be obtained with QCT.

[b]These sites are considered to be highly trabecular but the exact percentage of trabecular bone is not known.

[c]This site is often called the "proximal" site.

[d]This site is often called the "distal" site.

[e]Distance in mm indicates the separation distance between the radius and ulna at the site in question.

[f]This site is often called the ultra-distal site, but may be called simply "distal" as well.

posterior elements. The two-dimensional areal measurement employed in DPA and DXA measurements of the spine cannot do this. Although the posterior elements are eliminated from the scan path on a lateral spine study performed with DXA, elements of the cortical shell remain. Therefore, although the measurement of the spine in the lateral projection with DXA is a highly trabecular measurement of bone density, the measurement is not a measure of 100% trabecular bone.

THE SPINE IN DENSITOMETRY

Studies of the lumbar spine performed with DPA or DXA are generally acquired by the passage of photon-energy from the posterior to anterior direction. They are properly characterized as PA spine studies. Nevertheless, these studies are often called AP spine studies, probably because plain films of the lumbar spine are acquired in the AP projection. The Lunar Expert, a fan-array scanner, actually does acquire lumbar spine bone density images in the AP direction. Compared to plain radiography, however, the beam direction in a DXA study of the spine has less influence on the appearance of the image and little if any influence on the measured BMC or BMD. Studies of the lumbar spine may also be acquired in the lateral projection using DXA. Such studies may be performed with the patient in the supine or left lateral decubitus position, depending upon the type of DXA unit employed.

Vertebral Anatomy

The whole vertebra can be divided into two major components: the body and the posterior elements. The posterior elements consist of the pedicles, the lamina, the spinous
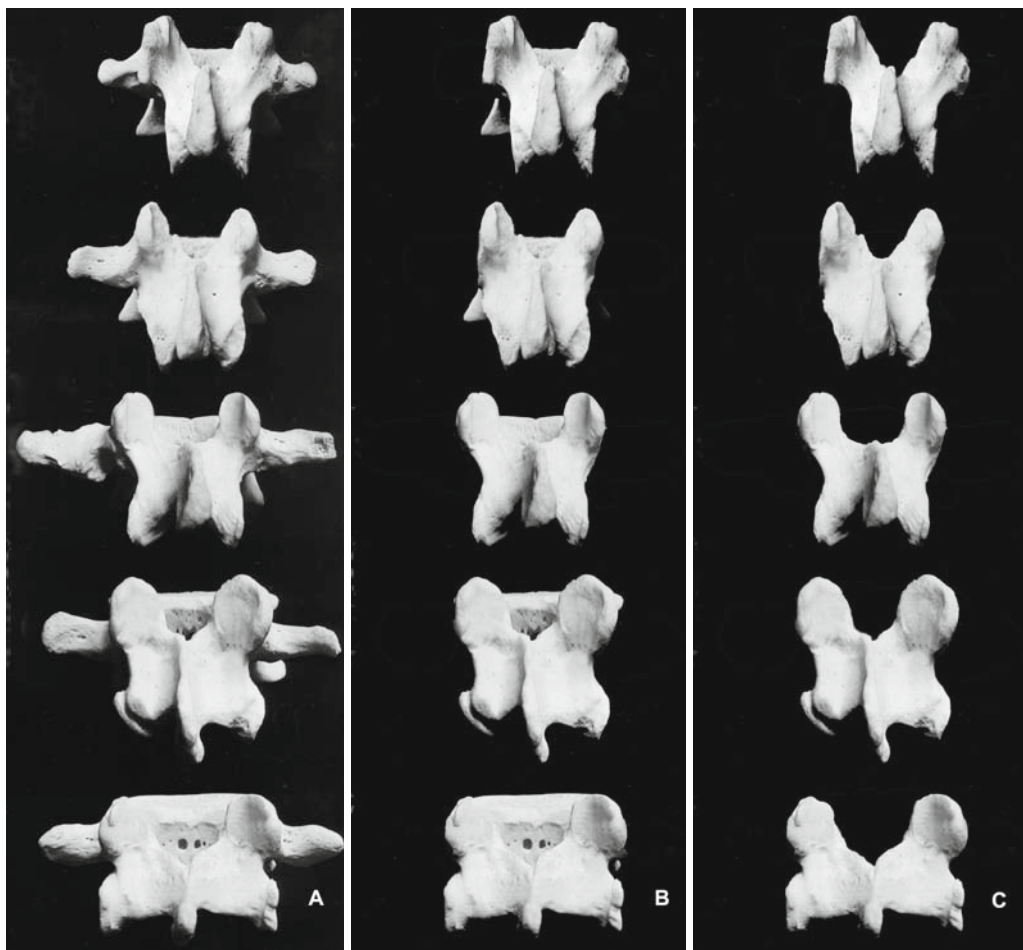
Fig. 2-3. The lumbar spine in the posterior view. **(A)** Intact vertebrae. **(B)** The transverse processes have been removed. **(C)** The vertebral bodies have been removed, leaving only the posterior elements (Adapted from McMinn RMH, Hutchings, RT, Pegington J, and Abrahams PH. Colour atlas of human anatomy. Third edition, 1993:83. © 1993 Mosby, with permission from Elsevier.).

process, the transverse processes, and the inferior and superior articulating surfaces. The appearance of the image of the spine on an AP or PA spine study is predominantly determined by the relative density of the various elements that make up the entire vertebra. Figure 2-3A is a photograph of a posterior view of the lumbar spine with the intervertebral discs removed. Figures 2-3B and 2-3C demonstrate the appearance of the spine as first the transverse processes and then the vertebral bodies are removed from the photograph. What remains in Fig. 2-3C is characteristic of the appearance of the lumbar spine on a PA DXA lumbar spine study and consists largely of the posterior elements. The posterior elements form the basis of the DXA lumbar spine image seen in Fig. 2-4. The transverse processes are eliminated from the scan field and the vertebral bodies are not well seen because they are both behind and equally or less dense than the posterior elements. In a study of 34 lumbar vertebrae taken from 10 individuals, age 61–88, the

ID:			SCAN DATE: 09/05/99

Bone Results
DEXA Calibration

Region	BMC* g	Area* cm²	BMD g/cm²
L1	12.88	10.97	1.174
L2	16.32	12.95	1.261
L3	17.39	13.10	1.327
L4	20.12	15.74	1.278
L1-L2	29.20	23.92	1.221
L1-L3	46.59	37.02	1.258
L1-L4	66.70	52.76	1.264
L2-L3	33.71	26.05	1.294
L2-L4	53.83	41.79	1.288
L3-L4	37.51	28.84	1.300

LUNAR®   IMAGE NOT FOR DIAGNOSIS   * Data for research only
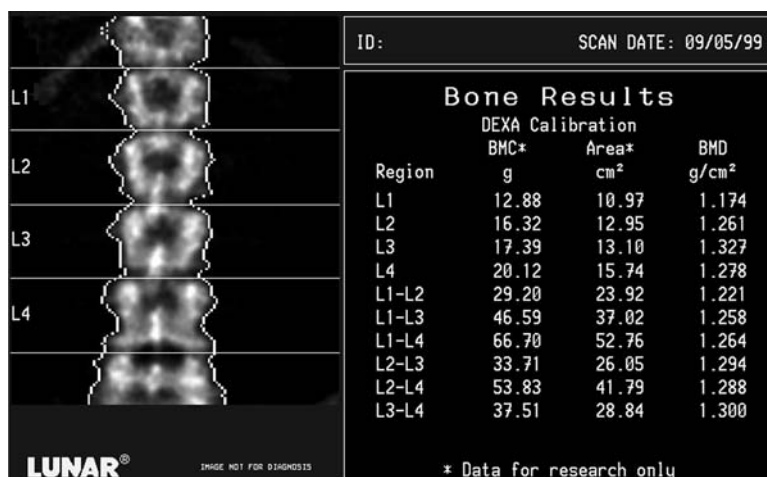
Fig. 2-4. A DXA PA spine study acquired on the Lunar DPX. The shapes of the vertebrae in this image are primarily created by the posterior elements. The shapes in this study are classic. The expected increase in BMC and area is also seen from L1 to L4. The increase in BMD from L1 to L3, with a decline from L3 to L4, is also typical.
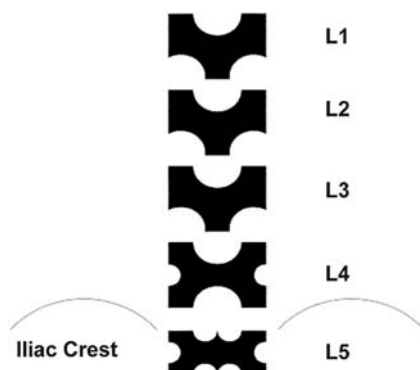
Fig. 2-5. A graphic illustration of the characteristic shapes of the lumbar vertebrae as seen on a DXA PA spine study.

average mineral content of the posterior elements was 47% of the mineral content of the entire vertebra (*12*).

The unique shapes of the posterior elements of the various lumbar vertebrae can be used as an aid in identifying the lumbar vertebrae. The posterior elements of L1, L2, and L3 have a U- or Y-shaped appearance. L4 can be described as looking like a block H or X. L5 has the appearance of a block I on its side. Figure 2-5 is a graphic illustration of these shapes. Compare these shapes to the actual posterior elements seen in Fig. 2-3C and the DXA lumbar spine study shown in Fig. 2-4. Although the transverse processes are generally not seen on a spine bone density study, the processes at L3 will sometimes be partially visible, since this vertebra tends to have the largest transverse processes. This fact can also be helpful in lumbar vertebral identification. Figures 2-6A and 2-6B
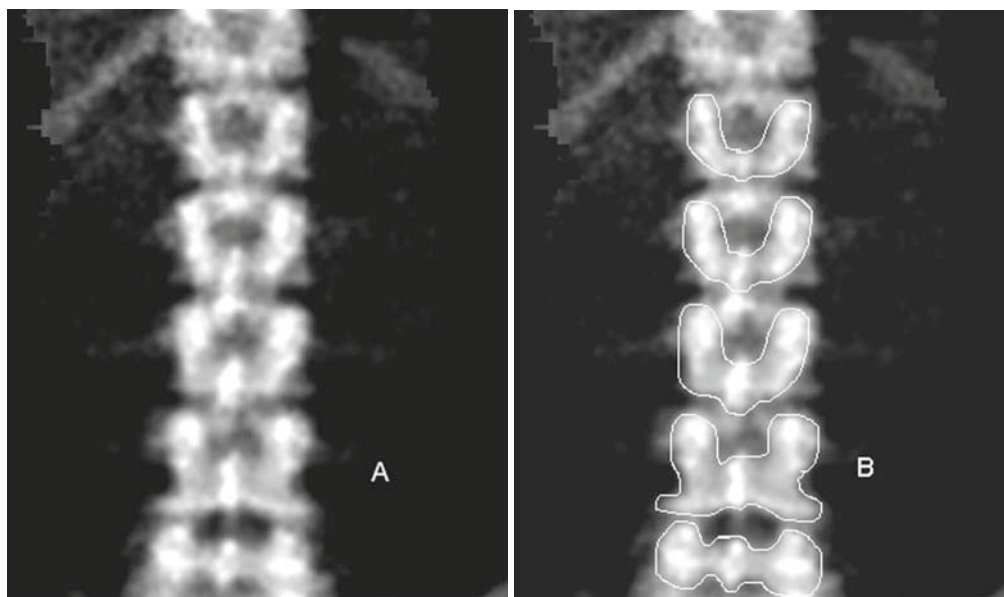
Fig. 2-6. (A) A DXA PA spine image acquired on the Lunar DPX. This is the spine image from the study shown in Fig. 2-4, with the intervertebral disk markers and bone-edge markers removed for clarity. **(B)** The shapes have been outlined for emphasis.

Table 2-2

Incremental Change in BMC and BMD Between Adjacent Vertebrae in 148 Normal Women Aged 50–60, as Measured by DXA

Vertebrae	Increase in BMC (g)	% Increase in BMC	Increase in BMD (g/cm²)	% Increase in BMD
L1–L2	2.07	13.7	0.090	7.9
L2–L3	2.43	14.8	0.050	4.3
L3–L4	1.13	5.0	–0.004[a]	–0.8[a]

[a]Not statistically significant

Adapted from ref. (*13*) with permission of the American Society for Bone and Mineral Research.

are the spine image only from the study shown in Fig. 2-4. In Fig. 2-6B, the shapes of the posterior elements have been outlined for emphasis.

On PA or AP DXA lumbar spine studies, L1 through L4 are quantified. Although L5 can be seen, it is not usually quantified because of potential interference from the pelvis. In fact, even if labeled on the scan, some software programs will not analyze L5 unless it is deliberately mislabeled L4. L1 frequently has the lowest BMC and BMD of the first four lumbar vertebrae. In a study of 148 normal women ages 50–60, Peel et al. (*13*) found that the BMC increased between L1–L2, L2–L3, and L3–L4 although the increase between L3 and L4 was roughly half that seen at the other levels as shown in Table 2-2. BMD increased between L1–L2 and L2–L3 but showed no significant change between L3 and L4. The average change between L3 and L4 was actually a decline of 0.004 g/cm². The largest increase in BMD occurred between L1 and L2. The apparent

discrepancies in the magnitude of the change in BMC and BMD between the vertebrae are the result of the progressive increase in area of the vertebrae from L1 to L4. The DXA PA lumbar spine study shown in Fig. 2-4 illustrates the progressive increase in BMC and area from L1 to L4 and the expected pattern of change in BMD between the vertebral levels.

Studies from Peel et al. (*13*) and Bornstein and Peterson (*14*) suggest that the majority of individuals have five lumbar vertebrae with the lowest set of ribs on T12. Bornstein and Peterson (*14*) found that only 17% of 1239 skeletons demonstrated a pattern of vertebral segmentation and rib placement other than five lumbar vertebrae with the lowest ribs on T12. Similarly, Peel et al. (*13*) found something other than the expected pattern of five lumbar vertebrae with the lowest ribs on T12 in only 16.5% of 375 women. An additional 7.2% had five lumbar vertebrae but had the lowest level of ribs on T11. Therefore, 90.7% of the women in this study had five lumbar vertebrae. Only 1.9% or seven women out of 375 had six lumbar vertebrae. In three of these women ribs were seen on L1. This was the only circumstance in which ribs were seen on L1, and 7.5% of the entire group had only four lumbar vertebrae. In the majority of cases here, the lowest ribs were seen on T11. Table 2-3 summarizes these findings.

Knowledge of the frequency of anomalous vertebral segmentation, the characteristic shapes created by the posterior lumbar elements on a PA lumbar spine study, and the expected incremental change in BMC and BMD can be used to label the vertebrae correctly. If the vertebrae are mislabeled, comparisons to the normative databases will be misleading. The expected effect of mislabeling T12 as L1 is a lowering of the BMC or BMD at L1, which would then compare less favorably to the reference values for L1. The BMC and BMD averages for L1–L4 or L2–L4 would also be lowered. The degree to which BMC is lowered by mislabeling is substantially greater than BMD as shown in Table 2-4 (*13*). The assumption that the lowest set of ribs is found at the level of T12 is often used as the basis for labeling the lumbar vertebrae. As can be seen from Table 2-3, this assumption would result in the vertebrae being labeled incorrectly in 13.3% of the population. As a consequence, all of the criteria noted above should be employed in determining the correct labeling of the lumbar vertebrae. This should obviate the need for plain films for the sole purpose of labeling the vertebrae in the vast majority of instances. Figure 2-7 is a PA spine study in which the labeling of the lumbar vertebra was not straightforward. The characteristic shapes of the vertebrae are easily

Table 2-3
Percentage of Women with Various Combinations of Numbers of Lumbar Vertebrae and Position of Lowest Ribs

No. of Lumbar Vertebrae	Position of Lowest Ribs	% of Women
5	T12	83.5
5	T11	7.2
4	T12	2.1
4	T11	5.3
6	T12	1.1
6	L1	0.8

Adapted from ref. (*13*) with permission of the American Society for Bone and Mineral Research.

Table 2-4
**The Effect of Mislabeling T12 as L1 on BMC and BMD
in AP-DXA Spine Measurements**

Measurement	Difference	Mean %
BMC		
L1	1.61 g	11.5
L2–L4	3.47 g	8.4
L1–L4	4.8 g	8.4
BMD		
L2–L4	0.035 g/cm^2	3.6
L1–L4	0.039 g/cm^2	3.5

Adapted from ref. (*13*) with permission of the American Society for Bone and Mineral Research.
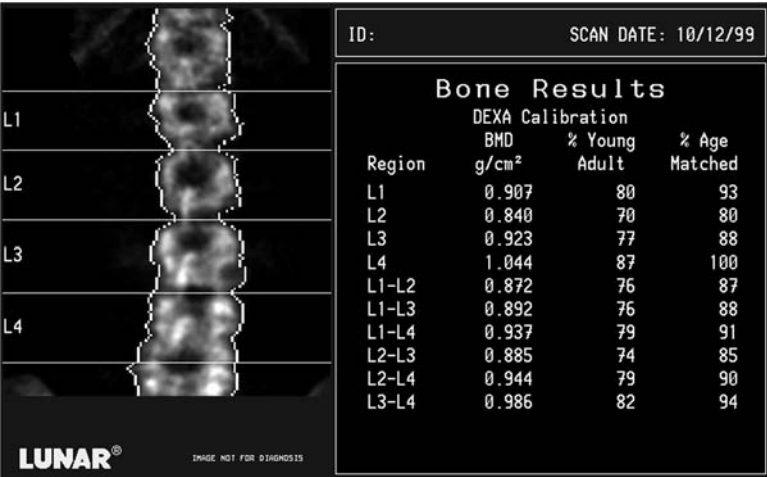
Fig. 2-7. A DXA PA spine study acquired on the Lunar DPX. The vertebra labeled L4 has a classic block H or X shape. No ribs are seen, however, protruding from the vertebra that should be T12. It is far more likely that this represents five lumbar vertebrae with the lowest ribs on T11 than six lumbar vertebrae with the lowest ribs on T12. Also note that the BMD at L1 is higher than at L2, which is unusual. A lateral lumbar spine X-ray of this patient, shown in Fig. 2-9, confirmed a fracture at L1.

seen, but no ribs appear to be projecting from what should be T12. Note the block H shape of the vertebra labeled L4 and the visible transverse processes on the vertebra labeled L3. Statistically, it is likely that there are five lumbar vertebrae here with the lowest set of ribs on T11. The appearance of L3 and L4 would also support this labeling. Plains films acquired for the purpose of diagnosing spine fracture confirmed that the labeling shown in Fig. 2-7 is correct.

Artifacts in PA or AP Spine Densitometry

The PA lumbar spine has been, and continues to be, used extensively in densitometry for diagnosis, fracture prediction, and monitoring. Unfortunately, it is also the skeletal site most often affected by structural changes and artifacts that may limit its utility.

VERTEBRAL FRACTURES

The BMD of a fractured vertebra will be increased because of the fracture itself. This increase in density could erroneously lead the physician to conclude that the bone strength is better and the risk for fracture lower than is the case. Vertebral fractures in osteoporosis frequently occur in the T7–T9 region and in the T12–L2 region (*15, 16*). Because DXA measurements of the lumbar spine are often employed in patients with osteoporosis, osteoporotic fractures in the lumbar spine, particularly at L1 and L2, are a common problem, rendering the measurement of BMD inaccurate if the fractured vertebrae are included. An increased precision error would also be expected if the fractured vertebrae were included in BMD measurements performed as part of a serial evaluation of BMD. Although a fractured lumbar vertebra can be excluded from consideration in the analysis of the data, this reduces the maximum number of contiguous vertebrae in the lumbar spine available for analysis. For reasons of statistical accuracy and precision, the BMD for three or four contiguous vertebrae is preferred over two vertebrae averages or the BMD of a single vertebra. Figure 2-8 illustrates a PA lumbar spine study in which a fracture was apparent at L3. Although the BMD at L3 is expected to be higher than either L2 or L4, it is disproportionately higher. The L2–L4 BMD will be increased because of the effect of the fracture on the BMD at L3. In the DXA PA lumbar spine study shown in Fig. 2-7, the image does not as readily suggest a fracture. The BMD at L1, however, is higher than the BMD at L2, which is unusual. A plain lateral film of the lumbar spine of this patient, shown in Fig. 2-9, confirmed a fracture at L1.
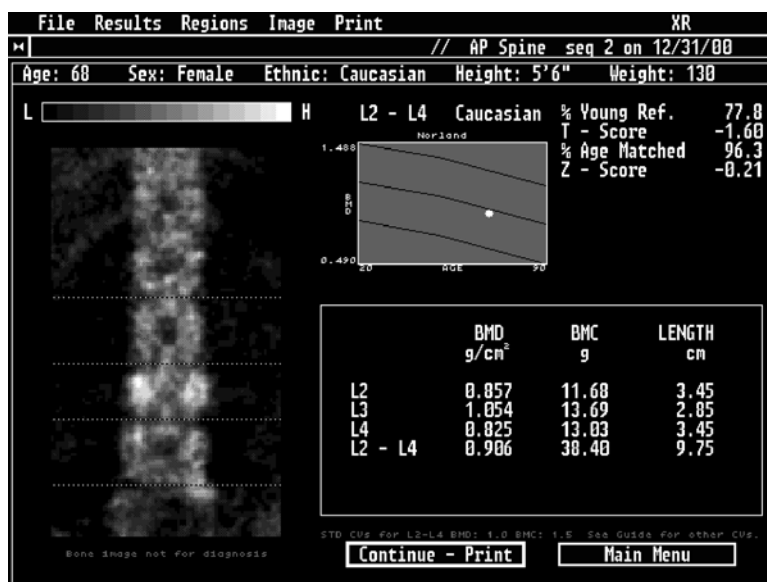
Fig. 2-8. A DXA PA spine study acquired on the Norland XR-36. The image suggests a loss of vertebral height and increased sclerosis at L3. Although the BMD at L3 is expected to be higher than at L2, the BMD at L3 here is markedly higher. These findings suggest a fracture at this level but this must be confirmed. In any case, the L2–L4 BMD will be increased by this structural change. Case courtesy of Norland, a CooperSurgical Company, Ft. Atkinson, WI.

Fig. 2-9. The lateral lumbar spine X-ray of the patient whose DXA study is shown in Fig. 2-7. A fracture at L1 is indicated by the *arrow*.

DEGENERATIVE CHANGES AND DYSTROPHIC CALCIFICATION

Other structural changes within the spine can affect BMD measurements. Osteophytes and facet sclerosis can increase the BMD when measured in the AP or PA projection. Aortic calcification will also potentially affect the BMD when measured in the AP or PA spine because the X-ray beam will detect the calcium in the aorta as it passes through the body on an anterior to posterior or posterior to anterior path. It is therefore useful to note how often these types of changes are expected in the general population and the potential magnitude of the effect these changes may have on the measured BMD in the lumbar spine.

The Effect of Osteophytes on BMD. In 1982, Krolner et al. (*17*) observed that osteophytes caused a statistically significant increase in the BMD in the AP spine when compared to controls without osteophytes. More recently, Rand et al. (*18*) evaluated a population of 144 postmenopausal women aged 40–84 years, with an average age of 63.3 years, for the presence of osteophytes, scoliosis, and aortic calcification. These women were generally healthy women referred for the evaluation of BMD because of suspected postmenopausal osteoporosis. Table 2-5 lists the percentages of these women found to have these types of degenerative changes. Based on these findings, Rand et al. estimated the likelihood of degenerative changes in the spine as being less than 10% in women under the age of 50. In 55-year-old women, however, the likelihood jumped to 40% and in 70-year-old women to 85%. Of these types of degenerative changes, however, only the presence of osteophytes significantly increased the BMD. The magnitude of the increase caused by the osteophytes ranged from 9.5% at L4 to 13.9% at L1. Cann et al. (*19*) also estimated the increase in BMD from osteophytes in the spine at 11%.

Table 2-5
Frequency of Specific Types of Degenerative Changes
in the Spines of 144 Women Aged 40–84

Type of Degenerative Change	% with Change (n)
Osteophytes	45.8 (66)
Osteochondrosis	21.5 (31)
Vascular calcification	24.3 (35)
Scoliosis	22.2 (32)
Any type	59.0 (72)

Adapted with kind permission of Springer Science and Business Media from ref. (*18*).

Fig. 2-10. A lateral lumbar spine X-ray of the patient whose DXA study is shown in Fig. 2-11. The *arrow* indicates a region of endplate sclerosis and osteophyte formation.

In 1997, Liu et al. (*20*) studied 120 men and 314 women, aged 60–99 years. Lumbar spine osteophytes were found in 75% of the men and 61.1% of the women. The effect of osteophytes on the BMD was sufficiently great to cause 50% of the men and 25% of the women with osteopenia to be misdiagnosed. About 20% of the men and 10% of the women with osteoporosis were misdiagnosed because of the effect of osteophytes on the BMD. In Fig. 2-10 osteophytes are clearly visible at L2 on the lateral lumbar radiograph. The appearance of this region on the DXA PA lumbar spine study in Fig. 2-11 suggests a sclerotic process at this level. Osteophytes and end-plate sclerosis are also seen on the plain film in Fig. 2-12. The effect on the DXA image of the lumbar spine, shown in Fig. 2-13 is dramatic. There is also a disproportionate increase in the BMD at L2 and L3 compared to L1 and L4.
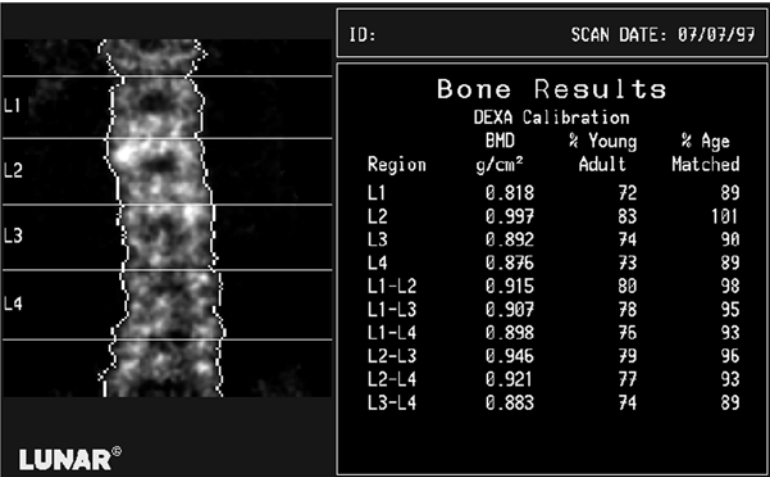
Fig. 2-11. A DXA PA spine study acquired on the Lunar DPX. A sclerotic process is suggested at L2 by the image. The BMD is also increased more than expected in comparison to L1 and is higher than L3, which is unusual. These findings are compatible with the endplate sclerosis and osteophytes seen in Fig. 2-10.
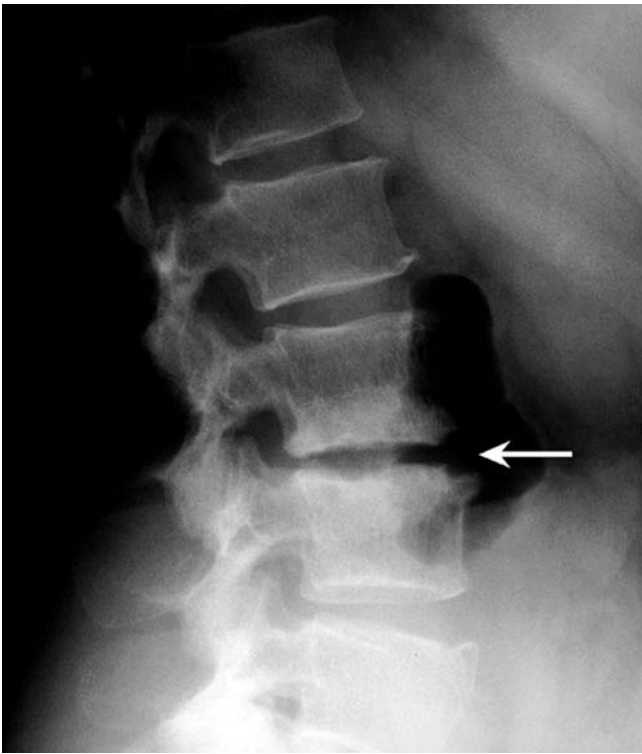
Fig. 2-12. A lateral lumbar spine X -ray of the patient whose DXA study is shown in Fig. 2-13. The *arrow* indicates a region of marked endplate sclerosis.
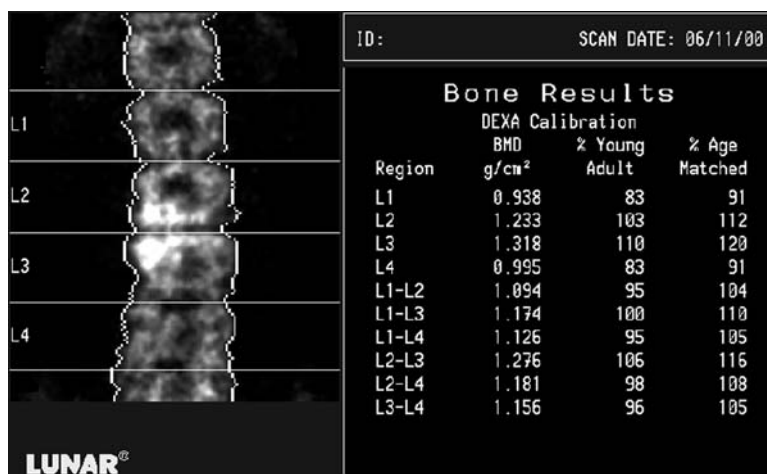
Fig. 2-13. A DXA PA spine study acquired on the Lunar DPX. The image dramatically suggests the sclerotic process seen on the X-ray in Fig. 2-12. There is a marked increase in the BMD at L2 and L3 compared to L1 and L4.

The Effect of Aortic Calcification on BMD. Although it did not significantly increase BMD, vascular calcification was seen in 24.3% of the 144 postmenopausal women studied by Rand et al. (*18*). In a study of aortic calcification in 200 women aged 50 or older by Frye et al. (*21*) the percentage of women with aortic calcification and the effect on BMD measured in the PA lumbar spine was noted. A grading system[2] for both linear calcifications and calcified plaques in the aorta was applied to lateral spine films with a grade of zero indicating neither type of calcification and a grade of two indicating the most severe degree. The percentage of women with any degree of aortic calcification and severe calcification is shown in Fig. 2-14. The percentage with any degree of aortic calcification was extremely low under age 60 but increased dramatically in women age 60 and older. The percentage of women with severe aortic calcification, however, remained low throughout the fifties, sixties, and seventies. Even in women aged 80 and older, the percentage did not exceed 30%. Table 2-6 summarizes the effect on BMD in women of any degree of aortic calcification and severe aortic calcification. Neither effect was statistically significant. These findings are similar to those of Frohn et al. (*22*), Orwoll et al. (*23*), Reid et al. (*24*), Banks et al. (*25*), and Drinka et al. (*26*) in which no significant effect of aortic calcification was seen on the BMD measured in the PA spine. The studies from Orwoll et al. (*23*) and Drinka et al. (*26*) were performed in men. A recent ex vivo study from Cherney et al. (*27*) quantified the effect of removal of the aorta on PA lumbar spine bone density. After choosing eight cadavers at random, PA lumbar spine DXA bone density studies were performed before and after the removal of the aorta. The age at death ranged from 67 to 87 years, with an average age of 79 years. Removal of the aorta resulted in an average decrease in PA lumbar spine

---

[2] This is not the same grading system as now used to quantify aortic calcification on plain films or lateral DXA images of the spine. See Chapter 13 for a discussion of the 24-point and 8-point grading systems in use today.
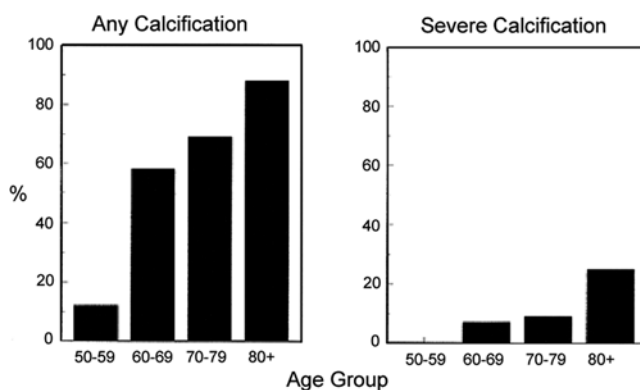
Fig. 2-14. The prevalence of aortic calcification in women aged 50 and over. From Frye MA et al. (*21*), with permission of Elsevier Science & Technology Journals.

Table 2-6
The Effect of Aortic Calcification on BMD in the Spine

| | BMD | | | |
Site	Observed	Expected	Difference	% of Expected
BMD spine				
Any grade 1 or 2	0.93	0.92	0.01	101.4
Any grade 2	0.94	0.89	0.05	106.7

Adapted from Frye MA et al. (*21*) with permission of Elsevier Science & Technology Journals.

BMD of 4.64%. The authors do not describe the severity of any observed aortic calcification. Nevertheless, their results are in keeping with those from Frye et al. (*21*) in which a small effect on lumbar spine bone density was observed with severe aortic calcification.

Aortic calcification is not easily seen on most DXA PA lumbar spine studies. In Fig. 2-15A, however, the faint outline of the calcified aorta is visible. The aorta is easily seen on the lateral DXA image in Fig. 2-15B. Figure 2-16 shows both studies. In this case, the effects of the calcified aorta on the BMD measurement can be eliminated on the DXA lateral spine bone density study. The ability to see aortic calcification when DXA images are acquired in the lateral projection has also led to a new application for DXA: quantifying aortic calcification. This is discussed in Chapter 13.

The Effect of Facet Sclerosis on BMD. Unlike aortic calcification, facet sclerosis can have a profound effect on the measured BMD in the AP or PA projection. In the study by Drinka et al. (*26*) noted earlier, 113 elderly men were evaluated with standard AP and lateral lumbar spine films and dual-photon absorptiometry of the lumbar spine. A grading system for facet sclerosis was developed with a grade of 0 indicating no sclerosis and a grade of 3 indicating marked sclerosis. As shown in Table 2-7, grade 1 sclerosis had no significant effect on the BMD. Grades 2 and 3, however, markedly increased the BMD at the vertebral levels at which the facet sclerosis
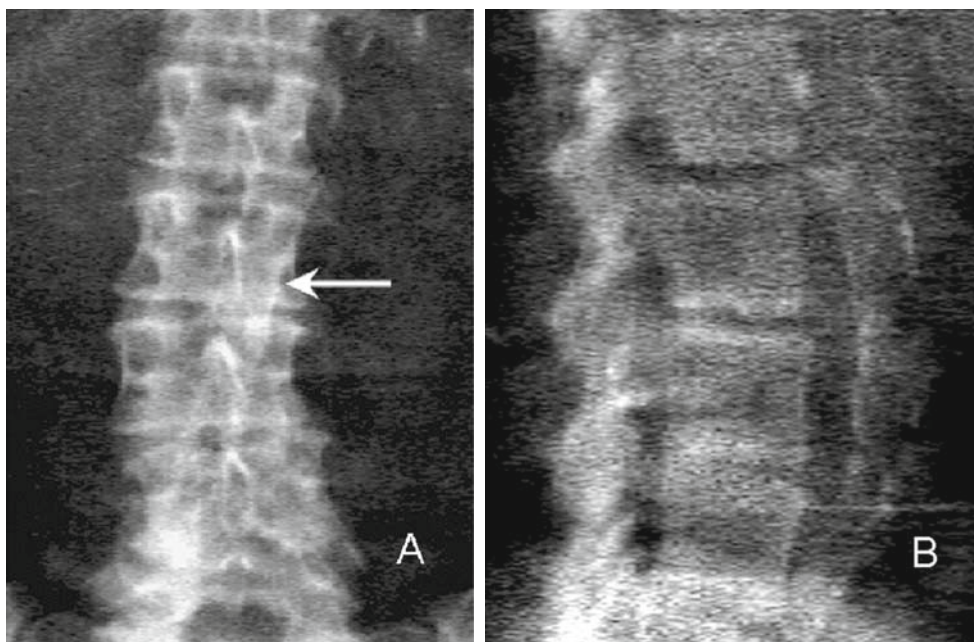
Fig. 2-15. PA and lateral DXA lumbar spine images acquired on the Hologic QDR-4500. The *arrow* seen in **(A)** indicates the faint outline of the calcified aorta that is easily seen on the lateral study in **(B)**. Case courtesy of Hologic, Inc., Bedford, MA.
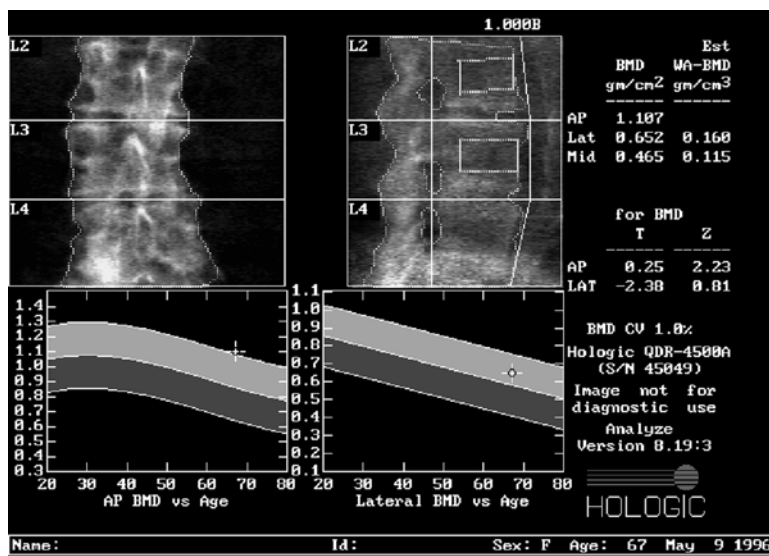
Fig. 2-16. A DXA PA and lateral lumbar spine study acquired on the Hologic QDR-4500. These are the analyzed studies for the images shown in Fig. 2-15. Case courtesy of Hologic, Inc., Bedford, MA.

was found. Figure 2-17 is a PA spine BMD study in which facet sclerosis is suggested at L3 by the appearance of the image. The BMD values at L3 and L4 are also markedly higher than expected, based on the values at L1 and L2. The plain film of this patient shown in Fig. 2-18 confirms facet sclerosis at the lower lumbar levels.

Table 2-7
The Increase in BMD from Facet Sclerosis

	Grade 2	Grade 3
L1	0.275	0.465
L2	0.312	0.472
L3	0.184	0.343
L4	0.034	0.247
Average	0.201	0.382

Values are in g/cm^2.
Adapted with kind permission of Springer Science and Business Media from Drinka et al. (*26*).
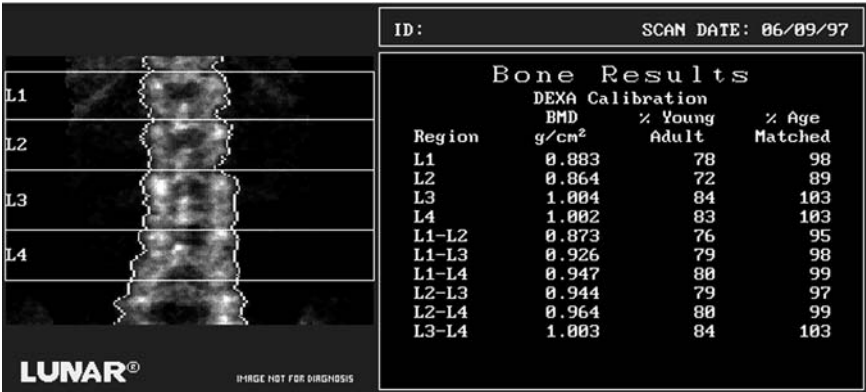
Fig. 2-17. A DXA PA lumbar spine study acquired on the GE Lunar DPX. There is a marked increase in the BMD between L2 and L3, which is maintained at L4. The image faintly suggests sclerosis in the region of the facet joints at L3 and L4. This is more dramatically seen in the plain film of this patient shown in Fig. 2-18.

OTHER CAUSES OF ARTIFACTS IN PA AND AP LUMBAR SPINE STUDIES

Potential causes of apparent increases in the BMD in the AP or PA lumbar spine have been identified by Stutzman et al. (*28*). These include pancreatic calcifications, renal stones, gallstones, contrast agents, and ingested calcium tablets in addition to osteophytes, aortic calcification, and fractures. The effect on the BMD of these artifacts would appear to be greater in the patient with low bone density than in the patient with high bone density (*29*, *30*). Using cadaveric specimens, Morgan et al. (*29*) placed a variety of commonly encountered artifacts, such as surgical clips, gallstones, calcium tablets, and kidney stones lateral to L1 or L3. One cadaveric specimen had a high BMD and the other had a low BMD. Surgical clips in the gallbladder region or a gallstone did not significantly affect the L1–L4 BMD in either cadaveric specimen. However, there was a significant effect on the L1–L4 BMD in the low BMD specimen from bra wires and calcium tablets lateral to L1 or L3. In a companion study, Morgan et al. (*30*) noted that some artifacts, because of their very high density, appear as "black hole" on a PA spine DXA study rather than white. This included tantalum surgical clips, which are often used in vascular surgery. Tantalum clips are useful for a variety of reasons, not the least of which is their lack of ferromagnetic potential, which allows for magnetic
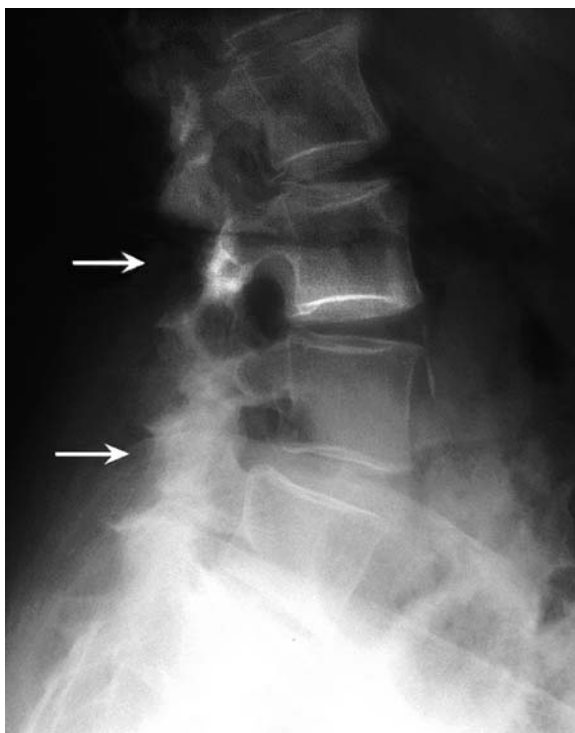
Fig. 2-18. A lateral lumbar spine X-ray of the patient whose bone density study is shown in Fig. 2-17. The *arrows* indicate sclerotic regions in the posterior elements.

resonance imaging. Tantalum pellets are also used as radiographic markers because they are radiopaque. Another artifact which produced a "black hole" was a lead bullet. In contrast, titanium or stainless steel clips appeared white. Once again, the most pronounced effects of the "black hole" artifact tantalum clips were seen in the low-BMD cadaveric specimen. When tantalum clips were placed over L3 of a cadaveric specimen with the high L1–L4 BMD, the L1–L4 BMD was largely unaffected. In the low-BMD cadaveric specimen, however, when eight tantalum clips were placed over L3 or L4 placed lateral to L3, the L1–L4 BMD was increased. A Hologic spine phantom was used to assess the effects of a 0.45-caliber lead bullet placed over L3.[3] The bullet created a "black hole" artifact at L3. The BMC, area, and BMD were all significantly greater at L3 and at L1–L4 with the bullet compared to the phantom BMD without the bullet overlying L3. The authors noted that their findings were obtained using a Hologic Discovery W. If the DXA software automatically excludes non-physiologic densities from the analysis, very dense objects overlying the spine would not be expected to increase the measured BMD. However, the effect of this approach is a "black hole" of another type in this case, the hole is in the data. Few studies exist on the effects of ascites on bone density measured in the PA projection. In one such study, Labio et al. (*31*) found that ascites can falsely lower the BMD measured in the PA projection in patients with cirrhosis. In the study

---

[3] See Chapter 4 for a discussion of spine phantoms, including the Hologic spine phantom.
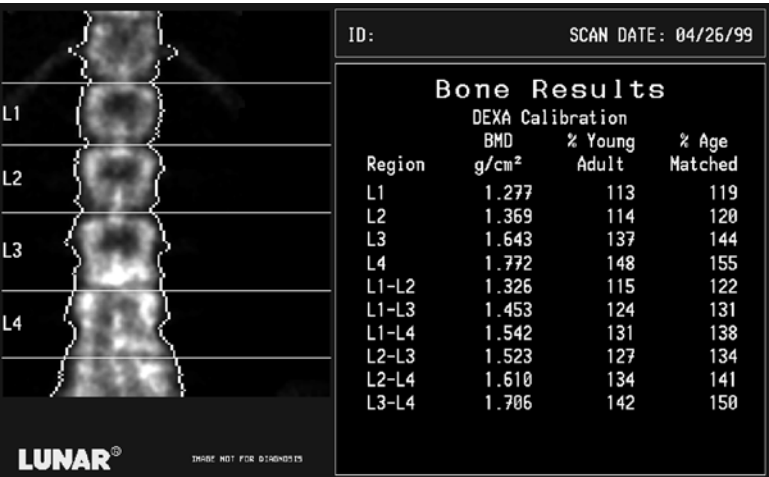
Fig. 2-19. A DXA PA lumbar spine study acquired on the Lunar DPX. The image suggests increased density at L3 and L4, but there is also a linear vertical lucency over L4. The BMD values are markedly increased at L3 and L4. This patient had previously undergone an L3–L4, L4–L5 interbody fusion and laminectomy at L4. Although the laminectomy alone would decrease the BMD at L4, the fusion mass has increased the BMD at L3 and L4 dramatically.
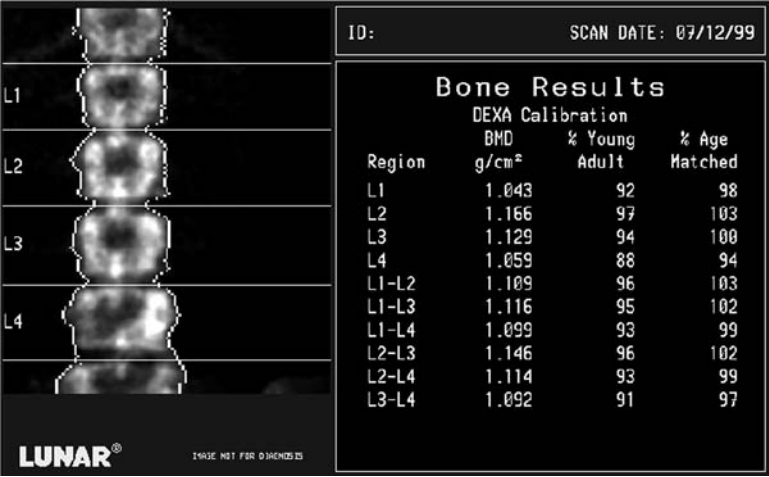
Fig. 2-20. A DXA PA spine study acquired on the Lunar DPX. The image is unusual at L4, with what appears to be an absence of part of the posterior elements. This was confirmed with plain films. This should decrease the BMD at L4.

noted previously from Cherney et al. (*27*), the removal of two intervertebral discs with chondrocalcinosis resulted in a decrease in BMD of 11.93%. Figures 2-19, 2-20, and 2-21 illustrate other structural changes in the spine that will affect the BMD measured in the PA projection.
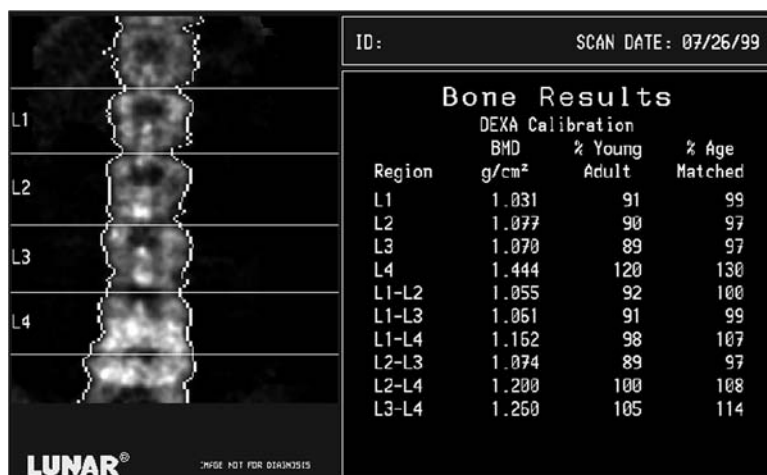
Fig. 2-21. A DXA PA spine study acquired on the Lunar DPX. The image suggests a marked sclerotic reaction at L4 and L5. There is also a marked increase in the BMD at L4 compared to L3. This sclerotic process was thought to be the result of an episode of childhood discitis. The patient was asymptomatic.

THE EFFECT OF VERTEBRAL ROTATION ON PA LUMBAR SPINE BONE DENSITY

Rotation of the vertebral bodies is often a component of idiopathic scoliosis although it is not frequently seen in adult-onset degenerative scoliosis. To study the effect of vertebral body rotation on bone density measured in the lumbar spine with DXA, Girardi and colleagues (*32*) utilized a cadaveric spine with intact soft tissue. The spine, which spanned the ninth thoracic vertebra to the sacrum, was mounted at both ends in the neutral midline position. Calibration markings on the mounts allowed for the spine to be rotated in 10° increments to a maximum of 60° in either direction. The bone density of L1 through L4 was measured with DXA in duplicate in the neutral position and at each 10° increment in both directions.

The vertebral segment area increased with increasing rotation up to 50° in either direction from midline and then decreased between 50° and 60°. The BMC remained relatively constant throughout rotation except at the extreme of 60° on either side of the midline at which point it decreased. Because BMD is determined by dividing the BMC by area, the increasing area with rotation resulted in BMD decreasing with rotation to either side of the midline. From neutral to 60°, the decrease in BMD was almost 20%. In clinical practice then, rotation of the spine for any reason should be expected to cause an apparent decrease in bone density when measured with DXA. This becomes relevant in the patient with roto-scoliosis, although the effect on BMD at the spine from the expected combination of rotation and facet sclerosis in such a patient is not straightforward.

The Spine in the Lateral Projection

The effect on BMD measured in the AP or PA projection from aortic calcification, facet sclerosis, osteophytes, and other degenerative changes in the spine can be nullified by quantifying the bone density of the spine in the lateral projection as shown in Fig. 2-15B. In addition, the highly cortical posterior elements and a portion of the

cortical shell of the vertebral body can be eliminated from the measurement, resulting in a more trabecular measure of bone density in the spine. The measurement is not a 100% trabecular measure as portions of the cortical vertebral body shell will still be included in the measurement. In addition to the elimination of artifact or confounding degenerative changes, the lateral spine BMD measurement is desirable in those circumstances in which a trabecular measure of bone density is indicated and particularly in circumstances in which changes in trabecular bone are being followed over time. The higher metabolic rate of trabecular bone compared to cortical bone should result in a much larger magnitude of change in this more trabecular measure of bone density compared to the mixed cortical-trabecular measure of bone density in the PA spine.

Vertebral identification in the lateral projection can be difficult. The lumbar vertebrae are generally identified by the relative position of the overlapping pelvis and the position of the lowest set of ribs. The position of the pelvis tends to differ, however, when the study is performed in the left lateral decubitus position compared to the supine position. Rupich et al. (*33*) found that the pelvis overlapped L4 in only 15% of individuals when studied in the supine position. Jergas et al. (*34*) reported a figure of 19.7% for L4 overlap for individuals studied in the supine position. In DXA studies performed in the left lateral decubitus position, pelvic overlap of L4 occurred in 88% of individuals in the study by Peel et al. (*13*). In the other 12%, the pelvis overlapped L5 in 5% and the L3–L4 disc space or L3 itself in 7%. As a consequence, while the position of the pelvis tends to identify L4 in most individuals scanned in the left lateral decubitus position, it also eliminates the ability to accurately measure the BMD at L4 in those individuals. The ribs are less useful than the pelvis in identifying the lumbar vertebrae. Rib overlap of L1 can be expected in the majority of individuals whether they are studied in the supine or left lateral decubitus position (*13*). This may not be seen, however, in the 12.5% of individuals whose lowest set of ribs is on T11.

While the location of the pelvis and the presence of rib overlap aid in identification of the vertebrae, they also limit the available vertebrae for analysis. When a lateral spine DXA study is performed in the left lateral decubitus position, L4 cannot be analyzed in the majority of individuals because of pelvic overlap. L1 is generally not analyzed because of rib overlap, regardless of whether the study is performed supine or in the left lateral decubitus position. Rupich et al. (*33*) also found that rib overlay L2 in 90% of individuals studied in the supine position. It was estimated that rib BMC added 10.4% to the L2 BMC. As a consequence, when lateral DXA studies are performed in the left lateral decubitus position, L3 may be the only vertebra that is not affected by either pelvic or rib overlap. In the supine position, L3 and L4 are generally unaffected. This means that depending upon the positioning required by the technique, the value from a single vertebra or from only a two vertebrae average may have to be used. This is undesirable, although sometimes unavoidable, from the standpoint of statistical accuracy and precision.

If the vertebrae are misidentified in the lateral projection, the effect on BMD can be significant. In the study by Peel et al. (*13*) misidentification of the vertebral levels would have occurred in 12% of individuals in whom the pelvis did not overlap L4 in the left lateral decubitus position. If L2 was misidentified as L3, the BMD of L3 was underestimated by an average of 5.7%. When L4 was misidentified as L3, the BMD at L3 was overestimated by an average of 3.1%. Although spine X-rays are rarely justified for the sole purpose of vertebral identification on a DXA study performed in the

PA or AP projection, this may occasionally be required for DXA lumbar spine studies performed in the lateral projection. Analysis may be restricted to only one or two verte-brae because of rib and pelvic overlap. This reduces the statistical accuracy and preci-sion of the measurement. Because of this reduction in accuracy, consideration should be given to combining lateral DXA spine studies with bone density assessments of other sites for diagnostic purposes.

THE PROXIMAL FEMUR IN DENSITOMETRY

Proximal Femur Anatomy

The gross anatomy of the proximal femur is shown in Fig. 2-22A and B. In densitom-etry, the proximal femur has been divided into specific regions of interest. The proximal femur studies shown in Fig. 2-23A and B illustrate these regions, which are based upon the anatomy shown in Fig. 2-22A and B. Ward's area is a region with which most physi-cians and technologists are not familiar. Ward's triangle, as it was originally called, is an anatomic region in the neck of the femur that is formed by the intersection of three trabecular bundles as shown in Fig. 2-24. In densitometry, Ward's triangle is a calculated region of low density in the femoral neck rather than a specific anatomic region. Because the region in densitometry is identified as a square, the region is generally now called Ward's area instead of Ward's triangle. The total femur region of interest encompasses all of the individual regions: the femoral neck, Ward's area, the trochanteric region, and the shaft. Each of these regions within this one bone contains a different percentage of trabecular and cortical bone as noted in Table 2-1.

Fig. 2-22. (A) The proximal femur as viewed from the front. The lesser trochanter is behind the shaft of the femur. **(B)** The proximal femur as viewed from behind. The lesser trochanter is clearly seen to be a posterior structure (Adapted from McMinn RMH, Hutchings, RT, Pegington J, Abrahams PH. Colour atlas of human anatomy. Third edition, 1993: 267–268. © 1993 Mosby, with permission from Elsevier.).
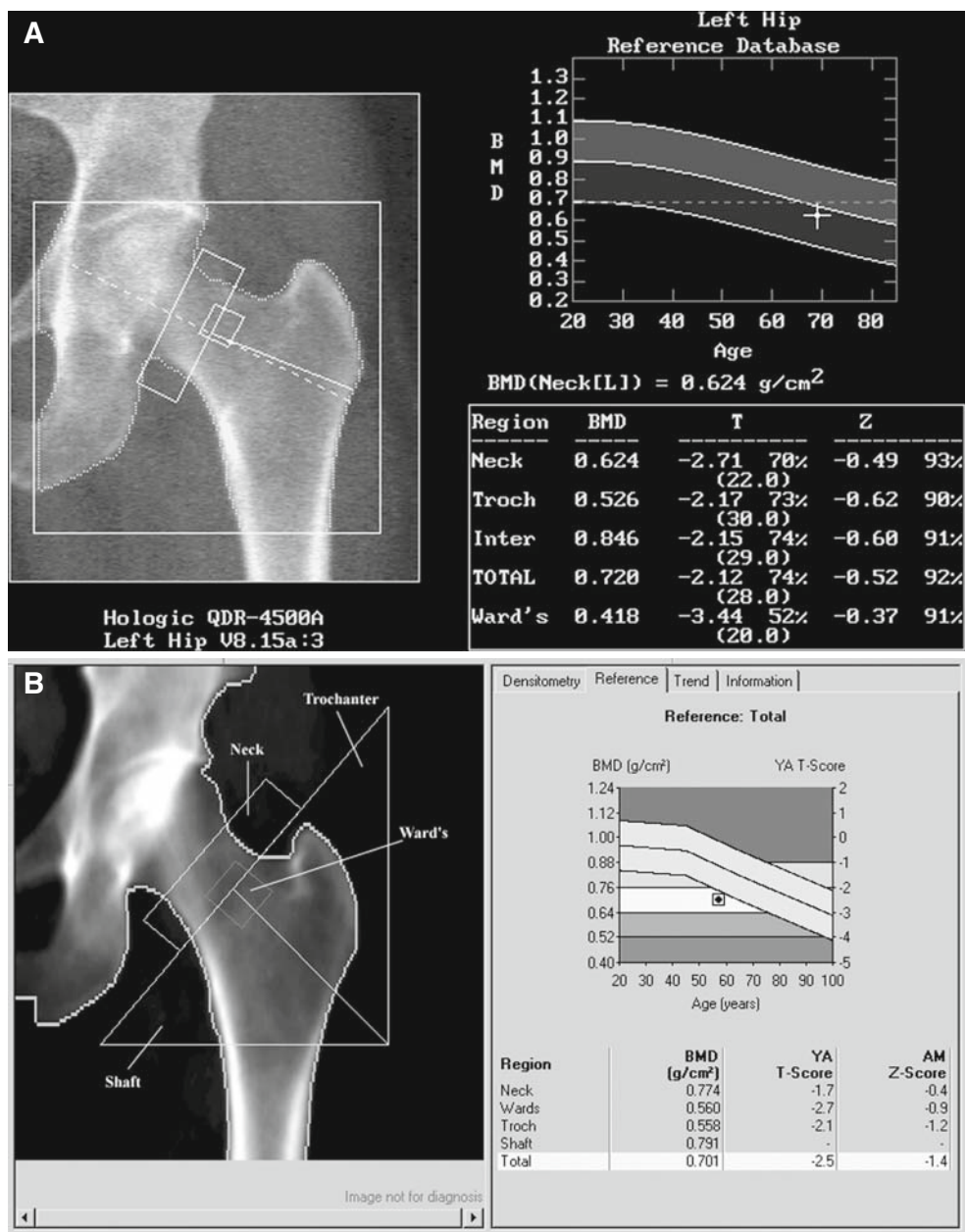
Fig. 2-23. DXA proximal femur studies. Five regions of interest are defined. **(A)** Hologic QDR 4500 DXA study. Case courtesy of Hologic, Inc., Bedford, MA. **(B)** Lunar Prodigy. Four regions of interest are labeled for emphasis on this study. The total ROI, which is not outlined, includes the neck, trochanter, and shaft.

The Effect of Rotation on BMD in the Proximal Femur

The lesser trochanter is an important anatomic structure from the perspective of recognizing the degree to which the femur has been rotated during positioning for a proximal femoral bone density study. Precision in proximal femur bone density testing is highly dependent upon reproduction of the degree of rotation of the proximal femur
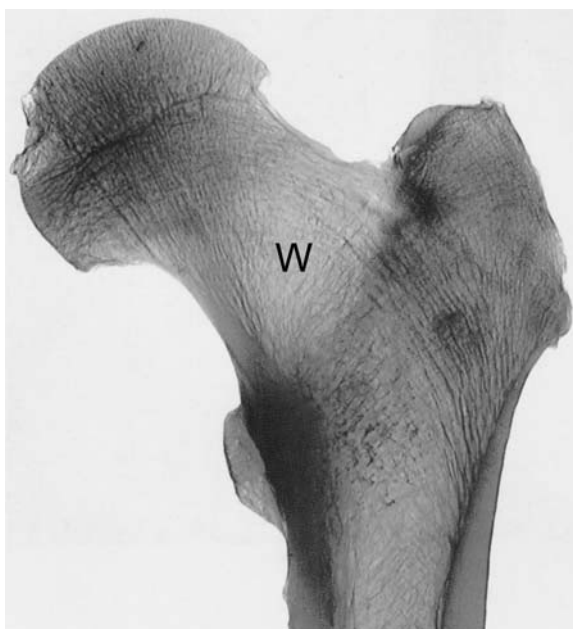
Fig. 2-24. Ward's triangle, indicated by the letter W, is formed by the intersection of bundles of trabeculae in the femoral neck (Adapted from McMinn RMH, Hutchings, RT, Pegington J, Abrahams PH. Colour atlas of human anatomy. Third edition, 1993:271. © 1993 Mosby, with permission from Elsevier.).

from study to study. In positioning the patient for a proximal femur study, internally rotating the femur 15–20° will bring the femoral neck parallel to the plane of the scan table. This rotation is accomplished with the aid of positioning devices provided by the manufacturers. In this neutral position BMD values in the femoral neck are the lowest. If the femoral neck rotation is increased or decreased from this position, the femoral neck BMD value will increase. Table 2-8 illustrates the magnitude of the increase in BMD in a cadaver study from Goh et al. (*35*). In another cadaver study from Cheng et al. (*36*), the mean increase in BMD at the femoral neck was 2.8% in the anteverted position compared to the desired neutral position with the femoral neck axis parallel to the plane of the scan table. The authors also noted that the BMD increased with increasing anteversion. The trochanteric BMD was also increased with anteversion but

Table 2-8
The Effect of Increasing Internal or External Rotation from the Neutral Position on the Femoral Neck BMD (g/cm^2) of Cadaveric Femurs

Cadaver No.	*Neutral*	*External Rotation from Neutral of*			*Internal Rotation from Neutral of*		
	0°	*15°*	*30°*	*45°*	*15°*	*30°*	*45°*
1	0.490	0.524	0.549	0.628	0.510	0.714	0.845
2	0.574	0.567	0.632	0.711	0.581	0.619	0.753
3	0.835	0.872	0.902	1.071	0.874	1.037	1.222
4	0.946	0.977	1.005	1.036	1.102	1.283	1.492

Reproduced with kind permission of Springer Science and Business Media from Goh et al. (*35*).

less than the femoral neck at 0.2%. The apparent length of the neck of the femur will decrease as rotation is increased or decreased from the neutral position. In the study from Cheng et al. (*36*) the femoral neck axis length decreased 2.4% with anteversion compared to the neutral position. When the neck of the femur is parallel to the plane of the scan table, the X-ray beam passes through the neck at a 90° angle to the neck. With changes in rotation, the neck is no longer parallel to the scan table and the beam enters the neck at angle that is greater or lesser than 90°. The result is an apparent shortening of the length of the neck and an increase in the mineral content in the path of the beam. The combination results in an apparent increase in BMD. In one of the few in vivo studies performed to look at the effects of rotation on proximal femur BMD, Lekamwasam et al. (*37*) found that BMD at the femoral neck and trochanter increased with increasing external rotation and decreased with internal rotation beyond the neutral position. Based on their established precision at the femoral neck, a significant change in BMD was seen in 12% of the subjects after internal rotation and 8% after external rotation. The only visual clue to consistent rotation is the reproduction of the size and shape of the lesser trochanter. Because the trochanter is a posterior structure, leg positioning in which the femur has not been rotated sufficiently internally tends to produce a very large and pointed lesser trochanter. Excessive internal rotation of the proximal femur will result in a total disappearance of the lesser trochanter. The size of the lesser trochanter in the DXA proximal femur image in Fig. 2-25A indicates correct internal rotation. This can be compared to the size of the lesser trochanter seen in the DXA proximal femur study in Fig. 2-25B. The lesser trochanter is very large and pointed, indicating insufficient internal rotation. Although this would be undesirable in a baseline study of the proximal femur, follow-up studies using the proximal femur in this patient should be done with this same degree of rotation. Any change in rotation from the baseline study would be expected to affect the magnitude of change in the BMD, decreasing the precision of the study.
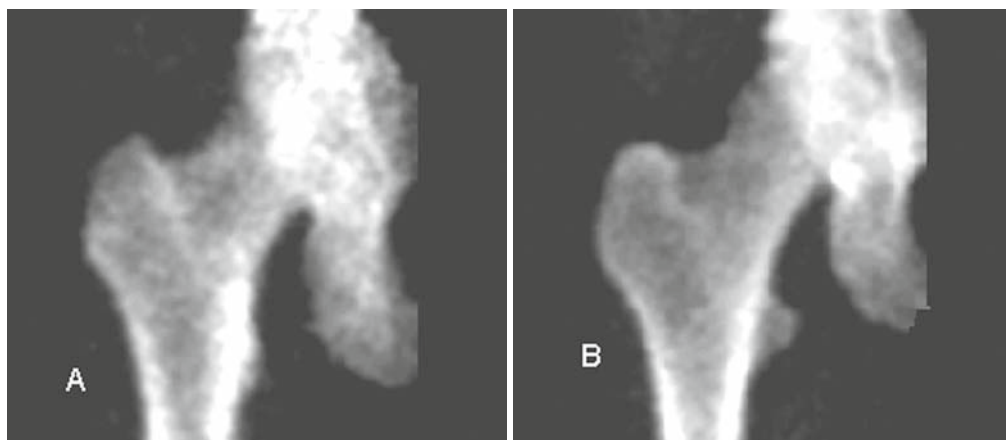
Fig. 2-25. Images of the proximal femur acquired during a DXA study. In **(A)** the lesser trochanter is clearly seen but is small and rounded, indicating proper internal rotation of the proximal femur during positioning. Compare this lesser trochanter to the lesser trochanter seen in **(B)**. This is the same patient seen in **(A)** but here the proximal femur was not rotated internally sufficiently causing the lesser trochanter to appear large and pointed.

The Effect of Leg Dominance on BMD in the Proximal Femur

In general, there does not seem to be a significant difference in the bone mineral density in the regions of the proximal femur between the right and left legs of normal individuals (*38*, *39*, *40*, *41*). Leg dominance, unlike arm dominance, does not appear to exert a significant effect on the bone densities in the proximal femur and is not used to determine which femur should be studied. When proximal femur bone density studies first became available, the default or automatic positioning mode for the proximal femur was the right side. This was subsequently changed to the left side. The reason for the change, however, only reflected the orientation of the machine and the technologist's ease of access to the left leg.

The Effect of Scoliosis, Osteoarthritis, Osteophytes, Surgery, and Fracture on BMD in the Proximal Femur

Structural changes and artifacts that interfere with DXA proximal femoral BMD measurements occur less often than at the spine. Osteoarthritic change in the hip joint may cause thickening of the medial cortex and hypertrophy of the trabeculae in the femoral neck, which may increase the BMD in the femoral neck and Ward's area (*42*). The trochanteric region is not apparently affected by such change and has been recommended as the preferred site to evaluate patients with osteoarthritis of the hip (*43*). Osteophytes in the proximal femur are apparently much less common than osteophytes in the lumbar spine (*20*). They also appear to have little effect on the bone densities measured in the proximal femur. In patients with scoliosis, however, lower bone densities have been reported on the side of the convexity (*44*). If a "worst-case" measurement is desired, the bone density in the proximal femur should be measured in the femur on the side of the convexity. Proximal femur fracture and surgically implanted prostheses will render measurements of bone density in the proximal femur inaccurate.

If osteoarthritis or some other process restricts the ability of the patient to rotate the femur properly, the study should not be done. An attempt should be made to scan the opposite proximal femur if possible. Similarly, if pain restricts the patient's range of motion such that the femur cannot be properly positioned, the study should not be done as the results will be not be valid.

Single vs. Dual Proximal Femur Bone Density Measurements

As noted earlier, studies suggest that leg dominance does not have a clinically significant effect on the mean BMD measured in the right and left proximal femurs and is thus not used to determine which femur should be measured (*38–41*). Artifact, degenerative change, or postioning difficulties may cause the densitometrist to decide to measure one side as opposed to the other. With the increasing speed of scan acquisition and the development of software, which can combine the performance of right and left proximal femur DXA scans into one study, some authorities have suggested that both proximal femurs be routinely measured for reasons of precision, diagnosis, and serendipity.

Precision is unquestionably improved when the mean of the right and left region of interest (ROI) is used instead of the BMD from either single ROI. Shepherd et al. (*45*) using the GE Lunar Prodigy and Hologic Dephi concluded that dual femur scan modes decreased the already superb precision by approximately 25% compared to single femur results. Mazess et al. (*46*) concluded that precision was improved by 30% compared to

single femur results. Similarly, White et al. (*47*) concluded that femoral neck precision was improved with the use of the mean bilateral femoral neck BMD rather than the femoral neck BMD from a single femur. The improvement in precision creates the potential to better detect changes in bone density and therefore the utility of the proximal femur ROIs for monitoring changes in BMD.

The potential benefit of studying both proximal femurs on the diagnosis of osteoporosis is not as straightforward. The World Health Organization (WHO) criteria[4] for the diagnosis of osteoporosis utilize specific cut points based on the number of standard deviations below the young adult mean bone density that the measured bone density lies. These criteria are now generally expressed in terms of the T-score. But because these are specific cut points, a change in the T-score of as little as 0.1 may result in a different diagnosis based on the WHO criteria. Because some treatment guidelines utilize T-score cut points as well, a change of as little as 0.1 in the T-score might result in the invocation of a different approach to clinical management based on the guideline. While the WHO diagnostic criteria and treatment guidelines from various organizations have proven to be extraordinarily useful, shifts in diagnostic categories or treatment approaches caused by potentially very small changes in the T-score are not a strong argument for the routine performance of bilateral proximal femur studies. Cole (*48*) has argued to the contrary. In a retrospective study of 313 postmenopausal women who underwent bilateral proximal femur studies, Cole found that the diagnosis changed from normal to osteopenia in 5.7% of the women when the lowest single T-score from either femur was used compared to the use of T-scores from only one femur, using WHO criteria and applying them to the total hip, femoral neck, or trochanter. The diagnosis changed from osteopenia to osteoporosis in 3.3%. Based on the 1998 National Osteoporosis Foundation treatment guidelines, the clinical management of the patient potentially changed in 5.4%. In a much larger study, Petley et al. (*41*) obtained BMD measurements of the PA lumbar spine and right and left femoral necks in 2372 women. The authors identified subjects with an osteoporotic femoral neck on one side and a normal or osteopenic femoral neck on the other. They then excluded those patients with an osteoporotic lumbar spine in order to determine the percent of patients in which knowledge of the second femoral neck might have changed the diagnosis from normal or osteopenic to osteoporotic. Importantly, they also excluded patients whose bone density differed between right and left femoral neck by less than the precision at the femoral neck. The authors found that there was diagnostic agreement between the two proximal femurs in 81.2% of the patients, leaving 18.8% in which there was not. When patients with an osteoporotic spine were then excluded, only 3.3% of the remaining patients had an osteoporotic femoral neck on one side and a normal or osteopenic femoral neck on the other. When the authors further excluded those patients whose right and left femoral neck BMD differed by less than the precision at the femoral neck, only 2.2% of the patients had an osteoporotic femoral neck on one side and a normal or osteopenic femoral neck on the other. The authors concluded that studies of both proximal femurs would have altered the categorization from normal or osteopenic to osteoporotic in 1.2% of the cases if only the right proximal femur had been studied and in 0.9% if only the left proximal femur had been studied. In this study

---

[4] See Chapter 9 for a discussion of the WHO criteria. They are also found in Appendix IV.
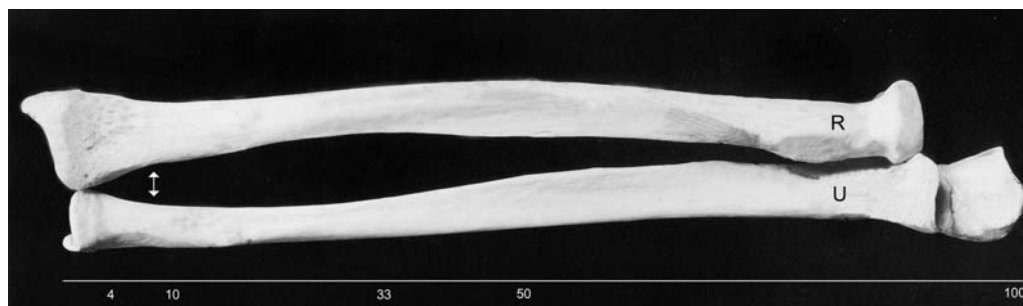
Fig. 2-26. The forearm. The *scale* at the *bottom* of the figure indicates ulnar length. The numbers reflect the percentage of ulnar length at which commonly measured sites are centered on either bone. The *arrow* between the two bones indicates the 8 mm separation point. R identifies the radius. U identifies the ulna (Adapted from McMinn RMH, Hutchings, RT, Pegington J, Abrahams PH. Colour atlas of human anatomy. Third edition, 1993:110. © 1993 Mosby, with permission from Elsevier.).

of 2372 women only three (0.1%) women had a normal femoral neck and an osteoporotic femoral neck. A higher percentage, 11.5% had a normal femoral neck and an osteopenic femoral neck. When the PA lumbar spine and proximal femur are studied, it would appear that there is little additional diagnostic yield from a bilateral femur study. However, if the PA lumbar spine is not studied or deemed not reliable, a stronger case can be made for a bilateral proximal femur study.

A final argument in favor of studying both proximal femurs is simply to ensure that a baseline study is obtained on both, in case one femur becomes unsuitable for study in the future. This is not clinically unreasonable, as the study of both proximal femurs adds little to the time of the study, radiation exposure remains very low and reimbursement is not changed from that for a single femur DXA study. There is no data at present to support this approach but that in no way diminishes the logic behind it.

THE FOREARM IN DENSITOMETRY

Nomenclature

The nomenclature used to describe the various sites in the forearm that are assessed with densitometry is confusing. Commonly measured sites are the 33% or one-third site[5], the 50%, and 10% sites, the 5 and 8 mm sites, and the ultradistal site. The sites designated by a percentage are named based on the location of the site in relationship to the overall length of the ulna. This is true for the site regardless of whether the site is on the ulna or the radius. In other words, the 50% site on the radius is located at a site on the radius which is directly across from the site on the ulna that marks 50% of the overall ulnar length, not 50% of the overall radial length. The 5 and 8 mm sites are located on either bone at the point where the separation distance between the radius and ulna is 5 or 8 mm respectively. In Fig. 2-26 the approximate location of these sites is

---

[5] Although a mathematical conversion of one-third to a percentage would result in a value of 33.3%, the site when named as a percentage is called the 33% site and is located on the radius or forearm at a location that represents 33%, not 33.3% of the length of the ulna.
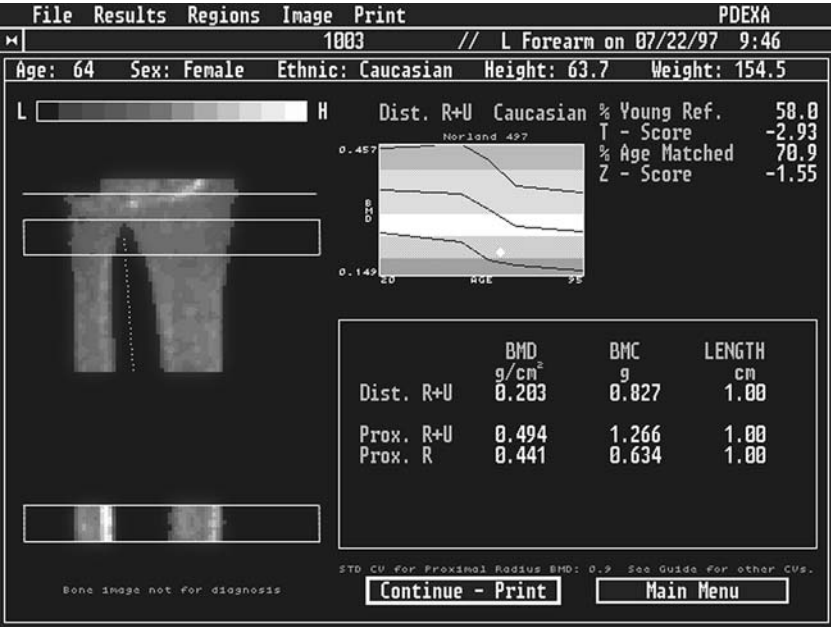
Fig. 2-27. A DXA study of the forearm acquired on the Norland pDEXA. Note the location of the regions of interest called the distal (dist.) and proximal (prox.) regions of interest. BMD values are given for the radius and ulna combined at both regions and for the radius alone at the proximal region of interest.

indicated. The 33% and 50% sites are both characterized as mid-radial sites while the 10% site is considered a distal site. The ultradistal site is variously centered at a distance of either 4% or 5% of the ulnar length. There is nothing inherent in the definition of distal, ultradistal, and proximal, however, that specifies the exact location of sites bearing these names. In Figures 2-27, 2-28, 2-29, and 2-30 the location of variously named regions of interest from several different DXA forearm devices can be compared.

The clinically important difference between these sites is the relative percentages of cortical and trabecular bone found at the site. Table 2-1 summarizes the percentages of cortical and trabecular bone at the various sites on the radius. These values are transferable to sites at the same location on the ulna.

The Effect of Arm Dominance on Forearm BMD

Unlike the proximal femur, arm dominance has a pronounced effect on the bone density in the forearm. In healthy individuals the BMC at the 33% radial site differs by 6% to 9% between the dominant and non-dominant arms (*49*). A difference of 3% has been reported at the 8 mm site (*50*). If the individual is involved in any type of repetitive unilateral arm activity, the difference between the dominant and non-dominant arm densities will be magnified to an even greater extent. Two studies of tennis players, an activity in which the dominant arm is subjected to repeated loading and impact, illustrated the effect of unilateral activity. In a study by Huddleston et al. (*51*) the BMC in the dominant forearm at the 50% radial site measured by SPA was 13% greater than in the non-dominant arm. In a more recent study from Kannus et al. (*52*) using DXA, the side-to-side difference in BMD in tennis players averaged 10.8% at the distal radius and 9.9%
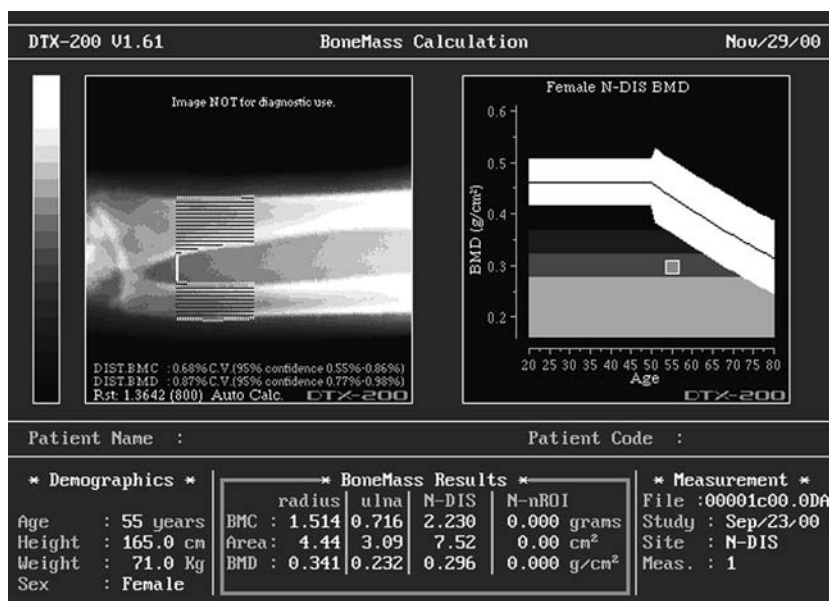
Fig. 2-28. A DXA study of the forearm acquired on the Osteometer DexaCare DTX-200. The region of interest is called the distal (DIS) region and begins at the 8 mm separation point. Values are given for each bone and for both bones combined. This distal region of interest is not the same as the distal region of interest shown in Fig. 2-27.
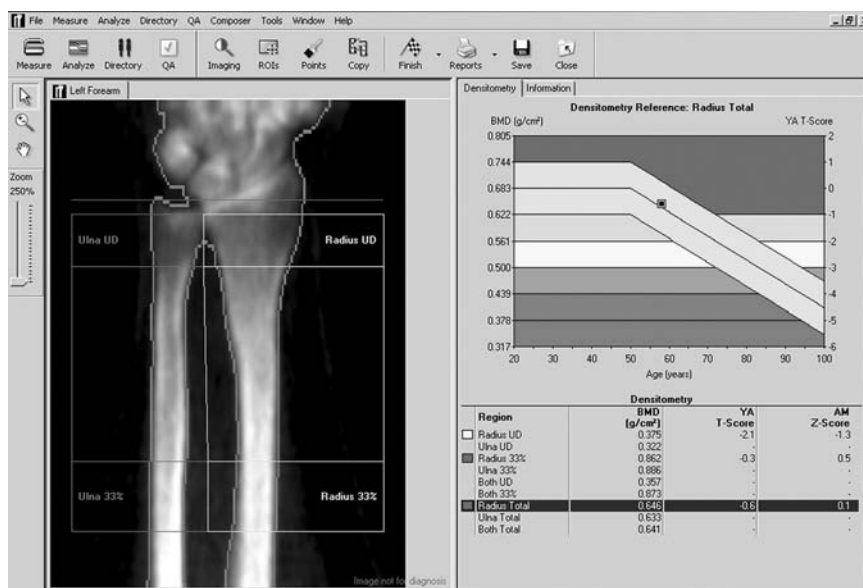
Fig. 2-29. A DXA study of the forearm acquired on the Lunar Prodigy. The two primary regions of interest are the ultradistal (UD) and 33% regions. These are similar but not identical in location to the distal and proximal regions seen in the study in Fig. 2-27.
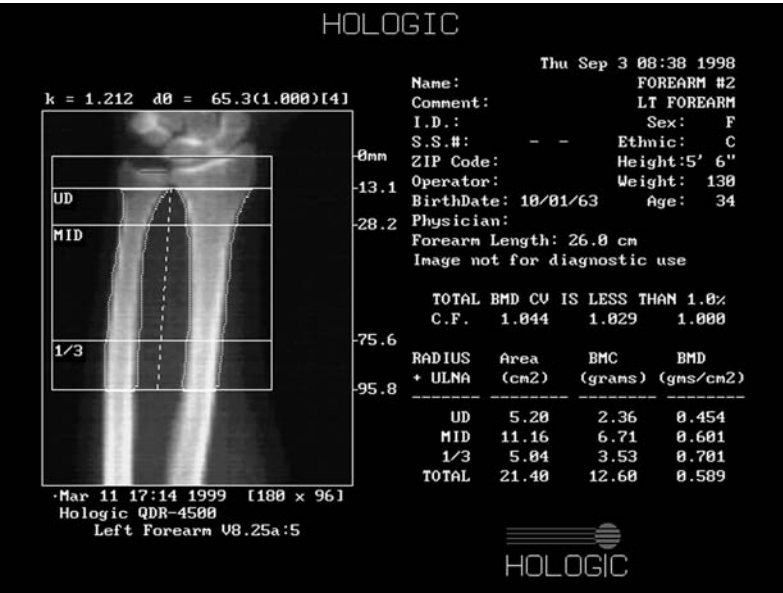
Fig. 2-30. A DXA study of the forearm acquired on the Hologic QDR-4500. Three regions of interest are shown here. An ultradistal (UD), mid, and one-third region of interest are indicated. The one-third region of interest is located similarly to the 33% region of interest shown in Fig. 2-29. Note that the mid region here is clearly not located at a point that would correspond to 50% of ulnar length. It is between the ultradistal and one-third sites.

at the mid-radius. The corresponding values in the non-tennis playing controls were only 3.4 and 2.5%, respectively. Because of these recognized differences, the non-dominant arm has traditionally been studied when the bone content or density is quantified for the purposes of diagnosis or fracture risk assessment. Most reference databases for the machines in current use have been created using the non-dominant arm. Comparisons of the dominant arm to these reference databases would not be valid. Some manufacturers supply databases for the dominant arm that can be used for comparisons if the dominant arm is to be studied. The operator's manual for the densitometry device should be consulted to determine which arm was used to create the database(s) provided by the manufacturer.

The Effect of Artifacts on BMD in the Forearm

The forearm sites are relatively free from the confounding effects of most of the types of artifacts that are often seen in the lumbar spine. The presence of a prior fracture in the forearm will affect the BMC or BMD measurements in the forearm close to the prior fracture site. A study from Akesson et al. (*53*) suggested that in women with a prior fracture of the distal radius, the BMC was increased by 20% at the distal radius of the fractured arm in comparison to the non-fractured arm, irrespective of arm dominance. It is obviously important for the technologist to ask if the patient has experienced a prior wrist or forearm fracture. Unfortunately, this same study from Akesson et al. noted that in a group of older women who were known to have previously had a distal radial fracture, many of the women did not recall the fracture or incorrectly recalled which

arm was fractured. It was noted, however, that the forearm most often fractured was the dominant forearm.

The effect of movement during a forearm scan was quantified by Berntsen et al. (*54*) using single-energy X-ray absorptiometry forearm studies performed as part of the Tromsø Study.[6] Over 7900 forearm studies were evaluated for the presence of movement artifacts, which were graded I–III depending on the severity. Movement artifacts were found in 14.2% of the studies. Berntsen et al. found that movement was more likely in older individuals with the prevalence of movement artifact increasing to 20% of the scans in the oldest age group. Movement artifact appeared to slightly decrease the measured BMD. The effect on precision was studied in a subset of 111 patients. The authors found a doubling of precision[7] when movement was present, which was independent of the severity of the movement artifact. Although this study was performed utilizing only one type of forearm densitometer, the authors noted that these results should be applicable to any forearm scan for which data acquisition requires 3–5 minutes.

THE METACARPALS, PHALANGES, AND CALCANEUS

Other skeletal sites can be studied using the techniques available today. The metacarpals, phalanges, and calcaneus were among the very first sites studied with the older techniques of radiographic photodensitometry and radiogrammetry. These sites are increasingly utilized today with the advent of computerized radiographic absorptiometry, computerized radiogrammetry, and peripheral DXA and ultrasound units. Figure 2-31 illustrates the anatomy of the hand and the location of the metacarpals and phalanges. The middle phalanges of the index, long, and ring fingers are the phalangeal regions most often quantified. Figure 2-32 illustrates the appearance of the phalanges on a computerized radiographic absorptiometry study while Fig. 2-33 illustrates the appearance of the metacarpals on a computer-assisted radiogrammetry study. The anatomy of the calcaneus[8] is illustrated in Fig. 2-34. The calcaneus contains an extremely high percentage of trabecular bone and is exquisitely sensitive to weight-bearing activities. Both the phalanges and the calcaneus have been shown to be useful sites for the prediction of hip fracture risk (*55, 56, 57*). The relative percentages of trabecular and cortical bone for the phalanges and calcaneus are found in Table 2-1.

BONE PHYSIOLOGY

Although the relevance of bone physiology to clinical densitometry may not be immediately apparent, the density of bone as measured in clinical practice is the outcome of the physiology and pathophysiology of bone. The densitometrist is generally not concerned with the development of bone or changes in bone that occur at the microscopic level. Nevertheless, the bone density at any given time and the changes in bone density

---

[6] The Tromsø Study is a population-based study, conducted in Tromsø, Norway, that focuses on lifestyle-related diseases such as osteoporosis.

[7] See Chapter 11 for a discussion of precision. Because precision is a measure of variability, an increase in precision is undesirable.

[8] The calcaneus is also known as the os calcis or heel.

Fig. 2-31. The dorsal surface of the hand. The numbering on the index finger would apply to the long, ring and small fingers as well. One, two and three are the distal, mid- and proximal phalanges. Four indicates the metacarpal. R and U indicate the radius and ulna, respectively. (Adapted from McMinn RMH, Hutchings, RT, Pegington J, Abrahams PH. Colour atlas of human anatomy. Third edition, 1993:112. © 1993 Mosby, with permission from Elsevier.

that the densitometrist observes and interprets are the direct outcomes of bone physiology and pathophysiology. A brief review of these processes is appropriate when considering skeletal anatomy in densitometry.

Bone is composed of both organic and inorganic materials. Approximately 70% of the weight of a bone is from its inorganic material (58). An additional 5–8% is from water and the rest is from its organic material. Of the inorganic material, approximately 95% is calcium phosphate crystalline hydroxyapatite and the remaining 5% are various impurities such as carbonate, chloride, or fluoride.[9] The organic material found in bone is primarily type I collagen. It also contains a variety of non-collagenous proteins and cells.

As noted previously, the bones in the skeleton belong to either the axial or appendicular skeleton. The long bones in the appendicular skeleton can be divided into four

---

[9] These impurities can replace the phosphate in the hydroxyapatite and may alter its physical properties.

Fig. 2-32. A radiographic absorptiometry analysis of the mid-phalanges of the index, long, and ringer fingers. Case provided courtesy of CompuMed, Inc., Los Angeles, CA.
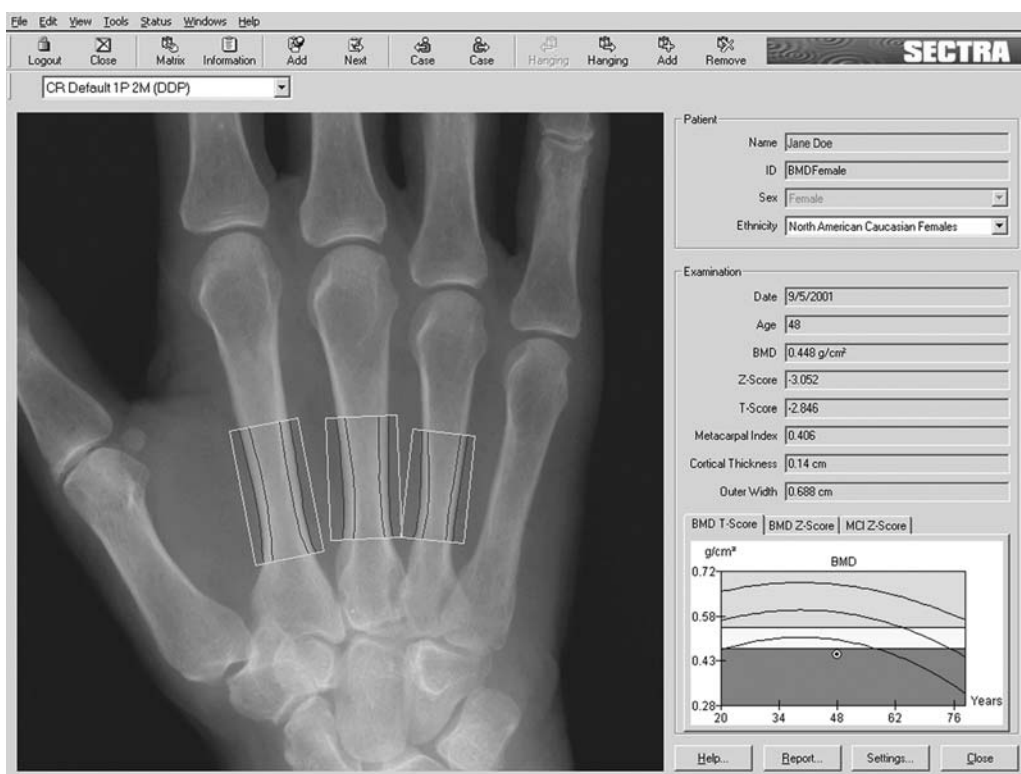
Fig. 2-33. An X-ray image from computer-assisted radiogrammetry of the metacarpals of the index, long, and ring finger. Case provided courtesy of Sectra Pronosco, Denmark.

Fig. 2-34. A lateral view of the bones of the left foot. The T indicates the talus. The C indicates the calcaneus (Adapted from McMinn RMH, Hutchings, RT, Pegington J, Abrahams PH. Colour atlas of human anatomy. Third edition, 1993:284. © 1993 Mosby, with permission from Elsevier.).

sections: the epiphysis, physis or growth cartilage, metaphysis, and diaphysis. The epiphysis is found at both ends of the long bone and develops from an ossification center that is separate from the rest of the bone. The growth cartilage separates the epiphysis from the metaphysis. After longitudinal growth has ceased in the adult, the growth cartilage disappears leaving only a remnant called the epiphyseal line to mark the boundary between the epiphysis and metaphysis. The metaphysis is a cone-shaped region that tapers to blend with the middle portion of the shaft of the long bone called the diaphysis. The cavity of a long bone is called the medullary canal and is bounded by cortex-marrow junction.

Within each bone are different surfaces such as the periosteal surface, cortical-endosteal surface, and trabecular-endosteal surface (*59*). These surfaces are also called envelopes because they create and bind specific spaces within the bone. The periosteum is the outermost bone surface. As an envelope, it encloses the hard and soft tissues within a bone. Both types of endosteal surfaces are the bone surfaces adjacent to marrow. The endosteal envelope encloses the majority of the soft tissues of the bone. The endosteal surfaces may thus be considered the innermost bone surfaces. Consequently, bone tissue itself is inside the periosteal envelope and outside the endosteal envelope. The response of bone cells to various stimuli can vary widely among the cells found in the periosteal and cortical-endosteal and trabecular-endosteal envelopes. The periosteal envelope increases throughout life, being predominantly a region in which net bone gain takes place. The cortical-endosteal envelope also expands throughout life, usually outpacing the increase in the periosteal envelope. As a consequence, the cortex of the bone tends to thin with advancing age. The trabecular-endosteal envelope is a bone surface with a high rate of metabolic activity in comparison to the other surfaces.

Bone Growth, Modeling, and Remodeling

The densitometrist works with bone at the macroscopic or gross level. From this perspective, bone appears to be a hard, inert substance. In fact, bone is extremely active at the microscopic level undergoing growth, modeling, or remodeling, depending on the stage of life. Longitudinal growth occurs in the skeleton of the child and adolescent from proliferation of cartilage at the growth plates, which subsequently undergo calcification. Modeling refers to a change in the shape or axis of a bone in response to mechanical or

physiologic stresses. Remodeling is the process in which old bone is removed and new bone is synthesized (*60*). This is a lifelong process by which the body renews the bone. Both modeling and remodeling are relevant to the work of a densitometrist although a densitometrist does not need to be expert in either. A basic understanding of the physiology and pathophysiology of the remodeling process, in particular, is adequate.

BONE MODELING

Bone modeling or the change in shape or orientation of the bone in response to physiologic or mechanical force is governed by Wolff's Law (*61*), which states:

> Every change in the form and function of bones, or of their function alone, is followed by certain definite changes in their internal architecture and equally definite secondary alteration in their external conformation, in accordance with mathematical laws.

In brief, Wolff's Law states "form follows function." The brilliance of bone modeling is meeting the needs of mechanical usage in the most efficient manner with the smallest amount of bone tissue necessary. This prevents the skeleton from being so heavy that mobility is impossible or so fragile that mobility results in fracture.

The emphasis in modeling is the change in shape or alignment of the bone. There is also a net gain of bone tissue that occurs during this process. This results in new periosteal bone with little gain in endosteal bone. Modeling, unlike remodeling, is largely absent after age 20.

BONE REMODELING

Parfitt posed the question of why bone, which survives for thousands of years after death, needs to remodel itself during life (*62*). At the microscopic level, the answer to this question would explain the events that trigger the bone remodeling process. A potential explanation lies in the basic functions of the skeleton.

The primary function of the skeleton is mechanical. According to Parfitt (*59*) the skeleton maintains the shape of the body and provides protection for the internal organs. It also provides a framework for the bone marrow and for the transmission of muscular contractions that result in movement and ambulation. A second function of the skeleton is the regulation of extracellular fluid (ECF) composition, in particular calcium homeostasis, through exchanges of the bone mineral with the extracellular fluid. Remodeling is postulated to be necessary for the skeleton to sustain both of these functions.

The mechanical competence of the skeleton is maintained by stochastic[10] and targeted remodeling. In theory, the purpose of stochastic remodeling is to *prevent* fatigue damage by removing bone before it reaches some critical age. That age may be different depending on the bone. Targeted remodeling would *repair* bone that has already undergone fatigue damage. It appears that a bone turnover rate of 2–5% per year is sufficient to maintain the skeleton's mechanical competence.

In the axial skeleton, adjacent to red marrow, the rate of bone turnover is 15–35% per year. This rate of bone turnover greatly exceeds the 2–5% per year needed to sustain mechanical competence. The comparatively excessive remodeling appears to sustain the ECF regulatory functions of the skeleton. This dichotomy in remodeling rates also

---

[10]Stochastic is an adjective that means random or subject to probabilities.

suggests that ECF regulatory functions are primarily limited to the trabecular bone of the axial skeleton, with the primary function of the trabecular bone of the appendicular skeleton being mechanical.

THE BASIC MULTICELLULAR UNIT IN BONE REMODELING

Bone remodeling is accomplished by the basic multicellular unit (BMU).[11] The BMU is a group of cells whose actions result in the resorption of bone and subsequent new bone formation to replace the resorbed bone. The end result of the activity of the bone BMU is the creation of a discrete packet of bone called the bone structural unit (BSU) (*60*). There can be many BSUs made at different times within any one bone. These are held together by a collagen-free connective tissue that histomorphometrists call a cement line.

Within the BMU are two major cell types: the osteoclast and the osteoblast. The BMU also contains blood vessels, nerves, and connective tissue. The osteoclast is a large, multinucleated cell of hematopoietic origin derived from macrophages (*63*). The osteoclast is the cell responsible for bone resorption. The lifespan of the osteoclast is not definitely known but is postulated to be only days. The cell does clearly undergo a preprogrammed death or apoptosis.

The osteoblast is the cell responsible for bone formation. It is presumed to originate from a pluripotent mesenchymal stem cell, although its origins and various stages of development are not well understood (*64*). It is believed to pass through an osteoprogenitor stage on its way to becoming a preosteoblast and, finally, a mature osteoblast. An osteoblast that has become encased in its own mineralized matrix further matures into an osteocyte. An osteoblast lying on a quiescent bone surface will develop into a flattened cell called a lining cell.

In cortical bone a tunnel is created by osteoclastic bone resorption. This resorption or erosion period lasts approximately 30 days (*60*). Preosteoblasts are drawn to the tunnel and mature into osteoblasts. Bone matrix is synthesized by the osteoblasts and after a period of time known as the mineralization lag time, it is mineralized. The formation period lasts about 90 days, during which time the erosion tunnel is refilled with new bone that has a central or Haversian canal. The new bone is laid down in layers of alternating direction called lamellar bone. The lamellar bone surrounding the Haversian canal is the newly formed BSU.

In trabecular bone, osteoclastic bone resorption occurs on the surface of the bone rather than by tunneling. Over a period of about 40 days, a resorption cavity is created. Preosteoblasts migrate into the resorption cavity and mature into osteoblasts. Matrix is synthesized and subsequently mineralized over a period of approximately 150 days. The resorption cavity is filled with this new, lamellar bone, becoming a trabecular BSU.

Under normal circumstances in the mature skeleton, bone resorption and bone formation are coupled. At any given remodeling site, bone formation predictably follows bone resorption such that resorbed bone is replaced with an equal amount of new bone. This predictable sequence of events in both cortical and trabecular bone remodeling is called

---

[11] The term basic multicellular unit (BMU) is considered synonymous with bone remodeling unit (BRU).

"ARF," an acronym for activation, resorption, and formation (60). In disease states like osteoporosis, even though the ARF sequence remains, resorption and formation may be uncoupled leading to an imbalance in resorption and formation and a net bone loss. The rate at which BMUs are activated initiating bone resorption is called the activation frequency. In some disease states, the activation frequency may increase or decrease producing changes in bone mass.

Ninety to 95% of the newly secreted bone matrix is type I collagen. Before the collagen fibrils are formed, procollagen molecules undergo cleavage of their extension peptides[12] These amino- and carboxy terminal peptides[12] from the procollagen molecule are quantifiable as measures of bone formation. During bone formation, osteoblasts secrete osteocalcin,[13] which is a protein containing 49 amino acids. Bone-specific alkaline phosphatase (BAP or BSAP) is found on the surface of osteoblasts. During bone formation, BSAP is released into the circulation. Both osteocalcin and BSAP can be quantified as measures of bone formation as well.

Once the triple helix type I collagen fibrils are formed, the mechanical strength of the collagen is enhanced by cross linking the fibrils with modified forms of the amino acid lysine. These collagen crosslinks are called pyridinium crosslinks. During bone resorption, free forms of pyridinoline and deoxypyridinoline are released and can be measured in the urine as markers of bone resorption. The C-terminal and N-terminal telopeptides associated with the cross linking sites on the collagen fibrils are also cleaved from the collagen fibrils during resorption and can be measured as markers of bone resorption as well.

The markers of bone resorption and bone formation are collectively called biochemical markers of bone remodeling or bone turnover. Assays for some of these markers are available for clinical use. In disease states characterized by high rates of bone remodeling, levels of markers of both bone formation and resorption may be increased while the converse is true in states of reduced bone remodeling. In clinical practice, it is not uncommon to measure two markers at any one time to assess the status of bone remodeling. One marker will be a formation marker such as BSAP and the second will be a marker of bone resorption, such as N-telopeptide. Measurable changes in the levels of these markers occur more quickly than changes in bone density, making them attractive as a means of assessing therapeutic efficacy of bone active interventions. Many of the anti-resorptive bone-active agents used in clinical medicine cause a reduction in the levels of biochemical markers as a result of their efficacy in reducing bone turnover. An anabolic agent like 1–34 rhPTH appears to stimulate bone formation and as a consequence, the levels of markers of bone formation are increased in response to therapy. In clinical practice, however, the precision[14] of biochemical markers is still poor compared to DXA for assessing therapeutic efficacy. Largely because of the poor precision, cost, and availability of markers, there are no general recommendations for the use of markers in clinical practice at the present time (65). However, when markers are used,

---

[12] The full name of these peptides is procollagen I carboxy-terminal or nitrogen-terminal extension peptide (PICP or PINP).

[13] Osteocalcin is also known as bone GLA protein.

[14] See Chapter 11 for a discussion of the importance of precision.

performance of markers in duplicate is generally recommended to improve the precision of the test.

High levels of bone turnover have been associated with increased risk of fracture, independent of the level of bone density (*66, 67, 68*). Both the number and the depth of the resorption cavities in trabecular bone have been proposed as a mechanism by which vertebral fractures may occur that is partially independent of bone density (*69, 70*). As a corollary, reductions in bone turnover that occur more quickly than changes in bone density in response to anti-resorptive therapies may be responsible for some of the initial rapid reduction in vertebral fracture risk seen with such therapies (*71*). Markers of bone remodeling are appearing in clinical practice as part of the assessment of patients with metabolic bone disorders and often in conjunction with the assessment of bone density. Although the densitometrist may not be directly involved with the interpretation of biochemical markers, an understanding of the origin and implications of these markers should prove increasingly useful.

REFERENCES

1. Recker RR. Embryology, anatomy, and microstructure of bone. In: Coe FL, Favus MJ, eds. Disorders of bone and mineral metabolism. New York: Raven Press, 1992;219–240.
2. American Medical Association. Current procedural technology 2007. Professional edition. Chicago, IL: AMA Press, 2006: 314.
3. Dempster DW. Bone remodeling. In: Coe FL, Favus MJ, eds. Disorders of bone and mineral metabolism. New York: Raven Press, 1992;355–380.
4. Schlenker RA, Von Seggen WW. The distribution of cortical and trabecular bone mass along the lengths of the radius and ulna and the implications for in vivo bone mass measurements. Calcif Tissue Res 1976;20:41–52.
5. Johnson LC. Morphologic analysis in pathology: the kinetics of disease and general biology of bone. In Frost HM, ed. Bone biodynamics. Boston: Little, 1964: 543–564.
6. Rockoff SD, Sweet E. Bleustein J. The relative contribution of trabecular and cortical bone to the strength of human lumbar vertebrae. Calcif Tissue Res 1969;3:163–175.
7. Nottestad SY, Baumel JJ, Kemmel DB, Recker RR, Heaney RP. The proportion of trabecular bone in human vertebrae. J Bone Miner Res 1987;2:221–229.
8. Eastell R, Mosekilde L, Hodgson SF, Riggs BL. Proportion of human vertebral body bone that is cancellous. J Bone Miner Res 1990;5:1237–1241.
9. Kuiper JW, Van Kuijk C, Grashuis JL. Distribution of trabecular and cortical bone related to geometry: a quantitative computed tomography study of the femoral neck. Invest Radiol 1997;32:83–89.
10. Werner C, Iversen BF, Therkildsen MH. Contribution of the trabecular component to mechanical strength and bone mineral content to the femoral neck. An experimental study on cadaver bones. Scan J Clin Lab Invest 1988;48:457–460.
11. Bonnick SL. Bone densitometry techniques in modern medicine. In Rosen C, ed. Osteoporosis: diagnostic and therapeutic principles. Totowa: Humana Press, 1996:89–112.
12. Louis O, Van Den Winkel P, Covens P, Schoutens A, Osteaux M. Dual-energy X-ray absorptiometry of lumbar vertebrae: relative contribution of body and posterior elements and accuracy in relation with neutron activation analysis. Bone 1992;13:317–320.
13. Peel NFA, Johnson A, Barrington NA, Smith TWD, Eastell R. Impact of anomalous vertebral segmentation of measurements of bone mineral density. J Bone Miner Res 1993;8:719–723.
14. Bornstein PE, Peterson RR. Numerical variation of the presacral vertebral column in three population groups in North America. Am J Phys Anthropo 1996;25:139–146.
15. Davis JW, Grove JS, Wasnich RD, Ross PD. Spatial relationships between prevalent and incident fractures. Bone 1999;24:261–264.
16. Nevitt MC, Ross PD, Palermo L, Musliner T, Genant HK, Thompson DE. Association of prevalent vertebral fractures, bone density, and alendronate treatment with incident vertebral fractures: effect of number and spinal location of fractures. Bone 1999;25:613–619.

17. Krolner B, Berthelsen B, Nielsen SP. Assessment of vertebral osteopenia-comparison of spinal radiography and dual-photon absorptiometry. Acta Radiol Diagn 1982;23:517–521.

18. Rand T, Seidl G, Kainberger F, et al. Impact of spinal degenerative changes on the evaluation of bone mineral density with dual energy X-ray absorptiometry (DXA). Calcif Tissue Int 1997;60:430–433.

19. Cann CE, Rutt BK, Genant HK. Effect of extraosseous calcification on vertebral mineral measurement. Calcif Tissue Int 1983;35:667.

20. Liu G, Peacock M, Eilam O, Dorulla G, Braunstein E, Johnston CC. Effect of osteoarthritis in the lumbar spine and hip on bone mineral density and diagnosis of osteoporosis in elderly men and women. Osteoporos Int 1997;7:564–569.

21. Frye MA, Melton LJ, Bryant SC, et al. Osteoporosis and calcification of the aorta. Bone Miner 1992;19:185–194.

22. Frohn J, Wilken T, Falk S, Stutte HJ, Kollath J, Hor G. Effect of aortic sclerosis on bone mineral measurements by dual-photon absorptiometry. J Nucl Med 1990;32:259–262.

23. Orwoll ES, Oviatt SK, Mann T. The impact of osteophytic and vascular calcifications on vertebral mineral density measurements in men. J Clin Endocrinol Metab 1990;70:1202–1207.

24. Reid IR, Evans MC, Ames R, Wattie DJ. The influence of osteophytes and aortic calcification on spinal mineral density in postmenopausal women. J Clin Endocrinol Metab 1991;72:1372–1374.

25. Banks LM, Lees B, MacSweeney JE, Stevenson JC. Do degenerative changes and aortic calcification influence long-term bone density measurements? Abstract. 8th International Workshop on Bone Densitometry 1991. Bad Reichenhall, Germany.

26. Drinka PJ, DeSmet AA, Bauwens SF, Rogot A. The effect of overlying calcification on lumbar bone densitometry. Calcif Tissue Int 1992;50:507–510.

27. Cherney DD, Laymon MS, McNitt A, Yuly S. A study on the influence of calcified intervertebral disk and aorta in determining bone mineral density. J Clin Densitom 2002;5:193–198.

28. Stutzman ME, Yester MV, Dubovsky EV. Technical aspects of dual-photon absorptiometry of the spine. Technique 1997;15:177–181.

29. Morgan SL, Lopez-Ben R, Nunnally N, et al. The effect of common artifacts lateral to the spine on bone mineral density in the lumbar spine. J Clin Densitom 2008;11:243–249.

30. Morgan SL, Lopez-Ben R, Nunnally N, et al. "Black hole artifacts"—a new potential pitfall for DXA accuracy? J Clin Densitom 2008;11:266–275.

31. Labio ED, Del Rosario DB, Strasser SI, McCaughan GW, Crawford BA. Effect of ascites on bone density measurement in cirrhosis. J Clin Densitom 2007;10:391–394.

32. Girardi FP, Parvataneni HK, Sandhu HS, et al. Correlation between vertebral body rotation and two-dimensional vertebral bone density measurement. Osteoporos Int 2001;12:738–740.

33. Rupich RC, Griffin MG, Pacifici R, Avioli LV, Susman N. Lateral dual-energy radiography: artifact error from rib and pelvic bone. J Bone Miner Res 1992;7:97–101.

34. Jergas M, Breitenseher M, Gluer CC, et al. Which vertebrae should be assessed using lateral dual-energy X-ray absorptiometry of the lumbar spine? Osteoporos Int 1995;5:196–204.

35. Goh JCH, Low SL, Bose K. Effect of femoral rotation on bone mineral density measurements with dual energy X-ray absorptiometry. Calcif Tissue Int 1995;57:340–343.

36. Cheng XG, Nicholson PH, Boonen S, et al. Effects of anteversion on femoral bone mineral density and geometry measured by dual energy X-ray absorptiometry: a cadaver study. Bone 1997;21:113–117.

37. Lekamwasam S, Lenora RSJ. Effect of leg rotation on hip bone mineral density measurements. J Clin Densitom 2003;6:331–336.

38. Bonnick SL, Nichols DL, Sanborn CF, Payne SG, Moen SM, Heiss CJ. Right and left proximal femur analyses: is there a need to do both? Calcif Tissue Int 1996;58:307–310.

39. Faulkner KG, Genant HK, McClung M. Bilateral comparison of femoral bone density and hip axis length from single and fan beam DXA scans. Calcif Tissue Int 1995;56:26–31.

40. Rao AK, Reddy S, Rao DS. Is there a difference between right and left femoral bone density? J Clin Densitom 2000;3:57–61.

41. Petley GW, Taylor PA, Murrills AJ, Dennison E, Pearson G, Cooper C. An investigation of the diagnostic value of bilateral femoral neck bone mineral density measurements. Osteoporos Int 2000;11:675–679.

42. Nevitt MC, Lane NE, Scott JC, et al. Radiographic osteoarthritis of the hip and bone mineral density. Arth Rheum 1995;38:907–916.

43. Preidler KW, White LS, Tashkin J, et al. Dual-energy X-ray absorptiometric densitometry in osteoarthritis of the hip. Influence of secondary bone remodeling of the femoral neck. Acta Radiol 1997;38:539–542.

44. Hans D, Biot B, Schott AM, Meunier PJ. No diffuse osteoporosis in lumbar scoliosis but lower femoral bone density on the convexity. Bone 1996;18:15–17.

45. Shepherd JA, Fan B, Lu Y, et al. Comparison of BMD precision for Prodigy and Delphi spine and femur scans. Osteoporos Int 2006;17:1303–1308.

46. Mazess RB, Nord RH, Hanson JA, Barden HS. Bilateral measurement of femoral bone mineral density. J Clin Densitom 2000;3:133–140.

47. White J, Harris SS, Dallal GE, Dawson-Hughes B. Precision of single vs. bilateral hip bone mineral density scans. J Clin Densitom 2003;6:159–162.

48. Cole RE. Improving clinical decisions for women at risk of osteoporosis: dual-femur bone mineral density testing. J Am Osteopath Assoc 2008;108:289–295.

49. Karjalainen P, Alhava EM. Bone mineral content of the forearm in a healthy population. Acta Radiol Oncol Radiat Phys Biol 1976;16:199–208.

50. Borg J, Mollgaard A, Riis BJ. Single X-ray absorptiometry: performance characteristics and comparison with single-photon absorptiometry. Osteoporos Int 1995;5:377–381.

51. Huddleston AL, Rockwell D, Kulund DN, Harrison B. Bone mass in lifetime tennis athletes. JAMA 1980;244:1107–1109.

52. Kannus P, Haapasalo H, Sievanen H, Oja P, Vuori I. The site-specific effects of long-term unilateral activity on bone mineral density and content. Bone 1994;15:279–284.

53. Akesson K, Gardsell P, Sernbo I, Johnell O, Obrant KJ. Earlier wrist fracture: a confounding factor in distal forearm bone screening. Osteoporos Int 1992;2:201–204.

54. Berntsen GKR, Tollan A, Magnus JH, Søgaard AJ, Ringberg T, Fønnebø V. The Tromsø study: artifacts in forearm densitometry-prevalence and effects. Osteoporos Int 1999;10:425–432.

55. Mussolino ME, Looker AC, Madans JH, et al. Phalangeal bone density and hip fracture risk. Arch Intern Med 1997;157:433–438.

56. Huang C, Ross PD, Yates AJ, et al. Prediction of fracture risk by radiographic absorptiometry and quantitative ultrasound: a prospective study. Calcif Tissue Int 1998;6:380–384.

57. Cummings SR, Black DM, Nevitt MC, et al. Bone density at various sites for prediction of hip fractures. Lancet 1993;341:72–75.

58. Lee CA, Einhorn TA. The bone organ system. In: Marcus R, Feldman D, Kelsey J, eds. Osteoporosis. Second edition. San Diego, CA: Academic Press, 2001: 3–20.

59. Parfitt AM. Skeletal heterogeneity and the purposes of bone remodeling. In: Marcus R, Feldman D, Kelsey J, eds. Osteoporosis. Second edition. San Diego, CA: Academic Press, 2001:433–447.

60. Eriksen EF, Axelrod DW, Melson F. Bone histomorphometry. New York: Raven Press, 1994:1–59.

61. Rasch PJ, Burke RK. Kinesiology and applied anatomy. Second edition. Philadelphia: Lee & Febiger, 1963:1–503.

62. Parfitt AM. Skeletal heterogeneity and the purposes of bone remodeling. In: Marcus R, Feldman D, Kelsey J, eds. Osteoporosis. Second edition. San Diego, CA: Academic Press, 2001:433–447.

63. Ross FP, Teitelbaum SL. Osteoclast biology. In: Marcus R, Feldman D, Kelsey J, eds. Osteoporosis. Second edition. San Diego, CA: Academic Press, 2001:73–105.

64. Lian JB, Stein GS. Osteoblast biology. In: Marcus R, Feldman D, Kelsey J, eds. Osteoporosis. Second edition. San Diego, CA: Academic Press, 2001:21–71.

65. Bonnick SL, Shulman L. Monitoring osteoporosis therapy: bone mineral density, bone turnover markers, or both? Am J Med 2006;119:S25–S31.

66. Riis BJ, Hansen MA, Jensen AM, Overgaard K, Christiansen C. Low bone mass and fast rate of bone loss at menopause: equal risk factors for future fracture. A 15-year follow-up study. Bone 1996;19:9–12.

67. Garnero P, Hausherr E, Chapuy M-C, et al. Markers of bone resorption predict hip fracture in elderly women: The EPIDOS Prospective Study. J Bone Miner Res 1996;11:1531–1538.

68. Melton LJ III, Khosla S, Atkinson EJ, O'Fallon WM, Riggs BL. Relationship of bone turnover to bone density and fractures. J Bone Miner Res 2002;12:1083–1091.

69. Parfitt AM. Letter to the editor. High bone turnover is intrinsically harmful: two paths to a similar conclusion. The Parfitt view. J Bone Miner Res 2002;17:1558–1559.

70. Riggs BL, Melton LJ, III. In reply. High bone turnover. The Riggs/Melton view. J Bone Miner Res 2002;17:1560.
71. Riggs BL, Melton LJ III. Editorial. Bone turnover matters: the raloxifene treatment paradox of dramatic decreases in vertebral fractures without commensurate increases in bone density. J Bone Miner Res 2002;17:11–14.

3

A Statistical Overview for the Non-statistician Densitometrist

CONTENTS

Many physicians in clinical practice have not had formal training in statistics. A basic knowledge of certain aspects of statistics is essential for the physician densitometrist. Quality control procedures for the various machines require some statistical analyses. The computer-generated reports of bone density data include statistical devices such as *T*- and *z*-scores and confidence intervals. To interpret serial studies, the physician must understand the concept of precision and be able to calculate the precision of repeat measurements in his or her facility. These concepts and others are discussed in this chapter.

THE MEAN, MEDIAN, MODE, VARIANCE, AND STANDARD DEVIATION

Most statistical textbooks begin with a discussion of the mean, variance, and standard deviation. This is appropriate here as well because many of the statistical devices used in densitometry begin with a calculation of the mean and standard deviation for a set of bone density measurements. The median and mode are encountered less frequently in densitometry, but are presented for the sake of completeness.

The Mean

The mean is the average value for a set of measurements. As an example, consider Mrs. B. who underwent three spine bone density studies on the same day. Between each study, she stood up and then resumed her position on the scan table. The results of her three studies are shown in Table 3-1. The average of the three spine bone density studies is simply the sum of the three studies divided by the number of studies, in this case, three. In statistical terminology, the average is called the mean. Statistical shorthand for the formula for calculating the average or mean is shown in Equation 1:

$$\bar{X} = \frac{\sum X}{n} \tag{1}$$

Table 3-1
Individual and Mean Spine BMD Values for Patient, Mrs. B

Patient	Scan 1	Scan 2	Scan 3	Mean or $\bar{X}$
Mrs. B.	1.011	1.030	1.022	1.021

Values are in g/cm^2.

The mean or $\bar{X}$ (pronounced X-bar) is equal to the sum, Σ, of all X measurements divided by the number of measurements, n. In this case, the mean of Mrs. B.'s three spine bone density measurements is 1.021 g/cm^2.

The Median

The median is much as it sounds—it's the middle value in a set of values. In other words, when there are an odd number of values in a data set, half of the values are above the median and half are below it. If there is an even number of values, then the median is generally said to be the average of the two middlemost values. The use of the median is not necessary in discussing the three values for Mrs. B., but it is often used in describing data when there are extreme or unusual values that could skew the mean in one direction or the other, which would result in a misleading characterization of the data if the mean were used. Statisticians would describe such data as not being normally[1] distributed. In data that are normally distributed, the mean and median will be the same.

The Mode

The mode is the most commonly occurring value in the data set. There is no mode in the spine bone density values obtained on Mrs. B., as presented in Table 3-1. If a fourth value was added for the sake of illustration and that fourth value was 1.011 g/cm^2, then 1.011 g/cm^2 would become the mode for this data set, because 1.011 g/cm^2 is the most commonly occurring value out of the four values for Mrs. B.

---

[1] The normal or Gaussian distribution is discussed later in this chapter.

The Variance and Standard Deviation

Although the average or mean value for the set of three measurements on Mrs. B. is 1.021 g/cm^2, it is reasonable to ask how much the individual measurements vary from the average measurement. This question can be answered by calculating the variance and standard deviation for this set of data.

The variance, abbreviated s^2, is the average of the squares of the differences between each individual measurement and the mean. The formula is as follows:

$$s^2 = \frac{\sum \left(X - \bar{X} \right)^2}{n - 1} \tag{2}$$

In Equation 2, each measurement, X, is substrated from the mean, $\bar{X}$, in order to find the difference between the measurement and the mean. Because some of the differences will be negative, the differences are squared to remove the negative sign. Each of the three squared differences is added and then the sum is divided by $n-1$, or the number of measurements minus 1, to find the average squared difference between the individual measurements and the mean. The rationale behind the use of $n-1$ instead of n to find the variance is discussed in Chapter 11.

Remember that the variance is the average of the squared differences between the individual values and the mean. The square root of the variance is called the standard deviation, written as s in statistical formulas and often abbreviated as SD in medical literature. It should be apparent now why the variance is abbreviated as s^2. Both the standard deviation and the variance are measures of variability in a set of data.

To calculate the variance for Mrs. B., the following calculations are made. First, the difference between each of the three measurements and the mean is calculated as shown in Equations 3 through 5:

$$1.011 - 1.021 = -0.010 \tag{3}$$

$$1.030 - 1.021 = 0.009 \tag{4}$$

$$1.022 - 1.021 = 0.001 \tag{5}$$

Then, each of the three differences is squared as shown in Equations 6 through 8:

$$(-0.010)^2 = 0.0001 \tag{6}$$

$$(0.009)^2 = 0.000081 \tag{7}$$

$$(0.001)^2 = 0.000001 \tag{8}$$

The three squared differences from Equations 6 though 8 are then added:

$$0.0001 + 0.000081 + 0.000001 = 0.000182 \tag{9}$$

Finally, this sum is divided by the number of measurements -1 as shown in Equation 10. This number is the variance:

$$s^2 = \frac{0.000182}{2} = 0.000091 \tag{10}$$

The square root of the variance is the standard deviation (*s* or SD). Therefore:

$$s = SD = \sqrt{0.000091} = 0.010 \tag{11}$$

The mean or average BMD based on the three spine bone density measurements on Mrs. B. is 1.021 g/cm^2. The variance and SD from this set of data on Mrs. B. are 0.000091 and 0.010 g/cm^2 (with rounding), respectively. Since the SD represents a measure of variability of the individual measurements about the mean, it is now reasonable to ask, what proportion or percentage the standard deviation is of the mean? This brings us to a discussion of the coefficient of variation.

COEFFICIENT OF VARIATION

The coefficient of variation is an important concept in bone densitometry because it is frequently used to describe the accuracy and precision of the various technologies. The coefficient of variation, abbreviated CV, is calculated by dividing the standard deviation, *SD*, by the mean, $\bar{X}$, for a set of data. The formula is as follows:

$$CV = \frac{SD}{\bar{X}} \tag{12}$$

The CV is expressed as a percentage by multiplying by 100. This is called the % coefficient of variation or %CV.

To calculate the CV for the three measurements on Mrs. B. the SD of 0.01 g/cm^2 is divided by the mean of 1.021 g/cm^2. This value is 0.010. To express this as a percentage, 0.010 is multiplied by 100 yielding 1.0%. The %CV is therefore 1.0%. The CV and %CV are measures of variability about the mean, just as are the variance and SD. The CV and %CV, however, are measures of proportional variability.

THE GAUSSIAN OR NORMAL DISTRIBUTION

The Gaussian[2] distribution is the classic, bell-shaped distribution of values that occurs when variations in data are caused by multiple, independent factors. This distribution of values is also called a "normal"[3] distribution. The Gaussian distribution or bell-shaped curve is centered on the mean. The width of the bell-shaped curve is determined by the magnitude of the SD. Approximately 68% of the values in the distribution will lie within ±1 SD of the mean and importantly 95% of the population lies within ±1.96 SD of the mean. This also implies, of course, that 5% of the population lies outside ±1.96SD of the mean. Areas under the normal distribution are described using the "z" distribution, in which the Z′ (pronounced z-prime) value indicates the number of SD from the mean. The importance of Z′ values is discussed in Chapter 11 in the calculation of the least significant change (LSC). When variations in the data from a population described by

---

[2] The Gaussian distribution is named after Johann Carl Friedrich Gauss (1777–1855), a German mathematician, astronomer, and physicist.

[3] Normal in this context simply means that the values follow the distribution described by Gauss. It should not be interpreted to mean that values that do not follow this distribution are abnormal.

the curve are largely due to a single factor, the data will not be normally distributed. In such cases, the distribution may be described as skewed or, in some cases, bimodal, but not Gaussian.

STANDARD SCORES

Standard scores allow you to compare values created from different scales to a common scale that is based on standard deviation units (1). Standard scores such as the *T*-score and *z*-score are used extensively but not exclusively in bone densitometry.

For example, imagine that a group of physicians, group A, was tested on their knowledge of bone densitometry. Arbitrarily, the highest score that could be made on the test was 75 and the lowest score that could be made was 25. A second group of physicians, group B, was also tested on their knowledge of bone densitometry. On this test, however, the highest score that could be made was 100 and the lowest score that could be made was 50. Sometime later, a physician from group A confided to a physician from group B that his score on the test was 70 and that he thought this score was generally above average for the test. The physician from group B, whose score was 75, was initially relieved to learn that he had outperformed his colleague on the test. Unfortunately, the physician from group B failed to recognize that two very different scales were used to grade the tests making it impossible to directly compare the raw scores of 70 and 75. The only way to compare how well the two physicians actually did is to convert their test scores to a third, common scale. This can be done using any one of several standard score scales. Figure 3-1 illustrates the relationships among several standard score scales, including the *T*-score, *z*-score, and Army General Classification Test (AGCT) scale. Each of these scales assigns an arbitrary value on the scale to the raw average value. For each SD change from the raw average value, the standard score increases or decreases by a pre-determined amount.
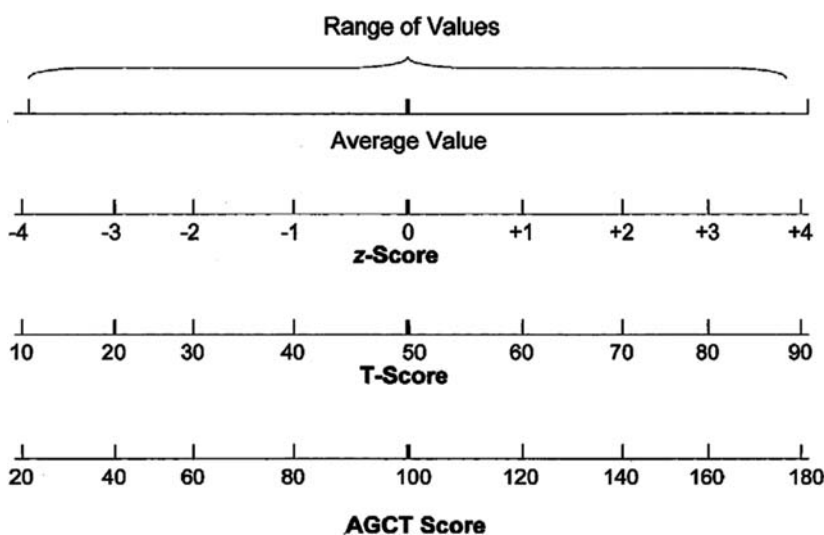
Fig. 3-1. Standard score scales. These scales are based on the standard deviation. Note that a true *T*-score has very different units from the *z*-score.

The z-Score in Statistics

In the *z*-score scale, the mean or average value for a set of raw data is arbitrarily assigned a *z*-score of 0. For each SD increase above or below the mean, the *z*-score increases by a value of 1. If the value lies above the mean, the *z*-score value is preceded by a + sign. If it lies below the mean, a − sign precedes it. If neither a + or − sign precedes the *z*-score, a + sign is assumed. In essence the *z*-score tells you how many standard deviations above or below the mean the value in question lies. For example, if the *z*-score is −3.2, the value in question lies 3.2 SD below the mean value. If the *z*-score is +1.5, the value in question lies 1.5 SD above the mean. *z*-scores are not unique to bone densitometry. Any type of numerical data can be converted to a *z*-score as long as the mean and standard deviation are known. Psychologists have used this type of scale extensively in psychological and I.Q. testing.

In order to compare the test scores of the two physicians from group A and group B, it becomes clear that it is necessary to calculate the mean and standard deviation for the test scores for group A and also for group B. When this is done, it is found that the average score for group A was a raw score of 60 with a standard deviation of 5. The average for group B was 80 with a standard deviation of 5. Since the physician from group A had a raw score of 70, his score is 10 points above the average. Because the standard deviation for this group was 5, the group A physician's raw score is 2 standard deviations above the mean. His *z*-score, therefore, is +2. Although the raw score of the physician from group B appears to be higher, since the average from group B was 80 and the standard deviation was 5, the *z*-score for the physician from group B is actually −1. The physician from group A has the better score in comparison to his peers than does the physician from group B.

The T-Score in Statistics

On the *T*-score scale the mean value is arbitrarily assigned a *T*-score value of 50. For each standard deviation change, the *T*-score increases or decreases by a value of 10 depending upon whether the value is above or below the mean. For example, if the value in question is 3 standard deviations above the mean, the corresponding *T*-score would be 80. If the value were 1.5 standard deviations below the mean, the *T*-score would be 35. For the two physicians from group A and group B discussed previously, their *T*-scores would be 70 and 40, respectively.

A *z*-score or *T*-score can be calculated for any set of numerical data for which you can calculate the mean and standard deviation. There is nothing inherent in the definition of these standard scores that limits their application to one kind of data. In bone densitometry, however, the *T*-score has undergone some modification and both the *T*-score and *z*-score have acquired specific characteristics, which are quite distinct from their use in general statistics.

Standard Scores on Bone Density Reports

T-scores and *z*-scores are found on the computer-generated bone densitometry printouts from virtually every manufacturer of bone density equipment. Figure 3-2 is the printout from a spine bone density study performed on an older Lunar DPX device. The individual BMD values for each vertebra are listed as well as the BMD values for each possible combination of contiguous vertebrae. The two columns adjacent to
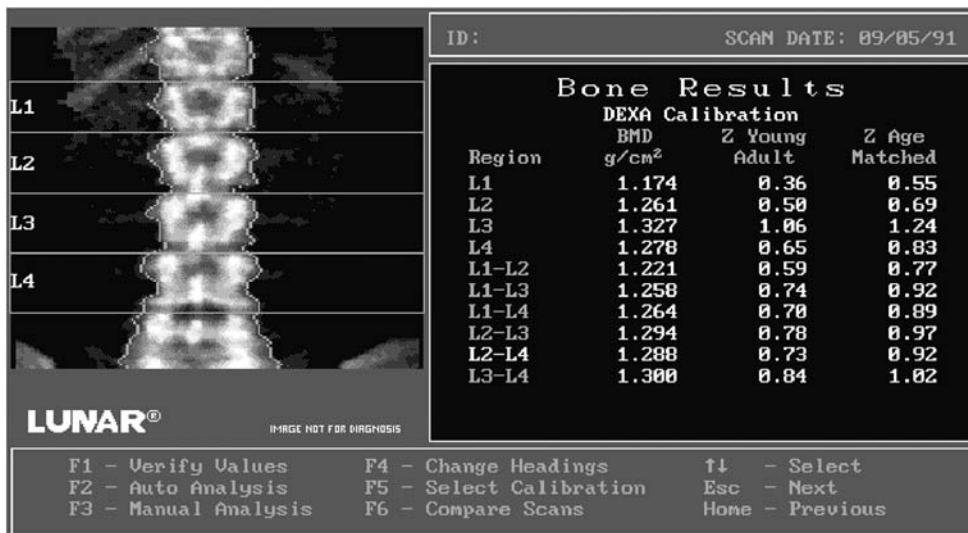
Fig. 3-2. A Lunar DPX PA spine study in which the standard scores are presented as young-adult z-scores and age-matched z-scores, reflecting the older, albeit, correct terminology for the standard score comparisons. The standard scores and BMD are listed for each vertebra and every possible combination of contiguous vertebrae.

the BMD values reflect z-scores. One column is entitled "young-adult z" and the other, "age-matched z." Based on an understanding of the z-score, it is clear that these z-scores indicate how many standard deviations above or below the mean value, the patient's BMD value lies. But what mean value and standard deviation were used to calculate these z-scores? The young-adult z-score was calculated using the average peak bone density and SD for the young adult. The column entitled age-matched z reflects the use of the average bone density that would have been predicted on the basis of the patient's age. In this case, the L2−L4 BMD average of 1.288 g/cm^2 has a young-adult z-score of 0.73 and an age-matched z-score of 0.92. This means that the L2−L4 BMD average is 0.73 standard deviations *above* the average peak bone density of the young adult and 0.92 standard deviations *above* the BMD that would have been predicted on the basis of the patient's age.

Figure 3-3 is a bone density printout from a spine study performed on a Hologic QDR-4500. The BMD values for each individual vertebra and the average BMD value for L1−L4 are evident. Adjacent to these values, two of the four columns are now entitled simply "T score" and "z score." There is nothing in the title of these columns to definitely indicate which average value is being used to calculate these standard scores. The "30.0" in parentheses next to the "T," however, indicates that the comparison is to the average bone density of a 30-year-old. Figure 3-4 is a Norland DXA PA spine study. A T-score of −0.5 and z-score of 0.72 are noted for the L2−L4 average BMD. When the formats used in these Hologic and Norland DXA studies are employed, the average value used to calculate the T-score is *always* the average peak BMD of the young adult. The average value used to calculate the z-score is *always* the average age-matched BMD. It is obvious however, that the values in the T-score column don't look like true T-scores. T-scores, after all, should be scores like 30 or 75. The use of either a + or
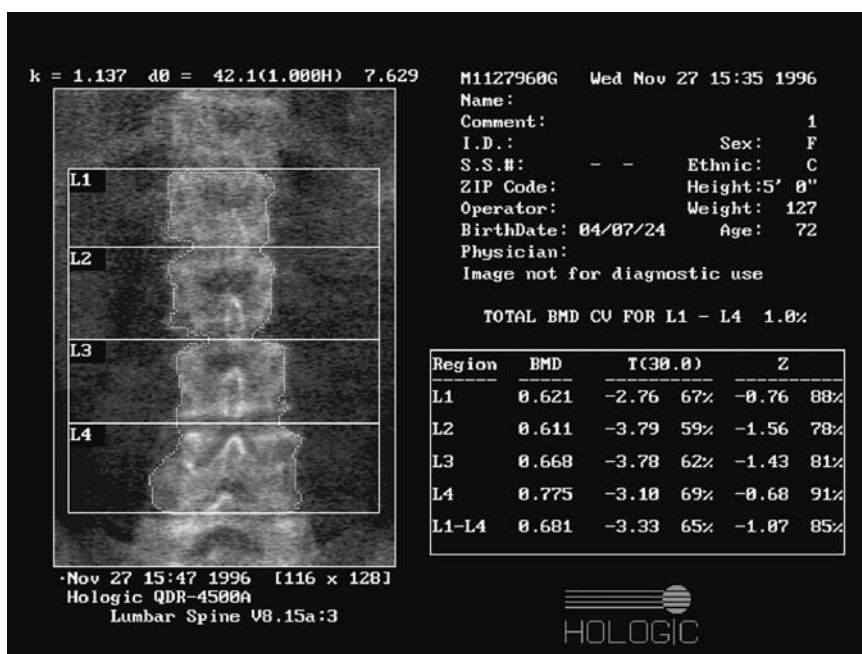
Fig. 3-3. A Hologic QDR 4500 PA spine study in which the standard scores are presented using the terminology of *T*-score and *z*-score, rather than young-adult *z*-score and age-matched *z*-score. This terminology has become the accepted format for standard score comparisons. These values, in addition to the BMD, are given for each vertebra and for the contiguous vertebrae of L1−L4. Study provided courtesy of Dr. Paul Miller, Colorado Center for Bone Research, Lakewood, CO.
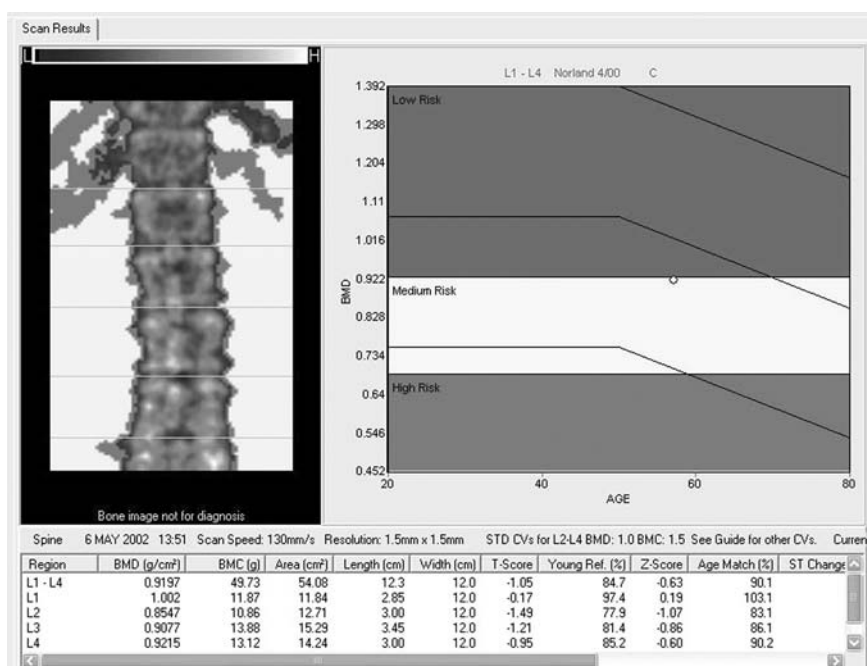
Fig. 3-4. A Norland XR DXA PA spine study. The *T*-score and *z*-score are given for the L1-L4 BMD. Study courtesy of Norland, a CooperSurgical Company, Ft. Atkinson, WI.

− sign to indicate the position relative to the mean value is not required with the traditional *T*-score. These values in the *T*-score column actually look more like *z*-scores. And in fact, that is exactly what they are. These are *z*-scores that, *in bone densitometry only*, are renamed *T*-scores. This allows one to understand without so stating that the reference average in use here is the young-adult peak BMD and that the reference average in use for the calculation of the *z*-score is the age-matched BMD. Therefore, the *T*-score of −3.33 for the L1−L4 average BMD seen on the Hologic QDR 4500 study means that the L1−L4 average BMD is 3.33 standard deviations below the average peak BMD of the young adult. This convention of renaming the young-adult *z*-score to the *T*-score has been adopted by virtually all manufacturers of bone density equipment and has also found its way into the bone density literature. In Fig. 3-5, a Lunar Prodigy PA spine study reflects the use of the *T*- and *z*-score terminology, although the abbreviations YA and AM for young-adult and age-matched still remain. It is important to remember that the young-adult *z*-score is identical to the *T*-score in this context. The age-matched *z*-score is identical to what is now simply called the *z*-score.

The International Society for Clinical Densitometry (ISCD) recommends that *T*- and *z*-scores be expressed to 1 decimal place only; that is, 2.1, not 2.13 (*2*). In addition, ISCD recommends the use of "T-score" and "Z-score" rather than the style used in the preceding discussion (*T*-score and *z*-score), which is often employed in statistical texts. This is appropriate, given the unique definitions of the T- and Z-score in densitometry. This ISCD position was reiterated in their 2007 guidelines, which can be found in their entirety in Appendix V (*3*).

There is one other important caveat in understanding what *T*- and *z*-scores mean in bone densitometry. The densitometrist must know if the *T*-score has been adjusted for race and if the *z*-score has been adjusted for race, weight, and/or ethnicity. Manufac-
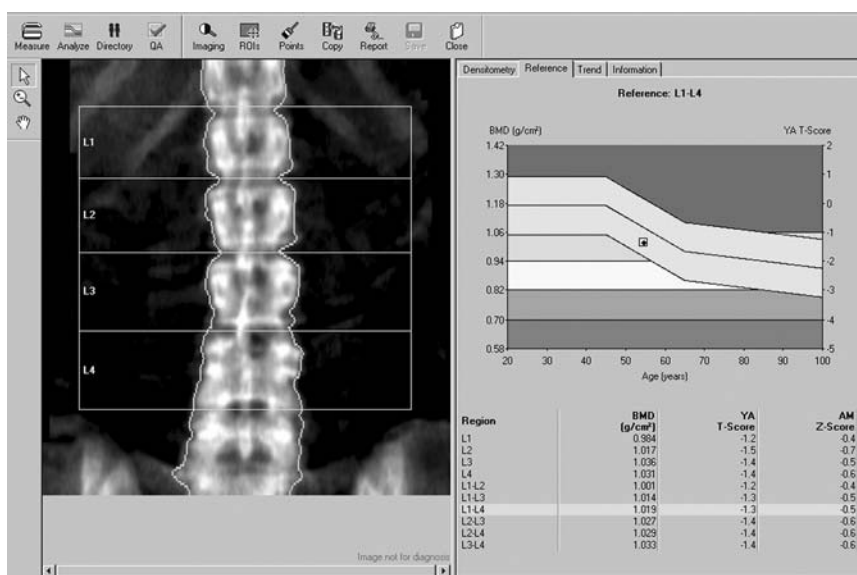
Fig. 3-5. A Lunar Prodigy DXA PA spine study. The older terminology of young-adult *z*-score and age-matched *z*-score has been replaced with YA (young-adult) *T*-score and AM (age-matched) *z*-score.

turers of densitometry devices approach this issue differently. For example, on some devices the *T*-score is *always* a comparison to a Caucasian young-adult no matter what the race or ethnicity of the patient actually is. On other devices, the *T*-score may be race-specific. A third possibility is that the user may configure how the *T*-score is determined. If the *T*-score is always a comparison to a young-adult Caucasian, then the *z*-score may be adjusted for race if the patient is not Caucasian. The *z*-score may also be adjusted for weight. On some devices, adjustments in the *z*-score for race and weight are options which can be enabled or disabled by the technologist. On other devices, no adjustment for weight in the *z*-score is possible. The operator's manual for the device should contain the relevant information. If it is not there, call the manufacturer.

MEASURES OF RISK

One of the many applications of densitometry is the assessment of risk for fragility fracture. There are several different measures of risk that are commonly used in bone densitometry: prevalence, incidence rate, incidence or absolute risk, relative risk, attributable risk, and odds ratios.

Prevalence and Incidence

Both prevalence and incidence rate can be considered as measures of a disease experience within a population. They differ principally in that prevalence is derived from observations of a population made at a single point in time while the incidence rate is derived from observations that are made only after observing a population over a period of time.

Prevalence

There are two ways of expressing prevalence: point prevalence and period prevalence. In this context it is not terribly important to distinguish between the two, but the information is presented here for the sake of completeness.

Point prevalence is the number of persons with a disease at the time of the observation divided by the total number of individuals in the population at risk for the disease. This is often expressed as a percentage. If the point prevalence is very small, it may be expressed as the number of cases per 1000 individuals in the population at risk in order to utilize whole numbers instead of fractions.

The period prevalence is the ratio of the number of individuals with a particular disease at a specific point in time *within a specified time interval* divided by the number of individuals in the population at risk for the disease *at the mid-point of that time interval.*

Both these measures of prevalence are considered rates. The point prevalence is the more commonly used measure of the two. If the term prevalence is used without a modifier, it is reasonable to assume that point prevalence is being discussed. For example, Melton et al. (*4*) reported that the prevalence of a bone density more than 2 SD below the young-adult mean in the spine in Caucasian women aged 50 and over was 31.8%. This figure is based on a one-time measurement of BMD at the spine in a group of women from Rochester, Minnesota, with extrapolation of the figures to the entire population of Caucasian women over age 50 in the United States in 1990. This is a point prevalence rate.

INCIDENCE

Like prevalence, there are two types of measures of incidence. One is a rate. The other is a risk. Incidence risk, however, is also called absolute risk. To clarify matters, incidence risk will be discussed under the heading of absolute risk in the next section.

The incidence rate, or simply incidence, is the number of new cases of any disease that have occurred within a specified period of time divided by the average number of individuals at risk for the disease multiplied by the length of the time interval. This value may be multiplied by 1000 and expressed as the incidence per 1000 person-years at risk. Other multipliers may be used as well. For example, Cooper et al. (*5*) reported that the vertebral fracture incidence rate in women in Rochester, Minnesota, was 145 per 100,000 person-years. *The number of individuals at risk for the disease in the population is not the same as the number of individuals in the population at the beginning of the time interval because, once having developed the disease, the individual is no longer considered at risk.* This is important in distinguishing the incidence rate from absolute risk.

Absolute, Relative, and Attributable Risk

ABSOLUTE RISK

As noted previously, incidence risk is also known as absolute risk. The term absolute risk will be used here. This is the number of individuals developing a disease within a specified period of time divided by the number of individuals at risk for the disease *at the beginning* of the time interval. In the context of this discussion, a certain level of bone density determines risk. The disease is fracture. For example, assume that 1000 women with the same level of bone density in the femoral neck are followed over a period of time. During the observation period, 160 of the women develop a hip fracture. The absolute risk for hip fracture in women with this level of bone density in the femoral neck is 0.16 (160 women with fractures ÷ 1000 women at risk at the beginning of the observation period). Expressed as a percentage, the absolute risk becomes 16%. These values used in the calculation of absolute risk were not taken from the literature. The numbers are for the purpose of illustration only.

RELATIVE RISK

Relative risk is the ratio of two absolute risks. In Fig. 3-6 the relationship between absolute risk and relative risk is illustrated. The values for absolute risk in Fig. 3-6 were not taken from the literature. They are used only for purposes of this exercise. For example, what is the relative risk for fracture for individuals who have a BMD that is equal to the mean or a SD score of 0 compared to the group with a BMD that is 1 SD below the mean or a SD score of −1?

This simply asks the question, what is the second group's risk (the group with the SD score of −1) compared to the first group's (the group with the SD score of 0)? Another way of putting this would be to say what is the second group's risk *relative* to the first group's risk?

As shown in Fig. 3-6, the group with the SD score of −1 has an absolute risk for fracture of 4%. The group with the SD score of 0 has an absolute risk for fracture of 2%. The relative risk is therefore 4% ÷ 2% or 2. An appropriate interpretation of this

RR AR/AR	AR	SD Score	AR	RR/SD
		+1	1%	
	2%	0	2%	2/1 = 2
16/2=8				4/2 = 2
		-1	4%	
or				8/4 = 2
		-2	8%	
2^3				16/8 = 2
	16%	-3	16%	

Fig. 3-6. The relationship between absolute risk, relative risk, and the standard deviation. Relative risk is the ratio of two absolute risks.

finding would be that there is a doubling of risk or a twofold increase in risk conferred by the decline in BMD of 1 SD.

In the medical literature data from the majority of the prospective fracture trials evaluating the ability of bone mass measurements to predict fracture risk are presented as the increase in relative risk per SD decline in bone density. For example, based on the prospective fracture trial from Melton et al. (6) the increase in relative risk for spine fracture when measured at the spine was 1.9 for each SD decline in bone density. In other words, when the absolute risk for fracture for any group was divided by the absolute risk for the group whose BMD was 1 SD higher, the ratio or relative risk was 1.9.

Using this data from Melton et. al. (6), how could the relative risk for spine fracture for an individual whose bone density is 3 SD below the mean at the spine be calculated? The relative risk for such an individual would be equal to 1.9^3 or 6.86. It would *not* be 1.9×3. Figure 3-6 illustrates this exponential relationship.

One of the limitations of relative risk is that the relative risk value alone does not convey information about the absolute risk for any particular group. After all, it would not matter if the absolute risks for two groups used to calculate the relative risk were $2\% \div 1\%$, $4\% \div 2\%$, or $50\% \div 25\%$. The relative risk would be 2 in each case. Nevertheless, relative risk is the strongest indicator of the strength of the relationship between a risk factor, such as low bone mass, and the disease outcome such as fracture. This is why early studies documenting the utility of bone density measurements in predicting fracture risk describe the findings in terms of relative risk. The use of relative risk to express an individual's risk for fracture based on a bone density measurement in clinical practice has become commonplace, because for many years it was the only reasonable means of expression. Today, however, absolute risk, which is far more relevant to the individual, should replace relative risk in clinical practice.

ATTRIBUTABLE RISK

Attributable risk does not appear frequently in bone density or osteoporosis literature but it is a useful concept to understand. Attributable risk is the difference between two absolute risks. It is the strongest indicator of the benefits of preventing the risk factor in reducing the occurrence of disease. For example, if the absolute risk for fracture was 10% in a group with a low BMD at the spine and 2% in a group with a higher BMD at the spine, the attributable risk would be $10\% - 2\%$ or 8%. In other words, 8% of the risk of fracture in the group with the lower BMD can be *attributed* to the difference in BMD between the two groups. If we could eliminate the difference in BMD between the two

groups by increasing the BMD in the group with the lower BMD, we could theoretically eliminate 8% of the fracture risk.

Odds Ratios

Odds ratios are similar to relative risk. The calculation of relative risk, however, requires knowledge of the absolute risk for the groups being compared. This requires data from a prospective study. When groups are evaluated retrospectively another measure of risk must be employed. In this circumstance, odds ratios are calculated. This is done by calculating the odds of disease for each of the two groups and then dividing to obtain the odds ratio.

For example, 1000 individuals are selected based on the individuals having a low spine bone density. The observation is made that 100 of these individuals have a spine fracture. In another group of 1000 individuals who are picked on the basis of having good spine bone densities, only five are observed to have a fracture. What are the odds of having a fracture for an individual in either group and what is the odds ratio of the low-BMD group compared to the high-BMD group?

The odds for fracture in either group are found by dividing the number of individuals with fracture in the group by the number in that group which has not experienced a fracture. Therefore, for the low-BMD group the odds are:

$$\frac{100}{1000 - 100} = \frac{100}{900} = 0.111 \tag{13}$$

The odds for the high-BMD group are:

$$\frac{5}{1000 - 5} = \frac{5}{995} = 0.005 \tag{14}$$

The odds ratio for the low-BMD group compared to the high-BMD group then is:

$$\frac{0.111}{0.005} = 22.2 \tag{15}$$

The interpretation of this odds ratio is that fracture is 22.2 times more likely in the low-BMD group compared to the high-BMD group. These values were not taken from the medical literature and are used for the purposes of illustration only.

For uncommon diseases, the relative risk and odds ratio will be very similar. For common diseases, however, the odds ratio will be greater than the relative risk.

CONFIDENCE INTERVALS

Remember Mrs. B. who had the three spine bone density tests for which the mean, standard deviation, and the coefficient of variation were previously calculated? What if three more measurements were performed on Mrs. B. the next day? After each measurement, Mrs. B. was asked to get up from the scan table and then resume her position just as she did for the first set of three measurements the day before. The values for the second set of measurements on Mrs. B. are shown in Table 3-2.

Although these values in Table 3-2 are very similar to the values seen in Table 3-1, they are not identical. The fact that the three scans do not produce identical results is not surprising. The ability of the machine to reproduce the results is not perfect. There is a

Table 3-2
Individual and Mean Spine BMD Values
for Patient, Mrs. B on Day 2

Patient	Scan 1	Scan 2	Scan 3	Mean or $\bar{X}$
Mrs. B (2nd Day)	1.024	1.015	1.018	1.019

Values are in g/cm^2.

small amount of error that is inherent in the testing regardless of how well the technician performs the test. This is true for any type of quantitative measurement used in clinical medicine today. The average value for the set of three measurements on the first and second day is different because the three measurements used to calculate each average are slightly different. The same thing would be true if three measurements were performed on Mrs. B. on third or fourth day. The average BMD value for each set of three measurements may be different because the individual measurements used to calculate the average may be slightly different. It is useful, therefore, to know what the range of *average* values would be if repeated sets of three measurements each were performed on Mrs. B. an infinite number of times. This range is called the confidence interval and is calculated by finding the standard error of the sample mean. The standard error is different from, but related to, the standard deviation. The formula for the standard error, abbreviated *SE*, is as follows:

$$SE = \frac{SD}{\sqrt{n}} \tag{16}$$

where *SD* is the standard deviation and *n* is the number of measurements. The standard deviation for the first set of three measurements on Mrs. B. was previously calculated as being 0.01 g/cm^2. The standard error, therefore, for that first set of three measurements is:

$$SE = \frac{0.01}{\sqrt{3}} = 0.006 \tag{17}$$

The value of 0.006 g/cm^2 is the standard error of the sample mean. The sample refers to the set of three measurements. The mean (or average) for this sample has already been calculated and found to be 1.021 g/cm^2. The standard error and sample mean are used to calculate the 95% confidence interval (CI) for the sample. The 95% confidence interval is bounded by the mean plus or minus two times the standard error.[4] The formula is written as follows:

$$95\% CI = \bar{X} \pm 2 \times SE \tag{18}$$

---

[4] The actual value by which the standard error is multiplied depends upon the sample size. For samples with an *n* of greater than 20, the value is very close to 2. For smaller samples, the value will be slightly larger. The formula shown here is a practical characterization of the calculation of the 95% confidence interval.

The 95% confidence interval based on the first set of three measurements on Mrs. B. is:

$$95\%CI = 1.021 \pm 2 \times 0.006 \tag{19}$$

$$95\%CI = 1.009 \; to \; 1.033 \tag{20}$$

The interpretation of the 95% confidence interval is that 95% of the means that would be obtained from an infinite number of sets of three scans each will fall within the range of 1.009–1.033 g/cm^2.

There are two characteristics of the standard error that become apparent upon reviewing the formula for its calculation. First, the standard error will always be smaller than the standard deviation. Second, the greater the number of measurements, or n, which make up the sample, the smaller the standard error will be. The smaller the standard error, the more narrow the confidence interval. The more narrow the confidence interval, the greater the likelihood that the average value from the limited sample of scans is representative of the average that would be obtained if Mrs. B. was tested an infinite number of times.

Another example of a confidence interval comes from Cummings et al. (7) who estimated a woman's lifetime risk of having a hip fracture. Using population-based data, it was calculated that the lifetime risk of hip fracture for a 50-year-old white woman was 15.6%. The 95% confidence interval for this risk was 14.8–16.4%. This very narrow confidence interval gives increasing credibility to the risk estimate of 15.6%.

Confidence intervals and statistical significance are closely related but confidence intervals tend to provide more useful clinical information. Many medical journals now require that confidence intervals be presented in addition to assessments of statistical significance for reported data. In densitometry, an understanding of confidence intervals is imperative in interpreting the significance of changes in the BMD over time. This is discussed in the following section on Precision and in greater detail in Chapter 11.

ACCURACY AND PRECISION

Quantitative measurement techniques should be both accurate and precise. In Fig. 3-7, the concepts of accuracy and precision are presented using the analogy of an archer's target. Five arrows have hit the target A. One arrow is in the bull's eye and the other four arrows are close. But of these four arrows, one arrow is off to the right, one is off to the left, one is below the bull's eye, and one is above it. The archer has, at least, hit the target and could be described as being reasonably accurate as he has placed one arrow in the bull's eye and the other four around it. But he certainly did not reproduce his shot each time. He is not, therefore, precise. Target B illustrates the abilities of an archer who is precise, but not very accurate. This archer has grouped all five arrows tightly in the upper right quadrant of the target. He has reproduced his shot each time, even though none of the shots was accurate. The skill of an archer who is both accurate and precise is illustrated in Fig. 3-7 by the five arrows grouped tightly around the bull's eye on target C.
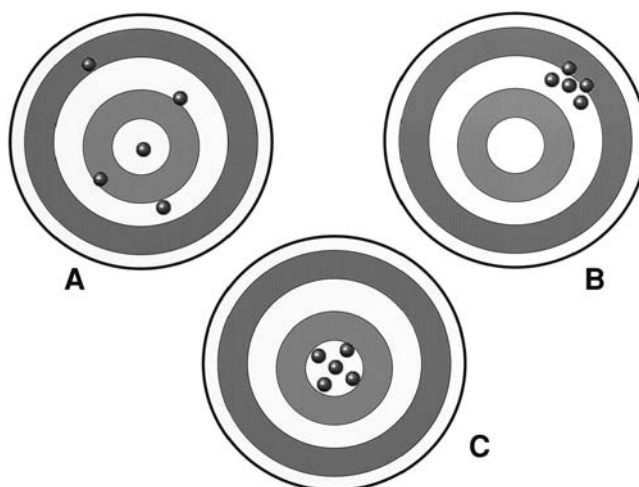
Fig. 3-7. Accuracy and precision. Target A illustrates accuracy without precision. Target B illustrates precision without accuracy. In target C, a high degree of both accuracy and precision is illustrated.

Accuracy

In bone densitometry, accuracy describes the degree to which the measurement of bone density reflects the true bone density. In other words, if the bone in question was removed from the body, measured, and then ashed and assayed, the true bone density could be determined. How close does a bone density measurement by any technique come to reproducing this *true* or *real* BMD? Accuracy can be described quantitatively by the SD or %CV, although the latter is used more often. Remember that the %CV describes the proportion by which the individual measurements vary from the mean value as a percentage. In the context of a discussion of accuracy, the mean value is synonymous with the true BMD. The SD used to calculate the CV or %CV represents the variability of the actual individual BMD measurements about this true BMD value. Therefore, if the accuracy of a DXA PA spine bone density measurement is said to have a %CV of 3–6%, this means that the measurements of BMD tend to vary about the true value by 3–6% of the true value or *real* BMD. Even though such a statement describing the accuracy of DXA may at first glance seem to be critical of the technology, remember that the % CV is describing the variability of the measurement about the true value. Therefore, the smaller the %CV the better.

In 1994, the International Organization of Standardization (ISO) recommended the use of the term "trueness" to describe what had been traditionally defined as accuracy (*8*) The term "accuracy" was then used to encompass both trueness and precision. Although the application of the ISO terminology in bone densitometry was recommended by Engelke and Glüer (*9*) in 2006, this terminology has not been adopted in North America.

Precision

The three spine bone density measurements on Mrs. B. on the same day, in fact, within a few minutes of each other, did not produce exactly the same result. This was true because there was a certain amount of error introduced by repositioning the patient

on the table in between measurements. There may also have been a small amount of error introduced during the analysis of the data by the technician. And finally, the technique itself is not perfect even when the technician exactly reproduces the positioning of the patient and the procedures used to analyze the data.

Precision is the ability to reproduce the measurement when it is performed under identical conditions when there has been no real biologic change in the patient. The International Organization of Standardization's sub-categories of precision, repeatability and reproducibility, are discussed in Chapter 11 (*8*). Like accuracy, precision is characterized by SD or %CV. The coefficient of variation for the first set of three measurements on Mrs. B. was calculated in the discussion of the CV earlier in this chapter and was found to be 0.010. Expressed as a percentage, the CV becomes 1.0%. In the context of precision, this means that the individual measurements tend to vary from the average of the measurements by 1.0% of the average BMD. Again, the smaller the %CV the better the precision of the technique.

When a bone density measurement is being performed for the purposes of diagnosing osteoporosis based on bone density criteria, the assessment of fracture risk, or to document the effects of any disease process on the bone density, accuracy is a vitally important attribute. Clearly, it is desirable for the measured bone density to be as close to the true or real bone density as possible. When the bone density measurement is one of a series of measurements being done to detect changes in the bone density over time, accuracy is far less important that precision. This is because it is the magnitude of the difference between measurements that is of interest. It becomes relatively unimportant whether the first measurement was accurate or not. In order to interpret serial changes in BMD, the densitometrist must have some quantitative idea of the precision of the testing being employed. If this is not known, there is no way to know if the changes being observed are real or simply due to the error inherent in the test. The calculation of precision for bone density measurements and the determination of significant change in BMD are discussed in detail in Chapter 11.

TYPES OF DATA

The particular type of data that is collected generally determines which type of statistical analysis is appropriate to use. Although the classification of some types of data is intuitive, some classifications are less intuitive or even arbitrary.

Quantitative Data

Quantitative data is basically numerical data. Within this broad category, numerical data may be continuous or discrete. Bone density data, for example, is continuous quantitative data, whereas the number of bone density measurements that a patient may have had is discrete quantitative data. Continuous data is numerical data that can be any fractional value on an interval scale. Height, weight, and blood pressure, as well as bone density are all types of continuous quantitative data. Any of these variables may be any one of many values on the scale on which they are measured, including fractional values. The potential values are not limited to whole numbers. In contrast, discrete quantitative data are data that can only be whole numbers, such as the number of children in a family or, as noted above, the number of bone density scans that a patient may have.

Qualitative or Categorical Data

If data are classified as belonging to categories, the data are considered qualitative data. Such data are discrete and generally consist of counts or the number of individuals belonging to each category. These type of data are also called categorical data. Categorical data can be ordinal or nominal, depending on whether there is a logical order to the categories. For example, individuals might be placed into height categories of tall, medium, or short (remember that the actual measurement of height is a continuous quantitative variable, which is different from the current example). This is clearly qualitative or categorical data. There also is a logical order to these categories, with medium in between tall and short. This is an example of ordinal data. Nominal data have no obvious order. Hair color, for example, cannot be ordered. Qualitative data count of the number of individuals with brown, blond, or black hair can be obtained, but the categories of brown, blond, or black hair have no apparent order. The word "apparent" is key here. It may be a matter of opinion in some cases as to whether there is a natural order to some types of qualitative data. For example, normal, osteopenia, and osteoporosis are categories into which individuals could be placed based on their bone density values. The number of individuals in each category is discrete, count, qualitative data. This data could also be considered ordinal since osteopenia could be viewed as being in between normal and osteoporotic, giving an obvious order to the categories. The classification of qualitative data as ordinal or nominal can be influenced by the statistician's interpretation of the meaning of the categories.

Data and Variables

In a strict sense, physicians and researchers acquire data. Statisticians analyze variables. Variables are simply data that are put into a form that makes them amenable to statistical analysis. Continuous quantitative data and ordinal categorical data are appropriate in their original form for statistical analysis and do not have to undergo any type of transformation to be analyzed statistically. The same is not always true for nominal categorical data, however. Nominal categorical data must often be transformed into dichotomous categories such as yes/no or present/absent. With only two possible outcomes, such data are also called binary data. For example, a group of women could be studied to determine which women have a spine fracture and which do not. The number of individuals in the categories of "fractured" and "not fractured" are count, categorical data. These are also nominal data because there is no obvious order to the categories of "fractured" and "not fractured." These categories represent a dichotomous situation. The categories could be re-named to simply "present" or "absent" in reference to the finding of fracture. They could also be considered as "yes" or "no" in response to the question, "Is a fracture present?" While this example seems relatively straightforward, the transformation is necessary for the statistician. When the statistician incorporates this type of binary data into a statistical analysis, it can be consolidated into only one variable. For example, for the purpose of statistical analysis, the statistician may employ the single variable representing the presence of a fracture.

CORRELATION

Correlation is a measure of the strength and direction of the association between two variables. It is generally expressed as a dimensionless number known as the correlation

coefficient. The most commonly used correlation coefficient is called Pearson's correlation coefficient. The correlation coefficient for a sample is denoted by the letter "*r*." Values for *r* can range from −1 to +1. The greater the numerical value of *r*, the stronger is the association between two variables. Therefore, the strongest associations would be indicated by an *r*-value of either +1 or −1. If the relationship between the two variables is a direct one, the sign in front of the *r*-value will be positive. If the relationship is an inverse one, the sign will be negative. For example, in a study reported by Takada et al. (*10*) an *r*-value of 0.56 was reported for bone density in the phalanges as measured by radiographic absorptiometry (RA) and bone density in the spine as measured by dual-energy X-ray absorptiometry (DXA). The correlation coefficient describes a direct relationship; that is, the BMD as measured by RA increased as the BMD measured by DXA increased. The association between the two variables was not a perfect one. Therefore, the bone density in the phalanges as measured by RA could not be perfectly predicted from the spine bone density measurement performed with DXA. Nevertheless, there was a direct association or relationship between the BMDs measured at both sites. In another study from Hansen (*11*), the strength of the association between body weight and BMD at a variety of skeletal sites was reported. The BMDs at the spine, forearm, femoral neck, and trochanter were all noted to be positively related to weight. That is, the BMD increased as weight increased. This association, therefore, will be expressed as a positive *r*-value. The *r*-values ranged from 0.20 to 0.35 between the weight and the BMDs at the various skeletal sites. Although these *r*-values were low and would tend to suggest that the strength of the association between weight and BMD was far from perfect, all of the *r*-values were statistically significant. One could conclude that the association between weight and BMD was positive or direct, but weak. Nevertheless, the *r*-values were statistically significant, implying that the association was unlikely to be due to chance. An example of an inverse correlation is the finding from Mazess et al. (*12*) of an *r*-value of −0.16 for the association between age and femoral neck BMD in a cross-sectional study of 218 women aged 20–39. This means that as age increased, the BMD in the femoral neck decreased. Although this value of *r* is again very small, it was statistically significant. Note that correlation does not prove cause and effect. It only quantifies the strength of a relationship or association.

STATISTICAL SIGNIFICANCE AND THE P VALUE

Statistical significance is virtually always discussed in the context of the likelihood of coming to an incorrect conclusion based on the acquired data. There are many ways to test for statistical significance. The choice of technique is determined by the nature of the study being performed. The various techniques for significance testing are not relevant to the discussion here. However, the results of significance testing are usually presented in the form of a "*P*" value. Traditionally, two levels of the *P* value have become synonymous with significant and very significant. Values of *P* that are ≤0.05 are considered significant. Values of *P* that are ≤0.01 are considered very significant. In the previous discussion of correlation, it was noted that Hansen (*11*) found a direct association between body weight and BMD at a variety of skeletal sites. These associations were expressed as correlation values of *r*, which ranged from 0.20 to 0.36. It was noted above that these correlations were weak but statistically significant. In fact, the correlations were very significant with a *P* value of <0.001. This value is interpreted

as meaning that there is less than 1 chance in 1000 of obtaining results such as those seen by Hansen if there is really no association at all between weight and BMD. Statistical significance, of course, does not necessarily imply medical or practical significance. That is for the clinician to decide.

REGRESSION ANALYSIS

Regression analysis is the development of a mathematical model based on real-world observations or measurements. The model is intended to describe mathematically the relationship between an independent variable or variables and a dependent variable. There are different types of regression analyses and a variety of reasons to employ them. No matter what the circumstance, an important caveat to remember about such mathematical models is: "All models are wrong. Some are useful." (*13*). The model is, after all, only a mathematical analogy for real world events.

Linear regression is common in the medical literature. The simplest mathematical model or equation in linear regression usually takes the form:

$$y = \alpha + \beta x \tag{21}$$

in which *y* is the dependent variable we would like to predict from our knowledge of *x*, the independent variable. The dependent variable *y* is a quantity that can be measured. It is important to note that there is only one *x* variable. The slope of the regression line is β and α represents the *y*-intercept, the value of *y* when *x* is zero. A third term, ε (epsilon), is usually added, representing random variability, but conceptually, it is not needed here. In multiple linear regressions, there are two or more *x* variables. As the name suggests, a plot of a linear or multiple linear regression equation results in a straight line. In nonlinear regression, there is again only one *x* variable, but a graph of *x* versus *y* results in a curve.

Two other common forms of regression analyses are logistic regression and proportional hazards regression. In logistic regression, there may be any number of *x* variables. The dependent variable, *y*, however, is a qualitative, binary variable. In other words, *y* represents a quality such as diseased or not diseased, normal or osteoporotic, and there can be only two choices. In proportional hazards regression there can again be any number of *x* variables and *y* is survival time. Other types of regression analyses are Poisson regression and ordinal regression. In these types of regression analyses, the dependent variable *y* is count data or ordinal data, respectively. The number of independent variables and the nature of the dependent variable basically determine the type of regression analysis that is appropriate for any given circumstance.

One of the more common uses of regression analysis is to determine if predictable relationships exist between variables. For example, does bone density decline predictably with age? Regression analysis can be performed using age as the independent variable *x* and bone density as the dependent variable *y* that we wish to predict. Regression analysis can also be performed to evaluate the relationship between one independent variable *x* and the dependent variable *y*, after adjusting for other independent variables. For example, we might wish to know if the risk for hip fracture increased with declining bone density after adjusting for the effects of age and sedative use. Bone density, age, and sedative use are independent *x* variables and fracture risk is the dependent *y* variable we wish to predict. Multiple regression analysis can be used in this

circumstance. Regression analyses can also be used to predict outcomes on the basis of independent variables. In other words, regression can be used to predict the risk of fracture based on knowledge of an individual's bone density, age, and sedative use.

STATISTICAL EVALUATIONS OF DIAGNOSTIC TESTS

In evaluating the clinical utility of any diagnostic test, including test instruments designed to select individuals for bone densitometry, several statistical measures are often used. The various measures are intended to indicate the probability of having or not having a particular disease based on the outcome of the test. Because bone density values are continuous data or variables, cut points must be selected that define the states of "diseased" and "non-diseased." Categories such as diseased and non-diseased are nominal data, as described earlier. Nominal data are necessary to determine probabilities. Cut points in bone densitometry are readily available by utilizing various T-scores or z-scores. The nominal data categories can then be described as at or above a certain standard score or, conversely, at or below a certain standard score. Once a cutpoint has been picked, a diagnostic test's utility in identifying diseased or non-diseased individuals can be characterized by its sensitivity, specificity, predictive value, and likelihood ratio. A receiver operating characteristic curve (ROC curve) can also be created to "test the test."

Sensitivity and Specificity

Sensitivity and specificity are easily illustrated by considering a population of 1000 women in whom the spine bone density has been measured. A cutpoint can be chosen, most simply by picking a T-score such as -2.5 to determine the exact percentages of women with spine T-scores of -2.5 or poorer and spine T-scores better than -2.5. The women with T-scores of -2.5 or poorer are considered diseased. Based on WHO criteria[5], they have osteoporosis. The women with T-scores better than -2.5 are considered non-diseased in this example. They do not have osteoporosis, although many of them may be osteopenic. By using the T-score to pick a cutpoint that defines the categories of diseased and non-diseased, quantitative continuous bone density data have been converted into two qualitative nominal data categories.

In this example, illustrated in Table 3-3, there are 500 women in the diseased group and 500 women in the non-diseased group. All of the women are asked to complete a questionnaire that elicits a history of various risk factors for low bone density, after which the questionnaire is scored. It is hoped that a score at or above a certain value will indicate a high probability of having a bone density T-score of -2.5 or poorer or of "being diseased." Those women with such a score would be considered as having a positive test.

Sensitivity is the ratio of the number of individuals with the disease who test positive to the total number of individuals with the disease. These individuals can be considered "true positives." Specificity is the ratio of the number of individuals without the disease

---

[5] See Chapter 9 for a discussion of the World Health Organization (WHO) criteria for the diagnosis of osteoporosis.

Table 3-3
The Results of a Diagnostic Test in 1000 Individuals with a
Disease Prevalence of 50%

	+ Test	− Test	Total
Diseased	400	100	500
Non-diseased	200	300	500
Total	600	400	1000

who test negative to the total number of individuals without the disease. These individuals are considered "true negatives." Both values can be expressed as a percentage by multiplying by 100. In Table 3-3, of the 500 women with the "disease," 400 tested positive. The sensitivity is calculated as follows:

$$\text{Sensitivity} = \frac{\text{Number of Diseased Individuals Who Test Positive}}{\text{Total Number of Diseased Individuals}} \quad (22)$$

$$\text{Sensitivity} = \frac{400}{500} = 0.80 \text{ or } 80\% \quad (23)$$

Specificity is calculated in a similar manner, using the 300 women without the disease who indeed tested negative and the total of 500 non-diseased women:

$$\text{Specificity} = \frac{\text{Number of Non} - \text{diseased Individuals Who Test Negative}}{\text{Total Number of Non} - \text{diseased Individuals}} \quad (24)$$

$$\text{Specificity} = \frac{300}{500} = 0.60 \text{ or } 60\% \quad (25)$$

Therefore, this particular questionnaire has a sensitivity of 80% and a specificity of 60% for identifying women with a bone density T-score of -2.5 or poorer at the lumbar spine.

Although this questionnaire correctly identified 80% of the women who were considered diseased, it failed to identify 20% of the diseased women. These women are said to have a false negative test. Mathematically, the false negatives are equal to 1-sensitivity. Similarly, although the questionnaire correctly identified 60% of the women who were not diseased, 40% of the non-diseased women had a positive test and were incorrectly labeled as diseased. These women are considered false positives. Mathematically, the false positives are equal to 1-specificity.

In the examples described above, the bone density or the disease status of the individual is known. In clinical practice, however, an individual completing such a questionnaire would not have previously had their bone density measured. The question the physician must answer is, "What is the probability that an individual with a positive test has the disease in question?" Or, the question may be, "How likely is it that an individual with a negative test does not have the disease?" The answer to these questions lies in the positive and negative predictive values for the test.

The positive predictive value (PPV or PV+) of a test is expressed as follows:

$$PPV = \frac{\text{Total number of individuals with the disease who test postive}}{\text{Total number of individuals who test positive}} \quad (26)$$

In the example in Table 3-3, 600 women tested positive but only 400 were actually diseased. Therefore:

$$PPV = \frac{400}{600} \text{ or } 0.66 \text{ or } 0.66\% \quad (27)$$

The negative predictive value (NPV or PV−) is calculated in an analogous fashion. In the same example, there were 400 women who had a negative test but only 300 women who had a negative test and were not diseased. Therefore:

$$NPV = \frac{\text{Number of individuals who are not diseased and test negative}}{\text{Total number of individuals who have a negative test}} \quad (28)$$

$$NPV = \frac{300}{100} \text{ or } 0.75 \text{ or } \% \quad (29)$$

In this example, then, if an individual has a positive test, there is a 66% chance that a diseased state or bone density *T*-score of −2.5 or less will be found. On the other hand, if the individual has a negative test, there is a 75% chance that a non-diseased state or bone density *T*-score better than −2.5 will be found.

Positive and negative predictive values of a test are highly dependent on the prevalence of the particular disease in the population (*14*). The positive and negative predictive values that were calculated from the data in Table 3-3 are appropriate for that population only, in which the prevalence of disease, defined as a *T*-score of −2.5 or poorer, is 50%. It is necessary to know the prevalence of the disease in the population being tested in order to correctly calculate the positive and negative predictive values of a test using its sensitivity and specificity. In addition, for positive and negative predictive values derived from a sample population to be useful in given patient population, the prevalence of disease must be the same in the two populations. To avoid this dependence on prevalence, likelihood ratios can be utilized to characterize the clinical utility of a test.

Likelihood Ratios

Likelihood ratios are also calculated using the sensitivity and specificity of a diagnostic test. The positive likelihood ratio (LR+) is the ratio of the probability of a positive test in diseased patients to the probability of a positive test in patients who are not diseased. Mathematically, this is expressed as follows:

$$LR+ = \frac{\text{Sensitiviity}}{1 - \text{Specificity}} \quad (30)$$

The negative likelihood ratio (LR−) is the ratio of the probability of a negative test in patients with the disease to the probability of a negative test in patients who are not

diseased. Mathematically, the LR− is expressed as follows:

$$\text{LR}- = \frac{1 - \text{Sensitivity}}{\text{Specificity}} \tag{31}$$

Likelihood ratios are less dependent on prevalence than predictive values. As an assessment of the utility of a diagnostic test, the greater the LR is from 1, the better is the ability of the test to discriminate between patients with and without the disease. The LR+ should be greater than 1. This suggests that it is more likely to find a positive test in a patient with the disease than in a patient without the disease. The LR− should be less than 1, which suggests that a negative test is less likely to be found in a patient with the disease than in a patient without the disease.

Receiver Operating Characteristic Curves

The sensitivity and specificity of a diagnostic test are dependent on the cutpoint chosen to identify the diseased population from the non-diseased population. If changing a cut point results in an increase in sensitivity, the specificity will decrease. Similarly, if the specificity is increased, the sensitivity will decrease. This relationship between sensitivity and specificity can be examined using a receiver operating characteristic (ROC) curve. Sensitivity is plotted on the y-axis and 1−specificity is plotted on the x-axis. By examining the ROC curve, the cutpoint that gives the optimum combination of sensitivity and specificity can be determined. The ROC curve also provides graphic evidence of the utility of the test. A stylized ROC curve is shown in Fig. 3-8. The points along the ROC curve should be above and not touch the dashed 45° line that has been added to the graphic. This 45° line represents equal values of sensitivity and 1−specificity or equal values for true positives and false positives. A test with such values would provide no useful information about the probability of a patient having the disease in question.

The area under the ROC curve (AUC or AUROC) measures the probability that, in randomly-paired diseased and non-diseased patients; the predicted probability of disease is greater for patients with the disease. Values for the AUC of 0.70 or less are unacceptable for a diagnostic test (*15*, *16*). A value of greater than 0.90 suggests superb
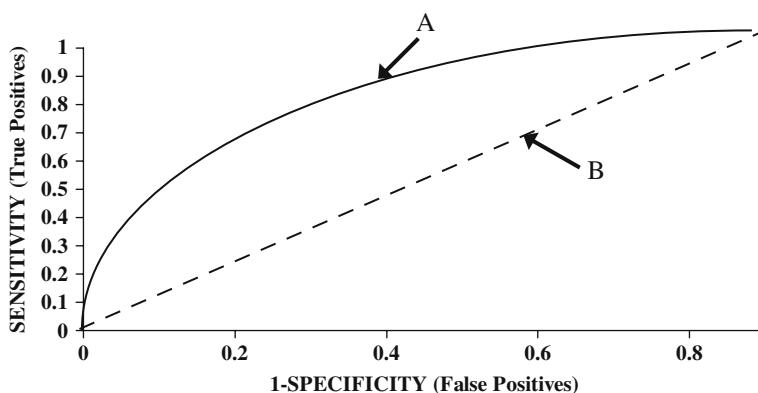
Fig. 3-8. A stylized ROC curve. Sensitivity is plotted on the *y*-axis and 1-specificity is plotted on the *x*-axis. The points on curve A should be above the dashed 45° line B for the test to have diagnostic utility as shown here.
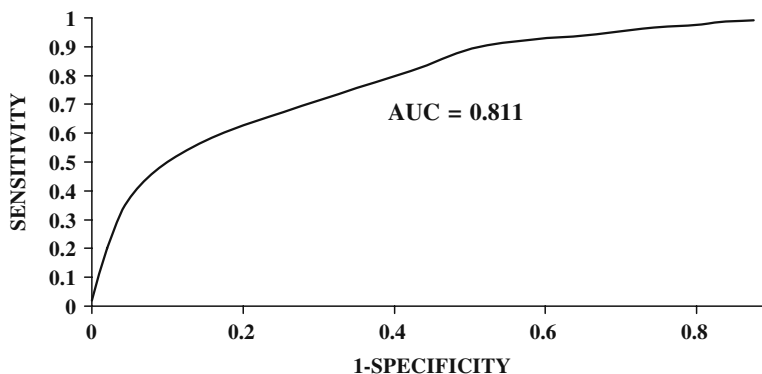
Fig. 3-9. The ROC curve from the development cohort of SCORE. The area under the curve (AUC) is 0.811. Note that all the points on the curve are above an imaginary 45° line. From Lydick et al. (*17*) with permission of the publisher. Permission conveyed by the Copyright Clearance Center.

predictive accuracy. For example, the development cohort ROC curve of the Simple Calculated Osteoporosis Risk Estimation (SCORE) questionnaire for identifying women with a bone density *T*-score of −2 or poorer is shown in Fig. 3-9. Here, the AUC is an acceptable 0.811 (*17*). SCORE is discussed in more detail in Chapter 8.

REGRESSION TO THE MEAN

Regression to the mean (RTM) is a statistical phenomenon that was first observed by Sir Francis Galton[6] in 1886. Galton was investigating the hereditary nature of height. In a study of a group of parents and their children, Galton (*18*) observed that the average or mean height of the children of the taller parents was closer to the mean height of all the children than was the mean height of their parents to the mean height of all the parents. The opposite was also true. The mean height of the parents of the taller children was closer to the mean height of all the parents than was the mean height of their children to the mean of all the children. This phenomenon was originally called regression toward mediocrity. Today it is called regression to the mean.

RTM is not a biological phenomenon. It is a statistical phenomenon that is created when certain conditions are met during data analysis. The three conditions (*19*) are as follows: (1) a variable is measured on two separate occasions; (2) the value of the variable can change because of biologic or measurement variability or both; and (3) a subgroup is defined based on a high or low value of the first measurement. In these circumstances, the average value of the second measurement for the subgroup will be closer to the mean of the first measurement for the entire group than was the average value of the first measurement of the subgroup. In other words, the mean of the subgroup at the time of the second measurement has regressed back toward the mean of the first measurement of the entire group. It should be clear that not only is this a

---

[6] Sir Francis Galton (1822–1911) was a physician as well as a statistician, geographer, meteorologist, and explorer. He is a considered a pioneer in statistical correlation and regression as well as in the science of fingerprint identification.

statistical phenomenon, it is a group phenomenon. Although RTM is an extremely important concept that affects the design of clinical trials and clinical trial data analysis, it has no relevance in the interpretation of serial bone density measurements made in individuals (*20*). This is an important distinction, because RTM has been inappropriately suggested as invalidating serial bone density measurements in individuals in clinical practice, as discussed in Chapter 11 (*21*).

REFERENCES

1. Phillips JL. Interpreting individual measures. In: Statistical Thinking. New York: W.H. Freeman and Company, 1982:62–78.
2. Writing Group for the ISCD Position Development Conference. Nomenclature and decimal places in bone density. J Clin Densitom 2004;7:45–50.
3. Baim S, Leonard MB, Bianchi ML, Hans DB, Kalkwarf HJ, Langman CB et al. Official positions of the International Society for Clinical Densitometry and executive summary of the 2007 ISCD Pediatric Position Development Conference. J Clin Densitom 2008;11:6–21.
4. Melton LJ, Chrischilles EA, Cooper C, Lane AW, Riggs BL. How many women have osteoporosis? J Bone Miner Res 1992;7:1005–1010.
5. Cooper C, Atkinson EJ, O'Fallon WM, Melton LJ. Incidence of clinically diagnosed vertebral fractures: a population-based study in Rochester, Minnesota, 1985–1989. J Bone Miner Res 1992;7:221–227.
6. Melton LJ, Atkinson EJ, O'Fallon WM, Wahner HW, Riggs BL. Long-term fracture prediction by bone mineral assessed at difference skeletal sites. J Bone Miner Res 1993;8:1227–1233.
7. Cummings SR, Black DM, Rubin SM. Lifetime risks of hip, Colles', or vertebral fracture, and coronary heart disease among white postmenopausal women. Arch Intern Med 1989;149:2445–2448.
8. International Organization of Standardization. Accuracy (trueness and precision) of measurement methods and results – Part 1: General principles and definition. 1st ISO 5725-1, Switzerland, ISO. International Standard. International Organization of Standardization, 1994: 1–17.
9. Glüer CC, Blake G, Lu Y, Blunt BA, Jergas M, Genant HK. Accurate assessment of precision errors: how to measure the reproducibility of bone densitometry techniques. Osteoporos Int 1995;5(4):262–270.
10. Takada M, Engelke K, Hagiwara S, Grampp S, Jergas M, Glüer CC, Genant HK. Assessment of osteoporosis: comparison of radiographic absorptiometry of the phalanges and dual X-ray absorptiometry of the radius and lumbar spine. Radiology 1997;202:759–763.
11. Hansen MA. Assessment of age and risk factors on bone density and bone turnover in healthy premenopausal women. Osteoporos Int 1994;4:123–128.
12. Mazess RB, Barden HS. Bone density in premenopausal women: effects of age, dietary intake, physical activity, smoking, and birth-control pills. Am J Clin Nutr 1991;53:132–142.
13. Campbell MJ. Statistics at Square Two. London: BMJ Books, 2001:3.
14. Hirsch RP, Riegelman RK. Statistical operations. Analysis of health research data. Cambridge: Blackwell Science, Inc., 1996:9–39.
15. Hanley JA, NcNeil BJ. The meaning and use of the area under a receiver operating characteristic (ROC) curve. Radiology 1982;143:29–36.
16. Swets JA. Measuring the accuracy of diagnosis systems. Science 1988;240:1285–1293.
17. Lydick E, Cook D, Turpin J, Melton M, Stine R, Byrnes C. Development and validation of a simple questionnaire to facilitate identification of women likely to have low bone density. Am J Man Care 1998;4:37–48.
18. Galton F. Regression towards mediocrity in hereditary stature. J Anthropol Inst 1886;15:246–263.
19. Bourke CJ, Daly LE, McGilvray J. Interpretation and uses of medical statistics. Oxford: Blackwell Scientific Publications;1985:147–148.
20. Bonnick SL. Monitoring osteoporosis therapy with bone densitometry: a vital tool or regression toward mediocrity? J Clin Endocrinol Metab 2000;85:3493–3495.
21. Cummings SR, Palermo L, Browner W, et al. Monitoring osteoporosis therapy with bone densitometry. Misleading changes and regression to the mean. JAMA 2000;283:1318–1321.

4   Quality Control

CONTENTS

Although much has been written about quality control procedures in densitometry, many of these articles have been concerned with data collection in clinical research rather than patient data collected as part of medical care. Quality control, while absolutely necessary in clinical research, is no less necessary in clinical practice. The original indications for bone mass measurements from the National Osteoporosis Foundation published in 1989 and the guidelines for the clinical applications of bone densitometry from the International Society for Clinical Densitometry published in 1996 called for strict quality control procedures at clinical sites performing densitometry (*1,2*). The Canadian Panel[1] of the International Society for Clinical Densitometry published specific guidelines for quality control procedures in 2002 (*3*). Such procedures are crucial to the generation of accurate and precise bone density data. When quality control is poor or absent, the bone density data may be incorrect. The interpretation made by the physician based on that incorrect information would be in error. The medical management of the patient may be adversely affected. The patient will also have been exposed to a small amount of radiation inappropriately and wasted time and money. In clinical trials, the results from hundreds or thousands of individuals are usually averaged and conclusions based on the average values. Small errors in machine performance are made insignificant by the averaging of so many results. In clinical practice, this luxury does not exist. Decisions are made based on one measurement from one patient, which means that *strict quality control in clinical practice is even more important than in clinical trials.* In spite of inherently superb accuracy and precision in today's densitometers,

---

[1] The Canadian Panel of the International Society for Clinical Densitometry represents the International Society for Clinical Densitometry in Canada and oversees the society's programs in Canada.

alterations in the functioning of the machines can and will occur. Quality control procedures to detect these alterations in machine function should be utilized by every clinical site performing densitometry regardless of the frequency with which measurements are performed.

Quality control procedures used in densitometry were derived from procedures originally developed for quality control in analytical chemistry and industry (*4*). The adaptation of these procedures for use in bone densitometry is generally credited to Drs. Orwoll and Oviatt (*5*). The most commonly used methods are control tables, visual inspection of a Shewhart chart, Shewhart rules, and the cumulative sum chart (CUSUM). All of these methods require that a phantom be scanned to establish a baseline value and then regularly to establish longitudinal values.

PHANTOMS

Manufacturers of X-ray-based bone densitometers routinely provide phantoms for use with their machines. Some phantoms, like the anthropomorphic Hologic spine phantom, are used with densitometers from other manufacturers. Other phantoms, such as the European Spine Phantom (ESP) or the Bona Fide phantom were developed independently of any one manufacturer and intended for use on multiple machines. The manufacturer-supplied phantom is often designed with the specific attributes of the manufacturer's machine in mind, making it the preferred phantom to use with that machine. The perfect phantom that could be used on all machines to test all things does not as yet exist.

Some, but not all, manufacturers provide two phantoms to be used for different purposes. One phantom may be used for daily quality assurance functions during which the mechanical operation and calibration of the machine are tested. The second phantom may be designed to mimic a region of the skeleton and used for quality control to detect a shift or drift in BMD values.

Phantoms that attempt to replicate a particular region of the skeleton are called anthropomorphic phantoms. These phantoms are made of hydroxyapatite or aluminum. Although hydroxyapatite is preferred by the Food and Drug Administration for such a phantom, aluminum is appropriate as well since aluminum behaves very much like bone when X-rayed. The phantom may be encased in an epoxy-resin or plastic block or placed within some other type of material to simulate human soft tissue. Water or uncooked rice can be used for this purpose. The perfect anthropomorphic phantom would replicate the size and shape of the bone or bones in question, have varying densities within a single bone or region, contain a range of densities likely to be encountered clinically, and be surrounded by a material that adequately mimics human soft tissue. Replicating the size and shape of the particular bone or bones and having a non-uniform density throughout the bone tests the edge-detection methodology of the particular system. In other words, it tests the machine's ability to distinguish bone from soft tissue. If the phantom bears no resemblance in size or shape to the particular bone or has very sharp, smooth edges, or if the density of the material is uniform within the bone, the edge-detection program of the machine will not be adequately tested. If the material surrounding the phantom does not adequately replicate human soft tissue, once again the ability of the machine to tell bone from soft tissue will not be maximally tested. In order to test a system's abilities at various levels of bone density, it is desirable to have a range of densities

contained within the phantom. At the same time, this range should reflect values that are likely to be encountered in clinical practice for the test to truly be useful. Most of the manufacturer-supplied phantoms in use today have some of these attributes but not all. Which attributes are emphasized by a manufacturer generally depends on those attributes that the manufacturer wishes to test as a part of the routine quality control program for their machine.

The European Spine Phantom

The development of the European Spine Phantom (ESP) was one attempt to develop a more perfect spine phantom that could be used on all central devices. It was developed independently of any manufacturer under the direction of the Committee d'Actions Concertés-Biomedical Engineering (COMAC-BME) (6).The ESP is a semi-anthropomorphic phantom. Its three vertebrae are made of hydroxyapatite and vary in density, with standardized BMDs of 500, 1000, and 1500 mg/cm^2 (7). The vertebrae are encased in a plastic and epoxy-resin material equivalent to about 10% fat that is molded into an oval shape with flattened sides measuring 28 cm by 18 cm. The phantom is shown in Fig. 4-1. The use of the ESP has generally been restricted to clinical research trials, primarily because of its expense. It was originally hoped that the ESP could be used to standardize BMD on any central bone densitometer. Unfortunately, this has not proven to be the case. It is an excellent phantom for cross-calibration of central DXA densitometers, however.
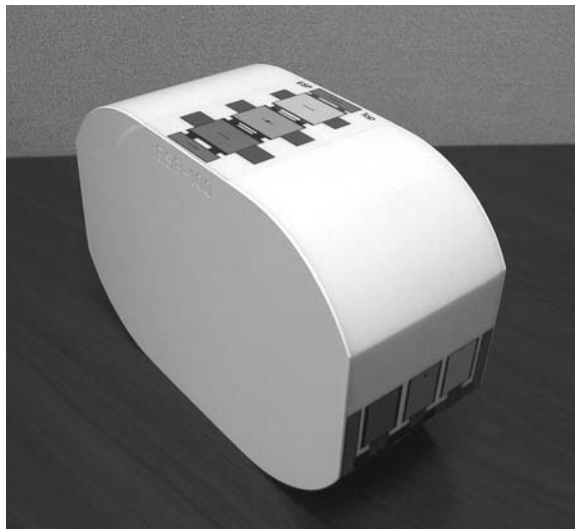
Fig. 4-1. The European Spine Phantom (ESP). Photo courtesy of Bio-Imaging Technologies Inc., Newtown, PA.

The Bona Fide Spine Phantom

The Bona Fide phantom is a calcium hydroxyapatite step wedge encased within an acrylic block. The acrylic provides a soft tissue equivalent of 26% fat while the phantom spans a range of densities from 0.7 to 1.5 g/cm^2 (8). The block may remain in its cloth carrying case during scanning, increasing ease of use. Like the ESP phantom,

Fig. 4-2. The Bona Fide Spine phantom. Photo courtesy of Bio-Imaging Technologies Inc., Newtown, PA.

the Bona Fide phantom is not manufacturer specific and is an excellent phantom for cross-calibration of central DXA devices. This phantom is shown in Fig. 4-2.

The Hologic Spine and Hip Phantoms

The Hologic anthropomorphic spine phantom, while intended for use with Hologic DXA devices, is often used with DXA devices from other manufacturers. The phantom itself consists of four anatomically correct vertebrae made of calcium hydroxyapatite. The vertebrae are encased in epoxy-resin to simulate soft tissue. The four vertebrae have similar densities and areas and the soft tissue simulation of the epoxy-resin approaches 60% fat. Each Hologic spine phantom will have a factory-specified L1–L4 BMD. Consistent daily calibration can be obtained with the Hologic anthropomorphic spine phantom, although the lack of a range of BMD values make it less suitable for cross-calibration of central DXA devices. The Hologic spine phantom is shown in Fig. 4-3. The Hologic anthropomorphic hip phantom has found less of a role in clinical medicine. It does not offer any quality control testing capabilities to the clinician that cannot be obtained with the anthropomorphic spine phantom other than proximal femur edge detection, which is under the control of the machine software, rather than the hardware (8).

The Lunar Spine Phantom

The Lunar spine phantom, shown in Fig. 4-4, is a rectangular aluminum bar which is intended to replicate the lower half of T12, all of L1–L4 and the upper half of L5. Each vertebra has a different density that is achieved by varying the thickness of the aluminum. The area of each vertebra is different as well. The densities of L1–L4 are 0.92, 1.076, 1.239, and 1.403 g/cm^2, respectively. The L2–L4 BMD is 1.256 g/cm^2. To simulate soft tissue, the aluminum phantom is submerged in a water bath with a depth of approximately 15 cm. The aluminum phantom is also available encased in an epoxy-resin block, avoiding the necessity of a water bath and improving ease of use.
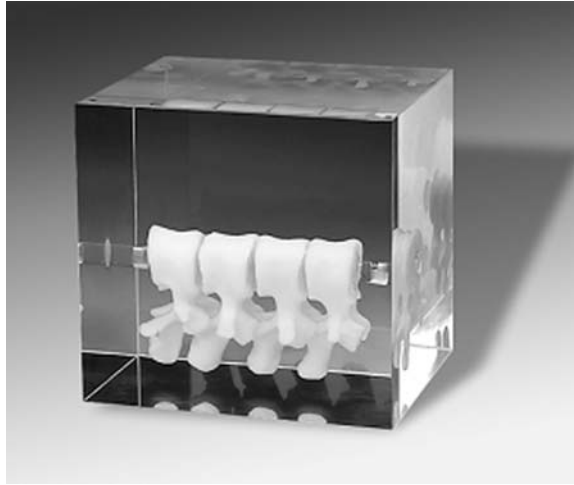
Fig. 4-3. The Hologic Spine phantom. Photo courtesy of Hologic, Inc., Bedford, MA.
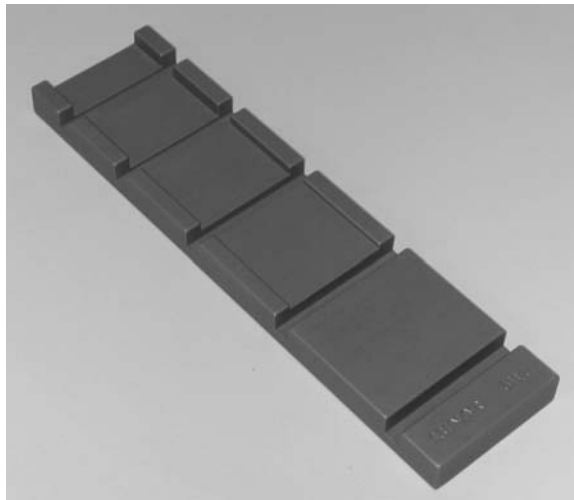
Fig. 4-4. The Lunar aluminum spine phantom. Photo courtesy of Bio-Imaging Technologies Inc., Newtown, PA.

The Norland Spine Phantom

The Norland spine phantom shown in Fig. 4-5, is an anthropomorphic spine phantom composed of hydroxyapatite equivalent materials. All Norland scanners are calibrated against a primary AP spine phantom with a BMD of 0.835 ± 0.01 g/cm^2 and against a primary body composition phantom (Tom Sanchez, Personal communication, CooperSurgical, Norland). Each scanner is factory-calibrated to within 1% for BMD and to within 2% for BMC, bone area, lean and fat mass. A transfer AP spine phantom, such as the one shown in Fig. 4-5, is shipped with every scanner to be used during initial and daily calibrations. As shown in Fig. 4-5, Norland Illuminatus software monitors
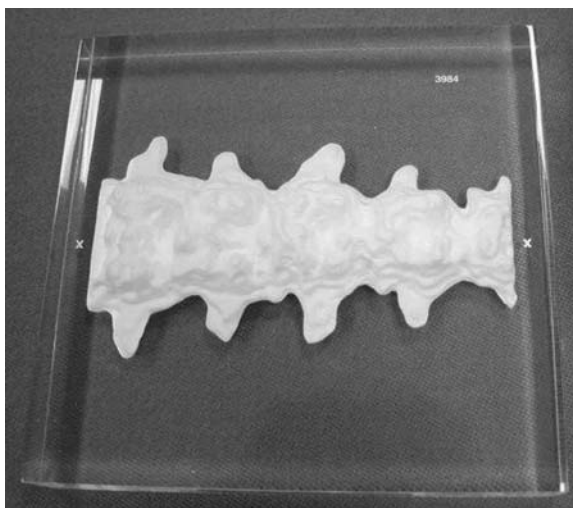
Fig. 4-5. The Norland spine phantom. Photo courtesy of Norland, a CooperSurgical Company, Ft. Atkinson, WI.

precision and accuracy for bone, lean and fat using Shewhart Chart protocols, which are discussed in the next section.

USING THE PHANTOM TO CREATE CONTROL TABLES AND CHARTS

Most daily quality assurance procedures to detect mechanical failures on today's densitometers are automated. The program will indicate a passing or failing condition. Before outright mechanical failure occurs, however, regular scanning of the quality control phantom and the application of Shewhart charts and rules or CUSUM charts can detect drifts or shifts in machine values that require correction in order to ensure continued accuracy and precision. Abrupt shifts in values are generally easy to detect. Drifts can be more subtle and therefore, more insidious. The confirmed occurrence of either indicates that the machine is OOC or "out of control."

Manufacturers generally recommend scanning the phantom 10 times on the same day without repositioning the phantom in between studies. This is also the procedure often used as part of quality control procedures in longitudinal clinical research trials. Subsequent phantom scans are then performed at least three times a week and on every day that a patient is scanned.

The average value of the 10 phantom scans should be calculated. The range that represents the average value ±1.5% should also be calculated. The average value + 1.5% and the average value –1.5% become the upper and lower limits of BMD within which all subsequent measurements of the phantom should fall. These upper and lower limits are called control limits. A control table as shown in Table 4-1 can then be created. One column lists the date of the phantom scan. The second column gives the actual BMD value. In the third column, a yes or no entry indicates whether the phantom BMD value fell within the established control limits.

A control graph offers some advantages over the control table. A control graph is created using the same average value from 10 consecutive phantom scans and control

Table 4-1
A Control Table

Date	Phantom Value	Within Control Limits
10/9/2000	1.179	Yes
10/10/2000	1.187	Yes
10/11/2000	1.162	No
10/11/2000	1.170	Yes
10/12/2000	1.184	Yes

Control limits of $\pm 1.5\%$ or 1.164–1.200 g/cm^2 were established based on a 10-phantom average BMD of 1.182 g/cm^2. The individual phantom values used to establish the mean $\pm 1.5\%$ are shown in Table 4-2.

limits based on $\pm 1.5\%$ of the average value. The vertical or "y" axis of the graph reflects the BMD values in g/cm^2. The horizontal or "x" axis reflects time in days. The BMD that corresponds to the 10-phantom average should be indicated by drawing a solid horizontal line across the graph. The upper and lower control limits values are similarly indicated by drawing a dashed line across the graph. Subsequent phantom values are easily tracked by plotting the results on the control graph. Such a graph is called a Shewhart chart.

The results of 10 scans of the anthropomorphic Hologic spine phantom that were performed on a Lunar DPX are shown in Table 4-2. The average value for the 10 scans was calculated as 1.182 g/cm^2. To find the upper and lower control limits, the average value was multiplied by 1.5%. This was determined to be 0.018 g/cm^2 (1.182 g/cm^2 $\times$ 0.015). Therefore, the range of values within which all subsequent phantom scan values should fall is 1.182 g/cm^2 $\pm$ 0.018 gm/cm^2 or from 1.164 g/cm^2 to 1.200 g/cm^2. Figure 5-5 is the Shewhart chart that was created for this set of 10 phantom scans onto which subsequent phantom scan values have been plotted. The phantom BMD values obtained over time from a scanner that is operating perfectly should randomly fall on either side of the 10-phantom BMD average value but remain within the control limit boundaries

Table 4-2
10 Hologic Spine Phantom Scans Performed on a Lunar DPX on the Same
Day to Establish a Baseline Phantom BMD Value for Quality Control

Phantom Scan	Date	BMD L1-L4 g/cm^2
Scan 1	4/22/2000	1.181
Scan 2	4/22/2000	1.173
Scan 3	4/22/2000	1.176
Scan 4	4/22/2000	1.180
Scan 5	4/22/2000	1.190
Scan 6	4/22/2000	1.174
Scan 7	4/22/2000	1.189
Scan 8	4/22/2000	1.192
Scan 9	4/22/2000	1.177
Scan 10	4/22/2000	1.187

The average value for the 10 phantom scans is 1.182 g/cm^2. The SD is 0.007 g/cm^2 and 1.5% of the average value is 0.018 g/cm^2.

of ±1.5%. If a value falls outside the boundaries, the phantom scan should immediately be repeated. If it falls outside the boundaries again, or "fails," the manufacturer should be contacted for additional instructions.

A visual inspection of the Shewhart chart can also provide more subtle clues to machine malfunction or a machine going OOC. The pattern of the values should be reviewed to ensure that the values appear to be randomly falling on either side of the average value in addition to being within the control limits. If this randomness appears to be lost, the machine may be drifting. If an imaginary straight line drawn through the center of the phantom values is above or below the average value, a shift may have occurred. In either of these cases, the manufacturer should again be contacted for instructions. An inspection of the Shewhart chart in Fig. 4-6 suggests a possible drift in values. Arrow #1 on the graph in Fig. 4-6 indicates a point at which it appears that the phantom values are no longer randomly scattered on either side of the average but instead are concentrated below the average. This suggests that the scan values may be starting to drift downward. These situations can and do occur even though the absolute BMD values obtained from the daily phantom scans remain within the established range and other daily quality assurance procedures continue to give "PASS" indications.

The control table described earlier is simpler to create and maintain than the Shewhart chart, but the ability to visually inspect the data for drifts or shifts is lost. The creation of a Shewhart control table or chart constitutes the minimum quality control program that should be in use in every facility performing densitometry.

The creation of an average baseline phantom value by scanning the phantom 10 times on the same day without repositioning may not reflect the day-to-day variability in machine values and the effects of repositioning that would be expected as the phantom is scanned over time. Several groups have consequently recommended that the baseline phantom value be established by scanning the phantom once a day for 15–25 consecutive days and then averaging these 15–25 scans. It is thought that this will more accurately reflect the day-to-day variability in machine values and result in fewer "false alarm failures." For example, the average BMD of the same Hologic spine phantom
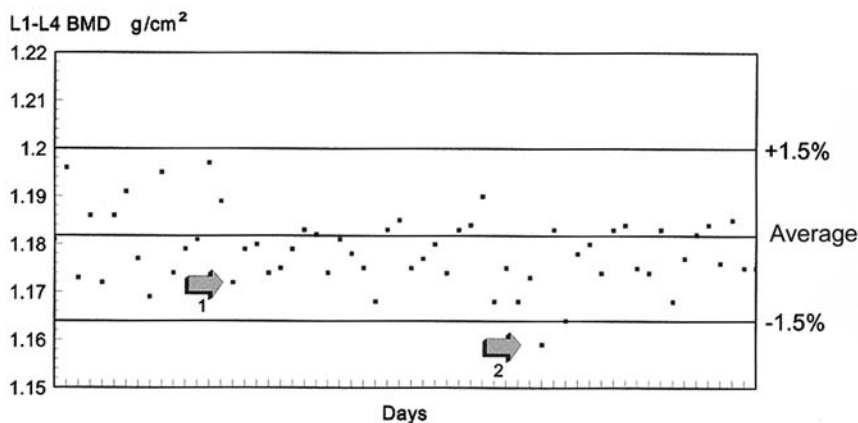
Fig. 4-6. A quality control chart with control limits of ±1.5%. The average BMD of the phantom was established by scanning the phantom 10 times on the same day. *Arrow 1* indicates a point at which values appear to be drifting downward. *Arrow 2* indicates a violation of the 1.5% rule.

Table 4-3
**25 Hologic Spine Phantom Scans Performed on a Lunar DPX on 25 Consecutive Days
to Establish a Baseline Phantom Value for Quality Control**

Phantom Scan	Date	BMD L1–L4 g/cm²	Phantom Scan	Date	BMD L1–L4 g/cm²
Scan 1	4/22/2000	1.181	Scan 14	5/14/2000	1.189
Scan 2	4/23/2000	1.172	Scan 15	5/15/2000	1.174
Scan 3	4/24/2000	1.176	Scan 16	5/16/2000	1.186
Scan 4	4/25/2000	1.172	Scan 17	5/20/2000	1.181
Scan 5	4/29/2000	1.180	Scan 18	5/21/2000	1.170
Scan 6	4/30/2000	1.185	Scan 19	5/22/2000	1.179
Scan 7	5/01/2000	1.179	Scan 20	5/23/2000	1.178
Scan 8	5/02/2000	1.176	Scan 21	5/28/2000	1.180
Scan 9	5/06/2000	1.177	Scan 22	5/29/2000	1.181
Scan 10	5/07/2000	1.169	Scan 23	5/30/2000	1.168
Scan 11	5/08/2000	1.180	Scan 24	6/03/2000	1.182
Scan 12	5/09/2000	1.167	Scan 25	6/04/2000	1.172
Scan 13	5/13/2000	1.179			

The average value for the 25 phantom scans is 1.177 g/cm². The SD is 0.006 g/cm² and 1.5% of the average value is 0.018 g/cm². Compare these average and SD values to those calculated for the 10 scans in Table 8-2.

when scanned on 25 consecutive days as shown in Table 4-3 was 1.177 g/cm² resulting in a range for the average $\pm$1.5% of 1.159–1.195 g/cm². In both cases, 1.5% of the mean value was 0.018 g/cm² but the range of acceptable values was different from that seen when the phantom was scanned 10 times on the same day without repositioning. Figure 4-7 is the graph of subsequent scans now plotted against the baseline phantom value obtained after scanning the phantom once on each of 25 consecutive days.
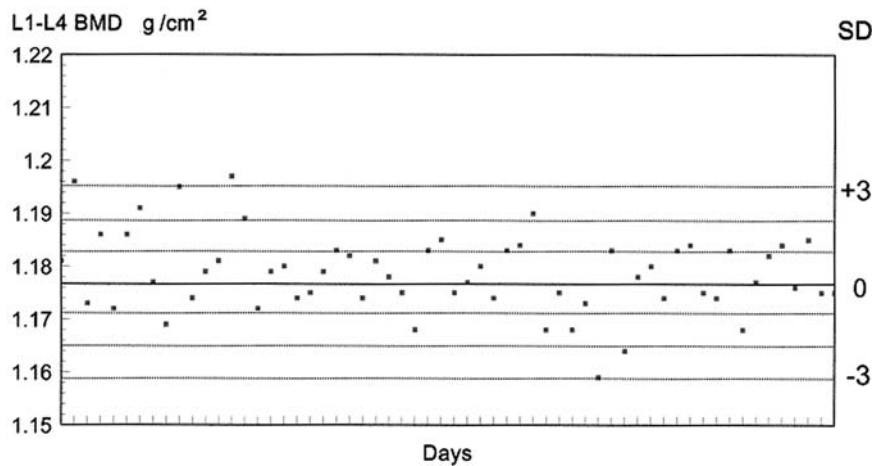
Fig. 4-7. A Shewhart chart for quality control. The average BMD of the phantom was established by scanning the phantom once on 25 consecutive days.

Notice in Fig. 4-7, when the mean was calculated using 25 scans performed on consecutive days, the same phantom values do not give any indication of a loss of random scatter. More sophisticated evaluations of this type of data can be done to determine if, in fact, there has been a shift in values. Nevertheless, this type of chart is the foundation of a good quality control program.

SHEWHART RULES AND CUSUM CHARTS

The field of analytical chemistry recognized the need for strict quality control many years ago. Like bone densitometry, analytical chemistry involves the use of machines for quantitative measurements. Techniques had to be developed to determine that the machines continued to function properly over long periods of time in order to ensure consistency in the results (*4*). The methods common to analytical chemistry have been adapted for use in bone densitometry (*5*). These methods utilize the BMD values from the phantom scans as described earlier: the average phantom value and the values from phantom scans performed over time. The two most commonly used methods for tracking machine performance are Shewhart rules and the CUSUM chart.

Shewhart Rules

Shewhart[2] rules have been used in analytical chemistry since the 1950s. In order to utilize Shewhart rules it is necessary to establish a baseline value and control limits for the phantom measurement and create a Shewhart chart as described earlier. Establishing the baseline phantom value by scanning the phantom on each of 15–25 consecutive days rather than multiple times on the same day is recommended. If, for some reason, this is impractical, a 10-phantom average created by scanning the phantom 10 times on the same day can certainly be used. Once the average value of the phantom scans is determined, the standard deviation (SD) for the set of scans should be calculated. A Shewhart chart can then be created onto which the BMD data from subsequent phantom measurements is plotted, as was done in Fig. 4-7. The y-axis of the graph should reflect both the actual BMD values and SD units as shown in Fig. 4-7. To utilize SD units, the average BMD is assigned a value of 0 on the y-axis of the graph and the SD tics are labeled +1 or −1, +2 or −2, and so on. In other words, the y-axis reflects both the measured BMD and the z-score[3] of the daily phantom BMD measurements. The average phantom value used to construct the Shewhart chart in Fig. 4-7 was previously found to be 1.177 g/cm². The SD was also previously found to be 0.006 g/cm² for this set of measurements. It is not necessary to calculate the z-score for each of the phantom measurements. When the measured BMD is plotted on the graph, it becomes visually apparent how many SDs from the average the value actually lies because of the SD or z-score scale on the y-axis. Remember that with a perfectly functioning machine, the

---

[2] Dr. William Andrew Shewhart (1891–1967) as a scientist with Western Electric; devised the basis for the application of statistical methods to quality control. In 1931, his book, *Economic Control of Quality of Manufactured Product*, was published in which he presented his methods for statistical sampling.

[3] In this context, *z*-score has nothing to do with reference population BMD data. It is simply the number of standard deviations above or below the average value.

values plotted on the graph are expected to be randomly scattered on either side (that is, above and below) of the average BMD or z-score of 0.

As these values are being plotted, "rules" are applied to detect trends or "failures" that may indicate a change in machine performance. These are called Shewhart rules or sensitizing rules (*9*). Different combinations of rules have been tested in densitometry in order to minimize false alarms and increase the ability of the Shewhart rules to detect true alterations in machine performance (*5, 10, 11*).

Shewhart rules are usually "set" at a certain level. In other words, a triggering or warning level is selected. When this level is exceeded, the Shewhart rules are applied. For example, Shewhart rules may be set at a warning level of the average ± 2 SD (*4*) If the phantom BMD value is more than 2 SD above or below the average BMD, the Shewhart rules are applied to detect potential machine failures. A machine failure is then deemed to have occurred if any one or more of the following Shewhart rules have been violated:

- A phantom BMD value exceeding the average ±3 SD
- Two consecutive phantom BMD values on the same side of the average exceeding the average by ±2 SD
- Two consecutive phantom BMD values differing by more than 4 SD
- Four consecutive phantom BMD values on the same side of the average exceeding the average by ±1 SD
- Ten consecutive phantom BMD values falling on the same side of the average regardless of their distance from the average

Not all violations of the rules will be found to be machine failures that require correction and as such, are considered "false alarms." In order to reduce the false alarms, a "filter" is sometimes applied to the "sensitizing rules." One such filter is to calculate the average BMD for 10 consecutive phantom measurements after a violation of one of the Shewhart rules has occurred. If this 10-scan average differs by more than 1 SD from the baseline average value, the violation is confirmed. Another method is to "set" the triggering of the rules at a higher level, such as the 3 SD deviation level. When this approach is employed, the occurrence of a single value outside the 3 SD limits then triggers the application of the other rules.

Without such "filters" or "triggers," Shewhart rules, although easy to use, produce a high false alarm rate. Even if a machine is in perfect working order, a violation of the Shewhart rules is expected to occur once every 39 scans (*11*). When the filter is added, the false alarm rate drops to once every 631 scans. Unfortunately, while the addition of the filter to Shewhart rules reduces the number of false alarms, it may also have the undesirable effect of delaying detection of true shifts in machine performance.

Shewhart rules may also be utilized by calculating the average ± a percentage of the average as was done in the quality control chart in Fig. 4-6 (*12*). For most of the central DXA scanners in clinical use today, repeat phantom measurements will generally result in a SD for the baseline set of phantom measurements that is roughly 0.5% of the average value. Consequently, 1.5% of the average value for the phantom BMD will approximately equal 3 SD. For example, when the statistics were calculated for the 10 phantom measurements performed on the same day shown in Table 4-2, the average was 1.182 g/cm^2 with a SD of 0.007 g/cm^2 and 1.5% of the average was found to be 0.018 g/cm^2. In this case, 1.5% of the average is equal to 2.6 SDs. In the case of the 25

phantom scans shown in Table 4-3 with a SD of 0.006, the 1.5% value of 0.018 g/cm^2 is equal to 3 SDs. The % values can be used to invoke the Shewhart rules. Using a value of 0.5% of the average as equaling 1SD, the Shewhart rules would be applied if a phantom value exceeded the baseline average value $\pm1\%$ (instead of the average ±2 SD). A violation would be deemed to have occurred in any of the following circumstances:

- A phantom BMD value exceeds the average by $\pm$ 1.5%
- Two consecutive phantom BMD values on the same side of the average exceed the average by $\pm1\%$
- Two consecutive phantom BMD values differ by more than 2%
- Four consecutive phantom BMD values on the same side of the average exceed the average by $\pm0.5\%$
- Ten consecutive phantom BMD values fall on the same side of the average regardless of their distance from the average

The 10-scan average filter described above would confirm a failure if the 10-scan average differed from the baseline average by more than 0.5% (instead of 1 SD).

In quality control "jargon," each of these rules has its own name. In the order listed above, the rules are known as the:

- 3 SD or 1.5% rule
- 2 SD twice or 1.0% twice rule
- Range of 4 SD or range of 2% rule
- Four $\pm$ 1 SD or Four $\pm$ 0.5% rule
- Mean $\times$ 10 rule

When any of the Shewhart rules are confirmed, the machine is OOC and the manufacturer should be consulted to determine the cause and corrective action. Once corrective action has been taken, a new phantom baseline BMD must be established by scanning the phantom as described earlier. A new Shewhart chart can then be constructed to monitor machine performance.

CUSUM Charts

CUSUM charts are not as easy to use as Shewhart charts and rules, but these are the types of charts employed by many professional densitometry quality control centers. This technique was originally developed for use in industry (*13*) and was subsequently adapted for use in bone densitometry (*11*, *14*, *15*). The principle underlying CUSUM charts is the expected random variation in the phantom measurement. Remember that even in a perfectly functioning machine, daily phantom BMD values are expected to randomly fall above or below the average phantom value. In other words, the daily phantom BMD value is expected to "vary about the average value." The magnitude of the variation, however, even though some measurements will be above (or greater) than the average value and some will be below (or less) than the average value, should remain relatively constant.

In order to utilize the CUSUM chart, a baseline spine phantom value must again be established by scanning the phantom 10 times consecutively or once on each of 15–25 consecutive days as was done previously for the application of Shewhart rules. For all subsequent scans, the difference between the average value and the subsequent value is

calculated. The differences are progressively summed and plotted on the CUSUM chart. Mathematically, this is expressed in Equation 1 as:

$$CS_n = \sum_{p=1}^{n} \left(BMD_p - BMD_{Mean}\right) \qquad (1)$$

where CS is the cumulative sum, n is the total number of measurements, BMD_{Mean} is the average phantom value and BMD_p is the phantom value for each of the n measurements. Each sequential value of CS is plotted on the graph. The vertical axis of the graph is marked in SD units of the average value. For a properly functioning machine, the values plotted on the CUSUM chart should be scattered in a horizontal pattern around 0 (0 is equal to the average phantom value). If the pattern is rising or falling, the machine is not functioning properly.

The construction of a CUSUM chart begins again with the data in Table 4-3. The phantom was scanned once each day for 25 consecutive days. The average value of the phantom was found to be 1.177 g/cm^2 and the SD was calculated to be 0.006 g/cm^2. Table 4-4 illustrates the calculations of the cumulative sum for the next 10 phantom measurements. Figure 4-8 illustrates the CUSUM plot for these 10 measurements and 30 additional measurements that followed. In Fig. 4-8, instead of BMD on the vertical axis, SD units or z-scores are utilized. The CUSUM plot for these 40 phantom scans clearly appears to be rising rather than being horizontal.

Table 4-4
Calculation of the Cumulative Sum for Sequential Phantom Scans

Date	Phantom BMD g/cm^2	Difference from Average Phantom Value g/cm^2	Cumulative Sum of the Differences g/cm^2	Cumulative Sum of the Differences Expressed in SD units (z-score)
6/5/2000	1.181	0.004	0.004	0.67 (0.004 ÷ 0.006)
6/6/2000	1.196	0.019	0.023 (0.004 + 0.019)	4.33 (0.023 ÷0.006)
6/10/2000	1.173	−0.004	0.019 (0.019 − 0.004)	3.17 (0.019 ÷0.006)
6/11/2000	1.186	0.009	0.028 (0.019 + 0.009)	4.67 (0.028 ÷0.006)
6/12/2000	1.172	−0.005	0.023 (0.028 − 0.005)	3.83 (0.023 ÷0.006)
6/13/2000	1.186	0.009	0.032 (0.023 + 0.009)	5.33 (0.032 ÷0.006)
6/17/2000	1.191	0.014	0.046 (0.032 + 0.014)	7.66 (0.046 ÷0.006)
6/21/2000	1.169	−0.008	0.038 (0.046 − 0.008)	6.33 (0.038 ÷0.006)
6/24/2000	1.195	0.018	0.056 (0.038 − 0.003)	9.33 (0.056 ÷0.006)
6/25/2000	1.174	−0.003	0.053 (0.056 − 0.003)	8.83 (0.053 ÷0.006)

The z-score of the cumulative sum is plotted on the CUSUM chart. The average phantom value is 1.177 g/cm^2 and the SD is 0.006 g/cm^2.

Although the CUSUM chart can be inspected visually to determine machine malfunction indicated by the non-horizontal plot, two methods have been developed to determine mathematically when control limits have been exceeded. A commonly used method involves the superimposition of a V-mask in which the slope of the arms on the mask is determined mathematically (14). The slope is normally some multiple of the standard error of the average phantom value. The stringency of the mask can be changed by increasing or decreasing the slope of the V-mask. The other method, called tabular
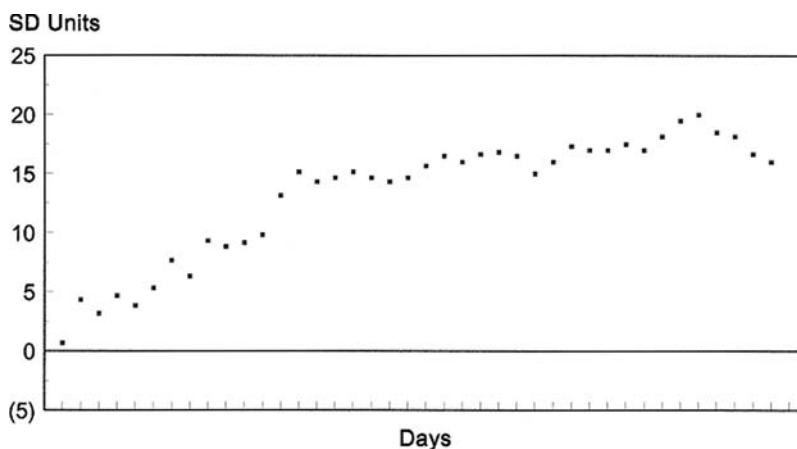
Fig. 4-8. A CUSUM chart. The values are clearly rising rather than being horizontal.

CUSUM, involves the mathematical calculation of upper and lower control limits (*11*). In either case, when values fall outside the control limits or the arms of the mask, an alarm is triggered indicating that the machine is OOC and that the manufacturer should be contacted.

CUSUM charts or tabular CUSUM are most easily performed with the help of sophisticated statistical software programs. Stand-alone software programs are available as well as add-ons for popular programs like Microsoft Excel. There is no reason, however, that clinical densitometry centers cannot employ CUSUM methodology although it is certainly less intuitive than Shewhart charts and rules. The additional benefit of using a CUSUM chart beyond the use of a Shewhart control chart is claimed to be the ability to detect smaller drifts sooner. It is not at all clear, however, that this is of benefit to the densitometrist.

AUTOMATED QUALITY CONTROL PROCEDURES

In recent years densitometry manufacturers have increasingly automated quality control procedures. Calibration standards may be contained within the devices and checked routinely at the touch of a button. Quality control graphs may be generated by the system software, on which phantom values over time are plotted. Shewhart rules may be automatically applied to the results, prompting messages of Pass, Fail, or notification of specific rule failures. Such innovations are indeed welcome but they are useless unless these procedures are performed on a regular basis. It is also imperative that the densitometrist knows what to look for and understand the information presented.

A quality control graph from a Norland XR-Series densitometer is shown in Fig. 4-9. The upper graph reflects the precision of the system (*16*). In the upper graph, the solid horizontal line reflects the average value for the 16 most recent scans. The dashed horizontal lines indicate ±2 SD about the average. The value of the SD used to establish this range is a value for the phantom that is entered into the computer during the setup of the system. The BMD values of the individual scans are plotted on the graph. Approximately 1 out of every 20 scans is expected to fall outside the range defined by the average ±2 SD simply because, statistically, this range will contain only 95% of the values. The
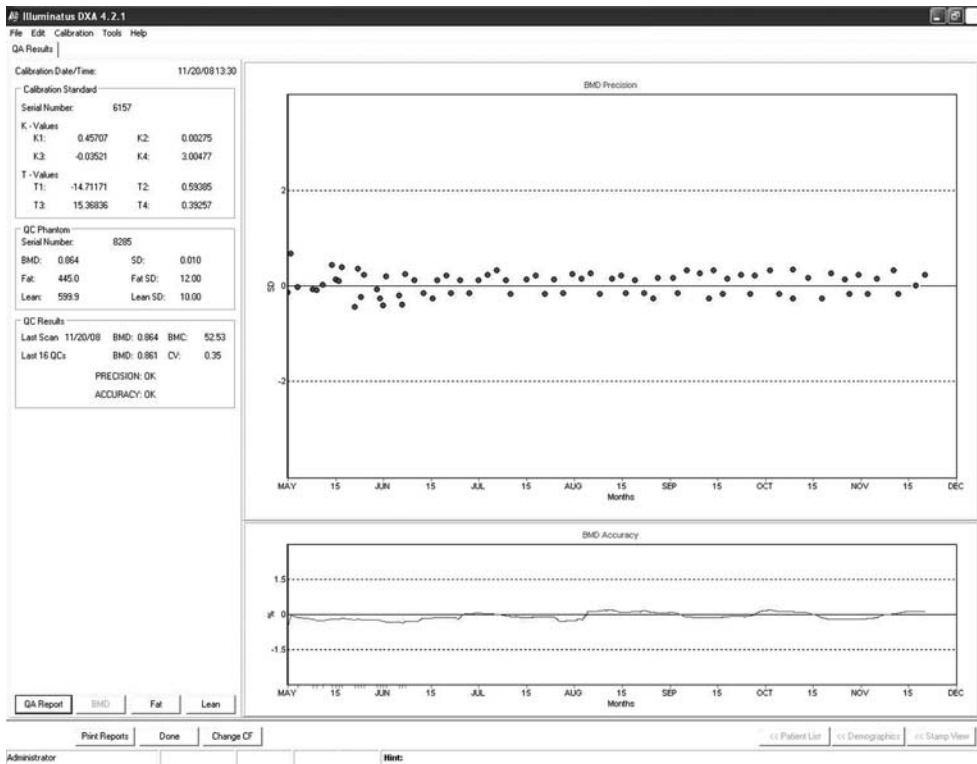
Fig. 4-9. The Norland XR Illuminatus quality control screen. The upper Shewhart chart tracks the precision of the machine while the lower Shewhart chart tracks accuracy. Courtesy of Norland, a CooperSurgical Company, Ft. Atkinson, WI.

computer will also calculate the SD for each set of 16 scans. This value is not plotted, but is used by the computer. Clearly, the average and SD will change as new phantom scans are performed and added to the set of the 16 most recent scans. This type of calculation is called a "moving average." The results are monitored for changes in the BMD as well as increases in the SD. Shewhart rules are applied to detect unacceptable changes in the BMD. The acceptable limits for an increase in the SD are calculated mathematically. If the system passes all tests, the notation of "OK" is seen after "PRECISION" at the bottom of the graph. Other messages may be seen, however, which should prompt a call to the manufacturer. For example, an "OUT OF RANGE" notation indicates that the SD from the most recent 16 scans has increased beyond acceptable limits. A "WARNING 1" notation indicates that a single phantom BMD value is more than 3 SD from the average. This is a violation of the Shewhart 3 SD rule. "WARNING 2" is a violation of either the Shewhart 2 SD twice or Range of 4 SD rule and "WARNING 3" is a violation of the Shewhart Four ±1 SD rule.

The lower graph reflects the accuracy of the system (*16*). The solid horizontal line represents the phantom BMD value that was entered into the computer during the setup of the system. The dashed horizontal lines indicate a range of ±1.5% about this value. The values plotted on this graph are the average BMD values for the last 16 phantom scans. If the average value for the 16 most recent phantom scans falls within ±1.5%

of the true phantom value, "OK" will be seen next to the word "ACCURACY" at the bottom of the graph. An "OUT OF RANGE" message will appear if the value falls outside those limits. If eight consecutive values fall on the same side of the true phantom value, a "TREND WARNING" message will appear.

The quality control graphs and calculations for the Norland pDEXA® are very similar to those of the XR-Series. The control limits for the accuracy of the pDEXA® system are ±2.5% instead of 1.5% (*17*).

Hologic scanners also provide automated quality control graphing procedures (*18*). The BMD of a phantom is established during the initial calibration procedures for the scanner. The control limits of ±1.5% of the phantom BMD value are defined on a graph onto which subsequent spine phantom BMD data is plotted. Underneath the graph, two tables are displayed. The table titled, "Reference Values" lists the average or mean value and SD for the spine phantom established during machine calibration. The table titled, "Plot Statistics" lists the number of phantom scans plotted (n), the mean, SD, and %CV for those scans. There are no sensitizing rules built into the quality control program in the computer. With this automated plot, however, Shewhart rules are easy to apply.

Other manufacturers have automated charting of phantom values. Figure 4-10 is such a chart from the Osteometer DTX-200 DexaCare®, a dedicated DXA forearm scanner. The dashed horizontal lines on the graph represent control limits of ±1.5%. None of the 85 phantom values has fallen outside the control limits and the values appear to be randomly scattered about the average value. If desired, the densitometrist can
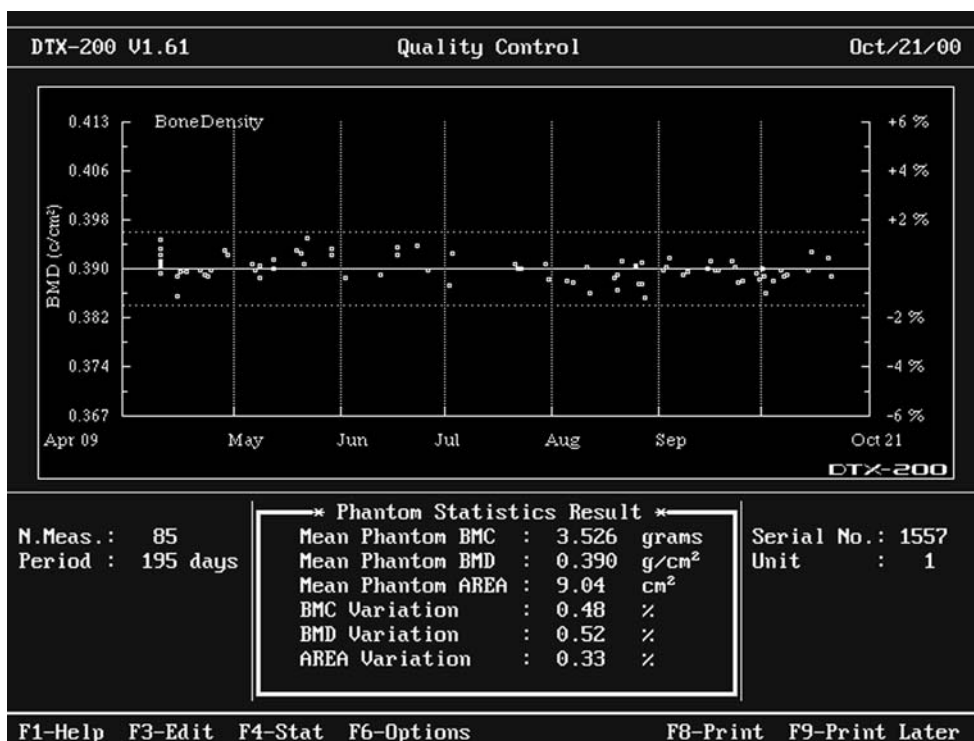
Fig. 4-10. The DTX-200 quality control screen. This is a Shewhart chart with control limits of ± 1.5%.
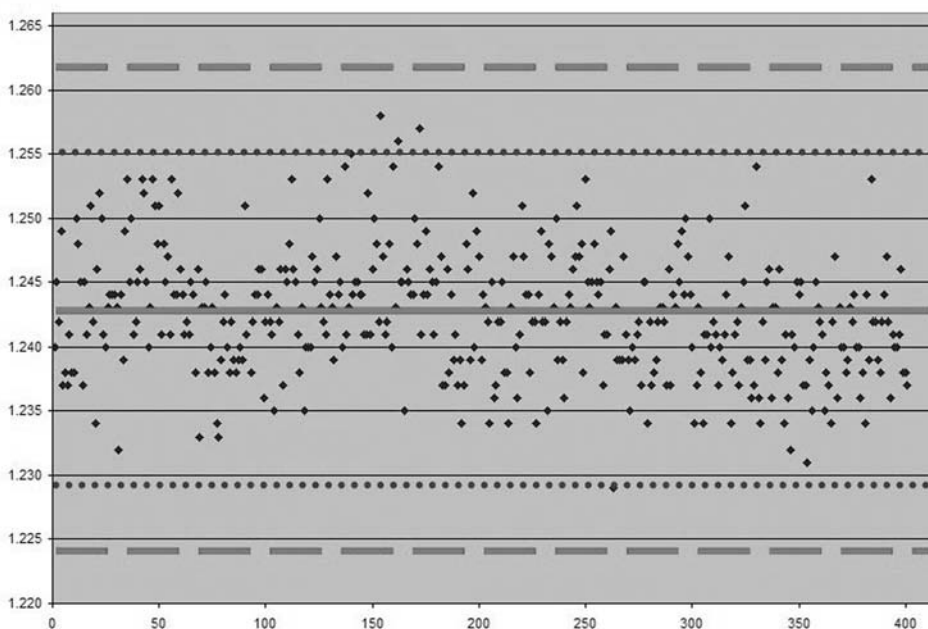
Fig. 4-11. A Shewhart control chart created within Microsoft Excel software. The mean phantom value is indicated by the solid horizontal line. This value was established by scanning the phantom on 25 consecutive days and calculating the average of the 25 scans. The *upper* and *lower dashed horizontal lines* indicate control limits of ±1.5% and the *upper* and *lower horizontal dotted lines* indicate control limits of ±1%. Phantom values, obtained over a 2-year period, have been plotted on the graph. As expected, the phantom values fall randomly on either side of the mean. Note that the overwhelming majority of the values are within 1% of the mean.

create a control chart, using the information in this chapter. Figure 4-11 is a Shewhart control chart that was created within Microsoft Excel in which L1-L4 phantom values from a central DXA device have been plotted over a period of 2 years. In this case, the Lunar aluminum spine phantom was scanned regularly on the GE Lunar Prodigy. The upper and lower dashed lines reflect control limits of the mean BMD ±1.5%, while the upper and lower dotted lines reflect control limits of ±1%. As can be seen in the figure, the majority of the phantom values were within the 1% control limits.

All densitometry centers should implement quality control procedures that minimally consist of control tables or charts with defined control limits of ± 1.5% for the average of 10 phantom scans performed on 1 day or 25 scans performed on consecutive days. Shewhart rules with a filter can then be implemented, using rules defined on the basis of % or SD, to further strengthen the quality control program. The application of CUSUM charts and calculations as performed at professional quality control centers is more labor intensive and not necessarily of greater benefit to the clinical densitometry center.

The recommendations (*3*) from the Canadian Panel of the International Society for Densitometry (ISCD) for a complete quality control program include not only the creation of a control chart with limits of 1.5% but the maintenance of logs and manuals for each densitometer that include the items listed in Table 4-5. These recommendations are certainly appropriate for densitometry facilities in the United States as well

Table 4-5

Recommendations from the Canadian Panel of the International Society for Clinical Densitometry for Documentation of a Quality Control Program

1. Current operating manual from equipment manufacturer
2. Appropriate positioning devices
3. Appropriate calibration standard
4. Calibration history for specific densitometer
5. Precision data and estimates of site-specific precision errors
6. Maintenance and upgrade records
7. Software version/upgrade records
8. Cross-calibration records in the event of an equipment change
9. Data and database archiving procedures
10. Local, provincial, and federal licensures of equipment as required
11. Medical physicist inspection reports as required

Reproduced from Khan et al. (*3*) with permission from Elsevier.

Table 4-6

International Society for Clinical Densitometry Guidelines for Quality Control Requirements for DXA Facilities

- Follow manufacturer's guidelines for system maintenance
- Perform weekly phantom scans, unless required more often by the manufacturer
- Plot and review data from calibration and phantom scans (such as using a Shewhart Chart with control limits of ±1.5%)
- Re-check and verify the mean phantom BMD after any service performed on the densitometer
- Establish corrective thresholds to trigger a repair request (such as two phantom scans outside of control limits or a post-service mean phantom BMD >1% from the pre-service mean phantom BMD)
- Maintain all service logs
- Comply with all government inspections, radiation surveys and regulatory requirements

as Canada. In its 2003 position statement, the full ISCD (*19*)issued guidelines for densitometry facility quality control programs. These recommendations remain in effect. The core and ancillary ISCD recommendations are shown in Tables 4-6 and 4-7. ISCD also recommended that the manufacturer's specific guidelines for system maintenance be followed.

REPLACING A DENSITOMETER

Replacing a densitometer in clinical practice is fortunately not a frequent event. Densitometers are extremely durable and rarely subject to such widespread component failure that replacement of the equipment becomes necessary. Software updates and upgrades to a device purchased years ago can keep that device's applications as current as most new models. Periodically, however, a densitometer must be replaced or a replacement simply becomes desirable. This creates a clinical dilemma for facilities at which patients are being followed when the original bone density measurement was made with the device being replaced.

Table 4-7
ISCD Recommendations for Additional Components of a Quality Control
Program for DXA Facilities

• Run the daily secondary calibration for the DXA system
• Keep service logs, which include:
   ○ Error messages
   ○ Technical problems
   ○ Problem resolution
   ○ Service reports
   ○ Regulatory inspections
   ○ Radiation surveys
• Performance of a precision study
• Written standard operating procedures
• Training manuals

Under ideal circumstances, provisions should be made to keep the old machine in use after the installation of the new machine until all patients who are currently being followed can be recalled and measured on both devices. This completes the follow-up on the old machine and creates a baseline on the new device. This may not be feasible as space requirements for densitometry within the facility immediately double and if the older device is being replaced because of component failures, it simply cannot be used. In addition, medically necessary repeat studies may not be required for at least a year, making this process lengthy.

Although the approach described above remains ideal, in most cases, it simply could not be done. Cross-calibration studies, either in vivo or in vitro, were recommended as an alternative, but until recently the resources required to do either were beyond the abilities of the majority of clinical densitometry facilities.

Original recommendations for an in vivo cross-calibration study called for between 60 and 100 patients whose bone densities spanned peak to osteoporotic values. Linear regression methods[4] were used to develop cross-calibration equations with a standard error of the estimate[5] of around 3% (20, 21). Once the cross-calibration equation was created, it was used to predict the value on the old machine from the value that was obtained on the new machine. With the help of a statistician or statistical software program, the 95% confidence interval for a predicted value for an individual was calculated.[6] In lieu of the in vivo cross-calibration study, in vitro study was recommended using a phantom. Recommendations for 60–100 phantom scans over a similar period of

---

[4] Linear regression involves the development of a mathematical model in order to predict one value from the measurement of another. Such models are useful but they are never perfect. Many statistical calculators or software programs can be used to calculate the regression equation.

[5] The standard error of the estimate (SEE) is also known as the standard deviation from the regression line. It is an estimate of the variability about the line of means predicted by the regression equation.

[6] The 95% confidence interval describes the range of values within which we can be 95% confident that the true value actually lies.

days were made. Linear regression was again used to create the predictive equation. It is important to remember that linear regression equations are useful for prediction only within the range of values that were used to create the equation in the first place. Therefore, subjects participating in a cross-calibration study or phantoms used in such studies must have bone densities similar to those likely to be encountered in clinical practice.

In vivo and in vitro cross-calibration studies and the predictive equations that come from such studies are extremely useful but they are still not as desirable as scanning patients being followed on both devices, as difficult as that may be. Pearson et al. (22) after comparing both in vivo and in vitro phantom cross calibrations, concluded that applying such calibrations to individual patients being followed over time was simply not possible because the error in such calibrations was too similar to the expected annual change in BMD. These authors noted that a new baseline BMD must be obtained for each patient when a new scanner is put into use. These concerns had been previously raised by Blake (23). In 2003, the International Society for Clinical Densitometry (19) stated as an official position of the society that a new baseline BMD should ideally be established on the new or replacement scanner rather than relying on previously published cross-calibration formulas derived using different DXA systems to predict the new baseline value.

Recognizing the practical difficulties of in vivo cross-calibration and the reality, albeit infrequent, of scanner replacement, ISCD expanded their position statement on the cross-calibration of DXA systems in clinical practice in 2005 (24). These positions were reiterated in 2007 and are reproduced in their entirety in Appendix V(25). ISCD stated that when a DXA device is replaced with the same make and model of device, cross-calibration could be accomplished by scanning 10 phantoms on each device. If more than 1% difference was observed between the mean BMD of each set of 10 phantoms, it was recommended that the manufacturer be contacted for assistance. Although this is entirely reasonable, it seems likely that manufacturers cannot promise to bring two systems to within ≤1% of the mean of 2 sets of 10 phantom values. When a DXA machine was replaced with a DXA machine from a different manufacturer or from the same manufacturer now utilizing a different technology, ISCD recommended the performance of an in vivo cross-calibration study involving 30 subjects. These 30 subjects should be representative of the facility's patient population in terms of the expected range of bone densities. Each of these 30 subjects should be scanned on the original device once and then scanned twice on the new system within 60 days. The ISCD cross-calibration tool,[7] available at www.iscd.org, can then be used to calculate the least significant change (LSC)[8] between the old and new machines. An LSC must be calculated for each skeletal region of interest (ROI) that may subsequently be used by the facility for monitoring skeletal change in a patient. This LSC should be used for patients whose baseline study was acquired on the original device and whose follow-up study is acquired on the new device. ISCD also noted that if this is not done, no comparison should be attempted

---

[7] The ISCD cross-calibration tool is available in the Members Only section of the web site at www.iscd.org. It can be downloaded and runs within Microsoft Excel.

[8] See Chapter 11 for a discussion of the LSC.

between studies on the old and new device. In this circumstance, it is necessary to establish new baseline values for a patient on the new device.

REFERENCES

1. Johnston CC, Melton LJ, Lindsay R, Eddy DM. Clinical indications for bone mass measurements: a report from the scientific advisory board of the National Osteoporosis Foundation. J Bone Miner Res 1989;4:S1–S28.
2. Miller PD, Bonnick SL, Rosen CJ. Consensus of an international panel on the clinical utility of bone mass measurements in the detection of low bone mass in the adult population. Calcif Tissue Int 1996;58:207–214.
3. Khan AA, Brown J, Faulkner K, et al. Standards and guidelines for performing central dual X-ray densitometry from the Canadian Panel of International Society for Clinical Densitometry. J Clin Densitom 2002;5:247–257.
4. Westgard JO, Barry PL, Hunt MR, Groth T. A multirule Shewhart Chart for quality control in clinical chemistry. Clin Chem 1981;27:493–501.
5. Orwoll ES, Oviatt SK, and the Nafarelin Bone Study Group. Longitudinal precision of dual-energy X-ray absorptiometry in a multicenter trial. J Bone Miner Res 1991;6:191–197.
6. Kalender W, Felsenberg D, Genant HK, Fischer M, Dequeker J, Reeve J. The European spine phantom – a tool for standardization and quality control in spine bone mineral measurements by DXA and QCT. Eur J Radiol 1995;20:83–92.
7. Pearson J, Dequeker J, Henley M, et al. European semi-anthropomorphic spine phantom for the calibration of bone densitometers: assessment of precision, stability and accuracy. The European Quantitation of Osteoporosis Study group. Osteoporos Int 1995;5:174–184.
8. Pearson D. Standardization and pre-trial quality control. In: Pearson D, Miller CG, eds. Clinical trials in osteoporosis. London, England: Springer, 2002:43–65.
9. Montgomery DC. Introduction to statistical quality control. New York: Wiley, 1992.
10. Orwoll ES, Oviatt SK, Biddle JA. Precision of dual-energy X-ray absorptiometry: development of quality control rules and their application in longitudinal studies. J Bone Miner Res 1993;8:693–699.
11. Lu Y, Mathur AK, Blunt BA, et al. Dual X-ray absorptiometry quality control: comparison of visual examination and process-control charts. J Bone Miner Res 1998;11:626–637.
12. Faulkner KG, Glüer C, Estilo M, Genant HK Cross-calibration of DXA equipment: upgrading from a Hologic QDR 1000/W to a QDR 2000. Calcif Tissue Int 1993;52:79–84.
13. BS5703: Guide to data analysis and quality control using Cusum techniques. London: British Standards Institution, 1980.
14. Pearson D, Cawte SA. Long-term quality control of DXA: a comparison of Shewhart rules and CUSUM charts. Osteoporos Int 1997;7:338–343.
15. Garland SW, Lees B, Stevenson JC. DXA longitudinal quality control: a comparison of inbuilt quality assurance, visual inspection: multi-rule Shewhart charts and Cusum analysis. Osteoporos Int 1997;7:231–237.
16. XR-Series X-Ray Bone Densitometer Operator's Guide. Ft. Atkinson, WI: Norland Medical Systems, Inc., 1993.
17. Model pDEXA Forearm X-ray Bone Densitometer Operator's Guide. Ft. Atkinson, WI: Norland Medical Systems, Inc., 1996.
18. QDR 4500 X-Ray Bone Densitometer User's Guide. Waltham, MA: Hologic, Inc.
19. The Writing Group for the ISCD Position Development Conference. Technical standardization for dual-energy X-ray absorptiometry. J Clin Densitom 2004;7:27–36.
20. Genant HK, Grampp S, Gluer CC, et al. Universal standardization for dual X-ray absorptiometry: patient and phantom cross-calibration results. J Bone Miner Res 1994;9:1503–1514.
21. Pearson D, Lawson N. Laboratory and instrument quality control. In: Pearson D, Miller CG, eds. Clinical trials in osteoporosis. London, England: Springer, 2002:137–154.
22. Pearson D, Horton B, Green DJ. Cross-calibration of DXA as part of an equipment replacement program. J Clin Densitom 2006;9:287–294.
23. Blake GM. Replacing DXA scanners: cross-calibration with phantoms may be misleading. Calcif Tissue Int 1996;59:1–5.

24. Shepherd JA, Lu Y, Wilson K, et al. Cross-calibration and minimum precision standards for dual-energy X-ray absorptiometry: the 2005 ISCD official positions. J Clin Densitom 2006;9:31–36.
25. Baim S, Leonard MB, Bianchi M, et al. Official positions of the International Society for Clinical Densitometry and executive summary of the 2007 ISCD pediatric position development conference. J Clin Densitom 2008;11:6–21.

5 Radiation Safety in X-Ray Densitometry

CONTENTS

Radiologists involved in the practice of densitometry have considerable background in radiation safety issues. This is not necessarily true for the non-radiologist physician densitometrist. Although radiation safety issues are not a major concern in the practice of densitometry, it is wise for the physician to be familiar with basic aspects of radiation safety, relating to protection of the public and protection of the technologist. This chapter is primarily intended for the non-radiologist.

X-ray densitometers expose patients to extremely small amounts of radiation in comparison to plain X-ray techniques. These amounts are often so small that they are biologically insignificant. Similarly, the technologist operating an X-ray densitometer on a regular basis is extremely unlikely to be exposed to a significant amount of radiation. Nevertheless, no amount of radiation should be considered inconsequential. The principle of "as low as reasonably achievable" (A.L.A.R.A.) should always be given the highest priority in the operation of these devices.

RADIATION BASICS

X-rays are a form of electromagnetic energy. Other forms of electromagnetic energy are radio and television waves, microwaves, radar, infrared, visible and ultraviolet light, and gamma (γ) radiation. These types of energies form the electromagnetic spectrum of energy. When energy is released and then transmitted through a substance it is called radiation. The substance through which the radiation has passed is said to have been "irradiated" or "exposed" to radiation. Ionizing radiation is radiation that causes the release of an electron from its orbit around an atom when the radiation passes through the substance containing that atom (*1*). X-rays and γ-rays are also forms of ionizing radiation.

Radiation Quantities

In X-ray densitometry the physician must be concerned with the amount of ionizing radiation to which both the patient and technologist are exposed. A review of the terminology describing these quantities is necessary before discussing the potential effects of ionizing radiation on living tissue and the exposure levels produced during various densitometry exams.

THE CURIE

The most basic unit of radiation is the Curie (Ci). This is used to quantify the amount of a radioactive material, not the radiation emitted by the material. The SI[1] unit equivalent to the Ci is the Becquerel (Bq). The formula for converting Ci to Bq is shown in Equation 1:

$$Ci \left(3.7 \times 10^{10}\right) = Bq \tag{1}$$

To use this equation, multiply the number of Ci by 3.7×10^{10} to determine the number of Bq. Amounts of radioactive material are described as being a certain number of milliCurie (mCi) or even microCurie (μCi).

THE ROENTGEN

The Roentgen (R), named for Wilhelm Roentgen who discovered X-rays, is used to describe a quantity of radiation exposure, but it is only used to describe the interaction of X-rays and γ-rays with air. The Roentgen is based on the electrical charge created by the liberation of electrons that occurs during ionization. In densitometry, the Roentgen is rarely used except to describe measured amounts of scattered radiation in the air when the devices are in use. This quantity is quite low and is generally expressed in milliRoentgens (mR). The Roentgen also has an SI counterpart, called the coulomb per kilogram (C/kg). The mathematical conversion of Roentgens to coulombs per kilogram is shown in Equation 2:

$$R \left(2.58 \times 10^{-4}\right) = C/kg \tag{2}$$

THE RAD

Rad is both an abbreviation and acronym for radiation absorbed dose. It is used in conjunction with any kind of ionizing radiation and any type of substance that has been exposed to ionizing radiation. The rad is commonly used to express the quantity of radiation received by a patient. The biologic effects of radiation are often associated with various quantities of radiation given as rads. The SI rad equivalent is the Gray[2] (Gy). The mathematical relationship between the rad and Gy is simple; 100 rads equal

---

[1] The system of units known as Le Systeme International d'Unites, or SI, and considered the preferred method of expressing scientific quantities.

[2] The Gray is named for Louis Gray (1905–1965), one of the creators of the Bragg-Gray theory used in radiation therapy.

1 Gy. This is expressed in Equation 3:

$$rad(0.01) = Gy \qquad (3)$$

For medical X-rays, 1 R is considered to be approximately equal to 1 rad because the radiation exposure to human tissue from 1 R is only about 5% more than 1 rad.

THE REM

Rem is also both an abbreviation and acronym for rad-equivalent man. The rem expresses the quantity of radiation received by a patient but unlike the rad, the quantity has been adjusted to reflect the type or quality of radiation involved (*2*). This recognizes that different types of ionizing radiation have different potentials to do harm. The conversion of rads to rems is expressed in Equation 4:

$$\text{Rem} = \text{rad} \times \text{quality factor} \qquad (4)$$

Medical X-rays are assigned a quality factor of 1. As a consequence, multiplying the number of rads by a medical X-ray quality factor of 1 does not change the value. For medical X-rays then, in the context of whole body exposure, a rad is equal to a rem. By extension, for medical X-rays, 1 R is also approximately equal to 1 rem. This is not true for all types of ionizing radiation, however. For example, alpha particle radiation from radon exposure has a quality factor of 20. Because radon is a gas, this exposure reflects the dose to the lungs. The exposure from medical X-rays in rads or rems is often called the skin dose.

The SI equivalent of the rem is the Sievert[3] (Sv). The mathematical relationship between the rem and Sievert is the same as between the rad and Gray. One hundred rems are equal to 1 Sv. This is expressed in Equation 5:

$$rem(0.01) = Sv \qquad (5)$$

THE EFFECTIVE DOSE EQUIVALENT

The effective dose equivalent (H_E) is a concept rather than a particular unit of measure. The concept was introduced in 1987 in an attempt to relate the magnitude of an exposure in rems or Sv to the *risk created by that exposure* (*3*). As noted in the discussion of the rem, the dose in rads must be multiplied by a quality factor for the type of ionizing radiation, recognizing that different types of radiation have different potentials to do harm. Similarly, different tissues or organs within the human body have different sensitivities to radiation. Some tissues are more sensitive than others. It matters then, what tissues are being irradiated in determining what the risk of that irradiation truly is. This is the concept behind the effective dose equivalent. Tissue weighting factors are assigned to the various tissues in the body. The H_E is determined by multiplying the value in rems or Sv by the tissue sensitivity weighting factor. Because the tissue weighting factor has no units of its own, the H_E is still expressed in rems or Sv.

---

[3] The Sievert is named for Rolf Maximilian Sievert (1896–1966), a Swedish medical physicist and founding member of the International Committee on Radiation Protection.

The body as a whole is assigned a tissue weighting factor of 1. Individual tissues or organs have sensitivity weighting factors less than 1 and vary widely. The ovaries and testes were assigned one of the highest values at 0.20–0.25(*4,5*) although recent recommendations from the International Commission on Radiological Protection (ICRP) have reduced this value to 0.05 (*6*). The thyroid's sensitivity is relatively low at 0.030.05. The red bone marrow, lungs, breasts, and colon are each assigned a sensitivity weighting factor of 0.12 (*6*). The H_E that is calculated for the exposure of any given area of the body is an expression of the risk that would result if the *entire body* was exposed to the same amount of radiation. For example, the H_E for a radiographic absorptiometry study of the phalanges on the Metriscan^{TM} is stated as being less than 0.0001 mrem or 0.012 µSv (*7*). This means that the risk of the radiation exposure from such a densitometry study of the phalanges is the same as if the entire body was exposed to less than 0.0001 mrem. This is not a measure of the amount of radiation exposure to the phalanges. The effective dose equivalent is an expression of the biologically important risk associated with any given amount of radiation exposure.

HARMFUL EFFECTS OF IONIZING RADIATION

Ionizing radiation has the potential to harm living tissue. In addition to medical X-rays, there are other sources of ionizing radiation. One important source found naturally in the environment is radon. Radon is a gas formed by the decay of uranium, which is normally found in small amounts in the earth. Materials that are derived from the earth, like concrete and brick, will therefore contain small amounts of radon to which everyone is exposed. The largest source of man-made ionizing radiation is medical X-rays. Other man-made sources include nuclear power generators, consumer products like smoke detectors and televisions, and industrial sources. In comparison to natural environmental radiation, man-made sources of ionizing radiation contribute very little to the total annual radiation exposure of an individual. Nevertheless, ionizing radiation does have the potential to do harm. The decision to expose a patient to ionizing radiation, no matter how small in amount, should not be made lightly.

Although ionizing radiation can cause an increase in the expected number of mutations, the mutations that result are not unique. In spite of the frightening and bizarre images seen in movies of giant crickets devouring Chicago after being exposed to ionizing radiation, the types of mutations that are actually seen are those that occur in nature. They simply will occur more frequently. Similarly, cancers that can result from high doses of ionizing radiation are not unique. The incidence of almost all types of cancer is increased after exposure to high doses of ionizing radiation but these are the same cancers seen in individuals who have not been exposed.

Acute Lethal Radiation Syndromes

Acute lethal radiation syndromes are mentioned here only for the sake of completeness. They *cannot occur* with the devices used in densitometry because the radiation doses required to produce them are thousands of times greater than those used in densitometry. DXA and SXA X-ray tubes are incapable of producing the high doses of radiation necessary to cause these syndromes because of their relatively low applied voltage and current. The peak kilovoltage (kVp) of the tube determines the amount of radiation that can be delivered by the tube. The X-ray tube current (mA) determines the

number of X-rays that are produced, which also affects the amount of radiation produced. In densitometry X-ray tubes, the kVp and mA are far too low to cause any of these syndromes. Nevertheless, the densitometrist should be aware of them, if only to reassure the anxious patient that they *cannot occur* with X-ray densitometry.

There are three different acute syndromes that ultimately result in death. The syndromes are called hematologic death, gastrointestinal (GI) death, and central nervous system (CNS) death. Doses of 200–1000 rads can cause nausea, vomiting, and diarrhea, hemorrhage, and a decrease in the white blood cell count leading to infection and fever. Hematologic death occurs within 10–60 days. Higher doses of 1000–5000 rads result in GI death in 4–10 days that is preceded by lethargy and shock as well as all the signs and symptoms seen with the hematologic death syndrome. Doses of more than 5000 rads result in CNS death within 3 days of exposure. Loss of coordination, meningitis, and the signs and symptoms seen in the GI and hematologic syndromes are also present. These types of syndromes were seen in the unfortunate victims of the Chernobyl nuclear power plant accident in 1986.

Local Tissue Damage from Radiation

Any tissue can suffer acute radiation damage if the dose is high enough. Like the acute lethal radiation syndromes, the doses employed in bone densitometry are much too low to cause immediate tissue damage but it may be necessary for the densitometrist to reassure the patient that such damage cannot occur.

THE SKIN

Reddening of the skin or erythema, can follow a single dose of 300–1000 rads. Persons who have undergone radiation therapy for cancer may have experienced erythema in the course of their therapy. The erythema may be followed by a sloughing of the skin called desquamation. The dose that has been determined to cause erythema in about 50% of the persons exposed is 600 rads (6 Gy) (*8*). This is again a dose that is thousands of times higher than the doses given with bone densitometry and as a consequence, erythema of the skin after a bone density study simply cannot occur.

THE OVARIES AND TESTES

The sensitivity of the ovaries to radiation changes with age. The ovaries are very sensitive in childhood and again after the age of 30 up until menopause. A radiation dose of 10 rads in a mature woman can cause a delay in menstruation (*7*). A higher dose of 200 rads can cause temporary sterility and a dose of 500 rads can cause permanent sterility. It is also possible that doses of 25–50 rads can produce genetic mutations in the oocytes without killing the oocytes such that birth defects could result if fertilization of one of these damaged oocytes was to occur. For this reason, some authorities have recommended delaying attempts at pregnancy for several months after receiving such a radiation dose.

The testes are also sensitive to radiation. Doses of 10 rads have been reported to cause a decrease in the number of sperms. Two hundred rads can produce temporary sterility and 500 rads can cause permanent sterility. Like the oocytes in the ovary, genetic mutations in surviving sperm are reason to advise men receiving such radiation doses to avoid attempts at inducing pregnancy for several months.

THE BONE MARROW AND BLOOD

Irradiation of the bone marrow can cause a drop in the number of red cells, white cells, and platelets. The most sensitive cell appears to be the white blood cell known as the lymphocyte. Another type of white blood cell, the granulocyte, is less sensitive. The platelets, the small cells responsible for clot initiation, are less sensitive than white blood cells and the red blood cells are the least sensitive of all. Radiation doses generally in excess of 25 rads are required to see a demonstrable effect on the most sensitive lymphocytes. The effect on the lymphocytes is rapid and recovery is slow. The drop in the number of the other cell types is less rapid and recovery is quicker.

Late Effects of Ionizing Radiation

As a practical matter, the late effects of ionizing radiation are more of a concern to those who work with radiation rather than to patients who undergo an occasional X-ray. Although late effects can follow a single high dose of radiation, there is greater concern that they will follow low doses received over a prolonged period of time such as might be seen in a radiologic technologist or physician working with an X-ray device. A physician or technologist, who works solely with X-ray densitometry, again because of the very low doses employed, will not accumulate sufficient radiation exposure to be at increased risk for these late effects.

The late effect of greatest concern is cancer. As noted earlier, radiation has been implicated as a cause of almost every type of cancer. Leukemia, thyroid cancer, skin cancer, bone cancer, lung cancer, and liver cancer have been strongly associated with certain types of ionizing radiation. It is difficult to state with certainty the exact amount of radiation that one must receive to be at increased risk for cancer. What does seem clear is that this amount is hundreds or even thousands of times higher than the amount to which a dedicated DXA or SXA technologist or non-radiologist-physician densitometrist would be exposed. Even the most basic radiation safety program will reduce the risk further still.

RADIATION DOSES IN DENSITOMETRY

The X-ray tubes used in densitometry devices have kVp and mA characteristics that prohibit the generation of high doses of radiation. The kVp and mA specifications for various devices are listed in the descriptions of the devices in Chapter 15. The densitometrist and technologist should be familiar with the patient doses for the various types of X-ray densitometry studies and how these doses compare to other types of radiation exposure. The point here is not to minimize the importance of any radiation exposure but to put the amount of exposure in perspective to allay inappropriate fears about the exposure.

A certain amount of radiation exposure occurs as a result of sources in the environment. The effective dose from natural background sources is estimated to be 0.6–0.7 mrem/day (6–7 μSv/day) or about 240 mrem/year (2400 μSv/year) (*4*). Living at higher altitudes such as a mile above sea level increases this environmental radiation by about 5 mrem/mos (50 μSv/mos). A PA spine DXA pencil-beam study generally results in an effective dose of only 0.1 mrem (1 μSv). QCT bone density studies do result in slightly higher effective doses than pencil-beam DXA PA spine studies. A QCT spine study may have an effective dose of about 3 mrem (30 μSv). By comparison, the effective dose for

a PA chest X-ray is about 5 mrem (50 µSv) and for a plain lateral lumbar spine film, about 70 mrem (700 µSv). The radiation doses for various types of densitometry studies, as provided by the manufacturers, are listed in Chapter 15. In some cases these are the skin doses and in others, the effective dose equivalents.

The kVp and mA of an X-ray tube was noted earlier as determining the amount of radiation produced by the tube. The skin and effective doses for bone densitometry studies will vary depending upon the scan speed and scan length (9). The dose will increase as the scan speed decreases and the scan length increases. On some devices, the technologist has the option of selecting the mA as well as the scan speed and scan length. Although decreasing the mA and increasing the scan speed decreases the skin and effective radiation doses, it also tends to reduce the precision of the measurement.

Multiple bone density studies will also result in greater effective dose equivalents. For example, it is not uncommon for a woman to undergo both PA spine and proximal femur bone density study on the same day. The total effective dose for that patient is the sum of the effective doses for the individual studies. It also makes a difference whether the woman is pre- or postmenopausal. The effective dose during a DXA proximal femur study will be greater for a premenopausal woman because the effect on the ovaries must be considered. For a postmenopausal woman, the effect on the ovaries is largely irrelevant. Skin doses may be higher in some projections because of higher mA values used in that scan mode, but if the scan length is shorter and important tissues are no longer in the beam path, the effective dose can still be comparable to other projections using lower mA values with resulting lower skin doses.

Fan-array DXA scanners tend to have higher effective doses per scan than pencil-beam scanners. This is because of higher X-ray tube voltages and currents that are employed in these scanners. For example, the effective dose for a PA lumbar spine study of L1-L4 on a Hologic QDR-1000, a pencil-beam DXA device, is estimated to be 0.05 mrem (0.5 µSv) (10). On a QDR-4500, a fan-array DXA device, this dose may increase to 0.67 mrem (6.7 µSv) (11). While the effective dose on the fan-array scanner is more than 10 times higher than the pencil-beam scanner, it is still no more than the effective dose from natural background radiation for 1 day.

The effective dose during a QCT spine bone density, like that of its DXA counterpart, will depend upon the kVp and mA. It will also depend upon the number of slices made during the study and the thickness of those slices. Usually three slices are made that are 8–10 mm thick. As a consequence, the area that is irradiated is quite small and the effective dose is much lower than might otherwise be anticipated. If a scout scan precedes the actual QCT examination for localization purposes, the effective dose is the sum of the effective doses of the scout scan and the actual QCT study. This total effective dose has been estimated at 6 mrem (60 µSv) but this may be an underestimation (4,8).

Plain lumbar spine films are occasionally obtained either prior to or after DXA spine studies to aid in vertebral identification or the assessment of vertebral deformities. This adds significantly to the effective radiation dose received by the patient. The effective dose from a lateral lumbar spine film alone may be 60–70 mrem (600–700 µSv). If a lateral thoracic film is obtained as well, the effective dose will be even higher. It is imperative then that both the densitometrist and technologist learn to identify the vertebrae based on their appearance on the densitometry image, their spatial relationships to other skeletal structures, and the various probabilities of types of segmentation to avoid needing plain spine film *solely* for the purpose of vertebral labeling.

Morphometry and vertebral imaging without morphometry, performed on some of the newer DXA devices, may also reduce the need for plain films in the assessment of vertebral deformities. These types of DXA scans can be performed rapidly with a much lower effective dose than plain films of the thoracic or lumbar spine. In addition to the added clinical value of assessing vertebral deformities at the time of the bone density study, the lower effective dose makes this new DXA application a safer alternative to plain films. The assessment of vertebral deformities with DXA is called vertebral fracture assessment (VFA). The effective dose for VFA on the Hologic QDR 4500 has been estimated as 4.1 mrem (41 μSv) in one of the slower scan modes. On the Lunar Expert-XL, the effective dose for VFA has been estimated at 3.8 mrem (38 μSv). Both of these doses are considerably lower than the 60–70 mrem (600–700 μSv) for lateral thoracic and lumbar spine films. VFA imaging with Hologic's Radiographic Vertebral Assessment[TM] (RVA[TM]) and GE Lunar's Dual-energy Vertebral Assessment[TM] (DVA[TM]) can be performed at a fraction of the effective dose for plain lateral spine films. The clinical utility of VFA is discussed in Chapter 13.

RADIATION PROTECTION PROGRAMS

Radiation protection programs, even in bone densitometry facilities, are based on the premise that any unnecessary radiation exposure is unacceptable, no matter how small. The guiding principle of all such programs in known as "ALARA," which stands for "as low as reasonably achievable." There are three aspects to any radiation protection program. One aspect is the protection of the public. Another is the protection of the patient. The final aspect is the protection of the technologists and physicians involved in the operation of radiologic devices. Limits for radiation exposure have been set for members of the public and for radiation workers such as technologists and physicians. "Members of the public" refers to individuals not undergoing radiologic procedures and who do not work with radiation producing devices or substances. These limits have changed over the years to reflect the increasing knowledge about the effects of ionizing radiation. They also differ slightly between the National Council on Radiation Protection (NCRP) and the ICRP. A member of the public may receive a dose of 0.1 rem (1 mSv) per year, while a radiation worker may receive a maximum dose of 5 rem (50 mSv) per year and still be considered to have exposures within permissible limits *(5, 6)*. According to the ICRP, the maximum dose for a radiation worker in a year should average 2 rem (20 mSv) over a 5-year period with no more than 5 rem (50 mSv) in any one year (*6*). The lifetime effective dose limit in rems for a radiation worker should not exceed his or her age in years (*5*).[4] While it is extremely unlikely that a member of the public who is consistently in the vicinity of a DXA device or a radiation worker dealing solely with DXA devices would ever exceed those limits, radiation protection programs can be designed to ensure this.

The exact requirements for any radiation protection program may vary from state to state. It is imperative, therefore, that the state regulations be reviewed to ensure compliance. In facilities in which the only radiologic device is a DXA device the regulations

---

[4] When expressed as mSv, the lifetime cumulative dose for a radiation worker should not exceed $10 \times$ age in years.

pertaining to radiation safety are generally minimal. But even in the absence of any regulations there are some simple but appropriate measures that should be considered.

Protection of the Public

The first measure is to "post" the room in which the densitometer is kept. "Posting" means placing radiation warning signs on the entrances to the room and restricting access. This is generally a requirement when radiation levels are 5 mrem/hr or more in the area housing the X-ray device. With most densitometers, radiation levels won't approach this threshold. Nevertheless, it seems reasonable to place warning signs on the entrances to the room and restrict access. This is simply a matter of fully informing the public and protecting expensive medical devices. The traditional X-ray warning sign is shown in Fig. 5-1. The fan blades of the sign are normally magenta in color on a yellow background. Professionally produced signs are inexpensive and available from a variety of X-ray supply companies.
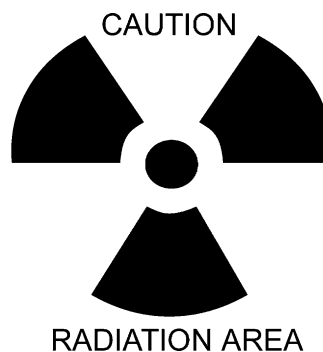
Fig. 5-1. A radiation warning sign. The fan blades are traditionally magenta on a yellow background.

Consideration should also be given to a radiation survey. A radiation physicist can document readings with a counter in and around the densitometer when the densitometer is in operation. Such readings should be taken at specific distances from the X-ray tube within the room and outside of the room. If there are offices or hallways that are frequented by the public that are next to the densitometry room, readings should be taken there as well. This would include offices on floors both above and below the densitometry room. The readings at each location should be documented in some way and signed and dated by the individual making the readings. It is quite likely that there will be no detectable counts on the counter when this is done. Nevertheless, this documentation can be invaluable in allaying unjustified fears about radiation exposure among members of the public.

Individuals who are not directly involved in the performance of a bone density test should not be in the densitometry room during testing. This is again an additional safeguard against even the smallest amount of unnecessary radiation exposure. If a radiation survey has been done so that no detectable counts have been documented at a specific distance from the X-ray tube, exceptions can be made on a case-by-case basis as long as the individual stays the documented safe distance away from the tube. If a radiation survey has not been done, allowing members of the public in the room is not advisable under any circumstances.

Protection of the Patient

The patient undergoing a bone density study is not technically considered a "member of the public" for radiation protection purposes. The densitometrist and technologist must assume the major role in protecting these individuals from unnecessary radiation. The physician-densitometrist is ultimately responsible for ordering the bone density study. It is the physician's responsibility, not the technologist's, to determine whether the bone density study is medically justified.

Patient's should always be asked if they have had a previous bone density study and if so, where, when, and on what type of machine. It is not uncommon for patient to have had a bone density study by any technique of the peripheral skeleton that suggests bone loss prompting the physician to request a study of the spine or proximal femur almost immediately. This is appropriate in many circumstances. On the other hand, if the patient is undergoing treatment for bone loss and being followed with bone density measurements, the bone density measurements should ideally be made on exactly the same machine every time. If the same machine is not used, then the next best choice is the same type of machine. If the patient's previous bone density study was at another facility on a different type of machine, it would be in the patient's best interests to return to that facility if possible. A test on another type of machine will not be interpretable in the context of judging a change in bone density *rendering that radiation exposure unjustified*. The timing of the repeat study is also an issue. Rarely are repeat studies justified more often than once a year at the spine and more often than every 2 years at the proximal femur. The most notable exception is patients receiving corticosteroids who may indeed undergo a follow-up spine bone density study after only 6 months. The appropriate timing of the repeat bone density study is determined by the precision of the measurement at the bone density facility at the particular skeletal site in question and by the expected rate of change in the bone density at that site. If the study appears to have been requested too soon, such that significant change in bone density is unlikely, then the medical justification for the test is lost. A test done too soon for the purposes of following therapy is a test that *exposes the patient to unnecessary radiation*.

It is also incumbent upon the technologist to perform every test correctly. This includes the correct choice of scan mode and speed when these attributes are modifiable, correct patient positioning, correct data acquisition and analysis. If it is not possible to position the patient correctly because of some arthritic or disease process, then the particular study should not be done. The physician should recognize that this is not the fault of the technologist. This is the expertise of the technologist in preventing the performance of an inappropriate bone density study.

Within the area there should also be signs that prompt a woman to disclose a pregnancy or the possibility of pregnancy. The wording for such a sign is shown in Fig. 5-2 in both English and Spanish. In clinical medicine, there is very little reason, if any, to perform a bone density study on a woman who is pregnant or who might be pregnant. *There are simply no emergency bone density studies*. Although it has been suggested that the effective doses are so low to the fetus that even asking about pregnancy is not necessary, there is simply no reason to abandon this precautionary measure (*12,13*). Although the sign is posted on the wall, it should not be assumed that the patient has read it. The patient should be asked the question directly, explaining that the risk is virtually negligible but that their safety is paramount and their response should be documented.

Pregnant?

If you are pregnant, or think you may be, tell the X-ray

technologist before having an X-ray taken.

———————————————————

¿Embarazo?

Si usted esta embarazada o cree que lo esta informe al

technologo antes de que le tomen los rayos-X.
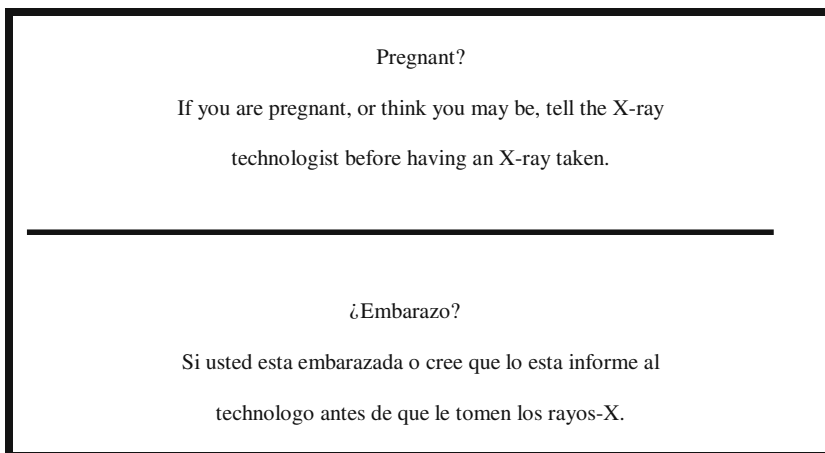
Fig. 5-2. A pregnancy warning sign in English and Spanish.

Another approach to this issue is the "10-day rule," which states that a radiologic exam should only be performed within 10 days of a woman's last menstrual period. In any case, it is far better to err on the side of caution in deciding whether to proceed with the examination; so, whenever there is any doubt about the possibility of a pregnancy, the test should be postponed.

Protective aprons, gonadal shields, and thyroid collars, while not routinely used in X-ray densitometry, should be available. On occasion it becomes clear that no amount of explanation will sufficiently allay a patient's fears about radiation. In that circumstance, a protective apron or shield should be made available to the patient if it will not interfere with the test. It is a simple matter with many of the peripheral X-ray densitometers to allow the patient to wear an apron during the study. This should always be used with children. In this circumstance, an apron with a thyroid collar is desirable. Gonadal shields can generally be used for men undergoing spine and proximal femur bone density studies without compromising either study.

Protection of the Technologist

The technologist who works solely with X-ray bone densitometers is unlikely to ever receive significant exposures. ALARA applies here as well, however. Protection for a technologist involves three concepts: time, distance, and shielding. Tracking radiation exposure over time is an additional safeguard.

Time, Distance, and Shielding

Longer scan times result in greater exposure, both for the patient and the technologist, for any given exposure rate. While the patient is exposed directly to the X-ray beam, the technologist is only concerned with any potential radiation leakage or scatter radiation. As noted previously the choice of the correct scan speed for a study is an integral part of radiation protection for the patient. It is also part of radiation protection for the technologist. Radiation leakage and scatter radiation are very low for X-ray densitometers, if they occur at all. The concept of ALARA demands, however, that the shortest appropriate scan speed be chosen for any particular study. This may not necessarily be

the shortest scan speed of which the machine is capable. It should simply be the shortest appropriate scan speed for that particular patient undergoing that particular study.

Shielding and distance can be considered together for X-ray densitometers in the context of the protection of the technologist. Because the leakage and scatter radiation are low to non-existent for pencil-beam DXA devices, the radiation exposure of a technologist should be well below permissible limits at distances of 3 ft (1 m) or more from the X-ray tube (*14*). For fan-array devices, this distance increases to about 10 ft (3 m). Ideally then, the technologist should remain in this minimum distance away from the X-ray tube when the machine is in operation. These recommended distances are based on the assumption that the densitometer is being maximally utilized. If studies are infrequent the potential radiation exposure of the technologist is greatly reduced. In any case, the technologist should not stand or sit within 3 ft of the X-ray tube when the machine is in operation. If this is not possible, a protective barrier should be utilized. When central DXA devices are considered, it should be recognized that the X-ray tube moves during patient scanning. The position of the tube during the entire scan must be considered in determining the necessary distance from the tube. This movement can also be used to the advantage of the technologist. For example, when the tube is homed to the head of the scan table, the technologist's workstation may be at an unacceptably short distance from the tube. When the tube is moved into position for a spine or proximal femur study, however, this distance will automatically increase. Similarly, additional distance may be obtained by performing right proximal femur studies rather than left.

PERSONNEL MONITORING DEVICES

Radiation monitoring devices, often called personnel monitoring devices, are inexpensive safeguards that allow a technologist to track exposure over a lifetime. A monitoring device does not protect the technologist from exposure, but the record that it provides can be used to ensure that the maximum permissible doses are not exceeded. These devices are generally required when it is anticipated that an individual may receive more than one-fourth of the maximum permissible dose. They should, however, be provided to any technologist who requests one, even if such exposures are not anticipated. The most common types of devices are film badges and thermoluminescent dosimeters (TLD).

Film badges have been in use since the mid-1940 s although they are giving way to TLDs. Special radiation dosimetry film is placed in the badge that is then worn for no more than 1 month. Film badges are not as sensitive to small exposures as are TLDs, which makes them less useful for the densitometry technologist. The TLD contains an entirely different material such as lithium fluoride. The TLD can generally be worn for up to 3 months at a time. Both the film badge and the TLD should be worn with their proper side to the front. Ideally they should be clipped to the collar, but a chest pocket or waistband is acceptable as long as a protective apron is not being worn.

Film badges and TLDs are obtained from certified laboratories to which they are then sent for analysis. The laboratory will provide a report back to the facility documenting the exposure of the wearer. A control badge or control TLD is provided with each shipment of new personnel monitors. This control should be kept at a location that is distant from the radiation-producing device. *The purpose of the control is to document any radiation exposure during the mailing of the personnel monitors*. This purpose is defeated if the control is kept in the room with the radiation producing device. Film badges and TLDs should not be exposed to extreme heat or high humidity, left in cars,

or worn during activities not related to the performance of the technologist's professional duties.

THE PREGNANT TECHNOLOGIST

If the technologist becomes pregnant, there are specific measures that can be taken to ensure the protection of the fetus, even though the risk is extraordinarily low if bone densitometry is the only potential source of occupational exposure. First, the technologist should inform her employer in writing that she is pregnant. A protective apron should be provided to be worn by the technologist. It is also reasonable for the technologist to wear a second personnel monitoring device at waist level under the apron to monitor exposure of the fetus. The maximum permissible dose to the fetus according the 1993 NCRP recommendations is 500 mrem (5 mSv) (5). It is extremely unlikely that a densitometry technologist would even remotely approach this level of exposure to a fetus but the concept of ALARA should always guide radiation protection efforts.

REFERENCES

1. Bushong SC. Concepts of radiation. In: Bushong SC, editor. Radiologic science for technologists. St. Louis: Mosby; 1993: 3–17.
2. Protection. In: Curry TS, Dowdey JE, Murry RC, editors. Christensen's physics of diagnostic radiology. Philadelphia: Lea & Febiger, 1990: 372–391.
3. National Council on Radiation Protection and Measurements. Ionizing radiation exposure of the population of the United States. [NCRP Report No. 93], 1–86.1993. Bethesda, NCRP. Recommendations of the National Council on Radiation Protection and Measurements.
4. Kalendar WA. Effective dose values in bone mineral measurements by photon absorptiometry and computed tomography. Osteoporos Int 1992; 2:82–87.
5. National Council on Radiation Protection and Measurements. Limitation of exposure to ionizing radiation. [NCRP Report No. 116], 1–88. 1993. Bethesda, NCRP. Recommendations of the National Council on Radiation Protection and Measurements.
6. ICRP. 2007 Recommendations of the International Commission on Radiological Protection. [ICRP Publication 103]. Ann ICRP 2007; 37:1–332.
7. Information on file. Alara, Inc., 2545 Barrington Court, Hayward, CA 94545.
8. Bushong SC. Early effects of radiation. In: Bushong SC, editor. Radiologic science for technologists. St. Louis: Mosby; 1993: 559–576.
9. Njeh CR, Fuerst T, Hans D, Blake GM, and Genant HK. Radiation exposure in bone mineral density assessment. Appl Radiat Isot 1999; 50:215–236.
10. Lewis MD, Blake GM, Fogelman I. Patient dose in dual X-ray absorptiometry. Osteoporos Int 1994; 1:11–15.
11. Patel R, Lewis MD, Blake GM, Batchelor S, et al. New generation DXA scanners increase dose to patient and staff. In: Current Research in Osteoporosis and Bone Mineral Measurement IV. London: British Institute of Radiology, 1996: 99.
12. Lloyd T, Eggli DF, Miller KL, Eggli KD, Dodson WC. Radiation dose from DXA scanning to reproductive tissues of females. J Clin Densitom 1998; 1:379–383.
13. Damilakis J, Perisinakis K, Vrahoriti H, et al. Embryo/fetus radiation dose and risk from dual X-ray absorptiometry examinations. Osteoporos Int 2002; 13(9):716–722.
14. Patel R, Blake GM, Batchelor S, Fogelman I. Occupational dose to the radiographer in dual X-ray absorptiometry: a comparison of pencil-beam and fan-beam systems. Br J Radiol 1996; 69:539–543.

6 Bone Density Data Among Technologies and Manufacturers

CONTENTS

The extraordinary advances in bone density technology over the last 40 years have enhanced the physician's ability to detect and manage metabolic bone disease. At the same time, these advances have created a dilemma as physicians have attempted to compare results obtained on early dual-photon (DPA) devices with today's dual-energy X-ray (DXA) devices. As DXA technology has advanced, data from pencil-beam systems are being compared with data from fan-array systems. Compounding this issue is that data from one manufacturer's DXA device may need to be compared to data from another manufacturer's device, which has been calibrated very differently. This situation is not dissimilar to circumstances created during the evolution of other types of quantitative measurement techniques used in clinical medicine. For example, the measurement of some parameter in blood may have initially been performed using one type of assay, only to be later replaced by a different assay. There may be different ranges of normal, depending upon the assay and even depending upon the laboratory. While it would be ideal for a patient being followed with a quantitative measurement technique for any reason to return year after year to the same laboratory to be tested using the same assay, this is not a reasonable expectation. In the context of bone densitometry, it is useful to have some ability to compare measurements originally made with DPA to measurements being made with DXA and between different types and makes of DXA devices. Although equations for making these types of comparisons are provided in this chapter, the margin of error is too great to justify monitoring changes in bone density with baseline and follow-up studies performed on DXA devices from different manufacturers if the situation is otherwise avoidable.

DPA TO DXA

With the passage of time, the need to compare older DPA results with DXA results has become less frequent. The means to do so is provided here more for historical interest than as a matter of necessity.

When DXA was approved for clinical use in 1988, it was immediately apparent that these systems offered substantial advantages over [153]gadolinium-based DPA systems. It was just as clear, however, that while the results obtained on any one patient with DXA were highly correlated with results from DPA, the BMD values were not identical. DPA is rarely used today having been replaced by DXA. Nevertheless, a DPA study may be part of a patient's medical record and circumstances may arise in which a physician would like to compare the older DPA results with those from today's modern DXA devices. Several studies have looked at the relationship between DPA and DXA values. Based on the findings from these studies, predictive equations were developed to allow the user to convert one device's values to the other. There is a margin of error in these predictions, which negates drawing quantitative conclusions about the magnitude of any change in BMD that may have occurred in the interval between the two studies. The comparisons do illustrate what a clinician might expect to see in such circumstances, however.

Hologic DXA and Lunar DPA

Kelly et al. (*1*) evaluated the relationship between BMD values in the spine in 85 individuals ranging in age from 21 to 78 years using the Lunar DP4, a [153]Gd DPA device, and the Hologic QDR-1000, a pencil-beam DXA device. The correlation for the measurement of spine BMD between the two devices was extremely good with $r = 0.98$. Not surprisingly, however, the two instruments did not give exactly the same results. Values obtained on the QDR-1000 were consistently lower than those obtained on the DP4. Equation 1 was derived to predict the DXA QDR-1000 values from the DPA DP4 values:

$$QDR_{BMD} = (0.84 \times DPA_{BMD}) - 0.033 \tag{1}$$

Pacifici et al. (*2*) evaluated lumbar spine BMD in 52 women using the Hologic QDR-1000 and the Lunar DP4. Again, the results were correlated with a statistically significant *r*-value of 0.94. The values in the spine obtained with the QDR-1000 were approximately 6.8% lower than those obtained with the DP4. The equation for predicting the DP4 spine value from the measurement of spine BMD with the QDR-1000 is shown in Equation 2:

$$DPA_{BMD} = 0.0242 + (1.0727 \times QDR_{BMD}) \tag{2}$$

A larger comparison trial was performed by Holbrook et al. (*3*) in which 176 individuals had lumbar spine bone density studies and 217 individuals had proximal femur bone density studies on both the Hologic QDR-1000 and the Lunar DP3 (an early DPA device). Once again, the values obtained with the DXA device were consistently lower than those obtained with the DPA device for both the spine and proximal femur. The average difference in this study was 16%. Nevertheless, the BMDs measured with the two devices were statistically correlated. In this study, equations were developed

to allow the conversion of values obtained with the Hologic QDR-1000 to Lunar DP3 values. Equations for the BMDs in the spine were given for individual vertebrae rather than an average and are shown in Equations 3, 4, 5, 6, 7, 8, and –9:

$$\text{L1 DP3}_{BMD} = 0.300 + (0.878 \times \text{L1 QDR}_{BMD}) \tag{3}$$

$$\text{L2 DP3}_{BMD} = 0.239 + (0.944 \times \text{L2 QDR}_{BMD}) \tag{4}$$

$$\text{L3 DP3}_{BMD} = 0.205 + (0.970 \times \text{L3 QDR}_{BMD}) \tag{5}$$

$$\text{L4 DP3}_{BMD} = 0.152 + (1.005 \times L4 \text{ QDR}_{BMD}) \tag{6}$$

$$\text{Neck DP3}_{BMD} = 0.1333 + (0.977 \times \text{Neck QDR}_{BMD}) \tag{7}$$

$$\text{Ward's DP3}_{BMD} = 0.146 + (0.983 \times \text{Ward's QDR}_{BMD}) \tag{8}$$

$$\text{Trochanter DP3}_{BMD} = 0.012 + (1.104 \times \text{Trochanter QDR}_{BMD}) \tag{9}$$

Lunar DXA and Lunar DPA

BMD values in the spine obtained with the Lunar DPX, the first clinically available DXA device from what is now GE Healthcare, were originally reported as being approximately 3% lower than those that would be obtained with the earlier gadolinium-based dual-photon absorptiometer, the Lunar DP3. This finding was based on an initial study of 41 subjects by Mazess et al. (*4*).

Lees and Stevenson (*5*) studied 70 subjects (2 men and 68 women) who underwent PA spine and proximal femur bone density studies using the Lunar DPX and Lunar DP3. The results between the two instruments were statistically significantly correlated. The *r*-value ranged from 0.96 at Ward's area in the proximal femur to 0.98 for the L2–L4 BMD. The BMD values in the lumbar spine were again lower on the DXA than on the DPA device. The equation for predicting the L2–L4 BMD for the DPX from a measurement of L2–L4 on the DP3 is shown in Equation 10:

$$\text{L2} - 4\text{DPX}_{BMD} = -0.110 + (1.052 \times \text{L2} - \text{L4 DP3}_{BMD}) \tag{10}$$

There was less difference between the BMD values in the femoral neck, Ward's area, and the trochanter obtained on the DPX and DP3 than in the lumbar spine. Unlike the spine, the DPX values at these sites in the proximal femur were slightly *higher* than the DP3 values for the same sites. Equations 11, 12, and 13 were used to predict the values that would be anticipated on the DPX from measurements of the proximal femur sites on the DP3.

$$\text{Neck DPX}_{BMX} = 0.028 + (1.002 \times \text{Neck DP3}_{BMD}) \tag{11}$$

$$\text{Ward's DPX}_{BMD} = 0.004 + (1.031 \times \text{Ward's DP3}_{BMD}) \tag{12}$$

$$\text{Trochanter DPX}_{BMD} = 0.043 + (0.955 \times \text{Trochanter DP3}_{BMD}) \tag{13}$$

Hologic DXA, Lunar DXA, and Lunar DPA

The general relationship between Lunar DP4 values, Hologic QDR-1000, and Lunar DPX values was summarized in a study from McClung and Roberts (*6*). Ninety-three

Table 6-1
The Ratio of BMD Values Obtained on the Lunar DP4, Lunar DPX,
and Hologic QDR-1000

Site	DPX/DP4	QDR/DP4	QDR/DPX
AP Lumbar Spine	0.90	0.78	0.87
Femoral neck	1.02	0.83	0.82
Ward's area	1.01	0.73	0.72
Trochanter	0.99	0.83	0.85

Calculated from data from ref. (6).

subjects underwent bone density measurement on all three machines of the PA spine and proximal femur. The ratio of mean values obtained for each combination of machines is shown in Table 6-1. Note that the PA spine values obtained with either DXA device are lower than those obtained with the DP4. The three regions in the proximal femur are lower when obtained with the QDR-1000 compared to the DP4 but are slightly higher than the DP4 in the femoral neck and Ward's area when obtained with the DPX. The Hologic QDR-1000 values are consistently lower than the Lunar DPX values at all sites.

Although these equations can be used to predict DXA values from earlier DPA measurements and vice-versa, the margin of error in these equations limits their utility to *exactly* predict BMD. They can be used to *approximate* the BMD, however. This is often reassuring to the patient who has previously had a DPA study and is now undergoing a DXA study. Even if there has been no change in the BMD over time, the spine BMD on the DXA study is expected to be lower. If the DXA device is a Hologic or Cooper Surgical Norland DXA device, the BMDs in the proximal femur are also expected to be lower. If the DXA device is a Lunar device, the BMDs in the proximal femur may be slightly higher.

DXA: FROM LUNAR TO HOLOGIC TO NORLAND

The central DXA devices from all the major manufacturers have inherently superb accuracy and precision in quantifying the bone density at virtually any skeletal site. The BMD in g/cm^{2}obtained on any one machine, however, will not be identical to the BMD obtained on a device from a different manufacturer. This is because they are calibrated differently. Comparison studies using combinations of machines provide conversion equations for the measurement of bone density on one device to the anticipated value on another device.

The Hologic QDR-1000, the Lunar DPX, and the Norland XR-26 were compared in an in vitro study by Arai et al (7), Solutions of various concentrations of potassium phosphate enclosed in an acrylic resin and submerged in water were used to simulate bone and soft tissue. The various concentrations of potassium phosphate were measured on each of the three machines to determine both the accuracy of the machines and the correlation between the BMDs measured by each of the machines. Each machine accurately measured the BMD. The correlation between each pair of machines was highly statistically significant with an *r*-value of 0.9999. The measured values were not identical, however. Values obtained with the Lunar DPX were 8.08% higher than those obtained

with the Norland XR-26 and 4.96% higher than those obtained with the Hologic QDR-1000. The QDR-1000 values were 2.96% higher than those obtained with the XR-26. An anthropomorphic Hologic spine phantom was also used in this study to compare the 3 DXA devices. The spine phantom was scanned 10 times on each manufacturer's machine. The BMD values obtained on the Lunar DPX were 16% higher than those obtained on the XR-26, while the values obtained on the QDR-1000 were 1.5% lower than the XR-26.

Hologic DXA and Norland DXA

In vivo comparisons of spine measurements made using the Norland XR-26 and the Hologic QDR-1000 were conducted by Lai et al. (*8*) in 65 subjects. The correlation for BMD at the spine was 0.990 and was highly significant. BMDs in g/cm^2 obtained on the Norland XR-26 tended to be lower than those obtained on the QDR-1000. Based on this study, Equation 14 resulted for predicting the Hologic BMD from the measurement of BMD on the Norland XR-26:

$$\text{Hologic QDR 1000 Spine}_{\text{BMD}} = -0.1 + \left(1.09 \times \text{Norland XR} - 26\,\text{Spine}_{\text{BMD}}\right) \quad (14)$$

Lunar DXA and Hologic DXA

The Lunar DPX and the Hologic QDR-1000 were compared in a study of 46 women by Pocock et al. (*9*). These women underwent lumbar spine and proximal femur studies on both machines on the same day. The correlations were extremely good with *r*-values of 0.98, 0.94, 0.96, and 0.96 for the lumbar spine, femoral neck, Ward's area, and the trochanter, respectively. The absolute BMD values were 16% lower on the QDR-1000 in the spine when compared to the DPX and 17% lower in the femoral neck. The equation for predicting the QDR BMD in the femoral neck based on a measurement of BMD in the femoral neck on the Lunar DPX is shown in Equation 15:

$$\text{QDR Femoral Neck}_{\text{BMD}} = 0.007 + (0.76 \times \text{DPX Femoral Neck}_{\text{BMD}}) \quad (15)$$

This is in keeping with the study from McClung and Roberts (*6*) in which the ratios of Hologic QDR values to Lunar DPX values at these sites as seen in Table 6-1 suggested similar findings.

STANDARDIZATION OF ABSOLUTE BMD RESULTS

It is clear from the extremely good correlations between DXA measurements of BMD at the spine and proximal femur using the central devices from the major manufacturers in the United States that these devices are indeed measuring the same thing. The BMD values in g/cm^2 obtained on the various machines may differ markedly because of differences in calibration and bone edge detection algorithms among the machines. Because of this, there has been a great deal of interest in developing a standardized BMD to which all DXA results could be converted, regardless of which manufacturer's machine was used.

Table 6-2
Conversion Formulas for BMDs of the AP Spine Between DXA Devices

Hologic QDR-2000 Spine$_{BMD}$ = (0.906 × Lunar DP - L Spine$_{BMD}$) – 0.025
Hologic QDR - 2000 Spine$_{BMD}$ = (0.912 × Norland X R 26 Spine$_{BMD}$) + 0.088
Lunar DPX-L Spine$_{BMD}$ = (1.074 × Hologic QDR 2000 Spine$_{BMD}$) + 0.054
Lunar DPX-L Spine$_{BMD}$ = (0.995 × Norland XR 26 Spine$_{BMD}$) + 0.135
Norland XR-26 Spine$_{BMD}$ = (0.983 × Lunar DPX-L Spine$_{BMD}$) – 0.112
Norland XR-26 Spine$_{BMD}$ = (1.068 × Hologic QDR 2000 Spine$_{BMD}$) – 0.070

Adapted from ref. (*10*) with permission from the American Society for Bone and Mineral Research.

Standardization of Central DXA Absolute BMD Values

In November 1990, the major manufacturers of DXA equipment agreed to work together in the area of standards as part of an international committee, known as the International Committee for Standards in Bone Measurement. Under the auspices of this committee a study of 100 healthy women (*10*) was performed in which each of the women underwent PA spine and proximal femur studies on the Hologic QDR-2000, the Norland XR-26 Mark II, and the Lunar DPX-L. The women ranged in age from 20 to 80, with an average age of 52.6 years. The difference in PA lumbar spine BMD was greatest between the Norland XR-26 and the Lunar DPX-L, averaging 0.118 g/cm^2 or 12.2%. The average difference between the Lunar DPX-L and the Hologic QDR-2000 was 0.113 g/cm^2 or 11.7%. The average difference in BMD at the PA lumbar spine between the Norland XR-26 and the Hologic QDR-2000 was the smallest at only 0.012 g/cm^2 or 1.3%.

Based on this data, equations were derived for the conversion of PA lumbar spine BMD obtained on any one of these manufacturer's machines to the BMD that would be expected to be obtained on each of the other two. The equations for each of the three pairs of scanners are shown in Table 6-2.

In order to derive an equation to convert each manufacturer's reported BMD to a standardized BMD (sBMD), the European Spine Phantom (ESP)[1] was scanned on each of the three devices. Equations were developed based on the BMD value for the central vertebra of the ESP averaging 1000 mg/cm^2 when scanned on each of the devices. These formulas are shown in Table 6-3. In November 1994, the Committee for Standards in DXA approved these formulas for the standardization of PA spine BMD values (*11*). Using these formulas, a PA spine sBMD obtained by scanning a patient on a Norland, Hologic or Lunar DXA device should be within 2–5% of the sBMD that would be obtained when the patient was scanned on either of the other two devices.

The value for the sBMD is multiplied by 1000 to convert it to mg/cm^2 rather than reporting it as g/cm^2. This serves to readily distinguish the sBMD from the non-standardized value. In other words, if the BMD obtained in the spine on a Lunar DPX-L is 0.985 g/cm^2, this value becomes 938 mg/cm^2 when reported as the sBMD (0.985 × 0.9522 = 0.9379 g/cm^2 × 1000 = 938 mg/cm^2). Using these formulas to convert the average spine BMD in the study population to the sBMD, the differences in

---

[1] See Chapter 4 for a discussion of the ESP.

<div align="center">

Table 6-3

Formulas for the Conversion of Manufacturer-Specific PA Spine BMDs to the Standardized BMD (sBMD)

</div>

$sBMD_{SPINE} = 1000(1.0761 \times \text{Norland XR-26 BMD}_{SPINE})$
$sBMD_{SPINE} = 1000(0.9522 \times \text{Lunar DPX-L BMD}_{SPINE})$
$sBMD_{SPINE} = 1000(1.0755 \times \text{Hologic QDR-2000 BMD}_{SPINE})$

Adapted from the (*10*) with permission from the American Society for Bone and Mineral Research.

BMD between the three machines were greatly reduced. Instead of an average difference of 12.2% between the Norland and Lunar values, the difference in the sBMD was only 2.8%. The difference between Hologic and Lunar was reduced to 2.2% and the difference between Hologic and Norland was reduced to 2.7%.

Conversion formulas were also developed by Genant et al. (*10*) for the femoral neck for each pair of scanners. These formulas are shown in Table 6-4.

<div align="center">

Table 6-4

Conversion Formulas for BMDs in the Femoral Neck Between DXA Devices

</div>

$\text{Hologic QDR-2000 Neck}_{BMD} = (0.836 \times \text{Lunar DPX-L Neck}_{BMD}) - 0.008$
$\text{Hologic QDR-2000 Neck}_{BMD} = (0.836 \times \text{Norland XR 26 Neck}_{BMD}) + 0.051$
$\text{Lunar DPX-L Neck}_{BMD} = (1.013 \times \text{Hologic QDR 2000 Neck}_{BMD}) + 0.142$
$\text{Lunar DPX-L Neck}_{BMD} = (0.945 \times \text{Norland XR 26 Neck}_{BMD}) + 0.115$
$\text{Norland XR-26 Neck}_{BMD} = (0.961 \times \text{Lunar DPX-L Neck}_{BMD}) - 0.037$
$\text{Norland XR-26 Neck}_{BMD} = (1.030 \times \text{Hologic QDR 2000 Neck}_{BMD}) + 0.058$

Adapted from ref. (*10*) with permission from the American Society for Bone and Mineral Research.

In December of 1996, the International Committee for Standards in Bone Measurement[2] approved formulas for the sBMD for the total femur region of interest (*12*). The total femur region of interest includes the femoral neck, Ward's area, the trochanter, and the shaft of the proximal femur. This region appears to have equal diagnostic utility but better precision than the femoral neck. The formulas for the sBMD for the total femur shown in Table 6-5 were based on the work by Genant et al. (*10*), from which the formulas for sBMD of the spine were also derived. The sBMD from any one of the three central DXA devices should fall within 3–6% of the sBMD on any of the other two.

<div align="center">

Table 6-5

Formulas for the Conversion of Manufacturer-Specific Total Femur BMD to the Standardized BMD (sBMD)

</div>

$sBMD_{TOTAL\ FEMUR} = 1000\ [(1.008 \times \text{Hologic BMD}_{TOTAL\ FEMUR}) + 0.006]$
$sBMD_{TOTAL\ FEMUR} = 1000[(0.979 \times \text{Lunar BMD}_{TOTAL\ FEMUR}) - 0.031]$
$sBMD_{TOTAL\ FEMUR} = 1000[(1.012 \times \text{Norland BMD}_{TOTAL\ FEMUR}) + 0.026]$

Adapted from ref. (*12*) with permission from the American Society for Bone and Mineral Research.

[2] Formerly the Committee for Standards in DXA.

Standardization of DXA BMD Results for the Femoral Neck, Trochanter, and Ward's Area

In 2001, Lu et al. (*13*) developed equations for an sBMD for the femoral neck, trochanter, and Ward's area based on information obtained from studies of the same 100 women whose data was previously used to create formulas for the sBMD of the spine and total femur (*10, 12*). The authors developed site-specific standardization formulas for the hip sub-regions. They compared the utility of the sub-region formulas in reducing the disparity in BMD results among the three manufacturers' devices to that of the total femur standardization formulas developed previously when both sets of formulas were applied to the hip sub-regions. The authors applied the formulas to bone density data from a multicenter clinical trial involving 3139 postmenopausal women. Bone density data was acquired on 51 Hologic, 17 Lunar, and 2 Norland DXA scanners. Table 6-6 shows the difference between scanners for each sub-region depending on whether no calibration, the total femur or sub-region calibration was used. The site-specific sub-region formulas were clearly superior in reducing the disparity between the machine-specific sub-region values compared to the total femur standardization formulas. As shown in Table 6-6, the overall variation in values at the femoral neck that appeared to be the result of using different manufacturers' scanners was 42%. Use of the total hip sBMD formula reduced this variation to 20% while use of the specific femoral neck sBMD formula reduced the variation to 0.2%. The basic formula for calculating the sBMD for the various regions in the proximal femur from the manufacturer's data is shown in Equation 16:

$$sBMD = 1000\,[a + (b \times BMD)] \qquad (16)$$

Table 6-6
Comparison of Baseline Mean BMD Among Manufacturers With and Without Standardization by Different Formulas

ROI	BMD	Hologic-Lunar	Hologic-Norland	Lunar-Norland	R^2 (%)[a]	p Value[b]
		Mean BMD Differences Between Scanner Types (mg/cm²)				
FN	No calibration	−130[c]	−64[c]	66[c]	42	<0.001
	Total hip calibration	−73[c]	−53[c]	−20[c]	20	<0.001
	FN calibration	6	5	0	0.2	0.0795
TR	No calibration	−96[c]	−31[c]	65[c]	21	<0.001
	Total hip calibration	−41[c]	−20[c]	21[c]	5	<0.001
	TR calibration	16[c]	4	12	0.6	<0.001
W	No calibration	−165[c]	−69[c]	95[c]	43	<0.001
	Total hip calibration	−112[c]	−59[c]	53[c]	24	<0.001
	W calibration	29[c]	7	−22[c]	2.6	<0.001

FN, femoral neck; TR, trochanter; W, Ward's area.
[a]R^2 is the percentage of BMD variation explained by scanner types with a lower value meaning less variation among manufacturers in the measured value.
[b]p value is based on F-test for the effect of manufacturers.
[c]p<0.001
Reproduced with kind permission from Springer Science + Business Media from Lu et al. (*13*).

Table 6-7
Standardization Formulas for Hip Sub-Regions and Total Hip

Manufacturer	Parameter	FN	TR	W	Total Hip
Hologic	a	0.019	–0.017	0.101	0.006
	b	1.087	1.105	0.940	1.008
Lunar	a	–0.023	–0.042	–0.106	–0.031
	b	0.939	0.949	0.980	0.979
Norland	a	0.006	0.057	0.001	0.026
	b	0.985	0.961	1.091	1.012

FN, femoral neck; TR, trochanter; W, Ward's area.
Reproduced with kind permission from Springer Science + Business Media from Lu et al. (*13*).

In this formula, a and b are regression parameters and are shown in Table 6-7 for each scanner type and sub-region. Multiplying by 1000, as shown in the formula, converts the original units of g/cm^2 to mg/cm^2 as was done for the sBMD of the PA spine and total femur.[3] The actual standardization formulas for the three sub-regions in the proximal femur are shown in Table 6-8. The equation from Lu et al. (*13*) is the equation used in the FRAX^{TM} Patch from the Oregon Osteoporosis Center that is discussed in Chapter 10.

Table 6-8
Standardization Formulas for Proximal Femur Sub-Regions

$$sBMD_{FEMORAL\ NECK} = 1000\ [(1.087 \times Hologic\ BMD_{FEMORAL\ NECK}) + 0.019]$$
$$sBMD_{FEMORAL\ NECK} = 1000\ [(0.939 \times Lunar\ BMD_{FEMORAL\ NECK}) - 0.023]$$
$$sBMD_{FEMORAL\ NECK} = 1000\ [(0.985 \times Norland\ BMD_{FEMORAL\ NECK}) + 0.006]$$
$$sBMD_{TROCHANTER} = 1000\ [(1.105 \times Hologic\ BMD_{TROCHANTER}) - 0.017]$$
$$sBMD_{TROCHANTER} = 1000\ [(0.949 \times Lunar\ BMD_{TROCHANTER}) - 0.042]$$
$$sBMD_{TROCHANTER} = 1000\ [(0.961 \times Norland\ BMD_{TROCHANTER}) + 0.057]$$
$$sBMD_{WARD'S} = 1000\ [(0.940 \times Hologic\ BMD_{WARD'S}) + 0.101]$$
$$sBMD_{WARD'S} = 1000\ [(0.980 \times Lunar\ BMD_{WARD'S}) - 0.106]$$
$$sBMD_{WARD'S} = 1000\ [(1.091 \times Norland\ BMD_{WARD'S}) + 0.001]$$

Derived from Lu et al. (*13*).

Standardization of Forearm DXA Results

The difficulty in creating an sBMD for forearm bone density is compounded by the multitude of potential sites in the forearm and the different definitions of those sites among the various manufacturers of forearm measurement devices. Shepherd and colleagues (*14*) have developed standardization equations for the ultradistal, mid, and proximal forearm for six devices, five of which employ DXA. The sixth device utilized radiogrammetry. The study was commissioned by the International Committee of Standards in Bone Measurement. The DXA devices used in the study were the Hologic

---

[3] The terms total hip and total femur are used interchangeably. Neither is exactly correct. Total femur is preferred but total hip is more commonly used.

QDR-4500A, the Osteometer DTX-200, the Aloka DCS-600EX,[4] the Lunar PIXI, and the Norland pDEXA. The Pronosco X-posure System,[5] which utilized computer-assisted radiogrammetry was the sixth device used.

One hundred and one women, age 20–80 years, were studied on each of the six devices. There were 13–19 subjects per decade. Women were excluded if they were pregnant, had a history of distal radial fracture, or had any bone diseases other than osteoporosis. Seventy-four percent of the women were white.

The regions of interest on the forearm with the six devices in question varied considerably.[6] The PIXI and the DTX-200 measured only one region of interest (ROI) on the forearm and while similar, the two regions were not identical in location or size. Similarly, the pDEXA measures a distal and proximal ROI while the QDR-4500A measures three regions of interest, two of which are similar, but not identical to the distal and proximal regions found on the pDEXA. There was no attempt to alter the manufacturers' ROIs in this study. In order to develop equations for all six devices for the ultradistal, mid, and proximal forearm, the single ROI from the PIXI and DTX-200 was used for all three sites. The distal ROI on the pDEXA was used in the standardized BMD equation for the mid region as well as the distal region. The standardized BMD equations for the 4 DXA devices available in the United States are shown in Table 6-9. The authors noted that these equations are specific for the devices in this study. Unlike the sBMD for the spine and proximal femur, the sBMD values for the forearm sites are reported in the original units of the measurement for the particular device.

Table 6-9
**Standardization Equations for the Ultradistal, Mid and Proximal
Forearm for 4 DXA Devices**

suBMD = (0.945 × PIXI BMD) + 0.015
suBMD = (1.158 × Hologic Radius + Ulna Ultradistal BMD) – 0.019
suBMD = (0.802 × Osteometer BMD) + 0.071
suBMD = (1.027 × Norland Distal BMD) + 0.084
smBMD = (1.011 × PIXI BMD) + 0.033
smBMD = (0.894 × Hologic Radius + Ulna Mid BMD) – 0.030
smBMD = (0.856 × Osteometer BMD) + 0.094
smBMD = (1.106 × Norland Distal BMD) + 0.105
spBMD = (1.091 × PIXI BMD) + 0.119
spBMD = (0.861 × Hologic Radius + Ulna one-third BMD) + 0.020
spBMD = (0.917 × Osteometer BMD) + 0.188
spBMD = (0.596 × Norland Proximal BMD) + 0.114

suBMD, standardized BMD for the ultradistal region; smBMD, standardized BMD for the mid region; spBMD, standardized BMD for the proximal region.

Adapted from ref. (*14*) with permission of the American Society for Bone and Mineral Research.

[4] This device is not available in the United States.

[5] This device is no longer sold in the United States. It has been replaced by dxr-online[TM] which utilizes the same technology for analysis of digital X rays sent via the Internet.

[6] See Chapter 2 for a discussion of the various regions of interest in the forearm.

The Utility of the sBMD

The sBMD is attractive as a means of comparing a BMD value obtained on one manufacturer's device with a BMD value obtained on another. This is useful in large population studies and clinical trials in which devices from several manufacturers must be used. The root-mean-square error in the calculation of the sBMD is estimated to be 4% for the PA spine and total femur and even larger for the proximal femur sub-regions (*13*). This means that the error in these conversions is simply too large to base important clinical decisions on the comparison of sBMD values obtained on different devices for an individual when monitoring changes in bone density in an individual on therapy. The development of the sBMD was a worthy effort but its clinical utility is limited.

DXA: MACHINE TO MACHINE WITHIN MANUFACTURERS

It is not uncommon for patients to have had a DXA study at another facility that must be compared to a DXA study at a second facility. Even if the studies have been performed on DXA machines from the same manufacturer, the results may vary slightly. If the machines have been properly calibrated and maintained using good quality control measures, the differences should be minimal. In a study performed at three different locations, three men and two women underwent duplicate total body and lumbar spine bone density studies at each location (*15*). The studies were performed on a Lunar DPX-L at one site and on a Lunar DPX at the other two locations. The differences in total body BMD among the three locations were less than 1.2% and the differences in lumbar spine BMD were less than 1.7%. When this is expressed as the percent coefficient of variation (%CV)[7] between testing locations, the %CV for total body BMD between sites was 0.7% and for the lumbar spine, 1.4%. Two similar studies using the Hologic QDR-1000 also demonstrated good agreement between BMD studies performed at different locations using Hologic DXA devices. The %CV at the spine between 13 locations in one study was 1.4% for the spine and 2.1% for the hip (*16*). In a second study, the %CV at the spine between eight locations for in vitro phantom measurements was 0.92%. For in vivo measurements on two subjects, the %CV at the spine was 3.68 and 1.85% at the femoral neck (*17*). Kolta et al. (*18*) studied the accuracy and precision of 62 DXA densitometers (51 Hologic, 11 Lunar) using the European Spine Phantom. The phantom was scanned five times without repositioning on each densitometer. In general, the results among devices from the same manufacturer were highly comparable, with in vitro 95% confidence limits of agreement of ± 0.026 g/cm^2 for Hologic devices and ± 0.025 g/cm^2 for Lunar devices. At the extreme, however, differences between devices from the same manufacturer were as much as 5.4% for Hologic and 3.6% for Lunar. While some of the inter-site variation seen in in vivo studies may be due to differences in positioning or analysis, differences in machine calibration may explain the variation seen in in vitro studies. Kolta et al. noted that only 36% of the devices in their study were calibrated within ± 0.5% and only 60% were calibrated within ± 1%. In contrast, Gaither et al. (*19*) found that 73% of 128 DXA devices (61 Hologic, 67 Lunar) were calibrated within

---

[7] See Chapter 3 for a discussion of the %CV.

±0.5% and 91% were within ±1.0%. These authors also noted a worst-case difference of 5% between devices from the same manufacturer.

These types of differences between machines from the same manufacturer are generally not large enough to result in different predictions of fracture risk. But because the diagnostic cut points used by the World Health Organization[8] are quite specific, a difference in BMD that results in a change in the T-score of as little as 0.1 can alter the diagnosis. The greater problem is in the serial assessment of changes in BMD. Current guidelines from the International Society for Clinical Densitometry (ISCD) (20) note that comparisons of BMDs obtained on different machines simply cannot be done unless the machines are cross-calibrated. For machines from the same manufacturer utilizing the same technology (for example, two fan array devices from the same manufacturer) ISCD recommends scanning a phantom 10 times with repositioning on each machine when the machines are within the same facility. If greater than a 1% difference is observed, it is recommended that the manufacturer be contacted to re-calibrate one machine if possible, to bring it within 1% or less of the other machine. If the machines are at different facilities, an in vivo cross-calibration study is preferable, but some type of cross-calibration must be done. Otherwise, no reasonable comparison can be made. Clearly inter-site variation between machines from the same manufacturers can be much larger than that indicated here if strict quality control and consistently correct positioning and analysis procedures are not observed at the densitometry facility.

DXA: PENCIL-BEAM TO FAN-ARRAY

The latest generation of central DXA scanners are fan-array scanners, which were first introduced with the Hologic QDR-2000 (21). The terminology reflects a change in design in these scanners in which a fan-shaped beam is projected through an entire scan line and captured by an array of detectors. This is markedly different from earlier pencil-beam devices in which a very narrow X-ray beam was projected in a plane that was perpendicular to the region of interest. This narrowed beam moved in tandem with a single detector in a rectilinear path across the region of interest. Fan-array technology such as found on the Hologic QDR-4500 and the Lunar Prodigy produces extraordinary skeletal image resolution and faster scan speeds. The extraordinary images such as those seen in Figs. 1-12, 1-13, 1-14, and 1-15 are utilized for skeletal morphometry. Dual-energy Vertebral Assessment™ (DVA™) and Instant Vertebral Assessment™ (IVA™) images of the spine are approved by the Food and Drug Administration for structural diagnosis, such as fracture. The physical dimensions of the proximal femur can be accurately and precisely measured with today's sophisticated computers as well. Some of these dimensions have been shown to be independent predictors of hip fracture risk as discussed in Chapter 13.

The difference in design between pencil-beam systems and fan-array systems introduced an additional issue in comparing data generated on any manufacturer's pencil-beam device and comparing it to data generated on the same manufacturer's fan-array device. Because the imaging geometry is different, there can be some magnification of

---

[8] See Chapter 9 for a discussion of the World Health Organization criteria for the diagnosis of osteoporosis based on the measurement of BMD.

the image that is dependent upon the distance of the region of interest from the beam and detectors and the angle of the beam. Theoretically, the BMC and area measurement should be altered to a similar degree causing a minimal effect on BMD (because BMD is calculated by dividing BMC by area). The effect has been estimated as approximately 3%/cm for BMC and area but < 0.5%/cm for BMD (*22*, *23*, *24*).

Using the Hologic spine phantom, Eiken et al. (*25*) compared the measurement of area, BMC, and BMD on the Hologic QDR-1000/W, a pencil-beam device, with that obtained on the Hologic QDR-2000, a fan-array device. As predicted, the BMC and area increased to a similar degree leaving the BMD unchanged when measurements were obtained on the QDR-2000 compared to the QDR-1000/W. Blake et al. (*23*) confirmed these findings using both in vitro spine phantom and in vivo spine and hip measurements on 20 subjects.

In a larger study, Faulkner et al. (*26*) evaluated the differences in BMD in the spine and proximal femur using the Hologic QDR-1000/W and the Hologic QDR-2000. Sixty-nine women underwent PA spine and proximal femur studies on both devices. At the spine, there were no statistically significant differences observed in the BMC, area, or BMD between the pencil-beam and fan-array device, although the actual BMD obtained with the fan-array device was slightly higher. In the proximal femur, BMD values obtained with the fan-array device were again all slightly higher than those obtained with the pencil-beam device. Although the differences in BMD for all regions in the proximal femur except the femoral neck were *statistically* significant between the two devices, the *actual* differences were *extremely small*. Similarly, BMC and area measurements were all slightly increased when obtained on the fan-array device for all regions in the proximal femur with the exception of the femoral neck.

Mazess and Barden (*27*) compared results obtained in 111 individuals on the Prodigy, a fan-array device, and the DPX-IQ, a pencil-beam device. The average values from duplicate scans on the Prodigy were compared to single scans on the DPX-IQ. The mean difference in PA spine BMD between the two densitometers was 0.002 g/cm^2. The mean difference in both femoral neck and total body BMD was 0.006 g/cm^2. These values were less than 1% of the mean BMDs in the various regions.

The differences in BMD between pencil-beam and fan-array devices are not large enough to be clinically significant in terms of the accuracy of the measurement or comparisons to the reference databases developed using pencil-beam devices. The differences can introduce an additional source of error into serial measurements, however. This potential change in BMD, which is the sole result of changing from a pencil-beam to a fan-array system must be kept in mind if the physician attempts to compare scans obtained on a patient over a period of time that were acquired using first one device and then the other. Once again, this really should not be done in the absence of cross-calibration of the machine.

REFERENCE DATABASES

Two of the most common applications of bone densitometry are the diagnosis of osteoporosis and the assessment of fracture risk. These applications depend upon comparisons of the BMD to the reference database that is supplied by the manufacturer of the bone densitometry equipment. The diagnosis of osteopenia or osteoporosis, using

World Health Organization criteria, depends upon comparing the patient's BMD to the average peak BMD of the young-adult and noting how many standard deviations below this value the patient's value lies. In other words, the diagnosis depends on the T-score.[9] Most fracture risk data in the medical literature is presented as the increase in relative risk per standard deviation decline in bone density from the age-adjusted mean bone density for the population that was studied.[10] Relative fracture risk for an individual patient is often calculated using this published data and the T-score or the *z*-score, although neither is technically correct. Lifetime or 10-year fracture risk probabilities are determined using a patient's T-score. Qualitative assessments of fracture risk typically utilize T-score cut points that coincide with the WHO criteria for the diagnosis of osteopenia and osteoporosis. Diagnosis and fracture risk predictions depend not just on the measurement of bone density but also on the standard scores that are determined from comparisons to the reference databases. The reference database then, can have a profound effect on both diagnosis and fracture risk assessment.

Manufacturer's "Native" Databases

It is logistically impossible to have every member of the population in a given country to undergo bone density measurements to create a reference database. Therefore, a sample of the population is studied to create a "reference" population. From this sample population, the average BMD value for the young-adult and for each age group is calculated. Depending upon the make-up of the individuals in the sample, a slightly different average or mean BMD will be obtained with each sample of the population that is studied. As was seen in Chapter 3, the standard deviation (upon which the *T*-score or young-adult *z*-score are based) that is calculated for the values from any given sample is dependent upon the average value of the sample and the number of individuals that make up that sample. Thus the standard deviation (SD) will also vary from sample to sample. Once the data are collected, different statistical methods can be employed to create the reference curves for the population. In the creation of their own or "native" reference databases, each manufacturer has necessarily utilized a different sample of the population and then applied the statistical methods that seemed most appropriate for that sample. All three major manufacturers of central DXA devices provide extensive reference databases for their machines. Methodological descriptions of the acquisition of these manufacturer-derived databases can be found in the operator's manuals for the devices and elsewhere. More detailed descriptions of the current databases currently in use in the United States are found in Appendices IX–XII.

These statistical and design issues confounded the recognized systematic differences in the measurement of bone mass and density between the different manufacturer's devices. As noted earlier, the BMD values in g/cm² from one machine can be converted using cross-calibration equations to the BMD in g/cm² that would be expected on another manufacturer's machine. The BMD values can also be converted to an sBMD. But the *T*-score or *z*-score from one manufacturer's database cannot be converted to the expected *T*- or *z*-score for another manufacturer's database because the average BMD

---

[9] See Chapter 3 for a discussion of the derivation of the *T*-score.

[10] See Chapter 10 for a discussion of predicting fracture risk with bone densitometry.

and SDs obtained from the different samples within a population used to create the specific reference databases will be different.

Pocock et al. (*9*) observed the effect of differences in the early reference databases between the Hologic QDR-1000 and the Lunar DPX on the % young-adult and % age-matched comparisons for the spine and femoral neck after studying 46 women. The % comparisons for the spine tended to be very similar on the two devices. At the femoral neck, however, the % young-adult comparisons were 6.2% lower on the QDR-1000. The % age-matched comparisons were 3.3% lower on the QDR-1000.

Other authors confirmed these observations. Laskey et al. (*28*) noted the effect of the differences in databases used for the Lunar DPX and the Hologic QDR-1000 for spine and proximal femur bone density. Fifty-three subjects underwent spine and proximal femur bone density measurements on the same day on both devices. Laskey, like Pocock (*9*), found that the comparisons of the measured BMD to the reference database for the young-adult or age-matched adult in the spine were similar. In the regions in the proximal femur, however, the differences were substantial. The magnitude of the difference approximated 1 SD. This difference was sufficiently great to have potential clinical ramifications. For example, when applying the WHO BMD criteria for the diagnosis of normalcy, osteopenia, or osteoporosis, the difference between normal and osteoporosis is 1.5 SD. Thus, a 1 SD difference could easily result in a markedly different diagnosis from one manufacturer's machine to another.

This problem was also studied by Faulkner et al. (*29*). T-scores and young-adult *z* scores[11] at the spine were compared for 83 women and in the proximal femur for 120 women who underwent bone density studies on a Lunar DPX and Hologic QDR-1000/W. The difference between the T-scores at the lumbar spine on the QDR-1000/W and the young-adult *z*-scores on the Lunar DPX was not statistically or clinically significant as it was less than 0.1 SD. At the femoral neck, however, there was a systematic difference of 0.9 SD.

Faulkner et al. (*29*) observed that these differences in the reference databases could be due to a combination of factors: different inclusion criteria, relatively small numbers of individuals used to calculate the average and SD young-adult values and different statistical methods employed in the calculation of the reference curves. Faulkner suggested correcting the proximal femur data from both manufacturers by employing proximal femur data that was obtained during the NHANES III[12] study of the United States population. The initial publication of NHANES III bone density data in 1995 (*30*) reported data collected between 1988 and 1991 using the Hologic QDR-1000. In this data set there were 194 non-Hispanic white women aged 20–29 whose bone density was used to calculate the young-adult average BMD value and SD in five regions in the proximal femur. The average BMD in the femoral neck for these young adults from NHANES III was 0.849 g/cm^2 with a SD of 0.11 g/cm^2. Faulkner substituted these values for the femoral neck young-adult average and SD values used in the QDR-

---

[11] The *T*-score and young-adult *z*-score are conceptually identical. At the time of this study, the standard score comparison to the average peak BMD was called the "young-adult z-score" on Lunar devices. The same comparison on Hologic devices was called the *T*-score. Lunar devices today utilize the *T*-score terminology.

[12] National Health and Nutrition Examination Survey III.

1000 reference database of 0.895 and 0.10 g/cm^2 respectively. The equivalent Lunar DPX BMD young-adult BMD was then calculated using the cross-calibration equation from Genant et al. (*10*). This resulted in a Lunar value of 1.000 g/cm^2 for the average young-adult BMD in the femoral neck compared to the value of 0.980 g/cm^2 used in the manufacturer-supplied database prior to October 1997. The SD for the young-adult of 0.11 g/cm^2 from NHANES III was substituted for the Lunar reported standard deviation of 0.12 g/cm^2. When the *T*-scores and young-adult *z*-scores were recalculated for each machine using the values based on the NHANES III data, the differences between the two manufacturer's databases largely disappeared.

NHANES III

NHANES III was conducted by the National Center for Health Statistics, Centers for Disease Control and Prevention. The first phase of bone density data collection occurred from 1988 to 1991. A second data collection phase took place from 1991 to 1994. There were no specific inclusion or exclusion criteria used to select individuals for bone density measurements in this study other than the presence of prior hip fracture or current pregnancy, which were grounds for exclusion. The individuals who received bone density measurements were otherwise part of a random sample of the population of the United States. All of the proximal femur bone density measurements were obtained on Hologic QDR devices. During the first phase, proximal femur bone density data was collected on 7116 men and women aged 20 and older (*30*). There were a total of 3217 non-Hispanic whites, 1831 non-Hispanic blacks, and 1840 Mexican-Americans in this study population. The addition of bone density data from the second phase increased the total sample to 14,646 men and women age 20 and older, 6181 of whom were non-Hispanic whites, 4021 of whom were non-Hispanic blacks, and 3858 Mexican-Americans (*31*). In this much larger sample, the non-Hispanic white female young-adult average values and SDs were based on 409 women rather than the 194 women used for this calculation from the phase 1 data only. The updated average BMD at the femoral neck for 20- to 29-year-old non-Hispanic white women from the complete 1998[13] NHANES III database was 0.858 g/cm^2 with a SD of 0.120 g/cm^2. At the total femur, the peak BMD was 0.942 g/cm^2 with an SD of 0.122 g/cm^2. The complete 1998 NHANES III non-Hispanic white database is found in Appendix IX.

With the development of the cross-calibration equations between manufacturers and the sBMD for the total femur, it became possible for the proximal femur data from NHANES III to be adopted as a common femur reference database for manufacturers even though the data was obtained solely on Hologic DXA devices. Based on the equations for sBMD, the total femur mean sBMD for U.S. white women aged 20–29 using the 1998 NHANES III reference data is 955 mg/cm^2 with an SD of 123 mg/cm^2 (*31*). Age-specific reference data using the sBMD for the total femur from NHANES III are shown in Appendix IX. Standardized 1995 NHANES III proximal femur data[14] were offered as part of the reference databases by manufacturers, either in conjunction with the native databases or as a replacement for the native proximal femur data after

---

[13] This is denoted as the 1998 NHANES III data because of the year in which it was published.
[14] This is denoted as the 1995 NHANES III data because of the year in which it was published.

September 1997. This does not eliminate the differences in the BMD in g/cm^2 because the use of a common proximal femur reference database in no way alters the differences in calibration among the devices from different manufacturers. The T-score comparison, however, is now based on the comparison to the same database—the 1995 NHANES III reference database. As a consequence, the marked disparities in reported proximal femur ROI T-scores among manufacturers have been greatly reduced. Manufacturers may still differ, however, in whether the NHANES III reference database is used only at the total hip or femoral neck or both. It should be noted, however, that these databases at present are based on the 1995 NHANES III data and not the 1998 NHANES data required by the World Health Organization 10-year fracture risk prediction algorithm called FRAX^{TM}.[15]

Database methodologic issues and their potential clinical ramifications remain for the spine and peripheral skeletal sites. NHANES III for the proximal femur is the only common reference database in use. Studies of other skeletal sites have suggested that a common reference database would reduce or eliminate diagnostic disagreement between different manufacturers' devices at those sites as well (*32, 33*). At present, however, there is no common database among the various devices for the PA or lateral spine, forearm sites, heel, or phalanges as measured by any technique.

AREAL AND VOLUMETRIC DENSITIES

It should be clear then, that BMD measurements with DXA are two-dimensional or areal measurements, whereas BMD measurements with QCT are three-dimensional or volumetric. Because DXA measurements are areal, bone size can affect the apparent BMD. In other words, it is possible for two vertebrae with identical volumetric densities to have different areal densities because of a difference in size. This is illustrated in Fig. 6-1. In Fig. 6-1A, each of the eight components of the cube is identical with a mineral weight of 2 g and dimensions of $1 \times 1 \times 1$ cm. Therefore, the face of the cube has a width of 2 cm and a height of 2 cm for a projected area[16] of 4 cm^2. The cube also has a depth of 2 cm. Its volume[17] then, is 8 cm^3. Because there are eight components of the cube, each weighing 2 g, the entire mineral weight of the cube is 16 g. Because areal density is the ratio of the bone mineral content to bone area, the areal density of this cube, such as might be seen with a DXA measurement, would be calculated as shown in Equation 17:

$$\frac{16 \text{ g}}{4 \text{ cm}^2} = 4.0 \text{ g/cm}^2 \tag{17}$$

The volumetric density of this cube, however, is the ratio of the bone mineral content to bone volume. This calculation is shown in Equation 18:

$$\frac{16 \text{ g}}{8 \text{ cm}^3} = 2.0 \text{ g/cm}^3 \tag{18}$$

---

[15] See Chapter 10 for a discussion of FRAX^{TM}.

[16] Area is calculated by multiplying the height x width.

[17] Volume is calculated by multiplying the height x width x depth.
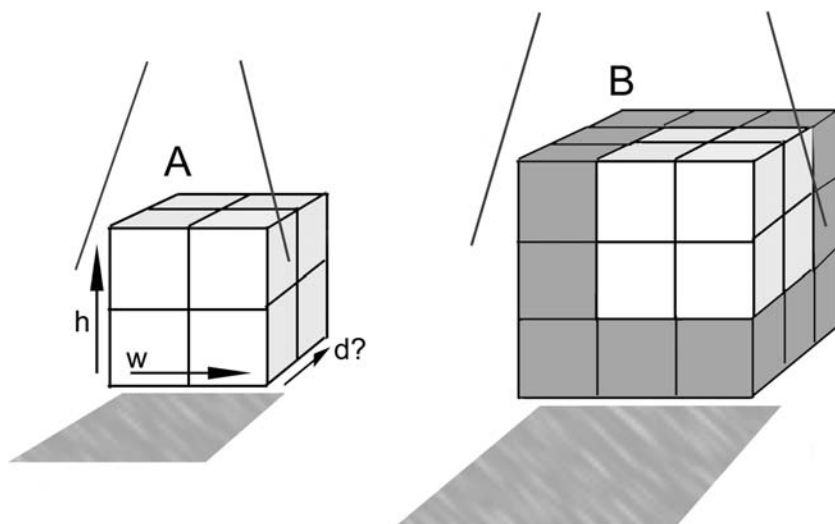
Fig. 6-1. The effect of bone size on areal BMD. The individual components of cube A are identical in size and volumetric density to the components of the larger cube B. Note that cube A will fit within cube B. The volumetric densities of cubes A and B are identical but a DXA areal density for cube A will be less than for cube B because of its greater depth. The depth of both cubes is unknown. Formulas in the text used to calculate the BMAD are based on assumptions about the relationship between the depth and height of the vertebrae (h-height; w-width; d-depth).

This eight-component cube, then, has an areal density of 4.0 g/cm^2 and a volumetric density of 2.0 g/cm^3. The cube in Fig. 6-1B has identical individual components as the cube in Fig. 6-1A, but the entire cube is larger. Instead of eight components, the cube in Fig. 6-1B has 27. Each of the components, however, is identical in size and mineral weight to the components that make up the cube in Fig. 6-1A. The areal density and volumetric density of the cube in Fig. 6-1B are calculated in Equations 19 and 20, respectively:

$$\frac{54 \text{ g}}{9 \text{ cm}^2} = 6.0 \text{ g/cm}^2 \tag{19}$$

$$\frac{54 \text{ g}}{27 \text{ cm}^3} = 2.0 \text{ g/cm}^3 \tag{20}$$

In this case then, the volumetric densities of the two cubes are identical, but the larger cube has the greater areal density. This reflects the effect of bone size on the two-dimensional areal measurement.

Bone Mineral Apparent Density

This issue has been recognized for some time, although no consensus has been reached on how to best correct for the effects of bone size on areal measurements. Different approaches have been proposed to calculate a volumetric bone density from the DXA areal measurement, which is then called the bone mineral apparent density or

BMAD (*34, 35*). An approach suggested by Carter et al. (*34*) is shown in Equation 21 and by Jergas et al. (*35*) in Equation 22:

$$BMAD = \frac{BMC}{pA^{1.5}} \text{ in which } pA = h \times w \tag{21}$$

$$BMAD = \frac{BMC}{pA \times w} \text{ in which } w = \frac{pA}{h} \tag{22}$$

The dimensions used in these equations are illustrated in Fig. 6-1. The effect of bone size on areal density is particularly important in pediatric densitometry, both in interpreting the results of single measurements and in following changes in bone density in growing children. It is also relevant in looking at the differences in bone density between men and women. At its most basic, smaller bones may have a lower areal bone density because of the effect of bone size. In addition, a change in bone size may cause a change in areal bone density, even though the volumetric bone density has not changed.

CALCULATING "AVERAGE" SPINE BONE DENSITIES

When bone density measurements are made in the lumbar spine in the PA projection with DXA, the BMD for three or four contiguous vertebrae is generally reported rather than the BMD for any single vertebra. In other words, the L1–L4 or L2–L4 BMD is reported for the lumbar spine rather than only using L1, L2, L3, or L4. The accuracy and precision for L1–L4 or L2–L4 are superior to the accuracy and precision for single vertebrae. The L1–L4 or L2–L4 BMD has been commonly called the "average" BMD. This is an accepted convention but somewhat misleading. The newer terminology of "total" BMD for L1–L4 is also an accepted convention but misleading for the same reason.

The BMD is calculated by the densitometry software for each individual vertebra and these values are provided on the bone density report as shown in Fig. 6-2. It is tempting to assume that the individual BMDs for each of the vertebrae included in the three or four vertebrae value are simply added and then the total divided by the number of vertebrae to find the "average" BMD. This is not correct. The correct approach is to add the BMC values for each of the vertebrae included in the three or four vertebrae value and divide this total by the sum of the individual areas of each of the included vertebrae. This is illustrated in Equation 23 for the L1–L4 BMD:

$$BMD_{L1-L4} = \frac{(BMC_{L1} + BMC_{L2} + BMC_{L3} + BMC_{L4})}{(Area_{L1} + Area_{L2} + Area_{L3} + Area_{L4})} \tag{23}$$

In DXA devices in which it is possible to exclude one or more vertebra from consideration, the resulting "average" BMD is calculated in an analogous manner. This "average" BMD then, is not really an average of the BMDs at the included individual vertebral levels at all. Nevertheless, it is an accepted convention in densitometry to refer to these quantities as the "average" BMD. In recent years, the L1–L4 BMD has been called the total spine BMD, analogous to the total hip BMD in the proximal femur.
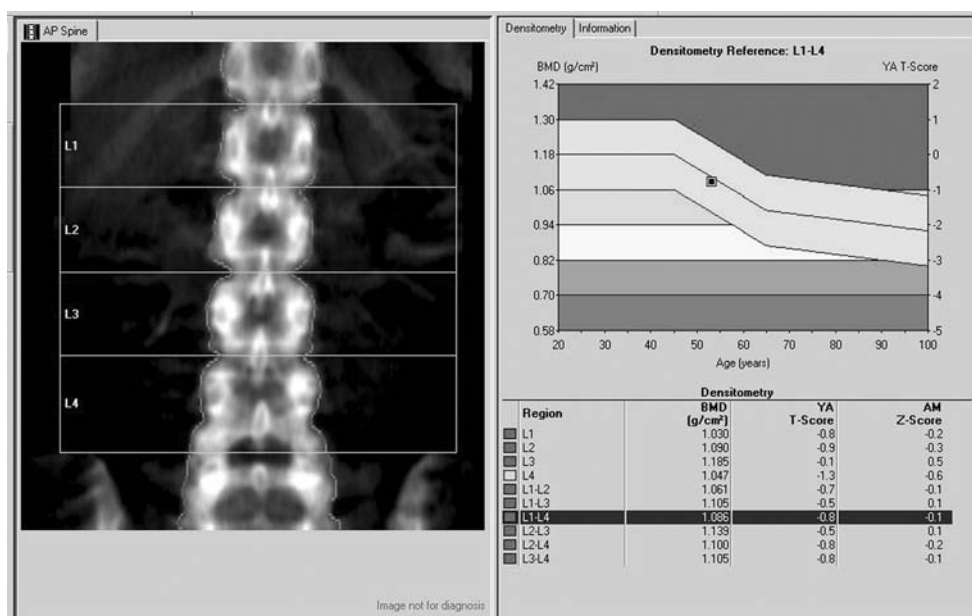
Fig. 6-2. A PA lumbar spine study on the Lunar Prodigy showing BMD values in g/cm² for each vertebra as well as every possible combination of contiguous vertebrae. Also note the classic shapes of the vertebral bodies in the bone density image as well as the height of the iliac crest and position of the lowest set of ribs.

REFERENCES

1. Kelly TL, Slovik DM, Schoenfeld DA, Neer RM. Quantitative digital radiography *versus* dual photon absorptiometry of the lumbar spine. J Clin Endocrinol Metab 1988;67:839–844.
2. Pacifici R, Rupich R, Vered I, Fischer KC, Griffin M, Susman N, Avioli LV. Dual energy radiography (DER): a preliminary comparative study. Calcif Tissue Int 1988;43:189–191.
3. Holbrook TL, Barrett-Connor E, Klauber M, Sartoris D. A population-based comparison of quantitative dual-energy X-ray absorptiometry with dual-photon absorptiometry of the spine and hip. Calcif Tissue Int 1991;49:305–307.
4. Mazess RB, Barden HS. Measurement of bone by dual-photon absorptiometry (DPA) and dual-energy X-ray absorptiometry (DEXA). Ann Chir Gynaecol 1988;77:197–203.
5. Lees B, Stevenson JC. An evaluation of dual-energy X-ray absorptiometry and comparison with dual-photon absorptiometry. Osteoporos Int 1992;2:146–152.
6. McClung M, Roberts L. Correlation of bone density measurements by 153-Gd and X-ray dual-photon absorptiometry. Abstract. J Bone Miner Res 1989;4:S368.
7. Arai H, Ito K, Nagao K, Furutachi M. The evaluation of three different bone densitometry systems: XR-26, QDR-1000, and DPX. Image Technol Inf Disp 1990;22:1–6.
8. Lai KC, Goodsitt MM, Murano R, Chesnut CH. A comparison of two dual-energy X-ray absorptiometry systems for spinal bone mineral measurement. Calcif Tissue Int 1992;50:203–208.
9. Pocock NA, Sambrook PN, Nguyen T, Kelly P, Freund J, Eisman JA. Assessment of spinal and femoral bone density by dual X-ray absorptiometry: comparison of Lunar and Hologic instruments. J Bone Miner Res 1992;7:1081–1084.
10. Genant HK, Grampp S, Gluer CC, et al. Universal standardization for dual X-ray absorptiometry: patient and phantom cross-calibration results. J Bone Miner Res 1994;9:1503–1514.
11. Steiger P. Standardization of spine BMD measurements. J Bone Miner Res 1995;10:1602–1603.
12. Hanson J. Standardization of femur BMD. J Bone Miner Res 1997;12:1316–1317.
13. Lu Y, Fuerst T, Hui S, Genant HK. Standardization of bone mineral density at femoral neck, trochanter, and Ward's triangle. Osteoporos Int 2001;12:438–444.

14. Shepherd JA, Cheng XG, Lu Y, et al. Universal standardization of forearm bone densitometry. J Bone Miner Res 2002;17:734–745.

15. Economos CD, Nelson ME, Fiatarone MA, et al. A multicenter comparison of dual-energy X-ray absorptiometers: in vivo and in vitro measurements of bone mineral content and density. J Bone Miner Res 1996;11:275–285.

16. Blake GM, Tong CM, Fogelman I. Inter-site comparison of the Hologic QDR-1000 dual-energy X-ray bone densitometer. Br J Radiol 1991;64:440–446.

17. Orwoll E, Oviatt SK, and the Nafarelin Bone Study Group. Longitudinal precision of dual-energy X-ray absorptiometry in a multicenter study. J Bone Miner Res 1991;6:191–197.

18. Kolta S, Ravaud P, Fechtenbaum J, Dougados M, Roux C. Accuracy and precision of 62 bone densitometers using a European spine phantom. Osteoporos Int 1999;10:14–19.

19. Gaither KW, Faulkner KG, Ostrem EC, Backman JK, Avecilla LS, McClung MR. Variations in calibration among like-manufacturer DXA systems. J Bone Miner Res 1996;11:S119.

20. Baim S, Leonard MB, Bianchi ML, et al. Official positions of the International Society for Clinical Densitometry and executive summary of the 2007 ISCD pediatric position development conference. J Clin Densitom 2008;11:6–21.

21. Steiger P, von Stetten E, Weiss H, Stein JA. Paired AP and lateral supine dual X-ray absorptiometry of the spine: initial results with a 32-detector system. Osteoporos Int 1991;1:190.

22. Mazess RB, Hanson JA, Payne R, Nord R, Wilson M. Axial and total body bone densitometry using a narrow-angle fan-beam. Osteoporos Int 2000;11:158–166.

23. Blake GM, Parker JC, Buxton FMA, Fogelman I. Dual X-ray absorptiometry: a comparison between fan-beam and pencil-beam scans. Br J Radiol 1993;66:902–906.

24. Pocock NA, Noakes KA, Majerovic Y, Griffiths MR. Magnification error of femoral geometry using fan-beam densitometers. Calcif Tissue Int 1997;60:8–10.

25. Eiken P, Barenholdt O, Bjorn Jensen L, Gram J, Pors Nielsen S. Switching from DXA pencil-beam to fan-beam. I: studies in vitro at four centers. Bone 1994;15:667–670.

26. Faulkner KG, Gluer CC, Estilo M, Genant HK. Cross-calibration of DXA equipment: upgrading from a Hologic QDR 1000/W to a QDR 2000. Calcif Tissue Int 1993;52:79–84.

27. Mazess RB, Barden HS. Evaluation of differences between fan-beam and pencil-beam densitometers. Calcif Tissue Int 2000;67:291–296.

28. Laskey MA, Crisp AJ, Cole TJ, Compston JE. Comparison of the effect of different reference data on Lunar DPX and Hologic QDR-1000 dual-energy X-ray absorptiometers. Br J Radiol 1992;65:1124–1129.

29. Faulkner KG, Roberts LA, McClung MR. Discrepancies in normative data between Lunar and Hologic DXA systems. Osteoporos Int 1996;6:432–436.

30. Looker AC, Wahner HW, Dunn WL, Calvo MS, Harris TB, Heyse SP, Johnston CC, Lindsay RL. Proximal femur bone mineral levels of US adults. Osteoporos Int 1995;5:389–409.

31. Looker AC, Wahner HW, Dunn WL, et al. Updated data on proximal femur bone mineral levels of US adults. Osteoporos Int 1998;8:468–489.

32. Greenspan SL, Bouxsein ML, Melton ME, et al. Precision and discriminatory ability of calcaneal bone assessment technologies. J Bone Miner Res 1997;12:1303–1313.

33. Grigorian M, Shepherd JA, Cheng XG, Njech CF, Toschke JO, Genant HK. Does osteoporosis classification using heel BMD agree across manufacturers? Osteoporos Int 2002;13:613–617.

34. Carter DR, Bouxsein ML, Marcus R. New approaches for interpreting projected bone densitometry data. J Bone Miner Res 1992;7:137–146.

35. Jergas M, Breitenseher M, Gluer CC, Yu W, Genant HK. Estimates of volumetric bone density from projectional measurements improve the discriminatory capability of dual X-ray absorptiometry. J Bone Miner Res 1995;10:1101–1110.

7

Selecting Patients for Bone Mass Measurements: Clinical Guidelines

CONTENTS

Clinical guidelines for the selection of patients for bone mass measurements and the timing of such measurements have been carefully crafted by major medical organizations knowledgeable in osteoporosis and bone densitometry. As practice guidelines, they are intended to help the physician determine when a bone mass measurement may be useful in the care of individual patients. There are also an increasing number of risk-based assessment questionnaires that may be administered by a medical professional or self-administered by the patient to determine if a high probability of low bone density exists. Such patients would also be considered appropriate candidates for a bone mass measurement. In this chapter, the clinical guidelines from major organizations will be reviewed and compared. Risk-based assessment questionnaires will be examined in the next chapter.

Guidelines for bone density testing first appeared in the 1980s. Guidelines vary in scope, depending on the interests and expertise of the issuing organization. Some organizations have issued multiple sets of guidelines over the years, revising or updating their guidelines as knowledge and technology advanced. Ultimately, however, there are far more similarities than differences between the versions of guidelines from any organization and among the guidelines from the different organizations.

GUIDELINES OF THE INTERNATIONAL SOCIETY FOR CLINICAL DENSITOMETRY

The International Society for Clinical Densitometry (ISCD)[1] has issued a series of guidelines since the inception of the society in the early 1990s. The first guidelines were published in 1996 (1). In the years that have followed, ISCD has held rigorous position development conferences to address specific issues in densitometry(2–5). Not all issues have been addressed at each development conference because of the complexity of the issues at hand and because not all issues needed to be re-addressed. ISCD has largely focused on the technical aspects of the performance of bone densitometry but as a matter of necessity, has also addressed issues of patient selection. As with guidelines from other organizations, previously issued guidelines have periodically been modified as demanded by advances in knowledge and technology. ISCD guidelines that are unchanged from previous years are restated in the 2007 positions.

1996 ISCD Guidelines

The 1996 guidelines (1) dealing with technical aspects of the performance of bone densitometry were developed by the International Society for Clinical Densitometry (ISCD) in 1994 during a meeting of an international panel of experts in bone densitometry and subsequently published in 1996. There were 22 members of this panel from eight countries. The guidelines addressed both the use and interpretation of bone mass measurements in the prevention, detection, and management of all diseases characterized by low bone mass with an emphasis on osteoporosis. The guidelines provided a broad overview of how bone mass measurements should be used regardless of specific clinical circumstances in which they were employed. Although they did not specifically deal with patient selection, a review of the 1996 ISCD guidelines is included here because of their importance and influence on the patient selection guidelines that followed. There were six major points on which the panel reached a consensus. Those points are summarized in Table 7-1.

The 1996 ISCD Guidelines are best appreciated if the scientific climate of the 1980s and early 1990s is understood. In the 1980s, medical conferences were awash in the "bone-mass measurement controversy." This controversy largely centered on whether a measurement of bone mass or bone density could be used to predict fracture risk. In a decade in which DPA and SPA were the predominant techniques, bone densitometry was not seen as useful for monitoring therapy. Indeed, therapeutic choices were

---

[1] The International Society for Clinical Densitometry was originally known as the Society for Clinical Densitometry.

Table 7-1
1996 Consensus Points from the International Society for Clinical Densitometry on the Clinical Utility of Bone Mass Measurements

1. Bone mass measurements predict a patient's future risk of fracture.
2. Osteoporosis can be diagnosed on the basis of bone mass measurements even in the absence of prevalent fractures.
3. Bone mass measurements provide information that can affect the management of patients.
4. The choice of the appropriate measurement site(s) for the assessment of bone mass or fracture risk may vary depending upon the specific circumstances of the patient.
5. The choice of the appropriate technique for bone mass measurements in any given clinical circumstance should be based on an understanding of the strengths and limitations of the different techniques.
6. Bone mass data should be accompanied by a clinical interpretation.

viewed (rightly or wrongly) as being so limited, that early detection of disease with bone mass measurements was perceived as having little value. The situation was further compounded by a lack of agreement on the actual definition of osteoporosis itself. In the late 1980s and early 1990s, however, rapid developments in the field made most of these controversies moot.

In 1988, DXA was FDA-approved for clinical use. The enhanced precision of DXA, particularly at the spine, made monitoring the effects of disease or therapy practical. In 1993, several major fracture trials (6–8) were published and added to a growing body of literature that effectively lay to rest the "bone-mass measurement controversy." There was no longer any question that the risk of fracture could be predicted with a single bone mass measurement. In 1994, the World Health Organization (9) published guidelines for the diagnosis of osteoporosis based on the measurement of bone density. Alendronate sodium and nasal spray salmon calcitonin, approved in 1995, were dramatic additions to the therapeutic armamentarium. These developments profoundly changed the field of densitometry and osteoporosis, but they had still been poorly communicated to the practicing physician, the public, insurers, and politicians. The ISCD Guidelines attempted to change that.

Another major goal of the ISCD Guidelines was to emphasize that all bone mass measurement techniques had potential value when they were properly used. The marketing competitiveness of the bone densitometry industry was, at times, misperceived by those outside the industry as meaning that some technologies were inferior to others. ISCD wished to emphasize that the devices which were FDA-approved for the measurement of bone density did exactly what they purported to do, which was measure the bone density accurately and precisely. Assuming that all techniques were available, ISCD stated that the choice of which technique to use should be determined by the intent of the measurement. The intent of the measurement determined which site or sites should be measured and whether the primary need was accuracy or precision at that site. Once these

determinations were made, a particular technique might be preferable to another in that specific circumstance but not necessarily in every circumstance that may follow. Another major emphasis of the ISCD guidelines was that the appropriate measurement site was determined by the intent of the measurement. One skeletal site was not appropriate for all of the potential uses of bone mass measurements. ISCD also strongly recognized the need for strict quality control of the machines and training for the operators. The guidelines also emphasized the need for an interpretation of the numeric data by a physician trained in densitometry.

2007 ISCD Guidelines

The complete 2007 ISCD guidelines (*5*) or positions are presented in Appendix V. Positions which are new in 2007 are in bold print. Positions not in bold print were established at earlier position development conferences. The 2003 positions (*3*) were the first ISCD positions to address patient selection for bone density testing. These were some of the first guidelines to address bone density testing in men as well as women, recommending bone density testing in men aged 70 years and older. The 2003 patient selection guidelines were reiterated in the 2005 guidelines (*4*). The 2007 ISCD guidelines (*5*) for patient selection largely still reflect the positions taken in 2003 (*3*) although there are notable additions to these positions in the 2007 guidelines. New in 2007 was the recommendation to consider bone density testing in women in the menopausal transition with clinical risk factors for fracture (*5*). Also new in 2007 was the recommendation to perform bone density testing in men under age 70 with clinical risk factors for fracture. Patient selection guidelines from the 2007 ISCD guidelines are shown in Table 7-2.

<div align="center">

Table 7-2

2007 ISCD Indications for Bone Density Testing

</div>

- Women aged 65 and older
- Postmenopausal women under age 65 with risk factors for fracture
- Women during the menopausal transition with clinical risk factors for fracture, such as low body weight, prior fracture, or high-risk medication use
- Men aged 70 and older
- Men under age 70 with clinical risk factors for fracture
- Adults with a fragility fracture
- Adults with a disease or condition associated with low bone mass or bone loss
- Adults taking medications associated with low bone mass or bone loss
- Anyone being considered for pharmacologic therapy
- Anyone being treated, to monitor treatment effect
- Anyone not receiving therapy in whom evidence of bone loss would lead to treatment

Women discontinuing estrogen should be considered for bone density testing according to the indications listed above.

NATIONAL OSTEOPOROSIS FOUNDATION GUIDELINES

The National Osteoporosis Foundation (NOF) has issued a series of guidelines, spanning a 20-year period. The various sets of guidelines are reviewed here. It is of interest that these guidelines have almost come full circle, with the 2008 guidelines closing resembling the original guidelines issued in 1988.

1988 NOF Guidelines

The 1988 NOF guidelines were developed in response to a report from the Office of Health Technology Assessment (OHTA) of the Public Health Service that had been submitted to the Health Care Finance Administration (HCFA). The report from OHTA concluded that the role of DPA and SPA in clinical practice had not been defined. The clinical indications from the NOF that were submitted to HCFA were published in 1989 in the *Journal of Bone and Mineral Research* (*10*). The NOF pointed out that the methods that were available to measure bone mass or density were safe, accurate, and precise. They also noted that important clinical decisions could be influenced by the results of the measurements. The four clinical circumstances in which the NOF believed that sufficient experience existed to support the use of bone mass measurements were based primarily on experience with SPA and DPA, as DXA had only been approved for clinical use in 1988. The four clinical indications for bone mass measurements were:

- In estrogen-deficient women, to diagnose significantly low bone mass in order to make decisions about hormone replacement therapy
- In patients with vertebral abnormalities or roentgenographic osteopenia to diagnose spinal osteoporosis in order to make decisions about further diagnostic evaluation and therapy
- In patients receiving long-term glucocorticoid therapy, to diagnose low bone mass in order to adjust therapy
- In patients with primary asymptomatic hyperparathyroidism, to identity low bone mass in order to identify those at risk of severe skeletal disease who may be candidates for surgical intervention

The NOF indications also noted the specific skeletal sites and techniques that should be used in these different circumstances. For an assessment of fracture risk in a postmenopausal woman, the NOF suggested that any site by any technique was appropriate. For the confirmation of spinal demineralization or the diagnosis of spinal osteoporosis, measuring the spine with DPA, DXA, or QCT was recommended. A measurement of the spine by DPA, DXA, or QCT was also recommended for the purposes of detecting bone loss from corticosteroids. To assess the effects of hyperparathyroidism on the skeleton a measurement of the spine by DXA, DPA, or QCT or a measurement of the radius by SPA was recommended.

DXA measurements of the forearm were not suggested as part of the evaluation of the patient with hyperparathyroidism as this capability was not in clinical use in 1988. The serial assessment of bone density for therapeutic efficacy or disease effect was also not mentioned in these indications because the indications were primarily based on the clinical experience with SPA and DPA. The precision of bone density measurements of the spine or proximal femur with DPA was not sufficient to make serial assessments feasible in most cases. In the text of the document, however, it was observed that the changes in bone density in the spine might be so rapid in the setting of corticosteroid-induced

osteoporosis that serial assessment of spine bone density with DPA could be considered. Measurements of the forearm with SPA were also not thought to be useful for serial assessments of therapeutic efficacy. Although the precision of SPA measurements of the forearm was excellent, the changes in BMD at the forearm sites were correctly thought to be too small to be detected in a clinically useful period of time.

The assessment of the estrogen-deficient woman with bone mass measurements specifically referred to making decisions about hormone replacement therapy. At the time of the 1988 NOF indications, there were no prescription alternatives to estrogen that were FDA-approved for the prevention[2] of osteoporosis.

Finally, the NOF emphasized that these measurements should not be done if intervention decisions would not be affected by the result of the test. They noted that women who received long-term estrogen replacement for reasons other than the prevention or treatment of osteoporosis did not need a measurement. The NOF also observed that measurements should not be done if sufficient quality control procedures were not in place to ensure the accuracy of the results.

1998 NOF Guidelines

In 1998, the NOF issued new guidelines for bone densitometry that addressed the detection and management of postmenopausal osteoporosis (*11*, *12*). The guidelines initially appeared in an extensive document on osteoporosis that was published in *Osteoporosis International* (*11*). With some modification, they subsequently appeared in the document titled "Physician's Guide to Prevention and Treatment of Osteoporosis." (*12*).

In the original 1998 document, extensive cost–benefit analyses were undertaken to determine the feasibility and benefits not only of measuring bone density but of treating women who were found to have a low bone mass. The authors of the paper insightfully noted that the conclusions were only as good as the evidence on which they were based and such evidence might change as new therapies became available or as more was learned about the pathophysiology of osteoporosis. In essence, however, the original 1998 NOF recommendations stated that it was cost–effective to assess bone density in all Caucasian women over the age of 60 regardless of other risk factors and in all Caucasian women between age 50 and 60 who had a strong risk factor for fracture (*13*). BMD testing was recommended for all women who had a vertebral fracture unless calcitonin was the only acceptable treatment option. In women who have had a non-vertebral fracture testing was recommended for women age 60 even without other risk factors and women age 50–59 with other risk factors. The risk factors for fracture that were emphasized in this report included a history of fracture after age 40, a history of hip, spine, or wrist fracture in a first-degree relative, weight equal to or less than 127 lbs, and current cigarette smoking. These risk factors were chosen because they were easy to determine in clinical practice and they were demonstrated as being independent predictors of hip fracture in the Study of Osteoporotic Fractures (*14*). In order to help the clinician determine when it would be cost effective to measure the bone density,

---

[2] Synthetic salmon calcitonin was clinically available but FDA-approved it for the treatment of osteoporosis in women who were more than 5 years postmenopausal. It was not FDA-approved for prevention.
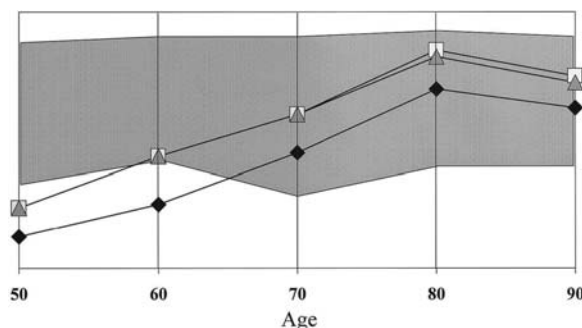
Fig. 7-1. Testing decision nomogram. If 5 years of alendronate therapy are being considered, a woman should undergo BMD testing if she falls into the shaded area based on her age and number of risk factors. ◇-no risk factors; ▲-1 risk factor; (☐-2 risk factors. Reproduced with kind permission of Springer Science and Business Media from ref. (*11*).

nomograms were developed that were specific for the presence or absence of a prior spine fracture and the therapy being considered. The clinician would use the number of remaining risk factors from the list given above to determine if the patient should be tested. An example of such a nomogram is shown in Fig. 7-1. Another nomogram was provided for women with spine fractures in whom alendronate therapy was being considered. Nomograms for women with and without spine fractures and each of the remaining therapies that were approved for clinical use in 1998 were also provided.

The complexity of these guidelines made them unsuitable for widespread clinical use. In response, the NOF developed a more succinct version of the 1998 guidelines, which were published in 1999 (*12*). In the introduction to the these guidelines, the NOF noted that the guidelines were primarily intended to be applied to postmenopausal Caucasian women because the data used to create the guidelines came from studies of that group. They also noted that their recommendations were based on measurements of bone density at the hip although they noted that BMD measurements at any site had value in predicting fracture risk. The NOF did not characterize any particular technique as being preferred, although measurements at the hip would, of necessity in 1999, have required the use of DXA.

In the 1998 clinical guidelines, the NOF recommended bone density testing in postmenopausal Caucasian women in the following circumstances:

- All women under age 65 who have one or more additional risk factors for osteoporotic fracture
- All women age 65 and older regardless of additional risk factors
- Postmenopausal women who present with fractures
- Women who are considering therapy if BMD testing would facilitate the decision
- Women who have been on hormone replacement therapy for prolonged periods

The risk factors to be considered in the postmenopausal women under age 65 were numerous but the same four risk factors used in the cost–benefit analyses were emphasized because of their association with hip fracture risk: a personal history of fracture as an adult, a history of fracture in a first-degree relative, current cigarette smoking, and body weight less than 127 lbs.

2003 NOF Guidelines

In the 2003 NOF guidelines (*15*), the selection criteria for bone mass measurements were reduced to only three, eliminating any reference to women who had been on hormone therapy for prolonged periods and the rather obvious admonition regarding women considering therapy if knowledge of the BMD would facilitate the decision to begin therapy. The three patient selection criteria for bone density testing as noted in 2003 were as follows:

- All women age 65 and older regardless of risk factors
- Younger postmenopausal women with one or more risk factors (other than being white, postmenopausal, and female)
- Postmenopausal women who present with fractures (to confirm the diagnosis and determine disease severity)

2008 NOF Guidelines

The 2008 NOF guidelines (*16*) for patient selection for bone density testing were the first NOF guidelines to include recommendations for men. They are also the most extensive guidelines issued by the NOF to date, covering a broad range of clinical circumstances in which bone density testing is appropriate. These recommendations are summarized in Table 7-3 and again in Appendix VI. In the 2008 guidelines, reference to women who had been receiving estrogen therapy was restored. While not identical, this recommendation was reminiscent of the 1998 recommendation. The reference to women in the menopausal transition was entirely new.

Table 7-3
2008 National Osteoporosis Foundation Indications for BMD Testing

- Women age 65 and older and men age 70 and older, regardless of clinical risk factors
- Younger postmenopausal women and men age 50–70 about whom you have concern, based on their clinical risk factor profile
- Women in the menopausal transition if there is a specific risk factor associated with increased fracture risk such as low body weight, prior low-trauma fracture, or high-risk medication
- Adults who have a fracture after age 50
- Adults with a condition (e.g., rheumatoid arthritis) or taking a medication (e.g., glucocorticoids, ≥ 5 mg/day for ≥ 3 months) associated with low bone mass or bone loss
- Anyone being considered for pharmacologic therapy for osteoporosis
- Anyone being treated for osteoporosis, to monitor treatment effect
- Anyone not receiving therapy in whom evidence of bone loss would lead to treatment
- Postmenopausal women discontinuing estrogen should be considered for bone density testing

Reprinted with permission from ref. (*16*). National Osteoporosis Foundation, Washington, DC 20037

OSTEOPOROSIS SOCIETY OF CANADA/OSTEOPOROSIS CANADA

The Osteoporosis Society of Canada issued guidelines in 1996, with updates in 2002 and 2006. This society is now known as Osteoporosis Canada.

1996 Osteoporosis Society of Canada Guidelines

In 1996, the Osteoporosis Society of Canada (OSC) published guidelines (*17*) that were originally developed during the 1993 Consensus Conference of the Osteoporosis Society of Canada. The clinical circumstances in which the OSC recommended bone density testing were:

- Menopause, because the decision to use hormone therapy may be aided by bone density measurement
- Amenorrhea in a younger woman for any reason, because amenorrhea can lead to osteopenia, in which case hormone therapy may be appropriate
- More than 3 months of treatment with supraphysiologic doses of glucocorticoids
- Asymptomatic, mild, primary hyperparathyroidism, because the bone density measurement may aid in a decision to recommend surgical intervention
- A strong family history of osteoporosis or the presence of other risk factors for osteoporosis, because the finding of a low bone density might result in the initiation of hormone therapy or other osteoporosis treatments
- Confirmation of radiographic osteopenia
- Monitoring osteoporosis therapy

2002 OSC Guidelines

In 2002, the OSC issued extensively revised and updated guidelines (*18*) for the diagnosis and management of osteoporosis in Canada. In these guidelines, the OSC recommended that all women age 65 and older have a bone density study. They also recommended BMD testing in individuals under age 65 (younger postmenopausal women and men over age 50) who had what the OSC deemed either one major risk factor or two minor risk factors for osteoporosis. The OSC noted that DXA was the optimum technology for risk assessment and that measurements of bone density with DXA at central sites (the PA lumbar spine and proximal femur) should be used for case finding. Repeat central DXA studies for the purposes of monitoring therapeutic efficacy were recommended after an interval of 1–2 years.

2006 Osteoporosis Canada Guidelines

In 2006, updated guidelines were published by Osteoporosis Canada[3] (*19*). There were no major changes from the 2002 guidelines (*18*) in regard to patient selection for bone density testing in these guidelines, although the 2006 guidelines focused almost exclusively on women. Osteoporosis Canada reiterated that bone density testing was appropriate for all women age 65 and older and for targeted case finding among women under the age of 65 (*19*). For targeted case finding, the identification of one major risk factor or two minor risk factors was sufficient to identify a woman over the age of 50 who

---

[3] Formerly the Osteoporosis Society of Canada.

was appropriate for bone density testing. The major risk factors that were emphasized as identifying a woman who should have a bone density test were: age > 65 years; fragility fracture after age 40; family history of osteoporotic fracture; and systemic glucocorticoid therapy of > 3 months. Minor risk factors included rheumatoid arthritis, smoking, excessive alcohol or caffeine intake, weight less than 57 kg, and chronic anticonvulsant therapy.

AMERICAN ASSOCIATION OF CLINICAL ENDOCRINOLOGISTS' GUIDELINES

1996 American Association of Clinical Endocrinologists' Guidelines

In 1996, the American Association of Clinical Endocrinologists (AACE) developed guidelines for the prevention and treatment of postmenopausal osteoporosis (*20*). As part of these guidelines, bone mineral density measurements were discussed. The specific clinical circumstances in which the AACE believed that bone mass measurements were appropriate were virtually identical to the 1988 guidelines from the NOF although they were clearly updated to reflect DXA's more precise measurements and the increase in available therapies. The clinical circumstances in which the AACE believed that bone mass measurements were appropriate were:

- For risk assessment in perimenopausal or postmenopausal women who are concerned about osteoporosis and willing to accept available intervention
- In women with X-ray findings that suggest the presence of osteoporosis
- In women beginning or receiving long-term glucocorticoid therapy, provided intervention is an option
- For perimenopausal or postmenopausal women with asymptomatic primary hyperparathyroidism in whom evidence of skeletal loss would result in parathyroidectomy
- In women undergoing treatment for osteoporosis, as a tool for monitoring the therapeutic response

Because these guidelines were for the prevention and treatment of postmenopausal osteoporosis only, the 1996 AACE guidelines for the use of densitometry dealt only with women. They also reflect the increase in available therapeutic options beyond hormone replacement therapy for the prevention or treatment of osteoporosis. With the availability of nasal spray calcitonin and alendronate sodium, a woman's choices for the prevention or treatment of this disease were no longer limited to hormone replacement therapy. The superior precision of DXA measurements also offered the ability to follow therapeutic efficacy over time with bone mass measurements.

AACE noted that a measurement of the spine, hip, radius, or calcaneus could be used for fracture risk assessment. They did not state whether they were recommending a global or site-specific fracture risk assessment.[4] Although it was observed that under ideal circumstances, a measurement of both the spine and hip would be performed at a baseline evaluation and again should follow-up be indicated, AACE stated that a bone density study of the hip was the preferred site for the first measurement.

---

[4] See Chapter 10 for a discussion of global and site-specific fracture risk predictions.

The 2001 AACE Guidelines

In 2001, AACE issued an update of its 1996 guidelines (*21*). Additional reports in the medical literature published between 1996 and January 2001 were reviewed in preparation for the 2001 guidelines. The 2001 guidelines for bone density testing were part of an extensive treatise on the pathophysiology, detection, and management of osteoporosis. Guidelines for bone density testing were given in two contexts: as part of the specific assessment for postmenopausal osteoporosis and as part of a variety of other clinical circumstances.

In 2001, AACE recommended that all women age 65 and older undergo an assessment for postmenopausal osteoporosis that included a bone density measurement. They also recommended assessments in adult women who presented with a history of fracture not caused by severe trauma and in postmenopausal women who had risk factors for osteoporosis such as body weight less than 127 lb (57.6 kg) or a family history of spine or hip fracture.

Unlike the 1996 recommendations, AACE specifically recommended in 2001 that DXA measurements of the spine or proximal femur or QCT measurements of the spine be used for the diagnosis of osteoporosis and for monitoring changes in bone density. If the patient had a normal bone density, AACE recommended that a follow-up measurement be considered every 3–5 years. For women in an osteoporosis prevention program, ACCE recommended a follow-up measurement every 1–2 years until stability of the bone density was demonstrated. For women undergoing treatment for osteoporosis, a yearly bone mass measurement was recommended until stability was demonstrated. Once stability was demonstrated, an interval of 2 years was recommended between measurements. AACE recommended that the measurement of bone density at peripheral sites *not* be used for diagnosis or monitoring but instead limited to assessment of fracture risk.

The broader recommendations for the use of bone densitometry in clinical practice were very similar to the recommendations issued in 1996. There was some change in the wording and the recommendations were expanded to include women 40 years of age and older with fractures and all women age 65 and older. The 2001 recommendations were as follows:

- For risk assessment in peri- and postmenopausal women with risk factors for fractures and willingness to consider intervention
- In women with X-ray findings suggestive of osteoporosis
- In women beginning or already receiving long-term glucocorticoids or other drugs associated with bone loss
- In all adult women with symptomatic hyperparathyroidism, other diseases, or nutritional conditions associated with bone loss if management would be affected by the outcome of the test
- For establishing skeletal stability and monitoring therapeutic response in women receiving treatment for osteoporosis
- In all women 40 years of age and older who have sustained a fracture
- In all women age 65 and older

The timing of repeat bone density testing was originally addressed in the 1996 AACE guidelines; however, the 2001 guidelines more clearly communicated AACE's recommendations. In 2001, AACE recommended:

- For patients with a normal BMD: consider a follow-up measurement in 3–5 years, if necessary
- For patients in an osteoporosis prevention program: repeat bone density testing every 1–2 years until stability of the bone mass is demonstrated. Once stability was achieved, AACE recommended follow-up measurements every 2–3 years
- For patients in an osteoporosis treatment program: repeated bone density testing was recommended yearly for 2 years and until stability was demonstrated. Once stability of the bone density was demonstrated, the follow-up interval increased to 2 years

The 2003 AACE Guidelines

Selected updates to the 2001 AACE guidelines were issued in 2003 (*22*). There were no changes, however, with regard to patient selection criteria for bone density testing in the context of postmenopausal osteoporosis. AACE continued to recommend testing in:

- All women age 65 and older
- All adult women with a history of low-trauma fracture
- All younger postmenopausal women with clinical risk factors for fracture

In 2003, as in 2001, AACE noted that DXA of the spine or hip or QCT of the spine could be used for the diagnosis of osteoporosis and monitoring therapy. AACE continued to recommend limiting peripheral bone density testing for the assessment of fracture risk. The recommendations for the timing of follow-up measurements did not change from 2001.

GUIDELINES FROM THE EUROPEAN FOUNDATION FOR OSTEOPOROSIS AND BONE DISEASE

1996 European Foundation for Osteoporosis and Bone Disease Guidelines

The 1996 European Foundation for Osteoporosis and Bone Disease (EFFO)[5] guidelines were some of the most practical guidelines ever issued for the clinical application of bone density measurements (*23*). Some of the clinical circumstances in which the EFFO believed that bone mass measurements should be considered are shown in Table 7-4.

The 1996 EFFO guidelines, like the 1996 ISCD guidelines, noted that the site of the bone density measurement should be determined by the intent of the measurement. While the EFFO observed that the hip may be less affected by changes of osteoarthrosis in the elderly and was the preferred site for a site-specific hip fracture risk assessment, they also observed that changes in BMD from therapeutic interventions were more likely to be documented in the spine. The EFFO also noted that the hip, wrist, or spine sites could be used for global fracture risk assessments in women around the time of menopause. While the EFFO recommended scanning only one site initially, they

[5] The EFFO was founded in 1987. In 1998 it joined with the International Federation of Societies on Skeletal Diseases to become the International Osteoporosis Foundation.

Table 7-4
Indications for Bone Mass Measurements from the EFFO Guidelines

1. Presence of strong risk factors
    a. Premature menopause (<45 years)
    b. Prolonged secondary amenorrhea
    c. Primary hypogonadism
    d. Corticosteroid therapy (>7.5 mg/day for 1 year or more)
    e. Conditions associated with osteoporosis
        i.   Anorexia nervosa
        ii. Malabsorption
        iii. Primary hyperparathyroidism
        iv. Post-transplantation
        v.   Chronic renal failure
        vi. Osteogenesis imperfecta
        vii. Neoplasm
        viii. Hyperthyroidism
        ix. Prolonged immobilization
        x.   Cushing's syndrome
2. Radiographic evidence of osteopenia and/or vertebral deformity
3. Previous fragility fracture, for example of the hip, spine, wrist, or upper
    humerus
4. Significant loss of height or thoracic kyphosis
5. Monitoring of treatment
    a. Hormone replacement treatment in patients with secondary osteoporosis
    b. Other agents, e.g. bisphosphonates, calcitonin, fluoride salts, vitamin D and
        its metabolites

Reproduced with kind permission from Springer Science+Business Media from ref. (*23*)

acknowledged that there might be clinical circumstances in which two sites were necessary in order to assess sites that were predominantly cortical or predominantly trabecular bone.[6]

The 1996 EFFO guidelines noted that the interval between BMD measurements for the detection of bone loss over time would vary with the anticipated rate of loss from the disease process. In some circumstances, the interval could be as short as 6 months. In others, the interval would be 2–3 years. In monitoring changes in BMD from a therapeutic intervention, the EFFO noted that the interval between measurements would again be determined by the agent being used and the site being measured. This statement reflects the combined effect of the expected rate of change from a particular agent at a given site and the precision of the measurement at that site.[7] They noted that the usual interval for such measurements was 1–2 years. The monitoring of women on hormone replacement therapy that was prescribed *for postmenopausal symptoms* was not recommended except

___

[6] See Chapter 2 for a discussion of the relative percentages of cortical and trabecular bone at various densitometry sites.

[7] See Chapter 11 for a discussion of the relationship between precision and rate of change in determining the interval between measurements.

in the case of complicating factors that might increase the woman's risk for secondary osteoporosis. If hormone replacement was prescribed specifically *for the treatment of osteoporosis*, the EFFO did recommend periodic monitoring because of the variability in response to hormone treatment.

1997 EFFO Guidelines

In 1997, the EFFO issued guidelines (*24*) which dealt with the broader issues of the diagnosis and management of osteoporosis. In these guidelines, patient selection was not discussed in as great a detail as in the 1996 guidelines (*23*) on bone density testing. In 1997, the EFFO (*24*) emphasized that the measurement of bone density was indicated in individuals with strong risk factors for osteoporosis in order to optimize selection of patients for treatment. The EFFO again emphasized that the choice of skeletal site should be determined by the intent of the measurement, noting that measurements of the spine, hip, or wrist may be appropriate in younger individuals, while the hip might be more appropriate in the elderly. The 1997 EFFO guidelines noted that the interval between measurements for monitoring therapy should generally not be less than 2 years.

2002 AMERICAN COLLEGE OF OBSTETRICIANS AND GYNECOLOGISTS RECOMMENDATIONS FOR BONE DENSITY SCREENING FOR OSTEOPOROSIS

In a press release (*25*) on February 28, 2002, the American College of Obstetricians and Gynecologists (ACOG) announced long-awaited recommendations for the use of bone densitometry. ACOG, like the NOF and AACE, recommended that all postmenopausal women 65 years of age and older be screened for osteoporosis. Similarly, they also recommended testing in postmenopausal women under the age of 65 with one or more risk factors. The risk factors ACOG noted in the press release were a personal history of fracture as an adult, Caucasian race, a history of alcoholism, and impaired eyesight after correction.

ACOG also noted that bone density testing might be useful in both pre- and postmenopausal women with other diseases or conditions associated with an increased risk for osteoporosis. The diseases and conditions emphasized in the press release are listed in Table 7-5. ACOG recommended that repeat testing for screening purposes should not occur more often than every 2 years. DXA was described by ACOG as the gold standard for bone density testing.

THE NORTH AMERICAN MENOPAUSE SOCIETY GUIDELINES

2002 The North American Menopause Society Guidelines

The North American Menopause Society (NAMS) published a comprehensive review of postmenopausal osteoporosis in the journal *Menopause* in 2002 (*26*). Included in the review were recommendations for bone density testing in the specific context of the prevention and management of postmenopausal osteoporosis. NAMS noted that measurement of BMD was the preferred method for diagnosing osteoporosis and that DXA is the "technological standard" for measuring BMD. NAMS stated that the total hip was the preferred region of interest to evaluate, particularly when measuring bone density in

Table 7-5
**ACOG: 2001 Recommendations for Bone Density Screening for Osteoporosis.
Diseases and Conditions Associated with an Increased Risk for Osteoporosis in
Which BMD Testing May Be Useful in Both Pre- and Postmenopausal Women.**
http://www.acog.org/from_home/publications/press_releases/nr02-28-02-1.htm

● Endometriosis	● Rheumatoid Arthritis
● Hemophilia	● Multiple Sclerosis
● Lymphoma	● Tobacco
● Leukemia	● Lithium
● Eating Disorders	● Heparin
● Nutritional Disorders	

women over 60 because of the increased likelihood of degenerative calcification in the spine that would affect spine measurements.[8] Nevertheless, spine measurements were described as useful in early postmenopausal women because of the faster rate of bone loss at that site compared to the rate seen at the proximal femur. Citing a report from the International Osteoporosis Foundation (IOF) published in 2000(*27*), NAMS stated that they generally supported the use of the total hip or femoral neck for the diagnosis of osteoporosis rather than other skeletal sites.

The NAMS recommendations, like those of the NOF, ACOG, and AACE included measuring bone density in all women age 65 years and older. They also recommended measuring bone density in postmenopausal women under the age of 65 who had at least one of the following risk factors: a non-spine fracture after menopause, weight less than 127 lbs., or a history of a first-degree relative with a spine or hip fracture. NAMS also recommended BMD measurements in premenopausal women who experienced fractures deemed to be low-trauma fractures and those with known causes of bone loss.

Like AACE, NAMS also addressed the frequency of repeat testing, in various clinical circumstances although the testing intervals tended to be longer than those recommended by AACE. In women not receiving a pharmacologic intervention for osteoporosis, NAMS stated that repeat testing should not be performed for 3–5 years. In women who were receiving treatment, a testing interval of 2 years was recommended. NAMS stated that peripheral sites should not be used to monitor therapy. Instead, they noted that peripheral site measurements should be used only for fracture risk assessments. NAMS recommended that diagnosis and monitoring be done using the spine or proximal femur.

2006 NAMS Guidelines

In the 2006, NAMS (*28*) continued to recommend BMD testing in postmenopausal women age 65 and older and in younger postmenopausal women with specific risk factors. The risk factors emphasized in 2006 were: fracture after menopause, body

---

[8] See Chapter 2 for a discussion of the effect of dystrophic calcification on the measurement of BMD in the spine.

weight $<$ 127 lbs (57.5 kg) or BMI $<$21 kg/m^2, parental hip fracture, and current smoking. Although NAMS continued to recommend testing in postmenopausal women with known medical causes of bone loss regardless of age, they no longer recommended testing in premenopausal women. Recommendations for the frequency of repeat testing did not change from 2002. The 2006 NAMS recommendations were a departure from the 2002 recommendations in the choice of skeletal site for the diagnosis of osteoporosis. In 2006, NAMS recommended the use of the PA lumbar spine, total hip, or femoral neck for the diagnosis of osteoporosis, much as ISCD (*4*) had done in 2005.

2002 UNITED STATES PREVENTIVE SERVICES TASK FORCE RECOMMENDATIONS

In September 2002, the United States Preventive Services Task Force (USPSTF) issued recommendations for bone density testing when screening for postmenopausal osteoporosis (*29*). Like the guidelines from the NOF, AACE, NAMS, and ACOG that preceded the release of these recommendations, the USPSTF recommended that women age 65 and older be tested for osteoporosis. Unlike previous guidelines, which also recommended testing for postmenopausal women younger than age 65 who had risk factors for osteoporosis, the USPSTF limited their recommendation for screening in younger postmenopausal women to those women ages 60–64 who were considered at high risk for osteoporosis. They made no comment on screening for postmenopausal women younger than age 60. The USPSTF also noted that there was no data to determine an upper age limit for screening.

In making these recommendations, the USPSTF did not direct the clinician to use a specific bone density technology or skeletal site. They also noted that the risk factors that should be considered in deciding whether to test the younger postmenopausal woman were difficult to identify. Body weight less than 154 lb (70 kg), increasing age, and no current use of estrogen were identified as strong predictors of low bone density.

The recommendations to screen women age 65 and older and women 60–64 at high risk for osteoporosis were classified by the USPSTF as Grade B recommendations. A Grade B recommendation meant that the USPSTF recommended that clinicians routinely provide such services to their patients based on finding fair evidence that the service was beneficial in improving outcomes and that such benefit outweighed any potential harm. The evidence supporting these recommendations was characterized as fair on the USPSTF scale of good, fair, and poor. A characterization of fair indicated that the USPSTF believed that the evidence was sufficient to determine the effect of the service on health outcomes but was limited by one or a number of factors.

The evidence reviewed by the USPSTF predominantly came from searches of MEDLINE spanning 1966 to May 2001, HealthSTAR spanning 1975 to May 2001, and Cochrane databases (*30*). No studies were identified that directly linked screening for postmenopausal osteoporosis using risk factors or bone densitometry to a reduction in osteoporotic fractures. It was primarily for this reason that the evidence for the screening recommendations from the USPSTF was characterized as fair rather than good. Numerous studies were identified that evaluated the associations between risk factors and low bone density and fractures as well as studies documenting the predictive

ability of bone densitometry for fracture risk. The USPSTF also reviewed published trials of the therapeutic agents approved by the Food and Drug Administration for either the prevention or treatment of postmenopausal osteoporosis or both.

Based on their review, the USPSTF estimated the effectiveness of screening 10,000 women with densitometry in reducing hip and spine fractures. Age-specific prevalence rates for osteoporosis and treatment effects based on clinical trial results were considered and an adherence to therapy rate of 70% was assumed. Available treatments were assumed to reduce the risk of hip fractures by 37% and spine fractures by 48%. The outcomes were also based on the assumption that bone density was measured at the femoral neck using DXA. Within this framework, it was estimated that bone density testing in 10,000 women age 65–69 would result in 1200 women being identified as osteoporotic, based on WHO criteria, and subsequently treated. Treatment of these women would prevent 14 hip fractures and 40 spine fractures, resulting in a number needed to screen to prevent 1 hip fracture of 731 and a number needed to screen to prevent 1 spine fracture of 248. In women age 70 and older, the number identified as osteoporotic would be higher because of the higher prevalence of disease in this age group and the number needed to screen to prevent one hip or one spine fracture, lower.

The USPSTF is an independent panel of experts in primary care (*31*). The first panel was convened in 1984 by the US Public Health Service. Its mission was to create age-, gender- and risk-based recommendations for services to be used in primary care using evidence-based medicine. In 1998, the Agency for Healthcare Research and Quality (previously known as the Agency for Healthcare Policy and Research) convened the third USPSTF panel. The members of the panel are experts representing various specialties of medicine who are selected from nominees based on their expertise in preventive and evidence-based medicine and primary care. Guidelines produced by the USPSTF panel are not considered official statements from the Agency for Healthcare Research and Quality, the Department of Health and Human Services, or the US Public Health Service.

WORLD HEALTH ORGANIZATION TASK FORCE RECOMMENDATIONS

1999 World Health Organization Recommendations

An interim report (*32*) from the World Health Organization (WHO) Task Force for Osteoporosis was published in 1999 in which recommendations for bone density testing for both[9] men and women were made. Bone density measurements were recommended if there was:

- Radiographic evidence of osteopenia or vertebral deformity
- Loss of height or thoracic kyphosis
- Previous low-trauma fracture
- Prolonged corticosteroid therapy
- Hypogonadism

---

[9] In these guidelines, reference to "individuals" was made rather than specifically men or women.

- Chronic disorders associated with osteoporosis
- A maternal history of hip fracture
- A body mass index less than 19 kg/m^2
- A low calcium intake

2003 World Health Organization Recommendations

In 2003, the WHO issued a new report (*33*) on the prevention and management of osteoporosis in which the indications for bone density testing noted in 1999 were largely reiterated. Low calcium intake was dropped as an indication for testing and two new indications were added: premature menopause (< 45 years) and prolonged secondary amenorrhea (> 1 year). The WHO noted that DXA was the gold standard technique and that the proximal femur was the preferred skeletal site to measure.

GUIDELINES FOR BONE DENSITY TESTING IN MEN ONLY

Determining when testing is appropriate in men has become increasingly important with the advent of prescription pharmacologic therapy for the treatment of osteoporosis in men. The prevalence of osteoporosis in men, while not as great as that in women, is high. In one study (*34*) the prevalence of osteoporosis in a population-based sample of 348 men was 19% when osteoporosis was defined as 2.5 SD or more below the average peak BMD for men. The major risk factors for osteoporosis in men are not dissimilar from those seen in women: cigarette smoking, advancing age, risk of falls, and the presence of diseases or the use of medications known to affect bone metabolism (*35–37*). Heavy alcohol consumption is considered a major risk factor in men, more so than in women. Other risk factors include a sedentary lifestyle, life-long low calcium intake, and low body weight.

In 2001, Orwoll published recommendations (*38*) for bone density testing in men, which did not differ considerably from the 1998 clinical guidelines for bone density testing in women from the NOF. Orwoll recommended testing in men in the following circumstances:

- Men with low-trauma fractures
- Men with prevalent spine deformities
- Men with radiographic evidence of osteopenia
- Men with medical conditions associated with an increased risk of bone loss such as hyperparathyroidism or overt hypogonadism
- Men receiving medications associated with an increased risk of bone loss such as corticosteroids

In 2002, ISCD (*39*) published a position paper on the diagnosis of osteoporosis in men and non-Caucasian women. Although the focus of this paper was the applicability of the World Health Organization criteria for the diagnosis of osteoporosis in Caucasian women to these other groups, recommendations were made for bone density testing in men. ISCD recommended bone density testing in the following groups of men:

- Men ≥70 years of age regardless of other risk factors
- Men with a prior history of fragility fracture
- Men with conditions known to increase the risk of bone loss and/or fracture such as hypogonadism, corticosteroid treatment, hyperparathyroidism, alcohol abuse, anticonvulsant use, and prior gastrectomy

As noted earlier in this chapter, the 2008 NOF guidelines (*16*) recommended bone density testing in a variety of different clinical circumstances applicable to both men and women. The NOF, like ISCD, also specifically recommended bone density testing in men age 70 and older.

The American College of Physician (ACP) issued guidelines for osteoporosis screening in men in 2008 (*40*). These guidelines were based on the evaluation of articles from the medical literature spanning 1990–2007. ACP recommended a careful assessment of clinical risk factors for osteoporosis in men prior to the age of 65, noting that men found to be at increased risk for osteoporosis were candidates for bone density testing. The risk factors noted by the ACP are listed in Table 7-6. ACP also noted that DXA was the preferred testing technology.

<div align="center">

Table 7-6

Risk Factors for Osteoporosis in Men According to the American College of Physicians (*40*)

</div>

- Age > 70 years
- Low body weight (BMI < 20–25 kg/m^2)
- Weight loss >10% (from young-adult weight or recently)
- Physical inactivity
- Corticosteroid use
- Androgen deprivation therapy
- Previous fragility fracture

HOW DO THE GUIDELINES COMPARE?

There is far more unanimity among the guidelines from the various organizations than differences. The four clinical circumstances in which bone mass measurements might be performed originally proposed to HCFA by the National Osteoporosis Foundation in 1988 have been repeated in subsequent guidelines from other organizations although additions to various guidelines have occurred over the years. The various guidelines have also noted the utility of central DXA in the serial assessment of bone density while recommending against the use of peripheral sites measured by any technique for this purpose. There was general agreement that hip fracture risk was best assessed by measuring the hip if the technology required to perform the hip measurement was available.

All of the guidelines emphasized to some degree that the measurement should not be performed if a decision to intervene would not be affected by the measurement. The need for strict quality control procedures in the performance of densitometry has also been uniformly emphasized.

A comparison of the major recommendations found in the more recent guidelines is shown in Table 7-7. The most glaring contrast among various versions of the guidelines

Table 7-7

A Comparison of Major Guidelines for Bone Density Testing for the Detection of Osteoporosis

	Women ≥ Age 65	Postmenopausal Women ≤ Age 64 and At Least One Risk Factor	Postmenopausal Women with Fractures	Men ≥ Age 70	Technique for Diagnosis	Site for Diagnosis [a]	Against Using Peripheral Sites for Monitoring
NOF 1998				—	DXA	Hip Preferred	—
NOF 2003				—	DXA	Hip Preferred, Spine	—
NOF 2008[g]					DXA	PA Lumbar Spine, Total Hip or Femoral Neck	
OSC 2002		[c]		[c]	DXA	PA Lumbar Spine Proximal Femur	
OC 2006		[c]		—	DXA	PA Lumbar Spine Proximal Femur	
WHO 1999	[b]	[b]	[c]	X[c]	DXA	Hip Preferred	—
WHO 2003	X[c]	X[c]		X[c]	DXA	Hip	—
IOF 2000	—	—	[d]	—	DXA	Total Hip	—
AACE 2001			[d]	—	DXA/QCT	Spine, Proximal Femur	
AACE 2003			[d]	—	DXA/QCT	Spine, Proximal Femur	
ACOG 2002				—	DXA	—	—
NAMS 2002				—	DXA	Total Hip Preferred, Femoral Neck or PA Lumbar Spine	
NAMS 2006				—	DXA	PA Lumbar Spine, Total Hip and Femoral Neck using the lowest T-score of the 3	

Guideline					Test	Measurement Site
USPSTF 2002	—	—	—	e	—	—
ISCD 2003	—	—	—		DXA[f]	PA Lumbar Spine, Proximal Femur (Total Hip, Femoral Neck or Trochanter)
ISCD 2005					DXA[f]	PA Lumbar Spine, Total Hip or Femoral Neck whichever is lowest (not Ward's or the Trochanter)
ISCD 2007[g]					DXA	A Lumbar Spine, Total Hip or Femoral Neck, whichever is lowest (not Ward's or the Trochanter)

NOF, National Osteoporosis Foundation; OSC, Osteoporosis Society of Canada; OC, Osteoporosis Canada; WHO, World Health Organization; IOF, International Osteoporosis Foundation; AACE, American Association of Clinical Endocrinologists; ACOG, American College of Obstetricians and Gynecologists; NAMS, North American Menopause Society; USPSTF, United States Preventative Services Task Force; ISCD, International Society for Clinical Densitometry.

[a]The term hip indicates that a specific region in the proximal femur was not specified.

[b]The WHO noted that hypogonadism, possibly to include all postmenopausal women, was justification for a measurement.

[c]A targeted case-finding approach based on the presence of risk factors is recommended, rather than using age as a criterion.

[d]Consideration was limited to low-trauma fractures.

[e]This recommendation was limited to postmenopausal women age 60–64.

[f]Methodologies other than DXA were not considered in these guidelines.

[g]Recommendations were also made for bone density testing in men in these guidelines but are not noted in this table.

X indicates a comment with significant limitations; — indicates no comment

within the same organization is the choice of skeletal site for the baseline measurement to diagnose osteoporosis and to which to apply the 1994 WHO criteria (*9*). For example, the 1996 guidelines from AACE (*20*) recommended the proximal femur as the preferred measurement site but the 2001 guidelines (*21*) noted that either the spine or proximal femur could be used. Although the WHO guidelines (*33*) continue to emphasize the proximal femur, ISCD (*5*) like AACE (*22*) and the EFFO (*23*) would not restrict a diagnostic measurement to the hip. These organizations would consider the PA lumbar spine as well. The preference for hipbone density measurements for diagnosis or fracture risk assessment is based on the ability of the hipbone density measurement to predict both spine and hip fracture risk and the relative lack of dystrophic changes at the hip that would affect the accuracy of the measurement. Although the hip can be used for follow-up measurements of bone density to assess therapeutic efficacy, this is not always clinically practical. The precision of proximal femur testing combined with the rates of change seen in the regions of interest in the proximal femur with currently available therapies result in a minimum wait of 2–3 years before efficacy can be assessed. Guidelines from the EFFO in 1996 noted that the spine, because of the greater percentage of trabecular bone, was more likely to demonstrate a greater response to therapeutic intervention than other sites. The precision of PA spine testing is also generally superior to that of proximal femur testing and equal to that of total hip testing. This combination of superior or equal precision and a greater expected magnitude of change makes the spine the preferred site for serial assessment of therapeutic efficacy. The dramatic improvement in the precision of the trochanteric region of interest (ROI) in the proximal femur seen with the newer fan-array DXA devices has given rise to a potential exception to the previous statement. Because the rate of change in the trochanteric ROI is similar to that seen in the PA spine, the use of the trochanteric ROI in the proximal femur for monitoring with the newer fan-array DXA devices may be as useful as the PA spine. No organization recommends the use of the trochanteric ROI for monitoring at this time, however.

REFERENCES

1. Miller PD, Bonnick SL, Rosen CJ. Consensus of an international panel on the clinical utility of bone mass measurement in the detection of low bone mass in the adult population. Calcif Tissue Int 1996;58:207–214.
2. Lenchik L, Leib ES, Hamdy RC, Binkley NC, Miller PD, Watts NB. Executive summary International Society for Clinical Densitometry position development conference Denver, Colorado July 20–22, 2001. J Clin Densitom 2002;5 Suppl:S1–S3.
3. Leib ES, Lewiecki EM, Binkley N, Hamdy RC. Official positions of the International Society for Clinical Densitometry. J Clin Densitom 2004; 7(1):1–6.
4. Binkley N, Bilezikian JP, Kendler DL, Leib ES, Lewiecki EM, Petak SM. Official positions of the international society for clinical densitometry and executive summary of the 2005 position development conference. J Clin Densitom 2006;9(1):4–14.
5. Baim S, Leonard BM, Bianchi ML, et al. Official positions of the international society for clinical densitometry and executive summary of the 2007 ISCD pediatric position development conference. J Clin Densitom 2008;11:6–21.
6. Cummings SR, Black DM, Nevitt MC, Browner W, Cauley J, Ensrud K, et al. Bone density at various sites for the prediction of hip fractures. Lancet 1993;341:72–75.
7. Melton LJ, Atkinson EJ, O'Fallon WM, Wahner HW, Riggs BL. Long-term fracture prediction by bone mineral assessed at different skeletal sites. J Bone Miner Res 1993;8:1227–1233.

8. Gardsell P, Johnell O, Nilsson BE, Gullberg B. Predicting various fragility fractures in women by forearm bone densitometry: a follow-up study. Calcif Tissue Int 1993;52:348–353.

9. World Health Organization. Assessment of fracture risk and its application to screening for post-menopausal osteoporosis. WHO technical report series. Geneva: WHO, 1994.

10. Johnston CC, Melton LJ, Lindsay R, Eddy DM. Clinical indications for bone mass measurements. A report from the scientific advisory board of the National Osteoporosis Foundation. J Bone Miner Res 1989;4(S2):1–28.

11. National Osteoporosis Foundation. Osteoporosis: review of the evidence for prevention, diagnosis, and treatment and cost-effectiveness analysis. Osteoporos Int 1998;S4:S7–S80.

12. National Osteoporosis Foundation. Physician's guide to prevention and treatment of osteoporosis. Belle Meade NJ: Excerpta Medica, 1999.

13. Osteoporosis: Review of the evidence for prevention, diagnosis, and treatment and cost-effectiveness analysis. Executive summary. Osteoporos Int 1998;S4:S3–S6.

14. Cummings SR, Nevitt MC, Browner WS, et al. Risk factors for hip fracture in white women. N Engl J Med 1995;332:767–773.

15. National Osteoporosis Foundation. Physician's guide to prevention and treatment of osteoporosis. 1–37. 2003. Washington, DC, National Osteoporosis Foundation.

16. National Osteoporosis Foundation. Clinician's guide to prevention and treatment of osteoporosis. 1–30. 2008. Washington, DC, National Osteoporosis Foundation.

17. Sturtridge W, Lentle B, Hanley DA. Prevention and management of osteoporosis: consensus statements from the scientific advisory board of the Osteoporosis Society of Canada. 2. The use of bone density measurement in the diagnosis and management of osteoporosis. CMAJ 1996;155:924–929.

18. Brown JP, Josse RG. 2002 clinical practice guidelines for the diagnosis and management of osteoporosis in Canada. CMAJ 2002;167:S1–S34.

19. Brown JP, Fortier M. Canadian consensus conference on osteoporosis, 2006 update. JOGC 2006;172:S95–S112.

20. Hodgson SF, Johnston CC. AACE clinical practice guidelines for the prevention and treatment of postmenopausal osteoporosis. Endocr Pract 1996;2:155–171.

21. Osteoporosis Task Force. American Association of Clinical Endocrinologists 2001 medical guidelines for clinical practice for the prevention and management of postmenopausal osteoporosis. Endocr Pract 2001;7:293–312.

22. Hodgson SF, Watts NB, Bilezikian JP et al. American Association of Clinical Endocrinologists medical guidelines for clinical practice for the prevention and treatment of postmenopausal osteoporosis: 2001 edition, with selected updates for 2003. Endocr Pract 2003;9(6):544–564.

23. Kanis J, Devogelaer J, Gennari C. Practical guide for the use of bone mineral measurements in the assessment of treatment of osteoporosis: a position paper of the European Foundation for Osteoporosis and Bone Disease. Osteoporos Int 1996;6:256–261.

24. Kanis JA, Delmas P, Burckhardt P, Cooper C, Torgerson D. Guidelines for diagnosis and management of osteoporosis. Osteoporos Int 1997;7(4):390–406.

25. ACOG releases recommendations for bone density screening for osteoporosis. Washington, DC: American College of Obstetricians and Gynecologists, 2002. (Accessed March 26, 2002, at http://www.acog.org/from_home/publications/press_releases/nr02-28-02-1.htm)

26. Management of postmenopausal osteoporosis: position statement of The North American Menopause Society. Menopause 2002;9:84–101.

27. Kanis JA, Gluer C-C. An update on the diagnosis and assessment of osteoporosis with densitometry. Committee of Scientific Advisors, International Osteoporosis Foundation. Osteoporos Int 2000;11:192–202.

28. Management of osteoporosis in postmenopausal women: 2006 position statement of The North American Menopause Society. Menopause 2006;13:340–367.

29. US Preventive Services Task Force. Screening for osteoporosis in postmenopausal women: recommendations and rationale. Ann Intern Med 2002;137:526–528.

30. Nelson HD, Helfand M, Woolf SH, Allan JD. Screening for postmenopausal osteoporosis: a review of the evidence for the US Preventive Services Task Force. Ann Intern Med 2002;137:529–541.

31. The New US Preventive Services Task Force. AHRQ Pub. No. 00-P046. Washington, DC: AHQR, February 2002. (Accessed October 19, 2002, at http://www.preventiveservices.ahrq.gov)

32. Genant HK, Cooper C, Poor G, et al. Interim report and recommendations of the World Health Organization Task-Force for osteoporosis. Osteoporos Int 1999;10:259–264.
33. WHO. Prevention and management of osteoporosis. [921], 1–192. 2003. Geneva, WHO. WHO Technical Report Series.
34. Melton LJ, Atkinson EJ, O'Connor MK, O'Fallon WM, Riggs BL. Bone density and fracture risk in men. J Bone Miner Res 1998;13:1915–1923.
35. Seeman E, Melton LJ, O'Fallon WM, Riggs BL. Risk factors for spinal osteoporosis in men. Am J Med 1983;75:977–983.
36. Jackson JA, Kleerekoper M. Osteoporosis in men: diagnosis, pathophysiology, and prevention. Medicine 1990;69:137–152.
37. Cauley JA, Smuda JM. Risk factors for fractures in men. In: Orwoll ES, ed. Osteoporosis in men. London, England: Academic Press, 1999:363–393.
38. Orwoll E. Perspective: assessing bone density in men. J Bone Miner Res 2000;15:1867–1870.
39. Binkley NC, Schmeer P, Wasnich RD, Lenchik L. What are the criteria by which a densitometric diagnosis of osteoporosis can be made in males and non-Caucasians? J Clin Densitom 2002;5:S19–S27.
40. Qaseem A, Snow V, Shekelle P, et al. Screening for osteoporosis in men: a clinical practice guideline from the American College of Physician. Ann Intern Med 2008; 148:680–684.

8 Selecting Patients for Bone Mass Measurements: Self-Assessment Indices

CONTENTS

Self-assessment indices are questionnaires or nomograms that utilize risk factors for low bone mass or osteoporosis to identify women who are likely to have a low bone density. Most indices have focused on women although self-assessment indices have begun to appear for men. Women and men who are identified in this fashion should be considered candidates for a bone density measurement. Although a man or woman can have a low bone density in the absence of any identifiable risk factors, these indices are useful in a variety of ways. They can help select those individuals who are less likely to have a low bone density as well as those who are more likely. Because most of these indices can be self-administered by the patient, they foster patient education and awareness and encourage the patient to initiate the discussion of bone density testing and osteoporosis with the physician.

In evaluating the utility of any one of these indices, it is useful to evaluate the process by which the index was created. In general, risk factors are identified and bone density measured in an initial group, called the development cohort. Regression analyses[1] are performed to determine which risk factors are significant predictors of having a

---

[1] See Chapter 3 for a discussion of regression analysis, sensitivity, and specificity, ROC curves and likelihood ratios.

predetermined level of bone density. Once the index is developed, it is then tested in a second group, called the validation cohort. Important measures of the utility of the index are the sensitivity, specificity, likelihood ratios, and the area under the receiver-operating characteristic (AUROC) curve. Before using any index the physician should determine if the development or validation cohort are similar to the population of patients in which the physician intends to use the index. It is also important to remember that most indices are designed to identify individuals likely to have a bone density that is at or below a specific level at one skeletal site only. Finally, determining what level of sensitivity and specificity is acceptable for these instruments is at least in part, a philosophical decision. A high sensitivity will ensure that most individuals with a low BMD are referred for testing. A high specificity will ensure that most individuals with a BMD not considered low are not referred for testing. In the former case, more individuals with a low BMD who might benefit from treatment will be identified. In the latter case, more unnecessary DXA studies may be avoided.

SIMPLE CALCULATED OSTEOPOROSIS RISK ESTIMATION

The Simple Calculated Osteoporosis Risk Estimation (SCORE) index was based on an analysis of the relationship between more than 350 variables and osteoporosis ([1]). The development cohort for SCORE consisted of community-dwelling women, 45 years of age and older, who were recruited from October 1994 to February 1995. There were 1279 postmenopausal women in this cohort. Eighty-nine percent of these women were Caucasian and their average age was 61.5 years. Each woman in this original development cohort completed a self-administered questionnaire to determine the presence or absence of factors possibly or probably associated with osteoporosis. Proximal femur and PA spine bone density studies were performed with DXA.

Through statistical analysis, the initial list of more than 350 variables was reduced to 123. The data was further evaluated at that point and any variable for which more than 4% of the responses from the questionnaire were missing was eliminated from consideration. This resulted in the number of variables considered for inclusion in a model to predict BMD being reduced to 101.

Multivariate linear regression[2] was used to develop the model for predicting the BMD T-score from the candidate variables. Statistically significant predictor variables were retained in the final model and the screening characteristics were determined for the model by calculating the specificity for the cutpoint value of probability that resulted in 90% sensitivity. The linear regression model was then simplified and the regression coefficients for each significant variable were reduced to integers. These integers are summed to give the SCORE, as shown in Table 8-1. For example, a 60-year-old Caucasian woman who weighs 120 lb, with no history of rheumatoid arthritis, a history of wrist fracture at age 57, and no history of estrogen use would have a SCORE of 16.[3]

---

[2] See Chapter 3 for a discussion of linear regression.

[3] The example is calculated as follows: +5 for race, 0 for no history of rheumatoid arthritis, +4 for the history of wrist fracture after age 45, +(3 × 6) for age, +1 for history of no estrogen use, and – (1 × 12) for weight. The sum is 16.

Table 8-1
Coefficients for Calculating SCORE (Simple Calculated Osteoporosis Risk Estimation)

Variable	Score	If Woman
Race	5	is NOT Black
Rheumatoid Arthritis	4	HAS Rheumatoid Arthritis
History of Fractures	4	for EACH TYPE (wrist, rib, hip) of nontraumatic fracture after age 45 (maximum score – 12)
Age	3	Times first digit of age in years
Estrogen	1	if NEVER received estrogen therapy
Weight	–1	Times weight divided by 10 and truncated to integer

Reproduced with permission of the publisher from ref. (*1*). Permission conveyed by the Copyright Clearance Center.

Table 8-2
Sensitivity and Specificity of SCORE for Various Threshold Values and Levels of Bone Mineral Density at the Femoral Neck Calculated Using Manufacturer's Reference Data

Threshold SCORE	Prediction of BMD ≤ –2 SD		Prediction of BMD ≤ –2.5 SD		Prediction of BMD ≤ –1 SD	
	Sensitivity	Specificity	Sensitivity	Specificity	Sensitivity	Specificity
0	0.993	0.124	0.996	0.103	0.980	0.199
1	0.986	0.167	0.992	0.140	0.963	0.256
2	0.976	0.203	0.992	0.176	0.948	0.305
3	0.966	0.257	0.992	0.223	0.924	0.368
4	0.942	0.340	0.974	0.294	0.872	0.447
5	0.925	0.417	0.954	0.361	0.831	0.529
6	0.894	0.497	0.936	0.433	0.776	0.602
7	0.816	0.578	0.883	0.520	0.694	0.678
8	0.737	0.672	0.822	0.614	0.616	0.787
9	0.674	0.746	0.769	0.692	0.540	0.845
10	0.604	0.824	0.708	0.772	0.456	0.902

Reproduced with permission of the publisher from ref. (*1*). Permission conveyed by the Copyright Clearance Center

As shown in Table 8-2, the SCORE threshold of 6 resulted in 90% sensitivity for identifying women with a femoral neck T-score ≤–2. The specificity at this cutpoint was 50%. When sensitivity is plotted against 1–specificity for the linear regression model, the area under the curve (AUC) for the resulting ROC is 0.811. The AUC is a measure of the probability that the predicted probability of low bone density is greater for women who have a low BMD between any two randomly paired low BMD and non-low BMD women. An AUC of around 0.8 is considered acceptable for a diagnostic test (*2*). This graph is shown in Fig. 3-8 as part of the discussion of ROC curves. In the worked

example of SCORE noted above, the SCORE of 16 is above the SCORE threshold of 6 for a high probability of a bone density T-score of ≤-2 at the femoral neck. As a result, the woman should be considered for bone density testing.

To validate the SCORE model, a second group of 259 women were recruited of whom 208 were postmenopausal. Ninety-four percent of these women were Caucasian and their average age was 63.1 years. Bone density was again measured with DXA and the SCORE questionnaire was completed. The sensitivity, specificity, and AUC for SCORE in both the development and validation cohorts are shown in Table 8-3.

Table 8-3
Summary of Results in Development and Validation Cohorts for SCORE Threshold of 6 for the Identification of a BMD ≤-2 at the Femoral Neck

Cohort	n[a]	Sensitivity	95% Confidence Interval	Specificity	95% Confidence Interval	AUC
Development	1102	0.89	0.86–0.92	0.50	0.47–0.52	0.77
Validation	185	0.91	0.81–0.96	0.40	0.30–0.52	0.72

[a]Number of women with no missing responses on all variables used in the predictor.
Adapted with permission of the publisher from ref. (*1*). Permission conveyed by the Copyright Clearance Center.

The SCORE questionnaire performed well in both the development and validation cohorts. Sensitivities of 0.89 and 0.91 indicate that 89% and 91% of the women in the two cohorts with femoral neck T-scores ≤-2 were at or above the SCORE threshold of 6 and would have been appropriately referred for bone density testing. In order to achieve this high degree of detection, the lower specificities of 0.50 and 0.40 in the two cohorts must be accepted. Fifty and 60% of the women in the two cohorts with femoral neck T-scores greater than -2 would also be referred for testing because their test scores were at or above the SCORE threshold of 6.

The initial publication of the design of the SCORE questionnaire and its utility was greeted with skepticism. Prior to the development of SCORE, most attempts to use clinical risk factors to select women for bone density testing had not resulted in adequate sensitivity and specificity. The questionnaire itself appeared deceptively simple in its final form, belying the very complex statistical analysis of more than 350 variables. It was also noted that 24% of the women in the validation cohort had rheumatoid arthritis. This cast doubt on the applicability and validity of the SCORE questionnaire to the general population in which such a high percentage of rheumatoid arthritis would not be expected. Finally, the femoral neck T-scores used in the development and validation phase of SCORE were based on the manufacturer's reference databases, not the NHANES III database (*3*). A Lunar DXA device was used in slightly more than half the cases in both cohorts with a Hologic or Norland DXA device used in the remaining cases. It was thus initially unclear how the adoption of the NHANES III database T-scores might affect the choice of the SCORE threshold for identifying individuals with a high probability of low bone mass at the femoral neck.

Other researchers attempted to validate the SCORE questionnaire in different study populations. Cadarette et al. (*4*) utilized the SCORE questionnaire in a population of 398 postmenopausal women with an average age of 64.5 years. Of the 398 women, 86.7% were Caucasian. Bone density was measured at the femoral neck and PA lumbar spine with a Hologic DXA device and T-scores were calculated using the manufacturer's

reference data. The original SCORE threshold of 6 was used to identify those women who had a high probability of having a T-score ≤–2 at the spine, femoral neck or both. The sensitivity and specificity for identifying women with a low BMD at either the spine or femoral neck in this study were 0.90 and 0.32, respectively. This means that 90% of the women with a low BMD at either the PA spine or femoral neck would be referred for bone density testing. Conversely, 68% of women with a BMD not considered low at either site would also be referred for testing, but 32% would not. When the analysis was restricted to identifying women with a low BMD at the femoral neck only, the sensitivity and specificity at a SCORE threshold of 6 were 0.904 and 0.29, respectively.

In a similar study, Von Mühlen et al. (5) studied 1013 postmenopausal Caucasian women who were part of the Rancho Bernardo osteoporosis study. The average age of these women was 72.5 years. Bone density was measured using a Hologic DXA device and T-scores were calculated for the femoral neck using the manufacturer's reference data. At the original SCORE threshold of 6, the sensitivity was an extremely high 0.98 but the specificity was only 0.125. The authors concluded that in these women who were much older than the original SCORE development and validation cohorts, the questionnaire had limited value for selecting women for a bone density measurement.

In 2000, Ungar et al. (6) writing in the *Journal of Clinical Densitometry* published the results from the use of the SCORE questionnaire in 307 postmenopausal women. The average age of the women was 58.4 years and 91% were Caucasian. The questionnaire was self-administered and the women then underwent PA lumbar spine and proximal femur bone density testing with either a Lunar or Hologic DXA device. PA spine T-scores were derived from the manufacturer's databases but the femoral neck T-scores were derived using the NHANES III reference database. Women with a T-score of –2.0 or lower at either skeletal site were considered as having low BMD.

Table 8-4 lists the sensitivity and specificity for different SCORE thresholds by age range for the 307 women in this study. At the original threshold of 6, the sensitivity and specificity for women aged 50–59 years were 0.96 and 0.51, respectively. In the older women, a SCORE threshold of 8 was required to achieve a sensitivity of 0.90. At this sensitivity, however, the specificity was only 0.20. The AU ROC for the older women was also poor at 0.594. The authors concluded that SCORE performed better in women in their fifties compared to women in their sixties and that SCORE thresholds higher than 6 were required in older women.

Table 8-4
Sensitivity and Specificity for Various SCORE Thresholds in Two Age Groups

Group	N	SCORE cut-point	Sensitivity	Specificity
50–59 y	183	6	0.96	0.51
		7	0.85	0.65
		8	0.74	0.77
60–69 y	124	8	0.90	0.20
		9	0.77	0.39
		10	0.72	0.58

Reproduced with permission from Elsevier from ref. (6).

OSTEOPOROSIS RISK ASSESSMENT INSTRUMENT

The Osteoporosis Risk Assessment Instrument (ORAI) questionnaire was developed by Cadarette et al. (7) using information obtained at the baseline visit for women participating in the Canadian Multicentre Osteoporosis Study[4] (CaMos). Nine hundred twenty-six women were participants in the development cohort and 450 participated in the validation cohort. The overwhelming majority of women in both cohorts were Caucasian. The average age was approximately 63 and three-fourths of the women had a femoral neck or lumbar spine T-score of –2 or better.

Information on risk factors was obtained from questionnaires that the women completed on enrollment in CaMos. The relationship between each risk factor and a low BMD at either the spine or femoral neck was evaluated using logistic regression techniques. The variables that were the best predictors of low BMD at either skeletal site were considered for inclusion in the final model to predict low BMD at either site. The six variables were age, weight, current estrogen use, menopause, physical activity, and previous minimal trauma fracture at age 45 or older. Models were tested that included from one to six variables. The sensitivity of the three variable model containing age, weight, and estrogen use was similar to the sensitivity of the models containing four, five, and six variables. Although the sensitivity of the model containing only the two variables age and weight was similar to the more complex models, the specificity was much lower. As a result, only the three variables of age, weight, and estrogen use were included in the final model.

Scores were assigned to the various risk factors by rounding the odds ratio for low BMD for that risk factor to the nearest integer. To ensure that few women with a low BMD at either site would be missed, threshold scores for recommending BMD testing were chosen to ensure 90% sensitivity. When the three-variable ORAI was tested in the validation cohort, its performance was similar to that seen in the development cohort. The sensitivity for identifying women with a PA lumbar spine or femoral neck T-score of –2 or poorer was 93.3% and the specificity was 46.4%.

In the ORAI scoring system, a woman was awarded from 0 to 15 points based on age, 0 to 9 points based on weight, and 2 points if she did not take estrogen. A score of 9 or greater indicated that a woman should be referred for testing. As a consequence of the scoring system, all women age 65 and older would be referred for testing. All women age 45 or older who weigh less than 60 kg (132 lb) would also be selected for testing. ORAI would also select women aged 55–64 years who weigh 60–70 kg and who are not currently taking estrogen.

THE STUDY OF OSTEOPOROTIC FRACTURES SIMPLE USEFUL RISK FACTOR SYSTEM

The Study of Osteoporotic Fractures Simple Useful Risk Factor System (SOFSURF) is a risk factor based statistical model for the prediction of a total hip BMD T-score of

---

[4] The Canadian Multicentre Osteoporosis Study (CaMos) is a population-based cohort study in which risk factors for osteoporosis, BMD, and osteoporotic fracture are being evaluated over a 5-year period.

Table 8-5
The SOFSURF Scoring System

Variable	Score
Weight < 150 lb	1
Current smoking	1
History of fracture after age 50	1
Weight < 130 lb[a]	2
Age > 65	0.2 for each year above 65

[a]This is in addition to the 1 point awarded for weight < 150 lb.
Adapted from ref. (8).

≤–2.5 in non-Black women age 67 years and older (8). Risk factor and bone density data from 8070 women in the very large Study of Osteoporotic Fractures were used to develop this prediction model. Weight and age were again strong predictors of total hip T-score as was seen in the development of the SCORE and ORAI instruments although those instruments focused on different skeletal sites. The scoring system for SOFSURF is shown in Table 8-5. In this development cohort, 85% of the women with a SOFSURF score greater than 3 had a total hip T-score of –2.5 or poorer. The AUROC for detecting this level of BMD at the total hip was 0.75.

ABONE

The ABONE instrument was proposed by Weinstein et al. (9) in 1999. ABONE is a mnemonic for age (A), bulk (B) and never estrogens (ONE). In the creation of the ABONE criteria, 1346 Caucasian, postmenopausal women underwent DXA testing of the spine and proximal femur and completed a risk factor questionnaire. Their average age was 62.2 years and they were an average of 16.2 years postmenopausal. Multivariate regression analysis was performed using the PA lumbar spine, total hip, and femoral neck T-score to determine which risk factors were independent predictors of osteoporosis. Osteoporosis was defined using World Health Organization criteria[5] and the NHANES III database[6] was used to calculate T-scores at the proximal femur. Among the potential risk factors that were evaluated were past or current use of steroids, thyroid replacement, heparin, oral contraceptives, estrogen, and alcohol. Caffeine intake, calcium intake, calcium supplementation, exercise, smoking history, family history of osteoporosis, and history of hysterectomy or oophorectomy were also evaluated.

The independent variables related to osteoporosis at the spine, total hip, and femoral neck were age and weight. Lack of postmenopausal estrogen use and lack of oral contraceptive use for at least 6 months were independent predictors for osteoporosis at any of the three sites.

In a subsequent publication (10) Weinstein et al. extended these observations to an additional 264 women. The addition of these 264 women increased the total number of

[5] See Chapter 9 for a discussion of the World Health Organization criteria for the diagnosis of osteoporosis based on measurement of the bone density.
[6] See Chapter 6 for a discussion of the NHANES III proximal femur database.

women studied to 1610 but did not change the average age or years postmenopausal. Multivariate regression analysis was again performed to determine which independent variables were significant predictors of osteoporosis. Age and years past menopause were positive predictors while weight was a negative predictor. Lack of either post-menopausal estrogen use or oral conceptive use for at least 6 months was also a signifi-cant predictor of osteoporosis. Ninety-five percent confidence intervals were calculated for age and weight to determine the best cutpoints for screening purposes. Based on these analyses, Weinstein and colleagues suggested that postmenopausal women greater than 65 years of age who weigh less than 140 lb at menopause or have never used estro-gens for more than 6 months be referred for bone density testing. A scoring system which awards 1 point for weight less than 140 lb at menopause or never use of estro-gens for more than 6 months was proposed such that any 65-year-old woman with an ABONE score of 1 or 2 would be referred for testing.

THE OSTEOPOROSIS SELF-ASSESSMENT TOOL

Koh and colleagues (*11*) developed the original Osteoporosis Self-Assessment Tool for Asians (OSTA) based on a study of 860 non-Caucasian, postmenopausal women from eight Asian countries. Risk factors were captured from a self-administered ques-tionnaire and bone density was measured by DXA in the proximal femur. Proximal femur T-scores were based on the manufacturer's reference data for Asian women. Statistical analysis was performed to determine which risk factors were independent predictors of BMD. The risk factors that were captured are listed in Table 8-6. These independent predictors were combined in a multivariable model from which risk factors were dropped one at a time until only statistically significant variables remained in the

Table 8-6
Risk Factors Evaluated in the Development of the OSTA Questionnaire

Age
Height
Weight
Race
Height loss
History of fracture
Age at menopause
History of rheumatoid arthritis
Calcium supplementation
Dietary calcium intake
Smoking history
Time spent in recreational physical activity
History of being bedridden
Sunlight exposure
Estrogen use
Thyroid hormone use
Corticosteroid use

Adapted with kind permission of Springer Science+Business Media from ref. (*11*).

model. An index was developed from the variables in the final model to identify those women with a high probability of having a femoral neck T-score of ≤–2.5.

The final model included 11 variables that were significantly and independently associated with femoral neck bone density: age, weight, current estrogen use, current thyroid hormone use, any fracture after age 45, spine fracture after age 45, Chinese or Thai ethnicity, and being from Malaysia, Hong Kong, or Taiwan. Each of these variables was assigned a value based on the regression coefficient for that variable in the statistical model. The index values for all 11 variables were then added for each woman.

The sensitivity and specificity for an OSTA cutpoint of –1 were 95% and 47%, respectively. The AUROC was 0.85. When thyroid hormone use and the three countries were dropped from the model, the AUROC was still 0.83. Dropping Chinese and Thai ethnicity and current estrogen use lowered the AUROC to only 0.80. Finally, dropping a history of any fracture or spine fracture after age 45 still resulted in an AUROC of 0.79. This left only age and weight in the final index. Using an OSTA cutpoint of –1 with only age and weight in the model, the sensitivity was 91% and the specificity was 45% for a femoral neck T-score ≤–2.5 in the development cohort. The two-variable index was validated in a cohort of 1123 Japanese women. A cutpoint of –1 resulted in a sensitivity of 98% and a specificity of 29% in this group.

The OSTA score is calculated by subtracting age in years from weight in kg, multiplying the result by 0.2 and truncating to an integer. For example, a 64-year-old Asian woman who weighs 56 kg would have an OSTA score of –1.[7] Using age and body weight to calculate the OSTA score, the authors identified three categories of risk. The low risk category included women with an OSTA score >–1. The women in the intermediate risk category had scores of –1 to –4 and the women in the high-risk category had scores <–4. Table 8-7 gives the total percentage of women in each group and the percentage with femoral neck T-scores ≤–2.5 for both the development and validation cohorts.

Table 8-7
Performance of the OSTA Index in the Development and Validation Cohorts by Risk Category for Femoral Neck T-Score ≤–2.5

Index Score	Asian Development Cohort		Japanese Validation Cohort	
	N (%), total	n (%) with T ≤–2.5	n (%)	n (%) with T ≤–2.5
< –4	62 (8%)	38 (61%)	281 (25%)	123 (44%)
–1 to –4	417 (52%)	62 (15%)	562 (50%)	56 (10%)
> –1	318 (40%)	10 (3%)	280 (25%)	4 (1%)

Adapted with kind permission of Springer Science+Business Media from ref. (*11*).

The OSTA index is easily transformed into a nomogram as shown in Fig. 8-1. Women in the high- and medium-risk category should be referred for bone density testing. It must be kept in mind that the cutpoint shown here is based on the original study of

---

[7] The OSTA score is calculated as follows: (56 – 64) × 0.2 = –1.6. This value is truncated to an integer resulting in an OSTA score of –1.
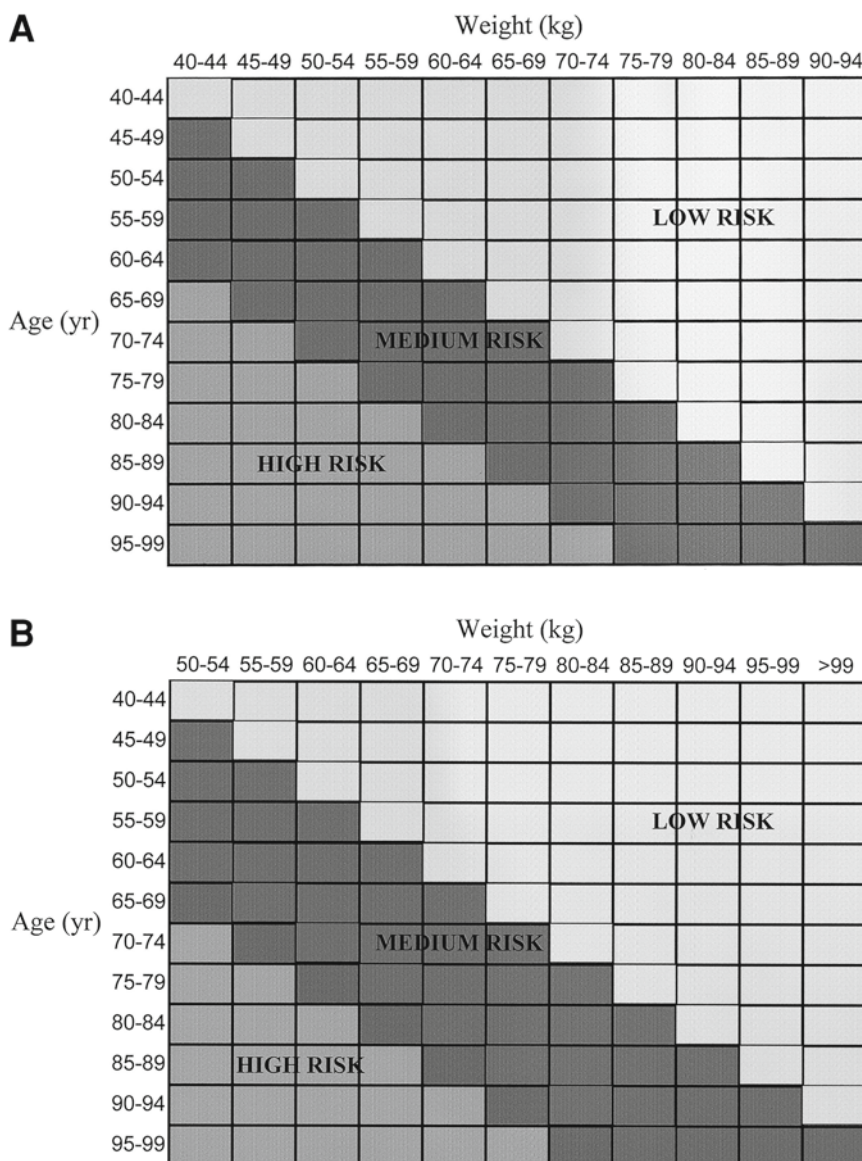
Fig. 8-1. (A) The OSTA nomogram for Asian women. **(B)** The OST nomogram for Caucasian women. The cells are shifted to the right, reflecting the effects of weight. Women in the high-and medium risk categories should undergo BMD testing because of a sufficiently high probability of osteoporosis at the femoral neck. These nomograms are found on the accompanying CD-ROM. ⓒ2001, Merck & Co., Inc., Whitehouse Station, NJ, USA. All rights reserved. Reproduced here with permission.

Asian women and is specific for predicting a T-score of –2.5 at the femoral neck. As will be seen, different cutpoints appear to be necessary if this index is to be used in other populations as well as for predicting different T-scores at other skeletal sites.

In 2002, Koh (*12*) reported the performance characteristics of the OSTA index in an additional group of 294 normal Singapore women with an average age of 59. The OSTA index calculated for each woman ranged from –10 to 7. The original OSTA cutpoints

of –1 and –4 were again used to establish high, moderate, and low risk categories. In this group, the index had a sensitivity of 90%, a specificity of 58%, and an AUROC of 0.82 for predicting a femoral neck T-score or –2.5 or poorer.

Koh (*13*) also attempted to utilize the OSTA index in 98 Asian men with an average age of 61 years. The calculated OSTA index values for these men ranged from –7 to 8. Using male Asian reference values to establish a T-score of –2.5 or poorer at the femoral neck, the original OSTA cutpoint of –1 resulted in a sensitivity of only 50% and a specificity of 78%.

Hochberg et al. (*14*) utilized the OSTA index to predict an osteoporotic femoral neck T-score in 140 Asian women who participated in the Fracture Intervention Trial in the United States. Utilizing an OSTA index cutpoint of 0[8] or less for the prediction of an osteoporotic femoral neck T-score based on reference data for Asian women, the sensitivity was 96% and the specificity was 37%. The positive likelihood ratio (LR+) was 1.52 and the negative likelihood ratio (LR–) was 0.12.

The OSTA index has also been utilized in Caucasian women. In this context, the name is shortened to the Osteoporosis Self-Assessment Tool (OST). Ben Sedrine and Reginster (*15*) reported the use of the OST index in 4035 Caucasian Belgian women with an average age of 61 and an overall prevalence of osteoporosis of 19%. Using the original OSTA index cutpoints of –1 and –4 to establish high, moderate, and low risk groups for a femoral neck T-score of –2.5 or poorer, 90% of the 3.4% of women in the high risk group were found to have osteopenia or osteoporosis. Thirty percent of the 4035 women were in the moderate risk group. Of these women 73% had either osteoporosis or osteopenia at the femoral neck. The authors noted that the prevalence of osteopenia and osteoporosis at the femoral neck was sufficiently high in the moderate-risk category to justify referral for a bone mass measurement when the OST index value was –1 or lower. This is the upper boundary of the moderate-risk group shown in the nomogram in Fig. 8-1A.

WEIGHT SELECTION CRITERIA

The use of weight alone as a criterion for selecting women for bone mass measurements was proposed in 1996 by Michaëlsson et al. (*16*) In this study reported in *Osteoporosis International*, only anthropomorphic measures were considered in predicting which individuals were likely to have a low bone density. The measures included height, weight, body mass index, waist-to-hip ratio, lean tissue mass, and fat tissue mass. Bone density was measured by DXA at the PA lumbar spine and femoral neck. Lean and fat tissue mass were determined using DXA total body studies. T-scores were calculated using the manufacturer's reference database for United States Caucasian women. Osteopenia and osteoporosis were defined using World Health Organization criteria for diagnosis. One hundred seventy-five women were studied, of whom 106 were postmenopausal. Their average weight was 148.6 lb (67.4 kg). The women were divided into tertiles based on weight. The sensitivity, specificity, and positive and negative predictive values for osteopenia and osteoporosis were calculated for the cutpoints between weight

---

[8] Note that the original OSTA index cutpoint value for women was –1 or below, not 0 or below.

Table 8-8
**Performance Characteristics of 154 lb (70 kg) Weight Criterion for Osteopenia
and Osteoporosis at the PA Lumbar Spine and Femoral Neck**

Site	Sensitivity	Specificity	PPV	NPV
PA Lumbar Spine				
Osteopenia	0.81	0.46	0.64	0.67
Osteoporosis	0.89	0.38	0.33	0.91
Femoral Neck				
Osteopenia	0.80	0.43	0.60	0.67
Osteoporosis	0.94	0.36	0.21	0.97

PPV, positive predictive value; NPV, negative predictive value
Adapted with kind permission of Springer Science+Business Media from ref. (*16*).

tertiles. The best sensitivity and negative predictive value was obtained for the weight cutpoint between the second and third tertile of 154 lb (70 kg). These are shown in Table 8-8. The authors suggested that women weighing 154 lb or less should undergo bone density measurements whereas women weighing more than 154 lb could reasonably be excluded from testing.

THE BLACK FRACTURE INDEX

The Fracture Index was developed by Black et al. (*17*) to identify women at high risk of osteoporotic fracture based on clinical risk factors *with* or *without* a bone density measurement. This is not exactly the same as a risk assessment tool to identify women with a high probability of having low bone mass. Nevertheless, women identified by this fracture risk assessment tool as being at high risk for fracture based on clinical risk factors alone (that is, without a measurement of BMD) would certainly be considered for bone density testing. For this reason, the Fracture Index is included in this discussion as well as the discussion in Chapter 10 on predicting fracture risk.

The Fracture Index is based on data that was obtained from 7782 women, aged 65 years and older, who participated in the Study of Osteoporotic Fractures (SOF).[9] Women in this trial provided complete medical histories and underwent physical examinations as well as anthropomorphic measurements and assessments of neuromuscular function. Bone density studies were performed with DXA of the proximal femur. Fracture assessments were performed every 4 months. Spine radiographs were obtained at an average of 3.7 years apart and total time for hip and non-vertebral fracture follow-up was 5 years.

To derive the index, the investigators considered previously identified (*18*) risk factors for hip fracture as well as other clinically identifiable risk factors. Some 20 different variables were initially considered in a logistic regression analysis. The final statistical model included those variables that were statistically significant for the prediction of hip

---

[9] The Study of Osteoporotic Fractures (SOF) is a prospective study of 9704 women at least 65 years of age. Caucasian women make up 99.7% of the study population.

fracture and were easily assessed in clinical practice. An additive scoring system was developed based on the final model. The scoring system is shown in Table 8-9.

Table 8-9
The Fracture Index Scoring System

	Point Value
1. What is your current age?	
Less than 65	0
65–69	1
70–74	2
75–79	3
80–84	4
85 or older	5
2. Have you broken any bones after age 50?	
Yes	1
No/Don't know	0
3. Has your mother had a hip fracture after age 50?	
Yes	1
No/Don't know	0
4. Do you weight 125 lb or less?	
Yes	1
No	0
5. Are you currently a smoker?	
Yes	1
No	0
6. Do you usually need to use your arms to assist yourself in standing up from a chair?	
Yes	2
No/Don't know	0
If you have a current bone density (BMD) assessment, then answer the next question	
7. BMD results: Total hip T-score	
T-score $\geq$ –1	0
T-score between –1 and –2	2
T-score between –2 and –2.5	3
T-score < –2.5	4

Adapted with kind permission from Springer Science+Business Media from ref. (*17*) with permission of the publisher

The same risk factors were used in the Fracture Index with or without a bone density measurement. As noted in Table 8-12, the maximum score without a bone density measurement is 11. With a bone density measurement, the maximum possible score is 15. The sensitivity and specificity were determined for all the possible scores for the index, both with and without a bone density measurement as well as the AUROC.

For the model without a BMD measurement, the AUROC was 0.714. For the model with a BMD measurement, the AUROC was 0.766. In the model without a bone density measurement, which is clearly the most relevant model to the discussion here, a score of

4 of higher[10] resulted in a sensitivity of 66.0% and a specificity of 66.3% for hip fracture. In the model that included a bone density measurement, a score of 6 or higher resulted in a sensitivity of 78.6% and a specificity of 61.7%.

The Fracture Index was validated in 6679 women with an average age of 80.5 years who participated in the EPIDOS study.[11] The women were divided into quintiles based on the Fracture Index score. Quintiles were derived for scoring both with and without the BMD measurement. As was seen in the SOF development cohort, the risk of hip fracture increased progressively with increasing Fracture Index values for both types of scoring. Without a BMD measurement, women with a Fracture Index value of 7 to 10 had a 10.4% risk of hip fracture. With a BMD measurement, those women who had Fracture Index values of 11 to 14 had a hip fracture risk of 14.1%.

The Fracture Index was also useful in identifying women at high risk of spine and other non-spine fractures in both the development and validation cohorts. The authors noted that risk factors other than BMD assessments were predictive of fracture but that the BMD measurement itself had additional predictive ability. As a consequence, they recommended BMD testing prior to initiating therapy whenever possible. The authors noted that age was the most important single component of the Fracture Index, in keeping with what has been found with other risk indices. Based on these findings, the authors recommended that postmenopausal women with a Fracture Index score of 4 or higher, in the absence of a BMD test, undergo additional evaluation. In the context of selecting women for bone density testing, it would seem reasonable to conclude that a Fracture Index score of 4 or higher is justification for a bone density measurement.

COMPARING THE PERFORMANCE OF SELF-ASSESSMENT QUESTIONNAIRES FOR WOMEN

Several studies (*19–22*) have compared the performance characteristics of the various indices. Cadarette and colleagues (*19*) compared the performance of the ORAI index to that of SCORE, ABONE, the 1998 NOF guidelines,[12] and the body weight criterion in a population of 2365 postmenopausal women age 45 and older who were participating in the CaMos study. These women were otherwise healthy women who had not taken hormone replacement therapy or any other bone-sparing agent or who had taken hormone replacement therapy for 5 years or more. The average age was 66.4 years and the average weight was 152 lb (69 kg). Bone density was measured at the femoral neck and T-scores were calculated using the manufacturer's reference data for Canadian women in whom the mean and SD were 0.857 g/cm^2 and 0.125 g/cm^2, respectively.[13] To compare

---

[10] The score of 4 is used as a dichotomous cutpoint. The sensitivity and specificity given here are for all scores of 4 or higher considered as a group, while a second group would be all scores of 3 or lower. The specificity and sensitivity for an exact score of 4, 5 or 6, etc. would be different.

[11] EPIDOS is a prospective study of risk factors for hip fracture in France. 7575 women aged 75 and older were recruited for the study during 1992 and 1993 and followed every 4 months for the duration of the study. The data presented here is based on a mean follow-up of 4 years.

[12] See Chapter 7 for a discussion of the 1998 NOF guidelines.

[13] The mean and SD at the femoral neck in the NHANES III non-Hispanic white female database are 0.858 g/cm^2 and 0.120 g/cm^2, respectively.

the performance of the 1998 NOF guidelines to the risk indices, the authors converted the NOF guidelines to an index scoring system in which 1 point was awarded for age 65 or older, weight less than 127 lb (57.6 kg), personal history of minimal trauma fracture after age 50, family history of fracture and current cigarette smoking. In keeping with the intent of the 1998 NOF guidelines, a score of 1 or greater would trigger a referral for bone density testing.

The performance characteristics of each index for identifying women with femoral neck T-scores at various levels are shown in Table 8-10. The original cutpoint[14] recommended by the creators of each index was used in this calculation. In this comparison, the performance characteristics of SCORE and ORAI were the best at all bone density levels. When the comparison was restricted to femoral neck T-scores at or below –2.5, SCORE, ORAI, and the weight criterion were equivalent based on the AUROC. SCORE, ORAI, and the NOF guidelines, selected 94% or more of the women with femoral neck T-scores below –2 and 96% of the women with femoral neck T-scores at or below –2.5. Of these three indices, ORAI had the highest specificity. ABONE and the weight criterion decision rules missed 20% of the women with femoral neck T-scores below –2 in this study suggesting that they were not useful for this purpose. The authors

Table 8-10
Performance Characteristics of Various Self-Assessment Risk Indices for Identifying Women Age 45 and Older Who Are Below Various Levels of Bone Density at the Femoral Neck

	Sensitivity	Specificity	AUROC
T-Score < –1			
NOF	87.9	25.6	0.64
SCORE	90.6	30.8	0.72
ORAI	83.2	43.7	0.71
ABONE	64.4	64.2	0.67
Weight	64.1	61.9	0.68
T-Score < –2.0			
NOF	93.7	19.8	0.67
SCORE	97.5	20.8	0.77
ORAI	94.2	31.9	0.76
ABONE	79.1	52.7	0.71
Weight	79.6	52.2	0.74
T-Score ≤ –2.5			
NOF	96.2	17.8	0.70
SCORE	99.6	17.9	0.80
ORAI	97.5	27.8	0.79
ABONE	83.3	47.7	0.72
Weight	87.0	47.6	0.79

[14] NOF guidelines 2; SCORE ≥ 6; ORAI ≥ 9; ABONE ≥ 2; Weight < 154 lb (70 kg)

suggested that because the ORAI index had superior specificity to SCORE and the NOF guidelines and greater simplicity when compared to SCORE, the ORAI index was the most useful.

SCORE, ORAI, SOFSURF, and OST were compared by Hochberg et al. (*22*) in a study of 17,572 Caucasian women ranging in age from 45 to 93 years who were initially screened for participation in the Fracture Intervention Trial (*23*). Twenty-one percent of these women had osteoporosis at the femoral neck using the WHO criteria of a T-score of –2.5 or poorer and the NHANES III proximal femur database. At approximately 90% sensitivity, both OST and SOFSURF had an acceptable 46% specificity for the prediction of an osteoporotic T-score at the femoral neck. The cutpoints, sensitivities, specificities, and likelihood ratios are shown in Table 8-11. The cutpoints for OST used in this study have been shifted up by one unit compared to those used in the original OSTA index for Asian women. The shift in the cutpoint for SCORE represents the effect of using the NHANES III reference database for the calculation of proximal femur T-scores and the prediction of a lower T-score than called for in the development of the SCORE index.

Table 8-11
Performance Characteristics of 4 Self-Assessment Risk Indices for the Prediction of Femoral Neck T-Scores ≤–2.5 in 17,572 Caucasian Women Screened for FIT

Index	Cutoff	Sensitivity	Specificity	LR +	LR −
OST	< 1 vs. ≥ 1	89%	46%	1.65	0.24
ORAI	> 10 vs. ≤ 10	92%	26%	1.24	0.31
SOFSURF	> 1 vs. ≤ 1	86%	46%	1.60	0.30
SCORE	> 11 vs. ≤ 11	89%	39%	1.45	0.30

Adapted with kind permission of Springer Science+Business Media from ref. (*14*).

The original development and validation cohorts for SCORE were utilized again in a comparison study of SCORE, ORAI, OST, and SOFSURF by Geusens et al. (*21*) As noted previously, in the original publication of the development and validation of the SCORE index femoral neck T-scores were calculated using the manufacturer's reference database instead of the NHANES III database (*1*). In this study, T-scores at the femoral neck were recalculated using NHANES III. The various indices were calculated as described in the original publications(*1, 7, 8, 11*). A single cutpoint was chosen for each index that provided approximately 90% sensitivity for the prediction of an osteoporotic femoral neck T-score of –2.5 or poorer. The sensitivity and specificity was also calculated for the same cutpoint for prediction of a femoral neck T-score of –2 or poorer. This resulted in slightly lower sensitivity and slightly higher specificity for the T-score of –2 or poorer. The results for the 1102 women from the SCORE cohorts are shown in Table 8-12.

The risk indices were compared by Geusens et al. (*21*) in three other study populations as well: 3374 Caucasian women aged 55 and older from the Rotterdam Study (*24*), 4204 postmenopausal women aged 50–80 from a Netherlands clinic study, and 23,833 postmenopausal women aged 55–81 years who were screened for the Fracture Intervention Trial (FIT). Femoral neck T-scores were calculated using the NHANES III

Table 8-12

Sensitivity and Specificity by Femoral Neck T-Score for Four Risk Indices from the Original SCORE Cohorts

Index	Cut Point	T-Score ≤–2.5		T-Score ≤–2.0	
		Sensitivity	Specificity	Sensitivity	Specificity
OST	< 2	88%	52%	84%	59%
ORAI	> 8	90%	52%	82%	58%
SCORE	> 7	89%	58%	80%	65%
SOFSURF	> –1	92%	37%	88%	42%

Reproduced with permission of the publisher from ref. (*21*).

reference data for the Rotterdam cohort and FIT cohort. T-scores for the PA lumbar spine in the SCORE cohort and the Netherlands clinic study cohort were calculated using the manufacturer's reference data.

The prevalence of femoral neck T-scores at or below –2.5 or –2.0 for the Rotterdam cohort and FIT cohort by risk index category is shown in Table 8-13. All four risk indices produced similar prevalences by risk category. The prevalence of PA lumbar spine T-scores for the SCORE cohorts and Netherlands clinic cohort by risk category is shown in Table 8-14. In order to obtain a sensitivity of 90% with the OST questionnaire for the prediction of a T-score of –2.5 or poorer at the PA lumbar spine, it was necessary

Table 8-13

Percentage of Individuals in Risk Index Categories with Femoral Neck T-Scores of –2.5 or Poorer or –2.0 or Poorer Using NHANES III Reference Data

Risk Index Category	FIT Screening Population		Rotterdam Study Population	
	T-Score ≤–2.5	T-Score ≤–2.0	T-Score ≤–2.5	T-Score ≤–2.0
Background Prevalence	21%	43%	19%	39%
OST				
>1 (low risk)	4%	16%	4%	16%
–3 to 1 (moderate risk)	23%	48%	22%	45%
<–3 (high risk)	57%	79%	57%	79%
ORAI				
<9 (low risk)	4%	17%	7%	21%
9 to 17 (moderate risk)	16%	37%	16%	36%
>17 (high risk)	41%	68%	46%	70%

Table 8-13
(continued)

Risk Index Category	FIT Screening Population		Rotterdam Study Population	
	T-Score ≤–2.5	T-Score ≤–2.0	T-Score ≤–2.5	T-Score ≤–2.0
SCORE				
<7 (low risk)	4%	15%	1%	4%
7 to 15 (moderate risk)	21%	46%	16%	35%
>15 (high risk)	51%	74%	38%	66%
SOFSURF				
<0 (low risk)	3%	11%	5%	16%
0 to 4 (moderate risk)	18%	40%	17%	39%
>4 (high risk)	53%	77%	51%	74%

Adapted with permission of the publisher from ref. (*21*).

Table 8-14
Prevalence of Low Spine BMD by OST Category and T-Score Cutoff

	SCORE Cohort		Netherlands Clinic Sample	
	T-Score ≤–2.5	T-Score ≤–2.0	T-Score ≤–2.5	T-Score ≤–2.0
Background Prevalence	17%	25%	17%	29%
OST				
>2 (low risk)	7%	11%	7%	15%
–3 to 2 (moderate risk)	21%	30%	23%	37%
<–3 (high risk)	38%	52%	50%	63%

Adapted with permission of the publisher from ref. (*21*).

to use a higher cutpoint than that for the femoral neck. The OST nomogram in Fig. 8-1B reflects the higher cutpoints for medium and high risk for Caucasian women in the FIT cohort for a femoral neck T-score of –2.5.

The authors of this study (*21*) noted that all four indices performed well. In addition, the re-evaluation of the original SCORE cohorts using NHANES III femoral neck reference data for the calculation of the T-score and SCORE's performance in the Rotterdam and FIT cohorts further validates the utility of the SCORE questionnaire. Nevertheless, the simplicity of the OST index may make it the most suitable for widespread clinical use.

THE MALE OSTEOPOROSIS RISK ESTIMATION SCORE

Only recently have self-assessment indices for men begun to appear. The Male Osteo-porosis Risk Estimation Score (MORES) is one such self-assessment index (*25*). The

authors utilized data collected from 2995 men age 50 and older from the third National Health and Nutrition Examination Survey (NHANES III). These men were randomly divided into two groups; the development cohort and the validation cohort. After evaluating several candidate risk variables in the development cohort, the authors developed a scoring system based on age, weight, and the presence of chronic obstructive pulmonary disease to identify men at increased risk for osteoporosis with a sensitivity of 90%.[15] The scoring system is shown in Table 8-15. The authors determined that a MORES value of 6 or greater in the development cohort resulted in a sensitivity of 0.91, specificity of 0.58, and area under the receiver operating characteristic curve (AUROC) of 0.822 for the identification of men found to be osteoporotic at the total hip using DXA. In the validation cohort, a MORES value of 6 or greater resulted in a sensitivity of 0.95, specificity of 0.61, and an AUROC of 0.842. Sensitivities and specificities were similar regardless of whether the man was Hispanic or non-Hispanic, white or black. Ultimately MORES correctly identified 93% of the men with osteoporosis in this sample from NHANES III. Of the criteria listed in Table 8-15, low weight, as has been seen with self-assessment indices for women, was the strongest predictor of osteoporosis in men. Use of a MORES value of 6 or greater would result in DXA testing in men age 50 and older weighing 154 lb or less.

Table 8-15
Male Osteoporosis Risk Estimation Score (MORES).

Risk Factor	Logistic Regression β Coefficient	MORES Points*
Age		
≤ 55 years[a]	0.00	0
56–74 years	1.29	3
≥ 75 years	2.03	4
Weight		
≤ 70 kg (≤154 lb)	3.07	6
> 70–80 kg (>154–176 lb)	1.86	4
> 80 kg (> 176 lb)[a]	0.00	0
COPD	1.32	3

COPD, chronic obstructive pulmonary disease

* Screening threshold is 6 points or greater

[a] Reference category

SUMMARY

All of these indices in their final form appear deceptively simple. In virtually all cases, however, hundreds of risk factors were actually evaluated using complex statistical analyses before the final index was developed. The indices rely on easily obtained information and each is dependent on weight and age (with the exception of the weight criterion) to some degree. The OST index in particular is easily reduced to a nomogram

[15] See Chapter 3 for a discussion of sensitivity, specificity, and area under the receiver operating characteristic curve (AUROC).

as shown in Fig. 8-1. Such a nomogram can be marked by the patient and brought to medical personnel for review. These indices are not intended to replace clinical judgment. They are also not intended to supplant the carefully crafted guidelines from various organizations discussed in Chapter 7. Nevertheless, the use of such indices can aid appropriate patient identification for bone densitometry and promote osteoporosis awareness and education. In using any risk index, however, the choice of the cutpoint is critical, as the cutpoint is specific for a given level of bone density at a particular skeletal site.

The SCORE questionnaire was originally developed to identify with 90% sensitivity those women with a high probability of having a femoral neck T-score of –2 or poorer at the femoral neck, using the manufacturer's reference data. A value of 6 on the SCORE index was determined as the appropriate cutpoint. Lowering the T-score to –2.5 and implementing the NHANES III reference data predictably altered the cutpoint to >7 in order to achieve 90% sensitivity in the same population, as demonstrated by Geusens et al. (*21*). Similarly the cutpoint for OST was adjusted from the original value to achieve 90% sensitivity with the lower femoral neck T-score, different reference database, and Caucasian rather than Asian population. Only the ORAI index was originally designed to identify women with low bone density at either the spine or femoral neck. The other indices primarily focused on the femoral neck. Nevertheless, it would appear that both SCORE and OST may be useful in identifying women with low bone density at the PA lumbar spine.

The use of these indices to create categories of low, moderate, and high risk provides more flexibility in identifying patients who potentially have low bone density and in deciding whom to test. The prevalence of low bone density in even the moderate risk categories is sufficiently great to justify the measurement of bone density in individuals in these categories.

REFERENCES

1. Lydick E, Cook K, Turpin J, Melton J, Stine R, Byrnes C. Development and validation of a simple questionnaire to facilitate identification of women likely to have low bone density. Am J Man Care 1998;4:37–48.
2. Hanley JA, McNeil BJ. The meaning and use of the area under a receiver operating characteristic (ROC) curve. Radiology 1982;143:29–36.
3. Looker AC, Wahner HW, Dunn WL, et al. Updated data on proximal femur bone mineral levels of US adults. Osteoporos Int 1998;8:468–489.
4. Cadarette SM, Jaglal SB, Murray TM. Validation of the simple calculated osteoporosis risk estimation (SCORE) for patient selection for bone densitometry. Osteoporos Int 1999;10:85–90.
5. Von Mühlen D, Lunde AV, Barrett-Connor E, Bettencourt R. Evaluation of the simple calculated osteoporosis risk estimation (SCORE) in older Caucasian women: the Rancho Bernardo study. Osteoporos Int 1999;10:79–84.
6. Ungar WJ, Josse R, Lee S, et al. The Canadian Score™ questionnaire. J Clin Densitom 2000;3:269–280.
7. Cadarette SM, Jaglal SB, Kreiger N, McIsaac WJ, Darlington GA, Tu JV. Development and validation of the Osteoporosis Risk Assessment Instrument to facilitate selection of women for bone densitometry. CMAJ 2000;162:1289–1294.
8. Black DM, Palermo L, Pearson J, Abbott T, Johnell O. SOFSURF: a simple, useful risk factor system can identify the large majority of women with osteoporosis. Bone 1998;23:S605.
9. Weinstein L, Ullery B, Bourguignon C. A simple system to determine who needs osteoporosis screening. Obstet Gynecol 1999;93:757–760.

10. Weinstein L, Ullery B. Identification of at-risk women for osteoporosis screening. Am J Obstet Gynecol 2000;183:547–549.
11. Koh LKH, Sedrine WB, Torralba TP, et al. A simple tool to identify Asian women at increased risk of osteoporosis. Osteoporos Int 2001;12:699–705.
12. Koh LKH. Identifying osteoporosis in a cohort of Singapore women using a simple clinical tool. Abstract. Osteoporos Int 2002;13:S116.
13. Koh LKH. Identifying osteoporosis in a cohort of Asian men using a simple clinical tool, which identifies osteoporosis in Asian women. Abstract. Osteoporos Int 2002;13:S120.
14. Hochberg MC, Thompson DE, Ross PD. Validation of a simple clinical risk index to identify postmenopausal Asian women with osteoporosis: The osteoporosis self-assessment tool for Asians (OSTA). Abstract. Osteoporos Int 2002;13:S115.
15. Ben Sedrine W, Reginster JY. Using the OST index to identify women at risk of osteoporosis: a validation study in Belgium. Abstract. Osteoporos Int 2002;13:S109.
16. Michaëlsson K, Bergström R, Mallmin H, Holmberg L, Wolk A, Ljunghall S. Screening for osteopenia and osteoporosis: selection by body composition. Osteoporos Int 1996;6:120–126.
17. Black DM, Steinbuch M, Palermo L, et al. As assessment tool for predicting fracture risk in postmenopausal women. Osteoporos Int 2001;12:519–528.
18. Cummings SR, Nevitt MC, Browner WS, et al. Risk factors for hip fracture in white women. N Engl J Med 1995;332:767–773.
19. Cadarette SM, Jaglal SB, Murray TM, McIsaac WJ, Joseph L, Brown JP. Evaluation of decision rules for referring women for bone densitometry by dual energy X-ray absorptiometry. JAMA 2001;286:57–63.
20. Siris E, Geusens P, Pols H, et al. Performance of self-assessment risk indices for encouraging appropriate use of bone density measurements among postmenopausal women. Abstract. J Bone Miner Res 2001;16:S341.
21. Geusens P, Hochberg MC, Van Der Voort DJM, et al. Performance of risk indices for identifying low bone density in postmenopausal women. Mayo Clin Proc 2002;77:629–637.
22. Hochberg MC, Thompson DE, Ross PD. Validation of risk indices to identify postmenopausal women with an increased likelihood of osteoporosis. Abstract. Osteoporos Int 2002;13:S111.
23. Black DM, Reiss TF, Nevitt MC, Cauley J, Karpf D, Cummings SR. Design of the fracture intervention trial. Osteoporos Int 1993;3:S29–S39.
24. Hofman A, Grobbee DE, de Jong PT, van den Ouweland FA. Determinants of disease and disability in the elderly: the Rotterdam Elderly Study. Eur J Epidemiol 1997;7:403–422.
25. Shepherd AJ, Cass AR, Carlson CA, Ray L. Development and internal validation of the male osteoporosis risk estimation score. Ann Fam Med 2007;5:540–546.

9 Diagnosing Osteoporosis

CONTENTS

Although the number of applications for bone densitometry has grown rapidly in the last few years, the use of densitometry to diagnose osteoporosis remains the most common application in clinical practice. What constitutes a diagnosis of osteoporosis, however, has continued to evolve.

CONCEPTUAL DEFINITIONS OF OSTEOPOROSIS

In 1991 (*1*) and again in 1993 (*2*), Consensus Development Conferences attempted to clarify the clinical definition of osteoporosis. The National Osteoporosis Foundation, the National Institutes of Health, and the European Foundation for Osteoporosis and Bone Disease sponsored these conferences. The definition of osteoporosis from the 1993 conference reflected only minor modifications from the 1991 conference. At the 1993 Consensus Development Conference (*2*) it was agreed that osteoporosis was:

> . . . a systemic skeletal disease characterized by low bone mass and microarchitectural deterioration of bone tissue, with a consequent increase in bone fragility and susceptibility to fracture.

The 1993 definition emphasized that both mass and architecture contributed to bone strength. The presence of a fracture was not required before a diagnosis of

osteoporosis was appropriate. Fracture, as an outcome of skeletal fragility, was separated from the disease, osteoporosis. This was similar to the approach taken with hypertension and hypercholesterolemia. Hypertension reflects the measurement of a quantity, the blood pressure, which has reached a level that places the individual at risk for the undesirable outcome of stroke. Hypercholesterolemia refers to the measurement of quantity, cholesterol, which has reached a level that places the individual at risk for the undesirable outcome of myocardial infarction. In both cases, the occurrence of the outcome is not required before the diagnosis of disease is made. In a strict sense, hypertension and hypercholesterolemia are not diseases in and of themselves. They are risk factors for the undesirable outcomes of stroke and myocardial infarction. They have been *made* diseases. Some would critically call this the "medicalization of risk factors." It is extremely useful, however, because quantifying those risk factors allows the clinician to determine the need for pharmacologic intervention to reduce the risk of the outcome. In the cases of hypercholesterolemia and hypertension, however, the diagnostic threshold, the threshold constituting unacceptable risk and the intervention threshold tend to be one and the same. The *implication* of the Consensus Conferences' definition of osteoporosis is also that the thresholds for diagnosis, unacceptable risk, and intervention would be the same. Unfortunately, the Consensus Conferences' definition lacked the specificity necessary to be implemented clinically. The specific level of low bone mass, architectural deterioration, or increased risk of fracture that was necessary for a diagnosis of osteoporosis was absent from the definition. Even in 1991 and 1993, bone density could be measured in all of its infinite variations. Quantifying architectural deterioration remains a challenge even today. Disagreement still abounds on how best to define fracture risk. So the question remains when using densitometry to diagnose osteoporosis: "How low is too low?"

1994 WORLD HEALTH ORGANIZATION CRITERIA FOR THE DIAGNOSIS OF OSTEOPOROSIS BASED ON THE MEASUREMENT OF BMD

In an extensive report published in 1994 (*3*), a World Health Organization (WHO) study group composed of 16 internationally known experts in the field of osteoporosis proposed criteria for the diagnosis of osteoporosis based on a specific level of bone density. The focus of the WHO study group was the study of world populations rather than the diagnosis of osteoporosis in individuals. While endorsing the prior 1991 and 1993 Consensus Development Conferences' definition of osteoporosis, the WHO study group recognized that their proposed criteria did not include any assessment of microarchitectural deterioration. In creating these criteria, the WHO attempted to reconcile the prevalence of the disease that would be created depending upon the level of bone density chosen with published lifetime fracture risk estimates. The study group noted that a cutoff value of 2.5 SD or more below the average value for healthy young women for bone density at the PA spine or proximal femur or for bone mineral content at the midradius would result in 30% of all postmenopausal women being labeled as osteoporotic. Fifty percent or more of these women will have sustained a fracture of the spine, femur, forearm, humerus, or pelvis. The diagnostic categories established by the study group of the WHO are shown in Table 9-1. Although the table refers to values of bone density in terms of the number of SD below the average value for a healthy young-adult, the

Table 9-1
World Health Organization Criteria for the Diagnosis of Osteoporosis in Caucasian Women

Diagnostic Category	Diagnostic Thresholds
Normal	Less than or equal to 1 SD below the young-adult mean
Osteopenia or Low Bone Mass	More than 1 SD below but less than 2.5 SD below the young-adult mean
Osteoporosis	2.5 SD or more below the young-adult mean
Severe or Established Osteoporosis	2.5 SD or more below the young-adult mean with fragility fracture(s)

values could also be expressed as the T-score or young-adult *z*-score, since these terms are used synonymously in densitometry. These guidelines for diagnosis were proposed for Caucasian women only. They were not originally intended to be applied to women of other races or ethnicities or to men. This is done in clinical practice, however, in the absence of any other diagnostic guidelines for these groups.

The WHO cautioned that "individuals will be categorized differently according to the site and technique of measurement and the equipment and the reference population used." They also emphasized that the use of bone density measurements for the diagnosis of osteoporosis should not be confused with the use of the technology for the prediction of fracture risk, noting that it was "important to distinguish between the diagnostic and prognostic use of bone mineral density measurement." They correctly pointed out that bone density values were risk factors for fracture as well as being used as criteria for the diagnosis of disease but that these two uses of the values were really quite distinct. The study group noted the analogy to hypertension and hypercholesterolemia described earlier in this section. While no other authoritative body has published proposed diagnostic levels of bone density for osteoporosis, a slightly higher cutoff level had been equated with the diagnosis of osteoporosis in the United States. In approving certain medications for the management or treatment of osteoporosis, the US Food and Drug Administration had recommended the use of these drugs in individuals with a bone density that was 2 SD or more below that of the young-adult. In essence, this equates a diagnosis of osteoporosis with a bone density that is 2 SD or more below that of the young-adult, in contrast to the lower cutoff proposed by the WHO of 2.5 SD or more below that of the young-adult.

The WHO Criteria, as they have come to be called, have been widely misquoted. In the original publication of the guidelines, as well as subsequent publications discussing them, confusion has arisen regarding the SD cut points for normal and osteoporosis. The cut points shown in Table 9-1 are correct (*4*). A normal bone density includes a bone density that is 1 SD below the average value for a young-adult (T-score of –1). Similarly, an osteoporotic bone density is considered present when the bone density is 2.5 SD or more below the average value for a young-adult (T-score of –2.5 or poorer). In some publications, a bone density T-score of –1 or –2.5 has been erroneously considered osteopenic. Osteopenia refers to a bone density T-score *between* –1 and –2.5.

THE 1999 AND 2003 WORLD HEALTH ORGANIZATION AND 2000 INTERNATIONAL OSTEOPOROSIS FOUNDATION AND 2002 INTERNATIONAL SOCIETY FOR CLINICAL DENSITMETRY RECOMMENDATIONS FOR THE APPLICATION OF THE 1994 WHO CRITERIA

The 1994 WHO criteria did not direct physicians to measure bone density at a specific site or region of interest for the diagnosis of osteoporosis. An interim report (*5*) from the WHO Task Force for Osteoporosis was published in 1999 in which it was stated that DXA of the proximal femur was preferred for diagnostic bone density measurements, particularly in elderly individuals. This statement was reiterated in the WHO 2003 document titled "Prevention and Management of Osteoporosis" (*6*). Physicians were not specifically directed in these reports, however, to limit the application of the WHO Criteria for diagnosis to BMD measurements made at the proximal femur.

In 2000, the International Osteoporosis Foundation (IOF) (*7*) also recommended that only bone density measured at the proximal femur be used for the diagnosis of osteoporosis, based on the WHO criteria. Although both the total femur and femoral neck were noted as useful in this regard, the IOF described the total femur as "optimal." In 2002, however, the International Society for Clinical Densitometry (*8*) stated that the WHO criteria could be utilized with bone density measurements at the PA spine, total femur, femoral neck, or trochanter. In 2005, the ISCD guidelines (*9*) were amended to exclude the trochanter. ISCD also stated that the WHO criteria should not be applied to measurements of bone density made at any peripheral site (*10*). Internationally, the femoral neck region of interest has become the preferred region of interest, particularly with the advent of FRAX[TM].[1] All of these positions strongly suggest that other skeletal sites, regardless of the technique by which they are measured, should not be used for the diagnosis of osteoporosis. The rationale behind these positions is both understandable and unfortunate and in no small way, reflects the inevitable confusion predicted by the WHO study group in 1994. Such positions also require that the identification of individuals at risk for fracture remain a separate issue from the diagnosis of osteoporosis because these positions would otherwise deny the established predictive ability of peripheral sites (*11*) for fracture.

THE CLINICAL DILEMMA

The WHO criteria were established to enable the WHO to study the prevalence of osteoporosis in large populations. Their intent was not to establish bone density criteria for the diagnosis of osteoporosis in *individuals*. As noted earlier, the WHO study group chose a cutpoint based on the number of SDs below the young-normal mean value that would result in a prevalence of osteoporosis that roughly coincided with published estimates of fracture risk. They chose the statistical device of the SD to avoid using specific levels of bone density or bone content that would be different for each technique and/or device. The bone density data that was considered in the creation of these guidelines

---

[1] See Chapter 10 for a discussion of FRAX[TM], the 10-year absolute fracture risk prediction algorithm from the World Health Organization.

came from the PA lumbar spine, proximal femur, and mid-radius as measured by DPA, DXA, and SPA. The WHO did not create only two classifications indicating the presence or absence of disease, but instead created four: normal, osteopenia, osteoporosis, and severe osteoporosis. The classifications actually recognized a gradient of fracture risk although only the last two were designated as representative of disease.

In spite of the warnings from the WHO study group that application of the criteria to individuals would result in a different diagnosis depending on the site measured, technique, and reference population used, the clinical community rapidly embraced the WHO criteria for use in individuals. The criteria provided the specificity that was lacking in the conceptual Consensus Conferences' definition of osteoporosis, enabling the use of densitometry for diagnosis. In the clinical application of these criteria, however, several issues immediately became apparent, all of which had been anticipated by the WHO.

In addition to the three skeletal sites considered by the WHO in the creation of the 1994 criteria (PA spine, proximal femur, and mid-radius), densitometrists can measure bone density at the phalanges, calcaneus, distal radius, distal and proximal forearm (radius and ulna combined), lateral spine, tibia, and total body. The bulk of the bone density data originally used by the WHO to create the 1994 criteria (*3*) came from studies performed with SPA, DPA, and DXA. SPA and DPA are largely obsolete but other techniques such as QUS, QCT, RA, and radiogrammetry[2] are now used clinically. For each site, on each device, from each manufacturer, data from a different population of individuals has been used to create the reference database. The peak bone density and SD are specific for that population, at that skeletal site, as measured by that device. The number of skeletal sites, devices, and techniques used today far exceed the number originally noted by the WHO in 1994. Although the WHO carefully considered both prevalence and fracture risk in choosing a cutpoint of 2.5 SD below the young-adult mean BMD or BMC, such considerations of prevalence and risk have largely been lost with the proliferation of devices, techniques, and sites. A measured value that is 2.5 SD below the young-adult mean value at some site by some technique based on some reference database may now reflect only the variability in the bone density in the population rather than a specific level of fracture risk.

There is no question that low bone density is predictive of fracture. This is essentially true, irrespective of where or how the bone density is measured (*11–14*). What we call low, however, is based on impressions created from comparisons to the reference database; specifically, the number of SDs below the young-adult average value or the T-score. How likely one is to be considered "low" is clearly dependent on the site, the technique, and the reference database. In the large prospective observational trial called the National Osteoporosis Risk Assessment (NORA), bone density and fracture data was evaluated in 149,524 white women (*14*). Bone density was measured in the phalanges with DXA (accuDEXA, Schick Technologies, Long Island City, NY), heel with SXA (Osteoanalyzer, Norland, a CooperSurgical Company, Ft. Atkinson, WI), heel with QUS (Sahara, Hologic, Inc., Bedford, MA), and forearm with DXA (pDEXA, Norland, a CooperSurgical Company, Ft. Atkinson, WI). After only 1 year of follow-up, 2259 women reported 2340 new fractures. All of the measurements, regardless of site, device,

---

[2] See Chapter 1 for a discussion of densitometry techniques.

or technique, predicted fracture equally well. Women with T-scores ≤–2.5 had a 2.15- to 3.94-fold increase in fracture risk compared with women with normal bone densities. Of note, however, was that the likelihood of having a T-score of –2.5 or less was dependent on where and how the bone density was measured. Only 2.9% of the women had a T-score of –2.5 or less based on QUS at the heel, compared to 4.1% based on SXA of the heel, 9.4% based on DXA of the forearm, and 12.0% based on DXA of the phalanges. The T-scores in NORA were derived from the manufacturers' reference databases.

Differences in the percentages of women diagnosed with osteoporosis depending on the measurement site and technique have been extensively documented. In 1996, Greenspan et al. (*15*) reported that the percentage could vary from 19% to 66% depending on the measurement site, even when all the sites were measured by the same DXA device. Varney et al. (*16*) published similar findings in 1999, with diagnostic percentages for osteoporosis of 4% at the trochanter, 6% at the total hip, 17% at the femoral neck, 34% at Ward's area, 20% at the PA lumbar spine, 12% at the ultradistal radius, and 27% at the 33% radius. This problem was highlighted by Faulkner et al. (*17*), who plotted the change in T-score by age in women for various skeletal sites as measured by different devices, using the manufacturers' reference databases. This graph is shown in Fig. 9-1. As the graph clearly shows, the T-scores for an average 60-year-old woman ranged from –0.7 at the heel by QUS to –2.5 at the spine by QCT. Such a woman could be diagnosed as normal, osteopenic, or osteoporotic depending on where and how the measurement was made.
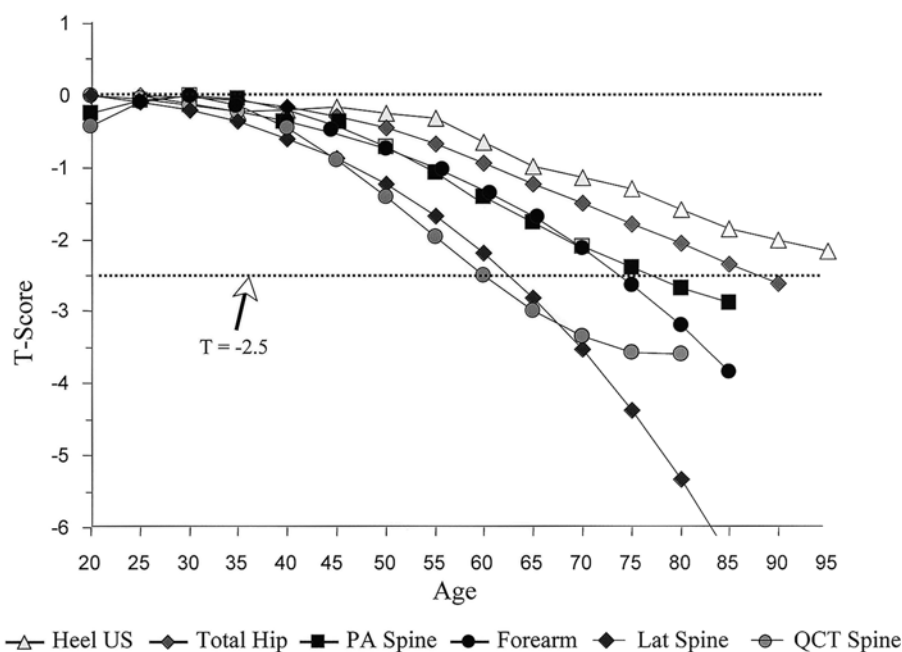

Fig. 9-1. The T-score regression on age for women by site and device, from the reference databases of the various manufacturers. The expected T-score for an average 60 year old woman ranges from –0.7 at the heel by QUS to –2.5 at the spine by QCT. Reproduced with permission of Elsevier from ref. (*17*).

Peripheral Site T-Score Equivalents for the Diagnosis of Osteopenia and Osteoporosis

The effect of different reference databases on diagnosis was discussed in Chapter 6. In addition to issues of reference databases, the multitude of sites and techniques adds considerations of different rates of bone loss and biologically different measures of bone density. The peripheral site data from NORA suggest a three-fold difference in the likelihood of being diagnosed "osteoporotic" using WHO criteria, depending on the site that is measured and the technique that is used. In recognition of this dilemma, investigators have attempted to determine T-scores or T-score ranges at non-spine, non-proximal femur sites that would identify similar percentages of individuals as osteopenic or osteoporotic based on WHO criteria at the spine and proximal femur itself.

Attempts to determine site, device, and manufacturer specific T-scores or T-score ranges at peripheral sites to identify women who are osteopenic or osteoporotic at the spine or proximal femur generally involve the calculation of sensitivity, specificity, and area under the receiver operating characteristic curve (AUROC or AUC), as discussed in Chapter 3. In a study from Pouillès et al. (*18*) 234 women ranging in age from 45 to 60 years underwent DXA studies of the PA lumbar spine and proximal femur (Lunar DPX-IQ) and pDXA forearm studies (Norland pDEXA). The average peak BMD and SD for each skeletal site was determined from studies of a group of young, healthy women, rather than from the manufacturers' reference databases. At the PA lumbar spine, the young-adult mean BMD and SD were 1.180 ± 0.12 g/cm^2. The values at the femoral neck were 0.990 ± 0.11 g/cm^2. At the forearm, the values for the distal region of interest were 0.347 ± 0.05 g/cm^2 and at the proximal region, 0.816 ± 0.06 g/cm^2. Using the WHO criteria of ≤-2.5 SD below the young-adult mean bone density for a diagnosis of osteoporosis, 17.5% of the women were osteoporotic at the spine and femoral neck combined. Fourteen percent were osteoporotic based on measurements at the proximal forearm and only 3.4% were osteoporotic based on measurements at the distal forearm. The authors then determined the number of SD below the young-adult mean BMD or T-score that would be required at the distal and proximal forearm for 95% sensitivity in diagnosing osteoporosis or a combination of osteopenia and osteoporosis at the spine and proximal femur. At the distal forearm, a T-score of –0.74 was required for 95% sensitivity for the diagnosis of osteoporosis at the central sites. The corresponding specificity was 59.5% and the AUROC was 0.80. At the proximal forearm, the T-score cutpoint was –0.73 with a corresponding specificity of 46.7% and an AUROC of 0.75. To detect both osteopenic and osteoporotic bone densities at the central sites, a T-score of +1.06 was required at the distal forearm and +0.53 at the proximal forearm for 95% sensitivity. The corresponding specificities were 23.3% and 23.4%, respectively.

In 115 women (average age 61 years) Varney et al. (*16*) measured bone density at the PA spine and proximal femur with DXA (Hologic QDR 4500A), at the phalanges with DXA (Schick accuDEXA), and at the heel with QUS (Hologic Sahara). Using the WHO criteria of a T-score of –2.5 to diagnose osteoporosis, 28% of the women were osteoporotic based on measurements at the spine, total hip, and femoral neck combined. Forty-nine percent were osteopenic and 23% were normal. The authors determined that a T-score of ≤-1.9 was necessary to diagnose a similar percentage of women as osteoporotic using QUS of the heel, using the estimated heel BMD in g/cm^2 as provided by the software. A T-score of ≤-1.4 for phalangeal DXA was required to diagnose a similar

percentage of women as osteoporotic. At these T-score thresholds, the sensitivity and specificity were 56% and 78% for heel QUS and 56% and 80% for phalangeal DXA, respectively. The authors also determined the equivalent T-score range for osteopenia for the two devices. For QUS of the heel, a similar percentage of women were diagnosed as osteopenic when osteopenia was defined as a T-score between –1.9 and +0.3. For DXA of the phalanges, the equivalent osteopenic range was between –1.4 and +0.4. The sensitivity and specificity for osteopenia using heel QUS was 86% and 48% and for phalangeal DXA, 89% and 59%, respectively.

T-score thresholds for phalangeal DXA were also determined by Mulder et al. (*19*). One hundred twenty-three women (average age 64.6 years) underwent PA spine, proximal femur, and forearm DXA measurements (Hologic QDR-4500) and phalangeal DXA measurements (Schick accuDEXA). In contrast to the definition used by Varney et al.(*16*) the authors of this study defined osteoporosis at a T-score of –2.5 or poorer at the femoral neck only. A T-score of –2.5 at the finger had a sensitivity of only 35% for osteoporosis at the femoral neck although the specificity was 88%. Better sensitivity was obtained with a phalangeal T-score of –1.0. At this T-score, the sensitivity for femoral neck osteoporosis was 85% although specificity fell to 49%. This phalangeal T-score threshold also had excellent sensitivity for femoral neck T-scores of –2 or poorer. Here the sensitivity was 82% with a specificity of 56%.

Fiter et al. (*20*) suggested that a T-score of –1.65 provided a better combination of sensitivity and specificity for phalangeal DXA for the diagnosis of osteoporosis at the PA lumbar spine or femoral neck. In a study of 230 postmenopausal women (average age 58.4 years), BMD was measured at the PA lumbar spine and femoral neck with DXA (Hologic QDR 1000) and at the middle phalanx with DXA (Schick accuDEXA). Applying the WHO criteria, the prevalence of osteoporosis was 33% based on measurements of the PA lumbar spine and femoral neck. At the middle phalanx, however, the prevalence of osteoporosis using the WHO threshold of 2.5 SD below the young adult mean value was only 18%. Based on an AUROC analysis, the authors determined that the optimum sensitivity and specificity for the middle phalangeal DXA measurement for diagnosing osteoporosis at the PA lumbar spine and femoral neck was a T-score of –1.65. At this T-score, the sensitivity was 75% with a specificity of 77%. The AUROC was 0.822.

Optimum T-score thresholds for a different heel QUS device were determined by Damilakis et al. (*21*) Bone density was measured at the PA lumbar spine, femoral neck, and total hip with DXA (Hologic QDR 1000), and at the heel with QUS (Ubis 3000, DMS, France) in 333 women, 42 to 79 years of age. Using the WHO criteria of a T-score of –2.5 or poorer, osteoporosis was found in 14% of the women at the spine, 13% at the femoral neck, and 10% at the total femur, for an average prevalence of 12%. Using a T-score of –2.5 or less based on the QUS measurement at the heel for BUA[3] resulted in only 1.5% of the women being diagnosed as osteoporotic. The SOS[4] T-score of –2.5 resulted in a diagnosis of osteoporosis in only 8.4%. In order to achieve a similar percentage of women diagnosed as osteoporotic as seen at the central sites by DXA,

---

[3] Broadband ultrasound attenuation, expressed as dB/MHz
[4] Speed of sound, expressed as m/s

the T-score thresholds for BUA and SOS had to be adjusted to –1.8 and –2.2, respectively. The authors also used sensitivity, specificity, and AUROC analyses to determine the optimum T-score thresholds for BUA and SOS for detecting osteoporosis at the femoral neck. In that analysis, the optimum T-score for BUA was –1.3. The sensitivity and specificity at this T-score was 68% and 83%, respectively, with an AUROC of 0.82. The optimum T-score threshold for SOS was –1.5. The sensitivity and specificity for the T-score of –1.5 was 63% and 79%, respectively. The AUROC was 0.75. The difference between the AUROC for the optimum BUA and SOS T-score thresholds was statistically significant, suggesting that BUA was a better predictor of low femoral neck bone density than was SOS.

Fordham et al. (*22*) attempted to define an optimum T-score threshold for the heel measured by DXA in 443 women with a mean age of 60 years. Bone density was measured at the PA lumbar spine and femoral neck with DXA (Lunar DPX-L) and with DXA at the heel (Lunar PIXI). Using the manufacturer's reference database, osteoporosis was considered to be present if either the PA lumbar spine or femoral neck T-score was –2.5 or less. Based on sensitivity, specificity, and AUROC analyses, the optimum heel T-score threshold for identifying women who were osteoporotic at the spine or femoral neck was ≤–1.3 for the entire group. At this T-score, the sensitivity was 69.6% and the specificity was 82.6%. The AUROC was 0.836. The authors also noted that the sensitivity and specificity varied by age. In women aged 50–64, a heel DXA T-score of ≤–1.3 had a sensitivity and specificity of 68% and 85%, respectively, with a false negative rate of 13%. In women age 65 and older, however, the same T-score threshold resulted in a sensitivity and specificity of 71% and 68%, respectively, with a false negative rate of 40%.

Pacheco et al. (*23*) also attempted to determine the optimum T-score threshold for BMD measured at the calcaneus by DXA for the diagnosis of osteoporosis at the PA lumbar spine, total femur, or femoral neck. Bone density was measured in 204 Caucasian women aged 20 and older at the heel (Lunar PIXI) and at the PA lumbar spine and proximal femur (Lunar DPX-L and Hologic QDR 4500). Osteoporosis was defined using the WHO criteria for the diagnosis of osteoporosis and femoral neck T-scores were calculated using the NHANES III reference database. At a T-score of –2.5 at the calcaneus, the sensitivity for osteoporosis at any of the three central sites was only 20.3% although the specificity was 97.1%. As in the study from Fordham et al. (*22*) the optimum T-score threshold at the calcaneus for the diagnosis of central osteoporosis based on a ROC curve analysis appeared to be a T-score of –1.3, which the authors noted coincided with a calcaneal BMD of 0.390 g/cm^2 on the Lunar PIXI.

Using a different heel DXA device (Norland Apollo), Sweeney et al. (*24*) measured bone density in the calcaneus in 119 women with an average age of 51.6 years. Bone density was also measured at the PA lumbar spine and femoral neck with DXA (Norland Eclipse). Using the established WHO criteria for the diagnosis of osteopenia and osteoporosis at the spine, 30% of the women were osteopenic and 17% were osteoporotic. At the femoral neck, 41% were osteopenic and 21% were osteoporotic. At the heel, 32% were osteopenic and only 2% were osteoporotic. The authors attempted to identify the heel DXA T-score threshold that would identify women with spine or femoral neck T-scores of –1 or less. Using a heel T-score of –1 or less resulted in a sensitivity of 58% and specificity of 88% for identifying women with a low bone density at the spine. The same heel T-score threshold resulted in a sensitivity of 51% and specificity of 93%

for identifying women with a low bone density at the femoral neck. The authors were particularly interested in maximizing sensitivity in women aged 40–65. They noted that a heel DXA T-score of ≤0.0 resulted in 100% sensitivity for low bone density at the femoral neck and 85% sensitivity for low bone density at the spine in this age group (Table 9-2).

Table 9-2

Equivalent T-Scores and T-Score Ranges at Peripheral Sites by Specific Devices for Osteopenia and Osteoporosis at the PA Lumbar Spine and/or Proximal Femur. The reader is referred to the text for specific definitions of optimum sensitivity and osteoporosis for the various studies as well as the methodology used for the diagnosis of osteoporosis

		Osteopenia		Osteoporosis	
Device	Site/ROI	Equal Prevalence	Optimum Sensitivity	Equal Prevalence	Optimum Sensitivity
pDEXA[a]	Distal		≤ +1.06		≤ −0.74
	Proximal		≤ +0.53		≤ −0.73
accuDEXA	Phalanges	−1.4 to +0.4[b]		≤ −1.4[b]	≤ −1.0[c]/ ≤ −1.65[d]
Sahara[b]	Heel BMD	−1.9 to +0.3		≤ −1.9	
UBIS[e]	Heel BUA			≤ −1.8	≤ −1.3
	Heel SOS			≤ −2.2	≤ −1.5
PIXI[f,g]	Heel				≤ −1.3
Apollo[h]	Heel		≤ 0.0*		≤ 0.0*

*Optimum sensitivity for detecting osteopenia and osteoporosis combined.
[a]From ref. 18.
[b]From ref. 16.
[c]From ref. 19.
[d]From ref. 20.
[e]From ref. 21.
[f]From ref. 22.
[g]From ref. 23.
[h]From ref. 24.

These observations have prompted organizations to specifically recommend that peripheral sites measured by any technique not be used for the diagnosis of osteoporosis in general and specifically when the WHO criteria are used. This is in spite of the recognized fact that bone density at peripheral sites is predictive of fracture and that considerations of bone density at the mid-radius were included in the development of the WHO criteria. It would also seem to be contradictory to the intent of the 1991 and 1993 Consensus Conferences' (*1*, *2*) definition of osteoporosis in which osteoporosis was defined as a disease of "... low bone mass ... characterized by an increase in bone fragility and susceptibility to fracture." If the measurement of bone density at peripheral sites is predictive of fracture and therefore indicative of bone fragility and increased susceptibility to fracture, bone density at peripheral sites should be used to diagnose osteoporosis. Clearly, however, the application of the specific T-score thresholds originally proposed by the WHO for the diagnosis of osteopenia and osteoporosis to the results from the myriad of sites, devices, and techniques available today is not appropriate.

Thus, the clinician is left with the seemingly contradictory but inescapable directive to utilize peripheral devices or measurements of BMD at peripheral sites for fracture risk prediction only but not for the diagnosis of osteoporosis.

Changing the Definition of Osteoporosis

There has been considerable debate as to whether T-scores and the WHO criteria should be retained or whether entirely new approaches to quantitatively defining osteoporosis should be pursued, although this debate appears to be waning. The 1991 and 1993 Consensus Conferences' (*1,2*) definition of osteoporosis and even the 2000 Consensus Conference (*25*) definition[5] ultimately defined osteoporosis as a state of increased risk for fracture. It would be preferable for the diagnostic threshold for osteoporosis to coincide with the level of bone density that constitutes an unacceptable level of fracture risk and therefore the potential intervention threshold, no matter what skeletal site or technique might be used for the measurement. This is not the case, however.

Lu et al. (*26*) compared the diagnostic agreement for osteoporosis between two normal reference population approaches and a risk-based approach in 7671 women from the Study of Osteoporotic Fractures (SOF). Bone density was measured at eight different regions of interest using a combination of DXA and SPA: the PA lumbar spine, total femur, femoral neck, trochanter, Wards' area, calcaneus, distal radius, and proximal radius. The first reference population approach utilized a T-score of –2.5 based on the manufacturers' reference databases for the diagnosis of osteoporosis. The second reference population approach used a SD score of –1, when the reference BMD was the mean BMD for 65-year-old women from the SOF population. The risk-based approach defined osteoporosis as a spine and/or hip fracture risk greater than 14.6% based on age and BMD. The best diagnostic agreement for osteoporosis among the eight different regions of interest was 69% using the risk-based approach. The poorest agreement of 25% was seen when young-normal reference data was used. Black (*27*), writing for a joint committee of the National Osteoporosis Foundation and International Society for Clinical Densitometry, proposed the development of risk-based T-score equivalents, based on the 5-year hip fracture risk in women aged 70–74 with femoral neck *T*-scores poorer than –2.5. Blake and Fogelman (*28*) have also suggested a hip fracture risk-based threshold approach. Conceptually, a risk-based definition of osteoporosis is far more clinically relevant than the population-based approach, which results from the sole reliance on the T-score. The development of such a definition is far from clear-cut, however. Decisions must be made as to the type of risk suitable to define the disease. Should it be global or all-fracture risk? Or should it be only hip fracture risk or spine fracture risk? Should the expression of risk be the current fracture risk, the 5-year or 10-year fracture risk or lifetime fracture risk? And finally, what level of risk is unacceptable? All of these issues generate strong opinions. At present, the recommendations to limit the use of the WHO criteria for diagnosis to the PA lumbar spine, total femur, and femoral neck are both reasonable and necessary. Nevertheless, a move to a risk-based definition of osteoporosis would serve the needs of the densitometrist and patient far

---

[5] At this NIH Consensus Conference osteoporosis was defined as a "skeletal disorder characterized by compromised bone strength predisposing a person to an increased risk of fracture."

better than a population-based approach and would enhance the utility of all measurement sites and devices. At present, though, none of the proposed risk-based approaches has supplanted the WHO criteria in clinical practice.

DIAGNOSING OSTEOPOROSIS IN MEN

The issues surrounding the appropriate criteria for the diagnosis of osteoporosis in men are not substantially different than those for women. The WHO criteria were derived from data on women and were intended to be applied only to women. Once again, in the absence of other criteria, they have been applied to bone density measurements in men as well. There is controversy as to whether a T-score of –2.5 at any skeletal site by any technique is appropriate for a diagnosis of osteoporosis in men. Additionally, whether the T-score that is used for a man should be calculated by using a female reference database rather than a male reference database has also been raised. Ultimately, the question once again becomes "What does the diagnosis of osteoporosis mean?" If it is meant to imply a certain level of fracture risk that is imparted by the bone density alone, then a sex-specific T-score calculation may not be necessary or appropriate. The choice of the T-score threshold for the diagnosis of osteoporosis in men would depend on the magnitude of risk that is deemed synonymous with the disease.

These issues were addressed by Faulkner and Orwoll (*29*) in the *Journal of Clinical Densitometry* in 2002. Using the manufacturers' reference databases for several skeletal sites and techniques, United States population estimates for the year 2000 and the WHO T-score cut points for women, they calculated the prevalence of osteoporosis in men age 50 and over. Calculations were done using both male and female reference databases. The results are shown in Tables 9-3 and 9-4. Using the same approach as the WHO, they then attempted to determine the T-score at each site/device that matched the prevalence of osteoporosis with a reported lifetime fracture risk estimate of 13%. As shown in Table 9-5, regardless of whether male or female reference databases were used, the T-score cutpoint at every site with the exception of the spine by QCT, was better than –2.5. If a T-score cutpoint of –2.5 was used, regardless of whether it was based on male

Table 9-3
Percentage of Men over the Age of 50 at or Below the Indicated T-Score Using Male Reference Data

T-Score	Femoral Neck	Total Femur	DXA Spine	Total Forearm	Heel Ultrasound	QCT Spine
–3.5	1%	0%	0%	1%	0%	8%
–3.0	4%	1%	1%	3%	2%	16%
–2.5	9%	4%	4%	8%	5%	28%
–2.0	20%	9%	11%	16%	13%	45%
–1.5	36%	20%	23%	29%	26%	62%
–1.0	55%	36%	40%	46%	44%	77%

Adapted from ref. (*29*), with permission of Elsevier.

Table 9-4
Percentage of Men over the Age of 50 at or Below the Indicated T-Score Using Female Reference Data

T-Score	Femoral Neck	Total Femur	DXA Spine	Total Forearm	Heel Ultrasound	QCT Spine
−3.5	0%	0%	0%	0%	0%	12%
−3.0	1%	0%	0%	0%	1%	22%
−2.5	6%	1%	2%	0%	3%	37%
−2.0	9%	3%	5%	0%	8%	54%
−1.5	19%	7%	12%	1%	18%	71%
−1.0	34%	16%	24%	2%	34%	84%

Adapted from ref. (*29*), with permission from Elsevier.

Table 9-5
T-Scores Thresholds at Different Skeletal Sites for Men Older than Age 50 that Best Correspond to Lifetime Risk for Osteoporotic Fracture

T-Score	Femoral Neck	Total Femur	DXA Spine	Total Forearm	Heel Ultrasound	QCT Spine
Male Norms	−2.3	−1.8	−1.9	−2.1	−2.0	−3.1
Female Norms	−1.7	−1.2	−1.5	−0.5	−1.7	−3.4

Adapted from ref. (*29*), with permission from Elsevier.

or female reference values, the lifetime fracture risks were underestimated. In contrast, a T-score of −2.5 at the spine by QCT overestimated the lifetime fracture risk.

In this same study, Faulkner and Orwoll examined the expected decline in T-scores in men by site and technique with age. This relationship is shown in Fig. 9-2. This
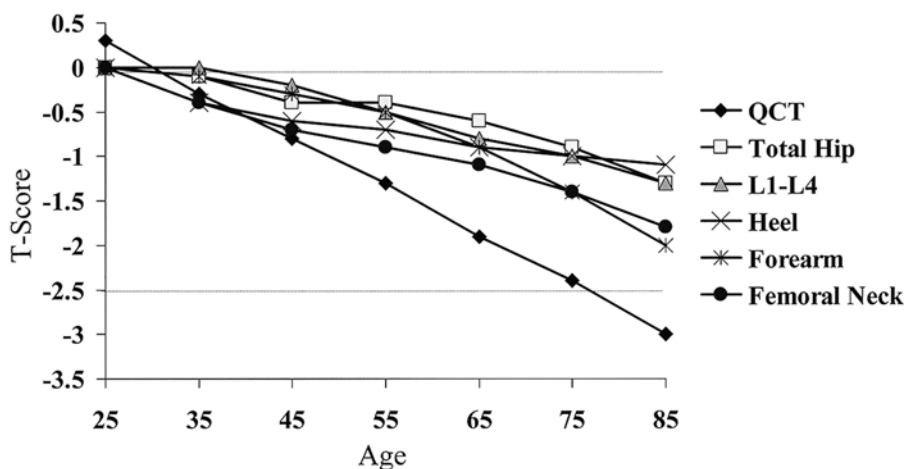

Fig. 9-2. The T-score regression on age for men by site and device, from the reference databases of the various manufacturers. The expected T-score for an average 65-year-old man ranges from −0.6 at the total femur by DXA to −1.9 at the spine by QCT. Reproduced with permission of Elsevier from ref. (*29*).

is similar to previously published findings in women (*17*). In Fig. 9-2, the decline in T-scores at the spine by QCT was the largest, falling below a T-score threshold of –2 by age 75. T-scores at other skeletal sites did not fall below –2 until the ninth decade. From the graph, it can be seen that T-scores for a man age 65 could range from –0.6 to –1.9, depending on the site and technique used for the measurement.

In 2002, ISCD (*30*) stated that osteoporosis in men should be defined as a T-score of –2.5 or poorer below the young-normal mean for *men*. This is in contrast to the recommendation of the IOF (*7*) in 2000 in which a T-score of –2.5 based on a *female* reference database was recommended as the diagnostic criteria for osteoporosis in men. An analysis of data from the EPOS[6] study (*31*) suggests that the IOF recommendation may actually be more appropriate when the primary issue is the implication for fracture risk from any given level of bone density. Using BMD and fracture data from 3461 men and women, the EPOS investigators determined that for any given age and spine bone density, the risk of spine fracture was similar in men and women. Incident spine fractures were more common in women than in men simply because, for any given age, bone density in women was lower than in men. Similarly, De Laet et al. (*32*), using mathematical models and data obtained from the Rotterdam study, suggested that hip fracture risk in men was lower than that in women overall, but appeared to be similar at the same level of femoral neck BMD. They noted that to capture the same proportion of hip fractures in men as in women, the BMD level must be higher than that for women and that the use of gender-specific T-scores would accomplish this. But because absolute risk for fracture was more relevant for intervention decisions, they proposed that the same levels of BMD be used for intervention decisions in men and women. As a consequence, if a given level of bone density in a woman would prompt an intervention to prevent fracture, that same level of bone density should prompt intervention in a man, regardless of the sex-specific T-scores. In an editorial in 2001 in the *Journal of Bone and Mineral Research*, Melton et al. (*33*) agreed that the absolute risk of fracture in men and women with the same BMD was similar although they also noted that relatively few men will reach the lowest levels of bone density that are associated with the greatest fracture risks in women. The authors observed that men are generally older than women at any given level of low bone density. Nevertheless, they concluded that it was not yet clear whether a female standard for the diagnosis of osteoporosis or risk assessment could reasonably be applied to men.

As noted earlier, these issues regarding the appropriate use of bone density to diagnose osteoporosis in men are similar to those for women. Conceptually, the 1991, 1993, and 2000 Consensus Conferences' definitions remain clinically relevant, linking the diagnosis of osteoporosis to an increased risk of fracture. How best to express this quantitatively remains at issue. In some cases, however, the T-score reflects more of the variability in bone density at a specific site when measured by a specific technique in a specific population than it reflects fracture risk. As a result, the diagnosis of osteoporosis and the prediction of fracture risk using bone densitometry must currently remain separate processes in men as well as women.

---

[6] The European Prospective Osteoporosis Study.

ADDITIONAL CONSIDERATIONS IN SITE SELECTION
FOR DIAGNOSIS

As noted in Chapter 2, the PA lumbar spine is commonly affected by dystrophic calcification in older adults, increasing the measured BMD and T-score. In particular, after the age of 60, the percentage of women having osteophytes in the lumbar spine is estimated at 61% (*34*). Calcification of the aorta, facet sclerosis, and intervertebral disk calcification can all have a significant effect on bone density measured at the PA lumbar spine (*35–40*). As a consequence, for diagnosis, the PA lumbar spine is less useful in individuals aged 60 and over. This age cutoff is somewhat arbitrary but generally appropriate. In individuals under age 60, the PA lumbar spine is an entirely appropriate skeletal site for the diagnosis of osteoporosis with bone densitometry.

In the proximal femur, the total hip and femoral neck are useful sites. The proximal femur is less affected by dystrophic changes than the PA spine, but it is not entirely free of such affects. Although the hip joint itself is not measured in a DXA proximal femur study, severe osteoarthritis of the hip joint can affect the bone density of the proximal femur (*41*, *42*). Therefore, if severe unilateral osteoarthritis is known or suspected, the proximal femur on the unaffected side should be measured. If this is not possible, the trochanteric region[7] becomes the preferable region of interest in the proximal femur as the effects of osteoarthritis of the hip joint are most notable in the femoral neck and Ward's area, both of which are included in the total hip region of interest.

If either hip has been fractured or undergone surgical instrumentation, it is not suitable for diagnostic assessment by densitometry. An additional consideration is the presence of scoliosis. In a study from Hans et al. (*43*) femoral neck bone density was 4.2% lower on the side of the spine convexity in a small study of 15 women with scoliosis. Consequently, the measurement of the proximal femur on the side of the convexity in scoliotic patients may provide the "worst case" bone density between the two femurs.

New developments in densitometry software have made possible the rapid study of both proximal femurs. While this may be desirable in specific circumstances, the question has arisen as to whether study of both proximal femurs should always be done when a proximal femur bone density measurement is performed to diagnose osteoporosis. Bone density in the various regions of the right and left femurs in individuals has consistently been found to be highly correlated when measured by DXA (*44–47*). Similarly, the average absolute differences in bone density in g/cm^2 between the right and left proximal femoral regions have been small and generally not statistically significantly different. Based on comparisons of both femurs in 198 women with an average age of 32.6 years, Bonnick et al. (*44*) found that the average difference was 0.7%, 0.2%, and 1.9% for the femoral neck, Ward's area, and trochanter, respectively. Only the difference observed at the trochanter was statistically significant, but all the differences were well within the precision error for the region of interest. Rao et al. (*45*) evaluated 131 women with an average age of 61 years. No significant difference was found between the femoral neck BMD in the right and left femurs in this study as well, with a

---

[7]Although ISCD does not recommend the use of the WHO criteria with trochanteric bone density measurements, the site does provide useful information when osteoarthritis of the hip joint makes results from the total hip and femoral neck suspect.

mean difference of about 1%. The differences in BMD between the right and left femurs at Ward's area and the trochanter were statistically significant but small, averaging 2–2.5%. In a very large study of 2372 women with an average age of 56.6 years, Petley et al. (*46*) did find a statistically significant difference between the right and left proximal femurs in the femoral neck, but again, the difference was quite small and not clinically relevant. The mean BMD of the right femoral neck in this study was 0.840 g/cm^2 while the mean BMD in the left femoral neck was 0.837 g/cm^2. The mean difference was 0.003 g/cm^2. The maximum difference observed in this study was 0.249 g/cm^2. Based on these findings, all of these authors concluded that there was little justification for the *routine* measurement of both proximal femurs in clinical practice. In a study of 61 women from Mazess et al. (*47*), however, it was noted that 32% of the women had differences between the right and left femoral necks of 0.5 SD and that 5% of the women had differences that exceeded 1 SD. In those 5% of women, a difference of 1 SD, or an entire T-score unit, could clearly affect not only the assignment of the WHO diagnostic category but treatment decisions as well. Nevertheless, it is difficult to justify routine measurement of both femurs in all women on this basis. In many centers, both the PA lumbar spine and proximal femur are studied during the initial evaluation. If this is the case, the clinical impact from scanning both proximal femurs instead of just one is likely to be small. In the very large study from Petley et al. (*46*) noted earlier, knowledge of the T-score at the second proximal femur altered the diagnosis to osteoporosis in only 2.2% of the patients when the PA lumbar spine had been studied as well. It is possible that a difference of even 0.1 SD could alter the assignment of diagnostic category when the WHO criteria are employed. If such an alteration will reasonably affect decisions to intervene, then the measurement of both femurs may be justified.

REFERENCES

1. Consensus Development Conference. Prophylaxis and treatment of osteoporosis. Am J Med 1991;90:107–110.
2. Consensus Development Conference. Diagnosis, prophylaxis, and treatment of osteoporosis. Am J Med 1993; 94:646–650.
3. World Health Organization. Assessment of fracture risk and its application to screening for postmenopausal osteoporosis. WHO technical report series. Geneva: WHO, 1994.
4. Personal communication. Dr. John Kanis to Dr. Leon Lenchik, March 29, 1999.
5. Genant HK, Cooper C, Poor G, et al. Interim report and recommendations of the World Health Organization Task-Force for osteoporosis. Osteoporos Int 1999;10:259–264.
6. WHO. Prevention and management of osteoporosis. [921], 1–192. 2003. Geneva, WHO. WHO Technical Report Series.
7. Kanis JA, Gluer C-C. An update on the diagnosis and assessment of osteoporsois with densitometry. Committee of Scientific Advisors, International Osteoporosis Foundation. Osteoporos Int 2000;11:192–202.
8. Hamdy RC, Petak SM, Lenchik L. Which central dual x-ray absorptiometry skeletal sites and regions of interest should be used to determine the diagnosis of osteoporosis? J Clin Densitom 2002;5: S11–S17.
9. Hans D, Downs RW, Duboeuf F, et al. Skeletal sites for osteoporosis diagnosis: the 2005 ISCD official positions. J Clin Densitom 2006;9:15–21.
10. Miller PD, Njeh CF, Jankowski LG, Lenchik L. What are the standards by which bone mass measurement at peripheral sites should e used in the diagnosis of osteoporosis? J Clin Densitom 2002;5: S39–S45.

11. Marshall D, Johnell O, Wedel H. Meta-analysis of how well measures of bone mineral density predict occurrence of osteoporotic fractures. BMJ 1996;312:1254–1259.

12. Cummings SR, Black DM, Nevitt MC, et al. Bone density at various sites for prediction of hip fracture. Lancet 1993;341:72–75.

13. Melton LJ, Atkinson EJ, O'Fallon WM, Wahner HW, Riggs BL. Long-term fracture prediction by bone mineral assessed at different skeletal sites. J Bone Miner Res 1993;8:1227–1233.

14. Miller PD, Siris ES, Barrett-Connor E, et al. Prediction of fracture risk in postmenopausal white women with peripheral bone densitometry: evidence from the National Osteoporosis Risk Assessment. J Bone Miner Res 2002;17:2222–2230.

15. Greenspan SL, Maitland-Ramsey L, Myers E. Classification of osteoporosis in the elderly is dependent on site-specific analysis. Calcif Tissue Int 1996;58:409–414.

16. Varney LF, Parker RA, Vincelette A, Greenspan SL. Classification of osteoporosis and osteopenia in postmenopausal women is dependent on site-specific analysis. J Clin Densitom 1999;2:275–283.

17. Faulkner KG, von Stetten E, Miller P. Discordance in patient classification using T-scores. J Clin Densitom 1999;2:343–350.

18. Pouillès JM, Tremollières FA, Martinez S, Delsol M, Ribot C. Ability of peripheral DXA measurements of the forearm to predict low axial bone mineral density at menopause. Osteoporos Int 2001;12:71–76.

19. Mulder JE, Michaeli D, Flaster ER, Siris E. Comparison of bone mineral density of the phalanges, lumbar spine, hip, and forearm for assessment of osteoporosis in postmenopausal women. J Clin Densitom 2000;3:373–381.

20. Fiter J, Nolla JM, Gómez-Vaquero C, Martínez-Aguilá D, Valverde J, Roig-Escofet D. A comparative study of computed digital absorptiometry and conventional dual-energy x-ray absorptiometry in postmenopausal women. Osteoporos Int 2001;12:565–569.

21. Damilakis J, Persinakis K, Gourtsoyiannis N. Imaging ultrasonometry of the calcaneus: optimum T-score thresholds for the identification of osteoporotic subjects. Calcif Tissue Int 2001;68:219–224.

22. Fordham JN, Chinn DJ, Kumar N. Identification of women with reduced bone density at the lumbar spine and femoral neck using BMD at the os calcis. Osteoporos Int 2000;11:797–802.

23. Pacheco EMB, Harrison EJ, Ward KA, Lunt M, Adams JE. Detection of osteoporosis by dual energy X-ray absorptiometry (DXA) of the calcaneus: is the WHO criterion applicable? Calcif Tissue Int 2002;70:475–482.

24. Sweeney AT, Malabanan AO, Blake MA, et al. Bone mineral density assessment: comparison of dual-energy x-ray absorptiometry measurements at the calcaneus, spine and hip. J Clin Densitom 2002;5:57–62.

25. Consensus Conference. Osteoporosis prevention, diagnosis, and therapy. JAMA 2001;285:785–795.

26. Lu Y, Genant HK, Shepherd J, et al. Classification of osteoporosis based on bone mineral densities. J Bone Miner Res 2001;16:901–910.

27. Black DM. A proposal to establish comparable diagnostic categories for bone densitometry based on hip fracture risk among Caucasian women over age 65. Abstract. J Bone Miner Res 2001;16:S342.

28. Blake GM, Fogelman I: Peripheral or central densitometry: does it matter which technique we use? J Clin Densitom 2001;4:83–96.

29. Faulkner KG, Orwoll E. Implications in the use of T-scores for the diagnosis of osteoporosis in men. J Clin Densitom 2002;5:87–93.

30. Binkley NC, Schmeer P, Wasnich RD, Lenchik L. What are the criteria by which a densitometric diagnosis of osteoporosis can be made in males and non-Caucasians? J Clin Densitom 2002;5: S19–S27.

31. The European Prospective Osteoporosis Study (EPOS) Group. The relationship between bone density and incident vertebral fracture in men and women. J Bone Miner Res 2002;17:2214–2221.

32. De Laet CEDH, Van Der Klift M, Hofman A, Pols HAP. Osteoporosis in men and women: a story about bone mineral density thresholds and hip fracture risk. J Bone Miner Res 2002;17:2231–2236.

33. Melton LJ, Orwoll ES, Wasnich RD. Does bone density predict fractures comparably in men and women? J Bone Miner Res 2001;12:707–709.

34. Liu G, Peacock M, Eilam O, Dorulla G, Braunstein E, Johnston CC. Effect of osteoarthritis in the lumbar spine and hip on bone mineral density and diagnosis of osteoporosis in elderly men and women. Osteoporos Int 1997;7:564–569.

35. Frye MA, Melton LJ, Bryant SC, et al. Osteoporosis and calcification of the aorta. Bone Miner 1992;19:185–194.
36. Frohn J, Wilken T, Falk S, Stutte HJ, Kollath J, Hor G. Effect of aortic sclerosis on bone mineral measurements by dual-photon absorptiometry. J Nucl Med 1990;32:259–262.
37. Orwoll ES, Oviatt SK, Mann T. The impact of osteophytic and vascular calcifications on vertebral mineral density measurements in men. J Clin Endocrinol Metab 1990;70:1202–1207.
38. Reid IR, Evans MC, Ames R, Wattie DJ. The influence of osteophytes and aortic calcification on spinal mineral density in post-menopausal women. J Clin Endocrinol Metab 1991;72:1372–1374.
39. Drinka PJ, DeSmet AA, Bauwens SF, Rogot A. The effect of overlying calcification on lumbar bone densitometry. Calcif Tissue Int 1992;50:507–510.
40. Cherney DD, Laymon MS, McNitt A, Yuly S. A study on the influence of calcified intervertebral disk and aorta in determining bone mineral density. J Clin Densitom 2002;5:193–198.
41. Nevitt MC, Lane NE, Scott JC, et al. Radiographic osteoarthritis of the hip and bone mineral density. Arth Rheum 1995;38:907–916.
42. Preidler KW, White LS, Tashkin J, et al. Dual-energy X-ray absorptiometric densitometry in osteoarthritis of the hip. Influence of secondary bone remodeling of the femoral neck. Acta Radiol 1997;38:539–542.
43. Hans D, Biot B, Schott AM, Meunier PJ. No diffuse osteoporosis in lumbar scoliosis but lower femoral bone density on the convexity. Bone 1996;18:15–17.
44. Bonnick SL, Nichols DL, Sanborn CF, Payne SG, Moen SM, Heiss CJ. Right and left proximal femur analyses: is there a need to do both? Calcif Tissue Int 1996;58:307–310.
45. Rao AK, Reddy S, Rao DS. Is there a difference between right and left femoral bone density? J Clin Densitom 2000;3:57–61.
46. Petley GW, Taylor PA, Murrills AJ, Dennison E, Pearson G, Cooper C. An investigation of the diagnostic value of bilateral femoral neck bone mineral density measurements. Osteoporos Int 2000;11:675–679.
47. Mazess RB, Nord RH, Hanson JA, Barden HS. Bilateral measurement of femoral bone mineral density. J Clin Densitom 2000;3:133–140.

10 Predicting Fracture Risk

CONTENTS

The risk of any outcome can be expressed in a variety of different ways, as was noted in Chapter 3. The more commonly used measures of risk are prevalence, incidence, absolute and relative risks, and odds ratios. All of these measures can be employed in the specific context of the assessment of fracture risk. In densitometry, other measures of risk are employed as well, such as the fracture threshold, lifetime risk, and remaining lifetime fracture probability. These are also quantitative measures of risk. Qualitative fracture risk assessments may also be useful. Although there is no question that a measurement of bone density can predict fracture risk, none of the measures used clinically to express fracture risk is ideal. The field as a whole, however, has moved toward the use of absolute risk, projected over varying lengths of time. A physician should ultimately use whichever expression of risk best conveys the implications for fracture, and therefore the need for pharmacologic intervention, based on the patient's BMD, age, and other risk factors.

THE PREVALENCE OF FRACTURE AT DIFFERENT LEVELS OF BMD

Prevalence describes the ratio of the number of individuals with a disease at a given point in time in a particular population to the number of individuals who are at risk for the disease. Prevalence can be used to answer the question of how common a disease is in a population that is at risk for the disease. In the context of this discussion, prevalence is used to answer the question, "How common is fracture at a given level of BMD?" This question was addressed by Mazess (1) in a study of 590 Caucasian women aged 50–89 years who underwent PA spine and proximal femur bone density

studies with DPA. Approximately 25% of these women had spine or hip fractures. The prevalence of spine or hip fracture or both at varying levels of L2–L4 or femoral neck BMD is shown in Tables 10-1 and 10-2. This type of risk assessment can be useful to a physician who is trying to determine the clinical significance of any given level of BMD in his or her patient, even if the patient has not yet fractured. Because the data shown in Tables 10-1 and 10-2 were based on measurements made with DPA, the ranges for spine BMD and for femoral neck BMD (depending upon the type of DXA device) should be adjusted downward in order to compare DXA measurements to this data. The equations for converting DPA data to DXA data are given in Chapter 6 and again in Appendix II.

Table 10-1
**The Prevalence of Spine or Hip Fracture or Both at Varying Levels of Spine BMD
Measured with Dual-Photon Absorptiometry**

L2–L4 BMD (g/cm^2)	N	Spine Fracture %	Hip Fracture %	Either/Both %
> 1.10	100	6.0	3.0	7.0
1.00–1.09	111	9.9	5.4	13.5
0.90–0.99	159	17.0	6.3	22.0
0.80–0.89	134	23.1	9.7	29.9
0.70–0.79	49	40.8	12.2	44.8
0.60–0.69	20	50.0	15.0	60.0

Adapted with permission from Elsevier from ref. (*1*) Elsevier Science Inc., 655 Avenue of the Americas, New York, NY, 10010-5107.

Table 10-2
**Prevalence of Spine or Hip Fracture or Both at Varying Levels of Femoral Neck BMD
Measured with Dual-Photon Absorptiometry**

Femoral Neck BMD (g/cm$^{2)}$	N	Spine Fracture %	Hip Fracture %	Either/Both %
> 0.80	133	3.8	0.0	3.8
0.70–0.79	178	10.6	3.4	12.9
0.60–0.69	164	21.3	10.4	31.1
0.50–0.59	89	32.6	29.2	51.7
0.40–0.49	26	38.5	46.2	76.9

Adapted with permission from Elsevier from ref. (*1*) Elsevier Science Inc., 655 Avenue of the Americas, New York, NY, 10010-5107.

FRACTURE RISK PREDICTION

Site-specific and Global Fracture Risk Prediction

Fracture risk predictions fall into two general categories. The prediction may be a site-specific fracture risk prediction or it may be a global fracture risk prediction. A site-specific fracture risk prediction is the prediction of the risk of fracture *at a specific site*. For example, the prediction of spine fracture risk is a type of site-specific fracture risk prediction. Similarly, the prediction of hip fracture risk is a type of site-specific fracture risk prediction. Site-specific fracture risk prediction does *not* necessarily mean that the measurement is being performed at a specific site. A global fracture risk prediction is

the prediction of the risk of having any and all types of osteoporotic fractures. Again, the terminology does not imply the measurement of bone density at a particular site.

Relative Risk Fracture Data

The studies that conclusively established the predictive capabilities of bone mass measurements for fracture risk generally reported the data as the increase in relative risk per standard deviation decline (SD) in bone density. In Chapter 3, it was noted that relative risk is the best indicator of the strength of the relationship between a risk factor (in this case, low bone mass or density) and an outcome (fracture). It is understandable therefore, that much of the information in the medical literature about the prediction of fracture risk from bone mass measurements is presented in the form of relative risk values. Relative risk is calculated from absolute risk data that is collected during prospective fracture trials. The ratio of the absolute risk for fracture between two groups constitutes the *relative* risk for fracture between the two groups. A relative risk of 1 implies that there is no difference in risk between the groups. It is possible that both groups have an increased absolute risk, but the risk of one group is no greater than the risk of the other group. Relative risk data thus obscures the actual magnitude of the absolute risk for either group. For example, if the absolute risk for fracture in group A is 50% compared to the absolute risk for fracture of 25% in group B, the relative risk of group A compared to group B is 2 (50 ÷ 25% = 2). This would be interpreted to mean that the risk in group A is two-fold greater than group B's. The relative risk would also be 2 however, if the absolute risk in group A was 2% and the absolute risk in Group B was 1% (2 ÷ 1% = 2). The interpretation is unchanged. Group A has a two-fold greater risk of fracture than group B.

Relative risk data can be used to establish which skeletal sites have the best predictive power for certain types of fracture risk predictions. The site that has a statistically significantly greater increase in relative risk for fracture per SD decline in bone mass or density will be the skeletal site that has the best predictive power for that type of fracture risk prediction.

GLOBAL FRACTURE RELATIVE RISK DATA

The sites on the forearm have been used in several classic fracture trials to assess global fracture risk as well as site-specific assessments of spine, hip, or forearm fracture risk. Hui et al. (*2*) evaluated radial bone mass in 386 community-based women and 135 retirement home-based women using SPA. Bone mass was measured at the mid-radius at baseline and the women were subsequently followed for the development of non-spine fractures for 1–15 years. During that time, 89 women had 138 non-spine fractures of various types. The statistical analysis revealed that for each SD decline in bone mass at the mid-radius, the relative risk for any type of non-spine fracture was 2.2 in the community-based women and 1.5 in the retirement-home women.

Gardsell et al. (*3*) also used the radius to evaluate global fracture risk in a study of 332 women over an average period of 14.6 years. The distal and mid-radius were measured using SPA. During the follow-up period, 100 women had one or more fragility fractures. The relative risk for fracture measured at the distal radius was 2.6 and at the mid-radius, 3.2.

The lumbar spine, femoral neck, and trochanter are also useful for global fracture risk prediction. In a study of 304 women, aged 30–94 years, who were followed for a median

of 8.3 years, 93 women experienced 163 new fractures (*4*). Bone mass was measured at baseline at five skeletal sites: the PA lumbar spine, femoral neck, and trochanter by DPA and the distal and mid-radius by SPA. The relative risk for all fractures measured at the spine, femoral neck, and trochanter was 1.5, 1.6, and 1.5, respectively when only those fractures that resulted from mild-to-moderate trauma were considered. The mid-radius was also predictive of global fracture risk for fractures resulting from mild-to-moderate trauma in this study with a relative risk of 1.5.

Other studies have quantified the increase in relative risk per SD decline in bone mass or density measured at different skeletal sites for the prediction of global fracture risk. In the Study of Osteoporotic Fractures (*5*), a 1 SD decrease in BMC at the mid-radius resulted in an age-adjusted increase in relative risk of 1.3 and at the distal radius 1.4. Measurements of BMD at the lumbar spine and femoral neck were also predictive of global fracture risk with comparable relative risk values of 1.35 and 1.41, respectively. The calcaneus was also equally predictive of global fracture risk with a relative risk of 1.51 for each SD decline in bone density. In another study (*6*) of 1098 women followed for an average of 4.5 years, a decrease of 2 SD in BMC at the mid-radius resulted in an increase in relative risk of 2.8 for any type of non-spine fracture. Relative risk values from the medical literature for global fracture risk prediction are summarized in Table 10-3.

Table 10-3
**Age-adjusted Increase in Relative Risk for Fracture for
Global Fracture Risk Prediction per Standard Deviation
Decrease in Bone Mass Measured at Various Skeletal Sites**

Site	*Global Fracture Risk RR*
AP Lumbar Spine	1.5[b], 1.35[b]
Total Femur	1.40[b]
Femoral Neck	1.6[b], 1.41[b]
Trochanter	1.5[b], 1.38[b]
Mid-Radius	1.5[a], 1.32[b], 3.2[a]
Distal Radius	1.42[b], 2.6[a]
Calcaneus	1.51[b]

[a] Per SD decrease in BMC
[b] Per SD decrease in BMD
From refs. (*2, 3, 4, 5*).

SITE-SPECIFIC SPINE FRACTURE RELATIVE RISK DATA

Several sites are useful for the site-specific prediction of spine fracture risk. In the study by Melton et al. (4) the increase in relative risk for spine fracture resulting from mild-to-moderate trauma for each SD decline in BMD or BMC was statistically significant not only at the spine itself, but also at the femoral neck, trochanter, and mid-radius. The relative risk values were 2.2, 2.0, 1.7, and 2.5, respectively. The greatest increase in relative risk of 2.5 was actually seen at the mid-radius, but the statistical analysis suggested that each of these four sites actually performed equally well.

Data presented in abstract form at the 19th Annual Meeting of the American Society for Bone and Mineral Research suggested that the phalanges and metacarpals as measured by radiographic absorptiometry (RA) were useful predictors of spine fracture risk.

In a study (*7*) of 251 women whose average age at baseline was 74 years, 18 spine fractures occurred during an average follow-up of 2.7 years. Based on RA measurements of the phalanges, the increase in relative risk per SD decline in BMD was 3.4. In another study (*8*) of 509 postmenopausal women with an average age of 74 at baseline, 37 fracture spine fracture cases were observed during an average follow-up of 2.7 years. The relative risk for spine fracture with RA of the metacarpals in this study was 1.9.

SITE-SPECIFIC HIP FRACTURE RELATIVE RISK DATA

Different skeletal sites for site-specific hip fracture risk prediction have been evaluated in several studies. In the study from Melton et al. (*4*), 10 fractures of the proximal femur from mild-to-moderate trauma occurred. Statistically significant increases in relative risk for hip fracture were found for BMD measured at the femoral neck, trochanter, and distal radius. The increases in relative risk for hip fracture from BMD measured at the spine or mid-radius did not reach statistical significance. In what is considered a sentinel study for demonstrating the predictive ability of the measurement of BMD for hip fracture risk prediction, Cummings et al. (*9*) evaluated 8134 women aged 65 and over. During an average follow-up period of 1.8 years, 65 hip fractures occurred (33 femoral neck, 32 intertrochanteric). Bone mineral density was measured at the lumbar spine and proximal femur with DXA (Hologic QDR-1000) and at the distal and mid-radius and os calcis with SPA (OsteoAnalyzer). Within the proximal femur, the total femur, femoral neck, trochanter, intertrochanteric, and Ward's triangle were measured. All of these regions of interest (ROIs) had statistically significant increases in relative risk for hip fracture for each SD decline in BMD. In this study, the ROIs in the proximal femur were clearly stronger predictors of hip fracture than the PA lumbar spine or radial sites. The os calcis[1] was also an excellent predictor of hip fracture risk, being out-performed by the proximal femur ROIs by the narrowest of margins. The age-adjusted increases in relative risk for hip fracture in the total femur, femoral neck, Ward's, trochanteric, and intertrochanteric regions were all very similar. They were 2.7, 2.6, 2.8, 2.7, and 2.5, respectively. The increase in relative risk at the os calcis was 2.0. Both the lumbar spine and distal radius had a relative risk of 1.6 per SD decline in BMD while the mid-radius had a relative risk of 1.5 per SD decline.

In the previously described study from Hui et al. (*2*), 30 hip fractures occurred in the retirement-community women.Based on measurements of the mid-radius with SPA in this group, the relative risk for hip fracture per SD decline in bone mass was 1.9.

Phalangeal bone density also appears to be useful as a predictor of hip fracture risk. During the National Health and Nutrition Examination Survey I (NHANES I) between 1971 and 1975, 3481 subjects underwent radiographic photodensitometry studies of the hand (*10*). At baseline, the ages of the subjects ranged from 45 to 74. During the follow-up period through 1987, 72 hip fractures occurred. The relative risk for hip fracture as calculated from radiographic photodensitometry measurements of the middle phalanx of the small finger was 1.57 for all subjects. When the analysis was restricted to Caucasian women, the relative risk was 1.56. The radiographic photodensitometry films were reanalyzed using the modern technique of RA. When the films were re-analyzed with RA,

---

[1] Os calcis and calcaneus are used interchangeably.

Table 10-4
Increase in Age-Adjusted Relative Risk for Spine or Hip Fracture per Standard
Deviation Decrease in Bone Mass as Measured at Various Skeletal Sites

Site	Spine Fracture Risk RR	Hip Fracture Risk RR
AP Lumbar Spine	2.2[b]	1.6[b]
Total Femur		2.7[b]
Femoral Neck	2.0[b]	2.6[b,] 2.8[b]
Ward's		2.8[b]
Trochanter	1.7[b]	2.7[b], 2.4[b]
Distal Radius		1.6[b], 3.1[b]
Mid-radius	2.5[a]	1.5[b,] 1.9[a]
Calcaneus		2.0[b]
Phalanges	3.4[c]	1.8[c]
Metacarpals	1.9[c]	

[a]Per SD decrease in BMC
[b]Per SD decrease inBMD
[c]Per SD decreaseinRA units
From refs. *(2, 4, 7, 8, 9, 10)*.

the relative risk for each SD decline in bone density was 1.81 for all subjects and 1.79 for Caucasian women only. Table 10-4 summarizes the increases in relative risk per SD decline in bone mass for site-specific fracture risk predictions from bone mass measured at different skeletal sites.

APPLYING RELATIVE RISK DATA IN CLINICAL PRACTICE

The values for relative risk discussed above were derived from specific study populations. The characteristics of each study population such as the mean age and the mean and SD for BMD at baseline make the increase in relative risk per SD decline in BMD unique for that population. Applying such relative risk data to an individual patient and utilizing the SD for the reference population supplied by the manufacturer to calculate the relative risk for the patient in question is clearly an extrapolation of the published data that may not be appropriate. In addition, relative risk values are generally calculated as age-adjusted values. Age-adjustment means that the effect of age has been accounted for or eliminated statistically such that only the effect of bone density on risk remains. Recall also that relative risk data obscures the magnitude of the absolute risks used to calculate it. These considerations profoundly affect the densitometrist's ability to use relative risk data in clinical practice.

The calculation itself of a patient's relative risk for various types of fracture using standard scores on the densitometry printout and published relative risk data is not difficult. The relationships between absolute risk, relative risk, and the magnitude of the SD decline in bone density that were discussed in Chapter 3 are the key to this calculation and its interpretation. For example, in the spine bone density study shown in Fig. 10-1, the L1–L4 BMD is 0.814 g/cm^2. The T-score of –2.12 indicates that the L1–L4 BMD is 2.12 SD below the average peak BMD of the young-adult. The z-score of –0.08 indicates that the L1–L4 BMD is 0.08 SD below the average BMD predicted for this woman's age. The age-adjusted increases in relative risk for fracture from Melton et al. (*4*) can be used to calculate the global and site-specific spine fracture relative risk.
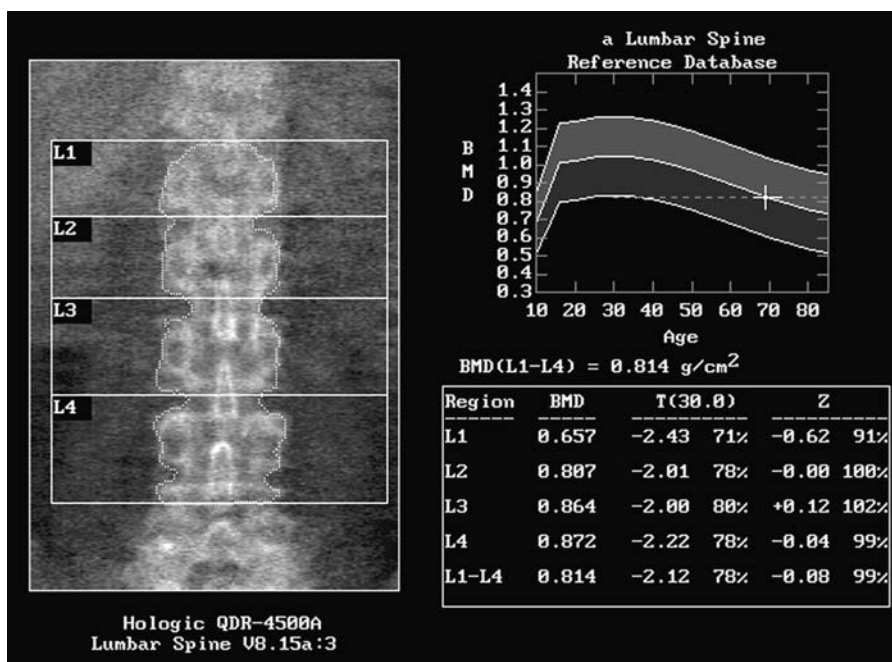
Fig. 10-1. Hologic QDR PA lumbar spine study in a 70-year-old Caucasian woman. The L1–L4 BMD is 0.814 g/cm^2. The *T*-score is –2.12 and the *z*-score is –0.08. The correct diagnosis is osteopenia. Use of relative risk fracture data with either the *T*- or *z*-score will lead to very different impressions of this patient's fracture risk.

Melton et al. found that for each SD decline in bone density when measured at the spine, the increase in relative risk for *any* type of low-to-moderate trauma fracture was 1.5. Therefore, the relative risk for global fracture in this patient compared to the individual who still has an average peak bone density, based on this measurement of bone density at the lumbar spine, is $1.5^{2.12}$ or 2.4. This is the increase in relative risk per SD decline in bone density raised to the power of the T-score.[2] Compared to the individual who has a spine bone density that would be predicted for the patient's age, the global fracture relative risk would be $1.5^{0.08}$ or 1.03. This is the increase in relative risk raised to the power of the *z*-score. A relative risk of 1.03, of course, is no increase in risk at all. *Strictly speaking, neither of these calculations is correct, although it is the best that can be done using relative risk data*. The reason that neither calculation is correct is because the strict interpretation of the finding of a 1.5 relative risk for global fracture per SD decline in spine BMD from the Melton study (*4*) is that an individual in the Melton study has a 1.5-fold higher risk for global fracture than another individual in the same study who has a BMD that is 1 SD higher. There is nothing here that a densitometrist can really use to quantify fracture risk in his or her individual patient. Because the data are age-adjusted, and the BMD study mean and SD are unique for the study population, the use of the individual patient's *T*- or *z*-score is not correct. The use of the patient's *z*-score

_____

[2] The minus sign in front of the T-score is disregarded.

is probably the better of the two standard scores on the bone density printout with which to use relative risk data but in this case, might lead to confusion. The patient would be diagnosed as osteopenic using World Health Organization criteria[3] and could conceivably meet the National Osteoporosis Foundation guidelines for prescription intervention and yet the use of the *z*-score with relative risk fracture data might lead the physician to conclude that she is not at increased risk for fracture.

Relative risks for site-specific spine fracture prediction are calculated in a similar fashion. Using an increase in relative risk per SD decline in BMD of 2.2 for spine fracture when measured at the spine, the calculation would be $2.2^{2.12}$ or $2.2^{0.08}$, depending upon the comparison the physician wishes to make. This results in relative risk values of 5.32 and 1.07, respectively. Once again, the use of the T-score resulted in a markedly different relative risk than the z-score. The relative risk value of 5.32 would be interpreted as meaning that the patient has a 5.32-fold higher risk of spine fracture than an individual whose bone density was identical to the average peak bone density. Unfortunately, the question that a relative risk value like this cannot answer is, "5.32-fold higher than what risk?" This is because the absolute risk of fracture is obscured when relative risk data are used.

Global fracture relative risk data for BMD measurements made at other sites can be calculated using data from Melton (*4*) as well as other authors (*2*, *3*, *5*). Similarly, the relative risk for a site-specific spine fracture risk prediction can be calculated from bone density measured at other sites using data from Melton (*4*) and others (*2*, *7*, *8*). The data from Cummings et al. (*9*) are most commonly used for the calculation of relative risk for site-specific hip fracture risk prediction.

Lifetime Risk Of Fracture

In 1992, Black et al. (*11*) proposed a method for calculating a woman's lifetime risk for hip fracture. The prediction was based on the woman's bone mass at menopause expressed as a percentile for her age, estimations of bone mass at subsequent ages, and then estimating her risk for hip fracture at each age. The risk of hip fracture at each age was based on two factors: the risk of fracture at a particular age derived from population-based data and the risk of fracture at a particular bone mass from prospective fracture trials. Based on a review of the literature at the time, an increase in relative risk for hip fracture of 1.65 for each SD decline in bone mass at the radius was used in the calculation of risk, based on the level of bone mass. Using this method, the lifetime risk of hip fracture for a 50-year-old Caucasian woman whose mid-radial bone mass was at the 10th percentile was 19%. If her bone mass was at the 90th percentile, her lifetime risk of hip fracture was 11%. The gradient of risk, therefore, between the 90th and 10th percentile was 1.7 (19 × 11% = 1.7). This model is obviously dependent upon the value chosen for the increase in relative risk per SD decline in bone mass. The authors noted if the increase in relative risk was 2.0 instead of 1.65, the lifetime risks for the 10th and 90th percentiles would be 21% and 9%, respectively. The gradient of risk would therefore increase to 2.3.

---

[3] See Chapter 9 for a discussion of the World Health Organization criteria for the diagnosis of osteoporosis.
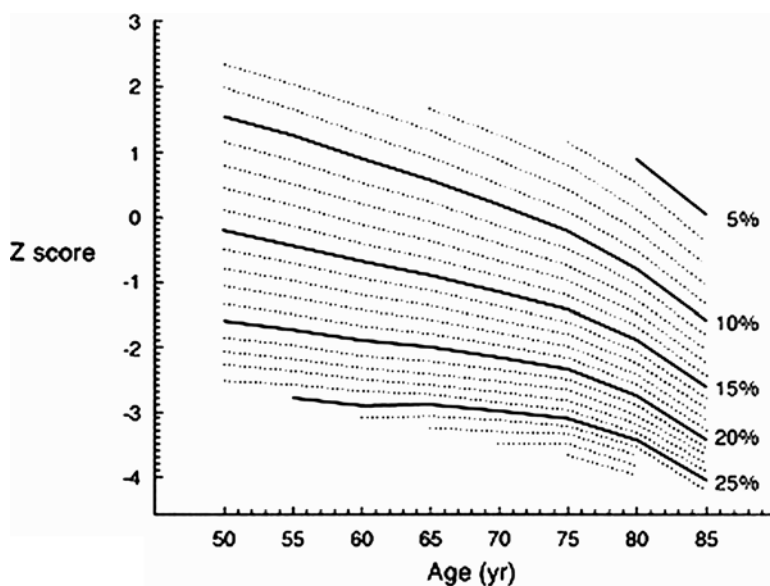
Fig. 10-2. Lifetime hip fracture risk as predicted from age and radial bone density. Z-scores are based on the average BMD of the 50-year-old woman. Reprinted with permission of Elsevier from ref. *12*.

In 1993, Suman et al. (*12*) developed a nomogram for predicting lifetime risk of hip fracture that was derived from the model developed by Black et al. (*11*). This nomogram is shown in Fig. 10-2. The *z*-scores utilized in the nomogram are based on the mean and SD for bone mass for 50-year-old Caucasian women. Like the concept of remaining lifetime fracture probability that is discussed next, lifetime fracture risk goes beyond the prediction of current fracture risk. A young individual with a slightly low bone mass and low current fracture risk will be identified as having a higher lifetime fracture risk. Similarly, an older individual with a low bone mass and high current fracture risk may have a lower lifetime fracture risk because of a shorter life expectancy.

Cummings et al. (*13*) published lifetime fracture risk data for hip fracture based on the femoral neck bone density T-score. These data are shown in Table 10-5. The risk of hip fracture used to determine lifetime hip fracture risk was derived from data from the

Table 10-5
Lifetime Risk (%) of Hip Fracture for White Women Based on Age and T-Score at the Femoral Neck

	Femoral Neck Bone Density T-Score							
Age, y	*−3.5*	*−3.0*	*−2.5*	*−2.0*	*−1.5*	*−1.0*	*−0.5*	*0*
50	49	41	33	27	21	16	13	10
60	47	40	33	27	21	17	13	10
70	46	39	33	27	21	17	13	10
80	41	35	30	24	20	16	12	10

Study of Osteoporotic Fractures in which the relative risk for hip fracture was 2.6 per SD decline in bone density at the femoral neck (*9*). The femoral neck T-scores are based on 1995 NHANES III reference data (*14*). Using Table 10-5, a 60-year-old Caucasian woman with a femoral neck T-score of –2.0 would have a lifetime hip fracture risk of 27%. An 80-year-old Caucasian woman with the same femoral neck T-score would have a lifetime hip fracture risk of 24%.

10-Year Fracture Probability

Lifetime fracture risk predictions appropriately emphasize that current or short-term fracture risk predictions may be misleading in the context of the need for pharmaco-logic intervention. Nevertheless, lifetime fracture risk predictions have been criticized for emphasizing a time frame that is too long to be clinically useful. Experts have argued that most patients will not take a medication over a lifetime. It is therefore argued that looking at risk over a shorter period of time better assesses the need for any potential benefit from an intervention. In response, 5- and 10-year fracture probability algo-rithms have been developed. Using fracture and mortality data from Malmö, Sweden, Kanis et al. (*15*) determined the 10-year probability of global and site-specific fractures. Tables 10-6, 10-7, 10-8, and 10-9 reflect the 10-year probability of fracture based on the patient's age and femoral neck T-score. The femoral neck T-score was again based on NHANES III 1995 reference data for Caucasian women (*14*). The relative risk of fracture at the hip and proximal humerus used to calculate 10-year fracture probabilities was 2.6 per SD decline in bone density at the femoral neck. Relative risk per SD decline in femoral neck bone density for spine fracture was assumed to be 1.8, for forearm fracture 1.4, and for global fracture 1.6. Tables 10-6 and 10-7 are 10-year global frac-ture risk predictions for women and men. Tables 10-8 and 10-9 are 10-year site-specific fracture risk predictions for women and men based on T-scores that define WHO diag-nostic categories of osteopenia and osteoporosis. The T-score thresholds of –1 and –2.5 correspond to femoral neck bone densities measured on Hologic DXA of 0.740 g/cm^2 and 0.577 g/cm^2 for both the men and women. The authors suggested that the similar

Table 10-6
Ten-Year Probability (%) of Sustaining Any Type of Osteoporotic Fracture (Hip, Spine, Shoulder, Forearm) in Men by Age and T-score at the Femoral Neck

	T-Score									
Age	*+1*	*+0.5*	*0*	*–0.5*	*–1.0*	*–1.5*	*–2.0*	*–2.5*	*–3.0*	*–4.0*
45	1.5	1.9	2.3	2.8	3.4	4.2	5.1	6.3	7.7	11.4
50	1.8	2.2	2.7	3.4	4.2	5.1	6.3	7.7	9.4	14.0
55	1.9	2.4	3.0	3.7	4.6	5.7	7.0	8.6	10.6	16.0
60	2.5	3.0	3.6	4.4	5.4	6.5	7.9	9.5	11.5	16.7
65	3.0	3.6	4.3	5.1	6.2	7.4	8.8	10.4	12.4	17.4
70	3.4	4.2	5.1	6.1	7.4	9.0	10.9	13.1	15.7	22.4
75	4.1	5.1	6.3	7.8	9.6	11.8	14.4	17.5	21.2	30.4
80	5.3	6.4	7.7	9.2	11.1	13.3	15.8	18.7	22.2	30.3
85	5.3	6.3	7.5	8.8	10.4	12.2	14.3	16.7	19.5	26.1

Adpated from ref. (*15*) with kind permission of Springer Science+Business Media.

Table 10-7
Ten-year Probability (%) of Sustaining Any Osteoporotic Fracture (Hip, Spine, Shoulder, Forearm) in Women by Age and T-Score at the Femoral Neck

					T-Score					
	+1	+0.5	0	–0.5	–1.0	–1.5	–2.0	–2.5	–3.0	–4.0
Age										
45	1.8	2.3	2.8	3.5	4.3	5.4	6.6	8.1	10.0	15.0
50	2.4	3.0	3.8	4.7	5.9	7.4	9.2	11.3	14.1	21.3
55	2.6	3.3	4.1	5.3	6.7	8.5	10.7	13.4	16.8	26.0
60	3.2	4.1	5.1	6.5	8.2	10.4	13.0	16.2	20.2	30.6
65	4.0	5.0	6.3	8.0	10.0	12.6	15.6	19.3	23.9	35.5
70	4.3	5.5	7.1	9.0	11.5	14.6	18.3	22.8	28.4	42.3
75	4.2	5.4	7.0	9.1	11.8	15.2	19.4	24.5	30.8	46.2
80	4.6	6.0	7.7	9.9	12.7	16.2	20.5	25.6	31.8	46.4
85	4.5	5.8	7.4	9.4	12.0	15.3	19.1	23.8	29.4	42.7

Adpated from ref. (*15*) with kind permission of Springer Science+Business Media.

Table 10-8
Ten-Year Probability (%) of Fracture at the Sites Shown by Age and Diagnostic Category in Men. The diagnostic category is based on the T-score at the femoral neck, using the 1995 NHANES III reference data for Non-Hispanic White women

Age	*Forearm Fracture*		*Hip Fracture*		*Spine Fracture*		*Shoulder Fracture*		*Any of These Fractures*	
	< –1	*< –2.5*	*< –1*	*< –2.5*	*< –1*	*< –2.5*	*< –1*	*< –2.5*	*< –1*	*< –.25*
45	1.9	2.7	1.2	3.3	1.6	3.0	0.8	1.1	4.7	7.6
50	1.8	2.5	2.0	5.2	2.2	4.0	0.7	1.0	5.7	9.2
55	1.9	2.8	1.9	5.2	2.6	4.9	0.6	0.9	6.4	10.4
60	2.3	3.2	2.6	6.2	3.0	5.1	1.0	1.3	7.6	11.6
65	2.0	2.7	4.1	8.8	3.5	5.7	1.7	2.3	8.8	13.0
70	1.2	1.7	6.2	13.7	4.8	8.0	2.0	2.7	10.8	16.2
75	1.5	2.1	9.5	21.4	5.6	9.7	1.9	2.6	14.1	21.5
80	1.7	2.3	11.0	21.2	6.0	9.7	2.4	3.1	16.6	23.2
85	1.3	1.6	9.6	16.9	5.2	7.7	2.8	3.5	16.0	21.4

Adpated from ref. (*15*) with kind permission of Springer Science+Business Media.

10-year probabilities of hip and spine fracture at the WHO diagnostic thresholds gave additional credibility to the position that the use of T-scores derived in women are applicable to men. Kanis et al. also pointed out that 10-year risks based on measurement of BMD at sites other than the femoral neck by DXA or by other techniques would be different. They noted that while data on fracture rates and mortality from Sweden were robust, fracture rates were high and mortality was low compared to other parts of the world.

Another approach (*16*) to 10-year fracture risk, which also suggested levels for intervention, was proposed using guidelines originally developed by the National Institutes of Health (NIH) (*17*) for the detection and treatment of high cholesterol in the prevention

Table 10-9

Ten-Year Probability (%) of Fracture at Sites Shown in Women by Age and Diagnostic Category. The diagnostic category is based on the T-score at the femoral neck, using the 1995 NHANES III reference data for Non-Hispanic White women

Age	Forearm Fracture		Hip Fracture		Spine Fracture		Shoulder Fracture		Any of These Fractures	
	< –1	*< –2.5*	*< –1*	*< –2.5*	*< –1*	*< –2.5*	*< –1*	*< –2.5*	*< –1*	*< –2.5*
45	3.6	5.2	0.8	2.2	1.1	2.1	1.2	1.7	6.1	9.9
50	5.1	7.3	1.1	2.9	1.9	3.5	1.6	2.3	8.6	13.9
55	5.8	8.4	2.0	5.1	2.5	4.6	1.7	2.5	10.3	16.8
60	6.7	9.3	3.3	7.8	3.6	6.4	2.8	4.0	13.2	20.5
65	7.5	10.2	5.0	10.9	5.3	9.0	4.0	5.4	16.8	24.9
70	7.9	10.6	8.3	16.7	6.7	10.9	4.8	6.5	20.7	29.8
75	8.0	10.4	11.8	21.5	6.9	10.7	5.3	7.0	23.6	32.6
80	7.6	9.5	14.6	23.8	7.1	10.2	5.7	7.2	26.6	34.4
85	6.1	7.4	14.7	21.9	6.9	9.4	6.4	7.8	26.7	33.1

Adpated from ref. (*15*) with kind permission of Springer Science+Business Media.

of heart disease. The NIH guidelines defined high risk for heart disease as a 10-year risk greater than 20%. Moderate risk was a 10-year risk from 10 to 20% and low risk, a 10-year risk of less than 10%. In an analogous fashion, the 10-year risk for all fractures (global fracture risk) for any given age and BMD that corresponded to 10 and 20% can be calculated and presented in graphic form as shown in Fig. 10-3. Interestingly, at age 65, a 20% 10-year risk for all fractures occurs at a T-score of –2.5, compatible with a World Health Organization diagnosis of osteoporosis. A T-score of –1 at age 65 results in a 10% 10-year fracture risk.
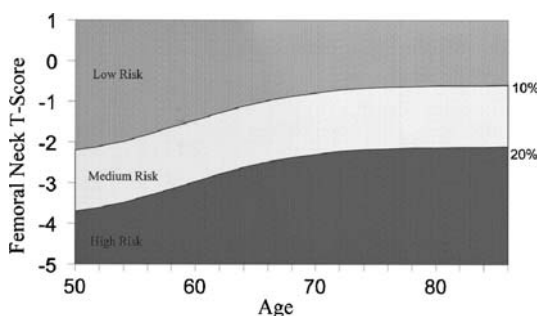

Fig. 10-3. 10-year global fracture risk stratified by risk probabilities of 10% and 20% based on age and femoral neck *T*-score. Reproduced courtesy of Dr. Ken Faulkner.

Remaining Lifetime Fracture Probability

Remaining lifetime fracture probability or RLFP is an approach to global fracture risk prediction that was proposed by Ross and Wasnich et al. (*18*) The concept of RLFP is based on the exponential increase in fracture risk as BMD declines and decreased survival after age 75. Therefore, while a 50-year-old woman and an 80-year-old woman may both have the same low bone density, their remaining lifetime fracture probability

will be quite different. Because the expected life span of the 80-year-old woman is much shorter than that of the 50-year-old, the RLFP for the 80-year-old will be less. RLFP is calculated based on the individual's current age and bone density, life expectancy, and anticipated rate of bone loss. These values are entered into a statistical model that predicts the number of osteoporotic fractures that the individual is expected to experience in her lifetime. For example, if the RLFP is 5, the individual is expected to suffer five osteoporotic fractures in her lifetime if no intervention is undertaken to slow the anticipated rate of bone loss and she lives a normal lifespan. The site(s) of the fractures cannot be specified. RLFP is a global fracture risk prediction. RLFP is one of the most concrete and easily understood modalities for expressing future fracture risk.

The fracture incidence and bone loss rate data on which the RLFP model was originally based were derived from the Kuakini Osteoporosis Study (*19*). The original implementation of RLFP (*20*) was based on measurements of bone mass at the calcaneus. Bone density measurements performed at other sites had to be converted to an equivalent calcaneal measurement. Using nomograms, the physician could find the calcaneal BMC on one scale and the patient's age on a second scale. By connecting the two values, the physician could find the RLFP on a third scale. RLFP predictions have now been recalculated for DXA measurements of the axial and appendicular skeleton and are available on the Internet at www.medsurf.com . After entering the patient's age, menopausal age, skeletal site measured, type of equipment used, and BMD, the RLFP calculation is presented as shown in Fig. 10-4. In this RLFP analysis, the RLFP was
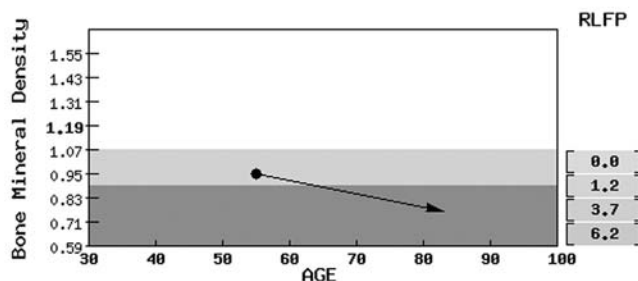

Fig. 10-4. The remaining lifetime fracture probability (RLFP) calculation from www.medsurf.com. At age 55 with a PA lumbar spine BMD of 0.945 g/cm^2 on a Lunar DXA device, the RLFP is 3.82. Reproduced courtesy of Dr. Richard Wasnich, Honolulu, HI.

3.82, indicating that the patient is expected to suffer 3.82 osteoporotic fractures in her lifetime without intervention. The probability of fracture in the next year is predicted to be only 1.5% but her 10-year fracture probability is 10.2%. It is also possible to calculate the effects on the RLFP of an intervention that reduces fracture risk or bone loss by a specified amount. In this case, an intervention that halts bone loss would reduce the RLFP to 0.76. Alternatively, an intervention that permanently reduces fracture risk by 50% is expected to reduce the RLFP to only 0.33. As noted above, the sites of the future fractures are not specified. RLFP is a global fracture risk prediction.

RLFP is based on a statistical model. When the RLFP model is applied to the United States population, the estimates of vertebral and non-vertebral fracture incidence are comparable to actual observations of fracture incidence (*21*). This observation provides external validation of the theory and application of RLFP.

The Fracture Threshold

Many experts in the field object strenuously to the concept of a fracture threshold, noting that it is more appropriate to emphasize the existence of a gradient of increasing risk for fracture as bone density declines. They correctly observe that there is no arbitrary level of bone density *above which no one fractures and below which everyone fractures*. Nevertheless, the concept of a fracture threshold can be useful in the clinical setting. It suggests a "cutoff" level of bone density above which it is desirable to stay in order to keep fracture risk at a minimum. Such a level of bone density could also be construed as an appropriate intervention threshold. It also emphasizes that bone density need not be returned to "normal" levels to reduce the risk of fracture.

In 1982, Riggs et al. (*22*) proposed a fracture threshold for BMD in the spine and proximal femur based on studies of 205 subjects (123 women, 82 men). Of these 205 subjects, 31 subjects (26 women, 5 men) had hip fractures and 84 women had vertebral fractures. BMD was measured with the older technique of DPA in the PA lumbar spine and proximal femur. The fracture threshold was defined as the 90th percentile for BMD in the proximal femur for subjects with hip fracture and in the spine for women with spine fracture. For women, the fracture threshold was 0.95 g/cm^2 at the femoral neck, 0.92 g/cm^2 at the intertrochanteric region, and 0.97 g/cm^2 at the lumbar spine.

Ross et al. (*23*) proposed that the fracture threshold be defined as the bone mineral content or density at which the risk of fracture doubled in comparison to premenopausal women. This recommendation was based on a prospective study of 1098 women who participated in the Kuakini Osteoporosis Study beginning in 1981. These women underwent BMC and BMD measurements at the proximal and distal radius and os calcis yearly with SPA and, beginning in 1984, lumbar spine BMD measurements with DPA. Four hundred eight women had spine films at baseline and provided the data used to calculate spine fracture incidence during four years of follow-up. Spine fracture prevalence was calculated based on data from subjects who had fractures prior to the first bone density measurement. The authors looked at a variety of ways to define the fracture threshold and the BMC or BMD levels at the various sites that resulted. These considerations are shown in Table10-10. They observed that the levels of BMC and BMD that corresponded to the 10th percentile of young-normals, the 80th percentile of prevalent spine fracture cases, or an absolute risk of fracture of 5% per decade also coincided with the level of BMC and BMD that resulted in a doubling of fracture risk in comparison

Table 10-10
A Comparison of Different Definitions for the Fracture Threshold

Definition	Proximal Radius (g/cm)	Distal Radius (g/cm)	Calcaneus (g/cm^2)	Lumbar Spine (g/cm^2)
Based on Young Normals				
10th Percentile	0.78	0.76	0.33	0.97
2 SD Below Mean	0.71	0.66	0.28	0.90
Based on Postmenopausal Women				
10th Percentile	0.59	0.52	0.22	0.74
2 SD Below Mean	0.49	0.42	0.17	0.60
Based on Prevalent Fracture Cases				
80th Percentile	0.78	0.75	0.33	0.94
Based on Incident Fracture Cases				
95th Percentile	0.78	0.67	0.31	0.94
Based on Increased Fracture Risk				
Absolute Risk of 5% per Decade	0.78	0.74	0.32	0.97
Doubling of Risk Relative to Age 45	0.77	0.78	0.32	0.94
Reference Values (mean and SD)				
Young Normals[a]	0.88 ± 0.08	0.89 ± 0.11	0.41 ± 0.07	1.13 ± 0.12
Postmenopausal Women[b]	0.73 ± 0.11	0.70 ± 0.13	0.31 ± 0.08	0.92 ± 0.15

[a] Premenopausal women, ages 30–45. Mean age 38 years, n = 128.
[b] Postmenopausal women, mean age 64. N = 1083.
Reprinted with permission from Elsevier from ref. (*23*).

to premenopausal women. They concluded that this level of bone density was the most appropriate definition of the fracture threshold.

Vega et al. (*24*) calculated a fracture threshold for femoral neck and trochanteric hip fractures based on cross-Sectional data from 75 women with atraumatic fractures of the proximal femur and 51 age-matched, non-fractured controls. The average age of the women was 70.1 years. In the hip fracture group, there were 36 femoral neck fractures and 39 trochanteric fractures. BMD was measured at the lumbar spine and proximal femur with DPA and at the mid-radius with SPA. The average BMD and SD in the femoral neck of the femoral neck fracture patients were 0.624 and 0.055 g/cm^2, respectively. For the trochanteric fracture patients, these values in the femoral neck were 0.548 and 0.066 g/cm^2. The authors defined the fracture threshold as the mean BMD plus 2 SD at the femoral neck as calculated from the BMD measurements in the fracture group. For fractures of the femoral neck, this value was 0.73 g/cm^2. For trochanteric fractures, this value was 0.68 g/cm^2. Using a spine fracture threshold of 0.97 g/cm^2 from Riggs et al. (*22*), the authors observed that 94% of the patients with trochanteric fracture and 74% of the patients with femoral neck fracture had spine BMD values that were also below the spine fracture threshold.

The fracture threshold concept can also be utilized to assess the benefit of any particular therapy. For example, a 57-year-old woman may have a bone density that is currently above the fracture threshold at a particular site. It is anticipated, however, that her bone

density will fall below the fracture threshold in the future at a point in time that will be determined by the rate of bone loss. Using statistical models, it can be anticipated that if the patient loses bone mineral density at a rate of 1% per year, she will fall below the fracture threshold by age 64. If the rate of bone loss is reduced to 0.5%, she will not reach the fracture threshold until age 72 gaining 8 years of relative protection from fracture.

Qualitative Risk Assessments

Qualitative fracture risk assessments are descriptions of risk as being "low," "moderate," or "high," or as "not increased," "increased," or "markedly increased." At its most basic, a qualitative assessment of fracture risk may be a statement of "not at risk" versus "at risk." This is an assessment of current fracture risk. In 2002, the Canadian Panel of the International Society for Clinical Densitometry recommended that bone density reports contain a qualitative assessment of fracture risk (*25*). Thresholds for moderate and high fracture risk or increased and markedly increased fracture risk are the same as the WHO diagnostic categories of osteopenia and osteoporosis. These types of qualitative assessments of risk are commonly seen on computer-generated printouts of bone density data. Caution must be used, however, as such assessments are inappropriate in individuals under age 50. In deciding whether a quantitative or qualitative assessment of risk is necessary or sufficient, the physician must decide what difference the type of assessment may make in the management of the patient. Will treatment be considered if the risk is reported as increased, without knowing the magnitude of the increase? This may or may not be an appropriate outcome. More sophisticated fracture risk prediction methodologies are quantitative rather than qualitative, providing more precise clinical guidance. There seems to be little reason to use qualitative risk prediction today when approaches like RLFP and the FORE 10-year FRC or the World Health Organization 10-year fracture risk prediction algorithm called FRAX^TM, which are discussed in detail later in this chapter, are readily available.

PREDICTING FRACTURE RISK IN MEN

The number of studies reporting fracture risk in men based on the decline in bone density has increased in recent years. As in so many of the studies on women, the increase in fracture risk is generally reported as the relative risk for fracture per SD decline in bone density. Other studies have reported absolute risk. The findings from these studies have led to two seemingly contradictory conclusions: women have a greater increase in relative risk for fracture per SD decline in BMD than do men but the absolute risk for fracture at any given level of BMD is the same in women and men (*26*). In Table 10-11, the age-adjusted relative risk values for fracture in men and women age 35 years and older from a population-based case-control study in Rochester, MN, are shown (*27*). The relative risks differ depending on the reference population used. Note that the relative risk for any type of fracture in men was 1.1 per SD decline in femoral neck BMD when the reference population was 20–29-year-old men. The same relative risk value in women was 2.4 when the reference population was 20–29- year-old women. An important difference in the calculation of these relative risk values was that the SD in men of 0.109 g/cm^2 was much smaller than the 0.119 g/cm^2 SD seen in women. In other studies in which the relative risks per SD decline in bone density have been similar, the

Table 10-11
Age-Adjusted Odds Ratios (and 95% Confidence Intervals) for Osteoporotic Fracture Per 1 SD Decrease in BMD by Skeletal Site Measured for Rochester, Minnesota Men and Women Depending on the Criterion Used for Establishing Normal Means and Standard Deviations

Study Group and Criterion	Total Hip	Femoral Neck	Skeletal Site Trochanter	AP Spine	Total Wrist
20–29 year *male* criteria					
Women	2.20 (1.50, 3.22)	2.25 (1.44, 3.51)	2.06 (1.38, 3.08)	1.67 (1.18, 2.36)	1.77 (1.27, 2.47)
Men	1.29 (0.97, 1.72)	1.10 (0.82, 1.48)	1.34 (1.00, 1.78)	1.15 (0.89, 1.48)	1.51 (1.12, 2.03)
20–49 year *male* criteria					
Women	2.66 (1.66, 4.29)	2.70 (1.56, 4.65)	2.48 (1.50, 4.10)	1.79 (1.21, 2.66)	1.67 (1.24, 2.26)
Men	1.38 (0.97, 1.97)	1.12 (0.78, 1.62)	1.44 (1.01, 2.07)	1.17 (0.88, 1.56)	1.45 (1.11, 1.90)
20–29 year *female* criteria					
Women	2.40 (1.57, 3.68)	2.43 (1.49, 3.95)	2.21 (1.42, 3.42)	1.66 (1.18, 2.33)	1.56 (1.20, 2.03)
Men	1.33 (0.97, 1.83)	1.11 (0.80, 1.54)	1.38 (1.01, 1.88)	1.14 (0.89, 1.47)	1.38 (1.09, 1.74)
Premenopausal *female* criteria					
Women	2.37 (1.56, 3.61)	1.28 (1.50, 4.08)	2.19 (1.42, 3.38)	1.61 (1.17, 2.23)	1.54 (1.20, 1.99)
Men	1.33 (0.97, 1.82)	1.11 (0.80, 1.55)	1.37 (1.00, 1.87)	1.14 (0.90, 1.44)	1.37 (1.09, 1.72)

Adapted from ref. (27) with permission of the American Society for Bone and Mineral Research.

magnitude of the SD in men and women was also similar. This suggests that the SD itself has a significant effect on the apparent sex-specific relative risk for fracture. This would be true even if the absolute risk for fracture at any given BMD was the same. Data from the Hawaii Osteoporosis Study do, in fact, suggest that the absolute risk for spine fracture is the same in men and women for any given level of calcaneal BMD (*28*).In an analysis of data (*29*) from the EPOS[4] study, the use of a common SD of 0.1 g/cm^2 resulted in a relative risk for spine fracture when bone density was measured at the PA lumbar spine of 1.4 in men and 1.5 in women. When bone density was measured at the femoral neck and the same SD of 0.1 g/cm^2 was used, the relative risk for spine fracture was 1.5 in men and 1.8 in women. In the Rotterdam study, as reported by De Laet et al. (*30*), hip fracture incidence was only slightly higher in women than in men for any given level of femoral neck BMD. De Laet et al. (*31*) concluded that hip fracture risk was the same in men and women at the same bone density. The authors noted that at the same level of low BMD, men were likely to be older than women. This meant that fewer men reach the same low levels of BMD than women. Second, the average BMD of men who experienced hip fractures was higher than that of women who experienced hip fractures. De Laet et al. (*31*) thus suggested that sex-specific SDs were appropriate when the primary goal was to identify a similar proportion of men who would fracture compared to women. If, however, the ultimate goal of using BMD in the prediction of fracture risk was the identification of individuals who would most benefit from intervention, *the same absolute BMD threshold that signals unacceptable risk would be appropriate in both men and women*. Note that in the 10-year fracture risk tables for *men* from Kanis et al. (*15*) in Fig. 10-7, the T-scores were derived using NHANES III femoral neck BMD data for *women*. In 2000, the Scientific Advisory Board of the International Osteoporosis Foundation (*32*) recommended that the diagnosis of osteoporosis in men be based on a *female* T-score of –2.5 at the hip. In 2002, however, the International Society for Clinical Densitometry (*33*) recommended the continued use of sex-specific SDs (T-scores) for men for diagnosis. This remains the current recommendation (*34*). From the standpoint of *predicting risk*, however, an approach that advocates the same BMD thresholds for varying levels of risk seems more appropriate for clinical decisions that may result in pharmacologic intervention. This is the approach that has been taken by the World Health Organization in the development and implementation of FRAX^{TM}.

FRAX^{TM}

FRAX^{TM} is a10-year absolute fracture risk prediction algorithm developed by the World Health Organization. It became available via Internet in 2008 at http://www.shef.ac.uk/FRAX /. FRAX^{TM} is the result of an extraordinary effort to use easily obtainable clinical risk factors with or without femoral neck BMD to predict the absolute 10-year probability of hip fracture or major osteoporotic fracture (spine, hip, humerus, wrist). While not perfect, FRAX^{TM} has rapidly become the standard for the prediction of fracture risk.

---

[4] EPOS is the European Prospective Osteoporosis Study and is a continuation of the European Vertebral Osteoporosis Study (EVOS). EVOS is a study of the prevalence of fracture in men and women conducted at 36 centers in 19 countries in Europe.

FRAX™ is relatively simple to use, assuming that the densitometrist has Internet access. When the mouse cursor is placed over the heading "Calculation Tool" a drop-down menu appears that allows the densitometrist to choose from nine different countries. In the case of the United States, four choices are available: US Caucasian, US Black, US Hispanic, and US Asian. Clicking with the left mouse button results in the appearance of the chosen FRAX™ algorithm. Figure 10-5 illustrates the FRAX™ screen that appears when US Caucasian is chosen.

Fig. 10-5. FRAX™, the World Health Organization 10-year absolute fracture risk prediction algorithm, available at http://www.shef.ac.uk/FRAX/. US Caucasian has been selected from a drop-down menu. Patient data has been entered including the femoral neck T-score. The 10-year probability of hip fracture and major osteoporotic fracture are calculated. Reproduced with the kind permission of the World Health Organization Collaborating Centre for Metabolic Bone Diseases, University of Sheffield, UK.

It is not necessary to enter the patient's name or ID in order to use the FRAX™ algorithm. There are 11 entries that are required for the calculation with the 12th, the femoral neck T- or z-score, being optional. The first item is the patient's age or birth date. Either one may be entered. Both are not necessary. Item 2 asks the user to click on the appropriate radio button for gender. Items 3 and 4 refer to weight and height. It is important to note that weight and height must be entered in kilograms (kg) and centimeters (cm). To the left of the screen are conversion calculators for original measurements made in pounds and inches. Once the conversion is complete, the data in kg and cm should be entered in Sections 3 and 4. Items 5-11 are questions about specific clinical risk factors. By default, the radio button for "no" is already selected. If necessary, change the appropriate radio button to "yes" simply by clicking on it. This will automatically remove the default selection of "no." Finally, if the femoral neck T- or z-score is available, that should be entered as well in Section 12, after selecting either T-score or z-score as appropriate. If the patient is a woman, the total hip T- or z-score could be entered instead. This is not appropriate for men.

Once the data is entered, use the left mouse button to click on "calculate." The algorithm then calculates the 10-year probability of hip fracture and the 10-year probability of a major osteoporotic fracture (clinical or symptomatic spine fracture, forearm fracture, proximal humerus fracture, and hip fracture). The small printer icon may be clicked to print the completed FRAX[TM] calculation.

The clinical risk factors that were included in the FRAX[TM] model were chosen after extensive reviews and meta-analyses of the medical literature in order to establish the magnitude of the relationship between the risk factor and fracture risk (*35–41*). Ultimately, the data used to create FRAX[TM] came from nine different study cohorts[5] around the world. The data was subsequently validated in 11 other cohorts in similar geographic locations (*42*). Two additional principles were applied to the choice of the risk factors for inclusion in the final FRAX[TM] algorithm. The first principle was that the risk imparted by the risk factor would be favorably modified by a therapeutic intervention (*43*). This data was available for BMD, age, gender, prior vertebral fracture, and glucocorticoids. In the absence of data showing that the risk was favorably modified by a therapeutic intervention, the second principle was that the risk factor must not be known to adversely affect the fracture risk reduction efficacy of an intervention. The specific risk factors that were ultimately chosen came to be known as the WHO 8: age, BMI, prior fracture, parental hip fracture, current smoking, glucocorticoid use, rheumatoid arthritis, and excessive alcohol consumption.

FRAX[TM] is not intended to calculate 10-year fracture risk probabilities in patients who are already being treated. In untreated patients, fracture probabilities can be calculated with FRAX[TM] with or without BMD. Inputting a T- or z-score, however, is clearly preferred to maximally refine the fracture risk prediction. The algorithm will accept an age value of 50–90. The BMI is automatically calculated from the data entered for height and weight. The risk factors have been simplified to dichotomized variables, requiring a "yes" or "no" response. The risk factor of "prior fracture" refers to fracture occurring as an adult in whom the fracture appears to have occurred spontaneously or as a result of a level of trauma, which would not result in fracture in a healthy individual. The subjectivity of this assessment is unavoidable. This risk factor captures prior morphometric spine, clinical spine, non-spine, and hip fractures. It is recognized that a "yes" response cannot convey the number, location or type of the pre-existing fracture (*43*). If multiple fractures have occurred, the algorithm may underestimate the 10-year fracture probability. When the risk factors are simplified to dichotomous variables, the inability to convey the effects of a "dose-response" are inevitable. This issue is also relevant to the ascertainment of smoking, use of glucocorticoids, and alcohol consumption. Rheumatoid arthritis is considered separately from other causes of secondary osteoporosis. This is because rheumatoid arthritis was found to impart a fracture risk that was independent of the BMD (*37*). Therefore, if "yes" is selected for rheumatoid arthritis, this will contribute to the calculation of the 10-year fracture probability regardless of whether a femoral neck T- or z-score is entered. The selection of "yes" or "no" for other secondary causes of osteoporosis has no effect in this circumstance on the fracture probability cal-

---

[5] The Rotterdam Study, the European Vertebral Osteoporosis Study (EVOS), the Canadian Multicentre Osteoporosis Study (CaMOS), Rochester, Sheffield, Dubbo, Hiroshima, and Gothenburg (two cohorts).

culation. If a BMD T- or z-score is not entered and "no" is selected for rheumatoid arthritis and "yes" is selected for other secondary causes of osteoporosis, the 10-year fracture probability calculation is affected by the selection of "yes" for other secondary causes of osteoporosis. If a BMD T- or z-score is entered, there is no effect of the "yes" response to other secondary causes of osteoporosis on the 10-year fracture probability. The stated rationale for the variable contribution of a "yes" response to other secondary causes of osteoporosis, depending upon the response to rheumatoid arthritis or the knowledge of the BMD was that the risk imparted by other secondary causes of osteoporosis was mediated through the BMD (*43*). Thus, when the BMD T- or z-score was inputted, the contribution to fracture risk was captured in the BMD.

FRAX^TM is primarily designed to utilize the femoral neck T- or z-score obtained with DXA. However, in women, the total hip T- or z-score could be substituted. This is not appropriate for men. Similarly, FRAX^TM is not intended to be used with T- or z-scores obtained at other skeletal sites or with other technologies. Although it is clearly stated that the T- or z-score for the femoral neck should be inputted in FRAX^TM, it is not overwhelmingly clear that what is required is the T- or z-score for non-Hispanic white women from the *1998 NHANES III database, regardless of the actual gender, race, or ethnicity of the patient*. This obviously creates a clinical dilemma is using FRAX^TM. DXA devices provide a gender-specific T-score. Most provide a T-score that is both gender and race/ethnicity specific. All DXA devices provide a z-score that is gender and race/ethnicity specific. If the patient is not a non-Hispanic white female, the T- or z-score will not be appropriate for use with FRAX^TM. Beyond this, however, none of the DXA devices in the United States utilize the 1998 NHANES III reference database (*44*). Instead, they utilize the 1995 NHANES III database (*45*). This means that even if the patient is a non-Hispanic white female, the T- and z-score are not appropriate for use with FRAX^TM.

To address this issue, a FRAX^TM Patch was created by Michael McClung, MD and Ned McKay-Mossman, MPH. This patch is available for free download from the Oregon Osteoporosis Center at http://www.orost.com or from the National Osteoporosis Foundation at http://www.nof.org. The download is a software program that will calculate the appropriate T-score at the femoral neck to be used with FRAX^TM. The FRAX^TM Patch is shown in Fig. 10-6. The only data which must be inputted are the machine type (that is, Hologic, GE Lunar, or Norland) and the actual femoral neck BMD in g/cm^2. The Patch does not calculate a z-score and therefore the use of the T-score as calculated by the FRAX^TM patch is the recommended value for use with FRAX^TM. The FRAX^TM patch uses the conversion equations[6] from Lu et al. (*46*) to convert non-Hologic femoral neck BMD values in g/cm^2 to Hologic equivalent values. The femoral neck T-score is then calculated using the mean BMD and SD for non-Hispanic white women aged 20–29 from the 1998 NHANES III database.

The 10-year fracture probabilities calculated from FRAX^TM have been incorporated into the 2008 National Osteoporosis Foundation guidelines for treatment (*47*). After refining the WHO FRAX^TM algorithm for data specific to the United States and the performance of extensive cost-effectiveness analyses (*48*, *49*), the NOF recommended

---

[6] See Chapter 6 for a discussion of conversion equations for BMD from one manufacturers' device to another.
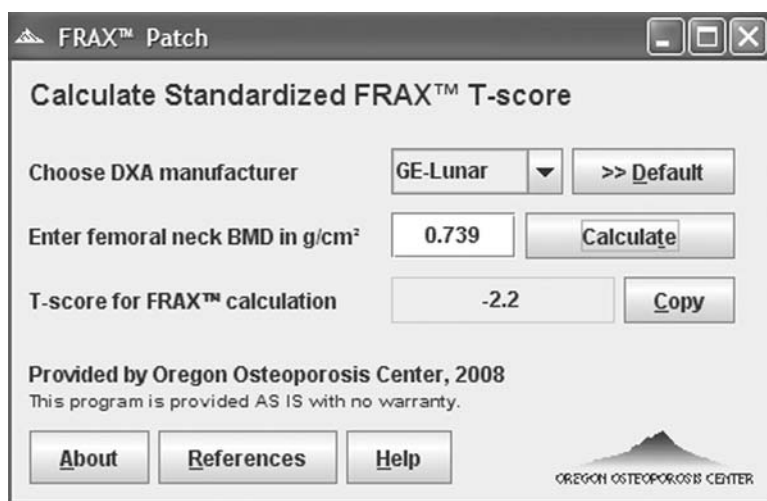
Fig. 10-6. The FRAX[TM] Patch. This utility converts the manufacturer-derived femoral neck BMD to the 1998 NHANES III Caucasian female T-score. The patch can be downloaded from the Oregon Osteoporosis Center web site at http://www.orost.com. Courtesy of Dr. Michael McClung.

that pharmacologic treatment be considered in an individual with an osteopenic bone density and a FRAX[TM] 10-year probability of hip fracture of ≥3% or a FRAX[TM] 10-year probability of major osteoporotic fracture of ≥20% (*47*).

FORE FRC

A second web-based 10-year absolute fracture risk prediction algorithm, called the FORE FRC (Foundation for Osteoporosis Education and Research Fracture Risk Calculator) is available from FORE at http://www.fore.org. In 2003, Ettinger et al. (*50*) developed a computer model for calculating the 5-year clinical spine, hip, and major osteoporotic fracture risk. This algorithm has been modified and expanded to become the FORE FRC and is, by intention, very similar to FRAX[TM]. However, the acceptable age range in the FORE FRC is slightly different at 45–85 years and the algorithm will accept weight and height entered in pounds and inches. It also requires that the T-score for the total hip be utilized instead of the femoral neck. The algorithm may be used in white, Asian, Black, or Hispanic men and women to predict the 10-year probability of a major osteoporotic fracture (spine, hip, humerus, and wrist) or hip fracture. This algorithm also provides a graphic representation of the results, which compares the patient's 10-year major osteoporotic fracture risk to the 10-year risk expected for the patient's age, which can be useful in explaining the results to the patient. A change in the background color of the graph at a 10-year risk of 20% indicates a qualitative assessment of high risk and also coincides with the 10-year major osteoporotic fracture probability cutpoint invoked by the National Osteoporosis Foundation (*47*) as justifying treatment in the presence of coexisting osteopenia. Like FRAX[TM], this algorithm is intended to calculate the 10-year fracture risks in *un*treated patients. Figure 10-7 shows the web-based FORE FRC and Fig. 10-8 the completed FORE FRC printout.

Fig. 10-7. The FORE FRC. This utility is similar but not identical to FRAX™. It is available at http://www.fore.org . Reproduced courtesy of the Foundation for Osteoporosis Research and Education.
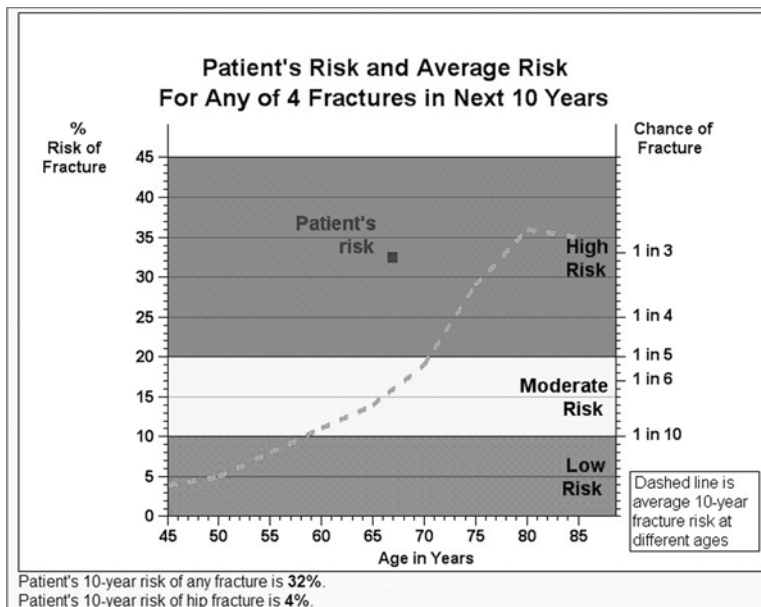

Fig. 10-8. The FORE FRC printout. Reproduced courtesy of the Foundation for Osteoporosis Research and Education.

THE BLACK FRACTURE INDEX

Another useful fracture risk assessment algorithm is the Black Fracture Index (*51*). This index is also discussed in detail in Chapter 8. The Black Fracture Index was based on the findings from the Study of Osteoporotic Fractures (SOF) in which 9704 women age 65 and older participated. In the development of the fracture index, data from 7782

women with DXA measurements of proximal femur bone density and complete fracture data were used. Reports of fracture were confirmed by review of X-ray films. Non-vertebral fractures resulting from major trauma were excluded from consideration. Risk factors were ascertained through direct questioning and responses to questionnaires. Women with a hip fracture prior to the measurement of bone density were excluded from the analysis. Hip and non-spine fractures were captured for 5 years after DXA proximal femur measurements were done and spine fractures for an average of 3.7 years.

In the final model, the included risk factors were age, fracture after age 50, maternal hip fracture after age 50, weight ≤125 lbs (57 kg), current smoking, and use of arms to stand from a chair (*51*). This is the only validated fracture risk prediction model that has retained ascertaining the use of arms to stand from a chair. This is not included in FRAX[TM] or the FORE FRC. The principles for the inclusion of specific risk factors in FRAX[TM] preclude considerations of the risk for falling because pharmacologic intervention will not reduce the risk of falling and there is some data to suggest that individuals at increased risk of falling may not have the same response to pharmacologic therapy (*52*) as an individual who is not at increased risk of falling. There is no question, however, that the inability to rise from a chair without the use of the arms is a significant risk factor for falling and therefore, for hip fracture (*53*). Such a finding may indicate upper leg musculoskeletal weakness or impairment of balance which may be amenable to other interventions. Nevertheless, such a patient does have an increase in the risk for hip fracture imparted by the inability to rise from a chair without using the arms. The Black Fracture Index is also the only risk calculator in current use that assesses fracture risk over a 5-year period instead of a 10-year period.

The fracture index is based on the responses to six questions (*51*). Depending upon the response, a score is awarded for each question, which is then totaled. The fracture index can be utilized with or without knowledge of the patient's total hip T-score. In the absence of knowledge of the total hip T-score, the index is intended to prompt the physician to evaluate the patient further and obtain a BMD if the fracture index score is sufficiently high. With the BMD, the fracture index score may be used to prompt consideration of pharmacologic intervention. The fracture index questions and scoring system are shown in Table 10-12. As can be seen from Table 10-12, the maximum or worst possible score when the total hip T-score is known is 15. The authors noted that at a fracture index score cutpoint of 6 out of 15, the model had a sensitivity of 78.6%, specificity of 61.7%, and a positive predictive value of 5.8% for hip fracture (*51*).

The Black Fracture Index was subsequently validated in 6679 women from the EPIDOS[7] study population. These women were an average age of 80.5 years, making them older than the average age of the woman in SOF. The resulting Black Fracture Index cut points for risk categories differed slightly in the EPIDOS cohort, but the overall relationship remained the same, with increasing scores indicating an increased risk of hip fracture.

---

[7]EPIDOS is a multicenter prospective study of 7575 women living at home aged 75–95 years, in France.

Table 10-12
Black Fracture Index Questions and Scoring

Risk Factor	Point Value
1. What is your current age?	
Less than 65	0
65–69	1
70–74	2
75–79	3
80–84	4
85 or older	5
2. Have you broken any bones after age 50?	
Yes	1
No/Don't know	0
3. Has your mother had a hip fracture after age 50?	
Yes	1
No/Don't know	0
4. Do you weight 125 pounds or less?	
Yes	1
No/Don't know	0
5. Are you currently a smoker?	
Yes	1
No	0
6. Do you usually need to use your arms to assist yourself in standing up from a chair?	
Yes	2
No/Don't know	0
7. BMD results: Total Hip T-score	
T-score $\geq$–1	0
T-score between –1 and –2	2
T-score between –2 and –2.5	3
T-score $\leq$ –2.5	4

Adapted from ref. (*51*) with kind permission of Springer Science+Business Media.
Note that the maximum or worst possible score is 15.

The Black Fracture Index is available as a computer program on a compact disc (CD) that was previously distributed by Procter & Gamble. With the permission of Procter & Gamble, this program is also available on the CD that accompanies this book. In the computer version of the Index, the age range into which the patient fits is selected from a drop-down menu. Five questions are then answered by clicking on "yes" or "no" and finally, the appropriate range in which the patient's total hip T-score lies is selected from a drop-down menu. The program will then calculate the Black Fracture Index score and also provide a graphic display of the 5-year fracture risks for women in SOF with the same Black Fracture Index score, as shown in Fig. 10-9. A score of 6 or higher indicates that additional evaluation and pharmacologic intervention may be warranted. It should be remembered that the women in SOF were a minimum of 65 years of age and were overwhelmingly Caucasian. The most appropriate patient then, in which to utilize the Black Fracture Index, is a Caucasian woman age 65 and older.
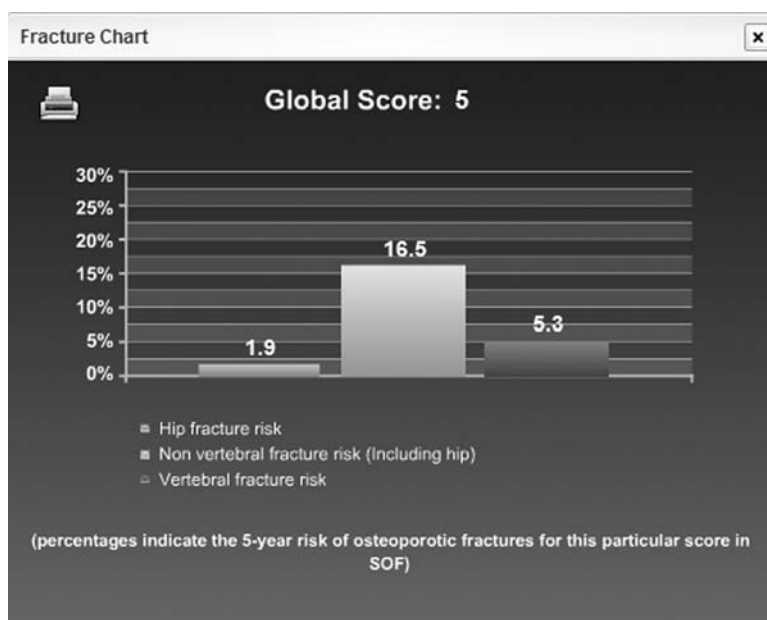
Fig. 10-9. The Black Fracture Index. This utility calculates a risk score and the 5-year absolute risks for women in SOF with the same score. The software is available on the CD that accompanies this book. Reproduced courtesy of Procter & Gamble, Inc.

LIMITATIONS OF FRACTURE RISK ALGORITHMS

None of the three absolute fracture risk prediction algorithms utilize spine BMD in the calculation of risk. FRAX[TM], FORE FRC, and the Black Fracture Risk Index all utilize a proximal femur region of interest in the calculations of risk. To paraphrase Ettinger (*54*) when the spine BMD is markedly lower than the femoral neck or total hip BMD, the densitometrist must take this into account in assessing fracture risk. Similarly, the reduction of risk factors to dichotomous variables (that is, "yes" or "no" responses) loses any dose-response effect on fracture risk. The densitometrist must recognize when the patient has multiple comorbidities within a given category of risk factor which could result in the patient's fracture risk being higher than that predicted by the algorithm. There may also be risk factors for fracture that are not utilized by one or the other of these algorithms for a variety of reasons. That certainly does not mean that the densitometrist should not consider them in the evaluation of the patient. Finally, FRAX[TM] and FORE FRC require Internet access. This seems to be an impediment to current use. FORE sent notices to 241 providers, inviting them to use the FORE FRC, but only 5% ever did (*54*). It seems likely that the response to FRAX[TM] would not be substantially different. In addition, the need to utilize the FRAX[TM] Patch prior to accessing FRAX[TM] creates one more, albeit small, barrier to use. Future developments may see the FRAX[TM] Patch incorporated into FRAX[TM] itself. FRAX[TM] and/or the FRC may become available through means other than the Internet. But even with these current limitations and caveats, there is no question that the prediction of absolute fracture risk

with algorithms like FRAX^{TM}, FORE FRC, and the Black Fracture Index represents a dramatic advance in the prediction of fracture risk. The use of relative risk in clinical densitometry reports is no longer appropriate.

REFERENCES

1. Mazess RB. Bone densitometry for clinical diagnosis and monitoring. In: DeLuca HF, Mazess R, eds. Osteoporosis: physiologic basis, assessment and treatment. New York: Elsevier Science Publishing Company, 1990:63–85.
2. Hui SL, Slemenda CW, Johnston CC. Baseline measurement of bone mass predicts fracture in white women. Ann Intern Med 1989;111:355–361.
3. Gardsell P, Johnell O, Nilsson BE. The predictive value of bone loss for fragility fractures in women: a longitudinal study over 15 years. Calcif Tissue Int 1991;49:90–94.
4. Melton LJ, Atkinson EJ, O'Fallon WM, Wahner HW, Riggs BL. Long-term fracture prediction by bone mineral assessed at different skeletal sites. J Bone Miner Res 1993;8:1227–1233.
5. Black DM, Cummings SR, Genant HK, Nevitt MC, Palermo L, Browner W. Axial and appendicular bone density predict fractures in older women. J Bone Miner Res 1992;7:633–638.
6. Wasnich RD, Ross PD, Heilbrun LK, Vogel JM. Prediction of postmenopausal fracture risk with use of bone mineral measurements. Am J Obstet Gynecol 1985;153;745–751.
7. Huang C, Ross PD, Yates AJ, Wasnich RD. Prediction of vertebral fractures by radiographic absorptiometry. Abstract. J Bone Miner Res 1997;12:S496.
8. Huang C, Ross PD, Davis JW, Imose K, Emi K, Wasnich RD. Prediction of single and multiple vertebral fractures by metacarpal BMD using Poisson regression. Abstract. J Bone Miner Res 1997;12:S496.
9. Cummings SR, Black DM, Nevitt MC, et al. Bone density at various sites for prediction of hip fracture. Lancet 1993;341:72–75.
10. Mussolino ME, Looker AC, Madans JH, et al. Phalangeal bone density and hip fracture risk. Arch Intern Med 1997;157:433–438.
11. Black DM, Cummings SR, Melton JL. Appendicular bone mineral and a woman's lifetime risk of hip fracture. J Bone Miner Res 1992;7:639–645.
12. Suman VJ, Atkinson EJ, O'Fallon WM, Black DM, Melton LJ. A nomogram for predicting lifetime hip fracture risk from radius bone mineral density and age. Bone 1993;14:843–846.
13. Cummings SR, Bates D, Black DM. Clinical use of bone densitometry. JAMA 2002;288:1889–1897.
14. Looker AC, Wahner HW, Dunn WL, et al. Proximal femur bone mineral levels of US adults. Osteoporos Int 1995;5:389–409.
15. Kanis JA, Johnell O, Oden A, Dawson A, De Laet C, Jonsson B. Ten year probabilities of osteoporotic fractures according to BMD and diagnostic thresholds. Osteoporos Int 2001;12:989–995.
16. Personal communication. KG Faulkner, PhD, Chief Scientist, GE Medical Systems Lunar.
17. Detection, evaluation, and treatment of high blood cholesterol in adults – third report of the National Cholesterol Education program (NCEP) expert panel. Washington, D.C.: US Department of Public Health, May, 2001. (NIH publication no. 01–3670).
18. Ross PD, Wasnich RD, MacLean CJ, Vogel JM. Prediction of individual lifetime fracture expectancy using bone mineral measurements. In: Christiansen C, Johansen JS, Riss BJ, eds. Osteoporosis 1987. Copenhagen, Denmark: Osteopress ApS, 1987:288–293.
19. Yano K, Wasnich RD, Vogel MJ, Heilbrun LK. Bone mineral measurement among middle-aged and elderly Japanese residents in Hawaii. Am J Epidemiol 1984;119:751–764.
20. Wasnich RD, Ross PD, Vogel JM, Davis JW. Osteoporosis: critique and practicum. Honolulu: Banyan Press, 1989.
21. Wasnich RD. Vertebral fracture epidemiology. Bone 1996;18:179S–183S.
22. Riggs BL, Wahner HW, Seeman E, et al. Changes in bone mineral density of the proximal femur and spine with aging. J Clin Invest 1982;70:716–723.

23. Ross PD, Wasnich RD, Heilbrun LK, Vogel JM. Definition of a spine fracture threshold based upon prospective fracture risk. Bone 1987;8:271–278.

24. Vega E, Mautalen C, Gomez H, Garrido A, Melo L, Sahores AO. Bone mineral density in patients with cervical and trochanteric fractures of the proximal femur. Osteoporos Int 1991;1:81–86.

25. Khan AA, Brown J, Faulkner K, et al. Standards and guidelines for performing central dual x-ray densitometry from the Canadian Panel of International Society for Clinical Densitometry. J Clin Densitom 2002;5:247–257.

26. Melton LJ, Orwoll ES, Wasnich RD. Does bone density predict fractures comparably im men and women? Osteoporos Int 2001;12:707–709.

27. Melton LJ, Atkinson EJ, O'Connor MK, O'Fallon WM, Riggs BL. Bone density and fracture risk in men. J Bone Miner Res 1998;13:1915–1923.

28. Ross PD, Lombardi A, Freedholm D. The assessment of bone mass in men. In: Orwoll ES, ed. Osteoporosis in men. San Diego: Academic Press, 1999:505–525.

29. The European Osteoporosis Study (EPOS) Group. The relationship between bone density and incident vertebral fracture in men nd women. J Bone Miner Res 2002;17:2214–2221.

30. De Laet CEDH, van Hout BA, Burger H, Weel AEAM, Hofman A, Pols HAP. Hip fracture prediction in elderly men and women: validation in the Rotterdam study. J Bone Miner Res 1998;13: 1587–1593.

31. De Laet CEDH, Van Der Klift M, Hofman A, Pols HAP. Osteoporosis in men and women: a story about bone mineral density thresholds and hip fracture risk. J Bone Miner Res 2002;17:2231–2236.

32. Kanis J, Glüer CC. An update on the diagnosis and assessment of osteoporosis with densitometry. Osteoporos Int 2000;11:192–202.

33. Binkley NC, Schmeer P, Wasnich RD, Lenchik L. What are the criteria by which a densitometric diagnosis of osteoporosis can be made in males and non-Caucasians? J Clin Densitom 2002;5: S19–S27.

34. Baim S, Leonard MB, Bianchi ML, et al. Official positions of the International Society for Clinical Densitometry and executive summary of the 2007 ISCD pediatric position development conference. J Clin Densitom 2008; 11:6–21.

35. Kanis JA, Johansson H, Oden A et al. A family history of fracture and fracture risk: a meta-analysis. Bone 2004;35(5):1029–1037.

36. Kanis JA, Johnell O, De Laet C et al. A meta-analysis of previous fracture and subsequent fracture risk. Bone 2004;35(2):375–382.

37. Kanis JA, Johansson H, Oden A et al. A meta-analysis of prior corticosteroid use and fracture risk. J Bone Miner Res 2004;19(6):893–899.

38. Kanis JA, Johansson H, Oden A et al. A meta-analysis of milk intake and fracture risk: low utility for case finding. Osteoporos Int 2005;16(7):799–804.

39. Kanis JA, Johansson H, Johnell O et al. Alcohol intake as a risk factor for fracture. Osteoporos Int 2005;16(7):
737–742.

40. Kanis JA, Johnell O, Oden A et al. Smoking and fracture risk: a meta-analysis. Osteoporos Int 2005;16(2):
155–162.

41. De Laet C, Kanis JA, Oden A et al. Body mass index as a predictor of fracture risk: a meta-analysis. Osteoporos Int 2005;16(11):1330–1338.

42. Kanis JA, Oden A, Johnell O et al. The use of clinical risk factors enhances the performance of BMD in the prediction of hip and osteoporotic fractures in men and women. Osteoporos Int 2007;18(8):1033–1046.

43. Kanis JA, Johnell O, Oden A, Johansson H, McCloskey E. FRAX and the assessment of fracture probability in men and women from the UK. Osteoporos Int 2008;19(4):385–397.

44. Looker AC, Wahner HW, Dunn WL, et al. Updated data on proximal femur bone mineral levels of US adults. Osteoporos Int 1998;8:468–489.

45. Looker AC, Wahner WH, Dunn WL, et al. Proximal femur bone mineral levels of US adults. Osteoporos Int 1995;5:389–409.

46. Lu Y, Fuerst T, Hui S, Genant HK. Standardization of bone mineral density at femoral neck, trochanter and Ward's triangle. Osteoporos Int 2001;12:438–444.

47. National Osteoporosis Foundation. Clinician's guide to prevention and treatment of osteoporosis. 1–30. 2008. Washington, D.C., National Osteoporosis Foundation.
48. Dawson-Hughes B, Tosteson AN, Melton LJ, III et al. Implications of absolute fracture risk assessment for osteoporosis practice guidelines in the USA. Osteoporos Int 2008;19(4):449–458.
49. Tosteson AN, Melton LJ, III, wson-Hughes B et al. Cost-effective osteoporosis treatment thresholds: the United States perspective. Osteoporos Int 2008;19(4):437–447.
50. Ettinger B, Hillier TA, Pressman A, Che M, Hanley DA. Simple computer model for calculating and reporting 5-year osteoporotic fracture risk in postmenopausal women. J Womens Health 2005;14(2):159–171.
51. Black DM, Steinbuch M, Palermo L et al. An assessment tool for predicting fracture risk in postmenopausal women. Osteoporos Int 2001;12(7):519–528.
52. McClung MR, Geusens P, Miller PD, et al. Effect of risedronate on the risk of hip fracture in elderly women. Hip Intervention Program Study Group. N Engl J Med 2001;344:333–340.
53. Bensen R, Adachi JD, Papaioannou A, et al. Evaluation of easily measured risk factors in the prediction of osteoporotic fractures. BMC Musculoskelet Disord 2005; 6:47.
54. Ettinger B. A personal perspective on fracture risk assessment tools. Menopause 2008; 15. Pub online 01 Aug 2008 d.o.i. 10.1097/gme.06013e31817f3e4d

11 Monitoring Changes in Bone Density

In following changes in bone density in individuals, a densitometrist is generally interested in disease progression or therapeutic efficacy. As densitometry has become more widespread, the awareness of the number of diseases with effects on skeletal density has also increased. Nevertheless, monitoring changes in bone density is still primarily done to assess therapeutic efficacy of bone active agents. An increase in bone density, or, depending on the agent, stabilization of the bone density is considered an appropriate surrogate for efficacy of the agent in reducing fracture risk. Although effects on bone density are not the only means by which therapeutic agents may reduce fracture risk, meta-analyses of the relationship between changes in bone density and spine fracture risk have consistently demonstrated a statistically significant relationship between increasing bone density and declining spine fracture risk (*1,2*). The same can be said of non-spine fractures and bone density, in which the relationship appears to be even stronger (*3*). This does not negate any potential effects of therapeutic agents on non-density factors in reducing fracture risk. It simply means that changes in bone density remain the best surrogate marker for fracture risk reduction in clinical practice. To properly follow changes in bone density and interpret the results, the densitometrist

must be thoroughly familiar with the concept of precision, which was introduced in Chapter 3.

THE CONCEPT OF PRECISION

The traditional definition of precision as used in bone densitometry is the closeness of agreement between test results in the setting of no real biologic change when the test is repeatedly performed in an identical fashion and under identical conditions. This definition remains in use today. However, in 1994, the International Organization of Standardization (ISO)[1] defined two subcategories of precision: repeatability and reproducibility (*4*). Repeatability refers to the closeness of agreement between test results when the tests are performed by the same technologist, on the same equipment, at the same location within a short period of time on the same subjects. Reproducibility refers to the closeness of agreement between tests results when the tests are performed on the same subjects using the same method but by different technologists, using different equipment at different locations. Repeatability, then, is likely to provide the best precision whereas reproducibility is likely to provide the worst. The ISO definition of repeatability is what densitometrists refer to as precision. Precision is generally expressed as the error of the technique. Consequently, the term precision error is sometimes used instead of simply precision. Remember that the precision or precision error expresses the undesirable variability in the technique; therefore, the smaller the value that represents the precision, the better. Like all quantitative tests in clinical medicine, the precision of bone density testing with any technique is not zero (which would be perfect). This is true even when the bone density test is performed in exact accordance with the manufacturer's recommendations every time. But if the test is not consistently performed in accordance with the manufacturer's recommendations, the technique becomes less precise.

The precision of bone density testing assumes great importance when the technique is used to follow changes in bone density over time. Because densitometry is not perfectly reproducible, the results on any given patient are not expected to be identical, *even if the bone density in the patient has not actually changed*. The only way that a physician can know that a real biologic change has occurred is to know if the precision error of the technique has been exceeded. This means that the precision must be quantified by performing a precision study. The precision, expressed as the root-mean-square standard deviation (RMS-SD) with the same units as the measurement or the root-mean-square % coefficient of variation (RMS-%CV), is then used to determine the minimum change in bone density that constitutes a real biologic change. This minimum change is called the least significant change (LSC). The LSC can then be used to determine the appropriate interval between follow-up measurements.

PERFORMING A PRECISION STUDY

The results of three PA lumbar spine DXA bone density measurements are shown in Table 11-1. This is Mrs. B., whose bone density studies were previously discussed

---

[1] Although the name of the organization is the *I*nternational *O*rganization for *S*tandardization, it is generally known as ISO and not IOS.

PA Spine DXA Studies	
Study #1	1.011 g/cm^2
Study #2	1.030 g/cm^2
Study #3	1.022 g/cm^2
Mean	1.021 g/cm^2
SD	0.010 g/cm^2
CV	0.010
%CV	1.0%

in Chapter 3 in the explanation of the mean, variance, and SD. Remember that these measurements on Mrs. B. were all performed within a few minutes of each other, with only enough time between studies to allow Mrs. B. to get off the scan table and be repositioned by the technologist. The same technologist positioned Mrs. B. perfectly for all three studies and also analyzed all three studies according to the manufacturer's recommendations. The mean or average value for these three studies was 1.021 g/cm^2.

Note that the numerical results of the three studies are not identical, even though each study was performed perfectly and no biologic change could have occurred in Mrs. B. in the brief period that elapsed between tests. This reflects the imperfect precision of bone densitometry. In looking at Mrs. B.'s measurements in Table 11-1 it is reasonable to ask, by how much does each of the three measurements vary from the mean value? This can be found by subtracting each of the three measurements from the mean value, as shown in Equations 1, 2, and 3:

$$\text{Scan \#1: } 1.011 - 1.021 = -0.010 \, \text{g/cm}^2 \tag{1}$$

$$\text{Scan \#2: } 1.030 - 1.021 = -0.009 \, \text{g/cm}^2 \tag{2}$$

$$\text{Scan \#3: } 1.022 - 1.021 = -0.001 \, \text{g/cm}^2 \tag{3}$$

The question then becomes, what is the representative variation from the mean for each of these measurements? An intuitive approach would be to find the average difference by adding the three differences found in Equations 1, 2, and 3 and dividing the sum by 3. This is neither mathematically correct nor possible, because the sum of the differences is 0, which cannot be divided. Instead, the formula in Equation 4 is used. The three differences are squared, to remove the minus signs. After squaring, they are added and the resulting total is divided by the number of measurements minus 1 (or in this case, 2). Then the square root is taken. The resulting value is the standard deviation (SD) for the set of three measurements on Mrs. B. The SD has the units of the measurement, g/cm^2, and is the appropriate expression of the representative variability about the mean for the three measurements on Mrs. B. The SD is also the appropriate expression of the precision of these three measurements.

$$SD_B = \sqrt{\frac{\sum\limits_{i=1}^{n_B} \left(X_{iB} - \bar{X}_B\right)^2}{n_B - 1}} \qquad (4)$$

In Equation 4, n_B is the number of measurements on Mrs. B., X_{iB} is the actual value of the ith measurement and $\bar{X}_B$ (pronounced X bar) is the mean BMD value for Mrs. B. The sum of the squared differences is divided by $n-1$ rather than n because, in this case, only two of the three measurements actually contribute independently to the calculation of the mean. In other words, if the average value and two of the three measured values that were used to calculate the average were known, the third measured value could always be determined mathematically. The third value is thus not independent. In the example presented, the SD for the set of three measurements on Mrs. B. is 0.010 g/cm² as shown in Table 11-1.

Now that the SD and mean value for the three measurements on Mrs. B. are known to be 0.010 g/cm² and 1.021 g/cm², respectively, it can be asked, "What proportion or percentage of the mean does the SD represent?" This is found by dividing the SD by the mean as shown in Equation 5. This quantity is called the coefficient of variation (CV). When multiplied by 100 and expressed as a percentage, it is called the percent coefficient of variation (%CV) as shown in Equation 6. The CV and %CV are alternative expressions of the precision of the measurement. For Mrs. B. the CV was 0.010 (after rounding) and the %CV, 1.0%.

$$CV = \frac{SD}{\bar{X}} \qquad (5)$$

$$\%CV = \frac{SD}{\bar{X}} (100) \qquad (6)$$

Although the SD, CV, or %CV for Mrs. B. could be used in determining significant changes in PA lumbar spine bone density over time for Mrs. B., calculating individual precision values for every patient in a clinical practice that might be followed with bone densitometry is not practical. It is necessary to establish representative precision values for each skeletal site used for monitoring at a bone densitometry facility. This is done by performing a short-term precision study.

Short-Term Precision Studies

A separate precision study must be done for each skeletal site that might be used in following a patient. The precision for multiple regions within a skeletal site, such as the five regions of interest within the proximal femur can be determined from a single proximal femur precision study.

The number of individuals and number of scans per individual needed for a precision study is determined by the degrees of freedom necessary to achieve the narrowest confidence limits for the precision estimate that are practical. Remember that one of the measurements on an individual will not contribute independently to the calculation of the mean for that individual. The number of measurements which do independently contribute are called the degrees of freedom (d.f.) for the study. For statistical validity, it is recommended that a short-term precision study have 30 d.f. (*5–7*). Thirty d.f. are

chosen to ensure that the upper limit for the 95% confidence interval of the precision value is no more than 34% greater than the calculated precision value. If only one person is studied, 31 tests must be performed to obtain 30 d.f. because one test will not contribute independently to the calculation of the mean. If 15 patients are studied, three tests per patient must be done because again, only two of the three tests per patient will be independent (15 × 2 = 30). The specific combinations of the number of patients and number of scans per patient that are recommended for a short-term precision study are shown in Table 11-2. A short-term precision study should be completed in two weeks to one month. All the scans on any one patient can be completed on the same day if desired.

Table 11-2
**Combination of Number of Patients and Scans per Patient
for 30 Degrees of Freedom in a Precision Study**

Number of Patients	Number of Scans per Patient
1	31
5	7
10	4
15	3
30	2

Leslie et al. (8) criticized the use of 30 d.f. in short-term precision studies, stating that 30 d.f. was insufficient for quantifying the precision in clinical practice. This criticism was based on comparing the LSC that was calculated using a precision value from a study with almost 200 d.f. (198 scan pairs at the PA lumbar spine, 193 scan pairs at the proximal femur) to the precision value from six smaller cohorts with 30 d.f., which were drawn from the larger precision population, and comparing the resulting determinations of significant change in a separate population. Depending on the particular LSC, 24.9–46% of the population was classified as having a significant change in lumbar spine BMD and 31.1–43.5%, at the total hip. This is not surprising, of course, because different LSCs would be expected to identify the significance of any change differently. The authors also noted that the RMS-SD for three of the six precision cohorts with 30 d.f. fell outside the 95% confidence limits for the precision of the much larger precision cohort with almost 200 d.f. This was also true in the case of one of the six 30 d.f. cohorts compared to the much larger precision cohort at the total hip. While this was a correct observation, it is irrelevant both statistically and clinically. Sample statistics would demand that a sample, such as the small cohort with 30 d.f. that was drawn from the larger population with almost 200 d.f. have a 95% confidence interval for the precision value that included the precision value of the much larger population from which the sample was drawn. That was in fact true for five of the six smaller cohorts at the lumbar spine and for all six of the smaller cohorts at the total hip. In any case, the authors noted that the recommendations for 30 d.f. in a short-term precision study represent a blend of accuracy, convenience, and practicality. Certainly as a practical matter, the confidence interval for the precision estimate cannot be narrowed appreciably without increasing the d.f. to at least 50 or even 100. This means many more patients would be needed and/or that more scans per patient would need to be done in the precision study.

The following is the method for determining short-term precision as recommended by Gluer et al. (*9*). Using the combination of 15 patients and three scans, each for the sake of example, the mean, SD, and CV should be found for each of the 15 sets of three measurements, just as was done for the set of three measurements on Mrs. B. Rather than reporting the arithmetic mean of the 15 SDs or 15 CVs (adding the 15 values and dividing by 15) as the precision value, the root-mean-square SD (RMS-SD) or the root-mean-square CV (RMS-CV) is calculated as shown in Equations 7 and 8. The RMS-SD and RMS-CV are preferred to the arithmetic mean SD and CV because the latter quantities tend to underestimate the Gaussian error.[2]

$$SD_{RMS} = \sqrt{\frac{\sum\limits_{i=1}^{m}\left(SD^2\right)}{m}} \qquad (7)$$

$$CV_{RMS} = \sqrt{\frac{\sum\limits_{i=1}^{m}\left(CV^2\right)}{m}} \qquad (8)$$

In Equations 7 and 8, *m* is the number of patients. Using these Equations, the 15 SDs or 15 CVs would be squared, summed and then divided by the number of patients, 15. Then the square root is taken resulting in the RMS-SD or RMS-CV for the group of 15 patients. The RMS-CV can be expressed as a percentage, the RMS-%CV, by multiply by 100.

In the following example, the short-term precision for the PA lumbar spine, using L1–L4, was calculated after three PA lumbar spine studies were performed on each of 15 patients within four weeks. The same technologist scanned all of the patients. Between each scan, the patient was repositioned. The individual values and the average value for each of the 15 patients are listed in Table 11–3. In all, 45 PA spine studies were performed (15 patients × 3 scans/patient = 45 scans).

Mathematical Procedures Used to Calculate Precision

Step 1. The mean or average BMD, SD, CV, and %CV for the set of three scans for *each* of the 15 patients must be calculated. These results are shown in Table 11-4. Note that Patient 1 in Table 11-3 and 11-4 is Mrs. B., for whom this calculation was made earlier.

Step 2. Although the precision for each of the 15 patients is now known, the precision for the group as a whole must now be calculated. This is done by finding the RMS-SD or RMS-CV for the group of 15 patients, using Equations 7 and 8, noted above.

Using Equation 7, each of the 15 SDs is squared. The 15 squared SDs are summed beginning with Mrs. B. who is patient number 1 and continuing through the total number of patients, *m*, which in this case is 15. The sum is divided by m, the number of patients or 15. Finally, the square root is taken. This is the RMS-SD in g/cm^2 and is the precision

---

[2] The Gaussian distribution is discussed in Chapter 3.

Table 11-3
**The Measured and Mean PA Lumbar Spine Values for 15
Patients in a Short-Term Precision Study. All values are in
g/cm^2**

Patient	Scan #1	Scan #2	Scan #3	Mean
1	1.011	1.030	1.022	1.021
2	0.925	0.940	0.918	0.928
3	1.164	1.160	1.170	1.165
4	0.999	1.010	1.008	1.006
5	0.900	0.920	0.905	0.908
6	0.955	0.960	0.960	0.958
7	1.000	1.010	1.150	1.053
8	0.875	0.849	0.869	0.864
9	0.898	0.920	0.901	0.906
10	1.111	1.009	1.100	1.073
11	0.964	0.949	0.960	0.958
12	1.000	0.985	0.992	0.992
13	1.200	1.185	1.205	1.197
14	1.165	1.170	1.180	1.172
15	0.909	0.915	0.904	0.909

Table 11-4
**The Mean, Standard Deviation (SD), Coefficient of
Variation (CV), and % Coefficient of Variation (%CV) for
Each of 15 Patients in a Short-Term Precision Study**

Patient	Mean (g/cm^2)	SD (g/cm^2)	CV	%CV
1	1.021	0.010	0.010	1.0
2	0.928	0.011	0.012	1.2
3	1.165	0.005	0.004	0.4
4	1.006	0.006	0.006	0.6
5	0.908	0.010	0.011	1.2
6	0.958	0.003	0.003	0.3
7	1.053	0.084	0.080	8.0
8	0.864	0.014	0.016	1.6
9	0.906	0.012	0.013	1.3
10	1.073	0.056	0.052	5.2
11	0.958	0.008	0.008	0.8
12	0.992	0.008	0.008	0.8
13	1.197	0.010	0.009	0.9
14	1.172	0.008	0.007	0.7
15	0.909	0.006	0.006	0.6

for the entire group. For the short-term precision study illustrated in Tables 11-3 and 11-4, the RMS-SD is 0.027 g/cm^2.

Because the precision may also be expressed as the CV, the RMS-CV for the entire group of 15 patients is determined using Equation 8. The steps are analogous to those

described above for Equation 7 and the calculation of the RMS-SD, except that the CV for each set of scans is used instead of the SD.

Using Equation 8, each of the 15 CV's that have been previously calculated are squared and then added. This sum is divided by the number of patients, m, and then the square root is taken. This is the RMS-CV for the entire group. To convert this value to the RMS-%CV, the RMS-CV is multiplied by 100. The RMS-%CV for the group of 15 patients is 2.61%.

The average BMD for the entire group used to determine the precision should be stated in addition to the RMS-SD, RMS-CV, or RMS-%CV. The average BMD for the group of 15 patients is found simply by adding all 45 values and dividing by 45. This value is 1.007 g/cm^2. The average BMD for the group should be stated because the precision may not be as good in osteopenic or osteoporotic populations as it is in normal populations. When the precision is expressed as a CV or %CV, part of the poorer precision in groups with a lower average BMD is a function of the smaller denominator in the calculation of the CV for each patient. For example, in the group of 15 patients with an average BMD of 1.007 g/cm^2 shown in Tables 11-3 and 11-4, the precision was found to be 0.027 g/cm^2 when the RMS-SD was used and 2.61 % when the RMS-%CV was used. If a precision study was done in a different group of 15 individuals and the RMS-SD for this group was also 0.027 g/cm^2, it would be correct to conclude that the precision was equal in the two groups. However, if the average BMD in the second group was lower, the RMS-%CV would appear to be poorer.

Part of the poorer precision may be real, however. As the bones become progressively demineralized and the BMD falls, the precision may not be as good as the precision in individuals with higher levels of BMD. In ideal circumstances, a precision study would be performed on different groups of individuals in whom the average BMDs of the various groups spanned normal to osteoporotic values. The appropriate precision value could then be applied in clinical circumstances based on the BMD of the patient in question. Another approach is to perform a precision study in each individual patient that will be followed. Neither are clinically practical suggestions. It is therefore important to remember that the precision value obtained in a short-term study of young, normal individuals represents the best possible precision. Nevertheless, this is an excellent population to test the basic skills of the technologist in positioning and analysis. In 2005, ISCD stated that the minimum acceptable precision for a technologist, expressed as the %CV was 1.9% at the lumbar spine, 1.8% at the total hip, and 2.5% at the femoral neck (10). If a young, healthy population is not representative of the patient population in whom the precision values would be used, a second precision study should be performed using individuals who more closely resemble the patient population in age and BMD.

Most authorities recommend that precision be expressed as the RMS-SD in the units of the measurement. Nevertheless, use of the arithmetic mean SD as well as the arithmetic mean %CV remains common in the literature. It should be noted that the arithmetic mean SD, CV, and %CV will appear better than their RMS counterparts.

Long-Term Precision Studies

A long-term precision study in which patients are followed over the course of at least a year would be preferable to a short-term precision study, but is logistically much

more difficult to do. The calculation of the precision value is also different, requiring the use of a statistical technique called linear regression since biological changes would be expected to occur during the longer time frame. Instead of the SD, a different quantity called the standard error of the estimate is calculated and used to express precision (*11*). Because of the longer time involved, the possibility of other errors in the test increases, such as errors from machine drift and differences in operator techniques. Consequently, long-term precision estimates tend to be poorer than short-term precision estimates. Although a long-term precision study is a more appropriate reflection of the relevant circumstances in clinical practice, the logistical difficulties of performing such a study make it impractical to do. As noted earlier, a short-term precision study, performed in its entirety by the same technologist, represents the absolute best-case precision.

APPLYING THE PRECISION VALUE TO SERIAL MEASUREMENTS

Assume that a postmenopausal woman, Mrs. C., underwent a PA lumbar spine bone density study and her physician elected to begin a bone active agent for the treatment of osteoporosis. Her baseline study revealed a BMD of 0.734 g/cm^2. How long should the physician wait before repeating the PA spine bone density study in the hope of seeing a significant change in BMD? When the repeat bone density study was performed, the PA spine bone density was 0.760 g/cm^2. This represented an absolute increase of 0.026 g/cm^2 or 3.54% from baseline. Was this a statistically significant increase given that the technology cannot perfectly reproduce the results of any bone density test even when there has been no real change in the BMD? Answering these questions begins with establishing the precision value for PA lumbar spine bone density testing and then using this value to determine the least significant change.

The Determination of Least Significant Change

Once the precision of the measurement at any given skeletal site is known, the magnitude of the change in bone density at that site that indicates real biologic change can be determined. This is called the least significant change (LSC). To determine the LSC, a decision must be made as to what level of statistical confidence is needed and how many measurements will be done at baseline and follow-up. Ideally, 95% statistical confidence is chosen, but 80% statistical confidence is generally more than adequate for clinical decisions. The formula for determining the LSC is as follows:

$$LSC = Z'\,(\text{Pr})\sqrt{\frac{1}{n_1} + \frac{1}{n_2}} \qquad (9)$$

where *Z'* (pronounced Z prime) is the value chosen based on the desired level of statistical confidence, Pr is the precision value as either the RMS-SD or the RMS-CV, n_1 is the number of baseline measurements and n_2 is the number of follow-up measurements.

The Z' value indicates the number of SD from the mean value. As noted in Chapter 3, in a normal or Gaussian distribution, 95% of the values will lie within ±1.96SD. This means, of course, that 5% of the values lie outside ±1.96 SD from the mean, 2.5%

more than +1.96 SD from the mean and 2.5% more than −1.96 SD from the mean. If, for example, the LSC was to be calculated at 95% confidence using a two-sided approach, as recommended by ISCD (7), the Z' value that is used, should be the Z' value that identifies the extreme 2.5% of values from each side or tail of the distribution. In this case, the Z' value would be 1.96. Tables of Z' values are found in statistical or mathematical texts. Z' values for various levels of confidence are shown in Table 11-5.

Table 11-5
Z Values for Various Levels of Statistical Confidence

Statistical Confidence Level (%)	Two-Sided Z' Value	1-Sided Z' Value
99	2.58	2.33
95	1.96	1.64
90	1.65	1.28
85	1.44	1.04
80	1.28	0.84

For any precision value and any number of baseline and follow-up measurements, the magnitude of the change needed for statistical significance, the LSC will be less at lower levels of statistical confidence. The magnitude of the LSC can also be reduced for any level of statistical confidence by increasing the number of measurements performed at baseline and follow-up. In clinical practice, one measurement is commonly done at baseline and again at follow-up. When 1 is substituted for both n_1 and n_2 in Equation 9, the sum under the square root sign becomes 2 as shown in Equation 10:

$$LSC = Z' \, (\mathrm{Pr}) \sqrt{\frac{1}{1} + \frac{1}{1}} = Z' \, (\mathrm{Pr}) \sqrt{2} \qquad (10)$$

The situation then, of one measurement at baseline and one measurement at follow-up effectively changes Equations 10 to 11, used for the calculation of the $_{1\times1}$LSC:

$$_{1x1}LSC = Z' \, (\mathrm{Pr}) \, 1.414 \qquad (11)$$

If two measurements are done at baseline and again at follow-up, the sum under the square root sign in Equation 9 becomes 1 as shown in Equation 12 for the calculation of the $_{2\times2}$LSC:

$$_{2x2}LSC = Z' \, (\mathrm{Pr}) \sqrt{\frac{1}{2} + \frac{1}{2}} = Z' \, (\mathrm{Pr}) \sqrt{1} \qquad (12)$$

This effectively changes the equation for the calculation of the $_{2\times2}$LSC to:

$$_{2x2}LSC = Z' \, (\mathrm{Pr}) \, 1 = Z' \, (\mathrm{Pr}) \qquad (13)$$

Thus, for any level of statistical confidence, the magnitude of the LSC is reduced by performing duplicate measurements at baseline and follow-up rather than single

measurement because the product of the Z' and precision values is being multiplied by only 1 instead of 1.414. The LSC is effectively reduced by approximately 30%.

If the Z values shown in Table 11-5 for 95 and 80% for a two-sided or two-tailed approach are substituted in the formulas for the $_{1\times1}$LSC and the $_{2\times2}$LSC the formulas become:

$$_{1x1}LSC^{95-2} = 1.96\,(\text{Pr})\,1.414 = 2.77\,(\text{Pr}) \tag{14}$$

$$_{1x1}LSC^{80-2} = 1.28\,(\text{Pr})\,1.414 = 1.81\,(\text{Pr}) \tag{15}$$

$$_{2x2}LSC^{95-2} = 1.96\,(\text{Pr})\,1 = 1.96\,(\text{Pr}) \tag{16}$$

$$_{2x2}LSC^{80-2} = 1.28\,(\text{Pr})\,1 = 1.28\,(\text{Pr}) \tag{17}$$

For example, if the RMS-SD precision of PA lumbar spine DXA studies at a facility was determined to be 0.015 g/cm^2, this value would be substituted in Equation 14 if 95% confidence was desired and one measurement was performed both at baseline and follow-up. In that case, the changes in Equation 14 are reflected in Equations 18 and 19:

$$_{1x1}LSC^{95-2} = 2.77\,(\text{Pr}) = 2.77\left(0.015\,g/cm^2\right) \tag{18}$$

$$_{1x1}LSC^{95-2} = 0.042\,g/cm^2 \tag{19}$$

For 80% confidence, the precision value of 0.015 g/cm^2 is substituted in Equation 15, resulting in an LSC of 0.027 g/cm^2. The RMS-%CV can be substituted in a similar fashion for the precision value in Equations 14, 15, 16, and 17 to give the LSC as a % change from baseline for the various levels of confidence and numbers of measurements.

When Should a Measurement Be Repeated?

The timing of the repeat measurement is a direct consequence of the LSC. The follow-up measurement(s) should be done when enough time has passed for the LSC to be achieved. Therefore, once the magnitude of the LSC has been determined, the time required between measurements is:

$$\text{Time Interval} = \text{LSC} \div \text{Expected rate of change per year} \tag{20}$$

The expected rate of change per year for the various therapeutic agents or disease states is determined from the available literature. For example, if the average increase in bone density after 1 year of therapy with some agent is 0.03 g/cm^2 and the LSC in Equation 19 of 0.042 g/cm^2 is used, the time interval required is:

$$\text{Time Interval} = \frac{0.042\,g/cm^2}{0.03\,g/cm^2/yr} = 1.4\,yr \tag{21}$$

The follow-up measurement should not be made for 1.4 years because it will take at least that long before the LSC can be expected to be reached. The LSC and expected rate of change can also be given as percentages. To calculate the LSC as a percentage change from baseline, the RMS-%CV value must be used as the precision value rather than the RMS-SD.

It is clear then, that the time interval required to see a significant change is not only dependent upon the precision at a site but the expected rate of change at that site as

Table 11-6
The Interval Between BMD Measurements Required to Obtain the
$_{1x1}LSC^{95-2}$ for Various Levels of Precision and Expected Rates of
Change

Precision as % CV	% Change/Year	Interval Between BMD Measurements	
		Months	Years
0.5	1	16.7	1.39
	3	5.60	0.46
	5	3.30	0.28
1.0	1	33.2	2.77
	3	11.0	0.92
	5	6.70	0.55
1.5	1	50.0	4.16
	3	16.6	1.39
	5	10.0	0.83
2.0	1	66.5	5.54
	3	22.2	1.85
	5	13.3	1.11
2.5	1	83.2	6.93
	3	27.7	2.31
	5	16.6	1.39

well. Therefore, if the precision at a particular site is excellent but the anticipated rate of change is very slow, the required time interval may be far too long to be acceptable for clinical purposes. Table 11-6 illustrates the interaction between precision and rate of change and the time interval to the LSC at the 95% confidence level for one measurement at both baseline and follow-up. Precision tends to be the best, and therefore, the precision values the lowest, at the PA lumbar spine, total hip, proximal radius, and heel. Rates of changes at these sites may be quite different, however. The preferred skeletal site for monitoring any particular therapy or disease state will be the site that provides the combination of superior precision and greatest rate of change. This will often be the PA lumbar spine and it is for this reason that the PA lumbar spine was noted as the preferred site for monitoring by ISCD (7).

A Case in Point

This case study illustrates the application of the precision and LSC values in clinical practice in order to answer the questions posed earlier in this chapter about Mrs. C., the postmenopausal woman who has begun therapy for the treatment of osteoporosis. Assume that the precision for PA lumbar spine studies at a bone densitometry facility was previously determined to be 1.5%. This is the RMS-%CV that was calculated from a study of 15 people, each of whom underwent three studies of the PA lumbar spine.[3] Such

---

[3] Although the RMS-SD is preferred to the RMS-%CV, the change in bone density from baseline seen with various therapeutic agents is generally given as a percentage in the medical literature, necessitating the use of the RMS-%CV for the calculation of the time to the LSC.

a precision study provides 30 d.f. This means that the calculated precision of 1.5%, at a statistical confidence level of 95%, is at worst actually 34% higher than that or 2.01% ([1.5 × 34%] + 1.5%). At this same facility, the precision for femoral neck bone density studies was established as 2.4%. At 95% confidence, the worst of this precision figure might actually be 3.2%.

Mrs. C., who has a recent diagnosis of osteoporosis, has just received a prescription for a potent antiresorptive agent as treatment for her osteoporosis. Her physician has requested that she have repeat bone density studies to assess the effectiveness of the therapy. When should Mrs. C.'s bone density studies be repeated? The follow-up measurements to assess therapeutic efficacy should not be made until sufficient time has passed to allow the LSC to be reached.

There are several factors to be considered in answering what would seem to be a straightforward question. First, what magnitude of change in bone density at the PA lumbar spine and femoral neck is expected over the course of a year with the particular agent that has been prescribed for Mrs. C.? How many measurements will be done at both baseline and follow-up? And finally, what level of statistical confidence is required for the clinical decision-making process. Ninety-five percent confidence is the most stringent criterion but 80% confidence is often more than sufficient.

For this example, assume that the therapeutic agent in question has been shown to produce an average increase of 5% from baseline in PA lumbar spine bone density and 2% in femoral neck bone density during the first year of treatment. One measurement of the PA lumbar spine and femoral neck has already been made and no additional baseline measurements are planned. Only one measurement of either the PA lumbar spine or femoral neck or both is planned at the time of follow-up. The time to the $_{1\times1}$LSC for both 95% and 80% confidence can be calculated.

The first step is to find the $_{1\times1}$LSC for 80% confidence and the $_{1\times1}$LSC for 95% confidence for each of the skeletal sites using the precision values that have been previously established. Equations 14 and 15 can be used to find these values by substituting the RMS-%CV precision values of 1.5% for the PA lumbar spine and 2.4% for the femoral neck into each of the equations. For the lumbar spine, the $_{1\times1}$LSC^{95} is 4.16% and the $_{1\times1}$LSC^{80} is 2.72%. At the femoral neck, the $_{1\times1}$LSC^{95} is 6.65% and the $_{1\times1}$LSC^{80} is 4.34%. Given the anticipated rate of change from the chosen therapeutic agent, the length of time it will take to equal or exceed any of these values is the earliest time that the follow-up study at either site should be performed.

If the average increase in PA lumbar spine bone density with this agent is 5% in the first year, then the $_{1\times1}$LSC^{95} of 4.16% should be exceeded within 1 year. Using Equation 20, the exact time can be determined to be 0.8 years. The $_{1\times1}$LSC^{80} at the lumbar spine can be reached even more quickly, by 0.54 years. At the femoral neck, however, given that the average increase in bone density is only 2% in the first year and the precision is slightly poorer than at the PA lumbar spine, the $_{1\times1}$LSC^{95} of 6.65% would not be reached for 3.33 years. Even the $_{1\times1}$LSC^{80} of 4.34% will not be reached for 2.17 years. It would be reasonable then to advise repeating only the PA lumbar spine bone density study in one year in anticipation of seeing a change in bone density sufficiently great to conclude that a significant change has occurred with 95% statistical confidence. Repeating the proximal femur bone density study in 1 year would not be reasonable since a significant change in bone density would probably not be detected then, given the precision of testing at the femoral neck and the relatively small anticipated change at that site.

One year later, Mrs. C. returns for her repeat PA spine bone density study. At the time of her original study, her L1–L4 PA lumbar spine bone density study was 0.734 g/cm^2. On her repeat study, the L1–L4 BMD was 0.760 g/cm^2. Is this a significant change? For the change to be significant, the LSC must be equalled or exceeded. In this example, the LSC has been given as a percentage, so the % increase from baseline for Mrs. C. must be calculated. In order to do this, the baseline BMD value is subtracted from the follow-up value. This difference is divided by the baseline value and multiplied by 100 to express it as a percentage. The formula and the practical application are shown in Equations 22, 23, and 24.

% Change from Baseline = [(Follow-up BMD − Baseline BMD)/Baseline BMD] × 100   (22)

% Change from Baseline = [(0.760 g/cm^2 − 0.734 g/cm^2)/0.734 g/cm^2] × 100   (23)

% Change from Baseline = 3.54%   (24)

The % change from baseline of 3.54% does not equal or exceed the $_{1\times1}$LSC^{95} of 4.16% so the change cannot be said to be significant at the 95% confidence level. It does exceed the $_{1\times1}$LSC^{80} of 2.72%, however, so the change can be said to be significant at the 80% confidence level.

MORE SOPHISTICATED ISSUES IN THE CALCULATION AND APPLICATION OF THE LSC

Determining the Level of Confidence for Any Magnitude of Change and Precision

In its 2002 position statement, ISCD (*7*) recommended that the LSC be calculated using a two-sided approach at 95% confidence and that changes in bone density be considered significant only if they equaled or exceeded this value. This is a stringent requirement. It is imperative to know how confident one can be that a real change has occurred, but the level of statistical confidence necessary to influence clinical decisions is generally not required to be 95%. For example, 80% is often more than adequate. If the change in BMD has not equaled or exceeded the LSC for 95% or even 80% confidence, the question then becomes how confident can you be that there has been a real change in the BMD? It is possible to calculate the level of confidence for any given precision value and change in BMD. This is essentially done by using Equation 9. The measured change, no matter what it is, is considered the LSC. Since the precision of the measurement and the number of measurements made at baseline and follow-up are also known, the equation can be solved for Z.´Once that is done, the confidence level can be determined. That is what has been done in the Statistical Confidence Calculator spreadsheet on the CD that accompanies this book. Table 11-7, from Dr. Ken Faulkner, is this type of calculation in tabular form for specific combinations of precision and change in BMD. For example, if the RMS-SD precision is 0.010 g/cm^2 and the measured change in BMD is 0.015 g/cm^2, the physician may be 71% confident that a real change in BMD has occurred. Whether this level of confidence is sufficient to warrant clinical consideration is a matter of judgment on the part of the physician.

Table 11-7
Levels of Statistical Confidence for Various Combinations of Precision and Change in BMD

Change in BMD (g/cm²)	Precision (g/cm²)									
	0.005 (%)	0.010 (%)	0.015 (%)	0.020 (%)	0.025 (%)	0.030 (%)	0.035 (%)	0.040 (%)	0.045 (%)	0.050 (%)
0.005	52	28	19	14	11	9	8	7	6	6
0.010	84	52	36	28	22	19	16	14	12	11
0.015	97	71	52	40	33	28	24	21	19	17
0.020	100	84	65	52	43	36	31	28	25	22
0.025	100	92	76	62	52	44	39	34	31	28
0.030	100	97	84	71	60	52	46	40	36	33
0.035	100	99	90	78	68	59	52	46	42	38
0.040	100	100	94	84	74	65	58	52	47	43
0.045	100	100	97	89	80	71	64	57	52	48
0.050	100	100	98	92	84	76	69	62	57	52
0.055	100	100	99	95	88	81	73	67	61	56
0.060	100	100	100	97	91	84	77	71	65	60
0.065	100	100	100	98	93	87	81	75	69	64
0.070	100	100	100	99	95	90	84	78	73	68
0.075	100	100	100	99	97	92	87	82	76	71
0.080	100	100	100	100	98	94	89	84	79	74
0.085	100	100	100	100	98	95	91	87	82	77
0.090	100	100	100	100	99	97	93	89	84	80
0.095	100	100	100	100	99	97	95	91	86	82
0.100	100	100	100	100	100	98	96	92	88	84

Table created by and reproduced courtesy of Ken Faulkner, Ph.D.

The Confidence Interval for the Change in BMD Between Two Measurements

Once it has been determined that a measured change in BMD is significant at some level of statistical confidence, the question remains as to what the actual change in BMD really is. As noted in the example above, with a precision of 0.010 g/cm^2 and a measured change of 0.015 g/cm^2, a physician may be 71% confident that a real change has occurred. The physician cannot be 71% confident that a change of 0.015 g/cm^2 has actually occurred. Because there is some statistical uncertainty in both the baseline and follow-up measurements, there is also uncertainty in the magnitude of the measured change. So how can the range of values in which the true change may lie be calculated? Table 11-8 illustrates the range of values for 99, 95, 90, 85, and 80% confidence intervals for a change in BMD between two measurements at various levels of precision. The values shown in the table for the various levels of precision and confidence are added and subtracted from the actual measured change. For example, if the precision of testing is 1.5% and the measured change is 3%, the actual range of change for the 95% confidence interval is $3 \pm 4.16\%$ or -1.16 to $+7.16\%$. Because the range of possible values contains 0, the measured change of 3% with a precision of 1.5% is not statistically significant at the 95% confidence level. On the other hand, if the precision is 1.25% and the change between two measurements is 4%, the 95% confidence interval for the change is $4 \pm 3.46\%$ or 0.54 to 7.46%. This range of values does not contain 0 and therefore the change of 4% is significant at the 95% confidence level. Obviously, this is a very wide confidence interval. It is perhaps disconcerting to note that while the measured change is statistically significant, the actual change may range from as little as 0.54% to as much as 7.46%. The 85% confidence interval is narrower. In this case, the range of values is $4 \pm 2.76\%$ or 1.24 to 6.76%. Defining these ranges is certainly less important than recognizing whether the measured change is statistically significant.

Table 11-8
Confidence Intervals for the Measured Change in BMD for Different Values of
Precision. All values are in %

Confidence Interval (%)	Precision, %CV				
	1	*1.25*	*1.5*	*1.75*	*2.0*
99	±3.65	±4.56	±5.48	±6.39	±7.30
95	±2.77	±3.46	±4.16	±4.85	±5.54
90	±2.33	±2.91	±3.50	±4.08	±4.66
85	±2.04	±2.55	±3.06	±3.57	±4.08
80	±1.81	±2.26	±2.72	±3.17	±3.62

One-Sided Determinations of the Least Significant Change

The LSC could be calculated using a one-sided approach rather than the currently recommended two-sided approach. The rationale behind doing so is based on two considerations. First, most serial bone density studies are done to monitor therapeutic efficacy. Second, therapeutic efficacy is generally said to be a significant increase in bone density or no change in the bone density. A logical extension of the last statement is that it is only the finding of a significant decline in BMD that would prompt the physician to potentially change the therapeutic approach. If that is the case, then the LSC could be

calculated in such a way that allows the densitometrist to more aggressively identify a statistically significant decline in bone density.

Assume that the densitometrist still wishes to calculate the LSC at 95% confidence, but that in this case, the intention is to be 95% confidence that a statistically significant decline in bone density has not occurred. The identification of potential bone loss is the only focus in this example. In this case, a one-sided approach to the calculation of the LSC is appropriate. Equations 11 or 14, depending upon whether one or two measurements were done at baseline and follow-up, are still applicable here. The difference is in the Z' value that is used. The Z' value is once again chosen on the basis of the level of statistical confidence that is desired, but Z' values for a one-sided approach are different than those used in a two-sided approach. Table 11-5 lists both types of Z' values for various levels of statistical confidence. In the case of 95% confidence, the one-sided Z value is 1.64. The use of 1.64 for the Z' value in Equation 11 is shown in Equation 25:

$$_{1x1}LSC^{95-1} = 1.64\,(\mathrm{Pr})\,1.414, \text{ which then becomes} \tag{25}$$

$$_{1x1}LSC^{95-1} = 2.32\,(\mathrm{Pr}) \tag{26}$$

Note that the magnitude of the LSC is now 2.32(Pr) when a one-sided approach at 95% confidence is used instead of 2.77(Pr) when a two-sided approach is used. In effect, this means that a smaller decline in BMD will now be called statistically significant. This is a more aggressive approach to the identification of bone loss on therapy and, while not currently recommended by ISCD, should be considered.

THE IMPORTANCE OF THE SHORT-TERM PRECISION STUDY

When properly performed, bone density measurements are the most precise quantitative measurements in use in clinical medicine today. But it should be clear that until precision studies are performed at a facility, the LSC cannot be determined for any level of statistical confidence, making the interpretation of serial studies impossible. The calculations necessary to determine precision are somewhat tedious but not complex. Such calculations are simple with a relatively inexpensive statistical calculator. On the CD-ROM that accompanies this book, a precision calculator program is included that utilizes Mircosoft® Excel. A similar program is available from the International Society for Clinical Densitometry.[4] Precision studies do not need to be done on a regular basis, but they should be done at least once. They should be repeated if a new technologist begins scanning or if there is a major equipment change. The patients who participate in precision studies to derive the values that will be used clinically should be representative of the patient population that will be subsequently monitored with the technique. If a densitometry facility employs two or more technologists who are equally likely to perform a patient's bone density study on any given day, then the precision study should

---

[4] At www.iscd.org an Excel spreadsheet is available at no cost for download by ISCD members that allows the physician to enter the bone density values obtained during a precision study. The precision is calculated automatically by formulas imbedded in the spreadsheet. The spreadsheet can only be used with Microsoft® Excel.

be performed by all of the technologists since this will be more representative of what is likely to occur in actual practice. It should be anticipated that the precision will not be quite as good as when only one technologist performs all the studies. It is not uncommon for precision studies to be performed with healthy young adults of normal body size and normal bone density. This type of precision study should be done to allow the technologist to test his or her skills in positioning and analysis. The precision value that results from such a study should not be used as the representative precision value for the facility, unless that is the type of patient the facility sees.

WHICH SKELETAL SITES SHOULD BE USED FOR MONITORING?

There are four basic rules that govern the choice of skeletal site for the purposes of monitoring the effects of disease or drugs on the skeleton.

1. Measure the skeletal site or type of bone (trabecular or cortical) that you expect to be affected.
2. Of the sites potentially affected, measure the site at which the greatest change in BMD is expected.
3. Of the sites potentially affected, measure the site at which you can measure the BMD with the best precision.
4. Peripheral sites are not used for monitoring by any technique.

Rule 1 is simply common sense. If a disease, drug, or procedure is not known to affect bone density in a particular region of the skeleton, it makes no sense to monitor that region. Knowing at which skeletal site the greatest effect is likely to be seen, as required by rule 2, is necessary to pick the skeletal site at which a change in BMD is most likely to be detected. This is because a certain magnitude of change is necessary to equal or exceed the LSC as discussed earlier. In addition, the greater the magnitude of the change, the sooner the change can be detected, making monitoring a more efficient process. Better precision, as required by rule 3, also increases the likelihood of detecting a significant change and detecting it more quickly. Table 11–6, seen earlier in this chapter, illustrates the relationship between rate of change, precision, and the time to the LSC. Ideally, the site that is chosen for monitoring is the site with the greatest anticipated rate of change and the best precision. Peripheral sites are not used for monitoring, regardless of the technique by which they are measured. Precision is generally excellent at peripheral sites but the anticipated rates of change are too slow to make monitoring clinically useful. As a practical matter then, rule 4 means that the skeletal sites used for monitoring are the spine and proximal femur.

As was noted in Chapter 2, the spine and proximal femur are both weight-bearing, central sites. The spine is part of the axial skeleton while the proximal femur is part of the appendicular skeleton. In considering the requirements of rules 1 and 2, however, the percentages of cortical and trabecular bone within the spine and various regions in the proximal femur are most pertinent. The area or size of the various regions of interest is relevant to rule 3. The PA spine is generally considered to be 66% trabecular bone. In the proximal femur, the regions of interest with the greatest percentage of trabecular bone are Ward's area and the trochanteric region. The exact percentage of trabecular bone in Ward's area is not defined but it is considered highly trabecular. The percentage of trabecular bone in the trochanteric region is approximately 50%. The greatest rates of

change are usually seen in skeletal regions that contain higher percentages of trabecular bone. This is because trabecular bone has a much higher metabolic rate than cortical bone. Precision, however, is often a function of the size of the area being measured. The larger the size, the better the precision tends to be. The greatest area is found in the PA spine by considering three or four of the lumbar vertebrae as one block. In the proximal femur, the greatest area is in the total femur region, followed by the trochanteric region.

In a position statement (*7*) from the International Society for Clinical Densitometry (ISCD) published in 2002, the PA lumbar spine was described as the preferred site for monitoring. The total femur region of interest was an alternate choice when the PA spine could not be measured for any reason. In recommending the PA lumbar spine as the preferred choice, the ISCD panel members noted that the PA lumbar spine provided the best combination of magnitude of change and precision. In the original publication there was no recommendation to use L1–L4 in preference to L2–L4. The precision of L1–L4 has rarely been compared to the precision of L2–L4. The area of L1–L4 will clearly be greater than that for L2–L4, and in general, the greater the area, the greater the precision will be. There is a point, however, past which further increases in area will not have a significant effect on improving precision. In a precision study in which the precision at L1–L4 was compared to that of L2–L4 on the Lunar Prodigy, Bonnick and Lewis (*12*) found excellent precision for both L1–L4 and L2–L4. In women aged 50–70, the RMS-SD and RMS-%CV values were 0.012 g/cm^2 and 1.1% for both combinations of vertebrae. In a younger group of women aged 20–49 years, the RMS-SD and RMS-%CV values were 0.009 g/cm^2 and 0.7% for L1–L4 and 0.011 g/cm^2 and 0.9% for L2–L4. Although these differences are statistically significant, their clinical significance is doubtful. It would seem then, that either L1–L4 or L2–L4 is appropriate for monitoring purposes in the PA lumbar spine.

The total femur was recommended by ISCD because of its greater area in the proximal femur. This does indeed result in excellent precision at the total femur. In the precision study from Bonnick and Lewis (*12*) noted above, the precision of the total femur on the Lunar Prodigy was 0.007 g/cm^2 or 0.7% in younger women (RMS-SD and RMS-%CV, respectively). In the group of older women the precision was 0.006 g/cm^2 and 0.7%. Rates of change at the total femur tend to be slow. They are often less than those seen in the femoral neck, a region with a much smaller area and certainly less than those seen in the trochanteric region. This slower rate of change is, in part, offset by the excellent precision, enabling the physician to detect a significant change in bone density within a reasonable period of time. The trochanteric region of interest, however, potentially offers a reasonable alternative to the PA lumbar spine for monitoring. Rates of change in the trochanteric region of interest are often similar to those seen in the PA lumbar spine because of its similar trabecular composition. The area of the trochanteric region is greater than that of the femoral neck although not as great as that of the total femur. With the advent of fan-array DXA scanning, the precision of trochanteric measurements has been dramatically improved. The precision of the trochanteric region of interest on the Lunar Prodigy was 0.008 g/cm^2 and 0.9% (RMS-SD and RMS%CV, respectively) in younger women and 0.009 g/cm^2 and 1.3% in the older women (*19*). Note that these RMS-SD values are even smaller than those seen at the PA lumbar spine and comparable to those seen at the total femur. The combination of rate of change and precision at the trochanter makes it a suitable site for

monitoring in the proximal femur and a reasonable choice if the PA lumbar spine cannot be monitored.

HOW FREQUENTLY SHOULD MEASUREMENTS BE REPEATED?

The frequency with which measurements should be made is determined by the time to the LSC, as discussed earlier. The time to the LSC is determined by the anticipated rate of change and the precision at the skeletal site being measured as well as the number of measurements made at baseline and at follow-up and the desired level of statistical confidence for the measured change. In the ISCD position (*12*) statement on serial bone density measurements, it was noted that an interval of less than 1 year was rarely indicated when measurements were made at the PA lumbar spine. It was also noted that an interval of 2 years at the total femur might not be sufficient to demonstrate a statistically significant change. Both of these statements are correct. The precision of PA lumbar spine bone density measurements is sufficiently good when combined with the rates of change generally seen at the PA lumbar spine to justify repeat measurements at the end of 1 year in anticipation of seeing a significant change in most circumstances, even at the 95% confidence level. In spite of superb precision at the total femur, the slower rates of change generally seen at this site may preclude seeing a significant change even after 2 years. The same statement would be true regarding the femoral neck region of interest. The potentially superb precision of the trochanteric region of interest with the newer DXA devices combined with rates of change comparable to those seen in the PA lumbar spine suggest that monitoring of the trochanteric region could be done in many cases at an interval of 1 year.

Once it has been determined that the bone density is stable or has significantly changed, the frequency with which testing should be repeated is unclear. In the context of assessing therapeutic efficacy of bone active agents, there is no evidence to date that suggests that therapeutic efficacy, once established, may subsequently be lost. As a consequence, the frequency of monitoring in this circumstance must be left to the discretion of the densitometrist. The frequency of repeat bone density studies in individuals not receiving therapy is discussed in Chapter 14.

REGRESSION TO THE MEAN AND MONITORING

In an article in the *Journal of the American Medical Association* in 2000, Cummings et al. (*13*) discussed whether regression to the mean (RTM) invalidated serial bone density measurements in clinical practice. The statistical concept of RTM was explained in Chapter 3. Cummings et al. used bone density data from the Fracture Intervention Trial (FIT) of alendronate in postmenopausal women as well as data from the Multiple Outcomes of Raloxifene Evaluation (MORE) trial in postmenopausal women. They limited their analysis to data obtained during the first 2 years of each trial in women who were compliant with the medication. They analyzed bone density data at the proximal femur in women by treatment assignment (active medication vs. placebo). The average change in bone density at the end of 1 year was calculated for each treatment assignment group. The women were then divided into subgroups based on their actual change in bone density during the first year. At the end of the second year, the change in bone density in each of the subgroups was compared to the change in bone density seen at the end of the first year in the same subgroups. The results were identical, regardless of treatment

assignment or clinical trial. The subgroups that gained bone density during the first year of the trial tended to lose bone density during the second. Conversely, the subgroups that lost bone density during the first year gained bone density during the second. The subgroups that had the greatest initial gains tended to show the greatest subsequent losses. The converse was again true in that the subgroups that had the greatest initial losses tended to have the greatest subsequent gains. Cummings et al. correctly noted that their observations were due to RTM. They further noted, however, that their "findings raise questions about the value of monitoring BMD during treatment." They suggested that because of RTM, individuals who appear to lose bone density during the first year of a therapy are likely to gain density during the second. Similarly, individuals who gain bone density during the first year of therapy will likely lose it during the second. These predictions would indeed make monitoring irrelevant if they were correct. They are not correct, however. As noted in Chapter 3, RTM is a statistical phenomenon that is created by a particular study design and analysis. The study design and analysis presented by Cummings et al. met all the necessary requirements to create RTM. First, a variable was measured on two separate occasions. In this case, the variable was the change in bone density during the first year and the change in bone density during the second year. Second, the value of the variable could change. The magnitude of the change in BMD during each of the 2 years could change because of the effects of therapy or simply because of precision errors. Third, subgroups were defined based on high or low values at the time of the first measurement. Here subgroups were indeed defined based on the change in bone density at the end of the first year. Having met these three conditions, the results of the Cummings' analysis were predictable. No matter what the change in the subgroup at the end of the first year, the change in that subgroup at the end of the second year would return toward or regress to the mean change at the end of the first year for the entire group. In other words, the conditions necessary to see RTM were created in this analysis and RTM was indeed observed. This is not clinically relevant, however. RTM is a statistical phenomenon, not a biologic one (*14*). It is also a group phenomenon, not an individual one. As a consequence, RTM has no relevance in following changes in BMD in individuals in clinical practice. The statistical issue of importance in serial bone density measurements is precision.

A FINAL CONSIDERATION

All of these careful considerations are rendered moot, however, if the follow-up study is performed on a different manufacturer's bone densitometer. Even a different device from the same manufacturer is less desirable than using the exact same densitometer for the follow-up study as was used for the baseline study.[5] Under ideal circumstances, the same technologist would perform both the baseline and follow-up study. Although sometimes difficult, it is the responsibility of the densitometrist to ensure that the follow-up study is performed under the exact conditions of the baseline study. Serial measurements made on devices from different manufacturers cannot be interpreted with any degree of clinical accuracy. The conversion equations described in Chapter 6 cannot be

---

[5] See Chapter 6 for a discussion of BMD data obtained different devices from the same manufacturer.

used for this purpose, as there is still too great a margin for error. The use of a different device for the follow-up study even though it is from the same manufacturer of the device used for the baseline study has the potential to increase the precision error and therefore, increase the LSC. The significance of the magnitude of any change in BMD becomes extremely difficult to determine. As a consequence, it is desirable to avoid this situation if at all possible.

REFERENCES

1. Wasnich RD, Miller PD. Antifracture efficacy of antiresorptive agents are related to changes in bone density. J Clin Endocrinol Metab 2000;85:231–236.
2. Cummings SR, Karpf DB, Harris F, et al. Improvement in spine bone density and reduction in risk of vertebral fractures during treatment with antiresorptive drugs. Am J Med 2002;112:281–289.
3. Hochberg MC, Greenspan S, Wasnich RD, Miller P, Thompson DE, Ross PD. Changes in bone density and turnover explain the reductions in incidence of nonvertebral fractures that occur during treatment with antiresorptive agents. J Clin Endocrinol Metab 2002;87:1586–1592.
4. International Organization of Standardization. Accuracy (trueness and precision) of measurement methods and results - Part 1: General principles and definition. 1st[ISO 5725-1], 1–17. 1994. Switzerland, ISO. International Standard. International Organization of Standardization.
5. Assessment of instrument performance: precision, installation of new equipment and radiation dose. In: Blake, GM, Wahner, HW, Fogelman, I, eds. The evaluation of osteoporosis. London: Martin Dunitz Ltd., 1999:147–172.
6. Bonnick SL, Johnston CC, Jr., Kleerekoper M et al. Importance of precision in bone density measurements. J Clin Densitom 2001;4(2):105–110.
7. Lenchik L, Kiebzak GM, Blunt BA. What is the role of serial bone mineral density measurements in patient management? J Clin Densitom 2002;5:S29–S38.
8. Leslie WD, Moayyeri A. Minimum sample size requirements for bone density precision assessment produce inconsistency in clinical monitoring. Osteoporos Int 2006;17:1673–1680.
9. Glüer CC, Blake G, Lu Y, Blunt, BA, Jergas, M and Genant, HK. Accurate assessment of precision errors: how to measure the reproducibility of bone densitometry techniques. Osteoporos Int 1995;5:262–270.
10. Shepherd JA, Lu Y, Wilson K et al. Cross-calibration and minimum precision standards for dual-energy X-ray absorptiometry: the 2005 ISCD Official Positions. J Clin Densitom 2006;9(1):31–36.
11. Verheij, LF, Blokland, JAK, Papapoulos, SE, Zwinderman, AH and Pauwels, EKJ. Optimization of follow-up measurements of bone mass. J Nucl Med 1992;33:1406–1410.
12. Bonnick SL, Lewis LA. The precision of PA spine, dualfemur and single femur bone density studies on the GE Lunar Prodigy, a DXA fan-array device. Abstract. J Clin Densitom 2002;5:S48.
13. Cummings SR, Palermo L, Browner W, et al. Monitoring osteoporosis therapy with bone densitometry. Misleading changes and regression to the mean. JAMA 2000;283:1318–1321.
14. Bonnick SL. Monitoring osteoporosis therapy with bone densitometry: a vital tool or regression toward mediocrity? J Clin Endocrinol Metab 2000;85:3493–3495.

12 Secondary Causes of Osteoporosis

CONTENTS

A general knowledge of secondary causes of bone loss and osteoporosis is useful and necessary in the practice of densitometry. It must be remembered that the bone density study provides information on the density of the bone at that moment only. It does not, by itself, identify any magnitude of bone loss and certainly cannot be used to identify the cause of any suspected bone loss. It is a single snapshot in time, telling the physician what the bone density is that day, but not how or why it got that way. Because of this, any time that the bone density is classified as low or osteoporotic, an evaluation of the patient for secondary causes of bone loss is appropriate. This evaluation would be performed by the patient's treating physician, and the extent of the evaluation would be guided by his or her knowledge of the patient. If the patient is well known to the physician, a review of the patient's medical records may be all that is warranted. It is also possible that additional testing or inquiry may be necessary to exclude causes of bone loss and conditions other than postmenopausal or age-related osteoporosis, as specific interventions may be necessary for successful treatment. Even if the densitometrist is not the treating physician, he or she may still be called upon to render an opinion as to the possible differential diagnoses for suspected bone loss and any appropriate evaluations necessary to exclude those possibilities. The International Society for Clinical Densitometry (ISCD) recommended in 2003 (1) that bone density reports contain a reminder to the referring physician that a "medical evaluation for secondary causes of low BMD may be appropriate." Specific recommendations regarding the nature of such an evaluation were considered optional. The ability to make specific recommendations, however, is desirable and often necessary in order to assist the referring physician.

An old but relevant admonition is, "you only find what you look for." It remains then to determine for what we should be looking, in whom is it reasonable to look, and how to look.

Z-SCORES AS AN INDICATION OF SECONDARY BONE LOSS

The z-score on the bone density printout itself compares the patient's bone density to the average bone density that is expected for an individual of the same age.[1] The z-score may be also be adjusted for the patient's weight and race, although these are options which may be disabled by the technologist. From a statistical perspective, a z-score that is poorer than −2 suggests the possibility of an underlying cause of secondary bone loss. This is because a z-score of 0 at any age implies that the patient's bone density is as expected for his or her age. In other words, if the patient has experienced the magnitude of bone loss over time that is expected for their age, the z-score will be 0. Statistically speaking, 95% of individuals should have a z-score from −2 to +2.[2] Only 2.5% should have a z-score poorer than −2. These patients must be considered suspect, in terms of secondary causes of bone loss, because it is statistically less likely that aging or the postmenopausal state alone would account for the magnitude of the suspected bone loss. After an evaluation, the patient may or may not be found to have a secondary cause of bone loss, but statistically the evaluation is justified.

The finding of a z-score that is better than −2 *does not* mean that the patient should not be evaluated for possible secondary causes of bone loss. This should *always* be considered, no matter what the z-score. In a study from Tannebaum et al. (*2*) 173 otherwise apparently healthy women with osteoporotic bone densities were evaluated for secondary causes of bone loss. Of the women with z-scores better than −1, 41.5% were found to have secondary causes. In the women with z-scores from −1 to −1.9, 42.7% had secondary causes of osteoporosis and 67.1% of the women with z-scores poorer than −2 also were found to have secondary causes of osteoporosis. Of all the women who were found to have secondary causes of osteoporosis, 60% had z-scores better than −2. At the same time, 32.9% of the women with z-scores poorer than −2 were not found to have any known secondary causes of osteoporosis. But a z-score poorer than −2 is a "red flag" that always merits attention.

POTENTIAL CAUSES OF SECONDARY BONE LOSS

One of the first studies looking at potential secondary causes of bone loss in men and women was published in 1989 from the University of Kansas (*3*). In this study, 300 patients (7 men and 293 women), ranging in age from 31 to 86, underwent bone density testing of the distal third of the radius by single-photon absorptiometry and of the spine by dual-photon absorptiometry.[3] A thorough medical evaluation was performed which included a 4-day dietary diary for calcium intake, complete blood count, serum chemistries, thyroid hormone, 25-hydroxyvitamin D levels, urinalysis, and a timed, fasting urine collection for calcium and creatinine. Most patients had thoracic and lumbar spine films as well. In this early study, osteoporosis was defined as the presence of two

---

[1] See Chapter 3 for a discussion of the z-score.

[2] Strictly speaking, the range is from −1.96 to +1.96; however, this is generally rounded to −2 to +2.

[3] See Chapter 1 for a discussion of the older techniques of single- and dual-photon absorptiometry.

or more atraumatic vertebral compression fractures or a lumbar spine bone density 10% or more below the value predicted for the patient's age.

Using this older definition, 180 of the 300 patients had osteoporosis. Of these 180 patients, 83 (46%) were found to have an additional condition or diagnosis that potentially contributed to bone loss. There were 128 diagnoses identified, with some patients having more than one diagnosis. In 11% of these patients, the diagnosis was made for the first time as a result of the evaluation. The diagnoses are illustrated in Table 12-1. While the authors noted a variety of potential limitations of their study, they correctly pointed out the value of a comprehensive evaluation for identifying conditions associated with bone loss and that the assessment of bone density "should not be performed in a medical vacuum."(*3*)

Table 12-1
Contributing Diagnoses in 83 of 180 Patients With Osteoporosis

Endocrine	Gastrointestinal
Glucocorticoid use (26)	Lactase deficiency (4)
Premature menopause (17)	Gluten-sensitive enteropathy (3)
Low serum 25-hydroxy	Malabsorption/surgery (2)
cholecalciferol (10)	Other
Hyperthyroid (7)	Chemotherapy (cancer/ arthritis) (8)
Iatrogenic (5)	Scoliosis (7)
Diabetes (5)	Rheumatoid arthritis (5)
Hyperparathyroid (3)	Poliomyelitis (4)
Paget's disease (3)	Kidney stones (4)
Polycystic ovary (1)	Alcohol abuse (4)
Hyperprolactinemia (1)	Prolonged bedrest (3)
Malignancy	Poor nutrition (2)
Multiple myeloma (2)	Seizure disorder with phenytoin (1)
Breast cancer (2)	Sarcoidosis (1)
Acute leukemia (1)	
Sarcoma (1)	
Hodgkin's disease (1)	

One of the largest studies to date is the analysis of the prevalence of secondary causes of osteoporosis in the Canadian Database of Osteoporosis and Osteopenia (CANDOO) population (*4*). Based on data presented in 2002, which had been collected from 5604 women and 561 men over the age of 50, secondary causes of osteoporosis were found in 41.4% of the women and 51.3% of the men. In comparing patients with fracture to those without fracture, the authors found secondary causes of osteoporosis in 45.9% of the fracture patients compared with 40.1% of the non-fractured patients. In general, the most common cause of secondary osteoporosis in this study was corticosteroid use.

In the study noted earlier from Tannebaum et al. (*12*) from Mount Sinai, New York, there were 56 previously undetected disorders that could potentially influence mineral metabolism that were identified in 44% of the 173 women with a mean age of 65.5 years. These diagnoses included hypercalciuria, malabsorption, hyperparathyroidism, vitamin D deficiency, exogenous hyperthyroidism, and Cushing's disease as shown in

Table 12-2
Secondary Contributors to Osteoporosis Identified in 173 Otherwise Healthy
Women with Osteoporosis. Personal communication Marjorie M. Luckey, MD

Diagnosis	% of 173 Otherwise Healthy Women with Osteoporosis
Vitamin D Deficiency (<20 ng/ml)	20%
Hypercalciuria	10%
Malabsorption	7%
Hyperparathyroidism	3%
Exogenous Hyperthyroidism	2%
Cushing's Disease	~1%
Other	1%

Table 12-2. Corticosteroid use was not identified as a cause in this study because women with a history of past or current corticosteroid use were excluded. In short, after excluding women from the study who were known to have conditions that could affect bone metabolism, almost half of the otherwise apparently healthy 173 women were found to have conditions that could affect the bone after careful evaluation. This speaks strongly of the need for a thorough medical evaluation once a low bone density is identified.

Freitag et al. (5) studied 272 individuals (258 women, 14 men) with an average age of 71.8 years, all of whom had T-scores at the lumbar spine, hip, or both of −2 or poorer. These were community-dwelling patients, living in the state of New York who had been referred for an initial evaluation after the finding of a low bone density or after the finding of a vertebral compression fracture or radiographic osteopenia. In this study, 24.7% of the patients were found to have conditions associated with bone loss or osteoporosis. Vitamin D deficiency, defined in this study as a 25-OH vitamin D level <16 ng/ml, was found in 17.9% of the patients. The authors noted that it was likely that vitamin D deficiency was underestimated in this study because some of the patients may have been advised to start vitamin D supplementation before being tested. Hypercalciuria, defined as >250 mg/24 hours was found in 6.3%. Hyperparathyroidism was found in two patients.

In a retrospective chart review at Brigham and Women's Hospital in Boston, MA, of 237 community-based women, Haden et al. (6) identified secondary causes of low bone density in 54%. These women had a median age of 56 years and median T-scores at the lumbar spine and femoral neck respectively of −2.35 and −3.25. Glucocorticoid use at a dose of ≥7.5 mg prednisone daily was found in 16.5%. Thyroid disease was found in 12.7% and premature ovarian failure without estrogen therapy in 11%. Organ transplantation was noted in 2.5%, gastrointestinal disorders such as sprue and inflammatory bowel disease were noted in 4.6%, rheumatoid disorders were noted in 3.0%, and 1.7% had hyperparathyroidism. The most common laboratory abnormality found in this study was a low 25-OH vitamin D level (defined as <15 ng/ml) in 16%. Abnormal serum and urine protein electrophoresis was found in 6% each and 4% were found to have suppressed TSH levels.

In a study of 377 individuals (285 women, 92 men) from Austria with osteoporosis, Deutschmann et al. (7) found that 63.9% had one or more identifiable secondary

causes. Lactose malabsorption was found in 18.6% of the patients and a history of hyperthyroidism was found in 13.3%. Hypercalciuria was found in 7.7% and hyperparathyroidism in 4.9%.

Although these studies vary by geographic location, patient age, and the nature of the referral center, the most common laboratory-detected secondary causes of bone loss would seem to be vitamin D insufficiency/deficiency, hypercalciuria, hyperthyroidism, malabsorption, and malignancy. Historically, corticosteroid use ranks as the most common secondary condition that could affect mineral metabolism. Extensive lists of conditions and drugs that could or are known to affect bone metabolism have been compiled by various authors and organizations. There are more similarities among them than differences. These lists tend to grow rapidly as more diseases and drugs are recognized as potentially affecting bone. Table 12-3 summarizes known conditions and drugs associated with bone loss or osteoporosis that should be considered in the evaluation of the patient (*8*).

AN APPROACH TO THE EVALUATION OF THE PATIENT

The long list of conditions in Table 12-3 which may contribute to or cause bone loss leading to osteoporosis should not be considered complete. Even when considerations are limited to the listed conditions, an evaluation to exclude every listed cause would be overwhelmingly complex and expensive. Some prioritizing, therefore, is in order. A careful medical history can exclude or increase suspicion of many of these conditions. Certainly the medical history can identify current or past medications and surgeries that may affect bone metabolism. The laboratory evaluation of the patient may be directed by findings in the medical history and physical examination. Even in the absence of significant findings in the medical history or physical examination, various authors have recommended approaches to the laboratory evaluation based on the prevalence of specific secondary causes of osteoporosis and cost–effectiveness analyses.

One of the first was the study from Tannebaum et al. (*12*) In this cross-sectional chart review study, the authors identified 664 postmenopausal women with osteoporosis aged 45 and older, who were seen consecutively in the Osteoporosis and Metabolic Bone Disease Program at Mount Sinai Medical Center. Based on a thorough medical history alone, the authors identified 355 (54%) of the women as having conditions or a history of medication use that could have an affect on bone metabolism. Out of the remaining 309 women, 173 met the authors' criteria for a complete battery of lab tests to exclude undetected causes of bone loss. Based on these findings, the authors' initially suggested that a cost-effective approach to the initial laboratory evaluation of postmenopausal women with osteoporosis would consist of measurements of the serum calcium, PTH, 24-hour urine calcium, and, in women on thyroid hormone replacement, a TSH (*2*). They noted that this approach identified 85% of all the observed disorders at a cost of $272 per diagnosis or $75 per patient tested, at the time this study was performed. In a subsequent analysis of these data as criteria for vitamin D insufficiency and deficiency were revised, the authors' found that the performance of a 25-OH vitamin D level instead of the measurement of PTH resulted in the identification of 92%

Table 12-3
Conditions, Diseases, and Medications that Cause or Contribute to Osteoporosis and Fractures

Lifestyle Factors		
Low calcium intake	Vitamin D insufficiency	Excess vitamin A
High caffeine intake	High salt intake	Aluminum (in antacids)
Alcohol (three or more drinks/d)	Inadequate physical activity	Immobilization
Smoking (active or passive)	Falling	Thinness
Genetic Factors		
Cystic fibrosis	Homocystinuria	Osteogenesis imperfecta
Ehlers-Danlos	Hypophosphatasia	Parenteral history of hip fracture
Gaucher's disease	Idiopathic hypercalciuria	Porphyria
Glycogen storage disease	Marfan syndrome	Riley-Day syndrome
Hemochromatosis	Menkes steely hair syndrome	
Hypogonadal states		
Androgen insensitivity	Hyperprolactinemia	Turner's & Klinefelter's syndromes
Anorexia nervosa and bulimia	Panhypopituitarism	
Athletic amenorrhea	Premature ovarian failure	
Endocrine disorders		
Adrenal insufficiency	Diabetes mellitus	Thyrotoxicosis
Cushing's syndrome	Hyperparathyroidism	
Gastrointestinal disorders		
Celiac disease	Inflammatory bowel disease	Primary biliary cirrhosis
Gastric bypass	Malabsorption	
GI surgery	Pancreatic disease	
Hematologic disorders		
Hemophilia	Multiple myeloma	Systemic mastocytosis
Leukemia and lymphomas	Sickle cell disease	Thalassemia
Rheumatic and Auto-immune diseases		
Ankylosing spondylitis	Lupus	Rheumatoid arthritis
Miscellaneous diseases		
Alcoholism	Emphysema	Multiple dystrophy
Amyloidosis	End stage renal disease	Parenteral nutrition
Chronic metabolic acidosis	Epilepsy	Post-transplant bone disease
Congestive heart failure	Idiopathic scoliosis	Prior fracture as an adult
Depression	Multiple sclerosis	Sarcoidosis
Medications		
Anticoagulants (heparin)	Cancer chemotherapeutic drugs	Gonadotropin-releasing hormone agonists
Anticonvulsants	Cyclosporine A and tacrolimus	Lithium
Aromatise inhibitors	Depo-medroxyprogesterone	
Barbiturates	Glucocorticoids ($\geq$ 5 mg/d of prednisone or equivalent for $\geq$ 3 mo)	

Reproduced with permission from ref. (*8*).

of all the observed disorders at a lower cost of $134 per diagnosis and $56 to $79 per patient screened (cost estimates are based on 2001 Medicare reimbursement rates) (*9*).

The American Association of Clinical Endocrinologists (AACE) issued guidelines in 2001 (*10*) and again in 2003 (*11*) for the prevention and treatment of postmenopausal osteoporosis. AACE recommended that the initial evaluation of the woman with osteoporosis should include a complete blood count, serum chemistries, and urinary calcium excretion. Based on the medical history or findings on physical examination, AACE recommended additional tests to be considered. These recommendations are summarized in Table 12-4. In the years that have followed these recommendations, the recognition of the prevalence of vitamin D insufficiency has prompted most authorities to recommend that the 25-OH vitamin D level be performed as part of the initial evaluation of the patient (*12*).

Table 12-4
Laboratory Assessment of the Woman with Osteoporosis as Recommended by the American Association of Clinical Endocrinologists

Initial Laboratory Tests
  Complete blood count
  Serum chemistry, including calcium, phosphorus, total protein, albumin, liver
    enzymes, alkaline phosphatase, creatinine, and electrolytes
  Urinary calcium excretion
Additional Tests as Indicated Based on the Medical History and Physical
 Examination
  TSH
  PTH
  25-OH vitamin D
  Urinary free cortisol and other tests for suspected adrenal hypersecretion
  Acid-base studies
  Biochemical markers of bone turnover
  Serum tryptase, urine N-methylhistamine, or other tests for mastocytosis
  Serum and/or urine protein electrophoresis
  Bone marrow aspiration and biopsy to exclude marrow based diseases
  Undecalcified iliac bone biopsy with double tetracycline labeling

PTH, parathyroid hormone; TSH, thyroid stimulating hormone
Reproduced with permission of the American Association of Clinical Endocrinologists ref. (*11*)

Jamal and colleagues recommended against any routine panel of laboratory tests for otherwise healthy women with osteoporosis in 2005 (*13*). Using data from over 15,000 women who had previously been screened for participation in the Fracture Intervention Trial (FIT) (*14*), the authors compared the prevalence of abnormal laboratory findings in women with osteoporosis to women with osteopenia or normal bone density, using World Health Organization criteria for the diagnosis of osteoporosis (*15*). The screening laboratory tests utilized in FIT are listed in Table 12-5. Note that a 25-OH vitamin D level was not done, as its importance was not recognized in 1993. The authors found that 57.1% of the women with osteoporosis had one or more abnormal test results compared to 58.3% of the women with osteopenia or normal bone density. These percentages are not statistically significantly different. In looking at specific test abnormalities, an abnormal TSH level was found significantly more often in women with osteoporosis

Table 12-5
Screening Laboratory Tests Performed in the Fracture
Intervention Trial

TSH	Total Bilirubin
PTH	AST
Calcium	ALT
Albumin	ALP
Phosphorus	BUN
Sodium	Creatinine
Potassium	CBC
Bicarbonate	Glucose

TSH, thyroid stimulating hormone; PTH, parathyroid hormone. AST, aspartate aminotransferase; ALT, alanine aminotransferase; ALP, alkaline phosphatase; BUN, blood urea nitrogen; CBC, complete blood count.

Reproduced with kind permission of Springer Science+Business Media from ref. (*13*). Note that 25-OH vitamin D levels were not done in this early trial.

than in women with osteopenia or normal bone densities. As a consequence, Jamal and colleagues suggested that a "routine" panel of laboratory tests was not useful in the evaluation of women with osteoporosis because the prevalence of abnormalities was not different from women without osteoporosis. The one exception appeared to be the measurement of TSH, for which abnormalities were found at a higher prevalence in women with osteoporosis than in women with osteopenia or normal bone density. The authors noted that a potential limitation of their findings was that only the prevalence of the abnormalities was assessed and not the clinical implications of their findings. This is a very important limitation. The clinical goal is to identify potential causes of bone loss in order to address them. Such causes of bone loss can be found in the woman with osteopenia as well as in the woman with osteoporosis. That the percentages of lab abnormalities were not different between the two groups is clinically irrelevant.

In 2006, the North American Menopause Society issued guidelines for the management of osteoporosis in postmenopausal women (*16*). In these guidelines, recommendations for "routine" laboratory tests included a complete blood count, serum calcium, 25-OH vitamin D, albumin, alkaline phosphatase, and urinary calcium. In 2008, the National Osteoporosis Foundation (*8*) recommended that biochemical testing generally be considered in patients with documented osteoporosis prior to the initiation of treatment. If a specific secondary cause of osteoporosis was suspected in a patient, the NOF recommended that relevant testing be pursued to identify or exclude the suspected secondary cause, noting such tests as the TSH, serum protein electrophoresis, cortisol, or antibodies suggestive of a gluten-sensitive enteropathy. In general, the initial evaluation recommended by AACE in 2003 (see Table 12-4), with the addition of a 25-OH vitamin D level for all patients and a TSH in individuals taking thyroid hormone replacement appears most appropriate. While this discussion has focused on the initial evaluation of the patient with low bone density or osteoporosis, the evaluation of the patient who does not respond as expected to osteoporotic therapies must also be considered. Co-morbid conditions, calcium and vitamin D deficiency, malabsorption, and other metabolic factors have been noted among the leading causes of apparent non-response to therapy (*17*). In any patient who appears to be a non-responder to prescribed therapy,

Table 12-6
Secondary Causes of Osteoporosis in Men

Hypogonadism	Anticonvulsants
Glucocorticoid excess	Thyrotoxicosis
Alcoholism	Immobilization
Gastrointestinal disorders/malabsorption	Hemochromatosis
Hepatic insufficiency	Systemic mastocytosis
Renal insufficiency	Neoplastic diseases
Cystic fibrosis	Eating disturbance
Hypercalciuria	Rheumatoid arthritis
Hyperparathyroidism	

Adapted with permission of the Elsevier from Orwoll ES. The clinical evaluation of osteoporosis in men. In ref. (*21*).

serious consideration must be given to the possibility of a previously undetected secondary cause of bone loss and the need for laboratory evaluation of suspected causes.

Special Considerations in Men with Low Bone Density or Osteoporosis.

Men are generally subject to the same secondary causes of bone loss or osteoporosis as are women. The basic approach to the laboratory testing, with the obvious exception of measuring the testosterone level, is the same as in women. Measurement of the total testosterone level is recommended in men (*18–20*). Hypogonadism, glucocorticoid excess, and alcoholism rank repeatedly as the major secondary causes of osteoporosis in men (*18–21*). Hypogonadism is a major cause of osteoporosis in men, just as it is in women. However, because hypogonadism is not expected in men, it is considered a secondary cause of osteoporosis. Secondary causes of osteoporosis in men are listed in Table 12-6.

SPECIFIC DISEASES AND CONDITIONS

The list of diseases, conditions, and medications use in Table 12-3 is not exhaustive. It is a list that changes daily as medical knowledge increases. While many of the components of that list can be identified or excluded based on the medical history, some cannot. In that setting, the densitometrist's medical background may leave him or her uncertain of the recommendations on how to proceed with laboratory testing. The following discussion highlights some of these conditions and the recommended laboratory testing, either because of their potential unfamiliarity to many densitometrists, the propensity for the diagnosis to be missed, or their marked prevalence as causes of secondary osteoporosis.

Vitamin D Insufficiency/Deficiency

In 1990, the concept of a continuum of effects on the bone with declining levels of 25-OH vitamin D was elucidated (*22*). Instead of the traditional concept of undesirable effects on the bone and calcium metabolism being seen only at very low 25-OH vitamin D levels, the effects of declining vitamin D levels on the bone were divided into 3 stages. In stage 1, calcium absorption is reduced, leading to depletion of skeletal calcium and osteoporosis. Biochemically, no abnormalities are found in stage 1 and there is no evidence of osteomalacia on bone biopsy. In stage 2, however, early changes of osteomalacia are found on bone biopsy, although clinically there are still no

biochemical abnormalities. Such patients will have depleted skeletal calcium reserves and osteoporosis because of the decline in calcium absorption. In stage 3, osteomalacia becomes apparent based on biochemical and histomorphometric measures.

This continuum of pathologic effects on the bone with ever-declining vitamin D stores required a reassessment of the traditional dichotomy between pathologically low and so-called normal vitamin D levels. A patient's vitamin D status is best assessed by the measurement of 25-OH vitamin D (*23*). The distinction between normalcy and disease had previously been set at 25-OH vitamin D level less than 20 nmol/L (8 ng/ml[4]), because this was the level associated with overt disease such as osteomalacia. At a level of 22 nmol/L (9 ng/ml) or higher, the 25-OH vitamin D level was considered normal. With the observations from Parfitt (*22*), it was clear that this was inappropriate. The question then became what should the 25-OH vitamin D level be for optimum bone health?

Based on a review of published literature, Heaney (*24*) observed that there was an established relationship between the malabsorption of calcium and increased fracture risk at 25-OH vitamin D levels below 80 nmol/L (32 ng/ml). At a round table discussion convened as part of the 5th International Symposium on the Nutritional Aspects of Osteoporosis, five of six experts in the field of vitamin D metabolism suggested that the minimum 25-OH vitamin D level for optimum bone health was between 70 and 80 nmol/L (28–32 ng/ml) (*25*). As a result of these observations, clinical terminology has changed such that a 25-OH vitamin D level of 75 nmol/L (30 ng/ml) or higher is now considered normal. A very low 25-OH vitamin D level of 20 nmol/L (8 ng/ml) or less is considered vitamin D deficiency. Values between 20 and 75 nmol/L represent vitamin D insufficiency.

Using these cut points and the newer terminology of vitamin D insufficiency, studies have identified a much higher prevalence of inadequate vitamin D than was previously thought to exist. Holick and colleagues (*26*) quantified the prevalence of vitamin D insufficiency and deficiency in 1536 community-dwelling postmenopausal women who were receiving pharmacologic intervention to prevent or treat osteoporosis. In this study, 52% of the women had 25-OH vitamin D levels <75 nmol/L (<30 ng/ml) and 18% had values <50 nmol/L (<20 ng/ml). The majority of women in this study lived above a latitude of 35° N, but the prevalence of vitamin D insufficiency appeared to be just as great in women living below the 35° N latitude. This finding suggested that populations living in the southern United States were not protected from vitamin D inadequacy from the sunshine in those regions. Binkley et al. (*27*) similarly reported that 51% of a convenience sample of adults living in Hawaii (latitude 21° N) had 25-OH vitamin D levels <75 nmol/L (<30 ng/ml). This finding is extremely important as it appears that below levels of 77 nmol/L (31 ng/ml) PTH begins to rise (*26, 28*). In 2005, Simonelli et al. (*29*) reported that 76 out of 78 consecutive patients who were hospitalized for hip or extremity fracture had 25-OH vitamin D concentrations below 75 nmol/L (30 ng/ml). The majority (81%) had 25-OH vitamin D levels <50 nmol/L (<20 ng/ml). In summary, it has become increasingly clear that vitamin D insufficiency is far more common than previously believed, regardless of the geographic location of the patient. Virtually all

---

[4] To convert nmol/L to ng/ml, multiply the nmol/L value by 2.496.

of the current prescription interventions for the treatment of osteoporosis have package labeling that states that disorders of mineral metabolism should be corrected before initiating therapy. This is for reasons of safety as well as efficacy of the prescription agent. In a study of 175 patients with osteoporosis treated with oral bisphosphonates Geller et al. (*30*) identified 39 patients with a significant decline in BMD in the absence of any other known cause of bone loss. Twenty of the 39 patients were subsequently found to have 25-OH vitamin D levels <75 nmol/L (<30 ng/ml). Correction of the 25-OH vitamin D level was associated with significant increases in both lumbar spine and proximal femur BMD. Deane and colleagues (*31*) reported a statistically significantly greater increase in BMD at the total hip with bisphosphonate treatment in 106 women with PTH levels of 41 ng/L or less compared to those with higher PTH levels. The lower PTH levels were seen in women with 25-OH vitamin D levels >70 nmol/L (> 28 ng/ml). In a study from Adami et al. (*32*) the odds ratio for incident fractures in vitamin D deficient women treated with alendronate, risedronate, and raloxifene was 1.77 compared to similarly treated vitamin D replete women. The identification of vitamin D insufficiency/deficiency is relatively straightforward. It is also an easily and inexpensively correctable cause of bone loss. The measurement of 25-OH vitamin D should be included in the evaluation of anyone suspected of bone loss or who is being treated with a pharmacologic agent for the prevention or treatment of osteoporosis.

Specific Considerations for Laboratory Tests Related to Vitamin D Insufficiency/Deficiency

Knowledge of the interpretation and pitfalls of some of the relevant laboratory tests may not be relevant to many densitometrists. Nevertheless, some densitometrists are asked for guidance in this regard. The discussion of vitamin D assays, correction of the serum calcium, and interpretation of 24-hour urine calcium values is relevant not only to evaluations for vitamin D insufficiency and deficiency but to evaluations for hyper- or hypoparathyroidism and malabsorption as well.

Vitamin D Assays. In 2004, Binkley and colleagues (*33*) published the results of a study, which highlighted inconsistencies in assays used to measure 25-OH vitamin D. The authors obtained serum for the measurement of 25-OH vitamin D from 10 healthy adults. The serum for each adult was then divided and 20 ng/ml of 25-OH vitamin D was added to one of the specimens. Aliquots from each of the two specimens for the 10 volunteers were sent to six different laboratories for analysis. The mean serum 25-OH vitamin D level in the 10 subjects differenced two-fold between the laboratories. Using a cut off of 80 nmol/L (32 ng/ml), the authors observed that the percent of subjects classified as insufficient ranged from 17–90%, depending on the laboratory. Binkley et al. (*33*) and others (*34*) have called for standardization of the measurement of 25-OH vitamin D and for the voluntary participation of laboratories performing such measurements in the international Vitamin D Quality Assessment Scheme (DEQAS). For a succinct explanation of DEQAS, the reader is referred to the report from Carter et al. (*34*)

An additional caveat in the interpretation of 25-OH vitamin D levels is the ability of the assay to measure both 25-OH vitamin D_3 and 25-OH vitamin D_2(*35*). The value will be reported as the total 25-OH vitamin D level. This total, however, is the sum of the 25-OH vitamin D_2 and 25-OH vitamin D_3. Over-the-counter vitamin supplements in the United States may contain either vitamin D_2 or vitamin D_3. Increasingly, manufacturers are using vitamin D_3 because of the recognition of the superiority of vitamin D_3 to

vitamin D_2(36). However, the only prescription form of vitamin D is vitamin D_2 in a 50,000 IU dose. If a patient is being treated with this form of vitamin D, it is imperative that the assay chosen accurately capture increments in 25-OH vitamin D_2 in order for the physician to assess the therapeutic response. If the assay does not accurately capture 25-OH vitamin D_2, the physician may be misled into thinking that the prescribed therapy is ineffective.

Correction of the Serum Calcium. In clinical practice it is common to measure the total serum calcium instead of the ionized serum calcium. Approximately 45% of the calcium is bound to serum proteins and about 50% is ionized (37). Because of the high protein binding, alterations in the levels of serum proteins, in particular albumin, can result in misleading results in the total serum calcium if it is not corrected for the albumin value. The formula for the correction is as follows:

$$[Ca]_{S_{Corrected}} = [Ca]_S + 0.8\,(4 - [Alb]_S) \tag{1}$$

 in which $[Ca]_{SCorrected}$ is the corrected serum calcium, $[Ca]_S$ is the total serum calcium, and $[Alb]_S$ is the serum albumin level. If the ionized calcium level is measured, no correction is necessary for the serum albumin level. Some authors suggested that the ionized calcium replace the measurement of total serum calcium in the investigation of disorders of mineral metabolism (38).

Interpretation of the 24-Hour Urine Calcium. The 24-hour urine calcium collection is performed to assist in the evaluation of hyper-or hypoparathyroidism, vitamin D insufficiency/deficiency, and various causes of malabsorption. Its interpretation, however, can be affected by the patient's calcium intake, weight, and, for women, estrogen repletion. Heaney and colleagues (39) studied 191 Caucasian women without known disorders of mineral metabolism with an average age of 40.4 years. Women were considered estrogen replete if they were premenopausal or postmenopausal receiving estrogen or hormone therapy. Postmenopausal women not receiving estrogen or hormone therapy were considered estrogen-deficient. During an inpatient evaluation, dietary calcium intake was controlled to match the patient's usual dietary calcium intake. The authors found that urinary calcium rose with calcium intake in both the estrogen-replete and estrogen-deprived women. This effect was more pronounced in the higher intake ranges than in the lower intake ranges. In addition, estrogen-replete women had 24-hour urine calcium values that were ~17% higher than the estrogen-deficient women with the same calcium intake. The authors therefore grouped their findings based on the estrogen status of the women and three categories of calcium intake: low, <500 mg/day; moderate, 500—1000 mg/day, high, >1000 mg/day. These findings are shown in Tables 12-7 and 12-8. As a rule of thumb, the authors suggested that in clinical practice, 250 mg of calcium per 24 hours should be considered the upper limit of normal regardless of calcium intake in an estrogen-replete woman. The corresponding figure in an estrogen-deficient woman was 300 mg per 24 hours. Using a weight-adjusted value, the authors recommended an upper limit of 4.1 mg/kg/day and 5.0 mg/kg/day for the estrogen-replete and estrogen-deficient woman, respectively. For both groups, the lower limit for 24-hour urine calcium was determined to be 40 mg/day.

Osteomalacia

Osteomalacia cannot be readily distinguished from osteoporosis based on the bone density study alone. Plain radiography of the skeleton may also not be helpful in an

Table 12-7

Ninety-Five Percent Probability Range for 24-Hour Urine Calcium in Estrogen-Replete, Normal Middle-Aged Women, by Calcium Intake Level

	Total Excretion (mg/day)			Weight-Adjusted Excretion (mg/kg/day)		
	Calcium Intake Level[a]			Calcium Intake Level[a]		
	Low	Moderate	High	Low	Moderate	High
Lower limit	39	54	66	0.65	0.77	0.98
Upper limit	194	269	327	3.23	3.84	4.89

[a]Low, <500 gm/day; moderate, 500–1000 mg/day; high, >1000 mg/day.
Reproduced with kind permission of Springer Science+Business Media from ref. (*39*).

Table 12-8

Ninety-Five Percent Probability Range for 24-Hour Urine Calcium in Estrogen-Deprived, Normal Middle-Aged Women, by Calcium Intake Level

	Total Excretion (mg/day)			Weight-Adjusted Excretion (mg/kg/day)		
	Calcium Intake Level[a]			Calcium Intake Level[a]		
	Low	Moderate	High	Low	Moderate	High
Lower limit	32	36	45	0.51	0.57	0.69
Upper limit	252	286	357	4.06	4.52	5.47

[a]Low, <500 gm/day; moderate, 500–1000 mg/day; high, >1000 mg/day.
Reproduced with kind permission of Springer Science+Business Media from ref. (*39*).

adult because the skeletal appearance is that of radiographic osteopenia. Trabeculae have been described as coarsened and indistinct in osteomalacia, but that appearance is common in osteoporosis as well. The finding of Looser's zones[5] is considered pathognomonic by some (*40*). Osteomalacia and osteoporosis may also coexist in a patient. Many diseases can cause osteomalacia. Of note, chronic renal insufficiency, renal transplantation, and hemodialysis may cause osteomalacia. Secondary hyperparathyroidism may occur in this setting, which can lead to the finding of an increased lumbar spine bone density from osteosclerosis in the spine. The classic appearance of the spine on plain films from osteosclerosis resulting from secondary hyperparathyroidism is the "rugger-jersey" spine. Clinically, signs and symptoms of osteomalacia include diffuse, non-specific bone pain, and muscle weakness. Fractures may occur as well. Whether signs and symptoms of hypocalcemia appear, such as oral numbness or carpal-pedal spasm depends on the cause of the osteomalacia. Ultimately, the measurement of 25-OH vitamin D becomes paramount in the diagnosis of vitamin D deficiency, which leads to osteomalacia.

[5] Looser's zones (pseudo-fractures) are focal accumulations of osteoid, which occur in cortical bone perpendicular to the long axis of the bone. They may be bilateral and symmetrical.

Primary Hyperparathyroidism

Because only about 20% of patients with hyperparathyroidism are symptomatic with kidney stones, overt bone disease, or proximal neuromuscular weakness (*41*), the diagnosis of hyperparathyroidism is now generally made when suspicion is raised by the finding of an increased serum calcium level. Suspicion should also be raised by the finding of bone loss at the one-third radial site[6] or at the femoral neck with a relatively preserved bone density at the spine. This is because of the predilection for cortical bone loss in hyperparathyroidism and the apparent protective effect of parathyroid hormone on trabecular bone at the spine. Primary hyperparathyroidism is diagnosed by finding an elevated serum calcium level in the presence of a high or inappropriately normal PTH (*42*). However, in some patients the serum calcium level may be normal in the presence of a high PTH. In such cases, it is imperative to establish that the 25-OH vitamin D level is > 50 nmol/L (> 20 ng/ml) and therefore not a likely cause of the increase in PTH. Similarly, medications such as thiazide diuretics and lithium that might increase the PTH level must be excluded (*41*). Finally, not all patients with primary hyperparathyroidism will have an elevated serum calcium level on every measurement. In some cases, only the ionized calcium is increased. The 24-hour urine calcium excretion is generally elevated in primary hyperparathyroidism. However, its primary utility is likely in helping to distinguish between primary hyperparathyroidism and familial benign hypocalciuric hypercalcemia (FBHH). FBHH is an autosomal dominant genetic disorder that is rare but which presents with hypercalcemia and a mildly elevated or inappropriately normal PTH level. However, in FBHH the calcium: creatinine clearance ratio is generally <0.01, whereas in primary hyperparathyroidism it is >0.02 (*42*). Imaging studies such as ^{99}Tc-labeled Sestamibi with SPECT are not used to diagnose primary hyperparathyroidism. They are instead used for pre-operative localization after the establishment of the diagnosis by the laboratory.

Celiac Disease

The treatment of celiac disease is generally the responsibility of a gastroenterologist. Nevertheless, a patient's initial or perhaps only presenting abnormality may be a low bone density. Otherwise, asymptomatic celiac disease must be considered as part of the differential diagnosis of low bone density and osteoporosis.

Celiac disease is thought to be an autoimmune disorder that occurs in genetically predisposed individuals (*43*). The environmental trigger is gluten, which is the major storage protein in wheat and similar grains. Although 50% of adults with celiac disease present with diarrhea, low bone density or osteoporosis can be the first manifestation of celiac disease. Celiac disease was previously thought to be uncommon in the United States in contrast to Europe. However, a study by Fasano and colleagues (*44*) suggested that the incidence of celiac disease in otherwise healthy adults in the United States with no family history of the disease was 1:133. In asymptomatic first-degree relatives of known celiac patients, the incidence was 1:22 and in second-degree relatives 1:39. It is clear that a family history of celiac disease is important in assessing an individual's

---

[6] See Chapter 2 for a discussion of naming conventions for radial and forearm sites.

risk for the disease, but an incidence of 1:133 in healthy, non-relatives of celiac patients suggests that the densitometrist is likely to encounter this disease.

The gold standard for the diagnosis of celiac disease remains the small bowel biopsy (*45*). Serologic testing, however, is extremely useful in identifying patients who should subsequently undergo biopsy. Serologic tests include antigliadin antibodies (AGA), tissue transglutaminase antibodies (tTGA), antiendomysial antibodies (EMA), and antireticulin antibodies. Antireticulin antibodies are generally no longer used, having been replaced by EMA and tTGA antibodies (*43*). tTGA and EMA are remarkably sensitive and specific for celiac disease and are superior in this regard to AGA testing in adults (*43,46*). The sensitivity of both the tTGA and EMA are reported as greater than 90% with a specificity of over 90% and 100%, respectively. Either serologic test is considered appropriate, although the American Gastroenterological Association Institute recommends that the tTGA be considered the test of choice (*47*).

These serologic tests are tests for IgA antibodies. IgA antibody deficiency is common in celiac disease and is estimated at 1:40 (*43*). In this circumstance, the EMA and tTGA will be negative. If celiac disease is still strongly suspected, it is recommended that total IgA levels be measured. If IgA deficiency is found, an IgG tTGA test can be performed.

Other laboratory abnormalities may be found in celiac disease. These include iron deficiency anemia, low serum calcium, low 24-hour urinary calcium excretion, and increased alkaline phosphatase (*48*).

Mastocytosis

Mastocytosis is discussed here, not because it is a common cause of secondary osteoporosis but because it can cause secondary osteoporosis and is easily missed. Mastocytosis is caused by an excess of normal mast cells. Although the disorder is often confined to the skin, other organ systems, like the skeleton, can be affected. Ninety percent of mastocytosis cases are cutaneous mastocytosis and approximately two-thirds of these are urticaria pigmentosa (*49*). Skin lesions, however, may or may not precede systemic manifestations of mastocytosis such as osteoporosis. Several mast cell products have been implicated in the development of low bone density and osteoporosis. These include heparin and prostaglandin D_2. If skin lesions are present, a biopsy of the lesion may be diagnostic. Hypocholesterolemia may be found in systemic disease as well as an increase in alkaline phosphatase and liver enzymes. One of the most sensitive tests for systemic mastocytosis is an elevated serum tryptase level. Other laboratory assessments may include urinary histamine levels or urinary N-methylhistamine. Marrow aspiration and biopsy may be necessary to establish the diagnosis.

Multiple Myeloma

Multiple myeloma is a malignant plasma cell disorder with an annual incidence of about 4.3 per 100,000 people (*50*). It occurs slightly more often in men than in women and is a recognized secondary cause of bone loss or osteoporosis. Abnormalities in the CBC, serum calcium, and creatinine, which are part of the routine evaluation of the patient with low bone density or osteoporosis, may raise suspicion of myeloma. Anemia may be found in 70% of patients with myeloma. Consequently, otherwise unexplained anemia on the CBC should prompt additional testing such as the serum protein electrophoresis (SPEP). Myeloma is characterized by a large increase in M protein, which appears as a spike on electrophoresis. This is due to the production of a monoclonal

immunoglobulin by the malignant plasma cells. The M protein can be detected by SPEP in about 82% of myeloma patients. When indicated, quantitative immunoglobulins can be performed to measure the levels of IgA, IgG, and IgM or less commonly, IgD or IgE. Hypercalcemia may also be found in about one-fourth of multiple myeloma patients and myeloma should be considered in cases of hypercalcemia in which the PTH level is normal. The serum creatinine is reported as elevated in approximately half (*50*).

REFERENCES

1. Indications and reporting for dual-energy x-ray absorptiometry. J Clin Densitom 2004;7(1):37–44.
2. Tannenbaum C, Clark J, Schwartzman K et al. Yield of laboratory testing to identify secondary contributors to osteoporosis in otherwise healthy women. J Clin Endocrinol Metab 2002;87(10)4431–4437.
3. Johnson BE, Lucasey B, Robinson RG, Lukert BP. Contributing diagnoses in osteoporosis. The value of a complete medical evaluation. Arch Intern Med 1989;149(5)1069–1072.
4. Brown JP, Ioannidis G, Adachi JD et al. Secondary causes of osteoporosis in patients registered in the Canadian Database of Osteoporosis and Osteopenia (CANDOO). J Bone Miner Res 2002;17:S261.
5. Freitag A, Barzel US. Differential diagnosis of osteoporosis. Gerontology 2002;48(2)98–102.
6. Haden ST, Fuleihan GE, Angell JE, Cotran NM, LeBoff MS. Calcidiol and PTH levels in women attending an osteoporosis program. Calcif Tissue Int 1999;64(4)275–279.
7. Deutschmann HA, Weger M, Weger W, Kotanko P, Deutschmann MJ, Skrabal F. Search for occult secondary osteoporosis: impact of identified possible risk factors on bone mineral density. J Intern Med 2002;252(5)389–397.
8. National Osteoporosis Foundation. Clinician's guide to prevention and treatment of osteoporosis. 1–30. 2008. Washington, D.C., National Osteoporosis Foundation.
9. Personal communication from Marjorie M. Luckey.
10. Hodgson SF, Watts NB, Bilezikian JP et al. American Association of Clinical Endocrinologists 2001 Medical Guidelines for Clinical Practice for the Prevention and Management of Postmenopausal Osteoporosis. Endocr Pract 2001;7(4)293–312.
11. Hodgson SF, Watts NB, Bilezikian JP et al. American Association of Clinical Endocrinologists medical guidelines for clinical practice for the prevention and treatment of postmenopausal osteoporosis: 2001 edition, with selected updates for 2003. Endocr Pract 2003;9(6)544–564.
12. Wagman, RB, Marcus R. Beyond bone mineral density—navigating the laboratory assessment of patients with osteoporosis. J Clin Endocrinol Metab 2002;87(10)4429–4430.
13. Jamal SA, Leiter RE, Bayoumi AM, Bauer DC, Cummings SR. Clinical utility of laboratory testing in women with osteoporosis. Osteoporos Int 2005;16(5)534–540.
14. Black DM, Reiss TF, Nevitt MC, Cauley J, Darpf D, Cummings SR. Design of the Fracture Intervention Trial. Osteoporos Int 1993;S3:S29–S39.
15. WHO Study Group. Assessment of fracture risk and its application to screening for postmenopausal osteoporosis. WHO, editor. [843], 1–129. 1994. Geneva. WHO Technical Report Series.
16. Management of osteoporosis in postmenopausal women: 2006 position statement of The North American Menopause Society. Menopause 2006;13(3)340–367.
17. Lewiecki EM. Nonresponders to osteoporosis therapy. J Clin Densitom 2003;6(4)307–314.
18. Ebeling PR. Clinical practice. Osteoporosis in men. N Engl J Med 2008;358(14)1474–1482.
19. Campion JM, Maricic MJ. Osteoporosis in men. Am Fam Physician 2003;67(7)1521–1526.
20. Tuck S, Francis R. Osteoporosis in men. In: Arden N, editor. Osteoporosis. London: Remedica; 2006; 163–;183.
21. Orwoll ES. The clinical evaluation of osteoporosis in men. In: Orwoll ES, editor. Osteoporosis in Men: The Effects of Gender on Skeletal Health. San Diego: Academic Press; 1999;527–552.
22. Parfitt AM. Osteomalacia and related disorders. In: Avioli LV, Krane SM, editors. Metabolic bone disease and clinically related disorders. 2nd ed. Philadelphia: WB Saunders; 1990;329–396.
23. Food and Nutrition Board, Institute of Medicine. Dietary reference intakes for calcium, magnesium, phosphorus, vitamin D, and fluoride. 1997. Washington, D.C., National Academy Press.
24. Heaney RP. Functional indices of vitamin D status and ramifications of vitamin D deficiency. Am J Clin Nutr 2004;80(6 Suppl):1706S–1709S.

25. Dawson-Hughes B, Heaney RP, Holick MF, Lips P, Meunier PJ, Vieth R. Estimates of optimal vitamin D status. Osteoporos Int 2005;16(7)713–716.

26. Holick MF, Siris ES, Binkley N et al. Prevalence of Vitamin D inadequacy among postmenopausal North American women receiving osteoporosis therapy. J Clin Endocrinol Metab 2005;90(6) 3215–3224.

27. Binkley N, Novotny R, Krueger D et al. Low vitamin D status despite abundant sun exposure. J Clin Endocrinol Metab 2007;92(6)2130–2135.

28. Chapuy MC, Preziosi P, Maamer M et al. Prevalence of vitamin D insufficiency in an adult normal population. Osteoporos Int 1997;7(5)439–443.

29. Simonelli C, Weiss TW, Morancey J, Swanson L, Chen YT. Prevalence of vitamin D inadequacy in a minimal trauma fracture population. Curr Med Res Opin 2005;21(7)1069–1074.

30. Geller JL, Hu B, Reed S, Mirocha J, Adams JS. Increase in bone mass after correction of vitamin D insufficiency in bisphosphonate-treated patients. Endocr Pract 2008;14(3)293–297.

31. Deane A, Constancio L, Fogelman I, Hampson G. The impact of vitamin D status on changes in bone mineral density during treatment with bisphosphonates and after discontinuation following long-term use in post-menopausal osteoporosis. BMC Musculoskelet Disord 2007;8:3.

32. Adami S, Giannini S, Bianchi G et al. Vitamin D status and response to treatment in post-menopausal osteoporosis. Osteoporos Int 2008;doi. 10.1007/s00198-008-0650-y.

33. Binkley N, Krueger D, Cowgill CS et al. Assay variation confounds the diagnosis of hypovitaminosis D: a call for standardization. J Clin Endocrinol Metab 2004;89(7)3152–3157.

34. Carter GD, Carter R, Jones J, Berry J. How accurate are assays for 25-hydroxyvitamin D? Data from the international vitamin D external quality assessment scheme. Clin Chem 2004;50(11)2195–2197.

35. Hollis BW. Editorial: The determination of circulating 25-hydroxyvitamin D: no easy task. J Clin Endocrinol Metab 2004;89(7)3149–3151.

36. Armas LA, Hollis BW, Heaney RP. Vitamin D2 is much less effective than vitamin D3 in humans. J Clin Endocrinol Metab 2004;89(11)5387–5391.

37. Disorders of mineral metabolism. In: Beers E, Berkow R, editors. The Merck Manual of Geriatrics. 3rd ed. Whitehouse Station: Merck Research Laboratories,2000;572–583.

38. Larsson L, Magnusson P. Ionized calcium or corrected total calcium? J Bone Miner Res 2003;18(8)1554–1555.

39. Heaney RP, Recker RR, Ryan RA. Urinary calcium in perimenopausal women: normative values. Osteoporos Int 1999;9(1)13–18.

40. Steinbach HL, Noetzli M. Roentgen appearance of the skeleton in osteomalacia and rickets. Am J Radiol 1964;91:955.

41. Bilezikian JP, Silverberg SJ. Clinical practice. Asymptomatic primary hyperparathyroidism. N Engl J Med 2004;350(17)1746–1751.

42. Bilezikian JP, Potts JT, Jr., Fuleihan G et al. Summary statement from a workshop on asymptomatic primary hyperparathyroidism: a perspective for the 21st century. J Clin Endocrinol Metab 2002;87(12)5353–5361.

43. Green PH, Cellier C. Celiac disease. N Engl J Med 2007;357(17)1731–1743.

44. Fasano A, Berti I, Gerarduzzi T et al. Prevalence of celiac disease in at-risk and not-at-risk groups in the United States: a large multicenter study. Arch Intern Med 2003;163(3)286–292.

45. Rostom A, Murray JA, Kagnoff MF. American Gastroenterological Association (AGA) Institute technical review on the diagnosis and management of celiac disease. Gastroenterology 2006;131(6) 1981–2002.

46. Vitoria JC, Arrieta A, Arranz C et al. Antibodies to gliadin, endomysium, and tissue transglutaminase for the diagnosis of celiac disease. J Pediatr Gastroenterol Nutr 1999;29(5)571–574.

47. AGA Institute Medical Position Statement on the Diagnosis and Management of Celiac Disease. Gastroenterology 2006;131(6)1977–1980.

48. Fitzpatrick LA. Secondary causes of osteoporosis. Mayo Clin Proc 2002;77(5)453–468.

49. Alto WA, Clarcq L. Cutaneous and systemic manifestations of mastocytosis. Am Fam Physician 1999;59(11)3047–3060.

50. Rajkumar SV, Kyle RA. Multiple myeloma: diagnosis and treatment. Mayo Clin Proc 2005;80(10)1371–1382.

13 New Applications for DXA

Densitometry has primarily been a quantitative measurement technique. The first skeletal images from a densitometer, as seen in Fig. 2-7 in an earlier chapter, were only vaguely reminiscent of the actual bone. The poor image quality had little effect on the ability to quantify the bone density, which was the primary purpose of the various techniques. Imaging, as a potential application of densitometry, has been anticipated for over a decade. Continued improvements in DXA technology combined with modern computer capabilities have resulted in dramatic improvements in imaging and acquisition speed.

LATERAL SPINE IMAGING

Truly remarkable images of the spine such as the RVA[TM] image from a Hologic Discovery[1] seen in Fig. 13-1 are possible today. When combined with the very low radiation exposure in comparison to conventional X-ray studies, the use of lateral spine DXA imaging for the diagnosis of vertebral fractures and assessment of aortic calcification has become a clinical reality.

The Relationship Between Prevalent Spine Fractures and Future Fracture Risk

A number of studies have demonstrated that the presence of a spine fracture is predictive of future fractures, independent of bone density (*1–7*). The strongest association is between existing spine fractures and future spine fractures with estimates of the increase

---

[1] RVA[TM] is a trademarked reference for radiographic vertebral assessment from Hologic. Specifications for the Hologic Discovery can be found in Chapter 15.

Fig. 13-1. An RVA image from the Hologic Discovery. The vertebrae are seen with remarkable clarity enabling structural diagnoses to be made at a fraction of the radiation exposure of plain spine films. Image courtesy of Hologic, Inc., Bedford, MA.

in risk from only one prevalent spine fracture of 3- to 11.1-fold. One of the first such studies was from Ross et al. (*1*). This study was performed in the same group of women from the Kuakini Osteoporosis Study who were described earlier in the discussion of the definition of a spine fracture threshold. In this study, the presence of one vertebral fracture at baseline resulted in a 5-fold increase in the risk for new vertebral fractures. If two vertebral fractures were present at baseline, the risk for new vertebral fractures increased 12-fold.

In a second study, Ross et al. (*3*) evaluated 380 postmenopausal women with an average age of 65 who were participants in a multicenter trial of etidronate therapy for postmenopausal osteoporosis. In this study, the presence of one or two spine fractures at baseline increased the risk of future spine fractures 7.4-fold.

Nevitt et al. (*2*) evaluated the effect of the number and location of prevalent spine fractures on future fracture risk using data from the Fracture Intervention Trial (FIT), a placebo-controlled, randomized trial of alendronate therapy in postmenopausal osteoporosis. Data from 6082 women were included in this analysis, roughly half of whom were receiving a placebo. Vertebral fractures at baseline were found in 1950 women. Four hundred sixty-two new vertebral fractures occurred in 344 women during an average of 3.8 years of follow-up. Nevitt et al. found that the presence of just one vertebral fracture at baseline resulted in a 3-fold increase in the risk for new vertebral fractures compared to women without a vertebral fracture at baseline. This was true even after adjustment for age, total hip BMD, and weight. Prevalent spine fractures appeared to be stronger predictors of incident spine fractures in the upper spine than in the lower spine.

Data obtained during the Study of Osteoporotic Fractures, a prospective study of 9704 women aged 65 and older, were analyzed by Black et al. (*4*) to determine the effect of prevalent spine fracture on future fracture risk. Seven thousand two hundred thirty-eight women had technically adequate films for morphometric evaluation of spine fracture at baseline and after an average follow-up of 3.7 years. Prevalent spine fractures were present at baseline in 1915 women. Two or more deformities were seen in 797 and four or more in 211. Over the follow-up period, 389 women developed new vertebral fractures. The risk for new vertebral fracture increased as the number of prevalent vertebral fractures increased. In women with one prevalent vertebral fracture the relative risk for new vertebral fracture was 3.2. For women with three or more prevalent vertebral fractures, the relative risk of new vertebral fracture was 10.6 even after adjustment for age.

In a population-based epidemiologic study (*5*) of vertebral fracture incidence between 1985 and 1994 in Rochester, MN, 820 residents (619 women, 201 men) were diagnosed as having one or more vertebral fractures. The residents were followed until death or the last clinical contact during the study period. The average age at the time of the first vertebral fracture was 67.3 years for women and 55.5 years for men. Compared to fracture incidence rates expected in the general population, the observed rate was almost three times higher in individuals age 35 or older with a prior vertebral fracture. The increase in risk for new vertebral fractures was 12.6-fold higher for both sexes combined and 11.1-fold higher for women alone.

Prevalent vertebral fractures have also been shown to be predictive of non-vertebral fractures. Two hundred fifty subjects (225 women, 25 men) with an average age of 74 years were evaluated for the presence of vertebral deformity at baseline and the subsequent development of non-vertebral fracture during a follow-up period of 3 years (*6*). During this period, 39 subjects suffered non-vertebral fractures of which 10 were hip fractures, 17 were forearm fractures, and 13 were at a variety of other skeletal sites. Twenty-seven of the 39 subjects who developed non-vertebral fractures had spine deformities at baseline. Spinal deformities were graded as mild or severe based on the number of vertebrae affected and/or the degree of deformity. After adjusting for age, sex, and BMD in the femoral neck (DXA), subjects with severe spinal deformities at baseline had a 4-fold increase in the risk of non-vertebral fracture (relative risk 4.1; 95% confidence interval 1.3–12.4). Subjects with mild spinal deformities had a relative risk of 1.5 for the development of non-vertebral fractures but this increase in relative risk was not significant at the 95% confidence level.

In the study from Black et al. (*4*) utilizing data from the Study of Osteoporotic Fractures, prevalent spine fractures were also predictive of non-spine fractures in general

and hip fractures, specifically. The risk of any non-spine fracture was increased 1.9-fold while the risk of hip fracture was increased 3.8-fold. The authors could not show a statistically significant increase in the risk for wrist fracture based on the finding of a prevalent spine fracture. In the Rochester, MN, population-based study from Melton et al. (5) the finding of a prevalent spine fracture resulted in a 2.3-fold increase in the risk for hip fracture. Unlike the study from Black et al., Melton and colleagues did find a significant increase in the risk of distal forearm fracture of 1.6.

Klotzbuecher et al. (7) reviewed the available literature in 2000 to summarize the known associations between prevalent fracture and future fracture risk of all types. They performed a literature search that spanned 1966 through 1999, identifying 15 publications that reported associations between prevalent spine fractures and subsequent fractures. Based on this review, Klotzbuecher et al. concluded that prevalent spine fracture increases the risk for future spine fracture 4.4-fold (95% confidence interval 3.6–5.4). The risk of subsequent hip fracture was increased 2.3-fold (95% confidence interval 2.0–2.8) and the risk of subsequent wrist fracture was increased 1.4-fold (95% confidence interval 1.2–1.7). The authors noted that in 5 of the 15 studies reviewed, the associations between prevalent spine fracture and subsequent fracture were reduced by only 20% or less when adjustments were made for BMD. Nevertheless, BMD was also a strong predictor of future fractures, independent of prior fractures. Klotzbuecher et al. concluded that BMD and prevalent fractures were complementary in the prediction of future fracture risk.

DIAGNOSING VERTEBRAL FRACTURES

The assessment of fracture risk is incomplete without an assessment of the presence of vertebral fracture. Only 33% of vertebral fractures are symptomatic (8). Of those fractures that are not clinically symptomatic, 78% remain unrecognized (9). It has also become sadly apparent, that vertebral deformities are not being recognized on plain films or that they are not regarded as clinically important (10–13). Identification of a vertebral fracture may result in a different diagnosis than would otherwise result based on the bone density alone. This may also result in a different approach to the management of the patient. In addition, the presence of vertebral fracture is unquestionably an independent predictor of fracture risk. A more aggressive effort to evaluate patients for vertebral fracture is clearly indicated.

A change in the size or shape of a vertebral body is characterized generically as a deformity. The "gold standard" for defining the types of vertebral deformities that is the result of bone fragility and therefore considered fractures remains controversial. Both semiquantitative and quantitative approaches for defining vertebral fractures are used clinically. Either can be applied to plain radiographs as well as densitometric spine images. In clinical trials in which vertebral fractures must be identified, both approaches are generally used.

Vertebral Fracture Assessment with Genant's Semiquantitative Technique

The semiquantitative (SQ) technique of Genant relies on the expertise of the observer rather than direct measurements of the physical dimensions of the vertebrae (14). Based on the physical appearance, vertebrae are characterized as being normal or deformed.
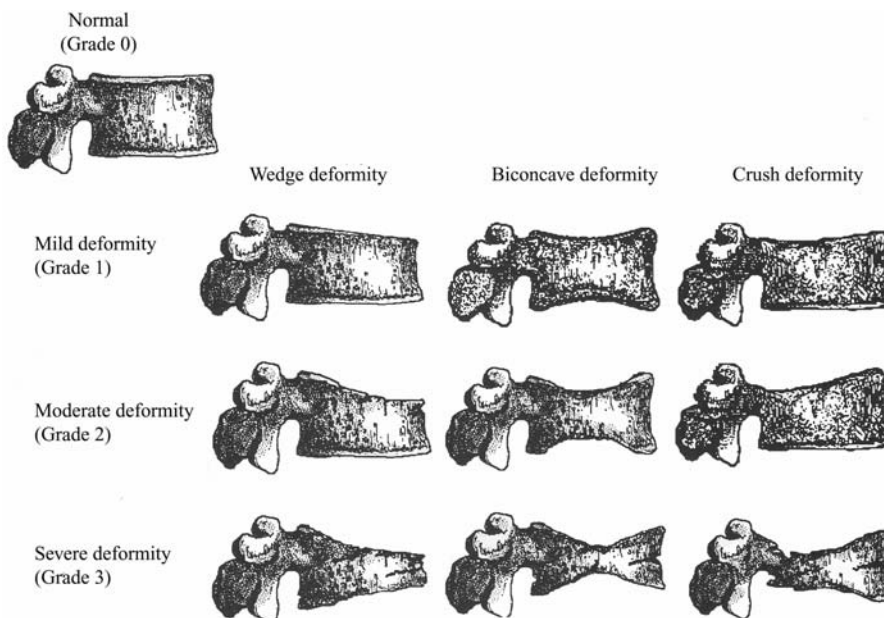
Fig. 13-2. The Genant semiquantitative vertebral fracture grading system. Reproduced courtesy of Dr. Harry Genant, San Francisco, CA.

The types of deformation are mild (grade 1), moderate (grade 2), and severe (grade 3). Deformed vertebrae are also described based on the shape of the deformation as wedged (anterior fracture), biconcave (middle fracture), or crushed (posterior fracture). These deformities are illustrated in Fig. 13-2. Although physical measurements are not made with this technique, a grade 1 deformity roughly corresponds to a 20–25% reduction in the anterior, middle, or posterior height of the vertebra and a 10–20% reduction in vertebral area. A grade 2 deformity is the result of a 25–40% reduction in any of the three heights and a reduction in vertebral area of 20–40%. A grade 3 deformity occurs when there is a 40% reduction in any of the three heights and a 40% reduction in vertebral area. This technique has been traditionally used with plain radiographs of the spine but semiquantitative vertebral fracture assessments can be performed with fan-array DXA spine images as well. In fact, some DXA software will automatically assign a fracture type and grade to a vertebral deformity, based on the Genant semiquantitative technique.

Vertebral Fracture Assessment with Quantitative Techniques

Quantitative techniques rely on physical measurements to diagnose vertebral fracture. Reference points are placed on each vertebral body. A common method is the placement of six points, one point at each corner of the vertebral body and one point at the midpoint of each of the endplates. Using these points, the anterior, mid-, and posterior heights (h_a, h_m, and h_p, respectively) of the vertebra are measured. The vertebral area is calculated as the polygon area defined by the six points. In addition to the heights themselves, the anterior-posterior height ratio (h_a/h_p) and the mid-posterior height ratio (h_m/h_p) are calculated. Other ratios include the wedge index ($I_w = h_p/h_a$) (15) and the biconcavity index (h_m/h_a) (16). These measurements were originally made from plain radiographs.

In recent years, measurements were made from digitized films. This is called morphometric radiography (MXR). With the advent of fan-array DXA spine imaging and morphometry software, quantitative vertebral morphometry can be performed using DXA as well, an approach which is called morphometric X-ray absorptiometry (MXA).

Different criteria have been proposed for the diagnosis of prevalent or incident[2] fracture based on quantitative morphometry. Several authorities have proposed that a prevalent fracture should be considered present if there is a 15% or greater reduction in the h_a/h_p or h_m/h_p ratio or the ratio of the posterior height of one vertebra to the posterior height of an adjacent vertebra (h_p/h_{pa}) when compared to the mean value for a normal population (17–19). A more stringent 20% reduction in these ratios has also been proposed. A reduction of 3 SD in the h_a/h_p or h_m/h_p compared to normative data to define vertebral fracture was proposed by Ross et al. and Eastell et al. (20, 21). McCloskey and Kanis (22, 23) also proposed utilizing a 3 SD reduction in any of the ratios combined with reductions in ratios calculated using a predicted posterior height. These morphometric definitions of vertebral fracture require comparisons to normative reference data for a population. Heights may also be adjusted for body size using the dimensions of the fourth thoracic vertebra (T4). In other words, the h_p for T12 can be adjusted or normalized for size by dividing it by the h_p at T4 in the individual. The resulting posterior dimension for T12 is then abbreviated nh_p, reflecting the normalization for size. Minne et al. (24) proposed defining vertebral fracture as being present when any of the three normalized heights was below the third percentile of the normal range. Because vertebrae are expected to have slightly different shapes depending on the vertebral level, individual heights must be compared to normal values that are specific for that vertebral level.

The definition of incident fractures tends to be more straightforward. A decrease of 15% in the h_a, h_m, or h_p from the baseline film is indicative of an incident fracture. Other authorities have proposed a reduction of 20–25% alone for the definition of an incident fracture (25) or this amount of reduction in any of the three heights in combination with a minimum absolute reduction of 4 mm (26).

Performance Comparisons of Semiquantitative and Quantitative Techniques

Quantitative techniques rely heavily on the accuracy of point placements as well as comparisons to reference databases. Point placement can be subjective and affected by the deformity itself or patient positioning. Differences of opinion exist regarding the validity and design of reference databases for vertebral morphometry, just as they do for bone densitometry. Genant's semiquantitative technique is based on the visual recognition of quantitative changes in vertebral shape. The performance of quantitative and semiquantitative techniques in identifying vertebral fractures has been compared in several studies (27–32). In order to compare the techniques, a "gold standard" for the diagnosis of vertebral fracture was generally created by a consensus reading of radiographs by experts. When done in this manner, the semiquantitative and quantitative approaches generally performed equally well but the criteria used to define fracture for the

---

[2] A prevalent fracture is a fracture that is already present at the time the patient is seen. An incident fracture is a fracture that develops at some point in time after the initial evaluation.

quantitative morphometry assessment profoundly effected the agreement between the two techniques. The combination of a semiquantitative and quantitative technique may be better than either alone. Spine imaging with fan-array densitometry combined with modern computer technology makes it possible for the densitometrist to utilize either or both approaches. Lateral spine images, such as the DVA[TM] image from a GE Lunar Prodigy[3] shown in Fig. 13-3, can be evaluated using Genant's semiquantitative method. Morphometric software can also be used to define and measure vertebral heights, as shown in Fig. 13-4.
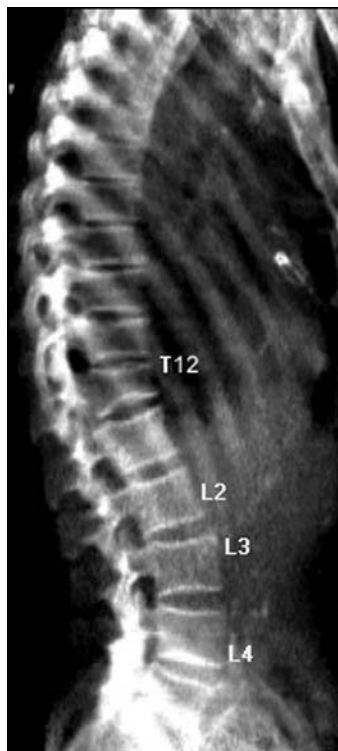
Fig. 13-3. A lateral spine DVA[TM] image from a Lunar Prodigy showing a grade 2 fracture at T12. Case courtesy of GE Medical Systems, Madison, WI.

Spine Imaging with DXA for Diagnosis of Vertebral Fracture

Using fan-array DXA spine imaging, the spine can be imaged from T4 to L5 in the lateral or PA projection. DXA spine imaging can be performed in seconds to minutes, depending on the scan mode, but always at a fraction of the radiation exposure of conventional spine radiographs. Fan-array DXA imaging also largely avoids the problem created by parallax[4] in plain radiography of the spine. Because the movement of the scan

---

[3] DVA[TM] is a trademarked reference to Dual-energy Vertebral Assessment as performed on GE Lunar fan-array DXA devices. Specifications for the GE Lunar Prodigy may be found in Chapter 15.

[4] Parallax refers to an apparent displacement of an object due to a change in the observer's position. In the case of spine radiography, it refers to the angle at which the X-ray beam passes
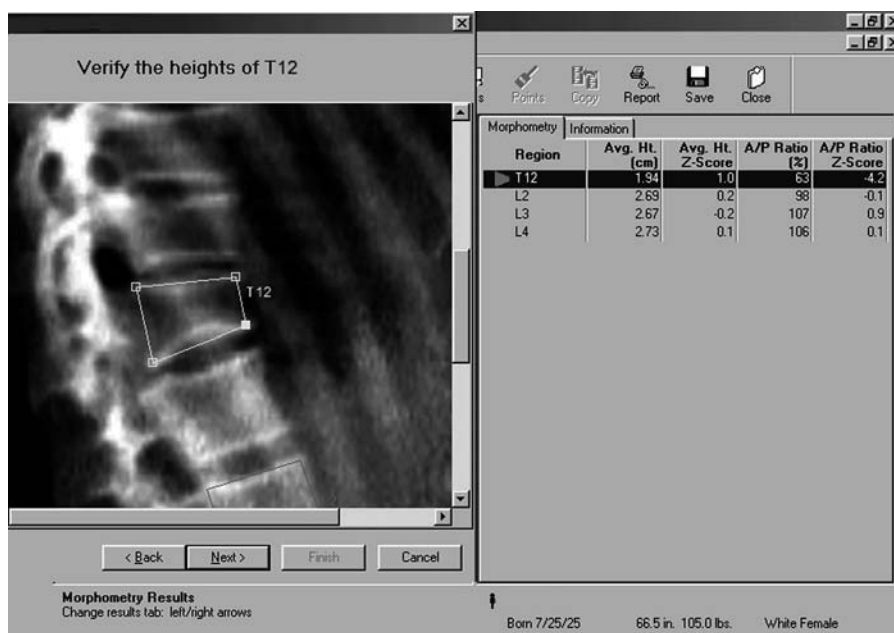
Fig. 13-4. Computerized morphometric analysis of vertebral heights for T12, as seen in Fig. 10-6. Case courtesy of GE Medical Systems, Madison, WI.

arm allows the DXA beam to be passed parallel to the vertebral endplates throughout the entire length of the spine, the vertebral dimensions are not distorted by the angle of the beam. If the patient has severe scoliosis, some parallax effect may be unavoidable.

In 1998, Rea et al. (*33*) evaluated 161 postmenopausal women for fracture using conventional lateral spine radiographs and fan-array lateral spine imaging. Both image types were evaluated using the Genant semiquantitative method. MXA correctly identified 91.9% of the grade 2 and grade 3 spine fractures. When the grade 1 (mild) fractures were included in the total, MXA correctly identified 77.4%. MXA also correctly identified 98.4% of the unfractured vertebrae. This suggests that DXA spine imaging and applying the Genant semiquantitative method was an excellent means of excluding the diagnosis of vertebral fracture. If a fracture was not seen using this technique, it was highly unlikely that a fracture was present at all and extremely unlikely that a grade 2 or grade 3 fracture was present. The agreement in fracture diagnoses between the visual assessment of DXA spine images and the semiquantitative assessment of standard spine radiographs for vertebrae that could be evaluated with both techniques was 96.3%.

Although DXA spine imaging spans T4−L5, it is not uncommon for the uppermost thoracic vertebrae to be poorly visualized. In the study noted above from Rea et al. (*33*) 94.9% of the vertebrae could be evaluated. T4 and T5 were the most common vertebrae that were too poorly visualized to be evaluated. In a study from Schousboe et al. (*34*) in which 342 women underwent DXA lateral spine imaging 92.1% or 4096

through the vertebral bodies. If the X-ray beam is not parallel to the vertebral endplates, the shape of the vertebrae may be distorted, making morphometric measurements inaccurate.

of the 4446 vertebrae studied could be evaluated. In this study, T4−T6 were less likely to be adequately visualized.

The inability to consistently evaluate T4−T6 on lateral DXA spine images does not present a significant problem in osteoporotic fracture identification. Several studies have demonstrated that the majority of fractures occur below these levels. The most common locations for vertebral fractures would appear to be T11-L1, followed by T7 and T8 (*2*, *31*, *34*, *35*). In studies that have utilized DXA spine imaging for spine fracture diagnosis, a surprising percentage of women with non-osteoporotic bone densities have been found to have fractures. In the study from Schousboe et al. (*34*) 27.4% of the patients aged 60 and older with osteopenic bone densities according to World Health Organization criteria were found to have vertebral deformities consistent with a diagnosis of fracture on DXA spine images. Forty-two percent of the patients aged 60 and older with osteoporotic bone densities were found to have vertebral deformities as well. In this study, the diagnosis of fracture on the DXA image was based primarily on the Genant semiquantitative method. Faulkner et al. (*36*) evaluated 231 women with a mean age of 65 with DXA spine imaging utilizing proprietary morphometric software in which a diagnosis of spine fracture was based on a reduction in vertebral height or height ratio of 3 SD or more from the expected mean value. Using this definition of prevalent fracture, more than half of the women were found to have vertebral fractures. Based on bone density at the PA lumbar spine or proximal femur, 46.7% of the women had osteopenia and 26.4% had osteoporosis. Of the women with osteopenia, 49.1% were found to have spine fractures. Over 72% of the women with osteoporosis were also found to have spine fractures based on these MXA measurements.

MXA, like densitometry, is a quantitative measurement technique. Like densitometry, then, the utility of MXA can be assessed in part by its reproducibility or precision.[5] After studying 48 normal postmenopausal women and 50 osteoporotic postmenopausal women, Ferrar et al. (*37*) concluded that the long-term precision of MXA was comparable to that of MXR. In this study, the RMS-SD was 0.60 mm in the normal women and 0.77 mm in the osteoporotic women. The RMS-SD for height ratios in the normal women was 0.03. These values were obtained using the "compare" feature. Use of the compare feature resulted in better precision than when the compare feature was not used. Rea et al. (*38*) also evaluated the long-term precision of MXA. They noted, as had Ferrer et al. (*37*), that the precision errors for MXA were substantially smaller than the 20–25% reduction in vertebral height, often used as a criteria for the diagnosis of incident vertebral fracture. The diagnosis of incident fracture from these images based on quantitative spine morphometry is therefore not adversely affected by the precision of the measurement technique. DXA spine imaging software from GE Lunar received 510(k) marketing clearance from the Food and Drug Administration in 2002 and was later followed by 510(k) clearance for Hologic DXA spine imaging software. The use of spine imaging for the assessment of vertebral fracture is called vertebral fracture assessment or VFA. The CPT[6] code for DXA-VFA is 77082 but insurance reimbursement eligibility varies widely.

---

[5] See Chapter 3 for a discussion of precision.
[6] See Appendix VIII for a listing and discussion of relevant CPT codes.

The potential contribution of VFA to the diagnosis of osteoporosis, prediction of fracture risk, and thus the decision to intervene with prescription medications must not be minimized. Even though a patient may have an osteopenic bone density, using WHO criteria,[7] the presence of a fracture implies that they have met the conceptual definitions of osteoporosis proposed by consensus conferences over the last decade. Such a patient would now meet the 2008 National Osteoporosis Foundation guidelines (39) for treatment. If a patient has an osteoporotic bone density by WHO criteria, but also has a fracture, their diagnosis would change to the WHO category of severe osteoporosis. In addition, the presence of a fracture clearly increases the risk of future fractures, over and above that implied by the bone density alone. These additional considerations must become part of the decision-making process for treatment. Consequently, in the absence of having current plain films of the spine with their attendant greater cost and radiation exposure to the patient, VFA with DXA should be considered an indispensable part of the evaluation of the patient's skeletal status.

VFA Patient Selection and Reporting

In 2007, the International Society for Clinical Densitometry (ISCD) published extensive guidelines on patient selection for VFA (40). All of these guidelines assume that current plain films of the spine are not available. These guidelines are summarized in Table 13-1 and also in Appendix V. ISCD also recommended the use of the Genant semiquantitative approach for the diagnosis of vertebral fracture with VFA. In reporting the VFA results, ISCD recommended that any such report document the methodology

Table 13-1
2007 ISCD Guidelines for VFA

- Consider VFA when the results may influence clinical management.
- Postmenopausal women with low bone mass (osteopenia) by BMD criteria, PLUS any one of the following:
  - Age greater than or equal to 70 years
  - Historical height loss greater than 4 cm (1.6 in.)
  - Prospective height loss greater than 2 cm (0.8 in.)
  - Self-reported vertebral fracture (not previously documented)
  - Two or more of the following;
    - Age 60–69 years
    - Self-reported prior non-vertebral fracture
    - Historical height loss of 2–4 cm
    - Chronic systemic diseases associated with increased risk of vertebral fractures (for example, moderate-to-severe COPD or COAD, seropositive rheumatoid arthritis, Crohn's disease)
- Men with low bone mass (osteopenia) by BMD criteria, PLUS any one of the following:
  - Age 80 years or older
  - Historical height loss greater than 6 cm (2.4 in.)
  - Prospective height loss greater than 3 cm (1.2 in.)

---

[7] See Chapter 9 and Appendix IV for a discussion of the WHO criteria for the diagnosis of osteoporosis based on the measurement of bone density.

<div align="center">

Table 13-1

(continued)

</div>

- Self-reported vertebral fracture (not previously documented)
- Two or more of the following;
  - Age 70–79 years
  - Self-reported prior non-vertebral fracture
  - Historical height loss of 3–6 cm
  - On pharmacologic androgen deprivation therapy or following orchiectomy
  - Chronic systemic diseases associated with increased risk of vertebral fractures (for example, moderate to severe COPD or COAD, seropositive rheumatoid arthritis, Crohn's disease)

- Women or men on chronic glucocorticoid therapy (equivalent to 5 mg or more of prednisone daily for three (3) months or longer).
- Postmenopausal women or men with osteoporosis by BMD criteria, if documentation of one or more vertebral fractures will alter clinical management.

---

used to determine fracture (SQ or MXA), unevaluable vertebrae, vertebral deformities, and unexplained vertebral and extra-vertebral pathology.

AORTIC CALCIFICATION ASSESSMENT

During the performance of lateral spine imaging with DXA for structural diagnoses in the spine, calcification in the abdominal aorta may be seen. This presents an opportunity to provide the referring physician and/or patient with information that is relevant to cardiovascular risk, even though the lateral spine imaging was not performed for this purpose. A significant increase in risk for cardiovascular events with osteoporotic total hip T-scores as well as vertebral fracture was reported by Tankó et al. (*41*). Others have found associations between low bone density and cardiovascular risk and mortality (*42–45*). Kiel et al. (*46*) also documented a significant relationship between a decline in metacarpal cortical area and the progression of aortic calcification in women over a 25-year follow-up. Bagger et al. (*47*) reported that the severity of aortic calcification was an independent predictor of hip fracture, with a statistically significant odds ratio of 2.3 while Naves et al. (*48*) reported a statistically significant odds ratio of 1.93 for all fractures and 2.45 for vertebral fractures. Similarly, Schulz et al. (*49*) reported a statistically significant odds ratio of 4.8 and 2.9 for spine and hip fractures respectively and the presence or absence of aortic calcification. The combination, therefore, of the assessment of BMD and the identification of vertebral fracture combined with the assessment of abdominal aortic calcification would seem highly desirable.

The prevalence of aortic calcification clearly increases with advancing age. In the study from Schulz et al. (*49*) the prevalence of any aortic calcification was 32.4% in women 50–54, 57.3% in women 55–59, 67.4% in women 60–64, and 74.2% in women 65–69. In women age 70 and older, the prevalence was over 90%. In the Framingham Heart Study, the prevalence of aortic calcification in women and men with a mean age of 61 was 57% and 68%, respectively (*50*).

In densitometry, concern regarding the prevalence of abdominal aortic calcification has largely centered around its potential effect on the measurement of BMD in the PA

lumbar spine.[8] In the lateral projection, the presence of aortic calcification does not affect the measurement of BMD or the identification of vertebral fracture. One use then, of identifying aortic calcification on a VFA image, is to document the presence of or lack of aortic calcification because of its potential effect on the BMD measured at the PA lumbar spine. But the presence of aortic calcification has far-reaching implications for cardiovascular event risk as well.

The predictive ability of aortic calcification for myocardial infarction (51) or stroke (52) was evaluated in the Rotterdam study.[9] Van der Meer et al. (51) categorized the degree of aortic calcification based on the measured length of the calcification in 6389 men and women who had not had a myocardial infarction prior to enrollment in the study. In this study, aortic calcification was assessed using lateral abdominal X-rays. The authors found a clear increase in the hazard ratio for myocardial infarction with increasing severity of aortic calcification based on the length of the plaque. The hazard ratio for the prediction of myocardial infarction for severe aortic calcification, defined as aortic calcification length of ≥2.5 cm, was 1.94. The hazard ratios for aortic calcification, carotid plaques, and carotid intima media thickness were equally high while the hazard ratio for peripheral atherosclerosis was lower.

Aortic calcification was also found to be an independent predictor of stroke in the Rotterdam study (52). In this analysis 6913 men and women with no history of stroke prior to enrolling in the study underwent assessment of aortic calcification on lateral abdominal X rays, assessment of carotid intima media thickness and carotid plaques, and peripheral atherosclerosis. During the mean 6.1 years follow-up, 378 stokes occurred. The relative risk (RR) for stroke was then calculated based on the severity category for each of the four measures of atherosclerosis. The RR for the per-category increase for aortic calcification was actually the highest at 1.21. The subjects were also divided into tertiles based on the length of the aortic calcification. There was clear increase in the RR with increasing length with the highest relative risk of 1.63 being seen in the tertile defined by an aortic calcification length of ≥2.5 cm.

The hazard ratios and RR for congestive heart failure (53) and coronary heart disease (50)by tertile of aortic calcification were also determined in the Framingham Heart Study.[10] In the original Framingham cohort were 5209 men and women who underwent evaluations every 2 years. Lateral spine radiographs were performed every 2 years from 1966 to 1970. These films were used to determine the severity of aortic calcification. In Table 13-2, the HR for congestive heart failure by tertile of abdominal aortic calcification for the 2214 participants who were free of coronary heart disease at baseline is shown (53). There was a clear increase in the HR for congestive heart failure with increasing abdominal aortic calcification. A clear increase in the RR for

---

[8] See Chapter 2 for a discussion of the potential effect of aortic calcification on BMD measured at the PA lumbar spine.

[9] The Rotterdam study is a prospective population-based cohort study of 7983 women and men age ≥55 years in which the incidence and causes of chronic disabling diseases were investigated.

[10] The Framingham Heart Study is a prospective epidemiologic cohort study begun in 1948 to identify potential risk factors for coronary heart disease.

Table 13-2
Hazard Ratio for Congestive Heart Failure by Tertile of
Abdominal Aortic Calcification Adjusted for Age and
Cardiovascular Risk Factors

AAC Tertile	Men n-883	Women n-1331
1	1.0	1.0
2	1.2	1.7
3	2.0	2.7

AAC; abdominal aortic calcification
n=2214 free of CHD at baseline; 24 point AAC score used.
Adapted with permission of Elsevier from ref. *53*.

coronary heart disease[11] with increasing abdominal aortic calcification was also demonstrated with a RR of 1.61 in men and 2.41 in women in the highest tertile of aortic calcification (*50*).

Aortic Calcification Scoring Systems

In the Framingham Heart Study, a 24-point grading system was used to determine the extent of abdominal aortic calcification, which was initially described by Kaupila et al. (*54*). The 24-point scale has since become the accepted standard for grading aortic calcification on plain films. Both the anterior and posterior walls of the aorta at each of four lumbar vertebral levels (L1-L4) are assigned a grade based on the length of the calcification seen in the wall. The scoring system is shown in Table 13-3. Because both the anterior and posterior aortic walls at each vertebral level could potentially receive a maximum combined score of 6, and four vertebral levels are evaluated, the worst possible score is 24. Using this methodology the inter-rater intraclass correlation was reported to be 0.93 and the intra-rater intraclass correlation was 0.98 (*54*). In the two studies noted previously for the assessment of the RR of coronary heart disease and the HR for congestive heart failure by tertile of aortic calcification, the third tertile corresponded to an AAC-24 score of ≥ 5.

Table 13-3
The AAC-24 Scale (*47*)

Aortic Calcification Length in the Anterior or Posterior Aortic Wall at L1, L2, L3, or L4	Score
None	0
$\leq 1/3$ of aortic wall	1
$> 1/3$ but $\leq 2/3$ of aortic wall	2
$> 2/3$ of aortic wall	3

[11] Coronary heart disease refers to angina, unstable angina, myocardial infarction, and coronary disease death.

Table 13-4
The AAC-8 Scale (*48*)

Calcification Length Relative to Vertebral Height	Score
None	0
1 Vertebra	1
> 1 but ≤ 2 Vertebrae	2
> 2 but ≤ 3 Vertebrae	3
> 3 Vertebrae	4

In 2006, Schousboe et al. (*55*) proposed a simplified abdominal aortic calcification scoring system, called the AAC-8. In this approach, the total length of aortic calcification, which spans L1-L4 is estimated for the anterior and posterior aortic walls separately. A possible score for each wall can range from 0 to 4, such that a maximum worst-case score is 8. The AAC-8 scoring system is shown in Table 13-4. The application of the AAC-8 to a lateral DXA image is shown in Fig. 13-5. Schousboe et al. then applied the AAC-24 and the AAC-8 scoring systems to plain radiographs and lateral DXA spine images which were acquired on a Hologic Delphi. Two readers assessed aortic calcification on the plain films and lateral DXA images using both scales. One reader assessed both sets of images using the AAC-8 scale as well several days after the AAC-24 assessment. The intraclass correlations using the AAC-24 scale for

Fig. 13-5. A lateral DXA spine image, with an AAC-8 score of 6/8 in a 76-year-old Caucasian woman with a total hip T-score of −1.2, femoral neck T-score of −1.4 and an L1−L4 T-score of −0.1. Image courtesy of Hologic, Inc., Bedford, MA.

Table 13-5

Intraclass Correlations Between Technologies and Between Readers in the Detection of Abdominal Aortic Calcification (24-Point Scale)

Comparison	Intraclass correlations (95% confidence intervals)
Lateral DXA vs. standard radiographs (reader 1)	0.81 (0.66–0.90)
Lateral DXA vs. standard radiographs (reader 2)	0.82 (0.69–0.90)
Reader 1 vs. reader 2 (on standard radiographs)	0.92 (0.88–0.95)
Reader 1 vs. reader 2 (on lateral DXA)	0.89 (0.80–0.94)

Reproduced with permission of Elsevier from ref. *55*

each reader and between the two readers are shown in Table 13-5. Because an AAC-24 score of ≥ 5 on plain radiographs was clearly associated with an increase in risk for congestive heart failure and cardiovascular events in the Framingham Heart Study, the authors evaluated the area under the receiver operator characteristic curve (AU-ROC)[12] for the identification of an AAC-24 score ≥5 on plain radiographs based on an AAC-24 score of ≥5 on lateral DXA images. For the two readers the AU-ROCs were 0.83 and 0.88.[13] The sensitivity of an AAC-24 score ≥5 on lateral DXA images for an AAC-24 score ≥5 on plain radiographs was 65% and 78% for the two readers and the specificity was 90% and 87%. The correlation of the AAC-8 score with the AAC-24 score on plain radiographs and lateral DXA images was 0.95 and 0.93, respectively.

Schousboe et al. (*56*) also studied 174 postmenopausal women age 55 and older to determine the AU-ROC for the identification of women with an AAC-24 score of ≥5 for the AAC-8 scale used with plain radiographs and lateral DXA images and the AAC-24 scale used with lateral DXA images. The lateral DXA images were obtained on a Hologic Discovery in the lateral decubitus position. The AU-ROC for the AAC-8 score using plain radiographs was 0.95. The AU-ROCs for the AAC-8 score and AAC-24 score for the lateral DXA images was 0.84 and 0.85, respectively. The sensitivity of the lateral DXA image AAC-8 score of ≥ 3 for the identification of women with an AAC-24 score of 5 on plain radiographs was 62% with a specificity of 96%. The positive and negative predictive values associated with a lateral DXA image AAC-8 score of ≥ 3 were 82% and 89%, respectively. An AAC-24 score ≥ 5 on lateral DXA imaging had a sensitivity and specificity of 59% and 97%, respectively, for the identification of women with an AAC-24 score ≥5 on plain radiographs. The positive and negative predictive values for the lateral DXA AAC-24 score ≥ 5 for an AAC-24 score ≥ 5 on plain radiographs was 85% and 88%. Importantly, an AAC score of 0 on either the 8 point or 24 point scale had a negative predictive value of 94% for an AAC-24 score ≥ 5 on plain radiographs.

---

[12] See Chapter 3 for a discussion of receiver operator characteristic curves.

[13] Diagnostic tests with an AU-ROC of 0.70–0.90 when compared to a "gold standard" test are considered to have acceptable predictive accuracy. An AU-ROC > 0.90 is superb.

Determining Aortic Calcification with DXA Lateral Spine Imaging

Most studies assessing the relationship between aortic calcification and the risk of myocardial infarction or stroke have utilized plain radiographs to quantify aortic calcification. However, Schousboe et al. (*57*) utilized lateral DXA imaging performed on a Hologic QDR4500 and both the AAC-24 scale and the AAC-8 scale to determine the odds ratio for myocardial infarction (MI) or stroke by tertile of AAC score. In a case control study of women aged 75 and older, 408 women sustaining an MI or stroke were matched with 408 controls. The women were divided into tertiles based on their AAC-8 and AAC-24 scores. The odds ratios for incident MI or stroke by tertile of AAC-8 and AAC-24 score for those with complete covariate data and after adjustment for multiple cardiovascular risk factors are shown in Table 13-6. Those women in the third tertiles of AAC-24 or AAC-8 scores had significantly increased odds ratios compared to the first tertiles. Schousboe et al. concluded that abdominal aortic calcification scored on VFA images was independently associated with incident MI or stroke.

Table 13-6
Association of AAC with Incident Myocardial Infraction or Stroke

AAC Scale	Tertile	Multivariable-Adjusted Odds Ratio (95% Confidence Interval)
AAC-24	First	1.0 (Reference)
	Second	0.88 (0.53–1.45)
	Third (>6)	1.67 (1.00–2.79)
AAC-8	First	1.0 (Reference)
	Second	1.38 (0.85–2.25)
	Third (>3)	1.80 (1.09–2.95)

n=420
Adapted from ref. (*57*).

Reporting Aortic Calcification on Lateral DXA Imaging

There are no guidelines for reporting aortic calcification on VFA images. However, it would seem appropriate to note the presence or absence of aortic calcification on the image. If the AAC-24 or AAC-8 scoring system is used, the particular system used should be stated and the score given. Because most physicians are unlikely to be familiar with the significance of any given score, it would be reasonable to include a comment on the significance of a finding of an AAC-24 score of 5 or higher or an AAC-8 score of 3 or higher, depending on the scoring system used. In addition, if no aortic calcification is seen, a comment regarding the very high negative predictive value of either AAC scoring system with VFA images for radiographic aortic calcification AAC-24 scores of 5 or greater is appropriate.

In 2006, Hologic received FDA 510(k) clearance for aortic calcification assessment with lateral spine imaging. Although there is no recommendation from any organization to perform lateral spine imaging for the *sole* purpose of identifying aortic calcification, the opportunity to detect aortic calcification, an important cardiovascular risk factor, on a VFA study should not be missed.

PROXIMAL FEMUR MORPHOMETRY

Interest in the measurement of the dimensions and geometry of the proximal femur as part of the assessment of fracture risk was spurred by the initial recognition of hip axis length as an independent predictor of hip fracture risk. Other measures have come under scrutiny as predictors of hip fracture risk as well. These are measures such as the neck-shaft angle and femoral neck width as well as segments of the hip axis length.

Hip Axis Length

Hip axis length (HAL) has been demonstrated to be a predictor of hip fracture risk that is independent of bone mineral density (*58*). As part of the Study of Osteoporotic Fractures, 8074 women aged 65 and older were evaluated with DXA (Hologic QDR-1000) measurements of the proximal femur. HAL was measured in 134 women without fractures and in 64 women who experienced hip fractures during 1.6 years of follow-up. A goniometer was used to measure HAL from the computer printout. HAL was defined as the distance from the inner pelvic brim to the outer edge of the greater trochanter along the femoral neck axis as shown in Fig. 13-6. Odds ratios for BMD and the risk of hip fracture and for HAL and the risk of hip fracture were calculated. For femoral neck BMD, each SD *decline* in BMD resulted in a 2.7-fold increase in the risk of hip fracture. For HAL, each SD *increase* in length resulted in a 1.9-fold increase in the risk of femoral neck fracture and a 1.6-fold increase in the risk of trochanteric fracture.
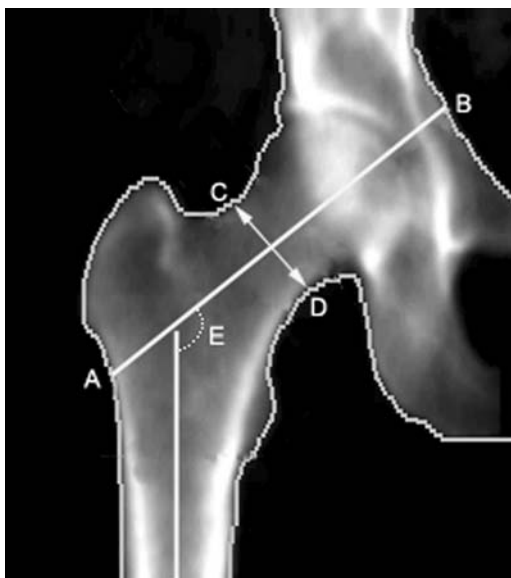
Fig. 13-6. The proximal femur image showing the HAL **(A−B)**, femoral neck width **(C−D)**, and neck-shaft angle **(E)**.

In 1994, Faulkner et al. (*59*) proposed automating the measurement of HAL on proximal femur bone density studies. Faulkner et al. re-analyzed the 198 proximal femur studies for which HAL had been determined manually (*58*) with modified proximal femur analysis software using a QDR-1000/W (Hologic, Inc.). The correlation between the manual and automated measurements was 0.98. The precision of the automated HAL

measurement was determined as the average SD from three measurements on each of 33 women. This value was 0.07 cm or 0.68%.

Duboeuf et al. (*60*) also found that HAL was a significant predictor of femoral neck fracture risk with an odds ratio of 1.64 based on an analysis of proximal femur studies from the EPIDOS[14] study. Unlike Faulkner (*58*), however, these authors concluded that HAL was not a significant predictor of trochanteric fracture. Other authors have attempted to partition the HAL into segments, to determine if any particular segment of HAL was more predictive of hip fracture than HAL itself. One such segment is the femoral neck axis length (FNAL), which is a segment of HAL that spans the base of the greater trochanter to the apex of the femoral head as shown in Fig. 13-7. Center et al. (*61*) measured the FNAL in 260 men and women from the Dubbo Osteoporosis Epidemiology Study[15] from proximal femur DXA studies in which the analysis software included a ruler that could be a manipulated for the measurement. In this study, FNAL was significantly correlated with current and maximum height. When FNAL was adjusted for current and maximum height, however, no difference was seen between hip fracture patients and non-fractured patients in the FNAL. Center et al. concluded that the FNAL had very little utility in improving hip fracture risk prediction.
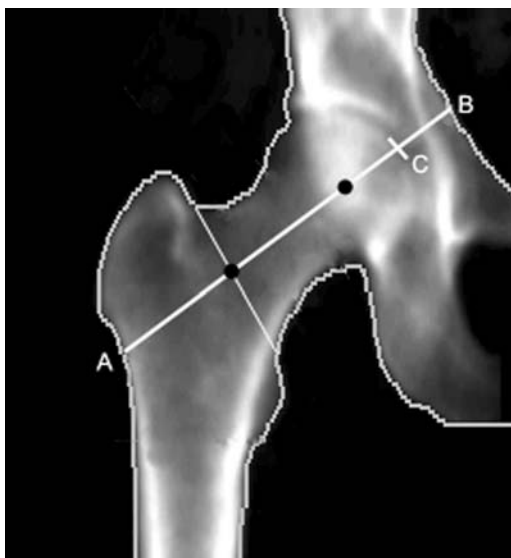
Fig. 13-7. The proximal femur showing the HAL **(A−B)** and its segments: the femoral neck axis length or FNAL **(A−C)**, and the intertrochanteric-head distance (■−●).

Bergot et al. (*62*) evaluated HAL and seven different segments of HAL, including the FNAL, from proximal femur DXA scans acquired on a Hologic QDR 1000/W. Comparisons of measurements in 49 women with non-traumatic hip fractures to measurements

---

[14] EPIDOS is a multicenter prospective study of 7575 women living at home aged 75–95 years in France. The data in this study are from 320 women from the Lyon and Montpellier centers.

[15] The Dubbo Osteoporosis Epidemiology Study is a case-control study involving 1902 men and women who were recruited between 1989 and 1993.

in 49 age-matched women and 49 age- and BMD-matched women were made to determine which HAL segments best discriminated between the three groups of women. The best discriminators between women with hip fractures and all non-fractured women were femoral neck BMD and HAL. Femoral neck BMD and HAL were also the best discriminators between the women with hip fracture and the non-fractured, age-matched women. The best discriminator between fractured women and low BMD-matched, non-fractured women was a different segment of HAL called the intertrochanteric-head center distance, defined by the line that begins at the center of the femoral head and ends at the intertrochanteric line, shown in Fig. 13-7. FNAL was not useful in discriminating between the groups. The authors noted that the intertrochanteric-head center distance is more difficult to measure than HAL because of the imprecision in marking the center of the femoral head. Normal values, as well as the magnitude of risk imparted by increases in the intertrochanteric-head center distance, must be established. This particular segment of HAL remains a focus of research interest.

HAL has been suggested as a possible explanation for the difference in hip fracture rates among various races. Cummings et al. (*63*) demonstrated that the mean HAL of predominantly American-born Asian and black women was significantly shorter than that of Caucasian women. Both Asian and black women are known to have a lower risk of hip fracture than Caucasian women. Nakamura et al. (*64*) demonstrated that the FNAL, a component of HAL, was significantly shorter in Japanese women than in Caucasian women, noting that hip fracture rates in Japanese are approximately half that seen in Caucasians. HAL is simple to measure and is now offered as an automated measurement commercially on proximal femur bone density studies. Figure 13-8 is a DualFemur® DXA study performed on a Lunar Prodigy showing the HAL measurement. The scale indicates the patient's value in comparison to the mean value predicted for height. Although this is clearly a non-modifiable risk factor, HAL can be useful for hip fracture risk stratification. Using the Lunar Prodigy, Bonnick and Lewis (*65*) reported RMS-SD and RMS-%CV precision values for HAL measurements of the left
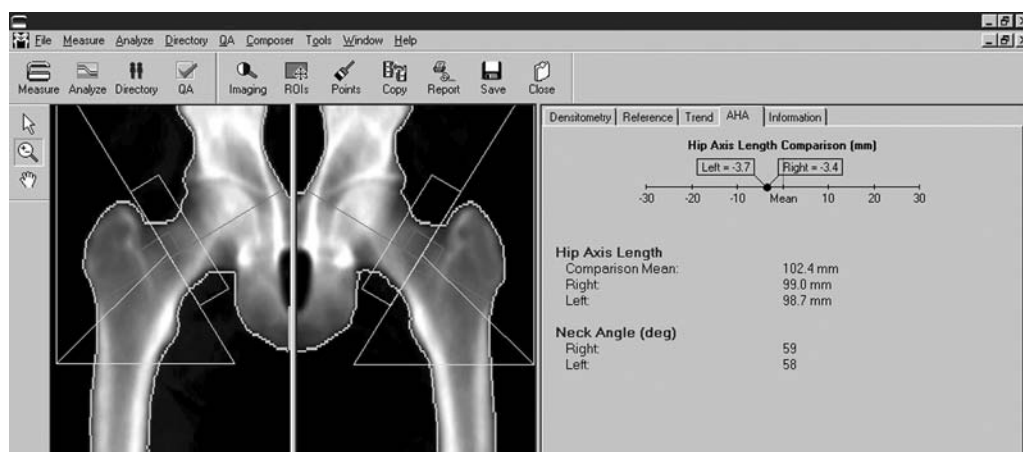
Fig. 13-8. A Lunar Prodigy DualFemur™ study with the HAL measurement. The HAL in both femurs is slightly shorter than predicted for height.

femur of 0.7 mm or 0.67% in women aged 20–49 and 0.6 mm or 0.53% in women aged 50–70.

The Femoral Neck-Shaft Angle

The femoral neck-shaft angle is another geometric measure that has been studied as a predictor of hip fracture risk. This angle is indicated by the letter "E" in Fig. 13-6. The studies to date have provided mixed results on the utility of this measure. Several studies (*66–69*) have found significantly greater femoral neck-shaft angles in hip fracture patients than in controls while others (*58, 62, 70*) have not. In the study from Bergot et al. (*62*) the neck shaft angle was not different in the hip fracture patients compared to the low-BMD non-fractured patients or the age-matched controls. The neck-shaft angle was 127.1° in the fracture patients compared to 127.2° in the low-BMD non-fractured patients and 125.6° in the age-matched control group. In contrast, in a study from Partanen et al. (*69*) the neck-shaft angle was statistically significantly greater in a group of 70 postmenopausal women with hip fractures (mean age 74.9 years) compared to a control group of 40 postmenopausal women (mean age 73.7) without hip fractures. In the fracture group, the mean neck-shaft angle was 133.7° compared to a mean of 128.3° in the control group. Partanen et al. also found that the neck-shaft angle was significantly greater in the 46 women with cervical fractures than in the 24 women with trochanteric fractures. The neck-shaft angle in the cervical fracture group was 135.7° compared to 130.3° in the trochanteric fracture group.

Femoral Neck Width

Femoral neck width is measured at the narrowest part of the femoral neck as indicated by line C-D in Fig. 13-6. An increase in neck width from periosteal bone apposition has been postulated as a response to a decrease in bone density. The result of the width increase should be an increase in the cross-sectional moment of inertia (CSMI). This would potentially compensate for the reduction in endosteal bone and theoretically reduce the risk of hip fracture. If this is so, the increase in femoral neck width in the presence of a low bone density should indicate a reduction in fracture risk compared to individuals with an average or reduced neck width and the same low bone density. Nevertheless, Bergot et al. (*62*) did not find a statistically significant difference in neck width between hip fracture patients and age- and BMD-matched non-fractured controls. The absolute neck width was slightly greater in the age- and BMD-matched non-fractured control group compared to the hip fracture patients at 3.20 cm compared to 3.17 cm. In this study the femoral neck width was greater in both the fracture group and age- and BMD-matched non-fractured group compared to the age-matched controls but again, not statistically significantly so. Other investigators (*66, 67*) have found a significant increase in femoral neck width in fracture patients compared to controls.

The Upper Femoral Neck

The upper femoral neck is a relatively new region of interest in the proximal femur. It is the superior half of the traditional femoral neck region of interest as shown in Fig. 13-9. Yoshikawa et al. (*71*) suggested that there was a greater decrease in bone density in the superior region of the femoral neck in women. They suggested that this
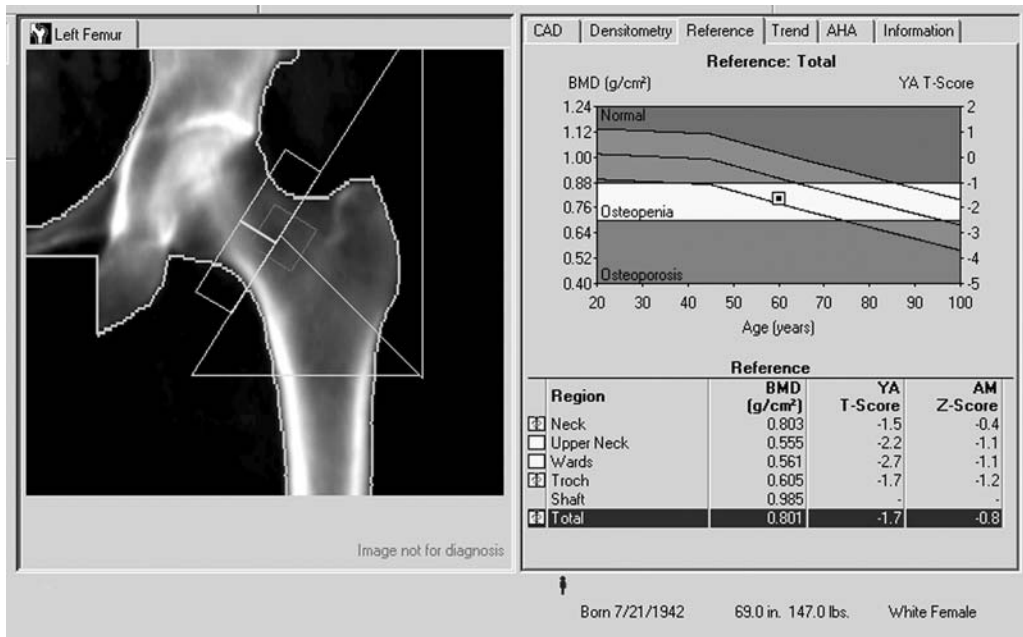
Fig. 13-9. A GE Lunar Prodigy study of the proximal femur showing the measurement of bone density in the upper femoral neck. Note that the upper femoral neck has a T-score of −2.2 in comparison to the T-score of −1.5 for the entire femoral neck.

would cause the center of mass to move in such a way as to place greater stress on the femoral neck, increasing the risk of fracture. The upper femoral neck region of interest was compared to the entire femoral neck region and to the lower femoral neck region for the prediction of neck and trochanteric hip fracture in the study from Duboeuf et al. (*60*). In this study, upper femoral neck BMD was highly predictive of femoral neck fracture with an odds ratio of 2.8 for each SD decline in bone density and outperformed the more traditional total femoral neck measurement. The lower femoral neck BMD was not predictive of femoral neck fracture. All three regions were predictive of trochanteric fracture and hip fracture in general.

Hip Structural or Strength Analysis

Hip structural or strength analysis (HSA) is based on work from Martin and Burr who demonstrated that the absorption curve generated during a single-photon absorptiometry forearm bone density study contained sufficient information to calculate the cross-sectional moment of inertia[16] (CSMI) (*72*). Further refinements led to the calculation of biomechanical parameters of bone strength from dual-energy X-ray absorptiometry (DXA) or quantitative computed tomography (QCT) proximal femur studies: the

---

[16] The CMSI is a measure of the distribution of the mineral within the cross-section. It is not a measure of bone strength but directly affects the section modulus, which is a measure of strength in bending.

mineralized bone surface cross-sectional area[17] (CSA), section modulus[18] (Z), and buck-ling ratio[19] (BR) (*71*, *73–75*).

There are two proprietary approaches to DXA-based HSA. In one approach 3 separate ROIs are defined at the femoral neck, intertrochanteric region and shaft (*73*). In a second approach, shown in Figure 13-10, parameters are calculated at the femoral neck (FN) to derive the femur strength index (FSI) (*71*, *76*). The FSI is essentially the ratio of femur strength to the fall forces on the femoral neck. The results of the HSA analysis utilizing this approach are shown in Figure 13-11.

Fig. 13-10. Proximal femur DXA hip structural analysis regions of interest. Shown is a Lunar Prodigy proximal femur hip strength analysis image. The femoral head is identified and a line that is parallel to the long axis of the femoral shaft is shown bisecting the femoral shaft. This line intersects the line that is parallel to the long axis of the femoral neck and bisects the femoral neck, creating the neck-shaft angle. The line bisecting the femoral neck is also used to measure HAL.

DXA-based HSA or its predecessor, dual-photon absorptiometry has been employed in clinical trials to study these parameters with aging, between genders, with bone active agents, and to predict fracture risk (*77–86*). In a cross-sectional study of 409 men and women from age 19 to 93, the CSMI declined at the FN in women but not in men although a decline in BMD was seen in both (*77*). In a cross-sectional study of 1044 pre- and postmenopausal women, the decline in CSMI was restricted to postmenopausal women although both demonstrated a decline in FN BMD (*78*). In 2719 non-Hispanic white men and 2904 non-Hispanic white women from the National Health and Nutrition Survey III (NHANES III) although FN and shaft BMD declined in both sexes, the

---

[17] The CSA is a measure of the bone mineral content in the cross section. It is directly proportional to the ability of the bone to withstand axial compression.

[18] The section modulus is a measure of the strength of the bone in bending. Note that the section modulus is indicated by the abbreviation "Z," which is unrelated to the z-score used in densitometry.

[19] The BR is the ratio of the diameter of the cross section to its cortical thickness. High BRs suggest the possibility of local failure or buckling due to an excessively thinned cortex.
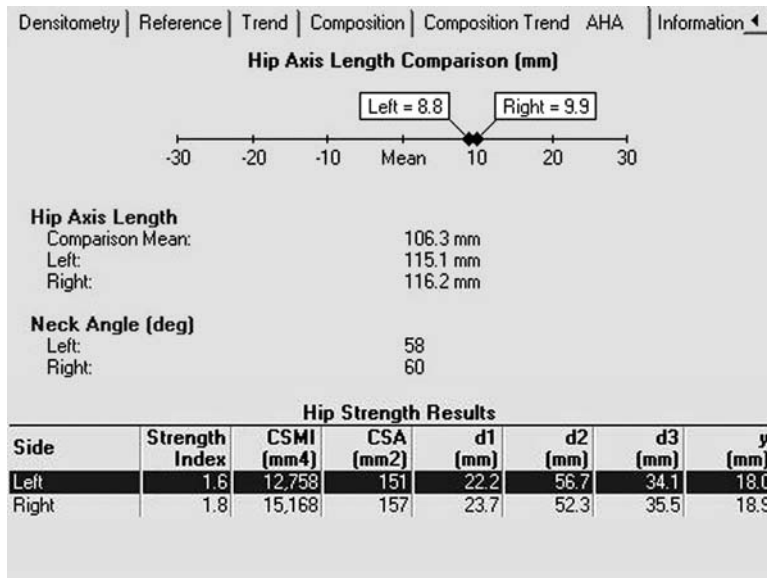
Fig. 13-11. Hip strength analysis results from a DualFemur™ study from a GE Lunar Prodigy. Data is provided for the HAL, neck-shaft angle and the FI (Fall Index) as well as the various parameters used in calculating the FI, such as the CSMI (cross-sectional moment of inertia). Data provided courtesy of GE Healthcare, Madison, WI.

pattern of change in the Z was different and gender dependent (*79*). The Z in women at both ROIs declined after age 50 but at a slower rate than BMD. In men, the femoral neck Z remained relatively constant after age 50 and increased at the shaft. The discordant behavior was attributed to a linear expansion in subperiosteal diameter which would preserve the CSMI and Z and therefore, mechanical strength.

In the Study of Osteoporotic Fractures, FN BMD declined over 3.5 years in elderly women regardless of current or past estrogen replacement therapy (ERT) (*80*). However, in the current ERT-users, Z increased at the FN and shaft whereas it remained unchanged in past- and never-users. In a prospective 3-year study of 373 women over the age of 65, CSA and Z increased significantly from baseline at the FN, intertrochanteric, and shaft in women receiving a combination of estrogen and alendronate or either agent alone while the BR was preserved or declined significantly (*81*). Placebo-treated women did not show significant increases in CSA at any ROI but had undesirable and significant increases in the BR at all three ROIs. In separate post-hoc subset analyses, Uusi-Rasi et al. reported the effects of raloxifene or teriparatide on DXA-HSA biomechanical strength parameters (*82*, *83*). In the MORE trial, 60 and 120 mg of raloxifene a day produced a 0.4–2% higher CSA, Z, and cortical thickness (CT) and 1–2% lower BR compared to placebo-treated women (*82*). In the Fracture Prevention Trial, treatment with either 20 μg or 40 μg of teriparatide a day for 1.8 years resulted in increases of 3.5–6.3% in CSA, 3.6–6.8 in Z, and decreases of 5.5–8.6% in the BR compared to placebo-treated women at the FN (*83*). Similar changes were seen at the intertrochanteric ROI.

Women with trochanteric hip fractures in a nested, case–control study from the EPI-DOS cohort had significantly decreased CSMI and CT and higher BR than controls (*84*). A decrease in CT, Z, and an increase in BR were all predictive of hip fracture in

general. However, after adjusting for BMD, the odds ratios (ORs) for fracture for the structural parameters lost statistical significance. The authors concluded that the HSA-derived biomechanical parameters were not superior to BMD for the prediction of fracture risk. In contrast, Ahlborg et al., in a prospective, case–control study of 96 men and women aged 60 and older, found that a lower CSMI or Z was a risk factor for hip fracture even after adjustment for BMD (85). They noted, however, that any improvement in fracture prediction beyond a conventional measurement of BMD was small. Similar conclusions were reached by Melton et al. in a study of 213 postmenopausal women (86). Here, hip BMD and HSA-structural parameters were all associated with moderate trauma and osteoporotic fractures in women but the best risk predictor was FN BMD.

Yoshikawa et al. (71) developed algorithms to calculate the CSMI as well as other measures of hip strength. Yoshikawa et al. noted that although BMD was an important predictor of hip fracture risk, BMD accounted for only 50% of the bone strength estimated from the CSMI. This suggested that the CSMI reflected elements of bone strength not captured in the measurement of BMD. In 2002, Crabtree et al. (87) reported the application of a test version of proprietary DXA software (GE Medical Systems) designed to assess hip strength. The subjects for this study were 68 women aged 60 and older who had recently suffered a hip fracture and 800 women age 60 and older without a hip fracture originally recruited as part of the EPOS study. All subjects underwent standard proximal femur DXA studies (Lunar DPX). The hip strength analysis (HSA) software uses the proximal femur DXA study to calculate measures reflecting the geometry and bone distribution within the proximal femur. In addition to standard measurements of proximal femur BMD, the program calculated the upper and lower femoral neck BMD, HAL, Cstress, and Femur Strength Index[20] (FSI). Cstress reflects the compressive stress from a fall on the greater trochanter. Typical units are N/mm^2. The calculation of the CSMI is necessary to calculate Cstress. The FSI is a dimensionless quantity that reflects the resistance to fracture from forces generated during a fall on the greater trochanter. In this study, HAL was significantly longer in the fracture patients than in the controls. Cstress was also significantly greater in the fracture patients than in the controls. The FSI was significantly lower in the fracture patients than in the controls. Femoral neck BMD, whether measured as a total, upper, or lower neck value, was significantly lower in the fracture patients than in the controls. Unlike the earlier study from Duboeuf et al. (60), Crabtree et al. (87) could not show that the upper femoral neck BMD was a better predictor of femoral neck fracture than total femoral neck BMD. The authors then attempted to develop a statistical model for the prediction of hip fracture status. They found that the combination of Cstress, age, and body mass index (BMI) in the model resulted in an area under the ROC curve (AU-ROC) of 0.875. The use of femoral neck BMD alone resulted in an AU-ROC of 0.827. The difference between these two AU-ROCs was statistically significant. Femoral neck BMD alone was better than Cstress alone, but the addition of femoral neck BMD to the model containing Cstress, age, and BMI did not improve the model's ability to predict hip fracture status. The authors concluded that the assessment of hip strength could enhance the prediction of hip fracture risk. Faulkner et al. evaluated the FSI in a cross-sectional study of

---

[20] This was originally called the Fall Index.

2506 women age 50 and older (*76*). Although the FSI was significantly lower in the hip fracture patients compared to non-fractured controls even after adjustment for FN BMD, the authors noted that the additional predictive power of the FSI in individuals might be small when compared to BMD.

The proprietary versions of HSA are now available commercially. Prospective fracture data that would allow the densitometrist to predict fracture risk from HSA measurements, however, is lacking.

HSA WITH QCT

HSA can also be performed with QCT. Three-dimensional imaging with QCT enables the estimation of CT around the circumference of the bone unlike the integral cortical thickness obtained with DXA. ROIs are again at the FN, intertrochanteric, and shaft regions in the proximal femur, but images along the length of the femoral neck can be acquired enabling the measurement of the biomechanical parameters and CT in progressive locations.

An advantage of DXA-based HSA is the wide availability of DXA. At the same point of care, measurements of density and biomechanical strength can be obtained. QCT-based HSA has the same potential but the availability of QCT is less than DXA. QCT, however, overcomes the two-dimensional limitation of DXA (*74, 75*). Because DXA is two-dimensional, the biomechanical parameters are valid for the fixed plane of the DXA-image only, which is not necessarily the relevant fracture plane. Although there is no population-based reference data for HSA biomechanical parameters, the desired direction of change in known making therapeutic monitoring is feasible. The precision of DXA-based HSA is approximately 1.5–2 times poorer than that of DXA-BMD (*88*). Precision of QCT-based HSA appears slightly better than DXA-based HSA (*89*). HSA strength parameters are predictive of hip fracture risk, but are not better predictors of hip fracture risk than conventional measurements of DXA-BMD.

BODY COMPOSITION ANALYSIS

Most full-size central DXA densitometers can be operated with software used to determine body composition from a total body bone density study. This application was first developed for dual-photon absorptiometers but the almost 1 hour scan time made such measurements clinically impractical. In contrast, today's DXA devices can perform total body scans in a matter of minutes. In spite of this dramatic improvement in speed, body composition assessment with DXA remains an underutilized application.

The assessment of body composition is much different from the measurement of weight, although certainly the two are related. The assessment of body composition is concerned with the percentage and distribution of fat and lean tissue in the body. Although many studies have associated extremes of weight with disease states, it is increasingly recognized that the percentage and distribution of fat and lean tissue is as or even more important than total body weight in various disease states. A brief review of other techniques used to assess body composition is useful in order to appreciate the unique aspects of body composition analysis with DXA.

The Body Mass Index

The body mass index (BMI) is only a first step in the assessment of body composition but it goes beyond the simple measurement of total body weight. The BMI relates the patient's weight to their height, using the following formula:

$$BMI = \left(\frac{Weight\ (lbs)}{Height\ (in)^2}\right) \times 703 \qquad (1)$$

For example, if a woman weighs 120 lbs and has a height of 62 in., her BMI is:

$$BMI = \left(\frac{120}{62^2}\right) \times 703 \qquad (2)$$

$$BMI = 21.95\ \text{lbs/in}^2 \qquad (3)$$

When using the metric system to measure height and weight, the formula changes to:

$$BMI = \left(\frac{Weight\ (kg)}{Height\ (cm)^2}\right) \times 10,000 \text{ or } BMI = \frac{Weight\ (kg)}{Height\ (m)^2} \qquad (4)$$

In the example given above, the patient's weight of 120 lbs and height of 62 in. converts to 54.53 kg and 1.575 m. The formula for BMI thus becomes:

$$BMI = \frac{54.43}{1.575^2} \qquad (5)$$

$$BMI = 21.94\ \text{kg/m}^2 \qquad (6)$$

The very slight differences in results are due to the effects of converting the original values to the metric system and rounding. However, in both cases, the BMI is essentially 22. The formula for calculating BMI is also called Quetelet's formula or index (90).

In 1995, the World Health Organization (WHO) used the BMI to define obesity in adults (91). In 1998, the WHO also defined categories of risk, based primarily on premature mortality for any given BMI (92). These divisions are shown in Table 13-7. The criteria apply to both women and men. Some DXA body composition software will

Table 13-7
The World Health Organization Criteria for Obesity and Risk for Premature Mortality Based on the BMI for Adults Age 20 and Older

Category	BMI (kg/m^2)	Risk
Underweight	< 18.50	Low (but other comorbidities increased)
Normal	18.50 – 24.99	Average
Overweight	≥ 25.00	
Preobese	25.00 –29.99	Increased
Obese class I	30.00 – 34.99	Moderate
Obese class II	35.00 – 39.99	Severe
Obese class III	≥ 40.00	Very severe

Adapted with the permission from ref. (92).

World Health Organization BMI Classification
Body Mass Index (BMI) = 26.0

Region	Tissue (%Fat)	Centile	T.Mass (kg)	Region (%Fat)	Tissue (g)	Fat (g)	Lear (g
Legs	38.1	-	-	36.4	21,467	8,188	13,27
Trunk	29.1	-	-	28.1	27,520	8,019	19,50
Android	24.5	-	-	24.1	3,420	838	2,58
Gynoid	39.3	-	-	38.3	9,885	3,889	5,99
Total	32.5	63	62.9	31.0	59,905	19,470	40,43
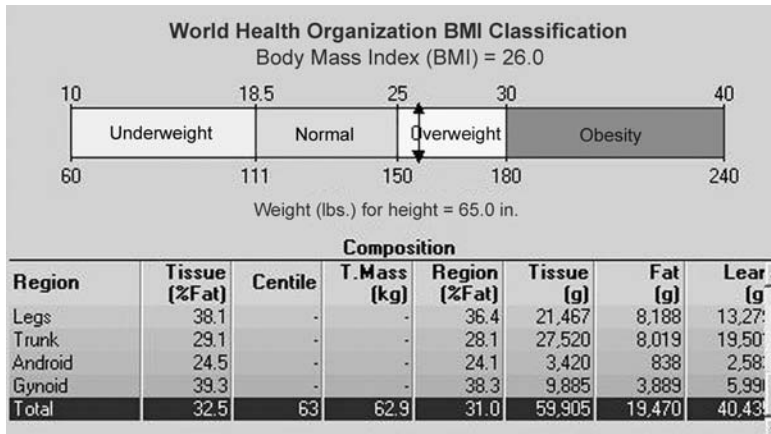
Fig. 13-12. Ancillary body composition data from a GE Lunar Prodigy body composition study in which the patient's BMI has been plotted on a scale representing the World Health Organization classification system for obesity.

calculate and plot the patient's BMI on a graphic scale that indicates the WHO classification. An example is shown in Fig. 13-12.

Although the BMI is an improvement over the assessment of weight alone, it does not address the actual percentage of total body fat or the distribution of fat in the body. The BMI obviously cannot distinguish the contribution to weight from either lean or fat tissue. As a consequence, individuals with a large muscle mass may actually have a BMI that results in a classification of overweight or obese, when clearly they are not. More sophisticated methods for body composition are required to distinguish the percentages of fat and lean tissue and the distribution of each within the body.

Body Composition Methods

The body can be divided into two major compartments: fat and fat-free. The fat-free compartment can be further divided into water, protein, and mineral. The various techniques used to measure body composition are characterized by the number of compartments that they measure. A two-compartment method measures fat and fat-free mass. If a method is described as a three- or four-compartment method, it is measuring fat-mass and two or three of the components of the fat-free mass.

The traditional "gold standard" for measuring body composition has been a two-compartment technique called underwater weighing (UWW).[21] Other two-compartment methods include measurement of skin-fold thickness, bioelectrical impedance, and air displacement plethysmography. Near infrared interactance (NIR) and DXA body composition assessments are three-compartment methods.

TWO-COMPARTMENT BODY COMPOSITION MEASUREMENT TECHNIQUES

Underwater Weighing. Underwater weighing (UWW) is one of the most widely used methods for assessing body composition, and, as noted earlier, has long been

---

[21] This technique is also known as hydrostatic weighing or hydrodensitometry.

considered the gold standard for these types of techniques. The principle behind UWW is that there is an inverse relationship between body fat and body density. That is, as one goes up, the other goes down. The major assumption in UWW is that the densities of the fat and fat-free mass in the body are constant (*93*). It is generally agreed that fat mass has a density of 0.9 g/cm^3 but the density of the fat-free mass is controversial. In the past, the density of the fat-free mass was assumed to be a relatively constant 1.1 g/cm^3. This does not appear to be true. Recall that the fat-free mass consists of water, protein, and bone mineral. Variations in any of these components may cause the density of the fat-free mass to change. Although the bone mineral is a small percentage of the fat-free mass, it contributes significantly to the density of the fat-free mass. As a consequence, changes in the amount of bone mineral have a greater influence on the total density of the fat-free mass than might otherwise be expected. This creates potential inaccuracies in the measurement of total body fat with UWW in which the amount of bone mineral is assumed, rather than measured. If the density of the fat-free mass is lower because of a decreased total body bone mineral content, the total body percent fat will be overestimated by UWW (*94*). The converse is also true; if the density of the fat-free mass is higher because the total body bone mineral is greater than assumed, UWW will underestimate total body percent fat.

The technique calls for the complete submersion of the individual in a tank of water. The individual is asked to exhale as much as possible and then, while holding their breath, they are submerged and weighed under water. Under ideal circumstances, no clothing of any kind is allowed for the measurement. This requirement is often waved but this will affect the accuracy of the measurement to a small extent as well. The amount of air left in the lungs after completely exhaling, the residual lung volume, must be measured since this is expected to provide some buoyancy to the body while underwater. In some institutions the residual lung volume is estimated, rather than measured, using equations that are specific for age, height, and gender.

The person's weight underwater can be calculated based on the Archimedes principle that there is a buoyant counter force equal to the weight of the water that is displaced by the body. Consequently, the weight of the body under water reflects the weight of the body minus the weight of the fluid that is displaced by the volume of the body. When combined with knowledge of the residual lung volume, the volume and density of the body can be estimated. The classic equation used to calculate the density of the fat mass from the total body density is the equation from Siri (*95*) in which

$$F = \left[4.95 \times \left(\frac{1}{D} \right) - 4.50 \right] \tag{7}$$

where F is the density of the fat mass and D is the density of the total body. In recent years, however, equations have been developed for the calculation of fat density that are age and gender specific.

Skinfold Measurements. Body fat can be estimated from multiple measurements of skinfold thickness. This is also considered a two-compartment method. In this method, it is assumed that the distribution of subcutaneous fat and internal fat is similar in everyone. This is a major assumption that is not necessarily valid. Nevertheless, there are equations that allow the calculation of percent body fat from skinfold thickness for men and women.

The technique requires that the skinfold thickness be measured at multiple sites. There are calipers made specifically for this purpose such as the Lange Skinfold Caliper and the Harpenden Skinfold Caliper. The number of sites measured varies from three to seven. The seven-site method calls for measurements of skinfold thickness at the chest, triceps, subscapular region, axilla, suprailiac region, abdomen, and thigh. The more commonly used three-site method calls for measurements at the chest, abdomen, and thigh in men and at the triceps, thigh, and suprailiac region in women.

The measurement of skinfold thickness at the various sites is then used in an equation to calculate the total body density. Equations have been developed by Durnin and Womersley (*96*) as well as Jackson and Pollock (*97, 98*) for this purpose, although Jackson and Pollock also combined gluteal or waist circumference with skinfold measurements to calculate body density. The classic formula to calculate total body density from the 7-skinfold thickness measurement in men is:

$$D = 1.112 - 0.00043499\,(X) + 0.00000055\,(X)^2 - 0.00028826\,(A) \qquad (8)$$

in which D is the total body density, X is the sum of the 7 skinfolds in mm, and A is the age in years. In women, the corresponding formula is:

$$D = 1.097 - 0.00046971\,(X) + 0.00000056\,(X)^2 - 0.00012828\,(A) \qquad (9)$$

For the 3-skinfold thickness measurement, specific equations also exist for men and women. For men:

$$D = 1.109380 - 0.0008267\,(X) + 0.0000016\,(X)^2 - 0.0002574\,(A) \qquad (10)$$

in which D is again the total body density, X is now the sum of the chest, abdomen, and thigh skinfolds and A is age in years. For women, the corresponding equation is:

$$D = 1.099421 - 0.0009929\,(X) + 0.0000023\,(X)^2 - 0.0001392\,(A) \qquad (11)$$

in which X is the sum of the triceps, thigh, and suprailiac skinfolds. Variations of these equations from other authors exist as well. With any of these equations, once the total body density is known, an equation such as Equation 7 in this chapter from Siri (*95*) can be used to calculate the percentage of total body fat. Today, these calculations are readily performed by computer programs. The accuracy and reproducibility of skinfold measurements are highly dependent on the skill of the individual making the measurements.

Bioelectrical Impedance Analysis. Bioelectrical impedance analysis (BIA) is also considered a two-compartment method. In this technique, the individual commonly stands barefoot on a metal foot plate from which an extremely low voltage electric current is sent up one leg and then down the other. The individual may also be asked to lie on a table with electrodes connected to both legs after which an undetectable low voltage electric current is transmitted through the body from the electrodes. Because fat is a very poor conductor of electricity and water, a component of the fat-free mass is a very good conductor of electricity, the resistance to the electric current can be used to estimate the percent body fat.

BIA is a popular method, often found in health clubs because of its ease of use and short measurement time (less than 1 minute). It is generally considered to overestimate

body fat in lean individuals and underestimate body fat in obese individuals. Because BIA results are highly dependent on total body water, the hydration status of the individual can profoundly affect the results. As a consequence, individuals are advised to abstain from eating or drinking in the 4 hours prior to the test, avoid exercise within 12 hours of the test, and abstain from alcohol for 48 hours prior to test. Immediately prior to testing, the individual is asked to empty their bladder. Diuretic use can also affect the results obtained with BIA.

Air Displacement Plethysmography. Air displacement plethysmography can be considered analogous to underwater weighing, except that it is the displacement of air instead of the displacement of water that is used to measure the density and volume of the body. One technique using air displacement is called the BOD POD® (Life Measurements Instruments, Concord, CA). This is an enclosed, egg-shaped, capsule-like structure. An individual undergoing the measurement sits very still within the capsule and breathes quietly during the 5-−8-minute measurement. A swim cap and tight fitting clothing are generally worn. As in underwater weighing, it is necessary to determine the residual lung volume, either by measurement or estimation. The equipment is relatively expensive which limits its availability, although less expensive models have become available. Measurements of body fat with the BOD POD® have been reported to be highly correlated with those made by underwater weighing (*99*). In a review of the published literature from December 1995 to August 2001, the average percent body fat in children and adults differed by less than 1% between the BOD POD® and UWW and by less than 1% between the BOD POD® and DXA in adults and less than 2% in children (*100*).

3-COMPARTMENT BODY COMPOSITION MEASUREMENT TECHNIQUES

Near Infrared Interactance. Near infrared interactance (NIR) for body composition analysis relies on the principles of infrared spectroscopy. A computerized spectrophotometer is used in this method. A probe, which emits an infrared light, is placed on the body. The infrared light passes through the fat and muscle and is then reflected back to the probe. The reflected light is quantified and used to calculate body density. The method is considered quite safe and is fast, convenient, and inexpensive. It requires no particular patient preparation. The NIR unit itself is generally small and portable. The Futrex-5000® (Futrex Inc., Gaithersburg, MD) is a commercial brand of a NIR body composition device. The accuracy of NIR has been compared to skinfolds and BIA using UWW as the reference technique (*101–103*). In general, the results obtained from skinfold measurements, BIA and NIR, were all highly correlated with the results from UWW. At the extremes of weight, skinfold measurements appeared to be more accurate than BIA or NIR, when UWW was used as the reference measurement but all three performed reasonably well in normal weight individuals.

Dual Energy X-ray Absorptiometry. Dual-energy X-ray absorptiometry (DXA) is a three-compartment method for the assessment of body composition because bone mineral is measured as well as the fat and fat-free mass. Unlike UWW or air displacement plethysmography, no assumption needs to be made regarding the amount of bone mineral because it is measured with the technique. Values are also not affected by the residual lung volume, making it unnecessary to either measure or estimate this value. The hydration status of the patient is still important (*104*, *105*). DXA body composition

studies go beyond the measurement of total body fat or fat-free mass. Unlike any other body composition technique, the distribution of fat in the body can be evaluated.

Although body composition software was originally developed for dual-photon absorptiometry, DXA's predecessor, the scan times approached an hour, making the study clinically impractical. The dramatically faster scan times of today's DXA units have reduced the time needed for DXA body composition studies to several minutes. Radiation exposure is reported as 0.037 mrem for the GE Lunar Prodigy™ (Madison, WI) and as low as 0.01 mGy for the Hologic Discovery™ (Bedford, MA) model A. In either case, radiation exposure is extremely low. Body composition software is generally offered as an option with full-size central DXA devices.

DXA total body bone and soft tissue images from a GE Lunar Prodigy ™ are shown in Fig. 13-13. The images seen in Fig. 13-13 are from the same woman, acquired during a total body bone and body composition study. The soft tissue image generally tends to be unflattering, even for a slim individual. The various regions of the body are
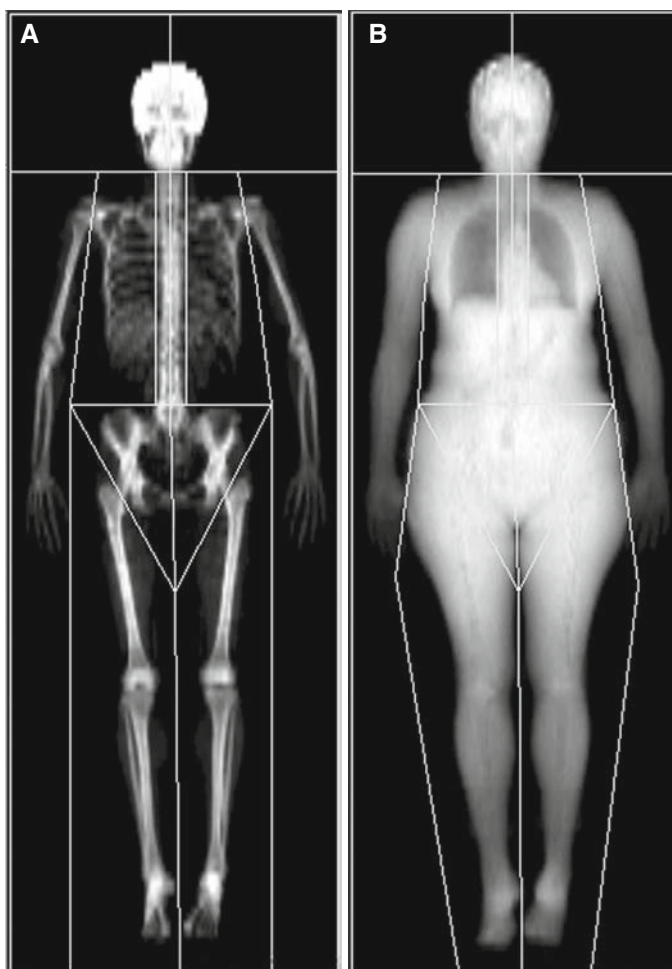
Fig. 13-13. The total body bone image (*left*) and body composition image (*right*) from a total body study on a Lunar Prodigy.
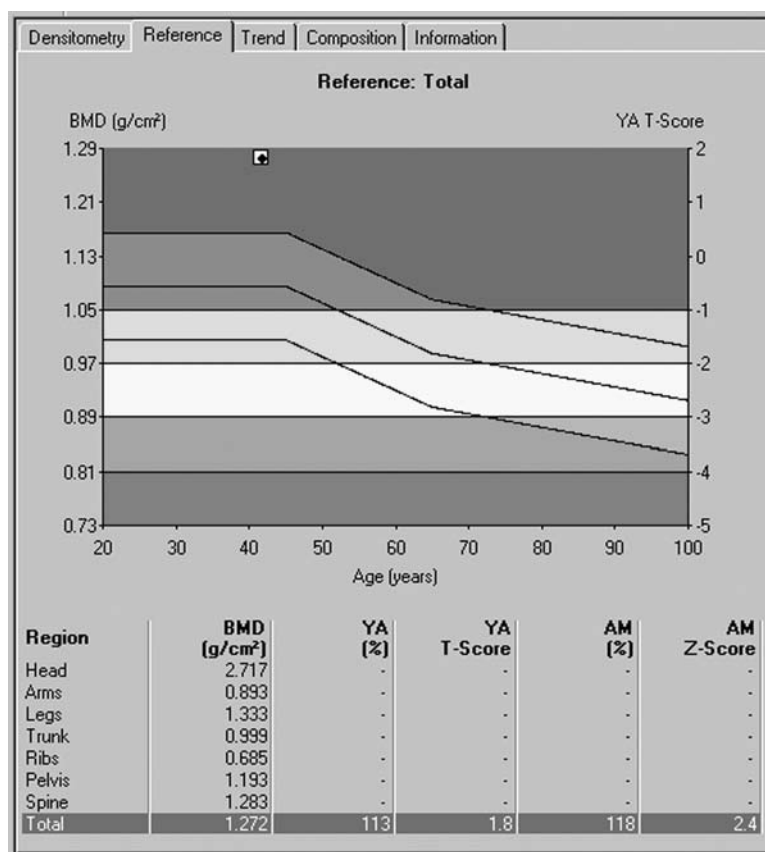
Fig. 13-14. The total body bone density data for the image shown in Fig. 13-13.

defined by the cuts on the image placed by the technologist. Figure 13-14 is the bone density data from this study and Fig.13-15 is the body composition data. Note that in the body composition data in Fig. 13-15, regional values as well as total body values are provided for the grams of fat, lean, and bone mineral. If the grams of fat, lean, and bone mineral are added, the total gram weight provides an extremely accurate assessment of the actual weight of the patient. In this particular case, adding the grams of fat, lean, and bone mineral results in a total gram weight of 56,440 grams or 56.4 kg. This is the derivation of the value listed in the column titled Total mass and in the row for Total values at the bottom of the printout. The total grams of tissue refer to the combined weight of the fat and lean mass. The region % fat values indicate the percentage of fat found in the indicated region when the gram weight of fat, lean, and bone mineral is considered. The tissue % fat refers to the percent of fat found in the indicated region when only the fat and lean gram weight is considered.

In Fig. 13-16, the total body image from a Hologic Discovery is shown. The bone density data from this study is shown in Fig.13-17 and the body composition data, in Fig. 13-18. The presentation of the data is similar but note that on the Discovery total body bone density and body composition data, a subtotal for every column is provided that excludes data from the head region. This is useful because it is often desirable to exclude the head from these analyses because of the marked density of the skull.
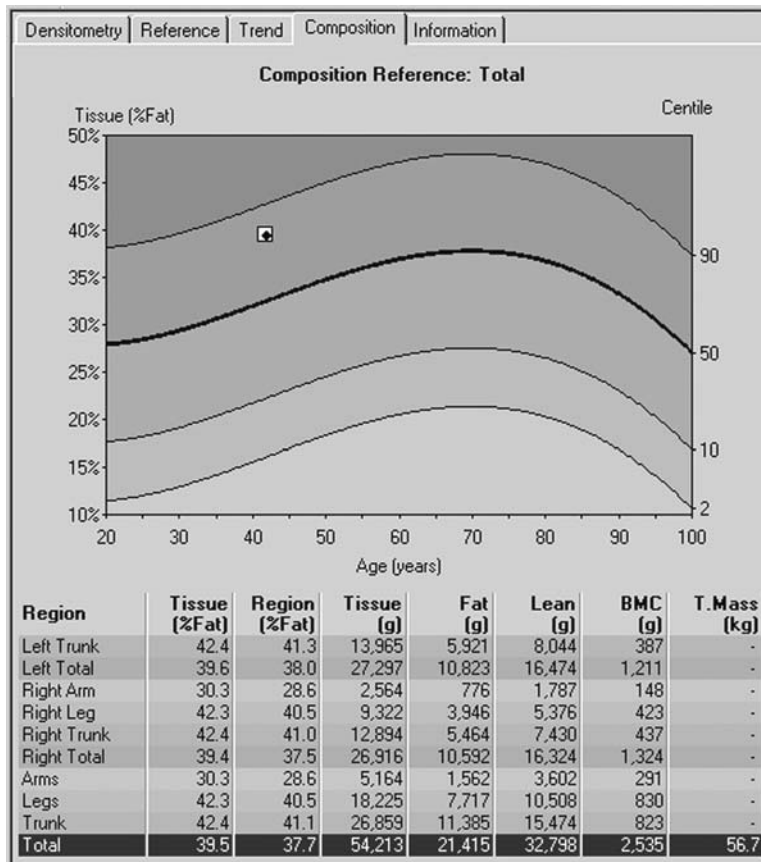
Fig. 13-15. The body composition data for the image shown in Fig. 13-13. The total grams of tissue reflect the grams of fat and lean tissue combined, excluding the grams of bone mineral. The % tissue fat thus reflects the % of fat in tissue only, exclusive of bone mineral. The % region fat reflects the % of fat in a region that includes both tissue and bone mineral. The total tissue mass in kg is an accurate measure of the patient's weight. Here, the value is 56.7 kg or 125 lbs.

In addition to the standard regions of interest shown in the body composition studies in Figs. 13-13 and 13-16, it is also possible to define unique regions of interest for analysis to describe more android or more gynoid distributions of fat. This is commonly done in research studies focusing on cardiovascular disease and the effect of fat distribution. The technologist may be asked to create region of interest boxes that are placed over the abdomen and thighs to make this type of assessment. Some versions of body composition software also provide these highly specialized regions of interest as shown in Fig. 13-19.

DXA body composition assessments of total body fat are highly correlated with those from UWW and skinfold measurements. In a study from Dalsky et al. (*106*) there were no significant differences in the average body fat results obtained in 63 men and women using all three techniques and the measurements were highly correlated. The correlation coefficient for UWW and DXA was 0.864 and for DXA and skinfolds, 0.917.

The precision of body composition measurements with DXA is excellent. In a study of 20 individuals measured four times on consecutive days, the percent coefficient of

Fig. 13-16. The image from a total body study performed on the Hologic Discovery. Case provided courtesy of Hologic, Inc., Bedford, MA.

DXA Results Summary:

Region	Area (cm²)	BMC (g)	BMD (g/cm²)	T-Score	PR (%)	Z-Score	AM (%)
L Arm	197.48	150.33	0.761				
R Arm	220.23	176.76	0.803				
L Ribs	105.72	81.56	0.771				
R Ribs	113.70	77.81	0.684				
T Spine	148.41	150.10	1.011				
L Spine	53.06	63.93	1.205				
Pelvis	207.06	261.46	1.263				
L Leg	363.05	426.29	1.174				
R Leg	369.04	435.21	1.179				
Subtotal	1777.76	1823.45	1.026				
Head	221.82	609.89	2.749				
Total	1999.58	2433.34	1.217	1.3	110	2.3	119

Total BMD CV 1.0%

Fig. 13-17. Total body bone density data for the image seen in Fig. 12-16. Note that a sub-total is provided for total body bone density, bone mineral content and area that excludes the head. Case provided courtesy of Hologic, Inc., Bedford, MA.

DXA Results Summary:

Region	BMC (g)	Fat (g)	Lean (g)	Lean+BMC (g)	Total Mass (g)	% Fat
L Arm	150.33	808.4	1941.2	2091.5	2899.9	27.9
R Arm	176.76	1010.0	2202.4	2379.2	3389.1	29.8
Trunk	634.86	5659.2	20279.8	20914.7	26573.9	21.3
L Leg	426.29	1921.0	6859.0	7285.3	9206.3	20.9
R Leg	435.21	2195.1	7379.5	7814.8	10009.8	21.9
Subtotal	1823.45	11593.7	38661.9	40485.4	52079.1	22.3
Head	609.89	792.2	2829.2	3439.1	4231.3	18.7
Total	**2433.34**	**12385.9**	**41491.1**	**43924.4**	**56310.4**	**22.0**

Fig. 13-18. The body composition results for the image seen in Fig. 12-16. The % Fat indicates the percentage of fat of the total tissue mass. The total mass in grams reflects the grams of bone mineral, lean, and fat tissue and is thus a measure of the patient's weight. A subtotal for each column is provided that excludes the head data. Case provided courtesy of Hologic, Inc., Bedford, MA.
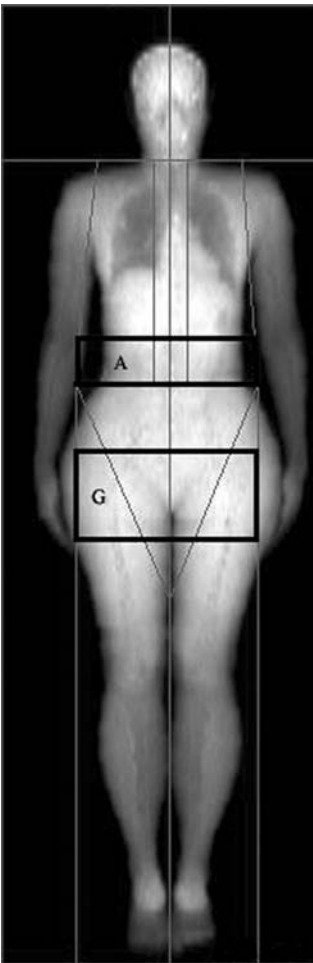
Fig. 13-19. Specialized regions of interest on a GE Lunar Prodigy body composition study. **(A)** indicates the android region of interest. **(G)** indicates the gynoid region of interest. Image provided courtesy of GE Healthcare, Madison, WI.

variation[22] for total body BMD was 0.62% and for total body percent fat, 1.89% (*107*). The precision of the total body fat mass, lean mass, and bone mineral content, expressed as the %CV, was 2.0, 1.11, and 1.09%, respectively. Regional measurement precision tended not to be as good as total body measurement precision. The authors also noted that, just as in following changes in bone density, the same scan mode should always be used when performing total body DXA studies to follow changes in body composition. Use of different scan modes is expected to reduce the precision of repeat measurements (*108*).

Using the same device for serial measurements of body composition is equally imperative in achieving good precision, just as it is in the measurement of bone density. As is recommended for following changes in bone density, changes in body composition assessed by DXA should be made on the basis of serial measurements on the same DXA device. In one study from Soriano et al. (*109*) although body composition measurements on 78 adults were highly correlated when performed on a GE Lunar DPX, GE Lunar DPX-L, GE Lunar Prodigy, and Hologic Dephi, there were significant differences in the % fat and bone mineral measurements among the devices. Although the body composition measurements performed on one manufacturer's device will be highly correlated with those from another, there will be differences in the absolute results because of differences in the manor in which the machines are calibrated. In a comparison of body composition measurements from devices from three different DXA manufacturers, Tothill et al. (*110*) found differences of 2.6–6.3% in the total body fat and as much as 13% in trunk fat. Even among devices from the same manufacturer, small differences have been found that could adversely affect the precision of serial measurements (*111*, *112*).

A final practical consideration is the height and weight of the patient to be studied. It is imperative that the entire body be included in the scan field. Therefore, the maximum height that can be accommodated will be determined by the table length and maximum scan length. In general, heights less than 6 feet (1.83 m) can be accommodated. The maximum weight that can be accommodated is largely a function of the construction of the scan table and may vary from manufacturer to manufacturer. Any height and weight limitations for a total body study should be provided by each manufacturer.

The Metabolic Syndrome

The measurement of body fat, and in particular abdominal fat or adipose tissue,[23] has assumed increasing importance in the evaluation and management of the patient with the metabolic syndrome. Current definitions of the metabolic syndrome are based in part, on the measurement of waist circumference, a surrogate measure for abdominal adiposity, rather than the BMI (*113*, *114*). The International Diabetes Federation (IDF) criteria and the American Heart Association/National Cholesterol Education Program

---

[22] See Chapter 11 for a discussion of the percent coefficient of variation and the number of subjects and studies needed for a valid precision study.

[23] Chemical fat is actually a component of adipose tissue. Fat can be found in other tissues as well. Similarly, adipose tissue also contains protein, minerals, and water. The terms fat and adipose tissue are unfortunately often used interchangeably, even though they are clearly not synonymous.

Table 13-8
International Diabetes Federation Criteria for the Diagnosis of the Metabolic Syndrome

Central Obesity Based on Waist Circumference $\geq$ 37″ (94 cm) for Europid men $\geq$ 31.5″ (80 cm) for Europid women	
And any two of these four criteria	TGY 150 mg/dL HDL $<$ 40 mg/dL for men $<$ 50 mg/dL for women BP Systolic $\geq$ 130 mmHg or Diastolic $\geq$ 85 mmHg FPG $\geq$ 100 mg/dL

TGY, triglycerides; HDL, high density lipoprotein; BP, blood pressure; FPG, fasting plasma glucose.

Table 13-9
American Heart Association/Updated National Cholesterol Education Program Criteria for the Diagnosis of the Metabolic Syndrome. For the diagnosis, the patient must meet three of the five listed criteria

Waist Circumference	$\geq$ 40″ (102 cm) in men $\geq$ 35″ (88 cm) in women
TGY $\geq$ 150 gm/dL	
HDL	$<$ 40 mg/dL in men $<$ 50 mg/dL in women
BP	Systolic $\geq$ 130 mmHg Diastolic $\geq$ 85 mmHg
FPG $\geq$ 100 mg/dL	

TGY, triglycerides; HDL, high density lipoprotein; BP, blood pressure; FPG, fasting plasma glucose.

(AHA/NCEP) criteria are shown in Tables 13-8 and 13-9. The waist circumference is unrelated to height, and although it correlates closely with the BMI, it is associated with risk factors for cardiovascular disease, independent of the BMI (*115*).

In addition to waist circumference, the waist-to-hip circumference ratio (WHR) or, much less often, the sagittal abdominal diameter (SAD) may be used as a surrogate for abdominal obesity or adiposity. In general, however, because the waist circumference is easily measured and strongly correlates with abdominal visceral fat (*116–120*), guidelines such as those from the IDF and AHA/NCEP have focused on the waist circumference in assessing risk. The correlation with abdominal visceral fat is important because increased visceral or abdominal adipose tissue is strongly associated with metabolic and cardiovascular disease risk, as well as a variety of chronic diseases (*121–126*). Abdominal visceral fat may be less sensitive to anti-lipolytic stimuli such as insulin and thus more likely to release free fatty acids into the circulation (*127*). Although visceral fat may release proportionally less free fatty acids into the circulation than subcutaneous fat, visceral fat-derived free fatty acids are released into the portal vein and therefore, into the liver, which may cause reduced hepatic insulin clearance, increased glucose production, and lipid

abnormalities. The contribution of subcutaneous fat to insulin resistance is not entirely clear and may depend on whether the subcutaneous fat is superficial or deep. In some studies deep subcutaneous fat has shown a much stronger association with insulin resistance than superficial subcutaneous fat (*128*, *129*).

Imaging modalities that are used to quantify abdominal fat or adipose tissue and abdominal visceral adipose tissue include MRI, CT, and DXA. MRI and CT are three-dimensional imaging techniques, whereas DXA is a two-dimensional technique. This means, of course, that MRI and CT can distinguish between visceral, deep, and superficial locations, whereas DXA cannot. In addition, MRI and CT measure adipose tissue (*130*). DXA measures fat. Of research interest then, is how well DXA-measured abdominal fat correlates with MRI- or CT-measured abdominal adipose tissue, and in particular, MRI and CT-measured abdominal visceral adipose tissue.

Park et al. studied 90 non-obese men ranging in age from 18 to 44 years to assess the correlation between DXA-derived abdominal fat and MRI-derived abdominal adipose tissue (*131*). Abdominal adipose tissue and total visceral adipose tissue were measured with whole body MRI, while visceral adipose tissue (VAT) area was measured by single slice MRI at the L4-L5 level. In addition to the standard trunk region of interest (ROI) four specialized ROIs were defined in this study for DXA measurements of abdominal fat: from the upper edge of L2 to the lower edge of L4; the upper edge of L2 to the iliac crest; the lower costal margin to the iliac crest; and the lower costal margin to the iliac crest excluding the spine. The correlations for abdominal and visceral adipose tissue measured by MRI and in the various DXA ROIs are shown in Table 13-10. The authors noted that the findings suggested that the ribs, spine, and pelvis had little influence on the measurement of soft tissue in the trunk.

Table 13-10
Correlation of DXA-Measured Fat with MRI-Measured Adipose Tissue.
All correlations are significant at p<0.01

DXA ROI	Total VAT	Abdominal AT
Standard trunk	0.825	0.960
L2-L4	0.852	0.974
L2-iliac crest	0.844	0.963
Lower costal margin-iliac crest	0.822	0.945
Lower costal margin-iliac crest without spine	0.818	0.948

DXA, dual-energy X-ray absorptiometry; VAT, visceral adipose tissue; AT, adipose tissue.
Adapted with permission of Macmillan Publishers Ltd. from ref. (*131*).

Snijder et al. (*132*) utilized slightly different ROIs to compare DXA-measured abdominal fat and CT-measured abdominal and visceral adipose tissue. In this study, 148 men and women aged 70–79 years underwent CT scans using a 10 mm slice thickness at the L4-L5 level as well as DXA total body scans, utilizing the standard trunk ROI and a manually created ROI, 3 pixels high, which rested on the tops of the iliac crests. CT-measured abdominal and visceral adipose tissue quantities converted to equivalent DXA-measured abdominal fat, taking into account the methodological differences in the two techniques. The correlation between CT-derived abdominal fat and DXA sub-region abdominal fat was very good at 0.96, although the DXA sub-region derived abdominal fat was significantly lower than the CT-derived abdominal fat. The correlations for

Table 13-11
Correlations Between CT-Visceral Fat and DXA Fat Measurements. All correlations are significant with P<0.001

| | CT Visceral Fat | | | |
| | Men | | Women | |
DXA Fat	White (41)	Black (33)	White (40)	Black (34)
Abdominal Subregion ROI	0.622	0.783	0.794	0.646
Trunk ROI	0.679	0.773	0.835	0.606
Total Body	0.586	0.747	0.763	0.514

DXA, dual-energy X-ray absorptiometry; CT, computerized tomography; ROI, region of interest.
Adapted with permission of Macmillan Publishers Ltd. from ref. (*132*).

DXA-derived abdominal fat and CT-derived visceral fat are shown in Table 13-11. The authors concluded that DXA was a good alternative to CT for predicting abdominal and visceral fat.

Glickman et al. (*133*) also compared DXA-derived measures of abdominal fat with CT-derived abdominal adipose tissue. Glickman et al. also evaluated the interrater reliability of three technologists. The authors utilized a specialized DXA ROI which was a quadrilateral box using a lower boundary at the L4-L5 disc space, and an upper boundary at the T12-L1 disc space. CT scanning spanned essentially the same region. As in the study from Snijder et al. (*132*), DXA-measured fat mass was significantly lower than CT-measured fat mass but was also significantly correlated with CT-measured fat mass ($r = 0.967$, $p < 0.0001$) (*133*). Among the three technologists who each analyzed 43 DXA studies using the manually created L1-L4 ROI, there were no significant differences in total mass, fat mass, or lean mass. The intraclass correlations were excellent at $r = 0.94$ for total mass, $r = 0.97$ for fat mass and $r = 0.89$ for lean mass (all, $p > 0.0001$).

The assessment of body composition in clinical medicine, particularly by DXA, is relatively new with the potential exception of the field of sports medicine. Body composition measurements are playing a role in the assessment and management of anorexia nervosa as well as Crohn's disease, celiac disease, and cystic fibrosis (*134*). However, the increasing prevalence of obesity and the metabolic syndrome has accelerated interest in the utility of readily available technologies such as DXA for the assessment of body composition and abdominal fat (*135*).

PEDIATRIC DENSITOMETRY

The application of DXA in pediatric medicine is a rapidly growing field. The rapidity of its growth, however, increases the likelihood of technical errors and misinterpretation of the results. One of the most important lessons to remember in pediatric densitometry is the admonition (*136*) from an expert in the field that "Children are not simply small adults." An extension of this statement relevant to the densitometrist is that an expert in adult densitometry is not automatically an expert in pediatric densitometry.

There are many issues in pediatric densitometry that are not concerns in adult densitometry, or which are of less concern. The pediatric skeleton is constantly changing

in terms of size and even shape. Ossification centers fuse in different bones at different ages. A child's chronological age does not necessarily reflect their bone age. The onset of puberty, at whatever age it occurs in the child, has a pronounced effect on the development of the skeleton. The densitometry software in pediatric densitometry must be able to detect bone edges in the setting of lower densities than often seen in adult densitometry. Radiation safety issues are not the same. Reference databases for adults are not appropriate in pediatric densitometry. Similarly, the use of the T-score in pediatric densitometry is not appropriate. And finally, the diagnosis of any degree of low bone mass or density should not be made on the basis of the mass or density measurement alone.

Pediatric Scan Acquisition and Analysis

The technical aspects of the performance of pediatric densitometry are not that different from those for adult densitometry. The greatest challenge in scan acquisition may indeed be keeping the child still during the scan. The shorter scan times needed by newer densitometers have helped to alleviate but not completely eliminate this problem. The manufacturer's directions for positioning and analysis should be followed for any given type of scan. It is preferable, however, that the acquisition software be software that is specifically designed for a pediatric population.

Bone edge detection algorithms that are unique to each manufacturer's DXA device enable the separation of bone from soft tissue. Edge detection algorithms designed with an adult population that has an expected range of bone densities in mind, may fail when used in a pediatric population with an anticipated lower body weight and lower bone mineral density (BMD). In essence, the machine may be unable to tell where the bone stops and starts. This will cause a failure in appropriate edge detection. The bone edges or bone map should be verified by the technologist during the analysis and corrected, if necessary. In a review of pediatric 34 pediatric bone density studies in which a diagnosis of osteoporosis, osteopenia, or low bone density was made, Gafni and Baron (*137*) found errors in bone mapping in seven or 21%. After recognition of these errors, three of the seven bone densities were found to be normal but two of the seven still could not be classified because of other errors.

Pediatric densitometry must be performed with these edge detection issues in mind. In 1993, Hologic, Inc. introduced a low-density spine (LDS) software option to be used in children as well as adults with low bone density. This was an operator-selected analysis mode rather than a scan acquisition mode. The effects of low-density edge detection became apparent when 100 bone density studies in children ages 2–18 years were analyzed using the LDS option as well as the standard analysis option (*138*). When the LDS option was used, the measured bone area and bone mineral content (BMC) increased significantly. Because the bone area increased to a greater degree than the BMC, the BMD decreased an average of 8.7% with the LDS option. Norland systems such as the XR-46™ and Excell™ utilize a dynamic filtration system that automatically adjusts the photon flux to accommodate differences in body size during scan acquisition. Systems like the GE Lunar Prodigy™ automatically select the best scan mode based on the height and weight of the patient and also employ specialized analysis algorithms for low bone density in the pediatric spine.

Radiation Safety Issues in Pediatric Densitometry

Radiation safety in densitometry in general was discussed in Chapter 5. As in adult densitometry, the overriding principle guiding radiation safety in pediatric densitometry is "as low as reasonably achievable" or ALARA. In pediatrics, however, the effective dose equivalent (H_E)[24] cannot be assumed to be the same as in adult densitometry. Body size may have a pronounced effect on the H_E because a smaller body size (less tissue thickness) may result in a greater dose to a specific organ and there is the potential for a proportionally greater amount of the body to be irradiated. Several studies have attempted to define H_E in children for total body, PA lumbar spine, and proximal femur studies on both pencil-beam and fan-array densitometers (*139–141*). Because the skin entrance doses are lower with pencil-beam systems than with fan-array systems, the H_E on a pencil-beam system will also be lower, all other things being equal. On the Lunar DPX-L, a pencil-beam DXA device, the H_E for a 5- and 10-year-old child for a PA lumbar spine study was estimated to be 0.28 and 0.20 µSv, respectively (*139*). For a total body study, the H_E values were 0.02 and 0.02 µSv. As expected, higher values for the H_E were found by Thomas et al. (*140*) and Blake et al. (*141*) for Hologic fan-array systems. Thomas et al. (*140*) estimated an H_E of 4.7 µSv for a 1-year-old for a PA lumbar spine study and values of 15.2 and 6.4 µSv for a proximal femur study in 1-year-old males and females in the fast array mode available on the QDR 4500. The difference between the males and females reflects the difference in the proportion of the gonads exposed to ionizing radiation. The effective doses calculated in this study are shown in Table 13-12. These calculations utilized the tissue weighting factors originally proposed by the ICRP in 1990 (*142*). H_E values for different Discover/QDR 4500 scan modes were calculated by Blake et al. (*141*) for 5-, 10-, and 15-year-old children as well as an adult using both the ICRP60 tissue weighting factors and the newer ICRP 2007 tissue weighting factors, in which, notably the tissue weighting factor for the gonads was decreased. These results are shown in Table 13-13. Blake et al. noted that the H_E values were lower in the express mode, available on the Discovery,

Table 13-12

Effective Dose for DXA Scans by a Hologic ADR 4500A Densitometer as a Function of Age

Age (year)	Lumbar spine scan[a] (fast array mode)	Total Body Scan		Hip Scan (fast array mode)		Forearm Scan[a]
		Male	Female	Male	Female	
1	4.7	3.4	3.5	15.2	6.4	0.14
5	3.3	2.9	3.0	13.2	6.1	0.10
10	2.7	2.5	2.7	8.3	5.6	0.066
15	2.2	2.0	2.2	6.3	4.7	0.03
Adult	2.2	1.8	2.1	5.1	4.6	0.03

[a] No difference between males and females

Reproduced with permission of Elsevier from ref. (*140*).

[24] See Chapter 5 for a discussion of the effective dose equivalent (H_E).

Table 13-13

Effective Doses (μSv) from Spine, Hip, and Total Body DXA Examinations for Different Discovery/QDR4500 Scan Modes

Scan length	Adult Default	15-year-old child		10-year-old child		5-year-old child	
		Scaled	Default	Scaled	Default	Scaled	Default
Spine scan modes							
Array (ICRP-60)	13.3	14.8	16.9	21.3	33.4	27.3	48.3
Fast (ICRP-60)	6.7	7.4	8.5	10.6	16.7	13.7	24.1
Express (ICRP-60)	4.4	5.0	5.6	7.1	11.1	9.1	16.1
Express (ICRP2005)	4.4	4.9	5.5	6.9	10.2	8.8	14.4
Hip Scan Modes							
Array (ICRP-60)	9.3	11.1	11.3	17.8	20.1	22.2	29.4
Fast (ICRP-60)	4.7	5.5	5.6	8.9	10.0	11.1	14.7
Express (ICRP-60)	3.1	3.7	3.9	5.9	6.7	7.4	9.8
Express (ICRP2005)	2.4	2.7	2.8	4.1	4.5	4.9	6.1
Whole body scans							
Discovery-A	4.2	–	4.2	–	4.8	–	5.2
Discovery-W	8.4	–	8.4	–	9.6	–	10.5

Scaled scan length refers to the shortened default scan length. ICRP2005 refers to the draft recommendations, which became ICRP2007. Slightly lower values for the H_E seen with the ICRP2005 tissue weighting factors primarily reflect the lower tissue weighting value given to the gonads.

Reproduced with permission of Elsevier from ref. (*141*).

compared to the fast or array modes. All of these authors noted that the H_E for the various scan types was very low. As was correctly pointed out by Blake et al., however, the real difference in risk is underestimated by the H_E in children compared to adults because of the greater sensitivity of growing tissues and the longer life expectancy of the child. In keeping with the principle of ALARA, the H_E should be kept as low as possible by using the fastest scan mode that is appropriate, shortening the scan length to accommodate the child, and by using careful technique to avoid scan re-starts and repeats.

Bone Age

Bone age is not necessarily the same as a child's chronological age. Bone age is a reflection of the developmental maturity of the skeleton. The presence of unfused and fused epiphyses is a reflection of developmental maturity. The epiphyses are secondary ossification centers at the ends of long bones and are responsible for longitudinal growth. The epiphyseal plate deposits cartilage, which subsequently becomes bone. Ultimately the epiphysis itself becomes engulfed in bone. Longitudinal growth stops and the epiphysis is then said to be "fused" with the rest of the bone. After fusion the only remnant of the ossification center is a line of demarcation called the epiphyseal line. The presence of unfused epiphyses will cause a DXA image that appears bizarre to the densitometrist accustomed to adult images such as the proximal femur image in Fig. 13-20. The greater trochanter is not completely formed or fused with the rest of the proximal femur. Ossification in the greater trochanter begins around the age of 3, but is not complete until
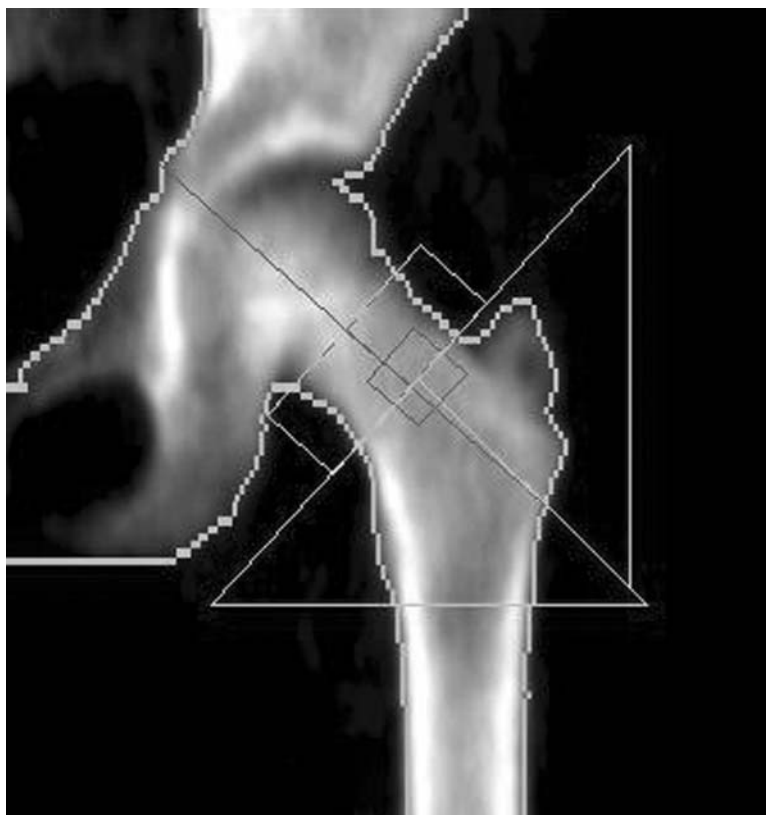
Fig. 13-20. A DXA image of a proximal femur in a child. The greater trochanter in particular appears unusual. The greater trochanter is not fully formed and will not completely fuse to the femoral neck and shaft until approximately 18 years of age.

around the age of 18 (*143*). Fusion of the femoral head and lesser trochanter to the proximal femur is also generally not complete until around the age of 18. The typical adult appearance of the vertebrae is not seen in young children. There are ring-like epiphyses on the upper and lower surfaces of the vertebral bodies that appear around the age of 16 but which do not fuse with the rest of the vertebral body until around the age of 25. Other regions that are commonly studied with DXA in which unfused epiphyses may be seen are the heel and the forearm. The secondary ossification center in the posterior calcaneus appears around the age of 7 and fuses at puberty. At the distal radius and ulna, secondary ossification centers appear by ages 1 and 5, respectively although neither fuses until around the age of 20.

The state of the secondary ossification centers in the hand is used to determine bone age. There are two techniques that are traditionally used to make this determination: the Greulich and Pyle method and the Tanner and Whitehouse method (*144*, *145*). The Greulich and Pyle method requires a comparison of all the bones in the hand and wrist against reference X rays for a wide range of ages. The technique has been modified in many centers to a comparison of the overall appearance of the child's hand to a

set of reference radiographs. The Tanner and Whitehouse method[25] requires a systematic assessment of the maturity of all the bones in the hand and wrist and employs a point scoring system to determine skeletal maturity. Although studies (*146*, *147*) have suggested that the two techniques give similar results, some authorities prefer the Tanner and Whitehouse method. Bone age is not determined from a DXA study. However, the interpretation of the bone density seen on a DXA study may well be affected by knowledge of the child's bone age. For example, if the child's bone age is less than their chronological age, their bone density would not be expected to be the same as their chronological peers.

Sexual Maturation Stage

Another important element in the interpretation of pediatric bone density measurements is knowledge of the level of sexual development of the child. This assessment is usually made by determining the Tanner[26] Stage (*148*). Tanner assigned 5 stages to puberty for both boys and girls, with Stage 1 indicating prepubertal development and Stage 5 indicating mature sexual development. The 5 stages in girls are based on the development of the breasts and pubic hair. For boys, the stages are based on the development of the genitalia and public hair. Tanner Stages are associated with different rates of linear growth (increase in height). In girls, the peak rate of linear growth is generally seen in Tanner Stage 3 around the age of 11.5 years. In boys, the maximum rate of linear growth occurs in conjunction with Tanner Stage 4 around the age of 13.5 years. In clinical practice, representative drawings are often used to allow the child to pick the body image that most closely matches their own. This is generally thought to be the least intrusive manner by which to make this determination. Parental permission is, of course, mandatory. Given that the Tanner Stage represents pubertal development, it is not surprising that it is linked to skeletal maturity and rates of increases in height. This is relevant information then, to the interpretation of a pediatric bone density study.

Considerations of Bone Size and Shape

The potential effect of changes in size on bone density was discussed in Chapter 6. Because the BMD obtained with DXA is a two-dimensional areal measurement, a larger bone may have a greater BMD than a smaller bone in spite of both having identical volumetric BMDs (*149*, *150*). The maturation of the skeleton and increases in height will cause changes in the shape and size of the bones, making this issue particularly relevant to pediatric densitometry. In addition, children with chronic diseases are often smaller than healthy children of the same age. The interpretation of areal density in such children must be made cautiously to avoid incorrectly diagnosing a child who simply has small bones from any cause as having an abnormally low bone mass for their age. Mølgaard et al. (*151*) proposed a three-step method to address the potential for misdiagnosis in a pediatric population because of changes in the size or shape of the bones. The authors

---

[25] The Tanner and Whitehouse method is often indicated by the abbreviation TW2 to indicate the method proposed in 1983 rather than an earlier method proposed in 1975.

[26] This is the same James Mourilyan Tanner as in the Tanner and Whitehouse bone age method.

noted that BMD was the ratio of the BMC divided by the bone area and that if the bone area was small, the BMC would potentially be reduced. They pointed out that it was important to know whether the low BMC was the result of a small bone area. Mølgaard et al. proposed the concept of BMC adjusted for bone area, which is also called "BMC for bone area." They also proposed an assessment of bone area adjusted for height or "bone area for height" and an assessment of height adjusted for age, also called "height for age." They suggested that this would address three potential causes of an apparent low BMD in a child: "light bones," "narrow bones," and "short bones." In essence, these three parameters address the following questions: Is the height appropriate for the age or does the child have "short bones?" Is the bone size or area appropriate for the child's height or does the child have "narrow bones?" Is the BMC appropriate for the bone area or does the child have "light bones?" The relevance of each of these findings to the health of the child may be quite different to the pediatrician. Figure13-21 shows the plot of these three parameters on centile scales[27] for the child whose total body bone density study is shown in Fig. 13-22. Data for the comparison of height for age comes from US Centers for Disease Control (*152*) growth statistics. BMC for bone area and bone area for height data are derived from the manufacturer's pediatric reference database. In
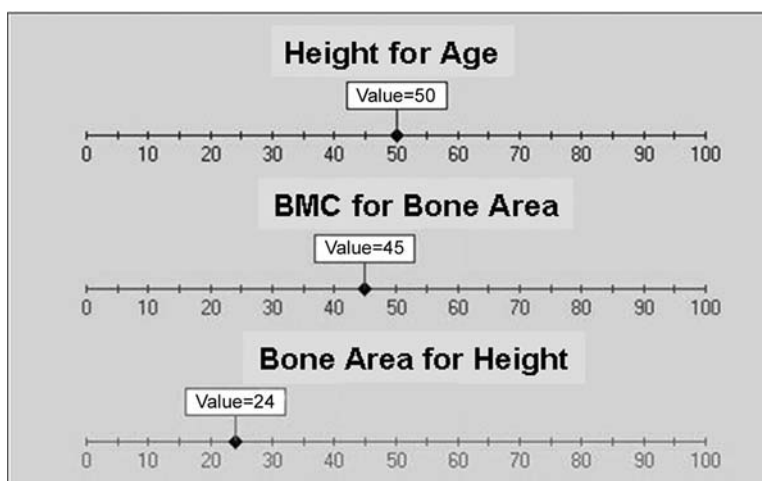
Fig. 13-21. Ancillary data provided as part of the pediatric total body study seen in Fig. 13-22. These centile line graphs provide necessary comparisons of the child's height for their age, bone area for their height and BMC for their bone area. This is useful in determining whether a low BMD in a child is the result of a truly decreased BMC or simply the result of bones that are smaller in size than an average child of the same age, sex, and ethnicity.

[27] A centile scale reflects values from 0 to 100. The terms centiles and percentiles are often used interchangeably. The location of the value plotted on the scale indicates the percentage of individuals in the population in question, who have a similar or poorer value. For example, if the centile scale reflects a value of 40, 40% of individuals in that population have the same or poorer value for the quantity in question. Conversely, 60% will have a higher value. If the value on the centile scale is 50, an appropriate interpretation is that half of the population will have a better value and half will have a poorer value. A centile value of 5 or less is generally a cause for concern although some circumstances may dictate concern at higher centile values.
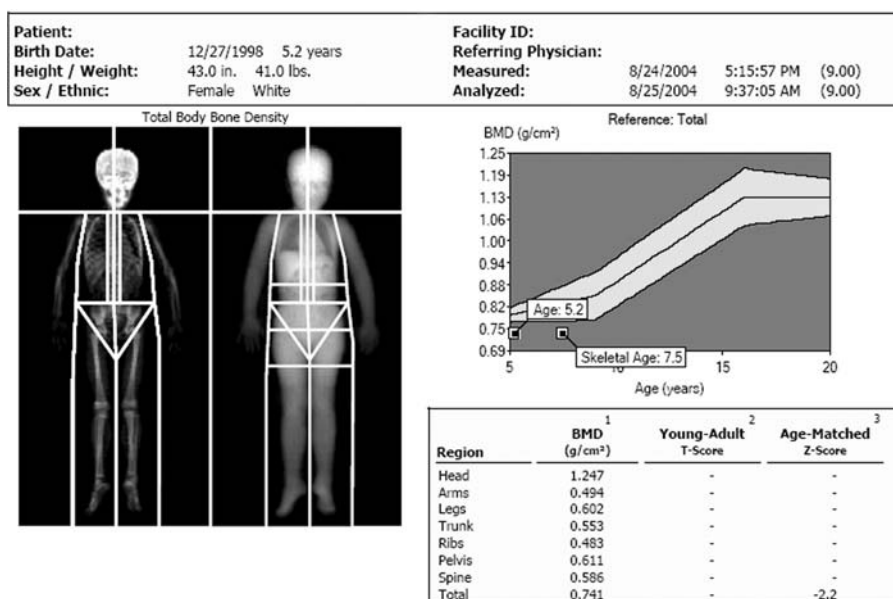
Fig. 13-22. A pediatric DXA total body study performed on the GE Lunar Prodigy for a 5-year-old girl. The total body bone image is on the left and the body composition image is on the right. Note that only the *z*-score is shown for the total body bone density. The bone age is also plotted on the age-regression graph and is shown as 7.5 years. This age was determined using the Tanner-Whitehouse method and inputted by the technologist prior to data acquisition. Case courtesy of GE Healthcare, Madison, WI.

this particular example, the total body bone density z-score shown in Fig.13-22 is −2.2. Why might this be? The centile scales shown in Fig. 13-21 suggest that the bone area for height is only in the 24th percentile while the height for age and BMC for bone area centiles are better. This suggests that the low BMD *z*-score may be in part determined by what Mølgaard et al. (*151*) called "narrow bones" and not solely due to a truly low BMC.

Skeletal Development and the Use of Standard Scores in Pediatric Densitometry

As noted in Chapter 3, the standard score called the T-score in densitometry indicates the number of standard deviations above or below the average peak bone density that the patient's bone density lies. The *z*-score, on the other hand, is the standard score comparison to the bone density that is predicted for the patient's age. Both are used in adult densitometry, although the T-score commands greater attention for its role in the diagnosis of osteoporosis based on the World Health Organization criteria[28] as well as for fracture risk prediction. Authorities in pediatric densitometry agree, however, that the use of T-scores in children for any purpose is *not* appropriate. To find that a child has a bone density that is less than the average peak bone density is expected because the child may not have reached the age by which peak bone density is achieved. Such a finding then, carries no particular significance and if misinterpreted, great potential harm.

---

[28] See Chapter 9 for a discussion of the World Health Organization criteria for the diagnosis of osteoporosis based on the measurement of bone density.

SKELETAL DEVELOPMENT

The exact age at which peak bone density is reached at any given skeletal site remains somewhat controversial. It is clear, however, that the age of peak bone density may be different between boys and girls and that the age of peak bone density may vary by skeletal site (*153*, *154*). The age at which peak bone density is achieved at any site may also be determined not just by the patient's chronological age, but by their bone age and pubertal status as well.

Changes in bone density in 778 Caucasian boys and girls, aged 2–20 years, were determined in a cross-sectional study by Zanchetta et al. (*155*) using DXA of the PA lumbar spine, proximal femur, and total body. In this study, BMD at the PA lumbar spine and proximal femur did not increase significantly after the age of 14 in girls. In boys, however, BMD at the spine increased throughout the age range of the study, but significant increases in proximal femur BMD were not seen in boys after the age of 16. Total body BMD in girls did not increase after the age of 16 but increased throughout the age range in boys. Nguyen et al. (*153*) also reported that total body peak BMD was reached earlier in girls than in boys, although at a later age than reported by Zanchetta et al. In a longitudinal study of 94 males and 92 females, aged 6–36 years with an average follow-up of 4.29 years, peak total body bone density was reached by the age of 20.8 years in females and 25.2 years in males.

Teegarden et al. (*156*) looked specifically at total body BMC and BMD with DXA in 247 girls and young women aged 11–32. They concluded that 99% of peak total body BMD and total body BMC is achieved by 22.1 years and 26.2 years of age, respectively. Based on a study (*154*) of 300 girls and women aged 6–32, these same authors concluded that peak BMD was achieved at the PA lumbar spine by age 23 although BMC and bone area continued to increase at the spine across the age range of this study. Peak BMD at the femoral neck was reached by the age of 18.5 years.

In another very large cross-sectional study by Sabatier et al. (*157*), changes in BMD, BMC, and bone area were determined in 574 girls aged 10–24 years. In this study, bone density measurements were made at the lumbar spine with DXA. Bone age was determined for girls less than age 20 using plain radiographs of the left hand and wrist with the Greulich and Pyle (*144*) method. Pubertal status was assessed using Tanner stages (*145*). Sabiatier et al. found that the BMD and BMC in the lumbar spine increased dramatically between the bone ages of 10 and 14 or until the first year after menarche.[29] Between the bone ages of 14 and 17 the PA lumbar spine BMD and BMC continued to increase, but at a slower rate. After the bone age of 17 or the 4th year after menarche, no additional significant increases in PA lumbar spine BMD or BMC were seen. The authors noted that bone age and pubertal status appeared to be more useful than chronological age in assessing skeletal status. They observed that lumbar spine BMC roughly doubled between the bone ages of 10 and 17 and that the period between the bone ages of 10 and 14 was particularly critical in the development of BMC.

The effect of pubertal state on the accumulation of bone mass had previously been observed by Theintz et al. (*158*). In a study of 98 girls and 100 boys aged 9–19 years,

---

[29] Menarche is defined as the age at which the first menstrual period occurs.

Theintz et al. found that BMC and BMD increased rapidly between the ages of 11 and 14. The rate of increase dropped dramatically, however, after the age of 16 or 2 years after menarche. In this study, 16 appeared to be the age of peak bone mass at the lumbar spine and femoral neck in girls. These findings are very similar to those from Sabatier (*157*). In boys, the increase in both BMC and BMD at the lumbar spine and proximal femur was greatest between the ages of 13 and 17. The rate of increase declined markedly after the age of 17 at both sites. No additional significant increases were seen at the femoral neck after the age of 17 in boys although significant increases in spine BMD were still seen. Finally, in the Bone Mineral Density in Childhood Study (BMDCS), 1554 children (761 boys, 793 girls) underwent DXA bone density testing at the PA lumbar spine, left proximal femur, nondominant forearm, and total body on the Hologic QDR 4500A, QDR 4500 W, or Delphi A (*159*). Based on 3-year data from 1442 children, the authors concluded that BMD was still increasing at all skeletal sites measured in girls aged 16 years and boys aged 17 years.

Although there are slight differences among the various studies that have attempted to determine the age of peak bone mass and density at various skeletal sites, the majority of these studies have concluded that peak bone mass is achieved at most sites by the age of 20. There is little disagreement that the overwhelming majority of peak bone density is attained by the age of 20. Increases in BMC and bone area may indeed continue, particularly at the spine, after the age of 20 (*154*). This would not necessarily be reflected as an increase in BMD because BMD is the ratio of BMC to area.

THE USE OF STANDARD SCORES IN PEDIATRIC DENSITOMETRY

An appreciation of the timing of peak bone density is critical to understanding why T-scores *must not be used* in the interpretation of bone density in children. This would be analogous to comparing the height of a 7-year-old to the height of a 35-year-old and concluding that the 7-year-old was abnormally short. Unfortunately, this misuse of the T-score is not widely appreciated. In the study cited earlier from Gafni and Baron (*137*) in 2002, the results of a review of 34 DXA bone density studies and the accompanying interpretations in children aged 4–17 years were reported. These children had been referred to the National Institutes of Health as possible participants in an osteoporosis treatment trial. All 34 children had a diagnosis of osteoporosis, osteopenia, or low bone mass based on the original bone density study interpretation. Gafni and Baron found that 88% or 30 of the 34 studies had at least one error in interpretation. In 21 of the 30 studies, the T-score had been used for diagnosis even though the *z*-score was also present on the printout. When the appropriate interpretation was made based on the *z*-score, 12 of these 21 children actually had a normal bone density. In 5 of the 21, an accurate diagnosis could not be made because of a lack of necessary information.

Printouts of DXA studies from major DXA manufacturers in which pediatric software is used do not display a T-score. This is seen in the printout from the total body study in Fig. 13-22 and the PA lumbar spine bone density study in Fig. 13-23. Note that only *z*-scores appear on the report. In the ancillary data for this study shown in Fig. 13-24, both the T-score and the % young adult comparisons are appropriately absent. This should be helpful in preventing this error in interpretation.
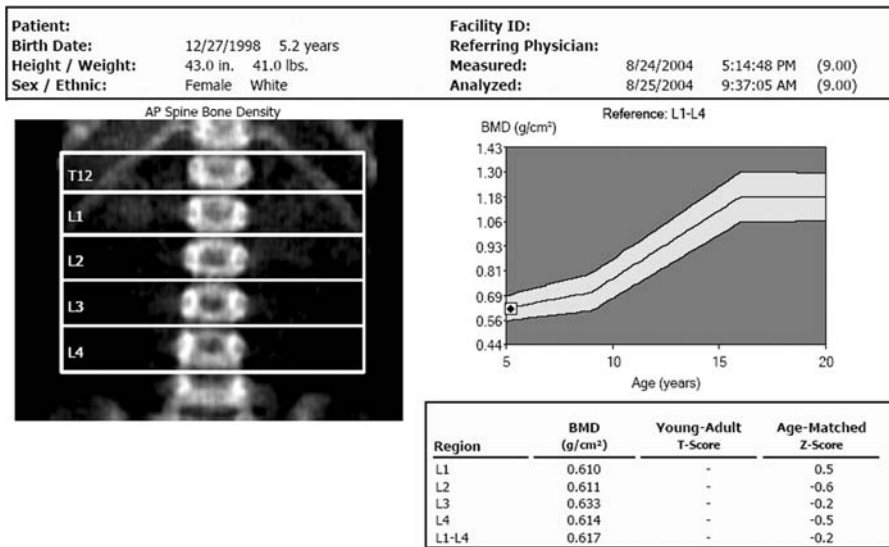
Fig. 13-23. A pediatric DXA PA lumbar spine study performed on the GE Lunar Prodigy for a 5 year old girl. The L1−L4 BMD is 0.617 g/cm^2. The z-score is −0.2. No T-score is provided. The use of the T-score in pediatric densitometry is not appropriate. The ancillary data for this study is seen in Fig. 13-24.

Fig. 13-24. Ancillary DXA PA lumbar spine data for the study shown in Fig. 13-23. Note that no T-score or % young-adult comparison is provided.

Pediatric Reference Databases

Even with the removal of the T-score from consideration, the validity of the z-score comparison is dependent upon the validity of the reference database. In the study from Gafni and Baron (*137*), the second most common error in interpretation of pediatric densitometry results was the use of a reference database that did not correctly reflect the patient's sex or ethnicity. As noted earlier, the BMD is expected to differ between boys and girls, particularly in adolescence. Use of a pediatric database that combines both genders as though there were no expected differences in BMD will lead to erroneous interpretations (*137*, *160*). In particular, boys may be misclassified as having low

bone mass. It is also clear from studies from Bachrach et al. (*161*) that the expected BMD differs among pediatric ethnic groups as well as between boys and girls. In general, she found that blacks had a greater areal bone density than non-blacks at the PA lumbar spine, proximal femur, and total body. For any age, the average BMD at the spine was 10% greater in black females and 3% greater in black males than in non-blacks. There were also differences among Asian, Hispanic, and Caucasian males and females, although the differences were not as great as those seen between blacks and non-blacks. Among the males, spine BMD was lower in Hispanics than in Asians or Caucasians. Total hip BMD and total body BMD was greater in Caucasian males than in Hispanic or Asian males. Among the females, Asians had a lower average femoral neck and total body BMD than Hispanics and Caucasians. Bachrach and colleagues also found that gender rather than ethnicity played a significant role in the timing of increases in BMD.

In the report from Gafni and Baron (*137*) noted earlier, there were seven instances in which an incorrect database had been used to interpret the pediatric bone density findings. When Gafni and Baron applied the correct database to determine the *z*-score, five of the seven children were no longer considered osteopenic or osteoporotic. They were, in fact, considered normal. In the other two cases, a determination could still not be made because of missing information. Gafni and Baron recommended that any reference database used to interpret pediatric bone density studies be specific for age, sex, and ethnicity. They also noted that an ideal database would consider body size and pubertal status as well.

The Bone Mineral Density in Childhood Study (*159*) noted earlier is an ongoing longitudinal study, from which pediatric reference databases are being created. In this study, it was clear that BMD values in childhood are not normally distributed[30] and that specific statistical procedures are necessary to create appropriate reference databases for children. The statistical approach used is called the LMS method, previously described by Cole and Green (*162*). Published reference curves from this study are currently limited by the relatively small number of Hispanic and Asian children and the length of follow-up. However, at study conclusion after 6 years, some of these limitations will be minimized. The data are specific for Hologic QDR 4500, Delphi, and Discovery systems, however. Pediatric reference databases on these types of Hologic devices utilize the BMDCS reference data, supplemented by Hologic native pediatric reference data, where appropriate (Personal communication, Kevin Wilson, Hologic, Inc.).

2003, 2004, and 2007 International Society for Clinical Densitometry Guidelines for Children

In 2003, ISCD issued guidelines for the use of bone densitometry to diagnose osteoporosis in children (*163*). ISCD emphasized that in males or females less than 20 years of age, the WHO criteria for the diagnosis of osteoporosis based on the measurement of BMD should *not* be used. ISCD stated that T-scores should *not* be used and should not appear in reports of bone densitometry in children; the z-score should be used instead. The PA lumbar spine and total body were recommended as the preferred skeletal sites

---

[30] See Chapter 3 for a discussion of the normal distribution.

in children. ISCD noted that while there was no agreement on standards for adjusting the BMD or BMC for bone size, pubertal stage, bone age, or body composition, any such adjustments should be clearly noted in the report. The need for an appropriate reference database for all z-score comparisons was stressed. In 2004, the Canadian Panel of the International Society for Clinical Densitometry (*164*) published guidelines for the diagnosis of osteoporosis in individuals less than 20 years of age, which mirrored the guidelines published earlier that year by the parent organization.

In 2007, ISCD convened the first Pediatric Position Development Conference to specifically address issues in pediatric densitometry. The recommendations from that conference are summarized in Appendix V. Importantly, ISCD reiterated the statement from earlier guidelines that the diagnosis of osteoporosis *should not be made in a child on the basis of the bone density alone* (*165*). According to the 2007 guidelines, such a diagnosis required the finding of a clinically significant fracture history and low bone density or low bone mineral content. Low bone mineral density or content was defined as a BMD or BMC z-score ≤ -2. DXA was the preferred bone density technique and the PA lumbar spine and total body (without the head) were the preferred skeletal sites for measurement. The need to utilize an appropriate reference database was again emphasized.

The Specialty of Pediatric Densitometry

In addition to studies of the development of peak bone density in children and its relationship to osteoporosis in later life, there are an ever-growing number of diseases in childhood in which the bone density may be adversely affected. One primary cause of osteoporosis in children is juvenile idiopathic osteoporosis (*166*). This disease is considered relatively rare. It usually occurs before puberty and is manifested by back pain, long bone fractures, and loss of height. There is often spontaneous resolution after 2–4 years but some individuals may develop permanent disabilities. Osteogenesis imperfecta (OI) is another cause of primary osteoporosis in children. OI is also often called "brittle bone disease" much as is adult osteoporosis. OI is the result of a genetic defect in collagen synthesis that results in skeletal fragility. Signs and symptoms of OI include a bluish discoloration of the sclerae, hearing loss, short stature, and fractures. There are six or more variants of OI (*167*). Type II is fatal. Type I is considered mild, while Type III is the most severe, non-fatal form of OI. Bisphosphonates are being evaluated as potential therapies in both juvenile idiopathic osteoporosis and OI (*168*, *169*). Other genetic defects that are associated with low bone density in childhood include Turner's syndrome, Down's syndrome, and Klinefelter's syndrome (*167*).

Secondary causes of osteoporosis or low bone mass in childhood are numerous, just as they are in adults (*170*). The list includes Cushing's syndrome, hyperthyroidism, hypopituitarism, and hypogonadism, as well as various nutritional deficiencies. Rheumatoid arthritis and inflammatory bowel disease in children are also associated with low bone density. Other diseases include sickle cell anemia, hemophilia, and cystic fibrosis. As in adults, certain drugs such as corticosteroids and anticonvulsants may cause bone loss. As the number of childhood cancer survivors increases, the effects of anti-neoplastic agents on bone mass have also become a concern. As has been the case in adult densitometry, the increasing application of densitometry in the pediatric population has resulted in an increasing number of diseases now known to have an adverse

effect on the skeleton of a child. This in turn will further increase the number of pediatric densitometry studies that are performed.

Perhaps the greatest problem faced in pediatric densitometry today is not its underutilization but rather, its misinterpretation when performed. It must always be remembered that "children are not simply small adults" (*136*). There is much more to consider in the interpretation of pediatric bone density results that the BMD itself, or even the *z*-score. Excellence in adult densitometry does not automatically confer excellence in pediatric densitometry. Densitometrists desiring expertise in this field are encouraged to pursue additional training, such as that offered by ISCD and publications such as the book by Sawyer et al. (*171*).

REFERENCES

1. Ross PD, Davis JW, Epstein RS, Wasnich RD. Pre-existing fractures and bone mass predict vertebral fracture incidence in women. Ann Intern Med 1991;114:919–923.
2. Nevitt MC, Ross PD, Palermo L, Muslinger T, Genant HK, Thompson DE. Association of prevalent vertebral fractures, bone density, and alendronate treatment with incident vertebral fractures: effect of number and spinal location of fractures. Bone 1999;25:613–619.
3. Ross PD, Genant HK, Davis JW, Miller PD, Wasnich RD. Predicting vertebral fracture incidence from prevalent fractures and bone density among non-black, osteoporotic women. Osteoporos Int 1993;3:120–126.
4. Black DM, Arden NK, Palermo L, Pearson J, Cummings SR. Prevalent vertebral deformities predict hip fractures and new vertebral deformities but not wrist fractures. J Bone Min Res 1999;14: 821–828.
5. Melton LJ, Atkinson EJ, Cooper C, O'Fallon WM, Riggs BL. Vertebral fractures predict subsequent fractures. Osteoporos Int 1999;10:214–221.
6. Burger H, van Daele PLA, Algra D, et al. Vertebral deformities as predictors of non-vertebral fractures. BMJ 1994;309:991–992.
7. Klotzbuecher CM, Ross PD, Landsman PB, Abbott TA, Berger M. Patients with prior fractures have an increased risk of future fractures: a summary of the literature and statistical synthesis. J Bone Miner Res 2000;15:721–739.
8. Cooper C, Atkinson EJ, O'Fallon WM, Melton LJ. Incidence of clinically diagnosed vertebral fractures: a population-based study in Rochester, Minnesota, 1985–1989. J Bone Miner Res 1992;7: 221–227.
9. Ensrud KE, Nevitt MC, Palermo L, et al. What proportion of incident morphometric vertebral fractures are clinically diagnosed and vice versa? Abstract. J Bone Miner Res 1999;14:S138.
10. Morris CA, Carrino JA, Lang P, Solomon DH. Incidental vertebral fractures on chest radiographs. Recognition, documentation, and treatment. J Gen Intern Med 2006;21(4):352–356.
11. Majundar SR, Kim N, Colman I, et al. Incidental vertebral fractures discovered with chest radiography in the emergency department: prevalence, recognition, and osteoporosis management in a cohort of elderly patients. Arch Intern Med 2005;165(8):905–909.
12. Gehlbach SH, Bigelow C, Heimisdottir M, May S, Walker M, Kirkwood JR. Recognition of vertebral fracture in a clinical setting. Osteoporos Int 2000;11(7):577–582.
13. Kim N, Rowe BH, Raymond G, et al. Underreporting of vertebral fractures on routine chest radiography. Am J Roentgenol 2004;182(2):297–300.
14. Genant HK, Wu CY, Van Kuijk C, Nevitt MC. Vertebral fracture assessment using a semiquantitative technique. J Bone Miner Res 1993;8:1137–1148.
15. Fletcher H. Anterior vertebral wedging-frequency and significance. AJR 1947;57:232–238.
16. Barent E, Nordin BEC. The radiological diagnosis of osteoporosis: a new approach. Clin Radiol 1960;11:166–174.
17. Black DM, Cummings SR, Stone K, Hudes E, Palermo L, Steiger P. A new approach to defining normal vertebral dimensions. J Bone Miner Res 1991;6:883–892.

18. Melton LJ, Kan SH, Frye MA, Wahner HW, O'Fallon WM, Riggs BL. Epidemiology of vertebral fractures in women. Am J Epidemiol 1989;129:1000–1011.

19. Smith-Bindman R, Cummings SR, Steiger P, Genant HK. A comparison of morphometric definitions of vertebral fracture. J Bone Miner Res 1991;6:25–34.

20. Ross PD, Davis JW, Epstein RS, Wasnich RD. Ability of vertebral dimensions from a single radiograph to identify fractures. Calcif Tissue Int 1992;51:95–99.

21. Eastell R, Cedel SL, Wahner HW, Riggs BL, Melton LJ. Classification of vertebral fractures. J Bone Miner Res 1991;2:207–214.

22. McCloskey E, Spector TD, Eyres KS, et al. The assessment of vertebral deformity: a method for use in population studies and clinical trials. Osteoporos Int 1993;3:138–147.

23. McCloskey EV, Kanis JA. The assessment of vertebral deformity. In: Genant HK, Jergas M, Van Kuijk C, eds. Vertebral fracture in osteoporosis. University of California, San Francisco: Radiology Research and Education Foundation, 1995:215–233.

24. Sauer P, Leidig G, Minne HW, et al. Spine deformity index versus other objective procedures of vertebral identification in patients with osteoporosis: a comparative study. J Bone Miner Res 1991;6: 227–238.

25. Black DM, Palermo L, Nevitt MC, Genant HK, Christensen L, Cummings SR. Defining incident vertebral deformity: a prospective comparison of several approaches. J Bone Miner Res 1999;14: 90–101.

26. Lunt M, Ismail AA, Felsenberg D, et al. Defining incident vertebral deformities in population studies: a comparison of morphometric criteria. Osteoporos Int 2002;13:809–815.

27. National Osteoporosis Foundation Working Group on Vertebral Fractures. Assessing vertebral fractures. J Bone Miner Res 1995;10:518–523.

28. Leidig-Bruckneer G, Genant HK, Minne HW, et al. Comparison of a semiquantitative and quantitative method for assessing vertebral fractures in osteoporosis. Osteoporos Int 1994;3:154–161.

29. Genant HK, Jergas M, Palermo L, et al. Comparison of semiquantitative visual and quantitative morphometric assessment of prevalent and incident vertebral fractures in osteoporosis: The Study of Osteoporotic Fractures Research Group. J Bone Miner Res 1996;11:984–996.

30. Grados F, Roux C, de Vernejoul MC, Utard G, Sebert JL, Fardellonne P. Comparison of four morphometric definitions and a semiquantitative consensus reading for assessing prevalent vertebral fractures. Osteoporos Int 2001;12:716–722.

31. Li J, Wu CY, Jergas H, Genant HK. Diagnosing prevalent vertebral fractures: a comparison between quantitative morphometry and a standardized visual (semiquantitative) approach. In: Genant HK, Jergas M, Van Kuijk C, eds. Vertebral fracture in osteoporosis. University of California, San Francisco: Radiology Research and Education Foundation, 1995:271–279.

32. Wu CY, Li J, Jergas M, Genant HK. Diagnosing incident vertebral fractures: a comparison between quantitative morphometry and a standardized visual (semiquantitative) approach. In: Genant HK, Jergas M, Van Kuijk C, eds. Vertebral fracture in osteoporosis. University of California, San Francisco: Radiology Research and Education Foundation, 1995:281–291.

33. Rea JA, Li J, Blake GM, Steiger P, Genant HK, Fogelman I. Visual assessment of vertebral deformity by X-ray absorptiometry: a highly predictive method to exclude vertebral deformity. Osteoporos Int 2000;11:660–668.

34. Schousboe JT, DeBold CR, Bowles C, Glickstein S, Rubino RK. Prevalence of vertebral compression fracture deformity by X-ray absorptiometry of lateral thoracic and lumbar spines in a population referred for bone densitometry. J Clin Densitom 2002;5:239–246.

35. Davis JW, Grove JS, Wasnich RD, Ross PD. Spatial relationships between prevalent and incident spine fractures. Bone 1999;24:261–264.

36. Faulkner KG, Barden HS, Weynand L, Burke P. Frequency of spine fractures assessed with LVA in normal, osteopenic, and osteoporotic postmenopausal women. J Bone Miner Res 2002; 17:S110.

37. Ferrar L, Jiang G, Eastell R. Longitudinal evaluation of morphometric X-ray absorptiometry for the identification of vertebral deformities. Osteoporos Int 2001;12:661–671.

38. Rea JA, Chen MB, Li J, et al. Vertebral morphometry: a comparison of long-term precision of morphometric X-ray absorptiometry and morphometric radiography in normal and osteoporotic subjects. Osteoporos Int 2001;12:158–166.

39. National Osteoporosis Foundation. Clinician's guide to prevention and treatment of osteoporosis. 1–30. 2008. Washington, D.C., National Osteoporosis Foundation.

40. Schousboe JT, Vokes T, Broy SB, et al. Vertebral fracture assessment: the 2007 ISCD official positions. J Clin Densitom 2008;11(1):92–108.

41. Tankó LB, Christiansen C, Cox DA, Geiger MJ, McNabb MA, Cummings SR. Relationship between osteoporosis and cardiovascular disease in postmenopausal women. J Bone Miner Res 2005;20(11):1912–1920.

42. von der Recke P, Hansen MA, Hassager C. The association between low bone mass at the menopause and cardiovascular mortality. Am J Med 1999;106:273–278.

43. Samelson EJ, Kiel DP, Broe KE, et al. Metacarpal cortical area and risk of coronary heart disease. The Framingham Study. Am J Epidemiol 2004;159:589–595.

44. Browner WS, Seeley DG, Vogt TM, Cummings SR. Non-trauma mortality in elderly women with low bone mineral density. Lancet 1991;338:355–358.

45. Trivedi DP, Khaw KT. Bone mineral density at the hip predicts mortality in elderly men. Osteoporos Int 2001;12:259–265.

46. Kiel DP, Kauppila LI, Cupples LA, Hannan MT, O'Donnell CJ, Wilson PW. Bone loss and the progression of abdominal aortic calcification over a 25-year period: the Framingham Heart Study. Calcif Tissue Int 2001;68(5):271–276.

47. Bagger YZ, Tankó LB, Alexandersen P, Qin G, Christiansen C. Radiographic measure of aorta calcification is a site-specific predictor of bone loss and fracture risk at the hip. J Intern Med 2006;259: 598–605.

48. Naves M, Rodríguez-García M, Díaz-López JB, Gómez-Alonso C, Annata-Andía JB. Progression of vascular calcifications is associated with greater bone loss and increased bone fractures. Osteoporos Int 2008;19(8):1161–1166.

49. Schulz E, Kiumars A, Liu X, Sayre J, Gilsanz V. Aortic calcification and the risk of osteoporosis and fractures. J Clin Endocrinol Metab 2004;89(9):4246–4253.

50. Wilson PW, Kauppila LI, O'Donnell CJ, et al. Abdominal aortic calcific deposits are an important predictor of vascular morbidity and mortality. Circulation 2001;103(11):1529–1534.

51. van der Meer IM, Bots ML, Hofman A, del Sol AI, van der Kuip DA, Witteman JC. Predictive value of noninvasive measures of atherosclerosis for incident myocardial infarction: the Rotterdam Study. Circulation 2004;109(9):1089–1094.

52. Hollander M, Hak AE, Koudstaal PJ, et al. Comparison between measures of atherosclerosis and risk of stroke: the Rotterdam Study. Stroke 2003;34(10):2367–2372.

53. Walsh CR, Cupples LA, Levy D, et al. Abdominal aortic calcific deposits are associated with increased risk for congestive heart failure: the Framingham Heart Study. Am Heart J 2002;144(4):733–739.

54. Kauppila LI, Polak JF, Cupples LA, Hannan MT, Kiel DP, Wilson PW. New indices to classify location, severity, and progression of calcific lesions in the abdominal aorta: a 25-year follow-up study. Atherosclerosis 1997;132(2):245–250.

55. Schousboe JT, Wilson KE, Kiel DP. Detection of abdominal aortic calcification with lateral spine imaging using DXA. J Clin Densitom 2006;9(3):302–308.

56. Schousboe JT, Wilson KE, Hangartner TN. Detection of aortic calcification during vertebral fracture assessment (VFA) compared to digital radiography. PLoS ONE 2007;2(1):e715.

57. Schousboe JT, Taylor BC, Kiel DP, Ensrud KE, Wilson KE, McCloskey EV. Abdominal aortic calcification detected on lateral spine images from a bone densitometer predicts incident myocardial infarction or stroke in older women. J Bone Miner Res 2008;23(3):409–416.

58. Faulkner KG, Cummings SR, Black D, Palermo L, Glüer CC, Genant HK. Simple measurement of femoral geometry predicts hip fracture: the study of osteoporotic fractures. J Bone Miner Res 1993;8: 1211–1217.

59. Faulkner KG, Mcclung M, Cummings SR. Automated evaluation of hip axis length for predicting hip fracture.
J Bone Miner Res 1994;9:1065–1070.

60. Duboeuf F, Hans D, Schott AM, et al. Different morphometric and densitometric parameters predict cervical and trochanteric hip fracture: the EPIDOS study. J Bone Miner Res 1997;12: 1895–1902.

61. Center JR, Nguyen TV, Pocock NA, et al. Femoral neck axis length, height loss, and risk of hip fracture in males and females. Osteoporos Int 1998;8:75–81.
62. Bergot C, Bousson V, Meunier A, Laval-Jeantet M, Laredo JD. Hip fracture risk and proximal femur geometry from DXA scans. Osteoporos Int 2002;13:542–550.
63. Cummings SR, Cauley JA, Palermo L, et al. Racial differences in hip axis lengths might explain racial differences in rates of hip fracture. Osteoporos Int 1994;4:226–229.
64. Nakamura T, Turner CH, Yoshikawa T, et al. Do variations in hip geometry explain differences in hip fracture risk between Japanese and white Americans? J Bone Miner Res 1994;9:1071–1076.
65. Bonnick SL, Lewis LA. The precision of PA spine, dual-femur and single-femur bone density studies on the GE Lunar Prodigy, a DXA fan-array device. J Clin Densitom 2002;5:S48.
66. Gomez Alonso C, Diaz Curiel M, Hawkins Carranza F, Perez Cano R, Diez Perez A. Femoral bone mineral density, neck shaft angle, and mean femoral neck width as predictors of hip fractures in men and women. Osteoporos Int 2000;11:714–720.
67. Gnudi S, Ripamonti C, Gualtieri G, Malavolta N. Geometry of proximal femur in the prediction of hip fracture in osteoporotic women. Br J Radiol 1999;72:729–733.
68. Karlsson KM, Sernbo I, Obrant KJ, Redlund-Johnell I, Johnell O. Femoral neck geometry and radiographic signs of osteoporosis as predictors of hip fracture. Bone 1996;18:327–330.
69. Partanen J, Jämsä T, Jalovaara P. Influence of the upper femur and pelvic geometry on the risk and type of hp fractures. J Bone Miner Res 2001;16:1540–1546.
70. Peacock M, Turner CH, Liu G, et al. Better discrimination of hip fracture using bone density geometry and architecture. Osteoporos Int 1995;5:167–173.
71. Yoshikawa T, Turner CH, Peacock M, et al. Geometric structure of the femoral neck measured using dual-energy X-ray absorptiometry. J Bone Miner Res 1994;9:1053–1064.
72. Martin RB, Burr DB. Non-invasive measurement of long bone cross-sectional moment of inertia by photon absorptiometry. J Biomech 1984;17:195–201.
73. Beck TJ, Ruff CB, Warden KE, et al. Predicting femoral neck strength from bone mineral data. A structural approach. Invest Radiol 1990;25:6–18.
74. Beck T. Measuring the structural strength of bones with dual-energy X-ray absorptiometry: principles, technical limitations, and future possibilities. Osteoporos Int 2003;14(S5):S81–S88.
75. Beck TJ. Extending DXA beyond bone mineral density: understanding hip structure analysis. Curr Osteoporos Rep 2007;5:49–55.
76. Faulkner KG, Wacker WK, Barden HS, et al. Femur strength index predicts hip fracture independent of bone density and hip axis length. Osteoporos Int 2006;17:593–599.
77. Beck TJ, Ruff CB, Scott WW, Jr, et al. Sex differences in geometry of the femoral neck with aging: a structural analysis of bone mineral data. Calcif Tissue Int 1992;50:24–29.
78. Beck TJ, Ruff CB, Bissessur K. Age-related changes in female femoral neck geometry: implications for bone strength. Calcif Tissue Int 1993;53(Sl)1:S41–S46.
79. Beck TJ, Looker AC, Ruff CB, et al. Structural trends in the aging femoral neck and proximal shaft: analysis of the Third National Health and Nutrition Examination Survey dual-energy X-ray absorptiometry data. J Bone Miner Res 2000;15:2297–2304.
80. Beck TJ, Stone KL, Oreskovic TL, et al. Effects of current and discontinued estrogen replacement therapy on hip structural geometry: the study of osteoporotic fractures. J Bone Miner Res 2001;16:2103–2110.
81. Greenspan SL, Beck TJ, Resnick NM, et al. Effect of hormone replacement, alendronate, or combination therapy on hip structural geometry: a 3-year, double-blind, placebo-controlled clinical trial. J Bone Miner Res 2005;20:1525–1532.
82. Uusi-Rasi K, Beck TJ, Semanick LM, et al. Structural effects of raloxifene on the proximal femur: results from the multiple outcomes of raloxifene evaluation trial. Osteoporos Int 2006;17:575–586.
83. Uusi-Rasi K, Semanick LM, Zanchetta JR, et al. Effects of teriparatide [rhPTH (1–34)] treatment on structural geometry of the proximal femur in elderly osteoporotic women. Bone 2005;36:948–958.
84. Szulc P, Duboeuf F, Schott AM, et al. Structural determinants of hip fracture in elderly women: re-analysis of the data from the EPIDOS study. Osteoporos Int 2006;17:231–236.
85. Ahlborg HG, Nguyen ND, Nguyen TV, et al. Contribution of hip strength indices to hip fracture risk in elderly men and women. J Bone Miner Res 2005;20:1820–1827.

86. Melton LJ, III, Beck TJ, Amin S, et al. Contributions of bone density and structure to fracture risk assessment in men and women. Osteoporos Int 2005;16:460–467.

87. Crabtree NJ, Kroger H, Martin A, et al. Improving risk assessment: hip geometry, bone mineral distribution, and bone strength in hip fracture cases and controls. The EPOS Study. Osteoporos Int 2002;13:48–54.

88. Khoo BC, Beck TJ, Qiao QH, et al. In vivo short-term precision of hip structure analysis variables in comparison with bone mineral density using paired dual-energy X-ray absorptiometry scans from multi-center clinical trials. Bone 2005;37:112–121.

89. Brown JK, Qiao Q, Weigert J, et al. Improved precision of hip structure analysis using optimized projection images from segmented 3D CT scans of the hip. J Bone Miner Res 2005;20(S1): S337.

90. Garrow JS, Webster J. Quetelet's index (W/H2) as a measure of fatness. Int J Obes 1985;9: 147–153.

91. World Health Organization. Physical status: the use and interpretation of anthropometry. Report of a WHO expert committee. 1–452. 1995. Geneva, World Health Organization. WHO Technical Report Series 854.

92. World Health Organization. Obesity: preventing and managing the global epidemic. Report of a WHO consultation on obesity. 1–158. 1998. Geneva, World Health Organization.

93. Wang J, Heymsfield SB, Aulet M, Thornton JC, Pierson RN. Body fat from body density: underwater weighing vs. dual-photon absorptiometry. Am J Physiol. 1989;256:E829–E834.

94. Heymsfield SB, Wang J, Lichtman S, et al. Body composition in elderly subjects: a critical appraisal of clinical methodology. Am J Clin Nutr 1989;50:1167–1175.

95. Siri WE. Body composition from fluid spaces and density: analysis of methods. University of California Radiation Laboratory Report 3349, 1956.

96. Durnin JVGA, Womersley J. Body fat assessed from total body density and its estimation from skinfold thickness: measurements on 481 men and women aged from 16 to 72 years. Br J Nutr 1974;32:77–97.

97. Jackson AS, Pollock ML. Generalized equations for predicting body density of men. Br J Nutr 1978;40:497–504.

98. Jackson AS, Pollock ML, Ward A. Generalized equations for predicting body density of women. Med Sci Sports Exerc 1980;12:175–182.

99. McCrory MA, Gomez TD, Bernauer EM, Molé PA. Evaluation of a new air displacement plethysmograph for measuring human body composition. Med Sci Sports Exerc 1995;27:1686–1691.

100. Fields DA, Goran MI, McCrory MA. Body-composition assessment via air-displacement plethysmography in adults and children: a review. Am J Clin Nutr 2002;75:453–467.

101. McLean KP, Skinner JS. Validity of Futrex-5000 for body composition determination. Med Sci Sports Exerc 1992;24:253–258.

102. Brodie DA, Eston RG. Body fat estimations by electrical impedance and infrared interactance. Int J Sports Med 1992;13:319–325.

103. Heyward VH, Cook KL, Hicks VL, et al. Predictive accuracy of three field methods for estimating relative body fatness of nonobese and obese women. Int J Sports Nutr 1992;2:75–86.

104. Horber FF, Thomi F, Casez JP, Fonteille J, Jaeger P. Impact of hydration status on body composition as measured by dual-energy X-ray absorptiometry in normal volunteers and patients on haemodialysis. Br J Radiol 1992;65:895–900.

105. Pietrobelli A, Wang Z, Formica C, Heymsfield SB. Dual-energy X-ray absorptiometry: fat estimation errors due to variation in soft tissue hydration. Am J Physiol 1998;274:E808–E816.

106. Dalsky GP, Kraemer W, Zetterlund AE, et al. A comparison of methods to assess body composition. Abstract. American College of Sports Medicine, Salt Lake City, UT, May 22–25, 1990.

107. Kiebzak GM, Leamy LJ, Person LM, Nord RH, Zhang ZY. Measurement precision of body composition variables using the Lunar DPX-L densitometer. J Clin Densitom 2000;3:35–41.

108. Black E, Petersen L, Kreutzer M, et al. Fat mass measured by DXA varies with scan velocity. Obes Res 2002;10:69–77.

109. Soriano JM, Ioannidou E, Wang J, et al. Pencil-beam vs fan-beam dual-energy X-ray absorptiometry comparisons across four systems: body composition and bone mineral. J Clin Densitom 2004;7: 281–289.

110. Tothill P, Avenell A, Love J, Reid DM. Comparisons between Hologic, Lunar, and Norland dual-energy X-ray absorptiometers and other techniques used for whole-body soft tissue measurements. Eur J Clin Nutr 1994;48:781–794.

111. Ellis KJ, Shypailo RJ. Bone mineral and body composition measurements: cross-calibration of pencil-beam and fan-beam dual-energy X-ray absorptiometers. J Bone Miner Res 1998;13:1613–1618.

112. Abrahamsen B, Gram J, Hansen TB, Beck-Nielsen H. Cross-calibration of QDR 2000 and QDR 1000 dual-energy X-ray densitometers for bone mineral and soft-tissue measurements. Bone 1995;16: 385–390.

113. Grundy SM. Metabolic syndrome scientific statement by the American Heart Association and the National Heart, Lung, and Blood Institute. Arterioscler Thromb Vasc Biol 2005;25(11):2243–2244.

114. Alberti KG, Zimmet P, Shaw J. The metabolic syndrome–a new worldwide definition. Lancet 2005;366(9491):1059–1062.

115. Zhu S, Wang Z, Heshka S, Heo M, Faith MS, Heymsfield SB. Waist circumference and obesity-associated risk factors among whites in the third National Health and Nutrition Examination Survey: clinical action thresholds. Am J Clin Nutr 2002;76(4):743–749.

116. Pouliot MC, Despres JP, Lemieux S, et al. Waist circumference and abdominal sagittal diameter: best simple anthropometric indexes of abdominal visceral adipose tissue accumulation and related cardiovascular risk in men and women. Am J Cardiol 1994;73:460–468.

117. Zamboni M, Turcato E, Armellini F, et al. Sagittal abdominal diameter as a practical predictor of visceral fat. Int J Obes Relat Metab Disord 1998;22(7):655–660.

118. Clasey JL, Bouchard C, Teates CD, et al. The use of anthropometric and dual-energy X-ray absorptiometry (DXA) measures to estimate total abdominal and abdominal visceral fat in men and women. Obes Res 1999;7(3):256–264.

119. Rankinen T, Kim SY, Perusse L, Despres JP, Bouchard C. The prediction of abdominal visceral fat level from body composition and anthropometry: ROC analysis. Int J Obes Relat Metab Disord 1999;23(8):801–809.

120. Onat A, Avci GS, Barlan MM, Uyarel H, Uzunlar B, Sansoy V. Measures of abdominal obesity assessed for visceral adiposity and relation to coronary risk. Int J Obes Relat Metab Disord 2004;28(8):1018–1025.

121. Larsson B, Seidell J, Svardsudd K, et al. Obesity, adipose tissue distribution, and health in men – the study of men born in 1913. Appetite 1989;13(1):37–44.

122. Despres JP, Moorjani S, Lupien PJ, Tremblay A, Nadeau A, Bouchard C. Regional distribution of body fat, plasma lipoproteins, and cardiovascular disease. Arteriosclerosis 1990;10(4):497–511.

123. Stevens J, Keil JE, Rust PF, Tyroler HA, Davis CE, Gazes PC. Body mass index and body girths as predictors of mortality in black and white women. Arch Intern Med 1992;152(6):1257–1262.

124. Stevens J, Keil JE, Rust PF, et al. Body mass index and body girths as predictors of mortality in black and white men. Am J Epidemiol 1992;135(10):1137–1146.

125. Folsom AR, Kaye SA, Sellers TA, et al. Body fat distribution and 5-year risk of death in older women. JAMA 1993;269(4):483–487.

126. Reeder BA, Senthilselvan A, Despres JP, et al. The association of cardiovascular disease risk factors with abdominal obesity in Canada. Canadian Heart Health Surveys Research Group: CMAJ 1997;157(Suppl 1):S39–S45.

127. Snijder MB, van Dam RM, Visser M, Seidell JC. What aspects of body fat are particularly hazardous and how do we measure them? Int J Epidemiol 2006;35(1):83–92.

128. Kelley DE, Thaete FL, Troost F, Huwe T, Goodpaster BH. Subdivisions of subcutaneous abdominal adipose tissue and insulin resistance. Am J Physiol Endocrinol Metab 2000;278(5):E941–E948.

129. Monzon JR, Basile R, Heneghan S, Udupi V, Green A. Lipolysis in adipocytes isolated from deep and superficial subcutaneous adipose tissue. Obes Res 2002;10(4):266–269.

130. Shen W, Wang Z, Punyanita M, et al. Adipose tissue quantification by imaging methods: a proposed classification. Obes Res 2003;11(1):5–16.

131. Park YW, Heymsfield SB, Gallagher D. Are dual-energy X-ray absorptiometry regional estimates associated with visceral adipose tissue mass? Int J Obes Relat Metab Disord 2002;26(7):978–983.

132. Snijder MB, Visser M, Dekker JM, et al. The prediction of visceral fat by dual-energy X-ray absorptiometry in the elderly: a comparison with computed tomography and anthropometry. Int J Obes Relat Metab Disord 2002;26(7):984–993.

133. Glickman SG, Marn CS, Supiano MA, Dengel DR. Validity and reliability of dual-energy X-ray absorptiometry for the assessment of abdominal adiposity. J Appl Physiol 2004;97(2):509–514.

134. Albanese CV, Diessel E, Genant HK. Clinical applications of body composition measurements using DXA. J Clin Densitom 2003;6:75–85.

135. Paradisi G, Smith L, Burtner C, et al. Dual-energy X-ray absorptiometry assessment of fat mass distribution and its association with the insulin resistance syndrome. Diabetes Care 1999;22(8): 1310–1317.

136. Bachrach LK. Bare-bones fact—children are not small adults. N Engl J Med 2004;351:924–926.

137. Gafni RI, Baron J. Overdiagnosis of osteoporosis in children due to misinterpretation of dual-energy X-ray absorptiometry (DEXA). J Pediatr 2004;144:253–257.

138. Leonard MB, Feldman HI, Zemel BS, et al. Evaluation of low-density spine software for the assessment of bone mineral density in children. J Bone Miner Res 1998;13:1687–1690.

139. Njeh CF, Samat SB, Nightingale A, McNeil EA, Boivin CM. Radiation dose and *in vitro* precision in paediatric bone mineral density measurement using dual X-ray absorptiometry. Br J Radiol 1997;70(835):719–727.

140. Thomas SR, Kalkwarf HJ, Buckley DD, Heubi JE. Effective dose of dual-energy X-ray absorptiometry scans in children as a function of age. J Clin Densitom 2005;8(4):415–422.

141. Blake GM, Naeem M, Boutros M. Comparison of effective dose to children and adults from dual X-ray absorptiometry examinations. Bone 2006;38(6):935–942.

142. International Commission on Radiological Protection. 1990 recommendations of the International Commission on Radiological Protection [ICRP Publication 60]. Ann ICRP 1991;21:1–201.

143. Abrahams PH, Marks SC, Hutchings RT. McMinn's Color Atlas of Human Anatomy 5th ed. Edinburgh: Elsevier Science Limited, 2003.

144. Greulich WW, Pyle SI, Waterhouse AM. A radiographic standard of reference for the growing hand and wrist. Chicago: Case Western Reserve University, 1971.

145. Tanner JM, Whitehouse RH, Cameron N, et al. Assessment of skeletal maturity and prediction of adult height, 2nd ed. London: Academic Press, 1983.

146. Milner GR, Levick RK, Kay R. Assessment of bone age: a comparison of the Greulich and Pyle and the Tanner and Whitehouse methods. Clin Radiol 1986;37:119–121.

147. King DG, Steventon DM, O'Sullivan MP, et al. Reproducibility of bone ages when performed by radiology registrars: an audit of Tanner and Whitehouse II versus Greulich and Pyle methods. Br J Radiol 1994;67:848–851.

148. Tanner JM. Growth of adolescents. Oxford: Blackwell Scientific Publishing, 1962.

149. Carter DR, Bouxsein ML, Marcus R. New approaches for interpreting projected bone densitometry data. J Bone Miner Res 1992;7:137–145.

150. Jergas M, Breitenseher M, Gluer CC, Yu W, Genant HK. Estimates of volumetric bone density from projectional measurements improve the discriminatory capability of dual X-ray absorptiometry. J Bone Miner Res 1995;10:1101–1110.

151. Mølgaard C, Thomsen BL, Prentice A, Cole TJ, Michaelsen KF. Whole body bone mineral content in healthy children and adolescents. Arch Dis Child 1997;76:9–15.

152. CDC, National Center for Health Statistics. Clinical growth charts. http://www.cdc.gov/nchs/about/major/nhanes/ growthcharts/cliical_charts.htm Accessed 01/05/2005.

153. Nguyen TV, Maynard LM, Towne B, et al. Sex differences in bone mass acquisition during growth: the Fels Longitudinal Study. J Clin Densitom 2001;4:147–157.

154. Lin Y-C, Lyle RM, Weaver CM, et al. Peak spine and femoral neck bone mass in young women. Bone 2003;32:546–553.

155. Zanchetta JR, Plotkin H, Alvarez Filgueira ML. Bone mass in children: normative values for the 2–20-year old population. Bone 1995;16:393S–399S.

156. Teegarden D, Proulx WR, Martin BR, et al. Peak bone mass in young women. J Bone Miner Res 1995;10:711–715.

157. Sabatier J-P, Guaydier-Souquières G, Laroche A, et al. Bone mineral acquisition during adolescence and early adulthood: a study in 574 healthy females 10–24 years of age. Osteoporos Int 1996;6: 141–148.

158. Theintz G, Buchs B, Rizzoli R, et al. Longitudinal monitoring of bone mass accumulation in healthy adolescents: evidence for a marked reduction after 16 years of age at the levels of lumbar spine and femoral neck in female subjects. J Clin Endocrinol Metab 1992;75:1060–1065.

159. Kalkwarf HJ, Zemel BS, Gilsamz V, et al. The bone mineral density in childhood study: bone mineral content and density according to age, sex, and race. J Clin Endocrinolol Metab 2007;92:2087–2099.
160. Leonard MB, Propert KJ, Zemel BS, Stallings VA, Feldman HI. Discrepancies in pediatric bone mineral density reference data: potential for misdiagnosis of osteopenia. J Pediatr 1999;135:182–188.
161. Bachrach LK, Hastie T, Wang MC, Narasimhan B, Marcus R. Bone mineral acquisition in healthy Asian, Hispanic, black, and Caucasian youth: a longitudinal study. J Clin Endocrinol Metab 1999;84:4702–4712.
162. Cole TJ, Green PJ. Smoothing reference centile curves: the LMS method and penalized likelihood. Stat Med 1992;11:1305–1319.
163. Lieb ES, Lewiecki M, Binkley N, Hamdy RC. Official positions of the International Society for Clinical Densitometry. J Clin Densitom 2004;7(1):1–5.
164. Khan AA, Bachrach L, Brown JP, et al. Standards and guidelines for performing central dual-energy X-ray absorptiometry in premenopausal women, men, and children: a report from the Canadian Panel of the International Society for Clinical Densitometry. J Clin Densitom 2004;7:51–63.
165. Baim S, Leonard MB, Bianchi M, et al. Official positions of the International Society for Clinical Densitometry and executive summary of the 2007 ISCD pediatric position development conference. J Clin Densitom 2008;11(1):6–21.
166. Krassas GE. Idiopathic juvenile osteoporosis. Ann NY Acad Sci 2000;900:409–412.
167. Saggese G, Baroncelli GI, Bertelloni S. Osteoporosis in children and adolescents: diagnosis, risk factors, and prevention. J Pediatr Endocrinol Metab 2001;14:833–859.
168. Shaw NJ, Boivin CM, Crabtree NJ. Intravenous pamidronate in juvenile osteoporosis. Arch Dis Child 2000;83:143–145.
169. Glorieux FH. Bisphosphonate therapy for severe osteogenesis imperfecta. J Pediatr Endocrinol Metab 2000;13:989–992.
170. van der Sluis IM, de Muinck Keizer-Schrama SMPF. Osteoporosis in childhood: bone density of children in health and disease. J Pediatr Endocrinol Metab 2001;14:817–832.
171. Sawyer AJ, Bachrach LK, Fung EB. Bone densitometry in growing patients. Totowa, NJ: Humana Press, 2007.

14 Reporting Densitometry

CONTENTS

The computer-generated printouts from densitometry devices have become increasingly sophisticated as the field of densitometry itself has matured. Skeletal images are clearer on the printouts with improvements in both image and printer resolution. In addition to the measured skeletal parameters from the device, World Health Organization (WHO) criteria (*1*) diagnoses, fracture risk assessments, and colorful graphic comparisons of the patient's BMD to their peers are commonly found. The addition of WHO diagnostic categories and fracture risk assessments to the densitometry printout is a departure from earlier practices in which such *clinical interpretations* of the numerical data were deemed inappropriate in the absence of a physician's review of the data. In fact, such densitometry computer-generated assessments are still inappropriate in the absence of a careful review by the densitometrist. It is also absolutely necessary that the densitometrist offer necessary clinical guidance to the referring physician based on the densitometry findings. Such guidance is far beyond the scope of the computer-generated printout.

ELEMENTS OF DENSITOMETRY REPORTS REQUESTED BY PRIMARY CARE PHYSICIANS

In 2001, Merck & Co., Inc. (Personal communication, 2002. Merck & Co., Inc.) conducted focus groups with primary care physicians to determine what was both wanted and needed in reporting the results of densitometry. When asked to rate the extent to which they used the technical report (the computer-generated printout) or the summary report (the physician interpretation) for clinical decisions, the primary care physicians assigned a score of 86 out of a possible 100 points to the summary report. According to these physicians, the top five components of the ideal report were risk factor identification, the T-score, diagnosis, fracture risk assessment, and treatment recommendations. It was also noted that comparisons to prior studies should be made when appropriate. In a separate focus group, physicians emphasized that the ideal report would only be one page long!

DENSITOMETRY CENTER REPORTING PRACTICES IN THE UNITED STATES

Based on a national survey of densitometry reporting practices, it is clear that the needs of primary care physicians are not being met. In 2002, Fuleihan et al. (2) summarized the reporting practices of 270 densitometry centers in the United States. These were centers that were listed in the National Osteoporosis Foundation database of densitometry centers in the United States who responded to a questionnaire on densitometry reporting practices. At 71% of the 270 centers, the PA spine and proximal femur were routinely measured. Thirteen percent of the centers measured only one site routinely and 11% routinely measured the spine, proximal femur, and forearm. In reporting the results of the studies, 89.6% included T-scores and 55.9% included z-scores as well. At 7.1% of the centers, T-scores were not reported and at 38.9%, z-scores were not reported. Only 64% of the centers mentioned the World Health Organization criteria for diagnosis and only 70% provided assessments of fracture risk. Of the centers reporting fracture risk, 65% based the risk assessment on the T-score while 6% utilized the z-score. Fourteen percent utilized both standard scores and 15% utilized neither standard score. In reporting fracture risk, 80% of the centers did not apply any age restriction to this assessment. Fracture risk assessments were limited to individuals over age 50 in only 7.5% and to individuals over age 65 in only 5%.

The findings from Fulheihan et al. continued to be disheartening in the realm of clinical guidance. Only 57% of the responding centers recommended patient evaluations for secondary causes of bone loss. The criteria for making such recommendations also varied. A T-score poorer than –2.5 was used by 25% of the centers and a z-score poorer than –2 was used in 18%. When specific tests were recommended, the most common recommendations included a measurement of serum calcium, parathyroid hormone (PTH), and thyroid stimulating hormone (TSH). Fifty-six percent recommended non-prescription interventions such as calcium, vitamin D, and exercise for the prevention of osteoporosis but only 52% recommended such interventions as part of therapy. Only 51% of the centers recommended prescription interventions for the prevention of osteoporosis while only 58% made recommendations for prescription interventions for treatment. In contrast, 74% of the centers did recommend a follow-up bone density measurement, with most recommending follow-up after a year. A detailed report, which included

recommendations for an evaluation for secondary causes of bone loss and treatment options, was employed by only 28% of the 270 centers. In summarizing the results of this study, the authors correctly concluded that densitometry reporting in the United States often failed to include clinical information necessary to assist physicians in the care of their patients and that such reporting was often not evidence-based. They noted that these issues must be addressed to optimize the clinical utility of densitometry. There is still no indication, however, that this has happened.

RECOMMENDATIONS FROM THE INTERNATIONAL SOCIETY FOR CLINICAL DENSITOMETRY FOR BONE DENSITY REPORTING

In 2004, the International Society for Clinical Densitometry (*3*) issued guidelines for the recommended components of the bone density report. These guidelines remain in effect today. The core components of a baseline DXA bone density report are listed in Table 14-1, as well as in Appendix V. The components of a follow-up DXA report are listed in Table 14-2, as well as in Appendix V. The list of core components would

Table 14-1

ISCD Recommendations for Core Components of a Baseline Bone Density Report

Demographics (name, medical record identifying number, date of birth, sex). Requesting provider.

Indications for the test.

Manufacturer and model of instrument used

Technical quality and limitations of the study, stating why a specific site or ROI is invalid or not included.

BMD in g/cm^2 for each site.

The skeletal sites, ROI, and, if appropriate, the side that were scanned.

The T-score and/or Z-score where appropriate.

WHO criteria for diagnosis in postmenopausal females and in men aged 50 and over.

Risk factors including information regarding previous non-traumatic fractures.

A statement about fracture risk. Any use of relative fracture risk must specify the population of comparison (e.g., young-adult or age-matched). The ISCD favors the use of absolute fracture risk prediction when such methodologies are established.

A general statement that a medical evaluation for secondary causes of low BMD may be appropriate.

Recommendations for the necessity and timing of the next BMD study.

Table 14-2

ISCD Recommendations for Core Components of a Follow-Up Bone Density Report

Statement regarding which previous or baseline study and ROI is being used for comparison.

Statement about the LSC at your facility and the statistical significance of the comparison.

Report significant change, if any, between the current and previous study or studies in g/cm^2 and percentage.

Comments on any outside study including manufacturer and model on which previous studies were performed and the appropriateness of the comparison.

Recommendations for the necessity and timing of the next BMD study.

seem to preclude the desired one-page length for a report, but it actually can be done. Although ISCD recommended inclusion of the BMD in g/cm^2 for each measured site, this seems redundant if the actual computer printouts are provided to the referring physician with the report. If the printouts are not provided, then clearly the BMD in g/cm^2 for each site must be stated in the report. According to ISCD, an optional item is a "recommendation for pharmacologic and nonpharmacologic interventions." ISCD correctly noted that the densitometrist was not in a position to recommend a *specific* pharmacologic agent and instead suggested referring to guidelines from such organizations as the American Association of Clinical Endocrinologists (*4*) or the National Osteoporosis Foundation (*5*) as supporting consideration of the patient for pharmacologic intervention by the referring physician. Although ISCD noted that such recommendations were an "optional" part of the report, such a recommendation goes to the heart of what these numbers mean. In that sense, such a recommendation is really not optional at all.

REPORTING THE DIAGNOSIS

The 1994 World Health Organization criteria (*1*) for the diagnosis of osteoporosis based on the measurement of BMD have become the accepted criteria with which to characterize the bone density. Nevertheless, a statement that these are the criteria being used is still appropriate for three reasons. The first reason, as noted in Chapter 9, is that both the International Osteoporosis Foundation (*6*) and the International Society for Clinical Densitometry (*7*) recommend limiting the use of the WHO criteria for diagnosis to specific skeletal sites or regions of interest. The second reason is that this immediately establishes the T-score cut points used to assign a diagnostic category. Using the PA lumbar spine and proximal femur DXA studies seen in Fig.14-1 from a 67-year-old postmenopausal woman, a statement regarding diagnosis might read:

Diagnosis: Osteoporosis, based on the L1–L4 T-score of –3.4, applying World Health Organization criteria and ISCD guidelines for diagnosis.

Such a statement is appropriate for this postmenopausal woman. The controversy surrounding both the use of the WHO criteria in men and the use of gender-specific reference databases for the calculation of the T-score was discussed in Chapter 9. Until this controversy is resolved, a statement regarding diagnosis in a man might read as follows:

Diagnosis: Osteoporosis, applying World Health Organization Criteria utilizing a gender-specific total hip T-score of –2.6 and ISCD guidelines for diagnosis.

In utilizing the WHO criteria, modifiers such as mild, moderate, or severe should *not* be used to describe the diagnostic category of osteopenia or low bone mass. In addition, the phrase "severe osteoporosis" should be used to describe *only* those individuals with a bone density 2.5 or more SD below the young-adult mean value *and* who have a presumed fragility fracture.

The third reason for stating that the WHO criteria are being used is simply to draw a distinction between instances in which the WHO criteria are not being used. One of the limitations of the WHO criteria is that the WHO criteria do not allow for an individual with an osteopenic T-score and presumed fragility fracture to be called osteoporotic. In
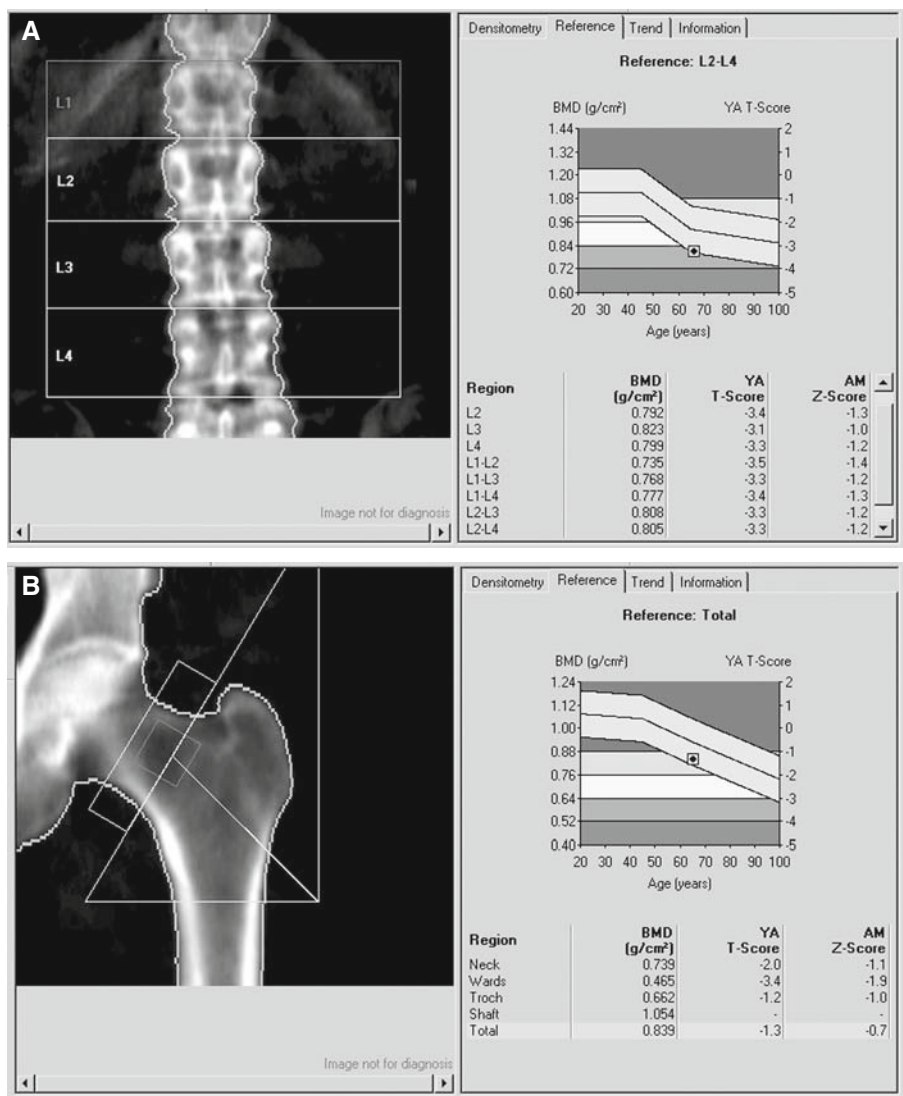
Fig. 14-1. (A) Lunar Prodigy PA lumbar spine study. **(B)** Lunar Prodigy proximal femur study on the same 67-year-old Caucasian woman.

such a case, it would be reasonable to point out that this individual meets the conceptual definition of osteoporosis as proposed by the 1991 and 1993 Consensus Development Conferences[1] (*8*, *9*) as well as the 2000 NIH Consensus Conference (*10*) even though they don't meet the WHO criterion for osteoporosis based on the BMD. In such a circumstance the statement might read:

Diagnosis: Osteoporosis, based on the finding of low bone density at [name of skeletal site] and history of fragility fracture, according to the 1991 and 1993 Osteoporosis

---

[1] *See* Chapter 9 for a discussion of the 1991 and 1993 consensus conferences' definition of osteoporosis.

Consensus Development Conferences' and 2000 NIH Consensus Conference definitions of osteoporosis.

The preceding statement is somewhat awkward but extremely important. Such a patient has proven that their skeleton is sufficiently fragile to fracture. They are at greater risk for future fracture than their bone density alone implies because of the presence of a fracture. If they are not appropriately diagnosed as osteoporotic by the densitometrist, they may not be given necessary consideration for pharmacologic intervention. The 2008 National Osteoporosis Foundation guidelines (5) note that such a patient should be considered for pharmacologic intervention, but without the *clinically appropriate* diagnosis of osteoporosis, such consideration may not be given.

REPORTING FRACTURE RISK

The previous discussion highlights the clinical dilemma of the densitometrist in explaining what these numbers mean, because the level of bone density that constitutes a WHO diagnosis of osteoporosis is not necessarily the same level of bone density that constitutes an unacceptable level of risk for fracture. The prediction of fracture risk is therefore a separate statement but often a more important statement than the diagnosis in terms of the need for pharmacologic intervention.

The expression of the implications of the bone density for the patient's future risk of fracture is fraught with difficulty. Relative risk data, whether used with the T-score or z-score is poorly understood and not useful clinically. In the past, the statement regarding the relative risk for fracture was the most accurate statement that the densitometrist could make. *That is no longer the case*. Instead, global or site-specific absolute fracture risk predictions such as remaining lifetime fracture probability (RLFP), the Black Fracture Index, the FORE FRC, and FRAX™ are clearly superior in their clinical utility to expressions of relative risk.[2] The overriding goal in any of these approaches is to ensure that the magnitude of the risk is recognized so that appropriate interventions are recommended. A typical statement utilizing FRAX™ for the patient whose proximal femur bone density is shown in Fig. 14-1B would be:

FRAX™ 10-Year Risk Prediction: Hip fracture: 28%. Major osteoporotic fracture: 3.3%.

These values were calculated after applying the FRAX™ patch to the femoral neck T-score, which resulted in a change in the T-score from –2.0 to –2.2. The patient's data, including a weight of 47.63 kg, height of 154.9 cm, and history of parental hip fracture were inputted into the FRAX™ algorithm along with the femoral neck T-score of –2.2 in order to calculate the 10-year fracture probabilities.

As noted in the study from Fuleihan et al. (2) many densitometry centers did not employ any age restriction on fracture risk predictions. This is inappropriate. The minimum age of a patient with which to utilize FRAX™ is 40. The minimum age for the FORE FRC is 45. The Black Fracture Index is appropriate for use in women aged 65 and older. Fracture risk predictions should not be made in otherwise healthy young adults, because there is no data to support doing so. It is also clear that for any given level of

---

[2] *See* Chapter 10 for a discussion of these methods for predicting fracture risk.

bone density, the risk of fracture is markedly less in these younger individuals than in older individuals.

RECOMMENDING EVALUATIONS FOR SECONDARY CAUSES OF BONE LOSS

Conspicuously absent from the top five elements of a report requested by primary care physicians was any reference to possible secondary causes of bone loss. This is all the more reason that such a statement *should* be included in densitometry reports. Statements reminding physicians to exclude secondary causes of bone loss are always appropriate in individuals with a low bone mass, regardless of the *z*-score. In postmenopausal women, estrogen-deficient bone loss is a diagnosis of *exclusion*. It is incumbent on the physician to prove that nothing else could have caused the apparent bone loss. In men, a search for secondary causes is equally important. Densitometrists may use the *z*-score to determine how aggressively to recommend such an evaluation, but the recommendation should always be made in some form. Statistically, a *z*-score of –2 or poorer is grounds for making an aggressive recommendation. A more aggressive recommendation could include not only a differential diagnosis of causes of bone loss but suggestions for specific tests to exclude such causes as well. More aggressive statements should always be prefaced with the phrase "if clinically indicated." The referring physician may be able to exclude many of the differential diagnoses based on his or her historical knowledge of the patient or based on previous tests. It should be made clear that the decision to pursue additional testing belongs to the referring physician. The routine recommendation for an evaluation for secondary causes, which should always be included in the report might be worded as follows:

> *Other Recommendations: Secondary causes of bone loss should be excluded clinically.*

More detailed and aggressive recommendations can be made based on published findings from studies of patients with osteoporosis such as those from Johnson et al. (*11*) and Tannenbaum et al. (*12*). These studies were discussed in Chapter 12. Using the data from these studies, an aggressive and detailed recommendation to exclude secondary causes of bone loss might read as follows:

> *Other Recommendations: Estrogen-deficient bone loss is a diagnosis of exclusion. Therefore, if clinically indicated, secondary causes of bone loss should be excluded. Such causes may include, but are not limited to, hyperparathyroidism, hyperthyroidism, hypercalciuria, Cushing's disease, rheumatoid arthritis, multiple myeloma, malabsorption, alcoholism, and use of medications such as corticosteroids, lithium, excessive thyroid hormone, anticonvulsants and GnRH agonists.*

An even more aggressive and detailed recommendation to exclude secondary causes of osteoporosis might read:

> *Other Recommendations: Estrogen-deficient bone loss is a diagnosis of exclusion. Therefore, if clinically indicated, secondary causes of bone loss should be excluded. Such causes may include, but are not limited to, hyperparathyroidism, hyperthyroidism, hypercalciuria, Cushing's disease, rheumatoid arthritis, multiple myeloma, malabsorption, alcoholism, and use of medications such as corticosteroids, lithium, excessive thyroid hormone, anticonvulsants and GnRH agonists. If clinically indicated, a laboratory evaluation that includes serum calcium, 25-OH vitamin D, 24-hour urinary calcium excretion and serum*

TSH (in patients receiving thyroid hormone) should be performed. Other tests that may be useful include a CBC,[3] SPEP,[4] IPEP,[5] and anti-tissue transglutaminase antibodies.[6]

TREATMENT RECOMMENDATIONS

There are two aspects to treatment recommendations: whom to treat and how to treat them. The National Osteoporosis Foundation (NOF) guidelines (*5*) for the treatment of postmenopausal osteoporosis are extremely useful as well as clear. In 2008, the NOF recommended that prescription interventions be considered for individuals who met any one of a variety of different criteria. It is relatively straightforward then, to make a statement such as:

Treatment Recommendations: Based on guidelines from the National Osteoporosis Foundation, consideration should be given to pharmacologic intervention.

The specific criterion met by the patient may also be cited. To recommend a specific treatment is a more difficult undertaking and generally not possible or even appropriate for the densitometrist. It is clear, however, that primary care physicians want suggestions in this regard (Personal communication, 2002. Merck & Co., Inc.). Given the diverse specialties of physicians involved in densitometry, some physicians may be more comfortable than others in making such recommendations. It should be possible, however, for any physician to remind the referring physician of the desirability of non-prescription interventions such as calcium and Vitamin D and to list the currently approved prescription interventions for the prevention and/or treatment of osteoporosis. A general statement regarding non-prescription interventions might be as follows:

Other Recommendations: A daily calcium intake of 1200 mg and vitamin D3 of 800– 1000 IU is recommended in accordance with the 2008 National Osteoporosis Foundation guidelines for individuals age 50 and older.

Prescription interventions are best summarized rather than specifically recommended, as decisions regarding the feasibility of any one intervention should be left to the referring physician. From a medical-legal perspective, it is important to distinguish between agents that are recommended for prevention, treatment, or both and to note the doses recommended for each. The following statements address these concerns:

The following anti-resorptive medications are FDA-approved for the prevention and treatment of postmenopausal osteoporosis: alendronate, 5 mg po daily or 35 mg po once weekly for prevention and 10 mg po daily or 70 mg po once weekly for treatment; risedronate, 5 mg po daily or 35 mg po once weekly for both indications with 75 mg po on 2 consecutive days once monthly or 150 mg po once monthly approved for treatment; ibandronate 2.5 mg po daily for prevention and treatment and 150 mg po once monthly and 3 mg IV every 3 months for treatment; raloxifene, 60 mg po daily for both indications. Reclast[7] 5 mg IV

---

[3] Complete blood count

[4] Serum protein electrophoresis

[5] Immuno protein electrophoresis

[6] These antibodies may be present in cases of non-tropical sprue.

[7] The trade name, Reclast, is used here to distinguish this form of zoledronate from Zometa, for which the dose, regimen, and indications are different.

once a year for treatment of postmenopausal osteoporosis and salmon calcitonin for treatment in women more than 5 years postmenopausal in a dose of 100 I.U. injected subq daily or 200 I.U. in one nasal spray daily. Several forms of estrogen replacement are approved for prevention only of postmenopausal osteoporosis. The minimum effective dose is specific for the preparation. The anabolic agent teripartide is FDA-approved for the treatment of postmenopausal osteoporosis in women who are at high risk for fracture for a period of no more than 2 years at a dose of 20 μg injected subq daily.

This very long statement clearly refers to therapies for women. If the nature of the report requires only a discussion of treatment, comments regarding preventive doses can be eliminated. If the issue is solely prevention, comments regarding treatment can be eliminated for the sake of brevity. For the treatment of osteoporosis in men, the following summary is appropriate:

Alendronate, in a dose of 10 mg po daily or 70 mg po once weekly and risedronate, in a dose of 35 mg po once weekly are FDA-approved to increase bone mass in men with osteoporosis. Teriparatide in a dose of 20 μg injected subq daily for period of no more than 2 years is indicated to increase bone mass in men with primary or hypogonadal osteoporosis who are at high risk for fracture.

Statements such as those noted above are lengthy but specific enough to be useful while still leaving final treatment decisions in the hands of the referring physician. If the densitometrist knows that such a statement would not be appreciated or needed by the referring physician, it is not necessary to include it in the report.

RECOMMENDING A FOLLOW-UP DENSITOMETRY STUDY

The timing of a follow-up study is based on the specific circumstances of patient management. If a prescription medication is started, either for prevention or treatment, the timing of the repeat study and the skeletal site to be used for that measurement are determined by the anticipated effects of the drug on the skeleton and the precision of the measurement at the chosen skeletal site.[8] To address all possible contingencies becomes quite difficult. As noted in Chapter 7 and again in Appendix VI, organizations such as the American Association of Clinical Endocrinologists (*4*) and the North American Menopause Society (*13*) have provided guidelines in this regard.

As a rule, the PA lumbar spine is the site of choice to monitor currently available therapies. Significant[9] changes in BMD at the PA lumbar spine from the bisphosphonates or teriparatide may be seen after a year. A more appropriate interval is 2–3 years if raloxifene is used. The longer interval would also be appropriate for salmon calcitonin. If the proximal femur is chosen as the site to monitor, a longer interval is required than at the spine for any therapy because of the effect of the combination of the rate of change and precision at the skeletal site. The minimum interval for proximal femur measurements to assess efficacy is generally 2 years. Of the various regions of interest in the proximal femur, ISCD (*14*) recommends the use of the total hip region of interest if the proximal

---

[8] *See* Chapter 11 for a discussion of monitoring changes in bone density.

[9] By significant, it is meant that changes, which equal or exceed the least significant change that are likely to be seen.

femur is used for monitoring. In general, proximal femoral measurements are less use-ful than the PA lumbar spine for monitoring the therapeutic efficacy of raloxifene and salmon calcitonin. Consequently, if therapy is begun, it is reasonable to recommend that the PA lumbar spine bone density study be repeated at an interval to be determined by the choice of therapy. From the standpoint of Medicare (*15*) reimbursement, however, a follow-up bone density study to assess treatment efficacy cannot be performed any ear-lier than 23 months after the baseline measurement.[10] Based on the bone density studies seen in Fig. 14-1, an appropriate statement might read:

> *Bone Densitometry Follow-up: A repeat study of the PA lumbar spine is recommended in 1 year if pharmacologic intervention is initiated, in accordance with recommendations from the American Association of Clinical Endocrinologists although such a study would not be eligible for Medicare reimbursement for 23 months.*

ASSESSMENT OF RISK FACTORS

Clinical risk factors (non-bone density factors) clearly increase the risk of both frac-ture and bone loss. Specific risk factors are also an integral part of the absolute fracture risk prediction algorithms such as FRAX^{TM}, the FORE FRC, and the Black Fracture Risk Index, which are discussed in Chapter 10. It is thus *mandatory* that the densit-ometrist assess the patient's clinical risk factors in order to provide an assessment of fracture risk and knowledgeable recommendations for follow-up and intervention. Such assessments can be done with self-administered questionnaires. It is a relatively sim-ple matter to construct a questionnaire that addresses the most significant and common risk factors for bone loss and fractures that are required by the absolute fracture risk prediction algorithms. Positive findings can be noted in the densitometry report and statements regarding fracture risk, selection for treatment, or timing of follow-up stud-ies can be amended accordingly. A sample questionnaire is shown in Appendix XIII and is also available on the CD-ROM that accompanies this book. Depending on the partic-ular patient population most often seen at a facility, modifications to the questionnaire should be made as the densitometrist deems appropriate.

REPORTING SERIAL STUDIES

When the results of a follow-up bone density study are reported, the appropriate emphasis is on the magnitude and significance of the change in BMD in g/cm^2 between studies, rather than the diagnostic category or prediction of fracture risk from the follow-up study. This distinction is not always understood by the referring physician or the patient. ISCD guidelines for reporting follow-up studies are noted in Table 14-2 and in Appendix V. It is imperative that the technical aspects of the baseline and follow-up study be identical. The report should indicate the equipment type, software versions and dates for both studies, and the regions of interest that are being compared at baseline and follow-up. The precision and least significant change (LSC) at the densitometry facility for the skeletal site(s) in question should be stated. Ideally, the precision should

---

[10] *See* Appendix VII for the provisions of the Bone Mass Measurement Act of 1997.

be expressed as the root-mean-square standard deviation (RMS-SD)[11] in g/cm^2. The absolute magnitude of the change in g/cm^2, the % change from baseline, and the statistical confidence level for the change should be reported. These values can be calculated with the statistical confidence calculator on the accompanying CD-ROM. Finally, recommendations for the timing of any repeat studies should also be made. If the measured change in BMD in g/cm^2 does not equal or exceed the LSC, this should be stated as well, in order to avoid any confusion on the part of the referring physician. Rather than stating that the LSC has not been equaled or exceeded, a more direct approach is advised in which the statement is made that the measured change in BMD does not exceed the precision error of the testing and therefore no change in the BMD must be assumed. If the patient is being followed to document therapeutic efficacy, the densitometrist may wish to further emphasize that no change in the BMD is considered an indication of efficacy.

THE CHALLENGE IN REPORTING DENSITOMETRY RESULTS

The knowledge that a densitometrist must bring to bear on the quantitative assessment of bone density to interpret the findings and place them in the appropriate clinical context is considerable. But the conclusions must be carefully crafted in the most succinct fashion possible. Long reports are simply not read. Vague statements will not be understood or appreciated. At present, it is not sufficient to simply say that the patient does or does not have osteoporosis or is or is not at increased risk for fracture. For the densitometry report to be useful it must be accurate, clear, and complete but also concise. Even though some have said that densitometrists should restrict their statements to a simple review of the numbers, referring physicians want and require more from the experienced densitometrist to better serve their patient's needs.

The best format for conveying this information is a matter of opinion. Narrations in the form of a letter may evoke a sense of frustration on the part of the busy clinician who feels he must search the letter for information relevant to the care of the patient. Shorter narrations that are followed by numbered conclusions may result in only the numbered conclusions being read. Any important information contained in the narration may be lost. It would also seem clear that the longer the letter or the greater the number of conclusions, the less likely it is that the pertinent information will be read. Addressing these issues at present is primarily a matter of trial and error and personal opinion. To meet the needs and requests of the primary care physician regarding reporting and to ensure that all the relevant information is reviewed and understood is a challenge. With these issues in mind, a reporting format that combines a brief series of numbered conclusions with short narrative paragraphs describing relevant technical issues would seem to be the best approach. The issues addressed by the numbered conclusions should be clearly identified and always given in the same order, from report to report.

The patient, whose bone density studies are shown in Fig. 14-1A and B, completed the patient questionnaire found in Appendix XIII of this book before the studies were done. She also underwent measurements of her weight and height, the latter being performed with a wall-mounted stadiometer. From the questionnaire, it was noted that she

---

[11] *See* Chapter 11 for a discussion of the RMS-SD.

had never taken hormone replacement, her mother had a hip fracture, and that this was her first bone density study. She did not smoke and did not acknowledge having any diseases or disorders or medication use known to be associated with an increased risk of bone loss or osteoporosis. The complete report from the densitometrist to the referring physician read as follows:

Dual Energy X-ray Absorptiometry Bone Density Report

Patient Name:	*Jane Doe*	*Technique:*	*DXA*
Patient Date of Birth:	*07/12/1943*	*Device:*	*GE Lunar Prodigy*
Referring Physician:	*John Smith, MD*	*Software Version:*	*11.4*
Date of Study:	*9/8/2008*	*Studies:*	*PA Lumbar Spine*
Technologist:	*S Jones, CDT*		*Left Proximal Femur*
Reason for testing:	*Osteoporosis*		

Conclusions and Recommendations

1. ***Current Diagnosis Based on BMD:*** *Osteoporosis, based on the L1–L4 T-score, applying World Health Organization criteria and ISCD guidelines for diagnosis.*
2. ***VFA Imaging for Diagnosis of Spine Fracture:*** *VFA imaging not requested. No history of spine fracture. No apparent height loss to suggest spine fracture.*
3. ***FRAX^{TM} 10-Year Risk Prediction: Hip fracture:*** *3.3%; Major osteoporotic fracture: 28%.*
4. ***Comparison to Previous Studies:*** *This is the patient's first bone density study.*
5. ***Treatment Recommendations:*** *This patient meets the 2008 National Osteoporosis Foundation criteria for consideration of pharmacologic intervention based on both the diagnosis of osteoporosis and the FRAX^{TM} 10-year hip and major osteoporotic fracture risk.*
6. ***Other Recommendations:*** *Secondary causes of bone loss should be excluded clinically. A daily intake of 1200 mg of calcium and 800–1000 IU of vitamin D3 is also recommended.*
7. ***Bone Densitometry Follow-up:*** *A repeat study of the PA lumbar spine is recommended in 1 year if pharmacologic intervention is initiated, in accordance with recommendations from the American Association of Clinical Endocrinologists although such a study would not be eligible for Medicare reimbursement for 23 months.*

Report Details

GENERAL

Studies were performed without difficulty. A standard bed pillow was placed under the patient's head for both studies. A foam black positioner was used during the PA lumbar spine study and an acrylic foot positioner was used for the left proximal femur study. The patient wore a hospital gown for both studies. Fracture risk interpretation is based on the measured BMD at the femoral neck, patient responses to a self-administered risk factor questionnaire and measured height and weight.

PA LUMBAR SPINE AND LEFT PROXIMAL FEMUR STUDY

Vertebral labeling is correct. The image does not suggest fracture or degenerative change. The left proximal femur was studied as a matter of convention. Significant differences in BMD between the femurs are not expected.
Please call if there are any questions concerning this report.
[Name of Densitometrist, CCD]

This report is actually only one page long, using a 12-point font, standard margins, and single line spacing. Note that the date of the study, patient's name, birth date, requesting provider, equipment manufacturer, model, software version, and skeletal sites measured are captured in the header of the report. The indications for the test are there as well, although this now reflects the appropriate ICD-9 diagnosis based on the test results. Headings are numbered and emphasized with a bold font for emphasis to ensure that they are read. In each case where it was appropriate and possible, guideline support from the various major organizations has been noted. Because the actual computer printouts of the bone density studies were included with the report, the BMD for each region of interest was not given in the report. The computer printouts were also signed by the densitometrist, indicating to the referring physician that the printouts had been reviewed by a physician. Item #2, which refers to VFA, serves several purposes. The first is to call the referring physician's attention to this application of DXA and the second is to suggest the need for an assessment, whether by clinical history or imaging, of prevalent vertebral fracture. It also highlights the densitometrist's assessment of the patient's history of vertebral fracture and height, both measured and historical. ISCD guidelines (*16*) emphasize a historical height loss of > 4 cm (1.6 in.) or a combination of factors which include age, patient-reported vertebral fracture, and historical height loss of 2–4 cm (0.8–1.6 in.), as indications for VFA. This statement also points out that VFA imaging was not requested and therefore, not done. The lack of direct knowledge of the patient's prevalent vertebral fracture status affects the diagnosis and fracture risk prediction. This statement, therefore, reflects the limitations placed on the densitometrist's interpretation. The recommendations for the timing of a repeat study highlights the discrepancy between what is medically appropriate and the limitations of insurance reimbursement. Both issues are important to the patient and should be noted. Finally, technical information regarding scan acquisition and the validity of the selected skeletal regions of interest were noted at the bottom of the report along with the basis for the fracture risk prediction.

If the more aggressive or detailed recommendations regarding the differential diagnosis of secondary causes of bone loss and/or additional laboratory tests are made, the report obviously becomes longer. The technical information regarding scan acquisition and the validity of the selected skeletal regions of interest must generally be moved to a second page. But the important recommendations can all be captured on the first page of the report. This is extremely important, as the second page of a report may not be immediately read.

This particular style of report is an attempt to meet the ISCD guidelines for reporting densitometry as well as the stated needs and desires of the referring physicians who have received such reports over the years. If other reporting formats are more appropriate for a particular practice they should certainly be used. But the report must be limited in length and to the point. And ultimately the point is to answer the question of the referring physician, which is "What do I need to do for my patient?" The densitometrist is responsible for device quality control, skeletal site selection, scan frequency, precision issues, data analysis, diagnosis, fracture risk assessment, therapeutic recommendations, and assessments of therapeutic efficacy. But the success or failure of the densitometrist and the promise of these marvelous technologies resides in the accuracy, clarity, and completeness of the reports sent to the physicians who have asked for assistance in the care of their patients.

REFERENCES

1. World Health Organization. Assessment of fracture risk and its application to screening for post-menopausal osteoporosis. WHO technical report series. Geneva: WHO, 1994.

2. Fuleihan GE, Stock JL, McClung MR, Saifi G. A national random survey of bone mineral density reporting in the United States. J Clin Densitom 2002;5:3–9.

3. Indications and reporting for dual-energy x-ray absorptiometry. J Clin Densitom 2004;7(1):37–44.

4. Hodgson SF, Watts NB, Bilezikian JP, et al. American Association of Clinical Endocrinologists medical guidelines for clinical practice for the prevention and treatment of postmenopausal osteoporosis: 2001 edition, with selected updates for 2003. Endocr Pract 2003;9(6):544–564.

5. National Osteoporosis Foundation. Clinician's guide to prevention and treatment of osteoporosis. 1–30. 2008. Washington, D.C., National Osteoporosis Foundation.

6. Kanis JA, Gluer C-C. An update on the diagnosis and assessment of osteoporosis with densitometry. Committee of Scientific Advisors, International Osteoporosis Foundation. Osteoporos Int 2000;11:192–202.

7. Hamdy RC, Petak SM, Lenchik L. Which central dual x-ray absorptiometry skeletal sites and regions of interest should be used to determine the diagnosis of osteoporosis? J Clin Densitom 2002;5: S11–S17.

8. Consensus Development Conference. Prophylaxis and treatment of osteoporosis. Am J Med 1991;90:107–110.

9. Consensus Development Conference. Diagnosis, prophylaxis, and treatment of osteoporosis. Am J Med 1993;94:646–650.

10. National Institutes of Health. Osteoporosis prevention, diagnosis, and therapy. JAMA 2001;285(6):785–795.

11. Johnson BE, Lucasey B, Robinson RP, Lukert BP. Contributing diagnoses in osteoporosis: the value of a complete medical evaluation. Arch Intern Med 1989;149:1069–1072.

12. Tannenbaum C, Clark J, Schwartzman K, et al. Yield of laboratory testing to identify secondary contributors to osteoporosis in otherwise healthy women. J Clin Endocrinol Metab 2002;87:4431–4437.

13. Management of osteoporosis in postmenopausal women: 2006 position statement of The North American Menopause Society. Menopause 2006;13(3):340–367.

14. Leib ES, Lewiecki EM, Binkley N, Hamdy RC. Official positions of the International Society for Clinical Densitometry. J Clin Densitom 2004;7(1):1–6.

15. Federal Register 42 CFR Part 410; Vol 63, No. 121, June 24, 1998.

16. Schousboe JT, Vokes T, Broy SB, et al. Vertebral fracture assessment: the 2007 ISCD official positions. J Clin Densitom 2008;11:92–108.

15 FDA-Approved Densitometry Devices

CONTENTS

The devices discussed in this chapter are available in the United States for clinical use. The specifications were provided by the manufacturers and are subject to change without notice as devices are continually upgraded to reflect advances in the technology. The categories of information provided by each manufacturer may vary slightly. All categories are not relevant to every device. This listing of devices is not intended to reflect all devices in use in the United States. This listing may also reflect devices in use in clinical and research settings but not necessarily still sold by manufacturers. Every attempt was made to ensure the accuracy of the information. The manufacturer should be contacted for the latest specifications. Manufacturer contact information can be found in Appendix I. The devices are grouped by type and listed alphabetically by model name.

COMPUTER-ENHANCED RADIOGRAMMETRY

dxr-online™

- Manufacturer: Sectra Pronosco, Herlev, Denmark
- Technique: Computerized radiogrammetry utilizing a standard digitized X-ray image
- Skeletal application(s): Metacarpals of the index, long, and ring fingers
- Results:

  - BMD (g/cm^2)
  - T-score, z-score
  - Graphical representation of the T- and z-score

- Patient scan time: Not applicable.
- Precision: 0.25–56%, depending on quality of image source.
- Radiation exposure: 1 μSv during plain film acquisition.

- Operation: Digitized hand film is transmitted over the Internet to be analyzed off-site. Image analysis algorithms are applied and are those previously employed in the Sectra Osteoporosis Package™ and the Pronosco X-posure System™ V2.

COMPUTER-ENHANCED RADIOGRAPHIC ABSORPTIOMETRY

Automated OsteoGram®

- Manufacturer: CompuMed Inc., Los Angeles, CA.
- Technique: Radiographic absorptiometry (RA) utilizing digital films of the hand with a computerized analysis.
- Skeletal application(s): Middle phalanges of the index, long, and middle fingers.
- Results:

    – BMD in arbitrary RA units
    – T-score and *z*-score
    – Diagnostic classification based on WHO criteria

- Patient scan time: Not applicable.
- Precision: < 1%.
- Quality control: Automated system checks to ensure quality and accuracy of image digitalization.
- Operation: Digital hand images are analyzed by proprietary software installed on the computer or workstation. The results are then printed.

Fig. 15-1. The CompuMed Automated Osteogram® Analysis System. Photograph courtesy of CompuMed Inc., Los Angeles, CA.

MetriScan™

- Alara, Inc., Fremont, CA
- Technique: Radiographic absorptiometry with storage phosphor technology
- Skeletal application(s): Middle phalanges of the index, long, and ring fingers

- Scan time: < 1 second
- Results:

    - Estimated phalangeal BMD in arbitrary RA units
    - % Young-adult and % age-matched comparisons
    - T-score and *z*-score
    - Diagnostic classification based on WHO criteria

- Precision: 1.1%
- Radiation exposure: 0.0001 mrem/scan (0.001 μSv/scan)
- Dimensions: 16 in. × 16 in. × 16 in. (40.6 cm × 40.6 cm × 40.6 cm)
- Weight: 41.5 lbs (18.8 kg)
- Environmental operating temperature: 64–95°F (18–35°C)
- Environmental operating humidity: 5–80%, non-condensing
- Scatter radiation: 0.0001 mrem/scan (0.001 μSv/scan) at 1 m
- Quality control: Automated
- Operation: Unit is self-contained and does not require a standard hand film. Data input from keypad on unit. Separate HP printer or printer as specified by Alara, Inc. for results output.

Fig. 15-2. The Alara MetriScan™. Photograph courtesy of Alara, Inc., Hayward, CA.

CENTRAL X-RAY DENSITOMETERS

Delphi™

- Manufacturer: Hologic, Inc., Bedford, MA
- Technology: Dual-energy X-ray absorptiometry

- Skeletal regions studied:

    – PA lumbar spine
    – Proximal femur
    – Forearm
    – IVA^{TM} lateral spine imaging (T4–L4)
    – Dual Hip^{TM}
    – Whole body (on Delphi with Whole Body)

- Scan time (in the 60 Hz scan mode):

    – PA lumbar spine and proximal femur 15 seconds
    – Forearm 30 seconds
    – Whole body 6.8 minutes
    – Single energy IVA^{TM} 10 seconds (for 15 in. scan length)

- Results:

    – BMD (g/cm^2)
    – BMC (g)
    – Area (cm^2)
    – T-score and z-score
    – sBMD (mg/cm^2)
    – NHANES III reference data for hip
    – Trend reports for serial monitoring

- Precision: <1.0%
- Radiation dose (in the 60 Hz scan mode):

    – PA lumbar spine and proximal femur 5 mR
    – Forearm 10 mR
    – Whole body 1.5 mR
    – IVA^{TM} 7 mR (15 in. scan length)

- Dimensions:

    – Delphi^{TM} 76 in. × 49.5 in. × 28 in. (193 cm × 126 cm × 71 cm)
    – Delphi^{TM} with Whole Body 79.5 in. × 48 in. × 28 in. (202 cm × 122 cm × 71 cm), 119 in. × 59 in. × 28 in. (302 cm × 150 cm × 71 cm) table extended

- Weight:

    – Delphi^{TM} 650 lb (296 kg)
    – Delphi^{TM} with Whole Body 680 lb (310 kg)

- Recommended dedicated floor space: 8 ft × 8 ft (2.4 m × 2.4 m)
- Scatter radiation: Less than 1.0 mR/hr (0.01 mSv/hr) measured at 6.6 ft (2.0 m) from the examination table for most scan modes
- Operating environmental temperature: 60–90°F (15–32°C)
- Operating environmental relative humidity: 20–80%, non-condensing
- X-ray source: Switched pulse at 140 kVp and 100 kVp for dual energy; 140 kVp for single-energy IVA^{TM}

- X-ray beam geometry: Fan
- Detectors: Multi-element detector array
- Scan path: Linear
- Quality control: Self-calibrating with Hologic Automatic Internal Reference system and automated quality control program
- Operation: IBM-compatible Pentium computer, Windows 98®-based operating system, HP DeskJet® printer, 17 in. monitor
- Accessories provided:

    – Anthropomorphic spine phantom
    – Medical imaging printer

- Options: Magneto optical disk storage; HP LaserJet® B&W printer; flat panel monitor; whole body, body composition analysis, and quantitative morphometry software; modem or network options

Fig. 15-3. The Hologic Delphi™. Photograph courtesy of Hologic, Inc., Bedford, MA.

Discovery™

- Manufacturer: Hologic, Inc., Bedford, MA
- Technology: Dual-energy X-ray absorptiometry
- Models: C*i*, W*i*, C, W, SL, and A
- Skeletal regions studied:

    – PA lumbar spine, all models
    – Proximal femur, all models
    – Forearm, all models
    – Dual Hip™, all models
    – IVA™, on models C, W, SL, and A
    – CAD*f*x, on models C, W, SL, and A
    – Whole body, on models W*i*, W, and A

- Scan time on models Ci and Wi (in the 60 Hz scan mode):

    – PA lumbar spine and proximal femur 30 seconds
    – Forearm 30 seconds
    – Whole body 6.8 minutes

- Scan time on models C, W, SL, and A (in the 60 Hz scan mode):

    – PA lumbar spine and proximal femur 10 seconds
    – Forearm 30 seconds
    – Single-energy IVA^{TM} 30 seconds
    – Whole Body 6.8 minutes (model W); 180 seconds (model A)

- Results:

    – BMD (g/cm^2)
    – BMC (g)
    – Area (cm^2)
    – T-score and z-score
    – NHANES III reference data for hip
    – Diagnosis using World Health Organization criteria
    – Fracture risk assessment
    – Vertebral fracture assessment (with IVA^{TM})
    – Trend reports for serial monitoring

- Precision: <1.0%
- Radiation dose (in the 60 Hz scan mode):

    – Models Ci and Wi PA lumbar spine and proximal femur 0.10 mGy
    – Models C, W, SL, and A, PA lumbar spine 0.007 mGy
    – Models C, W, SL, and A, Proximal femur 0.07 mGy
    – Models Ci and Wi Forearm 0.010 mGy
    – Models C, W, SL, and A Forearm 0.005 mGy
    – Models Wi, W, and A Whole body 0.015 mGy
    – Models C, W, SL, and A IVA^{TM} 0.07 mGy

- Dimensions:

    – Models Ci and C 76 in. × 41 in. (1.93 m × 1.05 m)
    – Models Wi, W, SL, and A 79.5 in. × 41 in. (2.02 m × 1.05 m)
    – Models Wi and W, table extended 119 in. × 59 in. (3.02 m × 1.50 m)
    – Model SL, table extended and C-arm rotated 79.5 in. × 59 in. (2.02 × 1.50 m)
    – Model A, table extended and C-arm rotated 119 in. × 59 in. (3.02 m × 1.50 m)

- Weight:

    – Control console, all models, 150 lb (68 kg)
    – Models Ci and C 650 lb (296 kg)
    – Models Wi and W 680 lb (310 kg)
    – Models SL and A 800 lb (365 kg)

- Recommended dedicated floor space: 8 ft × 8 ft (2.4 m × 2.4 m) to 8 ft × 10 ft (2.4 m × 3.1 m), depending on model
- Scatter radiation: Less than 1.0 mR/hr (0.01 mSv/hr) measured at 6.6 ft (2.0 m) from the examination table for most scan modes
- Operating environmental temperature: 60–90°F (15–32°C)
- Operating environmental relative humidity: 20–80%, non-condensing
- X-ray source: Switched pulse with 140 kVp peak
- X-ray beam geometry: Fan
- Detectors: Multi-element detector array
- Quality control: Self-calibrating with Hologic Automatic Internal Reference system and automated quality control program
- Operation: IBM-compatible Pentium computer, QDR for Windows XP operating systems, HP DeskJet® printer, 17 in. monitor, mouse, 56 K modem, CD-RW drive
- Options: Magneto optical disk storage; HP LaserJet® B&W printer; 15 in. flat panel monitor; modem or network options; IRIS package (includes DICOM, Physician's Report Writer); prosthetic hip software; and depending on model, decubitus lateral BMD, body composition, and sub-region analysis software, small animal capability.

Fig. 15-4. The Hologic Discovery™. Photo courtesy of Hologic, Inc., Bedford, MA.

DPX Bravo®

- Manufacturer: GE Healthcare, Madison, WI.
- Technology: Dual-energy X-ray absorptiometry
- Skeletal application(s):

  – PA spine
  – Proximal femur

- Scan time:

  – PA spine 90 seconds
  – Proximal femur 90 seconds

- Results:

  – BMD (g/cm^2)
  – BMC (g)
  – Area (cm^2)
  – % Young-adult and % age-matched comparisons
  – T-score and z-score
  – NHANES III total hip comparisons

- Precision:

  – PA spine <1%
  – Hip <1%

- Radiation dose:

  – PA spine or proximal femur 3 mR

- Dimensions:

  – 73.2 in. × 33.9 in. × 51.2 in. (186 cm × 86 cm × 130 cm)

- Power: 100–240 VAC +/– 10%, THD<5%, 600 VA
- X-ray filtration: constant potential, cerium K-edge filter
- X-ray beam geometry: SmartBeam^{TM}
- Quality control: Block phantom and aluminum spine phantom supplied by manufacturer Automated QA program with daily precision monitoring
- Software platform: Windows XP
- Accessories provided:

  – PA spine-positioning block
  – Foot positioner for proximal femur studies
  – Block phantom
  – Aluminum spine phantom
  – Washable table pad

- Options: DualFemur^{TM}, Forearm, OneVision, CAD, OneScan, Physician's Composer, TeleDensitometry, DEXTER PDA

DPX Duo$^{®}$

- Manufacturer: GE Healthcare, Madison, WI.
- Technology: Dual-energy X-ray absorptiometry/gynecology exam table
- Skeletal application(s):

  – PA spine
  – Proximal femur

- Scan time:

  – PA spine 90 seconds
  – Proximal femur 90 seconds

Fig. 15-5. The Lunar DPX Bravo®. Photo courtesy of GE Healthcare, Madison, WI.

- Results:

    – BMD (g/cm^2)
    – BMC (g)
    – Area (cm^2)
    – % Young-adult and % age-matched comparisons
    – T-score and *z*-score
    – NHANES III total hip comparisons

- Precision:

    – PA spine <1%
    – Hip <1%

- Radiation dose:

    – PA spine or proximal femur 3 mR

- Dimensions:

    – 73.2 in. × 33.9 in. × 57.9 in. (186 cm × 86 cm × 147 cm)

- Power: 100–240 VAC +/–10%, THD<5%, 600 VA
- X-ray beam geometry: SmartBeam™
- Quality control: Block phantom and aluminum spine phantom supplied by manufacturer. Automated QA program with daily precision monitoring
- Software platform: Windows XP
- Accessories provided:

    – PA spine-positioning block
    – Foot positioner for proximal femur studies

   – Block phantom
   – Aluminum spine phantom

- Exam table features

   – Two storage drawers
   – Paper roll disperser
   – Washable table pad
   – Extendable leg rests
   – Treatment pan

- Options: DualFemur, Forearm, OneVision, CAD, OneScan, Physician's Composer, Tele-Densitometry, DEXTER PDA

Fig. 15-6. The Lunar Duo®. Photo courtesy of GE Healthcare, Madison, WI.

DPX-IQ™

- Manufacturer: GE Healthcare, Madison, WI.
- Technology: Dual-energy X-ray absorptiometry
- Skeletal application(s):

   – PA spine
   – Proximal femur
   – Total body with soft tissue quantification (with full size table only)

- Scan time:

    - PA spine 2 minutes
    - Proximal femur 2 minutes
    - Total body 11 minutes

- Results:

    - BMD (g/cm^2)
    - BMC (g)
    - Area (cm^2)
    - % Young-adult and % age-matched comparisons
    - T-score and z-score
    - sBMD (mg/cm^2) for L2–L4 and total hip
    - NHANES III total hip comparisons

- Precision:

    - PA spine 0.5%
    - Hip 1%
    - Total body 0.5%

- Radiation dose:

    - PA spine or proximal femur < 3 mRem
    - Total body 0.02 mRem

- Dimensions:

    - Full-size table 95 in. × 42 in. × 52 in. (242 cm × 107 cm × 133 cm)
    - Compact table 71 in. × 40 in. × 52 in. (181 cm × 100 cm × 133 cm)

- Weight:

    - Full-size table 598 lbs (272 kg)
    - Compact table 550 lbs (250 kg)

- Recommended dedicated floor space:

    - Full-size table 9 ft × 7 ft (2. 7 m × 2.1 m)
    - Compact table 7 ft × 7 ft (2.1 m × 2.1)

- Operating environmental temperature: 65–80°F (18–27°C)
- Operating environmental relative humidity: 30–75%, non-condensing
- X-ray source: 134 KVp; 3.0 mA for PA spine and proximal femur studies (mA varies by skeletal site and scan mode)
- X-ray filtration: constant potential, cerium K-edge filter
- X-ray beam geometry: Pencil-beam
- Detectors: NaI
- Scan path: Rectilinear
- Quality control: Block phantom and aluminum spine phantom supplied by manufacturer
- Operation: IBM-compatible desktop Pentium^{TM} computer, SVGA monitor, printer

- Accessories provided:
    - PA spine-positioning block
    - Foot positioner for proximal femur studies
    - Block phantom
    - Aluminum spine phantom
- Options: Forearm, hand, lateral spine, and orthopedics software; forearm positioner; lateral spine positioner; encapsulated spine phantom

Fig. 15-7. The Lunar DPX Pro^{TM}. Photograph courtesy of GE Healthcare, Madison, WI.

DPX MD^{TM}

- Manufacturer: GE Healthcare, Madison, WI.
- Technology: Dual-energy X-ray absorptiometry
- Skeletal application(s):
    - PA spine
    - Proximal femur
    - DualFemur^{TM} (not available on compact model)
    - Total body (not available on compact model)
- Scan time:
    - PA spine and proximal femur 2 minutes
    - DualFemur^{TM} 4 minutes
    - Total body 8 minutes
- Results:
    - BMD (g/cm^2)
    - BMC (g)

- – % Young-adult and age-matched comparisons
  - – T-score and *z*-score
  - – sBMD (mg/cm^2)
  - – NHANES III reference data
  - – WHO diagnostic classification

- Precision:

  - – PA spine and total femur 1.0%
  - – DualFemur^{TM} 0.7%
  - – Total body 0.5%

- Radiation dose:

  - – PA spine 1 mrem
  - – Femur 1 mrem
  - – Total body 0.02 mrem

- Dimensions:

  - – Full size table 95 in. × 42 in. × 52 in. (242 cm × 107 cm × 133 cm)
  - – Compact table 71 in. × 40 in. × 52 in. (181 cm × 100 cm × 133 cm)

- Weight:

  - – Full-size table 598 lbs (272 kg)
  - – Compact table 550 lbs (250 kg)

- Recommended dedicated floor space:

  - – Full-size table 9 ft × 7 ft (2.7 m × 2.1 m);
  - – Compact table 7 ft × 7 ft (2.1 m × 2.1 m)

- Operating environmental temperature: 65–80°F (18–27°C)
- Operating environmental relative humidity: 30–75%, non-condensing
- X-ray source: 134 kV; 0.75 mA for PA spine, proximal femur, DualFemur^{TM} (mA varies by skeletal site and scan mode)
- X-ray filtration: Constant potential, cerium K-edge filter
- X-ray beam geometry: Pencil-beam
- Detectors: NaI
- Scan path: Rectilinear
- Quality control: Automatic test program
- Operation: IBM-compatible computer, printer
- Accessories provided:

  - – PA spine positioner
  - – Proximal femur positioner
  - – DualFemur^{TM} positioner
  - – Aluminum spine phantom

- Options: Lateral spine, Forearm/Hand, Pediatrics, Orthopedics, and Small Animal software; encapsulated phantom

DPX MD+^{TM}

- Manufacturer: GE Healthcare, Madison, WI.
- Technology: Dual-energy X-ray absorptiometry
- Skeletal application(s):

    – PA spine
    – Proximal femur

- Results:

    – BMD (g/cm^2)
    – BMC (g)
    – % Young adult and % age-matched comparisons
    – T-score and *z*-score
    – sBMD (mg/cm^2)
    – NHANES III reference data
    – WHO diagnostic classification

- Precision:

    – PA spine, proximal femur and total body 1.0%
    – DualFemur^{TM} < 1.0%

- Radiation dose:

    – PA spine and proximal femur 3.0 mrem
    – Total body 0.02 mrem

- Dimensions:

    – Full-size table 95 in. × 42 in. × 52 in. (242 cm × 107 cm × 133 cm)
    – Compact table 71 in. × 40 in. × 52 in. (181 cm × 100 cm × 133 cm)

- Weight:

    – Full-size table 598 lbs (272 kg)
    – Compact table 550 lbs (250 kg)

- Recommended dedicated floor space:

    – Full-size table 9 ft × 7 ft (2.7 m × 2.1 m)
    – Compact table 7 ft × 7 ft (2.1 m × 2.1 m)

- Operating environmental temperature: 65–80°F (18–27°C)
- Operating environmental relative humidity: 30–75%, non-condensing
- X-ray source: 134 kV; 0.75 mA for PA spine, proximal femur, DualFemur^{TM}
- X-ray filtration: Constant potential, cerium K-edge filter
- X-ray beam geometry: Pencil-beam
- Detectors: NaI
- Scan path: Rectilinear
- Quality control: Automatic test program
- Operation: IBM-compatible computer, printer

- Accessories provided:

    – PA spine positioner
    – Proximal femur positioner
    – Aluminum spine phantom

- Options: DualFemur™ with positioner (not available on compact model), total body with body composition (not available on compact model); encapsulated phantom

DPX-NT™

- Manufacturer: GE Healthcare, Madison, WI.
- Technology: Dual-energy X-ray absorptiometry
- Skeletal application(s):

    – PA spine
    – Proximal femur
    – DualFemur™
    – Total body with body composition

- Scan time:

    – PA spine 1 minute
    – Proximal femur 2 minutes
    – DualFemur™ 4 minutes
    – Total body 8 minutes

- Results:

    – BMD (g/cm^2)
    – sBMD (mg/cm^2)
    – T-score and *z*-score
    – NHANES III reference data
    – WHO diagnostic classification

- Precision:

    – PA spine 1.0%
    – Proximal femur 1.0%
    – Total body 1.0%
    – DualFemur™ < 1.0%

- Radiation dose:

    – PA spine 3.0 mrem
    – Proximal femur 3.0 mrem
    – Total body 0.02 mrem

- Dimensions: 95 in. × 42 in. × 52 in. (242 cm × 107 cm ×133 cm)
- Weight: 598 lbs (272 kg)
- Recommended dedicated floor space: 9 ft × 7 ft (2.7 m × 2.1 m)
- Operating environmental temperature: 65–80°F (18–27°C)
- Operating environmental relative humidity: 30–75%, non-condensing

- X-ray source: 134 kV; 1.5 mA for PA spine, proximal femur, DualFemur^{TM} (mA varies by skeletal site and scan mode)
- X-ray filtration: Constant potential, cerium K-edge filter
- X-ray beam geometry: Pencil-beam
- Detectors: NaI
- Scan path: Rectilinear
- Quality control: Automated QA program
- Operation: IBM-compatible computer running Windows NT
- Accessories provided:

    - PA spine positioner
    - Proximal femur positioner
    - DualFemur^{TM} positioner
    - Aluminum spine phantom

- Options: Encapsulated phantom

Excell^{TM}

- Manufacturer: CooperSurgical Norland, Trumball, CT.
- Technology: Dual-energy X-ray absorptiometry
- Standard application(s):

    - PA spine
    - Left and right proximal femur

- Scan time:

    - PA spine <1.5 minutes
    - Proximal femur <2 minutes

- Results

    - BMD (g/cm^2)
    - BMC (g)
    - Length (cm)
    - % Young-reference and % age-matched comparisons
    - T-score and z-score
    - sBMD (mg/cm^2) for L2–L4 and total hip
    - NHANES III proximal femur reference data

- Precision:

    - PA spine 1.0%
    - Proximal femur 1.2%

- Radiation dose: < 1.0 mRem in high speed scan mode
- Dimensions: 72 in. × 48 in. × 49 in. (182.8 cm × 122.0 cm × 124.5 cm)
- Weight: 400 lbs (181 kg)
- Recommended dedicated floor space: 7 ft × 7 ft (2.1 m × 2.1 m)
- Operating environmental temperature: 60–104°F (15–40° C)

- Operating environmental relative humidity: up to 80%, non-condensing
- X-ray source: 100 kV, 1.3 mA
- X-ray filtration: Samarium
- X-ray beam geometry: Pencil-beam
- Detectors: 2 NaI scintillation detectors
- Scan path: Rectilinear
- Quality control: Automated with 77-step calibration standard and quality control phantom
- Operation: IBM-compatible PC computer, HP DeskJet
- Accessories provided:

  - PA spine-positioning block
  - Hip sling with foot separator
  - 77-step calibration standard
  - Quality control phantom

- Options: Lateral spine, forearm, soft tissue composition, research, and small subject software

Fig. 15-8. The Norland Excell™. Photograph courtesy of Norland, a CooperSurgical Company, Ft. Atkinson, WI.

Excell™plus

- Manufacturer: CooperSurgical Norland, Trumball, CT.
- Technology: Dual-energy X-ray absorptiometry
- Skeletal application(s):

  - PA spine
  - Proximal femur

- – Forearm
- – Lateral spine

- Scan time:

  - – PA spine < 1.5 minutes
  - – Proximal femur < 2 minutes
  - – Forearm < 3 minutes,
  - – Lateral spine < 4 minutes

- Results:

  - – BMD (g/cm^2)
  - – BMC (g)
  - – Length (cm)
  - – % Young-reference and % age-matched comparisons
  - – T-score and z-score
  - – sBMD (mg/cm^2) for L2–L4 and total hip
  - – NHANES III total hip comparisons

- Precision:

  - – PA spine 1.0%
  - – Hip 1.2%
  - – Forearm 0.8%
  - – Lateral spine 2.4%

- Radiation dose:

  - – PA spine, proximal femur, forearm < 1.0 mrem
  - – Lateral spine < 2 mrem

- Dimensions: 72 in. × 48 in. × 49 in. (182.8 cm × 122.0 cm × 124.5 cm)
- Weight: 400 lbs (181 kg)
- Recommended dedicated floor space: 7 ft × 7 ft (2.1 m × 2.1 m)
- Operating environmental temperature: 60–104°F (15–40°C)
- Operating environmental relative humidity: Up to 80%, non-condensing
- X-ray source: 100 kV, 1.3 mA
- X-ray filtration: Samarium
- X-ray beam geometry: Pencil-beam
- Detectors: 2 NaI scintillation detectors
- Scan path: Rectilinear
- Quality control: Automated with 77-step calibration standard and quality control phantom
- Operation: IBM-compatible computer with Windows operating system, DeskJet printer, 15 in. SVGA monitor
- Accessories provided:

  - – PA spine-positioning block
  - – Hip sling with foot separator for use in proximal femur studies
  - – Lateral and forearm positioning aids

- – 77-step calibration standard
- – Quality control phantom

- Options: Software for research, small subject, or body composition; laptop computer; flat screen monitor; 17 in. SVGA monitor

Expert®-XL

- Manufacturer: GE Healthcare, Madison, WI
- Technology: Dual-energy X-ray absorptiometry
- Skeletal regions studied:

  - – PA spine
  - – Lateral lumbar spine
  - – Proximal femur
  - – Forearm and hand
  - – Total body
  - – Orthopedic hip
  - – Vertebral morphometry

- Scan times:

  - – PA spine and proximal femur 6 seconds
  - – Forearm/hand 10 seconds
  - – Lateral spine 24 seconds
  - – Total body 160 seconds
  - – Vertebral morphometry 38 seconds

- Results:

  - – BMD (g/cm^2)
  - – BMC (g)
  - – Area (cm^2)
  - – % Young-adult and % age-matched comparisons
  - – T-score and *z*-score
  - – Vertebral heights (mm) and vertebral height ratios

- Precision: 1.0%
- Radiation dose:

  - – PA spine and proximal femur 27 mrem
  - – Forearm/hand 12 mrem
  - – Lateral spine 190 mrem
  - – Total body 5 mrem
  - – Morphometry 120 mrem

- Dimensions: 108 in. × 71 in. (2.7 m × 1.8 m). Motorized C-arm 140° rotation with 78 in. (198 cm) longitudinal travel and 14 in. (36 cm) transverse travel
- Weight: 750 lb (340.2 kg)
- Recommended dedicated floor space: 12 ft × 10 ft (3.7 m × 3.1 m)
- Operating environmental temperature: 65–80°F (18–27°C)

- Operating environmental relative humidity: 30–75%, non-condensing
- X-ray source: 134 kV, 5 mA for PA spine, proximal femur, lateral spine, and morphometry
- X-ray beam geometry: Fan-beam
- Detectors: Dual-energy solid state
- Scan path: Linear
- Image resolution: 0.5 mm
- Quality control: Internal hydroxyapatite; Automated quality assurance program with spine phantom
- Operation: IBM-compatible, Pentium® based computer; Windows® environment; SVGA monitor; black and white laser printer; hand-held motor controller for C-arm rotation and table elevation
- Accessories provided: Spine phantom
- Options: Color printer; DICOM utilities

Fig. 15-9. The Lunar Expert®-XL. Photograph courtesy of GE Healthcare, Madison, WI.

Explorer^{TM}

- Manufacturer: Hologic, Inc., Bedford, MA
- Technology: Dual-energy X-ray absorptiometry
- Skeletal regions studied:

  – PA lumbar spine
  – Proximal femur
  – Dual Hip^{TM}
  – Forearm
  – Decubitus lateral spine
  – Whole body

- Scan time:

  – PA lumbar spine 122–163 seconds
  – Proximal femur 92–123 seconds
  – Forearm 62 seconds
  – Whole body 6.7 minutes
  – Decubitus lateral spine 163 seconds

- Results:

  – BMD (g/cm^2)
  – BMC (g)
  – Area (cm^2)
  – T-score and z-score
  – NHANES III reference data for hip

- Precision: <1.0% for PA spine and proximal femur
- Radiation dose (typical skin entrance dose):

  – PA spine 0.07–0.25 mGy
  – Proximal femur 0.07–0.094 mGy
  – Forearm 0.05 mGy
  – Whole body 0.012 mGy
  – Decubitus lateral spine 0.25 mGy

- Scan Region Dimensions at Pad Surface: 77.5 in. × 25.6 in. (1.97 m × 0.65 m)
- Weight:

  – System 720 lb (327 kg)
  – Console (Computer, Printer, Monitor) 75 lb (34.1 kg)

- Scatter radiation: Nominal 10 mGy/hr at 3.3 ft (1.0 m) from the examination table
- Operating environmental temperature: 59–90°F (15–32°C)
- Operating environmental relative humidity: 20–80%, non-condensing
- Operating footprint: 119 in. × 59 in. × 56 in. (3.02 m × 1.50 m × 1.42 m)
- X-ray source: Switched pulse at 100 and 140 kVp
- X-ray beam geometry: Fan beam
- Detectors: Multi-detector array
- Quality control: Self-calibrating with Hologic Automatic Internal Reference system and automated quality control program
- Operation: IBM-compatible Pentium computer.
- Options: Multiple reporting options. Forearm, prosthetic hip, decubitus lateral spine, body composition, and sub-region analysis, and pediatric software.

iDXA^{TM}

- Manufacturer: GE Healthcare, Madison, WI.
- Technology: Dual-energy X-ray absorptiometry

Fig. 15-10. The Hologic Explorer[TM]. Photograph courtesy of Hologic, Inc., Bedford, MA.

- Skeletal application(s):

    – PA spine
    – Single proximal femur
    – DualFemur[TM]
    – Dual-energy Vertebral Assessment (DVA)
    – Advanced hip assessment
      o Geometric parameters
      o Hip Axis Length (HAL)
    – Forearm
    – Total body BMD
    – Total body composition

- Scan time in standard mode for individual ˜66 in. tall

    – PA spine and proximal femur < 1 min each
    – DualFemur[TM] < 2 min
    – Total body < 7 min

- Results:

    – BMD (g/cm^2)
    – sBMD (mg/cm^2)
    – T-score and z-score
    – Fracture risk assessment based on WHO diagnostic classification
    – LUNAR® and NHANES III databases

- Precision:

    – PA spine 1.1%
    – Femoral neck 1.4%

- – Total femur 0.7%
- – Total body 0.5%

- Radiation dose, standard scan mode

  - – PA spine and proximal femur, 146 μGy each
  - – Total body 3 μGy

- Maximum patient weight: 450 lb (180 kg)
- Dimensions: 119 in. × 52 in. × 50 in. (302 cm × 131 cm × 127 cm)
- Weight: 779 lbs (353 kg)
- Minimum room size: 11 ft × 10.5 ft (3.5 m × 3.2 m)
- Scatter radiation: < 0.8 mR/hr (8 μSv/hr) at 39 in. (1 m) from x-ray source
- Operating environmental temperature: 65–81°F (18–27°C)
- Operating environmental relative humidity: 20–80%, non-condensing
- X-ray source: 100 kV; 0.188–2.500 mA (mA varies by skeletal site and scan mode)
- X-ray filtration: Dose efficient cerium K-edge filter
- X-ray beam geometry: Narrow angle fan-beam
- Detectors: High-definition CZT-HD (Cadium-zinc-telluride) staggered array
- Scan path: Rectilinear
- Quality control: Automated 6-point calibration and quality assurance with QA trending
- Operation: Windows operating system on IBM-compatible computer, printer
- Accessories provided:

  - – PA spine positioner
  - – DualFemur™ positioner
  - – Aluminum spine phantom
  - – 6-point calibration block phantom
  - – Washable table pad

- Options: DEXTER PDA, HL7, multi-user database

Fig. 15-11. The Lunar iDXA™. Photograph courtesy of GE Healthcare, Madison, WI.

Prodigy[TM]

- Manufacturer: GE Healthcare, Madison, WI.
- Technology: Dual-energy X-ray absorptiometry
- Skeletal application(s):

    – PA spine
    – Proximal femur
    – DualFemur[TM]
    – Customized regions of interest with metal removal
    – Total body and body composition

- Scan time:

    – PA spine and proximal femur 30 seconds
    – DualFemur[TM] 1 minute
    – Total body 5 minutes

- Results:

    – BMD (g/cm^2)
    – sBMD (mg/cm^2)
    – T-score and *z*-score
    – Fracture risk assessment based on WHO diagnostic classification
    – LUNAR® and NHANES III databases

- Precision:

    – PA spine and proximal femur 1.0%
    – DualFemur[TM] <1.0%
    – Total body < 1.0%

- Radiation dose:

    – PA spine and proximal femur 3.7 mrem
    – Total body 0.037 mrem

- Dimensions: 103.5 in. × 43.5 in. × 50 in. (263 cm × 111 cm × 127 cm)
- Weight: 600 lbs (272 kg)
- Recommended dedicated floor space: 9 ft × 7.5 ft (2.8 m × 2.3 m)
- Scatter radiation: < 0.3 mR/hr (3 μSv/hr) at 39 in. (1 m)
- Operating environmental temperature: 65–80°F (18–27°C)
- Operating environmental relative humidity: 20–80%, non-condensing
- X-ray source: 134 kV; 3.0 mA for PA spine, proximal femur, lateral vertebral assessment (mA varies by skeletal site and scan mode)
- X-ray filtration: Constant potential cerium K-edge filter
- X-ray beam geometry: Narrow angle fan-beam
- Detectors: Cadium-zinc-telluride (CZT)
- Scan path: Rectilinear
- Quality control: Automatic test program with QA trending
- Operation: Windows operating system on IBM-compatible Pentium® computer, printer

- Accessories provided:

    – PA spine positioner
    – DualFemur^{TM} positioner

    – Aluminum spine phantom

- Options: Pediatric, forearm, lateral spine, and lateral view^{TM}software; encapsulated phantom

Fig. 15-12. The Lunar Prodigy^{TM}. Photograph courtesy of GE Healthcare, Madison, WI.

QDR® 4500 A

- Manufacturer: Hologic, Inc., Bedford, MA.
- Technology: Dual-energy X-ray absorptiometry
- Skeletal regions studied:

    – PA spine
    – Proximal femur
    – Forearm
    – Whole body
    – Supine lateral lumbar spine

- Scan time (in the 60 Hz scan mode):

    – PA lumbar spine and proximal femur 10 seconds;
    – Lateral spine 120 seconds
    – Forearm 30 seconds
    – Whole body 3 minutes
    – Lateral imaging with morphometric X-ray absorptiometry (MXA) 7.5 seconds

- Results:

- – BMD (g/cm^2)
- – BMC (g)
- – Area (cm^2)
- – % Young-adult and % age-matched comparisons
- – T-score and z-score
- – sBMD (mg/cm^2) for L2–L4 and total hip
- – NHANES III total hip comparisons

- Precision: <1%
- Radiation dose (in the 60 Hz scan mode):

  - – PA lumbar 7 mR
  - – Proximal femur 7 mR
  - – Lateral spine 35 mR
  - – Forearm 5 mR
  - – Whole body 1 mR
  - – Lateral imaging with MXA 7 mR

- Dimensions: 79.5 in. × 41 in. × 28 in. (202 cm × 104 cm × 71 cm), 118.9 in. × 57 in. (302 cm × 145 cm) with C-arm rotated and table extended
- Weight: 800 lb (364 kg)
- Recommended dedicated floor space: 8 ft × 10 ft (2.4 m × 3.1 m)
- Scatter radiation: Less than 1.0 mR/hr (0.01 mSv/hr) measured at 6.6 ft (2.0 m) from the examination table for most scan modes
- Operating environmental temperature: 60–90°F (15–32°C)
- Operating environmental relative humidity: 20–80%
- X-ray source: Switched pulse, dual-energy
- X-ray beam geometry: Fan-beam
- Detectors: Multi-element detector array
- Scan path: Linear
- Quality control: Self-calibrating with patented Hologic Automatic Internal Reference System and automated quality control program
- Operation: IBM-compatible Pentium computer with Windows operating system, 17 in. monitor, HP LaserJet® B&W printer
- Accessories provided: Anthropomorphic spine phantom
- Options: Magneto optical disk storage; network configurations; body composition analysis software, MXA software, small animal software

QDR®4500 C

- Manufacturer: Hologic, Inc., Bedford, MA.
- Technology: Dual-energy X-ray absorptiometry
- Skeletal application(s):

  - – PA spine
  - – Proximal femur
  - – Forearm

Fig. 15-13. The Hologic QDR® 4500 A. Photograph courtesy of Hologic, Inc., Bedford, MA.

Fig. 15-14. The Hologic QDR® 4500 A. The gantry is rotated to perform supine lateral lumbar spine studies. Photograph courtesy of Hologic, Inc., Bedford, MA.

- Scan time (in the 60 Hz scan mode):
    - PA lumbar spine and proximal femur 15 seconds
    - Forearm 30 seconds
- Results:
    - BMD (g/cm^2)
    - BMC (g)

- – Area (cm^2)
- – % Young-adult and % age-matched comparisons
- – T-score and z-score
- – sBMD (mg/cm^2) for L2–L4 and total hip
- – NHANES III total hip comparisons
- – Fracture risk and diagnostic classification based on WHO criteria

- Precision: <1%
- Radiation dose (in the 60 Hz scan mode):

  - – PA lumbar spine 5 mR
  - – Proximal femur 5 mR
  - – Forearm 10 mR

- Dimensions: 79.5 in. × 41 in. × 28 in. (202 cm × 104 cm × 71 cm)
- Weight: 650 lb (296 kg)
- Recommended dedicated floor space: 8 ft × 8 ft (2.4 m × 2.4 m)
- Scatter radiation: Less than 1.0 mR/hr (0.01 mSv/hr) measured at 6.6 ft (2.0 m) from the examination table for most scan modes
- Operating environmental temperature: 60–90°F (15–32°C)
- Operating environmental relative humidity: 20–80%, non-condensing
- X-ray source: Switched pulse, dual energy, 140 V peak
- X-ray beam geometry: Fan-beam
- Detectors: Multi-element detector array
- Scan path: Linear
- Quality control: Self calibrating with patented Hologic Automatic Internal Reference System and automated quality control program
- Operation: IBM-compatible Pentium computer with Windows operating system, 17 in. monitor, HP DeskJet® printer
- Accessories provided: Anthropomorphic spine phantom
- Options: Magneto optical disk storage; network configuration; HP LaserJet® B&W printer

QDR®4500 SL

- Manufacturer: Hologic, Inc., Bedford, MA.
- Technology: Dual-energy X-ray absorptiometry
- Skeletal application(s):

  - – PA spine
  - – Proximal femur
  - – Forearm
  - – Supine lateral lumbar spine

- Scan time (in the 60 Hz scan mode):

  - PA lumbar spine and proximal femur 10 seconds
  - Lateral spine 120 seconds
  - Forearm 30 seconds
  - Lateral imaging with MXA 7.5 seconds

- Results:

  - BMD (g/cm^2)
  - BMC (g)
  - Area (cm^2)
  - % Youngadult and % age-matched comparisons
  - T-score and z-score
  - sBMD (mg/cm^2) for L2–L4 and total hip
  - NHANES III total hip comparisons

- Precision: $< 1\%$
- Radiation dose (in the 60 Hz scan mode):

  - PA lumbar spine 7 mR
  - Proximal femur 7 mR
  - Lateral spine 35 mR
  - Forearm 5 mR
  - Lateral imaging with MXA 7 mR

- Dimensions: 79.5 in. $\times$ 41 in. $\times$ 28 in. (202 cm $\times$ 104 cm $\times$ 71 cm), 79.5 in. $\times$ 57 in. (202 cm $\times$ 145 cm) with C-arm rotated and table extended
- Weight: 800 lb (364 kg)
- Recommended dedicated floor space: 8 ft $\times$ 8 ft (2.4 m $\times$ 2.4 m)
- Scatter radiation: Less than 1.0 mR/hr (0.01 mSv/hr) measured at 6.6 ft (2.0 m) from the examination table for most scan modes
- Operating environmental temperature: 60–90°F (15–32°C)
- Operating environmental relative humidity: 20–80%
- X-ray source: Switched pulse, dual-energy
- X-ray beam geometry: Fan-beam
- Detectors: Multi-element detector array
- Scan path: Linear
- Quality control: Self calibrating with patented Hologic Automatic Internal Reference System and automated quality control program
- Operation: IBM-compatible Pentium computer with Windows operating system, 17 in. monitor, HP DeskJet® printer
- Accessories provided: Anthropomorphic spine phantom
- Options: Magneto optical disk storage; network configurations; HP LaserJet® B&W printer; MXA software

QDR® 4500 W

- Manufacturer: Hologic, Inc., Bedford, MA.
- Technology: Dual-energy X-ray absorptiometry
- Skeletal regions studied:

    – PA spine
    – Proximal femur
    – Forearm
    – Whole body

- Scan time (in the 60 Hz scan mode):

    – PA lumbar spine and proximal femur 15 seconds
    – Forearm 30 seconds
    – Whole body 6.8 minutes

- Results:

    – BMD (g/cm^2)
    – BMC (g)
    – Area (cm^2)
    – % Young-adult and % age-matched comparisons
    – T-score and z-score
    – sBMD (mg/cm^2) for L2–L4 and total hip
    – NHANES III total hip comparisons

- Precision: < 1%
- Radiation dose (in the 60 Hz scan mode):

    – PA lumbar spine 5 mR
    – Proximal femur 5 mR
    – Forearm 10 mR
    – Whole body 1.5 mR

- Dimensions: 79.5 in. × 48 in. × 28 in. (202 cm × 122 cm × 71 cm), 118.9 in. × 59 in. × 28 in. (302 cm × 150 cm × 71 cm) with table extended
- Weight: 680 lb (310 kg)
- Recommended dedicated floor space: 8 ft × 10 ft (2.4 m × 3.1 m)
- Scatter radiation: Less than 1.0 mR/hr (0.01 mSv/hr) measured at 6.6 ft (2.0 m) from the examination table for most scan modes
- Operating environmental temperature: 60–90°F (15–32°C)
- Operating environmental relative humidity: 20–80%
- X-ray source: Switched pulse, dual-energy
- X-ray beam geometry: Fan-beam
- Detectors: Multi-element detector array
- Scan path: Linear
- Quality control: Self-calibrating with patented Hologic Automatic Internal Reference System and automated quality control program

- Operation: IBM-compatible Pentium computer with Windows operating system, 17 in. monitor, HP DeskJet® printer
- Accessories provided: Anthropomorphic spine phantom
- Options: Magneto optical disk storage; network configurations; HP LaserJet® B&W printer; body composition analysis software

XR-46™

- Manufacturer: CooperSurgical Norland, Trumball, CT
- Technology: Dual-energy X-ray absorptiometry
- Skeletal regions studied:

    – PA spine
    – Lateral spine
    – Proximal femur
    – Forearm
    – Whole body with soft tissue composition

- Scan time:

    – PA spine <1.5 minutes
    – Hip < 2 minutes
    – Forearm < 3 minutes
    – Lateral spine < 4 minutes
    – Whole body 5 minutes

- Results:

    – BMD (g/cm^2)
    – BMC (g)
    – % Young-reference and % age-matched comparisons
    – T-score and z-score
    – sBMD (mg/cm^2) for L2–L4 and Total hip based on NHANES III reference data

- Precision:

    – PA spine 1.0%
    – Hip 1.2%
    – Forearm 0.8%
    – Lateral spine 2.4%
    – Whole body BMD 1%.

- Radiation dose:

    – PA spine, hip, and forearm < 1.0 mrem
    – Lateral spine <5 mrem
    – Whole body < 0.1 mrem

- Dimensions: 103 in. × 48 in. × 51 in. (261.6 cm × 122.0 cm × 129.5 cm)
- Weight: 556.5 lbs (252.4 kg)
- Recommended dedicated floor space: 10 ft × 7 ft (3.1 m × 2.1 m)

- Operating environmental temperatures: 60–90°F (15–32°C)
- Operating environmental relative humidity: Up to 80%, non-condensing
- X-ray source: 100 kV, 1.3 mA
- X-ray filtration: 8-level automated samarium
- X-ray beam geometry: Pencil-beam
- Detectors: 2 NaI detectors
- Scan path: Rectilinear
- Quality control: Automatic with supplied calibration standard and QC phantom
- Operation: IBM-compatible computer, Windows software
- Accessories provided:

    – 77-step calibration standard
    – QC phantom
    – PA spine-positioning block
    – Hip sling with foot separator
    – Lateral spine positioner
    – Forearm positioner

- Options: Lateral spine, forearm, soft tissue composition, research, and small subject software

Fig. 15-15. The Norland XR-46™. Photograph courtesy of Norland, a CooperSurgical Company, Ft. Atkinson, WI.

XR-600™

- Manufacturer: CooperSurgical Norland, Trumball, CT
- Technology: Dual-energy X-ray absorptiometry
- Skeletal regions studied:

    – PA spine
    – Left and right proximal femur
    – Optional forearm

- Scan time:

  - PA spine ˜1 minute
  - Hip 1.5 minutes
  - Forearm 3 minutes

- Results:

  - BMD (g/cm^2)
  - BMC (g)
  - % Young-reference and % age-matched comparisons
  - T-score and *z*-score
  - NHANES III proximal femur reference data

- Precision:

  - PA spine 1.0%
  - Proximal femur 1.4%
  - Forearm 0.8%

- Radiation dose:

  - PA spine 3μSv
  - Proximal femur <15 μSv
  - Forearm <15 μSv

- Dimensions: 72 in. × 48 in. × 49 in. (182.8 cm × 122.0 cm × 124.5 cm)
- Weight: 400 lbs (181 kg)
- Recommended dedicated floor space: 7 ft × 7 ft (2.1 m × 2.1 m)
- Operating environmental temperatures: 60–90°F (15–32°C)
- Operating environmental relative humidity: Up to 80%, non-condensing
- X-ray source: 100 kV, 1.3 mA
- X-ray filtration: 8-level automated samarium
- X-ray beam geometry: Pencil-beam
- Detectors: Two NaI detectors
- Scan path: Rectilinear
- Quality control: Automatic with supplied calibration standard and QC phantom; auto-mated Shewhart Chart analysis to confirm absolute and trending performance
- Operation: IBM-compatible computer, Windows software
- Accessories provided:

  - 77-step calibration standard
  - QC phantom
  - PA spine-positioning block
  - Hip sling with foot separator
  - Forearm positioner

- Options: Research and small subject software

Fig. 15-16. The Norland XR-600™. Photograph courtesy of Norland, a CooperSurgical Company, Ft. Atkinson, WI.

XR-800™

- Manufacturer: CooperSurgical Norland, Trumball, CT
- Technology: Dual-energy X-ray absorptiometry
- Skeletal regions studied:

    - PA Spine
    - Right and left proximal femur
    - Forearm
    - Whole body with soft tissue composition

- Scan time:

    - PA spine ˜1 minute
    - Proximal femur 1.5 minutes
    - Forearm 3 minutes
    - Whole body 5 minutes

- Results:

    - BMD (g/cm^2)
    - BMC (g)
    - % Young-reference and % age-matched comparisons
    - T-score and z-score
    - NHANES III proximal femur reference data

- Precision:

    - PA spine 1.0%
    - Proximal femur 1.4%
    - Forearm 0.8%
    - Whole Body BMD 0.08%.

- Radiation dose:

    – PA spine 3μSv
    – Proximal femur <1.5μSv
    – Forearm μSv
    – Whole body 0.2μSv

- Dimensions: 103 in. × 48 in. × 51 in. (261.6 cm × 122.0 cm × 129.5 cm)
- Weight: 560 lbs (253 kg)
- Recommended dedicated floor space: 10 ft × 7 ft (3.1 m × 2.1 m)
- Operating environmental temperatures: 60–90°F (15–32°C)
- Operating environmental relative humidity: Up to 80%, non-condensing
- X-ray source: 100 kV, 1.3 mA
- X-ray filtration: 8-level automated samarium
- X-ray beam geometry: Pencil-beam
- Detectors: Two NaI detectors
- Scan path: Rectilinear
- Quality control: Automatic with supplied calibration standard and QC phantom; automated Shewhart Chart analysis to confirm absolute and trending performance
- Operation: IBM-compatible computer, Windows software
- Accessories provided:

    – 77-step calibration standard
    – QC phantom
    – PA spine-positioning block
    – Hip sling with foot separator
    – Forearm positioner

- Options: Research and small subject software

Fig. 15-17. The Norland XR-800™. Photograph courtesy of Norland, a CooperSurgical Company, Ft. Atkinson, WI.

PERIPHERAL X-RAY DENSITOMETERS

accuDEXA® Bone Mineral Density Assessment System

- Manufacturer: Lone Oak Medical Technologies (now managing Schick Technologies), Doylestown, PA.
- Technology: Dual-energy X-ray absorptiometry
- Skeletal application(s): Middle phalanx of the long finger
- Scan time: <1 minute
- Results:

    – BMD (g/cm^2)
    – % Young-adult and % age-matched comparisons
    – T-score and z-score
    – Diagnostic classification based on WHO criteria

- Precision: < 1%
- Radiation dose: 0.0003 μSv
- Dimensions: 14 in. × 15 in. × 14 in. (35.56 cm × 38.1 cm × 35.56 cm)
- Weight: 66 lbs (29.7 kg)
- Environmental operating temperature: 70–85°F (21–29°C)
- Environmental operating relative humidity: 20–80%
- X-ray Source:

    – Low energy 50 kVp, 0.5 mA
    – High energy 70 kVp, 0.9 mA

- X-ray filtration (High energy only): zinc
- Scatter radiation: 6.1 mR/hr at 1 m
- Quality control: Automatic, no user intervention required.
- Operation: Data input with touch pad on the device, data output with printer supplied by user (list of compatible printers available from manufacturer)

Apollo™

- Manufacturer: CooperSurgical Norland, Trumball, CT
- Technology: Dual-energy X-ray absorptiometry
- Skeletal application(s): calcaneus.
- Scan time: 15 seconds.
- Results:

    – BMD (g/cm^2)
    – BMC (g)
    – Area (cm^2)
    – % Young-reference and % age-matched comparisons
    – T-score and z-score
    – Fracture risk based on WHO diagnostic classification

- Precision: 1.8%
- Radiation dose: < 0.2 mrem

Fig. 15-18. The Lone Oak Medical Technologies accuDEXA™. A peripheral dual-energy X-ray absorptiometer. Photograph courtesy of Lone Oak Medical Technologies, Doylestown, PA.

- Dimensions: 22.5 in. × 17.5 in. × 14 in. (57.2 cm × 44.5 cm × 35.6 cm)
- Weight: 64 lbs (29 kg)
- Operating environmental temperature: 50–90°F (10–32°C)
- Operating environmental relative humidity: 20–95%, non-condensing
- X-ray source: 60 kV, < 0.3 mA
- X-ray filtration: Tin
- Detectors: Two solid state
- Quality control: Automatic with internal phantoms requiring < 5 minutes
- Operation: Hand-held console with fluorescent display. Unit on wheels with retractable handle. Built in floppy disc drive for data transfer. Built in parallel printer port for Canon BJC color printer or equivalent
- Options: Laptop configuration

DexaCare® G4

- Manufacturer: Osteometer MediTech, Inc., Hawthorne, CA.
- Distributed by CompuMed, Inc., Los Angeles, CA.
- Technology: Dual-energy X-ray absorptiometry
- Skeletal application(s): Forearm (ultra-distal, 8 mm distal, one-fourth distal)
- Scan time: 2 minutes, distal forearm
- Results:

    - BMD (g/cm^2)
    - BMC (g), area (cm^2)
    - % Young-adult and % age-matched comparisons
    - T-score and *z*-score

Fig. 15-19. The Norland Apollo[TM]. A peripheral dual-energy X-ray absorptiometer. Photograph courtesy of Norland, a CooperSurgical Company, Ft. Atkinson, WI.

- Precision: <1%
- Radiation dose: 0.1 μSv per scan
- Dimensions: 12.5 in. × 26 in. × 15.5 in. (32 cm × 66 cm × 40 cm)
- Weight: 49 lbs (22 kg)
- Environmental operating temperature: 58–86°F (15–30°C)
- X-ray source: 55 kV, 300 μA
- X-ray filtration: K-edge filtration
- Detectors: Solid state
- Imaging resolution: 0.4 mm × 0.4 mm
- Scatter radiation: < 0.25 μSv/hr at 1 m
- Calibration system: Line by line internal reference calibration
- Operation: IBM-compatible computer, printer

DTX-200 DexaCare®

- Manufacturer: Osteometer MediTech, Inc., Hawthorne, CA.
- Distributed by CompuMed, Inc., Los Angeles, CA., as the OsteoCare[TM] System
- Technology: Dual-energy X-ray absorptiometry
- Skeletal application(s): Forearm (ultra-distal, 8 mm distal, one-fourth distal)
- Scan time: Two minutes
- Results:

    – BMD (g/cm^2)
    – BMC (g), area (cm^2)

Fig. 15-20. The Osteometer DexaCare® G4. A peripheral dual-energy X-ray absorptiometer. Photograph courtesy of Osteometer MediTech, Hawthorne, CA.

Fig. 15-21. The Osteometer DexaCare® G4. A peripheral dual-energy X-ray absorptiometer. The forearm is placed into the well on the top of the machine. Photograph courtesy of Osteometer MediTech, Hawthorne, CA.

  –   % Young-adult and % age-matched comparisons
  –   T-score and *z*-score

- Precision: <1%
- Radiation dose: 0.1 μSv per scan
- Dimensions: 31 in. × 23 in. × 11 in. (79 cm × 59 cm × 28 cm)
- Weight: 114 lbs (52 kg)
- Environmental operating temperature: 58–86°F (15–30°C)
- X-ray source: 55 kV, 300 μA
- X-ray filtration: Tin, K-edge filtration
- Detectors: Solid state
- Imaging resolution: 0.4 mm × 0.4 mm
- Scatter radiation: < 0.25 μSv/hr at 1 m
- Quality control: Automated with forearm phantom supplied by manufacturer
- Operation: IBM-compatible computer, printer, unit on wheels for easy mobility

Fig. 15-22. The Osteometer DTX-200 DexaCare®. A peripheral dual-energy X-ray absorptiometer. Photograph courtesy of Osteometer MediTech, Hawthorne, CA.

Fig. 15-23. The Osteometer DTX-200 DexaCare®. A peripheral dual-energy X-ray absorptiometer. The forearm is placed into the well in the top of the machine. Photograph courtesy of Osteometer MediTech, Hawthorne, CA.

pDEXA ®

- Manufacturer: CooperSurgical Norland, Trumball, CT
- Technology: Dual-energy X-ray absorptiometry
- Skeletal application(s): Forearm
- Scan time: <5 minutes
- Results:

    – BMD (g/cm^2)
    – BMC (g)
    – area (cm^2)
    – % Young-reference and % age-matched comparisons
    – T-score and *z*-score

- Precision: <2.0%
- Radiation dose: <1.5 mrem at high speed
- Dimensions: 20.5 in. × 17 in. × 16.7 in. (52 cm × 43 cm × 42.5 cm)
- Weight: 59.4 lbs (27 kg)
- Environmental operating temperature: 60–82°F (15–28°C)
- Environmental operating relative humidity: Up to 80%, non-condensing
- X-ray source: 60 kV, <0.3 mA
- X-ray filtration: Tin
- Detectors: Two solid state
- Quality control: Automatic with manufacturer supplied calibration standard and QC phantom

- Operation: IBM-compatible laptop computer with Windows operating system, HP DeskJet printer and mouse.
- Options: IBM-compatible desktop computer with Windows operating system, 15 in. SVGA monitor, 15 in. flat panel display, 17 in. SVGA monitor, HP DeskJet

Fig. 15-24. The Norland pDEXA®. A peripheral dual-energy X-ray absorptiometer. Photograph courtesy of Norland, a CooperSurgical Company, Ft. Atkinson, WI.

PIXI® (Peripheral Instantaneous X-ray Imager)

- Manufacturer: GE Healthcare, Madison, WI.
- Technology: Dual-energy X-ray absorptiometry
- Skeletal application(s): Calcaneus, forearm
- Scan time: 5 seconds
- Results:

    – BMD (g/cm^2)
    – % Young-adult and % Age-matched comparisons
    – T-score and z-score

- Precision: <1.5%
- Radiation dose: 0.032 μSv
- Dimensions: 12 in. × 25 in. × 13 in. (30 cm × 63 cm × 33 cm)
- Weight: 66 lb (<30 kg)
- Environmental operating temperature: 64–81°F (18–27°C)
- X-ray source: Cone-beam geometry, 250 μA current
- Image resolution: 0.2 × 0.2 mm
- Quality control: Aluminum os calcis and forearm phantoms supplied by the manufacturer

- Operation: Laptop computer, printer
- Options: Portable color printer, reusable hard shipping case, soft-sided portability case, and cart

Fig. 15-25. The Lunar PIXI®. A peripheral dual-energy X-ray absorptiometer shown here in the configuration used to measure bone density in the calcaneus. The device can be re-configured and used to measure bone density in the forearm. Photograph courtesy of GE Healthcare, Madison, WI.

XCT 2000L[TM]

- Manufacturer: Stratec Medizintechnik, Pforzheim, Germany
- Distributor: Orthometrix, Inc., White Plains, NY
- Technology: Computerized tomography
- Skeletal application(s): Forearm
- Scan time: 90 seconds
- Results: BMD (mg/cm^3) for total bone and trabecular and cortical compartments
- Precision: ± 3 mg/cm^3 for trabecular bone; ± 9 mg/cm^3 for cortical bone
- Radiation dose: 0.03 mSv per scan
- Dimensions: 21.7 in. $\times$ 45.3 in. $\times$ 24.4 in. (55 cm $\times$ 115 cm $\times$ 62 cm)
- Weight: 143 lbs (65 kg)
- X-ray source: 58 kV, 180 μA (nominal)
- Detectors: 12 semiconductor detectors with amplifiers

- Operation: Pentium computer, monitor, and color printer
- Options: Magneto opticals for data backup
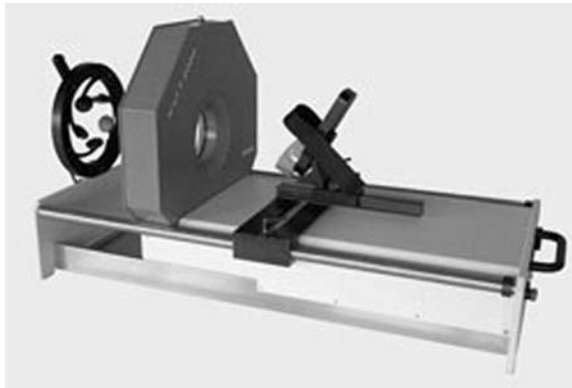
Fig. 15-26. The Stratec XCT 2000L^{TM}. A peripheral quantitative computed tomography device. Photograph courtesy of Orthometrix, Inc., White Plains, NY.

XCT 3000^{TM}

- Manufacturer: Stratec Medizintechnik, Pforzheim, Germany
- Distributor: Orthometrix, Inc., White Plains, NY
- Technology: Computerized tomography
- Skeletal application(s): Femur, tibia, forearm, mandible
- Scan time: 8 sec/step
- Results: BMD (mg/cm^3) for total bone and trabecular and cortical compartments; axial SSI, polar SSI
- Precision: < 1%
- Radiation dose: 1 mSv per scan
- Dimensions: 21.7 in. × 45.3 in. × 24.4 in. (55 cm × 115 cm × 62 cm)
- Path length for chair: 31.5 in. (80 cm)
- Weight: 176 lbs (80 kg)
- Operating temperature: 54–86°F (12–30°C)
- Operating humidity: 20–80% non-condensing
- X-ray source: 60 kV, 0.2–0.4 mA
- Detectors: 12 semiconductor detectors with amplifiers
- Operation: Pentium computer, DOS compatible; Windows, Unix, optional

ULTRASOUND BONE DENSITOMETERS

Achilles+^{TM}

- Manufacturer: GE Healthcare, Madison, WI.
- Technology:
    - Ultrasound
    - Transmitted through bone
    - Wet

Fig. 15-27. The Stratec XCT 3000™. A peripheral quantitative computed tomography device. Photograph courtesy of Orthometrix, Inc., White Plains, NY.

- Skeletal application(s): Calcaneus
- Scan time: 1 minute
- Results:

    - SOS (m/sec)
    - BUA (db/MHz)
    - Stiffness Index
    - % Young-adult and % age-matched comparisons
    - T-score and *z*-score

- Precision: 2.0% for Stiffness™ Index
- Dimensions: 20 in. × 13 in. × 24 in. (51 cm × 33 cm × 61 cm)
- Weight: 44 lbs (20 kg)
- Operating environmental temperature: 59–95°F (15–35°C)
- Operating environmental relative humidity: 20–80%
- Operation: Self-contained LCD touch screen, thermal printer, 50-measurement memory, built-in carrying handle
- Accessories provided:

    - Water-soluble ultrasonic gel
    - Premeasured surfactant

- Options: Laptop computer, external printer

Fig. 15-28. The Lunar Achilles+™. A peripheral quantitative ultrasound device shown here in the closed position. Photograph courtesy of GE Healthcare, Madison, WI.

Fig. 15-29. The Lunar Achilles+™. A peripheral quantitative ultrasound device shown here in use. Photograph courtesy of GE Healthcare, Madison, WI.

Achilles Express™

- Manufacturer: GE Healthcare, Madison, WI.
- Technology:

    - Ultrasound
    - Transmitted through bone
    - Dry

- Skeletal application(s): Calcaneus
- Scan time: 1 minute
- Results:

    - Stiffness Index
    - % Young-adult and % age-matched comparisons
    - T-score and *z*-scoree

- Precision: 2.0%
- Dimensions: 10 in. × 12 in. × 24 in. (25 cm × 31 cm × 61 cm)
- Weight: 22 lbs (10 kg)
- Operating environmental temperature: 59–95°F (15–35°C)
- Operating environmental relative humidity: 20–80%
- Operation: Self-contained LCD touch screen that swivels, thermal printer, 100 measurement memory; built-in carrying handle
- Accessories: Water-soluble ultrasonic gel

Fig. 15-30. The Lunar Achilles Express™. A peripheral quantitative ultrasound device. Photograph courtesy of GE Healthcare, Madison, WI.

Achilles InSight^{TM}

- Manufacturer: GE Healthcare, Madison, WI.
- Technology:

    – Ultrasound
    – Transmitted through bone
    – Dry

- Skeletal application(s): Calcaneus
- Scan time: 15 seconds
- Results:

    – Stiffness Index
    – % Young-adult and % age-matched comparisons
    – T-score and *z*-score
    – WHO classification
    – Heel image
    – Reference graph

- Precision: <2.0% CV
- Dimensions: 10 in. × 12 in. × 24 in. (25 cm × 31 cm × 61 cm)
- Weight: 22 lbs (10 kg)
- Operating environmental temperature: 59–95°F (15–35°C)
- Operation: Self-contained LCD touch screen that swivels, thermal printer, 100-measurement memory; built-in carrying handle. No gel required.
- Options: External computer, external color printer, Windows® XP user interface; external PC software

Fig. 15-31. The Lunar InSight^{TM}. A peripheral quantitative ultrasound device. Photograph courtesy of GE Healthcare, Madison, WI.

Fig. 15-32. The Lunar InSight™. A peripheral quantitative ultrasound device shown in use. Photograph courtesy of GE Healthcare, Madison, WI.

DTU-one UltraSure®

- Osteometer MediTech, Inc., Hawthorne, CA.
- Technology:
    - Imaging ultrasound
    - Transmitted through bone
    - Wet
- Skeletal application(s): Calcaneus
- Scan time: 3 minutes
- Results:
    - SOS (m/sec)
    - BUA (dB/MHz)
    - % Young-adult and % age-matched comparisons
    - T-score and *z*-score
- Precision:
    - SOS 0.2% (in vivo)
    - BUA 1.6% (in vivo)
- Dimensions: 21 in. × 11 in. × 17 in. (53 cm × 28 cm × 44 cm)
- Weight: 64 lbs (29 kg)
- Environmental operating temperature: 59–86°F (15–30°C)
- Image resolution: 0.6 mm
- Quality control: Automated with supplied phantom
- Operation: IBM-compatible computer with Windows operating system, monitor, printer
- Accessories provided: Phantom

Fig. 15-33. The Osteometer DTU-one Ultrasure®. A peripheral quantitative ultrasound device. Photograph courtesy of Osteometer MediTech, Hawthorne, CA.

Fig. 15-34. The Osteometer DTU-one Ultrasure®. A peripheral quantitative ultrasound device. Shown here in use. Photograph courtesy of Osteometer MediTech, Hawthorne, CA.

McCue C.U.B.A.Clinical^{TM}(Contact Ultrasound Bone Analyzer)

- Distributor: CooperSurgical Norland, Trumball, CT
- Technology:

  – Ultrasound
  – Transmitted through bone
  – Dry

- Skeletal application(s): Calcaneus
- Scan time: 1 minute
- Results:

  – BUA in db/MHz
  – % Young-reference and % age-matched comparisons
  – T-score and *z*-score

- Precision: 1.3% for BUA
- Dimensions: 17.8 in. × 13.9 in. × 10.2 in. (45.2 cm × 35.3 cm × 25.9 cm)
- Weight: 22 lb (10 kg)
- Environmental storage temperature: 23–122°F (–5–50°C)
- Environmental storage humidity: 10–95%
- Quality control: Internal phantom and external QA phantom
- Operation: Handheld controller or IBM-compatible computer with a minimum of 10 MB free hard drive space, 486DX2 microprocessor at 66 MHz, 1.44 MB floppy disc drive, serial port, Windows 3.1 or higher (Windows NT not supported) and Microsoft® Windows^{TM} supported printer (desktop or laptop computer equipment supplied by end user)
- Accessories provided:

  – Padded carrying bag for C.U.B.A.
  – Padded carrying bag for QA phantom, QA phantom
  – Bottle of ultrasound gel
  – Two anatomical foot inserts
  – C.U.B.A. plus+ software
  – Serial cable
  – Power cable
  – User's manual

Omnisense® 7000S Ultrasound Bone Sonometer

- Manufacturer: Sunlight Medical, Israel
- Technology:

  – Ultrasound
  – Axially transmitted along bone using Omnipath® technology
  – Dry

- Skeletal application(s): Distal one-third radius, proximal phalanx of the long finger, fifth metatarsal, tibial mid-shaft

Fig. 15-35. The McCue C.U.B.A. Clinical™. A peripheral quantitative ultrasound device. Photograph courtesy of Norland, a CooperSurgical Company, Ft. Atkinson, WI.

- Scan time: < 1 minute per site
- Results:

    – SOS (m/sec),
    – T-score and *z*-score

- Precision: 0.4% to 0.81% as the RMS %CV, depending upon the site
- Main unit dimensions: 15.4 in. × 5.1 in. × 13 in. (39 cm × 13 cm × 33 cm)
- Main unit weight: ~15 lbs (~7 kg)
- Quality control: Calibration free. Daily system verification with phantom required.
- Operation: Desktop PC with Windows XP interface, flat panel display, mouse or trackball, printer

Omnisense® 8000S Ultrasound Bone Sonometer

- Manufacturer: Sunlight Medical, Israel
- Technology:

    – Ultrasound
    – Axially transmitted along bone using Omnipath® technology
    – Dry

- Skeletal application(s): Distal one-third radius, proximal phalanx of the long finger, fifth metatarsal, tibial mid-shaft
- Scan time: < 1 minute
- Results:

    – SOS (m/sec),
    – T-score and *z*-score

Fig. 15-36. The Sunlight Omnisense™ 7000S. A peripheral quantitative ultrasound device. Photograph courtesy of Sunlight Medical Ltd., Rehovot, Israel.

Fig. 15-37. The Sunlight Omnisense™ 7000S. A peripheral quantitative ultrasound device. Shown here in use. Photograph courtesy of Sunlight Medical Ltd., Rehovot, Israel.

- Precision: 0.4–0.8% as the RMS %CV, depending upon the site
- Main unit dimensions: 14.8 in. × 5.4 in. × 11.2 in. (37.5 cm × 13.6 cm × 28.5 cm)
- Main unit weight: ∼14.3 lbs (∼6.5 kg)
- Operation: PC with Windows interface, printer; portable
- Accessories provided:

  – Soft carrying case

Sahara Clinical Bone Sonometer®

- Manufacturer: Hologic, Inc., Bedford, MA.
- Technology:

  – Ultrasound
  – Transmitted through bone
  – Dry

- Skeletal application(s): Calcaneus
- Scan time: < 10 seconds
- Results:

  – Estimated BMD (g/cm^2)
  – Quantitative Ultrasound Index (QUI) obtained from BUA and SOS
  – T-score and *z*-score

- Precision:

  – BMD 3% or 0.014 g/cm^2
  – QUI 2.6% or 2.2

- Dimensions: 17 in. × 14 in. × 12 in. (43 cm × 36 cm × 30 cm)
- Weight: 22 lbs (10 kg)
- Environmental operating temperature: 60–100°F (15–37.7°C)
- Environmental operating relative humidity: 20–80%, non-condensing
- Quality control: Daily, with supplied QC phantom
- Operation: Embedded microprocessor. Data and command input from touch pad on unit. Built-in strip printer.
- Accessories provided:

  – QC phantom
  – Sahara coupling gel
  – Alcohol wipes
  – Patient report forms
  – Operator training video

- Options

  – Carrying case
  – AC power cable
  – Spare battery

Fig. 15-38. The Hologic Sahara Clinical Bone Sonometer®. A peripheral quantitative ultrasound device. Photograph courtesy of Hologic, Inc., Bedford, MA.

Fig. 15-39. The Hologic Sahara Clinical Bone Sonometer®. A peripheral quantitative ultrasound device shown here in use. Photograph courtesy of Hologic, Inc., Bedford, MA.

16 Appendices

CONTENTS

I   **Appendix**

*Contact Information for Bone Densitometry
Manufacturers and Organizations of Interest*

MANUFACTURERS

The products listed by manufacturers refer to the products discussed in Chapter 15 but do not necessarily represent the entire line of densitometers available from the manufacturer. Every effort has been made to provide accurate and current contact information, but contact information is subject to change without notice.

Alara, Inc.

47505 Seabridge Drive   Web site: www.alara.com
Fremont, CA 94538-6546   Email: through website
Tel.: 800-410-2525
Fax: 510-315-5201

Product: MetriScan^{TM}

BeamMed Ltd. (Sunlight) Headquarters

8 Halapid St.   Web site: www.sunlightnet.com
P O Box 7520   Email: info@beammed.com
Petach Tikva 49170   Email: info@sunlightnet.com
Israel
Tel.: 972-3-923-6869 (technical
    support)
Fax.: 972-3-923-6867

Products: Sunlight Omnisense^{TM} 7000S, Sunlight Omnisense^{TM} 8000S

CompuMed, Inc.

5777 W. Century Blvd., Suite 360   Website: www.compumed.net
Los Angeles, CA 90045 US   Website: www.osteogram.com
Tel.: 310-258-5000   Email: osteocare@compumed.net
Fax: 310-645-5880   Email: osteogram@compumed.net

Products: Automated Osteogram® add-on software; distributor for the OsteoCare^{TM} system (Osteometer DexaCare® DTX-200) and the Osteometer DexaCare® G4

CooperSurgical, Norland

95 Corporate Drive
Trumball, CT 06611
Phone: 203-601-5200 (Corporate)
Fax: 203-601-1007 (Corporate)
Phone: 800-243-2974 (Customer
  Service)
Fax: 800-262-0105 (Customer Service)

Toll free: 800-645-3760 (Corporate)
Website: www.coopersurgical.com
Email: e-mail@coopersurgical.com
  (US)
Email: intl@coopersurgical.com
  (International)

Products: XR-46^{TM}, Excell^{TM}, Excell^{TM} plus, Apollo^{TM}, XR-600^{TM}, XR-800^{TM}, pDEXA$^{®}$, McCue C.U.B.A. Clinical^{TM}

GE Healthcare, Lunar

726 Heartland Trail
Madison, WI 53717-1915, US
Tel.: 608-828-2663
Fax: 608-826-7106

Toll free tel.: 1-888-795-8627
Website: www.gemedicalsystems.com
Email: through website

Products: EXPERT$^{®}$-XL, DPX Bravo$^{®}$, DPX Duo$^{®}$, DPX-IQ^{TM}, DPX MD^{TM}, DPX MD+^{TM}, DPX- NT^{TM}, DPX Pro^{TM}, Prodigy^{TM}, iDXA^{TM}, Achilles+^{TM}, Achilles Express^{TM}, Achilles Insight^{TM}, PIXI$^{®}$

Hologic, Inc.

35 Crosby Drive
Bedford, MA 01730-1401
Tel.: 781-999-7300
Tel.: 800-321-HOLX
Fax: 781-280-0669

Toll free tel.: 800-343-XRAY
Website: www.hologic.com
Customer support
Email: support@hologic.com

Products: QDR$^{®}$ 4500 A, QDR$^{®}$ 4500 C, QDR$^{®}$ 4500 SL, QDR$^{®}$ 4500 W, Delphi^{TM}, Discovery^{TM}, Explorer^{TM}, Sahara Clinical Bone Sonometer$^{®}$

Image Analysis, Inc.

1380 Burkesville Street
Columbia, KY 42728
Phone: 270-384-6400
Fax: 270-384-6405

Web site: www.n-vivo.com
Email: info@image-analysis.com

Products: QCT 3-D Plus software

Lone Oak Medical Technologies

3805 Old Easton Road
Doylestown, PA 18902
Phone: 888-818-4263
Phone: 215-230-7607
Fax: 215-230-7609

Website: www.loneoakmedical.com
Email: info@loneoakmedical.com

Product: accuDEXA® Bone Mineral Density Assessment System

Orthometrix, Inc.

106 Corporate Park Drive, Suite 102
White Plains, NY 10604
Tel.: (914) 694-2285
Fax: (914) 694-2286

Toll free: (877) 249-4229
Website: www.orthometrix.net
Email: info@orthometrix.net

Products: Distributor in North America of the Stratec XCT 2000L^{TM} and 3000^{TM}

Osteometer MediTech, Inc.

12515 Chadron Ave.
Hawthorne, CA 90250
Tel.: 310 978-3073
Fax: 310 676-0948

Toll free tel.: 866-421-7762
Website: www.osteometer.com
Email: info@osteometer.com

Products: DTX-200 DexaCare®, DTU-one Ultrasure^{TM}, DexaCare®G4

Sectra North America, Inc.

2 Corporate Drive, Suite 248
Shelton, CT 06484
Tel.: 203-925-0899
Fax: 203-925-0906

Web site: www.dxr-online.com
Email: dxr@dxr-online.com

Products: dxr-online^{TM}

Sectra Imtec AB

Teknikringen 20
SE-583 30 Linköping, Sweden
Tel.: 46 13 23 52 00
Fax.: 46 13 21 21 85

Web site: www.dxr-online.com
Email: dxr@dxr-online.com

Product: dxr-online^{TM}

Stratec Medizintechnik

Durlacher Strasse 35   Website: www.stratec-med.com
D-75172 Pforzheim   Email: info@stratec-med.com
Germany
Tel.: 49 (0) 7231 145420
Fax: 49 (0) 7231 145422

Products: XCT^{TM} 2000L, XCT 3000^{TM}

Wallach Surgical Devices, Inc.

235 Edison Road   Website: www.sunlightnet.com
Orange, CT 06477   Website: www.wallachsurgical.com
Tel: 800-243-2463   Email: wallach@wallachsurgical.com
Tel: 203-799-2000 (outside US)
Fax: 203-799-2002

Products: Distributors in the United States for Sunlight Omnisense^{TM} 7000S, Omnisense^{TM} 8000S

ORGANIZATIONS OF INTEREST

American Society of Radiologic Technologists

15000 Central Avenue, S.E.   Toll free: 800-444-2778
Albuquerque, NM 87123-3909   Website: www.asrt.org
Fax: 505-298-5063   Email: customerinfo@asrt.org

Foundation for Osteoporosis Education and Research

300 27th Street, Suite 103   Website: www.fore.org
Oakland, CA 94612   Email: info@fore.org
Tel.: (510) 832-2663
Fax: (510) 208-7174

International Society for Clinical Densitometry

342 North Main Street   Website: www.iscd.org
West Hartford, CT 06117-2507   Email: iscd@iscd.org
Tel.: 860-586-7563
Fax: 860-586-7550

National Osteoporosis Foundation

1232 22nd St., N.W.   Toll free: 800-231-4222
Washington, DC 20037-1202   Website: www.nof.org
Tel.: 202-223-2226   Email: through website

II Appendix

Conversion Formulas

PA SPINE CONVERSIONS BETWEEN CENTRAL DXA DEVICES[1] (1)

$$\text{Hologic QDR-2000 Spine}_{BMD} = (0.906 \times \text{Lunar DPX-L Spine}_{BMD}) - 0.025$$

$$\text{Hologic QDR-2000 Spine}_{BMD} = (0.912 \times \text{Norland XR-26 Spine}_{BMD}) + 0.088$$

$$\text{Lunar DPX-L Spine}_{BMD} = (1.074 \times \text{Hologic QDR-2000 Spine}_{BMD}) + 0.054$$

$$\text{Lunar DPX-L Spine}_{BMD} = (0.995 \times \text{Norland XR-26 Spine}_{BMD}) + 0.135$$

$$\text{Norland XR-26 Spine}_{BMD} = (0.983 \times \text{Lunar DPX-L Spine}_{BMD}) - 0.112$$

$$\text{Norland XR-26 Spine}_{BMD} = (1.068 \times \text{Hologic QDR-2000 Spine}_{BMD}) - 0.070$$

FEMORAL NECK BMD CONVERSIONS BETWEEN CENTRAL DXA DEVICES[1] (1)

$$\text{Hologic QDR-2000 Neck}_{BMD} = (0.836 \times \text{Lunar DPX-L Neck}_{BMD}) - 0.008$$

$$\text{Hologic QDR-2000 Neck}_{BMD} = (0.836 \times \text{Norland XR-26 Neck}_{BMD}) + 0.051$$

$$\text{Lunar DPX-L Neck}_{BMD} = (1.013 \times \text{Hologic QDR-2000 Neck}_{BMD}) + 0.142$$

$$\text{Lunar DPX-L Neck}_{BMD} = (0.945 \times \text{Norland XR-26 Neck}_{BMD}) + 0.115$$

$$\text{Norland XR-26 Neck}_{BMD} = (0.961 \times \text{Lunar DPX-L Neck}_{BMD}) - 0.037$$

$$\text{Norland XR-26 Neck}_{BMD} = (1.030 \times \text{Hologic QDR-2000 Neck}_{BMD}) + 0.058$$

STANDARDIZED BMD (sBMD) CALCULATIONS FOR PA SPINE FOR CENTRAL DXA DEVICES[2] (2)

$$\text{sBMD}_{SPINE} = 1000 (1.0761 \times \text{Norland XR-26 BMD}_{SPINE})$$

$$\text{sBMD}_{SPINE} = 1000 (0.9522 \times \text{Lunar DPX-L BMD}_{SPINE})$$

$$\text{sBMD}_{SPINE} = 1000 (1.0755 \times \text{Hologic QDR-2000 BMD}_{SPINE})$$

[1]Although specific models of the central DXA devices are noted in the equations, the formulas may be used to convert BMD measured on any model for a given manufacturer to the BMD for any model of the other manufacturer. It must be recognized, however, that the error in these conversions is too great to allow serial monitoring of BMD to be done using devices from different manufacturers.

[2]All equations are multiplied by 1000 to express the sBMD in mg/cm^2 instead of g/cm^2.

STANDARDIZED BMD (sBMD) CALCULATIONS FOR TOTAL HIP FOR CENTRAL DXA DEVICES[3] (3)

$sBMD_{TOTAL\ HIP} = 1000\ [(1.012 \times Norland\ XR\text{-}26\ BMD_{TOTAL\ HIP}) + 0.006]$

$sBMD_{TOTAL\ HIP} = 1000\ [(0.979 \times Lunar\ DPX\text{-}L\ BMD_{TOTAL\ HIP}) - 0.031]$

$sBMD_{TOTAL\ HIP} = 1000\ [(1.008 \times Hologic\ QDR\text{-}2000\ BMD_{TOTAL\ HIP}) + 0.006]$

STANDARDIZED BMD (sBMD) CALCULATIONS FOR HIP SUB-REGIONS FOR CENTRAL DXA DEVICES[4] (4)

$sBMD_{FEMORAL\ NECK} = 1000\ [(1.087 \times Hologic\ BMD_{FEMORAL\ NECK}) + 0.019]$

$sBMD_{FEMORAL\ NECK} = 1000\ [(0.939 \times Lunar\ BMD_{FEMORAL\ NECK}) - 0.023]$

$sBMD_{FEMORAL\ NECK} = 1000\ [(0.985 \times Norland\ BMD_{FEMORAL\ NECK}) + 0.006]$

$sBMD_{TROCHANTER} = 1000\ [(1.105 \times Hologic\ BMD_{TROCHANTER}) - 0.017]$

$sBMD_{TROCHANTER} = 1000\ [(0.949 \times Lunar\ BMD_{TROCHANTER}) - 0.042]$

$sBMD_{TROCHANTER} = 1000\ [(0.961 \times Norland\ BMD_{TROCHANTER}) + 0.057]$

$sBMD_{WARD'S} = 1000\ [(0.940 \times Hologic\ BMD_{WARD'S}) + 0.101]$

$sBMD_{WARD'S} = 1000\ [(0.980 \times Lunar\ BMD_{WARD'S}) - 0.106]$

$sBMD_{WARD'S} = 1000\ [(1.091 \times Norland\ BMD_{WARD'S}) + 0.001]$

STANDARD BMD CALCULATIONS FOR THE ULTRADISTAL (su), MID (sm), AND PROXIMAL (sp) FOREARM FOR 4 DXA DEVICES (5)

$suBMD = (0.945 \times PIXIBMD) + 0.015$

$suBMD = (1.158 \times Hologic\ Radius + Ulna\ Ultradistal\ BMD) - 0.019$

$suBMD = (0.802 \times Osteometer\ BMD) + 0.071$

$suBMD = (1.027 \times Norland\ Distal\ BMD) + 0.084$

$smBMD = (1.011 \times PIXI\ BMD) + 0.033$

$smBMD = (0.894 \times Hologic\ Radius + Ulna\ Mid\ BMD) - 0.030$

$smBMD = (0.856 \times Osteometer\ BMD) + 0.094$

$smBMD = (1.106 \times Norland\ Distal\ BMD) + 0.105$

$spBMD = (1.091 \times PIXI\ BMD) + 0.119$

$spBMD = (0.861 \times Hologic\ Radius + Ulna\ 1/3\ BMD) + 0.020$

$spBMD = (0.917 \times Osteometer\ BMD) + 0.188$

$spBMD = (0.596 \times Norland\ Proximal\ BMD) + 0.114$

[3]All equations are multiplied by 1000 to express the sBMD in mg/cm^2 instead of g/cm^2. The term total hip and total femur are interchangeable.

[4]All equations are multiplied by 1000 to express the sBMD in mg/cm^2 instead of g/cm^2.

METRIC/ENGLISH CONVERSIONS FOR UNITS OF MEASURE

English to Metric
    1 inch = 2.54 centimeters
    1 lb = 0.45 kg

Metric to English
    1 centimeter = 0.39 inches
    1 kg = 2.20 lb

Degrees in F = (1.8 C°)+ 32
    1 rad = 100 Gy
    1 rem = 100 Sv

Degrees in C = (F° − 32) × 0.555
    1 Gy = 0.01 rad
    1 Sv = 0.01 rem

MATHEMATICAL SYMBOLS AND DESIGNATIONS OF MULTIPLES

Symbol	Designation	Factor
G	giga-	10^9
M	mega-	10^6
k	kilo-	10^3
d	deci-	10^{-1}
c	centi-	10^{-2}
m	milli-	10^{-3}
μ	micro-	10^{-6}
n	nano-	10^{-9}
p	pico-	10^{-12}

REFERENCES

1. Genant HK, Grampp S, Gluer CC, et al. Universal standardization for dual x-ray absorptiometry: patient and phantom cross-calibration results. J Bone Miner Res 1994;9:1503–1514.
2. Steiger P. Standardization of spine BMD measurements. J Bone Miner Res 1995;10:1602–1603.
3. Hanson J. Standardization of femur BMD. J Bone Miner Res 1997;12:1316–1317.
4. Lu Y, Fuerst T, Hui S, Genant HK. Standardization of bone mineral density at femoral neck, trochanter, and Ward's triangle. Osteoporos Int 2001;12:438–444.
5. Shepherd JA, Cheng XG, Lu Y, et al. Universal standardization of forearm bone densitometry. J Bone Miner Res 2002;17:734–745.

III Appendix

Formulas for the Calculation of Precision and Least Significant Change

BASIC FORMULAS FOR THE SD$_{\text{RMS}}$, CV$_{\text{RMS}}$ AND LSC[1]

1). To calculate precision as the RMS-SD:

$$SD_{RMS} = \sqrt{\frac{\sum\limits_{i=1}^{m}(SD^2)}{m}}$$

2). To calculate precision as the RMS-CV:

$$CV_{RMS} = \sqrt{\frac{\sum\limits_{i=1}^{m}(CV^2)}{m}}$$

3). To calculate the least significant change (LSC):

$$LSC = Z'\,(\text{Pr})\sqrt{\frac{1}{n_1} + \frac{1}{n_2}}$$

FORMULAS FOR CALCULATING THE LSC USING A 2-SIDED OR 2-TAILED APPROACH

4). For one measurement at baseline and follow-up at 95% confidence:

$$_{1x1}LSC^{95-2} = 1.96\,(\text{Pr})\,1.414 = 2.77\,(\text{Pr})$$

5). For one measurement at baseline and follow-up at 80% confidence:

$$_{1x1}LSC^{80-2} = 1.28\,(\text{Pr})\,1.414 = 1.81\,(\text{Pr})$$

6). For two measurements at baseline and follow-up at 95% confidence:

$$_{2x2}LSC^{95-2} = 1.96\,(\text{Pr})\,1 = 1.96\,(\text{Pr})$$

7). For two measurements at baseline and follow-up at 80% confidence:

$$_{2x2}LSC^{80-2} = 1.28\,(\text{Pr})\,1 = 1.28\,(\text{Pr})$$

---

[1]*See* Chapter 11 for detailed explanations of the formulas.

FORMULAS FOR CALCULATING THE LSC USING A 1-SIDED OR 1-TAILED APPROACH

8). For one measurement at baseline and follow-up at 95% confidence:

$$_{1x1}LSC^{95-1} = 1.64\,(\text{Pr})\,1.414 = 2.32\,(\text{Pr})$$

9). For one measurement at baseline and follow-up at 80% confidence:

$$_{1x1}LSC^{80-1} = 0.84\,(\text{Pr})\,1.414 = 1.19\,(\text{Pr})$$

10). For two measurements at baseline and follow-up at 95% confidence:

$$_{2x2}LSC^{95-1} = 1.64\,(\text{Pr})\,1 = 1.64\,(\text{Pr})$$

11). For two measurements at baseline and follow-up at 80% confidence:

$$_{2x2}LSC^{80-1} = 0.84\,(\text{Pr})\,1 = 0.84\,(\text{Pr})$$

Various Combination of Number of Patients and Scans per Patient for 30° of Freedom in a Precision Study

Number of Patients	Number of Scans per Patient
1	31
5	7
10	4
15	3
30	2

Z′ Values for Various Levels of Statistical Confidence – Two-Sided Approach

Statistical Confidence Level (%)	Z′ Value
99	2.58
95	1.96
90	1.65
85	1.44
80	1.28

Z′ Values for Various Levels of Statistical Confidence – One-Sided Approach

Statistical Confidence Level (%)	Z′ Value
99	2.33
95	1.64
90	1.28
85	1.04
80	0.80

**The Interval Between BMD Measurements Required to Obtain the $_{1\times1}LSC^{95}$
for Various Levels of Precision and Expected Rates of Change**

Precision as % CV	% Change/Year	Interval Between BMD Measurements	
		Months	*Years*
0.5	1	16.7	1.39
	3	5.60	0.46
	5	3.30	0.28
1.0	1	33.2	2.77
	3	11.0	0.92
	5	6.70	0.55
1.5	1	50.0	4.16
	3	16.6	1.39
	5	10.0	0.83
2.0	1	66.5	5.54
	3	22.2	1.85
	5	13.3	1.11
2.5	1	83.2	6.93
	3	27.7	2.31
	5	16.6	1.39

Levels of Statistical Confidence for Various Combinations of Precision and Change in BMD

Change in BMD (g/cm^2)	Precision (g/cm^2)									
	0.005	*0.010*	*0.015*	*0.020*	*0.025*	*0.030*	*0.035*	*0.040*	*0.045*	*0.050*
0.005	52%	28%	19%	14%	11%	9%	8%	7%	6%	6%
0.010	84%	52%	36%	28%	22%	19%	16%	14%	12%	11%
0.015	97%	71%	52%	40%	33%	28%	24%	21%	19%	17%
0.020	100%	84%	65%	52%	43%	36%	31%	28%	25%	22%
0.025	100%	92%	76%	62%	52%	44%	39%	34%	31%	28%
0.030	100%	97%	84%	71%	60%	52%	46%	40%	36%	33%
0.035	100%	99%	90%	78%	68%	59%	52%	46%	42%	38%
0.040	100%	100%	94%	84%	74%	65%	58%	52%	47%	43%
0.045	100%	100%	97%	89%	80%	71%	64%	57%	52%	48%
0.050	100%	100%	98%	92%	84%	76%	69%	62%	57%	52%
0.055	100%	100%	99%	95%	88%	81%	73%	67%	61%	56%
0.060	100%	100%	100%	97%	91%	84%	77%	71%	65%	60%
0.065	100%	100%	100%	98%	93%	87%	81%	75%	69%	64%
0.070	100%	100%	100%	99%	95%	90%	84%	78%	73%	68%
0.075	100%	100%	100%	99%	97%	92%	87%	82%	76%	71%
0.080	100%	100%	100%	100%	98%	94%	89%	84%	79%	74%
0.085	100%	100%	100%	100%	98%	95%	91%	87%	82%	77%
0.090	100%	100%	100%	100%	99%	97%	93%	89%	84%	80%
0.095	100%	100%	100%	100%	99%	97%	95%	91%	86%	82%
0.100	100%	100%	100%	100%	100%	98%	96%	92%	88%	84%

Table created by and reproduced courtesy of Ken Faulkner, Ph.D.

Confidence Intervals for the Measured Change in
BMD for Different Values of Precision

Confidence	Precision, %CV				
Interval	1%	1.25%	1.5%	1.75%	2.0%
99%	±3.65	±4.56	±5.48	±6.39	±7.30
95%	±2.77	±3.46	±4.16	±4.85	±5.54
90%	±2.33	±2.91	±3.50	±4.08	±4.66
85%	±2.04	±2.55	±3.06	±3.57	±4.08
80%	±1.81	±2.26	±2.72	±3.17	±3.62

All values are in %.

$_{1\times1}LSC^{99\text{-}2}$ for Different Values of
Precision Expressed as the %CV

Precision (%CV)	$_{1\times1}LSC^{99}$ (%)
0.50	1.83
0.75	2.74
1.00	3.65
1.25	4.56
1.50	5.48
1.75	6.39
2.00	7.30
2.25	8.21
2.50	9.13
2.75	10.04
3.00	10.95
3.25	11.86
3.50	12.78

$_{1\times1}LSC^{95\text{-}2}$ for Different Values of
Precision Expressed as the %CV

Precision (%CV)	$_{1\times1}LSC^{95}$ (%)
0.50	1.39
0.75	2.08
1.00	2.77
1.25	3.46
1.50	4.16
1.75	4.85
2.00	5.54
2.25	6.23
2.50	6.93
2.75	7.62
3.00	8.31
3.25	9.00
3.50	9.70

$_{1\times1}LSC^{90\text{-}2}$ for Different Values of
Precision Expressed as the %CV

Precision (%CV)	$_{1\times1}LSC^{90}$ (%)
0.50	1.17
0.75	1.75
1.00	2.33
1.25	2.91
1.50	3.50
1.75	4.08
2.00	4.66
2.25	5.24
2.50	5.83
2.75	6.41
3.00	6.99
3.25	7.57
3.50	8.16

$_{1\times1}LSC^{85\text{-}2}$ for Different Values of
Precision Expressed as the %CV

Precision (%CV)	$_{1\times1}LSC^{85}$ (%)
0.50	1.02
0.75	1.53
1.00	2.04
1.25	2.55
1.50	3.06
1.75	3.57
2.00	4.08
2.25	4.59
2.50	5.10
2.75	5.61
3.00	6.12
3.25	6.63
3.50	7.14

$_{1 \times 1}$**LSC $^{80\text{-}2}$ for Different Values of
Precision Expressed as the %CV**

Precision (%CV)	$_{1 \times 1}LSC^{80}$ (%)
0.50	0.91
0.75	1.36
1.00	1.81
1.25	2.26
1.50	2.72
1.75	3.17
2.00	3.62
2.25	4.07
2.50	4.53
2.75	4.98
3.00	5.43
3.25	5.88
3.50	6.34

IV Appendix

World Health Organization Criteria for the Diagnosis of Osteoporosis Based on the Measurement of Bone Density (1)

Diagnosis	Bone Density Criteria	T-Score Criteria
Normal	Not more than 1 SD below the young adult peak bone density	–1 or better
Osteopenia	More than 1 but less than 2.5 SD below the young adult peak bone density	Between –1 and –2.5
Osteoporosis	2.5 SD or more below the young adult peak bone density	–2.5 or poorer
Severe or Established Osteoporosis	2.5 SD or more below the young adult peak bone density and a fracture	–2.5 or poorer + a fracture

In 2003, the WHO noted that DXA was considered the "gold standard" technique and that the hip was the preferred skeletal site for diagnosis *(2)*.

1. WHO. Assessment of fracture risk and its application to screening for postmenopausal osteoporosis. [843], 1–129. 1994. Geneva, WHO. WHO Technical Report Series.
2. WHO. Prevention and management of osteoporosis. [921], 1–192. 2003. Geneva, WHO. WHO Technical Report Series.

V   Appendix

2007 ISCD Official Positions

The official positions that are new or revised since 2005 are in bold type.
© Copyright ISCD, October 2007. Supersedes all prior "Official Positions" publications.

Indications for Bone Mineral Density (BMD) Testing

- Women aged 65 and older
- Postmenopausal women under age 65 with risk factors for fracture
- **Women during the menopausal transition with clinical risk factors for fracture, such as low body weight, prior fracture, or high-risk medication use**
- Men aged 70 and older
- **Men under age 70 with clinical risk factors for fracture**
- Adults with a fragility fracture
- Adults with a disease or condition associated with low bone mass or bone loss
- Adults taking medications associated with low bone mass or bone loss
- Anyone being considered for pharmacologic therapy
- Anyone being treated, to monitor treatment effect
- Anyone not receiving therapy in whom evidence of bone loss would lead to treatment

Women discontinuing estrogen should be considered for bone density testing according to the indications listed above.

Reference Database for T-Scores

- Use a uniform Caucasian (non-race adjusted) female normative database for women of all ethnic groups*
- Use a uniform Caucasian (non-race adjusted) male normative database for men of all ethnic groups*
- The NHANES III database should be used for T-score derivation at the hip regions

 *Note: Application of recommendation may vary according to local requirements

Central DXA for Diagnosis

- The WHO international reference standard for osteoporosis diagnosis is a T-score of –2.5 or less at the femoral neck

  - The reference standard from which the T-score is calculated is the female, white, age 20–29 years, NHANES III database

- Osteoporosis may be diagnosed in postmenopausal women and in men age 50 and older if the T-score of the lumbar spine, total hip, or femoral neck is –2.5 or less*

  - In certain circumstances the 33% radius (also called 1/3 radius) may be utilized

445

*Note: Other hip regions of interest, including Ward's area and the greater trochanter should not be used for diagnosis. Application of recommendation may vary according to local requirements.

- Skeletal sites to measure

    - Measure BMD at both the PA spine and hip in all patients
    - Forearm BMD should be measured under the following circumstances:
        - Hip and/or spine cannot be measured or interpreted
        - Hyperparathyroidism
        - Very obese patients (over the weight limit for DXA table)

- Spine Region of Interest (ROI)

    - Use PA L1–L4 for spine BMD measurement
    - Use all evaluable vertebrae and only exclude vertebrae that are affected by local structural change or artifact. Use three vertebrae if four cannot be used and two if three cannot be used
    - BMD based diagnostic classification should not be made using a single vertebra
    - If only one evaluable vertebra remains after excluding other vertebrae, diagnosis should be based on a different valid skeletal site
    - Anatomically abnormal vertebrae may be excluded from analysis if:
        - They are clearly abnormal and non-assessable within the resolution of the system or
        - There is more than a 1.0 T-score difference between the vertebra in question and adjacent vertebrae
    - When vertebrae are excluded, the BMD of the remaining vertebrae is used to derive the T-score
    - The lateral spine should not be used for diagnosis, but may have a role in monitoring

- Hip ROI

    - Use femoral neck or total proximal femur, whichever is lowest
    - BMD may be measured at either hip
    - There are insufficient data to determine whether mean T-scores for bilateral hip BMD can be used for diagnosis
    - The mean hip BMD can be used for monitoring, with total hip being preferred

- Forearm ROI

    - Use 33% radius (sometimes called one-third radius) of the non-dominant forearm for diagnosis. Other forearm ROI are not recommended

Fracture Risk Assessment

- A distinction is made between diagnostic classification and the use of BMD for fracture risk assessment
- For fracture risk assessment, any well-validated technique can be used, including measurements of more than one site where this has been shown to improve the assessment of risk

Use of the Term "Osteopenia"

- The term "osteopenia" is retained, but "low bone mass" or "low bone density" is preferred.
- People with low bone mass or density are not necessarily at high fracture risk.

BMD Reporting in Postmenopausal Women and in Men Age 50 and Older

- T-scores are preferred.
- The WHO densitometric classification is applicable.

BMD Reporting in Females Prior to Menopause and in Males Younger Than Age 50

- Z-scores, not T-scores, are preferred. This is particularly important in children.
- A Z-score of –2.0 or lower is defined as "below the expected range for age", and a Z-score above –2.0 is "within the expected range for age."
- **Osteoporosis cannot be diagnosed in men under age 50 on the basis of BMD alone.**
- **The WHO diagnostic criteria may be applied to women in the menopausal transition.**

Z-Score Reference Database

- Z-scores should be population specific where adequate reference data exist. For the purpose of Z-score calculation, the patient's self-reported ethnicity should be used.

Serial BMD Measurements

- Serial BMD testing can be used to determine whether treatment should be started on untreated patients, because significant loss may be an indication for treatment.
- Serial BMD testing can monitor response to therapy by finding an increase or stability of bone density.
- Serial BMD testing can evaluate individuals for non-response by finding loss of bone density, suggesting the need for reevaluation of treatment and evaluation for secondary causes of osteoporosis.
- Follow-up BMD testing should be done when the expected change in BMD equals or exceeds the least significant change (LSC).
- Intervals between BMD testing should be determined according to each patient's clinical status: typically one year after initiation or change of therapy is appropriate, with longer intervals once therapeutic effect is established.
- In conditions associated with rapid bone loss, such as glucocorticoid therapy, testing more frequently is appropriate.

Phantom Scanning and Calibration

The Quality Control (QC) program at a DXA facility should include adherence to manufacturer guidelines for system maintenance. In addition, if not recommended in the manufacturer protocol, the following QC procedures are advised:

- Perform periodic (at least once per week) phantom scans for any DXA system as an independent assessment of system calibration.
- Plot and review data from calibration and phantom scans.
- Verify the phantom mean BMD after any service performed on the densitometer.
- Establish and enforce corrective action thresholds that trigger a call for service.
- Maintain service logs.
- Comply with government inspections, radiation surveys and regulatory requirements.

Precision Assessment

- Each DXA facility should determine its precision error and calculate the LSC.
- The precision error supplied by the manufacturer should not be used.

- If a DXA facility has more than one technologist, an average precision error combining data from all technologists should be used to establish precision error and LSC for the facility, provided the precision error for each technologist is within a pre-established range of acceptable performance.
- Every technologist should perform an in vivo precision assessment using patients representative of the clinic's patient population.
- Each technologist should do one complete precision assessment after basic scanning skills have been learned (e.g., manufacturer training) and after having performed approximately 100 patient-scans.
- A repeat precision assessment should be done if a new DXA system is installed.
- A repeat precision assessment should be done if a technologist's skill level has changed.
- To perform a precision analysis:

  - Measure 15 patients 3 times, or 30 patients 2 times, repositioning the patient after each scan
  - Calculate the root mean square standard deviation (RMS-SD) for the group
  - Calculate LSC for the group at 95% confidence interval

- The minimum acceptable precision for an individual technologist is:

  - Lumbar Spine: 1.9% (LSC=5.3%)
  - Total Hip: 1.8% (LSC=5.0%)
  - Femoral Neck: 2.5% (LSC=6.9%)
  - Retraining is required if a technologist's precision is worse than these values

- Precision assessment should be standard clinical practice. Precision assessment is not research and may potentially benefit patients. It should not require approval of an institutional review board. Adherence to local radiologic safety regulations is necessary. Performance of a precision assessment requires the consent of participating patients.

Cross-Calibration of DXA Systems

- When changing hardware, but not the entire system, or when replacing a system with the same technology (manufacturer and model), cross-calibration should be performed by having one technologist do 10 phantom scans, with repositioning, before and after hardware change.

  - If a greater than 1% difference in mean BMD is observed, contact the manufacturer for service/correction

- When changing an entire system to one made by the same manufacturer using a different technology, or when changing to a system made by a different manufacturer, one approach to cross-calibration is:

  - Scan 30 patients representative of the facility's patient population once on the initial system and then twice on the new system within 60 days
  - Measure those anatomic sites commonly measured in clinical practice, typically spine and proximal femur
  - Facilities must comply with locally applicable regulations regarding DXA
  - Calculate the average BMD relationship and LSC between the initial and new machine using the ISCD DXA Machine Cross-Calibration Tool (www.ISCD.org)

- Use this LSC for comparison between the previous and new system. Inter-system quantitative comparisons can only be made if cross-calibration is performed on each skeletal site commonly measured
  - Once a new precision assessment has been performed on the new system, all future scans should be compared to scans performed on the new system using the newly established intra-system LSC

- If a cross-calibration assessment is not performed, no quantitative comparison to the prior machine can be made. Consequently, a new baseline BMD and intra-system LSC should be established.

BMD Comparison Between Facilities

- It is not possible to quantitatively compare BMD or to calculate a LSC between facilities without cross-calibration.

Vertebral Fracture Assessment Nomenclature

- Vertebral Fracture Assessment (VFA) is the correct term to denote densitometric spine imaging performed for the purpose of detecting vertebral fractures.

Indications for VFA

- Consider VFA when the results may influence clinical management.
- **Postmenopausal women with low bone mass (osteopenia) by BMD criteria, PLUS any one of the following:**

  - **Age greater than or equal to 70 years**
  - **Historical height loss greater than 4 cm (1.6 in.)**
  - **Prospective height loss greater than 2 cm (0.8 in.)**
  - **Self-reported vertebral fracture (not previously documented)**
  - **Two or more of the following;**
    - **Age 60 to 69 years**
    - **Self-reported prior non-vertebral fracture**
    - **Historical height loss of 2 to 4 cm**
    - **Chronic systemic diseases associated with increased risk of vertebral fractures (for example, moderate to severe COPD or COAD, seropositive rheumatoid arthritis, Crohn's disease)**

- Men with low bone mass (osteopenia) by BMD criteria, PLUS any one of the following:

  - **Age 80 years or older**
  - **Historical height loss greater than 6 cm (2.4 in)**
  - **Prospective height loss greater than 3 cm (1.2 in)**
  - **Self-reported vertebral fracture (not previously documented)**
  - **Two or more of the following;**
    - **Age 70 to 79 years**
    - **Self-reported prior non-vertebral fracture**
    - **Historical height loss of 3 to 6 cm**
    - **On pharmacologic androgen deprivation therapy or following orchiectomy**
    - **Chronic systemic diseases associated with increased risk of vertebral fractures (for example, moderate to severe COPD or COAD, seropositive rheumatoid arthritis, Crohn's disease)**

- **Women or men on chronic glucocorticoid therapy (equivalent to 5 mg or more of prednisone daily for three (3) months or longer).**
- **Postmenopausal women or men with osteoporosis by BMD criteria, if documentation of one or more vertebral fractures will alter clinical management.**

Methods for Defining and Reporting Fractures on VFA

- The methodology utilized for vertebral fracture identification should be similar to standard radiological approaches and be provided in the report.
- Fracture diagnosis should be based on visual evaluation and include assessment of grade/severity. Morphometry alone is not recommended because it is unreliable for diagnosis.
- **The Genant visual semi-quantitative method is the current clinical technique of choice for diagnosing vertebral fracture with VFA.**
- Severity of deformity may be confirmed by morphometric measurement if desired.

Indications for Following VFA With Another Imaging Modality

- The decision to perform additional imaging must be based on each patient's overall clinical picture, including the VFA result.
- **Indications for follow-up imaging studies include:**
    - **Two or more mild (grade 1) deformities without any moderate or severe (grade 2 or 3) deformities**
    - **Lesions in vertebrae that cannot be attributed to benign causes**
    - **Vertebral deformities in a patient with a known history of a relevant malignancy**
    - Equivocal fractures
    - Unidentifiable vertebrae between T7–L4
    - Sclerotic or lytic changes, or findings suggestive of conditions other than osteoporosis

Note: VFA is designed to detect vertebral fractures and not other abnormalities.

Baseline DXA Report: Minimum Requirements

- Demographics (name, medical record identifying number, date of birth, sex).
- Requesting provider.
- Indications for the test.
- Manufacturer and model of instrument used
- Technical quality and limitations of the study, stating why a specific site or ROI is invalid or not included.
- BMD in g/cm^2 for each site.
- The skeletal sites, ROI, and, if appropriate, the side, that were scanned.
- The T-score and/or Z-score where appropriate.
- WHO criteria for diagnosis in postmenopausal females and in men age 50 and over.
- Risk factors including information regarding previous non traumatic fractures.
- A statement about fracture risk. Any use of relative fracture risk must specify the population of comparison (e.g., young- adult or age-matched). The ISCD favors the use of absolute fracture risk prediction when such methodologies are established.
- A general statement that a medical evaluation for secondary causes of low BMD may be appropriate.
- Recommendations for the necessity and timing of the next BMD study.

Follow-Up DXA Report

- Statement regarding which previous or baseline study and ROI is being used for comparison.
- Statement about the LSC at your facility and the statistical significance of the comparison.
- Report significant change, if any, between the current and previous study or studies in g/cm^2 and percentage.
- Comments on any outside study including manufacturer and model on which previous studies were performed and the appropriateness of the comparison.
- Recommendations for the necessity and timing of the next BMD study.

DXA Report: Optional Items

- Recommendation for further non-BMD testing, such as X-ray, magnetic resonance imaging, computed tomography, etc.
- Recommendations for pharmacological and non pharmacological interventions.
- Addition of the percentage compared to a reference population.
- Specific recommendations for evaluation of secondary osteoporosis.

DXA Report: Items That Should not be Included

- A statement that there is bone loss without knowledge of previous bone density.
- Mention of "mild," "moderate," or "marked" osteopenia or osteoporosis.
- Separate diagnoses for different ROI (e.g., osteopenia at the hip and osteoporosis at the spine).
- Expressions such as "She has the bones of an 80-year-old," if the patient is not 80 years old.
- Results from skeletal sites that are not technically valid.
- The change in BMD if it is not a significant change based on the precision error and LSC.

Components of a VFA Report

- Patient identification, referring physician, indication(s) for study, technical quality and interpretation.
- A follow-up VFA report should also include comparability of studies and clinical significance of changes, if any.
- **VFA reports should comment on the following**
  - **Unevaluable vertebrae**
  - **Deformed vertebrae, and whether or not the deformities are consistent with vertebral fracture**
  - **Unexplained vertebral and extra-vertebral pathology**
- Optional components include fracture risk and recommendations for additional studies.

General Recommendations for Non Central DXA Devices: QCT, pQCT, QUS, and pDXA

The following general recommendations for QCT, pQCT, QUS, and pDXA are analogous to those defined for central DXA technologies. Examples of technical differences amongst devices, fracture prediction ability for current manufacturers and equivalence study requirements are provided in the full text documents printed in the *Journal of Clinical Densitometry*.

- **Bone density measurements from different devices cannot be directly compared.**
- **Different devices should be independently validated for fracture risk prediction by prospective trials, or by demonstration of equivalence to a clinically validated device.**
- **T-scores from measurements other than DXA at the femur neck, total femur, lumbar spine, or one-third (33%) radius cannot be used according to the WHO diagnostic classification because those T-scores are not equivalent to T-scores derived by DXA.**
- **Device-specific education and training should be provided to the operators and interpreters prior to clinical use.**
- **Quality control procedures should be performed regularly.**

Baseline Non Central DXA Devices (QCT, pQCT, QUS, pDXA) Report: Minimum Requirements

- **Date of test**
- **Demographics (name, date of birth or age, sex)**
- **Requesting provider**
- **Names of those receiving copy of report**
- **Indications for test**
- **Manufacturer, and model of instrument and software version**
- **Measurement value(s)**
- **Reference database**
- **Skeletal site/ROI**
- **Quality of test**
- **Limitations of the test including a statement that the WHO diagnostic classification cannot be applied to T-scores obtained from QCT, pQCT, QUS, and pDXA (other than one-third (33%) radius) measurements**
- **Clinical risk factors**
- **Fracture risk estimation**
- **A general statement that a medical evaluation for secondary causes of low BMD may be appropriate**
- **Recommendations for follow-up imaging**

   Note: A list of appropriate technical items is provided in the QCT and pQCT sections of the full text documents printed in the *Journal of Clinical Densitometry.*

Non Central DXA Devices (QCT, pQCT, QUS, pDXA) Report: Optional Items

- **Report may include the following optional item:**

    - **Recommendations for pharmacological and non pharmacological interventions**

QCT and pQCT

- **Acquisition**

    - **With single-slice QCT, L1-L3 should be scanned; with 3D QCT, L1-L2 should be scanned**

- **Fracture Prediction**

    - **Spinal trabecular BMD as measured by QCT has at least the same ability to predict vertebral fractures as AP spinal BMD measured by central DXA in**

> postmenopausal women. There is lack of sufficient evidence to support this position for men
- There is lack of sufficient evidence to recommend spine QCT for hip fracture prediction in either women or men
- pQCT of the forearm at the ultra-distal radius predicts hip, but not spine, fragility fractures in postmenopausal women. There is lack of sufficient evidence to support this position for men

- **Therapeutic Decisions**

  - Central DXA measurements at the spine and femur are the preferred method for making therapeutic decisions and should be used if possible. However, if central DXA cannot be done, pharmacologic treatment can be initiated if the fracture probability, as assessed by QCT of the spine or pQCT of the radius using device specific thresholds, and in conjunction with clinical risk factors, is sufficiently high

- **Monitoring**

  - Trabecular BMD of the lumbar spine measured by QCT can be used to monitor age-, disease-, and treatment-related BMD changes
  - Trabecular and total BMD of the ultra-distal radius measured by pQCT can be used to monitor age-related BMD changes

- **Reporting**

  - For QCT using whole body CT scanners the following additional technical items should be reported:
    - Tomographic acquisition and reconstruction parameters
    - kV, mAs
    - Collimation during acquisition
    - Table increment per rotation
    - Table height
    - Reconstructed slice thickness, reconstruction increment
    - Reconstruction kernel

- For pQCT using dedicated pQCT scanners, the following additional technical items should be reported:

  - Tomographic acquisition and reconstruction parameters
  - Reconstructed slice thickness
  - Single / multi-slice acquisition mode
  - Length of scan range in multi-slice acquisition mode

QUS

- **Acquisition**

  - The only validated skeletal site for the clinical use of QUS in osteoporosis management is the heel

- **Fracture Prediction**

  - Validated heel QUS devices predict fragility fracture in postmenopausal women (hip, vertebral, and global fracture risk) and men over the age of 65 (hip and all non-vertebral fractures), independently of central DXA BMD

- Discordant results between heel QUS and central DXA are not infrequent and are not necessarily an indication of methodological error
- Heel QUS in conjunction with clinical risk factors can be used to identify a population at very low fracture probability in which no further diagnostic evaluation may be necessary. (Examples of device-specific thresholds and case findings strategy are provided in the full text documents printed in the *Journal of Clinical Densitometry*.)

- **Therapeutic Decisions**

  - Central DXA measurements at the spine and femur are preferred for making therapeutic decisions and should be used if possible. However, if central DXA cannot be done, pharmacologic treatment can be initiated if the fracture probability, as assessed by heel QUS, using device specific thresholds and in conjunction with clinical risk factors, is sufficiently high. (Examples of device-specific thresholds are provided in the full text documents printed in the *Journal of Clinical Densitometry*.)

- **Monitoring**

  - QUS cannot be used to monitor the skeletal effects of treatments for osteoporosis

pDXA
- **Fracture Prediction**

  - Measurement by validated pDXA devices can be used to assess vertebral and global fragility fracture risk in postmenopausal women, however its vertebral fracture predictive ability is weaker than central DXA and heel QUS. There is lack of sufficient evidence to support this position for men
  - Radius pDXA in conjunction with clinical risk factors can be used to identify a population at very low fracture probability in which no further diagnostic evaluation may be necessary. (Examples of device-specific thresholds and case findings strategy are provided in the full text documents printed in the *Journal of Clinical Densitometry*.)

- **Diagnosis**

  - The WHO diagnostic classification can only be applied to DXA at the femur neck, total femur, lumbar spine and the one-third (33%) radius ROI measured by DXA or pDXA devices utilizing a validated young-adult reference database

- **Therapeutic Decisions**

  - Central DXA measurements at the spine and femur are the preferred method for making therapeutic decisions and should be used if possible. However, if central DXA cannot be done, pharmacologic treatment can be initiated if the fracture probability, as assessed by radius pDXA (or DXA) using device specific thresholds and in conjunction with clinical risk factors, is sufficiently high. (Examples of device-specific thresholds are provided in the full text documents printed in the *Journal of Clinical Densitometry*.)

- **Monitoring**

  - pDXA devices are not clinically useful in monitoring the skeletal effects of presently available medical treatments for osteoporosis

Skeletal Health Assessment In Children and Adolescents (Males and Females ages 5-19)

Fracture Prediction and Definition of Osteoporosis

- **Fracture prediction should primarily identify children at risk of clinically significant fractures, such as fracture of long bones in the lower extremities, vertebral compression fractures, or two or more long-bone fractures of the upper extremities.**

- **The diagnosis of osteoporosis in children and adolescents should NOT be made on the basis of densitometric criteria alone.**

  - **The diagnosis of osteoporosis requires the presence of both a clinically significant fracture history and low bone mineral content or bone mineral density.**
    - **A clinically significant fracture history is one or more of the following:**
      - **Long bone fracture of the lower extremities**
      - **Vertebral compression fracture**
      - **Two or more long-bone fractures of the upper extremities**

  - **Low bone mineral content or bone mineral density is defined as a BMC or areal BMD Z-score that is less than or equal to -2.0, adjusted for age, gender and body size, as appropriate.**

DXA Assessment in Children and Adolescents With Disease That May Affect the Skeleton

- **DXA measurement is part of a comprehensive skeletal health assessment in patients with increased risk of fracture.**

- **Therapeutic interventions should not be instituted on the basis of a single DXA measurement.**

- **When technically feasible, all patients should have spine and total body less head (TBLH) BMC and areal BMD measured**

  - **Prior to initiation of bone-active treatment.**
  - **To monitor bone-active treatment in conjunction with other clinical data.**

- **In patients with primary bone diseases or potential secondary bone diseases (e.g., due to chronic inflammatory diseases, endocrine disturbances, history of childhood cancer, or prior transplantation (non-renal)), spine and TBLH BMC and areal BMD should be measured at clinical presentation.**

- **In patients with thalassemia major, spine and TBLH BMC and areal BMD should be measured at fracture presentation or at age 10 years, whichever is earlier.**

- **In children with chronic immobilization (e.g., cerebral palsy) spine and TBLH BMC and areal BMD should be measured at fracture presentation.**

  - **DXA should not be performed if contractures prevent the safe and appropriate positioning of the child.**

- **The minimum time interval for repeating a bone density measurement to monitor treatment with a bone-active agent or disease processes is six months.**

DXA Interpretation and Reporting in Children and Adolescents

- **DXA is the preferred method for assessing BMC and areal BMD.**
- **The PA spine and TBLH are the most accurate and reproducible skeletal sites for performing BMC and areal BMD measurements.**

- **Soft tissue measures in conjunction with whole body scans may be helpful in evaluating patients with chronic conditions associated with malnutrition (such as anorexia nervosa, inflammatory bowel disease, cystic fibrosis), or with both muscle and skeletal deficits (such as idiopathic juvenile osteoporosis).**

- **The hip (including total hip and proximal femur) is not a reliable site for measurement in growing children due to significant variability in skeletal development and lack of reproducible ROI.**

- **In children with linear growth or maturational delay, spine and TBLH BMC and areal BMD results should be adjusted for absolute height or height age, or compared to pediatric reference data that provide age-, gender-, and height-specific Z-scores.**

- **An appropriate reference data set must include a sample of the general healthy population sufficiently large to characterize the normal variability in bone measures that takes into consideration gender, age, and race/ethnicity.**

- **When upgrading densitometer instrumentation or software, it is essential to use reference data valid for the hardware and software technological updates.**

- **Baseline DXA reports should contain the following information:**

    - **DXA manufacturer, model, and software version**
    - **Referring physician**
    - **Patient age, gender, race/ethnicity, weight, and height**
    - **Relevant medical history including previous fractures**
    - **Indication for study**
    - **Bone age results, if available**
    - **Technical quality**
    - **BMC and areal BMD**
    - **BMC and areal BMD Z-score**
    - **Source of reference data for Z-score calculations**
    - **Adjustments made for growth and maturation**
    - **Interpretation**
    - **Recommendations for the necessity and timing of the next DXA study are optional**

- **Serial DXA testing**

    - **Should be done only when the expected change in areal BMD equals or exceeds the LSC**
    - **Serial DXA reports should include the same information as for baseline testing, but additionally include:**
        - **Indications for follow-up scan**
        - **Comparability of studies**
        - **Interval changes in height and weight**
        - **BMC and areal BMD Z-scores adjusted or unadjusted for height or other adjustments**
        - **Percent change in BMC and areal BMD and interval change in Z-scores**
        - **Recommendations for the necessity and timing of the next BMD study are optional**

- **Accurate interpretation of serial DXA results requires knowledge of the LSC for all sites measured and for all technologists at the DXA testing facility.**

- **Terminology**

    - **T-scores should not appear in pediatric DXA reports.**
    - **The term "osteopenia" should not appear in pediatric DXA reports.**
    - **The term "osteoporosis" should not appear in pediatric DXA reports without knowledge of clinically significant fracture history.**
    - **"Low bone mineral content or bone mineral density for chronologic age" is the preferred term when BMC or BMD Z-scores are less than or equal to -2.0.**

pQCT in Children and Adolescents

- **Reference data are not sufficient for the clinical use of pQCT for fracture prediction or diagnosis of low bone mass.**
- **When the forearm is measured, the non-dominant forearm should be used.**
- **Measurements sites should include the metaphysis and diaphysis.**
- **Determination of the precision error, LSC, and monitoring time interval should be performed as described for DXA.**
- **pQCT reports should include:**

    - **Manufacturer, model, and software version**
    - **Referring physician**
    - **Patient age, gender, race/ethnicity, weight, and height**
    - **Relevant medical history including previous fractures**
    - **Indication for measurement**
    - **Bone age results, if available**
    - **Measurement site**
    - **Limb length**
    - **Scan acquisition and analysis parameters**
    - **Scan technical quality**
    - **Reference data source for Z-score calculation**
    - **Metaphyseal total and trabecular vBMD and Z-scores**
    - **Diaphyseal BMC, cortical vBMD, cortical thickness, cross-sectional moment of inertia, SSI results, and Z-scores.**
    - **Adjustments made for growth and maturation**
    - **Interpretation**

- **Quality control procedures should be performed as described for central DXA.**

DXA Nomenclature

- DXA – not DEXA.
- T-score – not T score, t-score, or t score
- Z-score – not Z score, z-score, or z score

DXA Decimal Digits

Preferred number of decimal digits for DXA reporting:

- BMD: 3 digits
  (example, 0.927 g/cm2)

- T-score: 1 digit
  (example, -2.3)

- Z-score: 1 digit
  (example, 1.7)

- BMC: 2 digits
  (example, 31.76 g)

- Area: 2 digits
  (example, 43.25 cm2)

- % reference database: Integer
  (example, 82%)

GLOSSARY

BMC – bone mineral content

BMD – bone mineral density

DXA – dual-energy X-ray absorptiometry

ISCD – International Society for Clinical Densitometry

LSC – least significant change

NHANES III – National Health and Nutrition Examination Survey III

PA – posterior anterior

pDXA – peripheral dual-energy x-ray absorptiometry

pQCT – peripheral quantitative computed tomography

QC – quality control

QCT – quantitative Computed Tomography

QUS – quantitative Ultrasound

ROI – region(s) of interest

SSI – strain strength index

TBLH – total body less head

VFA – Vertebral Fracture Assessment

vBMD – volumetric BMD

WHO – World Health Organization

These 2007 guidelines were reproduced with the permission of the ISCD.

Accessed at: http://www.iscd.org on July 17, 2008.

VI Appendix

Guidelines[1] for Bone Density Testing from Other Major Organizations

2008 NATIONAL OSTEOPOROSIS FOUNDATION GUIDELINES FOR BONE DENSITY TESTING

Bone density should only be measured if it will affect the patient's treatment decision. It is not routinely recommended in children or adolescents or healthy young men or premenopausal women. The following are indications for BMD testing:

1. All postmenopausal women age 65 and older
2. All men age 70 and older
3. Younger postmenopausal women and men age 50–70 if there is concern based on their clinical risk factor profile
4. Women in the menopausal transition if there is a specific risk factor associated with increased fracture risk, such as low body weight, prior low-trauma fracture, or high risk medication
5. Adults with a condition (e.g., rheumatoid arthritis) or taking a medication (e.g., glucocorticoids, $\geq$ mg/day for $\geq$3 months) associated with low bone mass or bone loss
6. Anyone being considered for pharmacologic therapy for osteoporosis
7. Anyone being treated for osteoporosis, to monitor treatment effect
8. Anyone not receiving therapy in whom evidence of bone loss would lead to treatment
9. Postmenopausal women discontinuing estrogen should be considered for bone density testing

National Osteoporosis Foundation. Clinician's Guide to Prevention and Treatment of Osteoporosis. National Osteoporosis Foundation, Washington, D.C. 2008

AMERICAN ASSOCIATION OF CLINICAL ENDOCRINOLOGISTS 2003 MEDICAL GUIDELINES FOR CLINICAL PRACTICE FOR THE PREVENTION AND MANAGEMENT OF POSTMENOPAUSAL OSTEOPOROSIS

BMD measurements as part of the assessment for postmenopausal osteoporosis should be performed in the following settings:

1. All women 65 years of age and older

---

[1]These guidelines and others are discussed in detail in Chapter 8.

2.   All adult women with a history of fracture not caused by severe trauma
3.   Younger postmenopausal women who have clinical risk factors for fractures (low bone weight less than 57.6 kg or a family history of spine or hip fracture)

BMD measurements for monitoring changes in BMD may be performed with following frequency:

1.   For patients with "normal" baseline BMD, consider a follow-up measurement every 3–5 years, although patients with a bone density well above the minimal acceptable level may not need further BMD testing.
2.   For patients in an osteoporosis prevention program, perform a follow-up measurement every 1–2 years until bone mass stability is documented. After BMD has stabilized, perform follow-up measurements every 2–3 years.
3.   For patients on a therapeutic program, perform a follow-up measurement yearly for 2 years. If bone mass has stabilized after 2 years, perform a follow-up measurement every 2 years. Otherwise, continue with annual follow-up measurements until stability of bone mass is achieved.

AACE Osteoporosis Task Force. American Association of Clinical Endocrinologists medical guidelines for clinical practice for the prevention and management of postmenopausal osteoporosis: 2001 edition, with selected updates for 2003. Endocr Pract 2003;9:544–563.

AMERICAN COLLEGE OF OBSTETRICIANS AND GYNECOLOGISTS GUIDELINES FOR BONE DENSITY MEASUREMENTS

Bone density measurements should be made in:

1.   All postmenopausal women 65 years of age or older
2.   Postmenopausal women under 65 years of age who have one or more risk factors
3.   All postmenopausal women who have sustained a fracture

Bone density measurements may be useful in:

1.   Pre- or postmenopausal women with diseases or conditions associated with an increased risk of osteoporosis

ACOG releases recommendations for bone density screening for osteoporosis. Washington, D.C.: American College of Obstetricians and Gynecologists, 2002. (Accessed March 26, 2002, at http://www.acog.org/from_home/publications/press_releases/nr02-28-02-1.htm)

2006 POSITION STATEMENT ON MANAGEMENT OF POSTMENOPAUSAL OSTEOPOROSIS FROM THE NORTH AMERICAN MENOPAUSE SOCIETY

Bone mineral density should be measured in:

1.   Postmenopausal women who are at least 65 years of age regardless of risk factors
2.   Postmenopausal women with medical causes of bone loss, regardless of age

BMD testing should be considered in:

1. Postmenopausal women younger than age 65 with one or more of the following risk factors: fracture after menopause, body weight $<$ 127 lb or BMI $<$ 21 kg/m^2, parental hip fracture, current smoking.

   Management of osteoporosis in postmenopausal women: 2006 position statement of the North American Menopause Society. Menopause 2006;13:340–367.

UNITED STATES PREVENTIVE SERVICES TASK FORCE RECOMMENDATIONS FOR BONE DENSITY TESTING

Bone density should be measured in:

1. All postmenopausal women 65 years of age and older
2. All postmenopausal women age 60–64 at high risk for osteoporosis

U.S. Preventive Services Task Force. Screening for osteoporosis in postmenopausal women: recommendations and rationale. Ann Intern Med 2002;137:526–528.

VII Appendix

Bone Mass Measurement Act of 1997

Medicare recipients are potentially eligible for reimbursement of bone mass measurements performed in the following circumstances:

- An estrogen-deficient woman at clinical risk for osteoporosis, based on medical history and other findings
- An individual with vertebral abnormalities demonstrated by X ray suggesting osteoporosis, osteopenia or fracture
- An individual being monitored to assess efficacy of an FDA-approved drug therapy
- An individual receiving or expected to receive corticosteroids $\geq$ 7.5 mg of prednisone for $>$ 3 months
- An individual with primary hyperparathyroidism

Frequency Standards

At least *23* months must have passed since the month the last measurement was performed except. . .

- For monitoring patients on long-term glucocorticoid therapy
- For allowing a confirmatory baseline measurement to permit future monitoring if the initial test was performed with a technique that is different from the proposed monitoring method

Federal Register 42 CFR Part 410; Vol 63, No. 121, June 24, 1998.

VIII Appendix

CPT/HCPCS Codes for Bone Densitometry

Technique	Skeletal Site	CPT Code	HCPCS Code
Dual-energy x-ray absorptiometry[a,d]	PA Spine Lateral Spine Pelvis Proximal Femur	77080	
Dual-energy x-ray absorptiometry	Vertebral Fracture Assessment	77082	
Dual-energy x-ray absorptiometry[b]	Body Composition	0028T	
Dual-energy x-ray absorptiometry	Forearm Heel Phalanges	77081	
Single-energy x-ray absorptiometry	Heel		G0130
Quantitative ultrasound[c]	Heel	76977	
Radiographic absorptiometry	Hand	77083	
Computer-assisted radiogrammetry	Phalanges Forearm	77083	
Quantitative-computed tomography[a]	PA spine Proximal Femur	77078	
Quantitative-computed tomography	Forearm Heel	77079	
Single-photon absorptiometry	Forearm	78350	
Dual-photon absorptiometry[a,e]	PA Spine Proximal Femur Total Body	78351	

[a]In the description of the code, the skeletal sites noted are characterized as axial sites, even though anatomically the proximal femur and pelvis are part of the appendicular skeleton.

[b]This is a temporary, CPT Level I Category III code.

[c]The code for quantitative ultrasound indicates both the procedure and the interpretation.

[d]There is no specific code for a dual-energy x-ray total body bone density study. However, the 77080 code describes a dual-energy x-ray study of one or more sites such as the spine, pelvis, and proximal femur.

[e]This code is described as dual photon absorptiometry, one or more sites. Therefore, total body bone density studies are not excluded by this code.

CPT^{TM} codes are Level I codes developed and maintained by the AMA. These are five digit codes that are widely accepted for reporting services by healthcare providers. The modifier "-TC" is attached to the code to indicate billing for the technical component.

HCPCS (Healthcare Common Procedure Coding System) codes, pronounced "hick-picks," are Level II codes that are developed and assigned by the Health Care Finance Administration (HCFA). They are intended to meet the needs of Medicare and Medicaid and allow coordination of government programs by providing a uniform reporting system of procedures. HCPCS codes *begin* with a letter and are followed by four digits.

CPT Level I Category III codes are temporary codes assigned to new or emerging technologies. They allow data collection for the particular procedures. Category III codes consist of four digits *followed* by a letter. If a Category III code is available for a procedure, it must be used. Procedures assigned a Category III code may eventually receive a Category I code. Category III codes are not assigned for longer than 5 years however.

REFERENCES

AMA. HCPCS 2008. Medicare's National Level II Codes: Color-coded Complete Drug Index. Chicago, IL: AMA Press, 2007.

AMA. CPT 2009. Professional edition. Chicago, IL: AMA Press, 2008.

IX Appendix

1998 NHANES III Proximal Femur Reference Data

Table IX-1

NHANES III Femoral Neck BMD Data for Non-Hispanic White Women as Acquired on the Hologic QDR-1000

Age	N	Mean BMD (g/cm^2)	SD (g/cm^2)
20–29	409	0.858	0.120
30–39	518	0.825	0.120
40–49	444	0.791	0.125
50–59	450	0.737	0.121
60–69	454	0.681	0.119
70–79	556	0.619	0.110
80+	420	0.573	0.108

Table IX-2

NHANES III Trochanter BMD Data for Non-Hispanic White Women as Acquired on the Hologic QDR-1000

Age	N	Mean BMD (g/cm^2)	SD (g/cm^2)
20–29	409	0.708	0.099
30–39	518	0.699	0.101
40–49	444	0.676	0.104
50–59	450	0.637	0.105
60–69	454	0.595	0.108
70–79	556	0.550	0.106
80+	420	0.509	0.108

Table IX-3
NHANES III Total Femur BMD Data for Non-Hispanic White Women as Acquired on the
Hologic QDR-1000

Age	N	Mean BMD (g/cm^2)	SD (g/cm^2)
20–29	409	0.942	0.122
30–39	518	0.931	0.129
40–49	444	0.907	0.135
50–59	450	0.863	0.138
60–69	454	0.797	0.139
70–79	556	0.728	0.128
80+	420	0.668	0.134

Table IX-4
Standardized NHANES III Total Femur BMD Data for Non-Hispanic White Women as
Acquired on the Hologic QDR-1000

Age	N	Mean BMD (mg/cm^2)	SD (mg/cm^2)
20–29	409	955	123
30–39	518	945	130
40–49	444	920	136
50–59	450	876	139
60–69	454	809	140
70–79	556	740	129
80+	420	679	135

Table IX-5
NHANES III Femoral Neck BMD Data for Non-Hispanic White Men as Acquired on the
Hologic QDR-1000

Age	N	Mean BMD (g/cm^2)	SD (g/cm^2)
20–29	382	0.934	0.137
30–39	416	0.887	0.134
40–49	409	0.839	0.124
50–59	393	0.813	0.125
60–69	477	0.788	0.135
70–79	445	0.754	0.131
80+	408	0.698	0.140

Table IX-6
NHANES III Trochanter BMD Data for Non-Hispanic White Men as Acquired on the Hologic QDR-1000

Age	N	Mean BMD (g/cm^2)	SD (g/cm^2)
20–29	382	0.778	0.118
30–39	416	0.762	0.112
40–49	409	0.737	0.107
50–59	393	0.740	0.120
60–69	477	0.736	0.129
70–79	445	0.711	0.127
80+	408	0.670	0.137

Table IX-7
NHANES III Total Femur BMD Data for Non-Hispanic White Men as Acquired on the Hologic QDR-1000

Age	N	Mean BMD (g/cm^2)	SD (g/cm^2)
20–29	382	1.041	0.144
30–39	416	1.024	0.143
40–49	409	0.988	0.139
50–59	393	0.977	0.142
60–69	477	0.955	0.155
70–79	445	0.915	0.150
80+	408	0.846	0.159

Table IX-8
NHANES III Standardized Total Femur BMD Data for Non-Hispanic White Men as Acquired on the Hologic QDR-1000

Age	N	Mean BMD (mg/cm^2)	SD (mg/cm^2)
20–29	382	1055	146
30–39	416	1038	144
40–49	409	1002	140
50–59	393	990	143
60–69	477	969	157
70–79	445	928	151
80+	408	859	161

Table IX-9
NHANES III Femoral Neck BMD Data for Non-Hispanic Black Women as Acquired on the
Hologic QDR-1000

Age	N	Mean BMD (g/cm^2)	SD (g/cm^2)
20–29	492	0.950	0.133
30–39	538	0.913	0.130
40–49	404	0.915	0.153
50–59	241	0.852	0.158
60–69	255	0.770	0.128
70–79	144	0.722	0.138
80+	55	0.632	0.115

Table IX-10
NHANES III Trochanteric BMD Data for Non-Hispanic Black Women as Acquired on the
Hologic QDR-1000

Age	N	Mean BMD (g/cm^2)	SD (g/cm^2)
20–29	492	0.753	0.113
30–39	538	0.733	0.114
40–49	404	0.752	0.127
50–59	241	0.700	0.130
60–69	255	0.646	0.117
70–79	144	0.613	0.117
80+	55	0.539	0.118

Table IX-11
NHANES III Total Femur BMD Data for Non-Hispanic Black Women as Acquired on the
Hologic QDR-1000

Age	N	Mean BMD (g/cm^2)	SD (g/cm^2)
20–29	492	1.026	0.134
30–39	538	1.003	0.140
40–49	404	1.020	0.159
50–59	241	0.959	0.173
60–69	255	0.877	0.153
70–79	144	0.825	0.153
80+	55	0.711	0.145

Table IX-12
**Standardized NHANES III Total Femur BMD Data for Non-Hispanic Black Women as
Acquired on the Hologic QDR-1000**

Age	N	Mean BMD (mg/cm^2)	SD (mg/cm^2)
20–29	492	1040	135
30–39	538	1017	142
40–49	404	1034	160
50–59	241	972	175
60–69	255	890	154
70–79	144	837	154
80+	55	723	146

Table IX-13
**NHANES III Femoral Neck BMD Data for Non-Hispanic Black Men as Acquired on the
Hologic QDR-1000**

Age	N	Mean BMD (g/cm^2)	SD (g/cm^2)
20–29	460	1.074	0.168
30–39	450	1.005	0.158
40–49	335	0.935	0.145
50–59	196	0.908	0.169
60–69	255	0.854	0.148
70–79	147	0.815	0.154
80+	49	0.769	0.189

Table IX-14
**NHANES III Trochanteric BMD Data for Non-Hispanic Black Men as Acquired on the Hologic
QDR-1000**

Age	N	Mean BMD (g/cm^2)	SD (g/cm^2)
20–29	460	0.871	0.141
30–39	450	0.823	0.135
40–49	335	0.789	0.126
50–59	196	0.789	0.138
60–69	255	0.763	0.132
70–79	147	0.724	0.143
80+	49	0.699	0.163

Table IX-15
NHANES III Total Femur BMD Data for Non-Hispanic Black Men as Acquired on the Hologic
QDR-1000

Age	N	Mean BMD (g/cm^2)	SD (g/cm^2)
20–29	460	1.174	0.169
30–39	450	1.126	0.165
40–49	335	1.079	0.160
50–59	196	1.058	0.183
60–69	255	1.013	0.166
70–79	147	0.970	0.171
80+	49	0.920	0.192

Table IX-16
Standardized NHANES III Total Femur BMD Data for Non-Hispanic Black Men as Acquired
on the Hologic QDR-1000

Age	N	Mean BMD (g/cm^2)	SD (g/cm^2)
20–29	460	1190	171
30–39	450	1141	166
40–49	335	1094	162
50–59	196	1072	185
60–69	255	1027	168
70–79	147	984	173
80+	49	933	194

Table IX-17
NHANES III Femoral Neck BMD Data for Mexican-American Women as Acquired on the
Hologic QDR-1000

Age	N	Mean BMD (g/cm^2)	SD (g/cm^2)
20–29	479	0.874	0.111
30–39	428	0.867	0.125
40–49	320	0.848	0.127
50–59	174	0.758	0.116
60–69	283	0.711	0.112
70–79	103	0.646	0.123
80+	40	0.556∗	0.106

*Unreliable estimate

Table IX-18
**NHANES III Trochanteric BMD Data for Mexican-American Women as Acquired on the
Hologic QDR-1000**

Age	N	Mean BMD (g/cm^2)	SD (g/cm^2)
20–29	479	0.696	0.092
30–39	428	0.703	0.109
40–49	320	0.701	0.100
50–59	174	0.637	0.109
60–69	283	0.601	0.104
70–79	103	0.535	0.112
80+	40	0.450*	0.111

*Unreliable estimate

Table IX-19
**NHANES III Total Femur BMD Data for Mexican-American Women as Acquired on the
Hologic QDR-1000**

Age	N	Mean BMD (g/cm^2)	SD (g/cm^2)
20–29	479	0.950	0.113
30–39	428	0.961	0.137
40–49	320	0.960	0.132
50–59	174	0.877	0.138
60–69	283	0.819	0.124
70–79	103	0.732	0.146
80+	40	0.611*	0.150

*Unreliable estimate

Table IX-20
**NHANES III Standardized Total Femur BMD Data for Mexican-American Women as Acquired
on the Hologic QDR-1000**

Age	N	Mean BMD (g/cm^2)	SD (g/cm^2)
20–29	479	963	114
30–39	428	975	138
40–49	320	973	133
50–59	174	890	139
60–69	283	832	125
70–79	103	744	147
80+	40	622*	151

*Unreliable estimate

Table IX-21
NHANES III Femoral Neck BMD Data for Mexican-American Men as Acquired on the Hologic QDR-1000

Age	N	Mean BMD (g/cm^2)	SD (g/cm^2)
20–29	623	0.982	0.137
30–39	429	0.922	0.127
40–49	354	0.870	0.121
50–59	156	0.857	0.130
60–69	298	0.827	0.123
70–79	124	0.798	0.135
80+	47	0.709	0.119

Table IX-22
NHANES III Trochanteric BMD Data for Mexican-American Men as Acquired on the Hologic QDR-1000

Age	N	Mean BMD (g/cm^2)	SD (g/cm^2)
20–29	623	0.787	0.111
30–39	429	0.756	0.106
40–49	354	0.737	0.100
50–59	156	0.743	0.103
60–69	298	0.730	0.109
70–79	124	0.710	0.111
80+	47	0.639	0.120

Table IX-23
NHANES III Total Femur BMD Data for Mexican-American Men as Acquired on the Hologic QDR-1000

Age	N	Mean BMD (g/cm^2)	SD (g/cm^2)
20–29	623	1.060	0.135
30–39	429	1.035	0.131
40–49	354	1.011	0.128
50–59	156	1.007	0.131
60–69	298	0.984	0.143
70–79	124	0.947	0.132
80+	47	0.854	0.127

Table IX-24
NHANES III Standardized Total Femur BMD Data for Mexican-American Men as Acquired on the Hologic QDR-1000

Age	N	Mean BMD (mg/cm^2)	SD (mg/cm^2)
20–29	623	1074	136
30–39	429	1049	132
40–49	354	1025	129
50–59	156	1021	132
60–69	298	998	144
70–79	124	961	133
80+	47	867	128

Adapted with permission of the publisher from Looker AC et al. Updated data on proximal femur bone mineral levels of US adults. Osteoporos Int 1998;8:468–489.

X Appendix

Norland DXA Reference Data[1]

Table X-1
Norland DXA Caucasian Female PA Spine Reference Data. Active Date 4/00. All values are in g/cm² with the exception of the total spine sBMD which is in mg/cm²

Region	Young Reference	SD	Age 20 BMD	Age 50 BMD	Age 80 BMD
L1	1.029	0.155	1.034	1.034	0.779
L2	1.097	0.163	1.094	1.094	0.824
L3	1.115	0.171	1.108	1.108	0.885
L4	1.082	0.169	1.063	1.063	0.893
L1–L4	1.086	0.159	1.074	1.074	0.851
L2–L4	1.102	0.162	1.087	1.087	0.869
Total Spine sBMD	1186	175	1170	1170	935

Table X-2
Norland DXA Caucasian Female Proximal Femur Reference Data. Active 4/00. All values are in g/cm²

Region	Young Reference	SD	Age 20 BMD	Age 50 BMD	Age 80 BMD
Femoral Neck	0.987	0.117	0.981	0.873	0.655
Trochanter	0.787	0.109	0.775	0.699	0.599
Ward's	0.851	0.125	0.848	0.674	0.441

[1]Reproduced with permission of Norland A CooperSurgical Company, Ft. Atkinson, WI.

Table X-3
Norland DXA Caucasian Female Total Hip sBMD Reference Data Based on NHANES III. Values are in mg/cm^2

Region	Young Reference	SD	Age 20 BMD	Age 25 BMD	Age 35 BMD	Age 45 BMD	Age 55 BMD	Age 65 BMD	Age 75 BMD	Age 85 BMD
Total Hip sBMD	956	123	956	956	944	920	876	809	740	679

Table X-4
Norland Caucasian Female Forearm Reference Data for Central DXA Devices. Active 7/98. Values are for the hydroxyapatite calibration. All values are in g/cm^2

Region	Young Reference	SD	Age 20 BMD	Age 50 BMD	Age 90 BMD
Distal Forearm	0.3567	0.0539	0.3567	0.3589	0.2279
Proximal Forearm	0.8552	0.07484	0.8552	0.8731	0.5463
Proximal Radius	0.8481	0.07472	0.8481	0.8575	0.5369

Table X-5
Norland DXA Caucasian Male PA Spine Reference Data. Active Date 4/00. All values are in g/cm^2 with the exception of the total spine sBMD, which is in mg/cm^2

Region	Young Reference	SD	Age 20 BMD	Age 50 BMD	Age 80 BMD
L1	1.105	0.167	1.096	1.066	1.036
L2	1.171	0.186	1.158	1.127	1.097
L3	1.181	0.191	1.165	1.146	1.127
L4	1.134	0.199	1.126	1.126	1.126
L1–L4	1.148	0.176	1.130	1.119	1.107
L2–L4	1.164	0.184	1.146	1.133	1.121
Total Spine sBMD	1253	198	1233	1219	1206

Table X-6
Norland DXA Caucasian Male Proximal Femur Reference Data. Active 4/00. All values are in g/cm^2 with the exception of the total hip sBMD, which is in mg/cm^2. Total hip sBMD is based on Norland reference data

Region	Young Reference	SD	Age 20 BMD	Age 50 BMD	Age 80 BMD
Femoral Neck	1.108	0.125	1.111	0.940	0.770
Trochanter	0.933	0.113	0.925	0.838	0.751
Ward's	0.908	0.126	0.905	0.680	0.456
Total Hip sBMD	1147	123	1150	1027	903

Table X-7

Norland DXA Caucasian-Hispanic Female PA Spine Reference Data. Active Date 4/00. All values are in g/cm^2 with the exception of the total spine sBMD, which is in mg/cm^2

Region	Young Reference	SD	Age 20 BMD	Age 50 BMD	Age 80 BMD
L1	1.054	0.152	1.041	1.041	0.775
L2	1.124	0.159	1.100	1.100	0.820
L3	1.133	0.167	1.112	1.112	0.882
L4	1.084	0.165	1.066	1.066	0.892
L1–L4	1.101	0.156	1.080	1.080	0.848
L2–L4	1.115	0.158	1.091	1.091	0.866
Total Spine sBMD	1200	170	1174	1174	932

Table X-8

Norland DXA Caucasian-Hispanic Female Proximal Femur Reference Data. Active 4/00. All values are in g/cm^2 with the exception of the total hip sBMD which is in mg/cm^2. Total hip sBMD is based on Norland reference data

Region	Young Reference	SD	Age 20 BMD	Age 50 BMD	Age 80 BMD
Femoral Neck	0.995	0.116	0.993	0.871	0.656
Trochanter	0.779	0.108	0.772	0.698	0.560
Ward's	0.846	0.124	0.849	0.674	0.442
Total Hip sBMD	1022	118	1010	920	741

Table X-9

Norland DXA Caucasian-Hispanic Male PA Spine Reference Data. Active Date 4/00. All values are in g/cm^2 with the exception of the total spine sBMD, which is in mg/cm^2

Region	Young Reference	SD	Age 20 BMD	Age 50 BMD	Age 80 BMD
L1	1.109	0.167	1.096	1.065	1.034
L2	1.176	0.187	1.160	1.125	1.089
L3	1.183	0.191	1.166	1.142	1.119
L4	1.138	0.199	1.122	1.122	1.122
L1–L4	1.152	0.176	1.130	1.118	1.106
L2–L4	1.168	0.185	1.147	1.130	1.113
Total Spine sBMD	1257	199	1234	1216	1198

Table X-10

Norland DXA Caucasian-Hispanic Male Proximal Femur Reference Data. Active 4/00. All values are in g/cm^2 with the exception of the total hip sBMD, which is in mg/cm^2. Total hip sBMD is based on Norland reference data

Region	Young Reference	SD	Age 20 BMD	Age 50 BMD	Age 80 BMD
Femoral Neck	1.107	0.126	1.109	0.939	0.769
Trochanter	0.928	0.114	0.919	0.835	0.751
Ward's	0.900	0.128	0.898	0.678	0.457
Total Hip sBMD	1146	124	1147	1025	903

Table X-11

Norland DXA Hispanic Female PA Spine Reference Data. Active Date 4/00. All values are in g/cm^2 with the exception of the total spine sBMD which is in mg/cm^2

Region	Young Reference	SD
L1	1.088	0.126
L2	1.149	0.122
L3	1.144	0.126
L4	1.080	0.121
L1–L4	1.112	0.119
L2–L4	1.123	0.117
Total Spine sBMD	1207	128

Table X-12

Norland DXA Hispanic Female Proximal Femur Reference Data. Active 4/00. All values are in g/cm^2 with the exception of the total hip sBMD, which is in mg/cm^2

Region	Young Reference	SD
Femoral Neck	0.982	0.111
Trochanter	0.740	0.103
Ward's	0.800	0.125
Total Hip sBMD	1021	109

Table X-13
**Norland DXA Asian Female PA Spine Reference Data. Active Date 4/00.
All values are in g/cm^2 with the exception of the total spine sBMD,
which is in mg/cm^2**

Region	Young Reference	SD
L1	1.005	0.129
L2	1.061	0.132
L3	1.090	0.130
L4	1.036	0.127
L1–L4	1.043	0.125
L2–L4	1.062	0.126
Total Spine sBMD	1142	135

Table X-14
**Norland DXA Asian Female Proximal Femur Reference Data. Active
4/00. All values are in g/cm^2 with the exception of the total hip sBMD
which is in mg/cm^2**

Region	Young Reference	SD
Femoral Neck	0.866	0.113
Trochanter	0.697	0.108
Ward's	0.712	0.128
Total Hip sBMD	929	117

Table X-15
**Norland DXA Black Female PA Spine Reference Data. Active Date 4/00.
All values are in g/cm^2 with the exception of the total spine sBMD,
which is in mg/cm^2**

Region	Young Reference	SD
L1	1.206	0.140
L2	1.256	0.139
L3	1.259	0.136
L4	1.216	0.127
L1–L4	1.239	0.126
L2–L4	1.243	0.127
Total Spine sBMD	1338	137

Table X-16
Norland DXA Black Female Proximal Femur Reference Data. Active
4/00. All values are in g/cm^2 with the exception of the total hip sBMD,
which is in mg/cm^2

Region	Young Reference	SD
Femoral Neck	1.046	0.140
Trochanter	0.797	0.125
Ward's	0.852	0.164
Total Hip sBMD	1081	140

Table X-17
Norland DXA Black Male PA Spine Reference Data. Active Date 4/00.
All values are in g/cm^2 with the exception of the total spine sBMD,
which is in mg/cm^2

Region	Young Reference	SD
L1	1.232	0.184
L2	1.291	0.204
L3	1.309	0.215
L4	1.279	0.201
L1–L4	1.271	0.191
L2–L4	1.293	0.202
Total Spine sBMD	1391	218

Table X-18
Norland DXA Black Male Proximal Femur Reference Data. Active 4/00.
All values are in g/cm^2 with the exception of the total hip sBMD, which
is in mg/cm^2

Region	Young Reference	SD
Femoral Neck	1.161	0.205
Trochanter	0.933	0.181
Ward's	0.939	0.217
Total Hip sBMD	1188	198

XI Appendix

Hologic DXA Reference Data[1]

Table XI-1
Hologic DXA PA Lumbar Spine L1–L4 Reference Data for Caucasian Women. Active date11/4/91. Peak BMD 1.047 g/cm^2. All BMD values are in g/cm^2

Age	BMD	SD
20	1.019	0.110
25	1.040	0.110
30	1.047	0.110
35	1.041	0.110
40	1.024	0.110
45	0.999	0.110
50	0.967	0.110
60	0.892	0.110
70	0.815	0.110
80	0.752	0.110
85	0.731	0.110

[1]Reproduced courtesy of Hologic, Inc., Bedford, MA. T-scores on Hologic printouts are based on gender-specific comparisons to Caucasian reference databases. However, this output may be user-configured on some Hologic devices.

Table XI-2
Hologic DXA Supine Lateral Lumbar Spine L2–L4
Reference Data for Caucasian Women. Active date 7/27/92.
Peak BMD 0.82 g/cm². All BMD values are in g/cm²

Age	BMD	SD
20	0.820	0.084
25	0.813	0.084
30	0.803	0.084
35	0.789	0.084
40	0.770	0.084
45	0.746	0.084
50	0.716	0.084
55	0.680	0.084
60	0.636	0.084
65	0.584	0.084
70	0.523	0.084
75	0.453	0.084
80	0.373	0.084
85	0.283	0.084

Table XI-3
Hologic DXA Total Hip Caucasian Female Reference Data
Based on NHANES III. Active Date 2/1/97. Peak BMD
0.942 g/cm². BMD values are in g/cm²

Age	BMD	SD
20	0.942	0.122
25	0.942	0.122
30	0.939	0.122
35	0.933	0.122
40	0.922	0.122
45	0.907	0.122
50	0.886	0.122
55	0.860	0.122
60	0.827	0.122
65	0.793	0.122
70	0.759	0.122
75	0.725	0.122
80	0.691	0.122
85	0.657	0.122

Table XI-4
**Hologic DXA Femoral Neck Caucasian Female Reference
Data Based on NHANES III. Active Date 2/1/97. Peak
BMD 0.849 g/cm^2. BMD values are in g/cm^2**

Age	BMD	SD
20	0.849	0.111
25	0.849	0.111
35	0.831	0.111
45	0.803	0.111
55	0.732	0.111
65	0.682	0.111
75	0.618	0.111
85	0.569	0.111

Table XI-5
**Hologic DXA Trochanteric Caucasian Female Reference
Data Based on NHANES III. Active Date 2/1/97. Peak
BMD 0.703 g/cm^2. BMD values are in g/cm^2**

Age	BMD	SD
20	0.703	0.101
25	0.703	0.101
35	0.703	0.101
45	0.681	0.101
55	0.635	0.101
65	0.594	0.101
75	0.546	0.101
85	0.504	0.101

Table XI-6
**Hologic DXA Intertrochanteric Caucasian Female Reference
Data Based on NHANES III. Active Date 2/1/97. Peak
BMD 1.100 g/cm^2. BMD values are in g/cm^2**

Age	BMD	SD
20	1.086	0.155
25	1.086	0.155
35	1.100	0.155
45	1.077	0.155
55	1.032	0.155
65	0.952	0.155
75	0.860	0.155
85	0.776	0.155

Table XI-7
Hologic DXA Ward's Caucasian Female Reference Data
Based on NHANES III. Active Date 2/1/97. Peak BMD
0.734 g/cm^2. BMD values are in g/cm^2

Age	BMD	SD
20	0.734	0.117
25	0.734	0.117
35	0.695	0.117
45	0.634	0.117
55	0.535	0.117
65	0.470	0.117
75	0.403	0.117
85	0.361	0.117

Table XI-8
Hologic DXA Ultradistal Forearm Caucasian Female
Reference Data. Active date 10/25/91. Peak BMD
0.412 g/cm^2. All values in g/cm^2

Age	BMD	SD
20	0.412	0.051
25	0.410	0.051
30	0.407	0.051
35	0.404	0.051
40	0.398	0.051
45	0.392	0.051
50	0.384	0.051
55	0.374	0.051
60	0.362	0.051
65	0.348	0.051
70	0.331	0.051
75	0.312	0.051
80	0.291	0.051
85	0.266	0.051

Table XI-9
Hologic DXA Mid Forearm Caucasian Female Reference Data. Active date 10/25/91. Peak BMD 0.588 g/cm². All values in g/cm²

Age	BMD	SD
20	0.588	0.053
25	0.585	0.053
30	0.581	0.053
35	0.575	0.053
40	0.568	0.053
45	0.558	0.053
50	0.546	0.053
55	0.532	0.053
60	0.514	0.053
65	0.494	0.053
70	0.470	0.053
75	0.442	0.053
80	0.410	0.053
85	0.374	0.053

Table XI-10
Hologic DXA 1/3 Forearm Caucasian Female Reference Data. Active date 10/25/91. Peak BMD 0.684 g/cm². All values in g/cm²

Age	BMD	SD
20	0.684	0.058
25	0.681	0.058
30	0.677	0.058
35	0.671	0.058
40	0.663	0.058
45	0.653	0.058
50	0.641	0.058
55	0.626	0.058
60	0.608	0.058
65	0.586	0.058
70	0.561	0.058
75	0.532	0.058
80	0.499	0.058
85	0.462	0.058

Table XI-11
Hologic DXA Total Forearm Caucasian Female Reference
Data. Active date 10/25/91. Peak BMD 0.564 g/cm^2. All
values in g/cm^2

Age	BMD	SD
20	0.564	0.051
25	0.561	0.051
30	0.557	0.051
35	0.552	0.051
40	0.546	0.051
45	0.537	0.051
50	0.526	0.051
55	0.513	0.051
60	0.497	0.051
65	0.478	0.051
70	0.456	0.051
75	0.430	0.051
80	0.401	0.051
85	0.368	0.051

Table XI-12
Hologic DXA Whole Body Bone Density Caucasian Female
Reference Data. Active date 10/25/91. Peak BMD
1.136 g/cm^2. All values are in g/cm^2

Age	BMD	SD
20	1.136	0.095
25	1.127	0.095
30	1.116	0.095
35	1.103	0.095
40	1.088	0.095
45	1.071	0.095
50	1.052	0.095
55	1.031	0.095
60	1.008	0.095
65	0.983	0.095
70	0.957	0.095
75	0.928	0.095
80	0.897	0.095
85	0.864	0.095

Table XI-13
**Hologic DXA PA Lumbar Spine L1–L4 Caucasian Male
Reference Data. Active date 11/4/91. Peak BMD
1.091 g/cm². All values in g/cm²**

Age	BMD	SD
20	1.091	0.110
25	1.091	0.110
35	1.091	0.110
45	1.068	0.110
50	1.053	0.110
55	1.038	0.110
60	1.023	0.110
65	1.008	0.110
70	0.993	0.110
75	0.978	0.110
80	0.963	0.110
85	0.947	0.110

Table XI-14
**Hologic DXA Total Hip Caucasian Male Reference Data
Based on NHANES III. Active Date 2/1/97. Peak BMD
1.033 g/cm². BMD values are in g/cm²**

Age	BMD	SD
20	1.033	0.151
25	1.033	0.151
35	1.014	0.151
45	0.995	0.151
55	0.975	0.151
65	0.957	0.151
75	0.910	0.151
85	0.842	0.151

Table XI-15
**Hologic DXA Femoral Neck Caucasian Male Reference Data
Based on NHANES III. Active Date 2/1/97. Peak BMD
0.930 g/cm². BMD values are in g/cm²**

Age	BMD	SD
20	0.930	0.136
25	0.930	0.136
35	0.885	0.136
45	0.845	0.136
55	0.814	0.136
65	0.790	0.136
75	0.749	0.136
85	0.698	0.136

Table XI-16
**Hologic DXA Trochanter Caucasian Male Reference Data
Based on NHANES III. Active Date 2/1/97. Peak BMD
0.777 g/cm^2. BMD Values are in g/cm^2**

Age	BMD	SD
20	0.777	0.126
25	0.777	0.126
35	0.754	0.126
45	0.743	0.126
55	0.738	0.126
65	0.739	0.126
75	0.705	0.126
85	0.667	0.126

Table XI-17
**Hologic DXA Intertrochanteric Caucasian Male Reference
Data Based on NHANES III. Active Date 2/1/97. Peak
BMD 1.195 g/cm^2. BMD values are in g/cm^2**

Age	BMD	SD
20	1.195	0.181
25	1.195	0.181
35	1.188	0.181
45	1.171	0.181
55	1.149	0.181
65	1.117	0.181
75	1.058	0.181
85	0.974	0.181

Table XI-18
**Hologic DXA Ward's Caucasian Male Reference Data Based
on NHANES III. Active Date 2/1/97. Peak BMD
0.785 g/cm^2. BMD values are in g/cm^2**

Age	BMD	SD
20	0.785	0.141
25	0.785	0.141
35	0.712	0.141
45	0.637	0.141
55	0.579	0.141
65	0.541	0.141
75	0.487	0.141
85	0.44	0.141

Table XI-19
**Hologic DXA Ultradistal Forearm Caucasian Male
Reference Data. Active date 10/25/91. Peak BMD
0.509 g/cm^2. All values in g/cm^2**

Age	BMD	SD
20	0.509	0.056
25	0.506	0.056
30	0.503	0.056
35	0.498	0.056
40	0.493	0.056
45	0.488	0.056
50	0.481	0.056
55	0.474	0.056
60	0.467	0.056
65	0.458	0.056
70	0.449	0.056
75	0.440	0.056
80	0.429	0.056
85	0.418	0.056

Table XI-20
**Hologic DXA Mid Forearm Caucasian Male Reference Data.
Active date 10/25/91. Peak BMD 0.695 g/cm^2. All values in
g/cm^2**

Age	BMD	SD
20	0.695	0.055
25	0.694	0.055
30	0.692	0.055
35	0.690	0.055
40	0.686	0.055
45	0.682	0.055
50	0.677	0.055
55	0.671	0.055
60	0.663	0.055
65	0.654	0.055
70	0.644	0.055
75	0.632	0.055
80	0.618	0.055
85	0.603	0.055

Table XI-21
**Hologic DXA Total Forearm Caucasian Male Reference
Data. Active date 10/25/91. Peak BMD 0.679 g/cm^2. All
values in g/cm^2**

Age	BMD	SD
20	0.679	0.054
25	0.678	0.054
30	0.675	0.054
35	0.673	0.054
40	0.669	0.054
45	0.664	0.054
50	0.658	0.054
55	0.650	0.054
60	0.641	0.054
65	0.631	0.054
70	0.618	0.054
75	0.604	0.054
80	0.587	0.054
85	0.569	0.054

Table XI-22
**Hologic DXA PA Lumbar Spine L1–L4 Black Female
Reference Data. Active date 11/4/91. Peak BMD
1.150 g/cm^2. All values in g/cm^2**

Age	BMD	SD
20	1.119	0.110
25	1.142	0.110
30	1.150	0.110
35	1.143	0.110
40	1.124	0.110
45	1.097	0.110
50	1.062	0.110
60	0.979	0.110
70	0.895	0.110
80	0.826	0.110
85	0.803	0.110

Table XI-23
Hologic DXA Total Hip Black Female Reference Data Based on NHANES III. Active date 11/25/96. Peak BMD 1.031 g/cm². All values are in g/cm²

Age	BMD	SD
20	1.030	0.156
25	1.030	0.156
35	1.004	0.156
45	1.031	0.156
55	0.945	0.156
65	0.879	0.156
75	0.832	0.156
85	0.755	0.156

Table XI-24
Hologic DXA Femoral Neck Black Female Reference Data Based on NHANES III. Active date 11/25/96. Peak BMD 0.951 g/cm². All values are in g/cm²

Age	BMD	SD
20	0.951	0.142
25	0.951	0.142
35	0.913	0.142
45	0.925	0.142
55	0.839	0.142
65	0.769	0.142
75	0.728	0.142
85	0.670	0.142

Table XI-25
Hologic DXA Trochanteric Black Female Reference Data. Based on NHANES III. Active date 11/25/96. Peak BMD 0.761 g/cm². BMD values are in g/cm²

Age	BMD	SD
20	0.760	0.123
25	0.760	0.123
35	0.734	0.123
45	0.761	0.123
55	0.691	0.123
65	0.646	0.123
75	0.620	0.123
85	0.572	0.123

Table XI-26

Hologic DXA Intertrochanteric Black Female Reference Data Based on NHANES III. Active date 11/25/96. Peak BMD 1.220 g/cm^2. All values are in g/cm^2

Age	BMD	SD
20	1.203	0.190
25	1.203	0.190
35	1.187	0.190
45	1.220	0.190
55	1.128	0.190
65	1.042	0.190
75	0.988	0.190
85	0.891	0.190

Table XI-27

Hologic DXA Ward's Area Black Female Reference Data Based on NHANES III. Active date 11/25/96. Peak BMD is 0.834 g/cm^2. BMD values are in g/cm^2

Age	BMD	SD
20	0.834	0.147
25	0.834	0.147
35	0.762	0.147
45	0.746	0.147
55	0.613	0.147
65	0.545	0.147
75	0.496	0.147
85	0.444	0.147

Table XI-28
**Hologic DXA PA Lumbar Spine L1–L4 Black Male
Reference Data. Active date 11/25/96. Peak BMD
1.198 g/cm². All values in g/cm²**

Age	BMD	SD
20	1.198	0.110
25	1.198	0.110
35	1.198	0.110
45	1.173	0.110
50	1.156	0.110
55	1.140	0.110
60	1.123	0.110
65	1.107	0.110
70	1.090	0.110
75	1.074	0.110
80	1.057	0.110
85	1.040	0.110

Table XI-29
**Hologic DXA Total Hip Black Male Reference Data Based
on NHANES III. Active date 11/25/97. Peak BMD
1.033 g/cm². All values in g/cm²**

Age	BMD	SD
20	1.177	0.172
25	1.177	0.172
35	1.125	0.172
45	1.062	0.172
55	1.053	0.172
65	1.025	0.172
75	0.973	0.172
85	0.900	0.172

Table XI-30
**Hologic DXA Femoral Neck Black Male Reference Data
Based on NHANES III. Active date 11/25/96. Peak BMD
1.073 g/cm². All values in g/cm²**

Age	BMD	SD
20	1.073	0.156
25	1.073	0.156
35	1.008	0.156
45	0.918	0.156
55	0.903	0.156
65	0.870	0.156
75	0.811	0.156
85	0.756	0.156

Table XI-31
Hologic DXA Trochanteric Black Male Reference Data
Based on NHANES III. Active date 11/25/97. Peak BMD
0.880 g/cm^2. All values in g/cm^2

Age	BMD	SD
20	0.880	0.138
25	0.880	0.138
35	0.829	0.138
45	0.773	0.138
55	0.789	0.138
65	0.775	0.138
75	0.730	0.138
85	0.691	0.138

Table XI-32
Hologic DXA Intertrochanteric Black Male Reference Data
Based on NHANES III. Active date 11/25/96. Peak BMD
1.361 g/cm^2. All values in g/cm^2

Age	BMD	SD
20	1.361	0.206
25	1.361	0.206
35	1.322	0.206
45	1.258	0.206
55	1.232	0.206
65	1.198	0.206
75	1.143	0.206
85	1.052	0.206

Table XI-33
Hologic DXA Ward's Black Male Reference Data Based on
NHANES III. Active date 11/25/96. Peak BMD
0.926 g/cm^2. All values in g/cm^2

Age	BMD	SD
20	0.926	0.173
25	0.926	0.173
35	0.824	0.173
45	0.708	0.173
55	0.661	0.173
65	0.62	0.173
75	0.554	0.173
85	0.501	0.173

Table XI-34
**Hologic DXA PA Lumbar Spine L1–L4 Hispanic Female
Reference Data. Active Date 11/25/96. Peak BMD
1.047 g/cm^2. BMD values are in g/cm^2**

Age	BMD	SD
20	1.019	0.110
25	1.040	0.110
30	1.047	0.110
35	1.041	0.110
40	1.024	0.110
45	0.999	0.110
50	0.967	0.110
60	0.892	0.110
70	0.815	0.110
80	0.752	0.110
85	0.731	0.110

Table XI-35
**Hologic DXA PA Lumbar Spine L1–L4 Hispanic Male
Reference Data. Active date 11/25/96. Peak BMD
1.091 g/cm^2. All values are in g/cm^2**

Age	BMD	SD
20	1.091	0.110
25	1.091	0.110
35	1.091	0.110
45	1.068	0.110
50	1.053	0.110
55	1.038	0.110
60	1.023	0.110
65	1.008	0.110
70	0.993	0.110
75	0.978	0.110
80	0.963	0.110
85	0.947	0.110

XII Appendix

Lunar Reference Data[1]

Table XII-1
Lunar PA Lumbar Spine L2–L4 DXA Reference Data for Caucasian Women. Peak L2–L4 BMD is 1.200 g/cm^2. The SD is 0.12 g/cm^2

Age	BMD (g/cm^2)
20	1.200
25	1.200
30	1.200
35	1.200
40	1.200
45	1.200
50	1.153
55	1.105
60	1.058
65	1.010
70	0.970
75	0.960
80	0.950
85	0.940

[1]Reproduced courtesy of GE Healthcare, Madison, WI.

Table XII-2
**Lunar PA Lumbar Spine L1–L4 DXA Reference
Data for Caucasian Women. Peak L2–L4 BMD
is 1.180 g/cm^2. The SD is 0.12 g/cm^2**

Age	BMD (g/cm^2)
20	1.180
25	1.180
30	1.180
35	1.180
40	1.180
45	1.180
50	1.133
55	1.085
60	1.038
65	0.990
70	0.950
75	0.940
80	0.930
85	0.920

Table XII-3
**Lunar Femoral Neck DXA Reference Data for
Caucasian Women. Peak femoral neck BMD is
0.980 g/cm^2. The SD is 0.12 g/cm^2**

Age	BMD (g/cm^2)
20	1.000
25	0.990
30	0.980
35	0.970
40	0.960
45	0.950
50	0.915
55	0.880
60	0.845
65	0.810
70	0.790
75	0.770
80	0.750
85	0.730

Table XII-4
Lunar Trochanteric DXA Reference Data for
Caucasian Women. Peak trochanteric BMD is
0.790 g/cm^2. The SD is 0.11 g/cm^2

Age	BMD (g/cm^2)
20	0.790
25	0.790
30	0.790
35	0.790
40	0.790
45	0.790
50	0.770
55	0.750
60	0.730
65	0.710
70	0.690
75	0.670
80	0.650
85	0.630

Table XII-5
Lunar Total Femur DXA Reference Data for
Caucasian Women. Peak total femur BMD is
1.000 g/cm^2. The SD is 0.12 g/cm^2

Age	BMD (g/cm^2)
20	1.010
25	1.005
30	1.000
35	0.995
40	0.990
45	0.985
50	0.955
55	0.925
60	0.895
65	0.865
70	0.838
75	0.810
80	0.783
85	0.755

Table XII-6
**Lunar PA Lumbar Spine L2–L4 DXA Reference
Data for Caucasian Men. Peak L2–L4 BMD is
1.240 g/cm². The SD is 0.12 g/cm²**

Age	BMD (g/cm²)
20	1.240
25	1.240
30	1.240
35	1.240
40	1.240
45	1.230
50	1.219
55	1.209
60	1.198
65	1.188
70	1.177
75	1.167
80	1.156
85	1.146

Table XII-7
**Lunar PA Lumbar Spine L1–L4 DXA Reference
Data for Caucasian Men. Peak L2–L4 BMD is
1.220 g/cm². The SD is 0.12 g/cm²**

Age	BMD (g/cm²)
20	1.220
25	1.220
30	1.220
35	1.220
40	1.220
45	1.210
50	1.199
55	1.189
60	1.178
65	1.168
70	1.157
75	1.147
80	1.136
85	1.126

Table XII-8
**Lunar Femoral Neck DXA Reference Data for
Caucasian Men. Peak femoral neck BMD is
1.070g/cm² . The SD is 0.13 g/cm²**

Age	BMD (g/cm²)
20	1.111
25	1.090
30	1.070
35	1.050
40	1.030
45	1.010
50	0.990
55	0.970
60	0.950
65	0.930
70	0.910
75	0.890
80	0.870
85	0.850

Table XII-9
**Lunar Trochanteric DXA Reference Data for
Caucasian Men. Peak trochanteric BMD is
0.930 g/cm² . The SD is 0.11 g/cm²**

Age	BMD (g/cm²)
20	0.945
25	0.938
30	0.930
35	0.923
40	0.915
45	0.908
50	0.900
55	0.893
60	0.885
65	0.878
70	0.870
75	0.863
80	0.855
85	0.848

Table XII-10
Lunar Total Femur DXA Reference Data for
Caucasian Men. Peak total femur BMD is
1.090 g/cm^2. The SD is 0.13 g/cm^2

Age	BMD (g/cm^2)
20	1.120
25	1.105
30	1.090
35	1.075
40	1.060
45	1.045
50	1.033
55	1.020
60	1.008
65	0.995
70	0.980
75	0.965
80	0.950
85	0.935

XIII Appendix

Densitometry Patient Demographic and Risk Factor Questionnaire

This questionnaire can also be found on the accompanying CD-ROM. The contents and format should be modified, if necessary, to meet the specific needs of the physician's practice. In its current form, the questionnaire is primarily intended to elicit responses that are needed to utilize absolute fracture risk prediction algorithms like FRAX™, the FORE FRC, and the Black Fracture Index. These fracture risk prediction algorithms are discussed in Chapter 10. A computerized version of the Black Fracture Index may also be found on the accompanying CD-ROM.

Densitometry Patient Questionnaire

Name:_____

Date of Birth:_____ Age:_____ Sex: F   M

Race/Ethnicity: Caucasian   Hispanic   Black   Asian   Native   American   Other

Current Weight:_____

Current Height:_____   Height at age 20:_____

Rate your overall health: Excellent   Good   Fair   Poor

For Women Only

1. Are you postmenopausal?   Yes   No
   If *yes*, at what age did you become menopausal?_____

2. Have you had a hysterectomy (removal of the uterus)?   Yes   No
   If *yes,* at what age?_____

3. Have you had both ovaries removed?   Yes   No
   If *yes,*at what age?_____

4. Do you take or have you ever taken estrogen or hormone replacement?   Yes   No
   If yes, what kind, what dose and when?

   _____

   _____

   _____

For Everyone

5. Have you been told that you have osteoporosis?   Yes   No
If *yes*, when?_____

6. Have you been told that you have low bone mass (osteopenia)   Yes   No
If *yes*, when?_____

7. Have you ever had a bone density test before?   Yes   No
If *yes,* when and where was it performed?

_____

_____

_____

If yes, what were you told about the results?

_____

_____

_____

8. Did your mother ever break her hip?   Yes   No

9. Did you father ever break his hip?   Yes   No

10. Have you had a broken bone since the age of 45?   Yes   No
    If *yes*, which bones have you broken and at what age?

_____

_____

11. Can you get up from a chair without using your arms?   Yes   No

12. Do you currently smoke?   Yes   No

13. Do you have rheumatoid arthritis?   Yes   No

14. Have you taken steroid pills for 3 months or more?   Yes   No

15. Do you have type I (insulin-dependent) diabetes?   Yes   No

16. Do you have three or more servings of alcoholic beverages a day? Yes   No

For Everyone-Osteoporosis Medications

17. Do you take or have you ever taken any of the following medications?

Drug	Yes, currently	In the past, but not now	Start Date	Stop Date	Never taken
Fosamax					
Actonel					
Boniva					
Reclast					
Evista					
Miacalcin					
Fortéo					

For Everyone

18. Do you have night-lights in your bedroom?	Yes	No
19. Do you have safety bars in your bathroom?	Yes	No
20. Do you have throw rugs in your home?	Yes	No
21. Do you have epilepsy?	Yes	No
22. Have you ever had hyperthyroidism?	Yes	No
23. Have you ever had hyperparathyroidism?	Yes	No
24. Have you ever had sprue or celiac disease?	Yes	No
25. Do you have Crohn's Disease?	Yes	No
26. Do you have ulcerative colitis?	Yes	No
27. Have you ever had cancer? If *yes,* what kind and when?	Yes	No

_____

_____

28. Have you ever had cancer chemotherapy?	Yes	No
29. Have you ever had any part of your stomach removed surgically?	Yes	No
30. Have you ever had an intestinal bypass operation?	Yes	No

For Everyone-Nutritional Supplements

31. Do you take a calcium or combination
    calcium + Vitamin D supplement?   Yes   No
    If *yes*, what kind and how many per day?

_____

_____

32. Do you take a multivitamin?   Yes   No
    If *yes,* what kind?

_____

33. Do you take an entirely separate Vitamin D supplement?   Yes   No
    If *yes*, what kind and how much?

_____

_____

For Everyone-Other Medications

34. Do you take or have you ever taken any of the following medications?

Testosterone replacement	Yes	No
Lithium	Yes	No
Thyroid hormone	Yes	No
If yes, what kind and what dose?		

_____

_____

Insulin	Yes	No
Dilantin®	Yes	No
Lupron® (leuprolide) or Zoladex® (goserelin)	Yes	No
Femara® (letrozole)	Yes	No
Arimedex® (anastrozole)	Yes	No
Anti-depressants	Yes	No

XIV Appendix

The CD-ROM Companion

There are four folders on the CD-ROM: the Densitometry Patient Demographic and Risk Factor Questionnaire, the Precision Calculator Companion, the Black Fracture Index, and the CME Review. Put the CD-ROM into the CD-ROM drive of your computer. The CD is self-launching and will open automatically. All the folders can be accessed from the opening page. This is the simplest way to access the contents of the CD-ROM Companion. The folders may also be accessed through MY COMPUTER or through WINDOWS EXPLORER. To view the Densitometry Patient Questionnaire, Microsoft Word must be installed on your computer. The Precision Calculator Companion requires Microsoft Excel. The Black Fracture Index and the CME Review are stand-alone programs. Microsoft Word and Microsoft Excel may also be used to open their respective programs directly.

THE PRECISION CALCULATOR COMPANION

There is only one Microsoft Excell workbook file in this folder. There are two spreadsheets in the workbook. The first spreadsheet is the Precision Calculator Companion. Instructions are given on the spreadsheet. This spreadsheet allows the user to calculate precision as the RMS-SD and RMS-%CV for a group of 15 patients studied three times each. The spreadsheet will also calculate the $_{1 \times 1}\text{LSC}^{95}$ for this level of precision.

The second spreadsheet is the Statistical Confidence Calculator. The instructions are included on the spreadsheet. This spreadsheet allows the user to calculate the absolute and percent change from baseline for two studies as well as the level of statistical confidence for measured change and any precision value. In other words, even though a measured change in BMD may not be statistically significant at the 95% confidence level, the Statistical Confidence Calculator indicates the level of statistical confidence at which there would be significance.

Each spreadsheet can be printed once the calculations are completed. The instructions will not be visible on the printout. The spreadsheets are locked but not password protected. This was done to prevent inadvertent erasure of the formulas. As long as the spreadsheets are not deliberately unlocked, it is not possible to erase the formulas embedded in the spreadsheets.

THE DENSITOMETRY PATIENT DEMOGRAPHIC AND RISK FACTOR QUESTIONNAIRE

There is only one file in the Densitometry Patient Questionnaire folder, which is the Densitometry Patient Demographic and Risk Factor Questionnaire. The questionnaire is not protected in any way and can be altered to suit your individual practice needs.

THE BLACK FRACTURE INDEX

The Black Fracture Index is discussed extensively in Chapter 10. It is a 5-year absolute fracture risk prediction algorithm, which utilizes several easily obtainable clinical risk factors and total hip BMD to derive a Fracture Index Score. The 5-year fracture risks for women in the Study of Osteoporotic Fractures with the same score are displayed graphically. Procter & Gamble graciously gave permission for the distribution of this software on the CD-ROM that accompanies this book.

THE CME REVIEW FOR
BONE DENSITOMETRY IN CLINICAL PRACTICE:
APPLICATION AND INTERPRETATION THIRD EDITION

To begin the review, click on the link from the CD Companion launch page. Follow the on-screen instructions. This is a 100 multiple-choice question review. Each question has only one right answer. Select the answer you believe to be correct and then click on SUBMIT. You will immediately be told if the answer is correct or incorrect. If incorrect, close the dialog box by clicking on the X in the upper right hand corner, return to the question and make another selection. Keep trying until you get the correct answer. You must click on SUBMIT for the answer to be recorded by the program. After obtaining the correct answer, close the dialog box as before and go to the next question. You may stop the review at any time and resume at a later date. After obtaining the correct answer on all 100 questions, you may complete and print a certificate of completion. Identifying data must be entered on the certificate prior to printing. Completion of the requested identifying information and course evaluation on the certificate is required for processing of CME credit. Successful completion of the Review will result in the awarding of 30 hours of Category 1 continuing education credit. The certificate of completion, course evaluation, and processing fee of $150.00 should be sent to:

Foundation for Osteoporosis Education and Research
300 27th Street, Suite 103
Oakland, CA 94612

Funds must be in US dollars. Checks should be made out to FORE.

Index